



UNIVERSITÀ DEGLI STUDI DI PAVIA
DOTTORATO IN SCIENZE CHIMICHE
E FARMACEUTICHE
XXIX CICLO

Coordinatore: Chiar.mo Prof. Mauro Freccero

TOWARDS THE DISCOVERY OF NOVEL SIGMA RECEPTOR
MODULATORS: ORGANOLITHIUM-METHODS BASED
SYNTHESIS AND BIOLOGICAL EVALUATIONS

Tutore

Chiar.ma Prof.ssa Simona Collina

Chiar.mo Dr. Vittorio Pace

A handwritten signature in black ink, appearing to be 'Simona Collina', written over the printed name.

Tesi di Dottorato di

RUI MARTA

a.a. 2015- 2016



universität
wien

DISSERTATION / DOCTORAL THESIS

Titel der Dissertation /Title of the Doctoral Thesis

„Towards the discovery of novel sigma receptor
modulators: organolithium-methods based synthesis and
biological evaluations“

verfasst von / submitted by

Dott. Marta Rui

angestrebter akademischer Grad / in partial fulfilment of the requirements for the degree of
Doktorin der Naturwissenschaften (Dr.rer.nat.)

Wien 2016/ Vienna 2016

Studienkennzahl lt. Studienblatt /
degree programme code as it appears on the student
record sheet:

A 796 610 449

Dissertationsgebiet lt. Studienblatt /
field of study as it appears on the student record sheet:

Pharmazie

Betreut von / Supervisors:

Prof. Vittorio Pace
Prof. Simona Collina

*“Do not think of yourself, think of others.
Think of the future that awaits you,
think about what you can do and
do not fear anything.”*

- Rita Levi Montalcini -

ABSTRACT

My three-year-project has been focused on two main topics, Sigma Receptors (SRs) and Lithium carbenoids, as briefly summarized in the following paragraphs.

1. Sigma Receptors as novel targets for the cancer treatment.

The driving force of my project work has been the need of finding “druggable” proteins as new molecular targets to treat cancer conditions. In the discovery of novel anticancer agents, able to guarantee a result with poor side effects, SR modulators are fit for purpose. Briefly, Sigma Receptors are involved in a large number of physiological functions including learning and memory processes, depression and anxiety, schizophrenia, analgesia and cancer. There are two subtypes of Sigma Receptors: S1R and S2R based on anatomical distribution, pharmacological and pathological activities. S1Rs are well known and several modulators have been identified so far. Particularly, S1R agonists are proved to exert neuroprotective and neuroplastic effects whereas S1R antagonists give rise to beneficial activities against neuropathic pain and cancer. Conversely, S2Rs still present enigmatic aspects, both from a structural and pharmacological point of view. However, numerous experimental evidences show the overexpression of this molecular target in cancer cells and the scientific community strongly supports the idea that S2R modulators may have antiproliferative and proapoptotic effects. Accordingly, we spent some of our efforts in identifying new anticancer agents, acting *via* SR modulation. In detail, we generated a QSAR model, using the activity data published in literature and our in-house library. This approach allowed to identify the structural features that guarantee a high affinity towards both SR subtypes. From this study emerged that compounds presenting a bulky aminic portion, *i.e.* 4-benzylpiperidine, possess pan-SR affinity. Therefore, we designed and synthesized a compound series of racemic and enantiomeric arylalkyl(alkenyl)-4-benzylpiperidine derivatives. On the bases of binding profile towards S1R and S2R and of its cytotoxic properties towards a panel of cancer cell lines, we select **RC-106** as the most promising antiproliferative agent. We believe that **RC-106** may be considered a valuable anticancer candidate and an in depth investigation of its anticancer properties is in progress. Lastly, a biotin-pan-SR conjugate has been designed as pharmacological tool able to enhance the uptake of antiproliferative molecules in cancer cells, as well as to avoid side effects. Although several attempts have been carried out, up to now, the desired product has not been obtained.

2. Lithium carbenoids, useful homologating agents.

During my experience at the University of Vienna, I studied the reactivity/stability of lithiumcarbenoids toward enone substrates. The final aim of this study was to verify the applicability of these reagents towards ketone derivatives of **RC-106**, in order to obtain key intermediate for future functionalization. The introduction of methylene groups in the drug structure may lead to a modification of its pharmacological properties and therefore homologation reactions represent important synthetic steps useful to obtain bioactive compounds. Particularly, carbenoid-mediated homologations are valuable alternative to the traditional and sometimes hazardous C-C bond forming reactions. Carbenoids are characterized by the presence of an electron-donating and an electron-withdrawing substituent, these elements confer to the carbon center an ambiphilic activity. Carbenoids may act as nucleophiles or as electrophiles, depending on the experimental conditions and, thanks to their versatility towards different substrates, they are considered important reagents in organic chemistry. The work presented herein is part of this scenario and it is a pursuance of the prior publication of Pace and co-workers, which developed a strategy to carry out a chemoselective 1,2-addition of LiCH_2Cl to cyclic enones. Once the applicability of the lithium carbenoids towards these ketones has been confirmed, the reactivity/stability of these species has been investigated in depth. Therefore, we focused on the study of the parameters that may influence the behavior of monohalomethylithium reagents, using a syringe pump instrument. Interestingly, from this work unexpected products emerged. Indeed, under particular conditions, a double homologation may occur, furnishing aldehydes. We analyzed this surprising reaction and disclosed the mechanism that took place.

RIASSUNTO

Il mio progetto di dottorato si è focalizzato su due argomenti principali, come brevemente descritto nei paragrafi successivi: i Recettori Sigma (RS) e Carbenoidi di Litio.

1. I Recettori Sigma come nuovi target molecolari per il trattamento del cancro.

La forza trainante di questo progetto di tesi è stata l'esigenza di individuare proteine "druggable" quali nuovi *targets* molecolari per il trattamento del cancro. Da dati di letteratura è emerso che i Recettori Sigma (RS) rispondono a tale requisito. Brevemente, i RS sono coinvolti in numerose funzioni fisiologiche, compresi i processi di apprendimento e memoria, depressione e ansietà, schizofrenia, analgesia e cancro. Due sottotipi recettoriali dei RS sono stati scoperti: RS1 e RS2. Essi presentano diversa distribuzione anatomica e differenti attività farmacologiche e patologiche. RS1 e i suoi modulatori sono noti da tempo. In particolare, è accertato che gli agonisti dei RS1 hanno effetto neuroprotettivo e neuroplastico, invece gli antagonisti dei RS1 sono utili contro il dolore neuropatico e il cancro. Differentemente dai RS1, i RS2 presentano ancora degli aspetti enigmatici, sia da un punto di vista strutturale che farmacologico. Tuttavia, numerose evidenze sperimentali dimostrano che questi sottotipi recettoriali sono sovra-espressi in cellule tumorali e la comunità scientifica supporta fortemente l'idea che i modulatori dei RS2 potrebbero avere effetto anti-proliferativo e pro-apoptotico. Di conseguenza, abbiamo rivolto la nostra attenzione verso l'identificazione di nuovi agenti antitumorali, che agiscono attraverso la modulazione dei RS. Nel dettaglio, un modello QSAR è stato generato, utilizzando l'attività di molecole note da letteratura e la nostra libreria di composti. Questo approccio ha permesso di identificare le caratteristiche strutturali che promuovono un'alta affinità nei confronti di entrambi i sottotipi recettoriali dei RS. Da questo studio è emerso che i composti che possiedono una porzione amminica ingombrante, ad esempio la 4-benzilpiperidina, possiedono affinità sia per RS1 che per RS2. Pertanto, abbiamo progettato e sintetizzato una serie di arilalchil(alchenil)-4-benzilpiperidine, in forma racemica ed enantiomerica. Sulla base dei profili di *binding* nei confronti dei RS1 e dei RS2 e le loro proprietà citotossiche verso un *pool* di linee cellulari tumorali, abbiamo selezionato **RC-106** come agente anti-proliferativo più promettente. Noi riteniamo che **RC-106** potrebbe essere considerate un candidato antitumorale molto promettente, di conseguenza ulteriori valutazioni biologiche sono in atto. Infine, è stato progettato un coniugato biotina-pan RS al fine di ottenere uno strumento farmacologico capace di aumentare l'ingresso di molecole anti-proliferative in cellule tumorali, così come per evitare gli effetti collaterali tipici delle terapie antitumorali tradizionali. Nonostante i

numerosi tentativi per ottenere il prodotto desiderato, al momento non abbiamo individuato la strategia giusta per accedere al coniugato.

2. Carbenoidi di litio, utili agenti di omologazione.

Durante la mia esperienza presso l'Università di Vienna, ho studiato la reattività/stabilità dei litiocarbenoidi nei confronti di chetoni α,β -insaturi. Lo scopo ultimo di questo studio sarà quello di verificare se tali reagenti possono essere applicati verso derivati chetonici di **RC-106**, al fine di ottenere degli intermedi chiave per future funzionalizzazioni. L'introduzione di gruppi metilenici in una struttura di interesse farmaceutico può comportare la modifica delle sue proprietà farmacologiche. Pertanto, le reazioni di omologazione rappresentano importanti *step* sintetici utili per ottenere composti bioattivi. In particolare, le omologazioni mediate dai carbenoidi sono delle alternative preziose alle tradizionali e qualche volta pericolose reazioni C-C. I carbenoidi sono caratterizzati dalla presenza di un gruppo elettron-donatore e da un sostituente elettron-attrattore, questi elementi conferiscono al carbonio attività ambifiliche. Infatti, i carbenoidi possono agire sia da nucleofili che da elettrofili, in funzione delle condizioni sperimentali e, grazie alla loro versatilità nei confronti di diversi substrati, sono considerati degli importanti reagenti in chimica organica. Il lavoro riportato in questa tesi è parte di questo scenario ed è una continuazione della pubblicazione precedente di Pace e collaboratori, i quali hanno sviluppato una strategia per effettuare un'addizione 1,2-chemosellettiva di LiCH_2Cl a chetoni α,β -insaturi ciclici. Una volta che la fattibilità di queste reazioni è stata confermata, la reattività/stabilità di queste specie è stata approfondita. Pertanto, ci siamo focalizzati sullo studio dei parametri che possono influenzare il comportamento dei reagenti di monoalometillitio, utilizzando una *syringe pumpe* come strumento. Inoltre, da questo lavoro prodotti inaspettati sono emersi. Infatti, in condizioni particolari, una doppia omologazione può avvenire, fornendo delle aldeidi. Abbiamo analizzato questo risultato sorprendente e abbiamo dimostrato il meccanismo che ha luogo.

ABSTRAKT

Mein dreijähriges Projekt fokussierte sich auf zwei Hauptthemen, Sigmarezeptoren (SRs) und Lithiumcarbenoide, welche in den anschließenden Absätzen kurz zusammengefasst werden.

1. Sigmarezeptor Modulatoren als neuartige Targets in der Krebsbehandlung.

Die Motivation hinter meinem Projekt war die Notwendigkeit, neue „druggable“ Proteine als Targets zur Behandlung von Krebserkrankungen aufzufinden. Auf der Suche nach neuartigen krebzbekämpfenden Wirkstoffen, welche unter geringen Nebenwirkungen ihre Wirkung entfalten, sind SRs Modulatoren geeignet. Sigmarezeptoren sind in einer Vielzahl an physiologischen Funktionen involviert, unter anderem Lern- und Erinnerungsprozesse, Depressionen und Angstzustände, Schizophrenie, Analgesie und Krebs. Es gibt dabei zwei Unterarten von Sigmarezeptoren: S1R und S2R, basierend auf anatomischer Verteilung sowie pharmakologischer und pathologischer Aktivitäten. S1Rs sind gut bekannt und bisher wurden mehrere Modulatoren entdeckt. Insbesondere wurde für S1R-Agonisten gezeigt, dass sie neuroprotektive und neuroplastische Effekte haben, wohingegen S1R-Antagonisten zu positiven Wirkungen gegen neuropathischen Schmerzen und Krebs führen. Im Gegensatz dazu ist S2R immer noch nicht hinreichend bekannt, sowohl in struktureller als auch in pharmakologischer Hinsicht. Zahlreiche experimentelle Ergebnisse zeigen aber eine Überausscheidung dieses Targets in Krebszellen und die Wissenschaft unterstützt die Idee, dass S2R-Modulatoren antiproliferative und proapoptische Effekte haben könnte. Damit einhergehend verwenden wir einigen Aufwand dafür, Antikrebs-Wirkstoffe zu finden, die via SR-Modulation wirken. Genau gesagt haben wir ein QSAR-Modell erstellt, basierend auf in der Literatur veröffentlichter Daten und Daten aus unserer hauseigenen Bibliothek. Dieser Ansatz hat es erlaubt, die strukturellen Eigenschaften zu identifizieren, die eine hohe Affinität gegenüber beiden SR-Subtypen garantieren. Aus dieser Studie ging hervor, dass Verbindungen mit sperrigen Amin-Gruppen, z.B. 4-Benzylpiperidin, pan-SR affin sind. Daher entwarfen und synthetisierten wir eine Reihe an razemischen und enantiomeren Arylalkyl(alkenyl)-4-Benzylpiperidin-Derivaten. Auf Grund des Bindungscharakters bezüglich S1R und S2R, sowie den cytotoxischen Eigenschaften einer Menge an Krebszelllinien, wählten wir RC-106 als den vielversprechendsten antiproliferativen Wirkstoff. Wir glauben, dass RC-106 ein vielversprechender Kandidat für einen Antikrebs-Wirkstoff ist, weitergehende Untersuchungen dieser Eigenschaften sind im Gange. Zu guter Letzt wurde ein Biotin-Pan-SR-Konjugat als pharmakologisches Werkzeug entworfen, das dazu fähig ist, die Aufnahme an

antiproliferativen Molekülen in Krebszellen zu erhöhen und Nebenwirkungen zu vermeiden. Trotz wiederholten Versuchen wurde nicht das gewünschte Produkt gefunden.

2. Lithiumcarbenoide, nützliche homologierende Stoffe

Während eines Aufenthaltes an der Universität Wien wurden die Reaktivität und Stabilität der Lithiumcarbenoide gegenüber Enonsubstraten untersucht. Das Hauptziel dieser Untersuchung war die Anwendbarkeit dieser Reagenzien gegenüber Ketonderivaten des RC-106 zu verifizieren, um das Hauptzwischenprodukt für spätere Funktionalisierung zu gewinnen. Die Einführung einer Methylen-Gruppe in der Wirkstoffstruktur kann zu einer Modifikation ihrer pharmakologischen Eigenschaften führen, somit stellen Homologisierungsreaktionen wichtige Synthese-Schritte dar, welche dem Auffinden bioaktiver Verbindungen dienen. Vor allem carbenoidgesteuerte Homologierungen sind wertvolle Alternativen zu den manchmal gefährlichen C-C Reaktionen. Carbenoide sind von der Gegenwart elektronenspendender und elektronenziehender Substituenten charakterisiert, diese Elemente geben dem Kohlenstoffzentrum eine ambiphile Aktivität. So können Carbenoide abhängig von den experimentellen Bedingungen als Elektrophile und Nukleophile agieren, was ihrer Vielfältigkeit gegenüber unterschiedlicher Substrate zuzurechnen ist. Sie werden als bedeutende Reaktanden der Organischen Chemie gesehen. Die dabei ausgeübte Tätigkeit ist Teil dieses Szenarios und eine Fortsetzung der vorangehenden Publikationen von Pace et al., welche Strategien zu einer chemoselektiven 1,2-Addition von LiCH_2Cl zu zyklischen Enonen entwickelten. Sobald die Anwendbarkeit dieser Lithiumcarbenoide gegenüber diesen Ketonen bestätigt wurde, konnten Reaktivität und Stabilität dieser Spezies weiter untersucht werden. Somit richtete sich der Fokus auf die Untersuchung der Parameter mit einem Spritzpumpen-Apparat, welcher das Verhalten von Monohalomethylithium-Reagenzien beeinflussen könnte. Unerwartete Produkte wurden dabei erhalten. Tatsächlich kann unter besonderen Bedingungen eine doppelte Homologisierung stattfinden, bei welcher Aldehyde angefügt wurden. Die unerwartete Reaktion wurde untersucht und der grundlegende Mechanismus dahinter gefunden.

TABLE OF CONTENTS

FOREWORD	1
Chapter 1 - SIGMA RECEPTORS	5
1. INTRODUCTION	7
1.1. Sigma 1 Receptor (S1R)	10
1.2. Sigma 2 Receptor (S2R)	12
1.3. S1R and S2R modulators	13
2. THE RESEARCH	19
2.1. Background	21
2.2. MY Ph.D. project	23
3. CONCLUSION AND OUTLOOK	45
4. EXPERIMENTAL SECTION	49
4.1. Compounds characterizations and biological evaluations	51
4.2. Materials and methods	54
4.3. Synthesis of biotin derivative 21 (SA3)	54
4.3.1. Preparation of compound 19	54
4.3.2. Preparation of compound 20	55
4.3.3. Preparation of compound 21 (SA3)	55
4.3.4. ¹ H and ¹³ C NMR Spectra of Compounds 19-21	57
5. REFERENCES	59
Chapter 2 - LITHIUM CARBENOIDS	67
1. INTRODUCTION	69
1.1. Lithium carbenoids	73
1.2. Generation of monohalolithium carbenoids	76
1.3. Carbon electrophiles for carbenoids	78

2. THE RESEARCH	85
2.1. Background	87
2.2. My Ph.D. project	90
3. CONCLUSION AND OUTLOOK	101
4. EXPERIMENTAL SECTION	105
4.1. Materials and methods	107
4.2. General Procedure for the Chemoselective Addition of LiCH ₂ Cl to Ketones, to obtain halohydrins	107
4.3. General Procedure for the conversion of the halohydrins into epoxides	132
4.4. General Procedure for the Chemoselective Addition of LiCH ₂ Cl to Ketones to obtain aldehydes	138
4.5. General Procedure for the Chemoselective Addition of LiCH ₂ Cl to Ketones to obtain epoxides	180
5. REFERENCES	187
ACKNOWLEDGEMENTS	195
APPENDIX	197
MR1: Tripodo, G.; Mandracchia, D.; Collina, S.; Rui, M.; Rossi, D. New perspectives in cancer therapy: the biotin-antitumor molecule conjugates. <i>Med.Chem.</i>	
MR2: Rossi, D.; Marra, A.; Rui, M.; Laurini, E.; Fermaglia, M.; Pricl, S.; Schepmann, D.; Wuensch, B.; Peviani, M.; Curti, D.; Collina, S. A step forward in the sigma enigma: A role for chirality in the sigma ₁ receptor-ligand interaction? <i>Med. Chem. Comm.</i>	
MR3: Rossi, D.; Marra, A.; Rui, M.; Brambilla, S.; Juza, M.; Collina, S. "Fit-for-purpose" development of analytical and (semi-preparative enantioselective high performance liquid and supercritical fluid chromatography for the access to a novel sigma(1) receptor agonist. <i>J. Pharmac. Biomed. Anal.</i>	
MR4: Monticelli, S.; Parisi, G.; Rui, M.; de la Vega Hernandez, K.; Murgia, I.; Urban, E.; Langer, T.; Pace, V. The Use of the Comins-Meyers Amide in Synthetic Chemistry: an Overview. <i>Natural Product Communications.</i>	
MR5: Rui, M.; Rossi, D.; Marra, A.; Paolillo, M.; Schinelli, S.; Curti, D.; Tesei, A.; Cortesi, M.; Zamagni, A.; Laurini, E.; Pricl, S.; Schepmann, D.; Wünsch, B.; Urban, E.; Pace, V.; Collina, S. Synthesis and biological evaluation of new aryl-alkyl(alkenyl)-4-benzylpiperidines, novel Sigma Receptor (SR) modulators, as potential anticancer-agents. <i>Eur. J. Med. Chem.</i>	
MR6: Rui, M.; Marra, A.; Pace, V.; Juza, M.; Rossi, D.; Collina, S. Novel enantiopure sigma	

receptor (SR) modulators: quick preparation via (semi)-preparative chiral HPLC and absolute configuration assignment. *Molecules*.

MR7: Rossi, D.; Rui, M.; Di Giacomo, M.; Schepmann, D.; Wuensch, B.; Monteleone, S.; Liedl, K.R.; Collina, S. Gaining in Pan-Activity Towards Sigma 1 and Sigma 2 Receptors. SAR studies on arylalkylamines. *Bioorg. Med. Chem.*

MR8: Collina, S.; Bignardi, E.; Rui, M.; Rossi, D.; Gaggeri, R.; Cortesi, M.; Zamagni, A.; Tesei, A. Are Sigma modulators an effective opportunity for cancer treatment? A patent overview (1996-2016). *Exp. Opin. Ther. Pat.*

MR9: Pace, V.; Castoldi, L.; Monticelli, S.; Rui, M.; Collina, S. New Perspectives in Lithium Carbenoids Mediated Homologations. *Synlett*.

ABBREVIATIONS

1,2-DCE	1,2-Dichloroethane
4-NPCF	4-nitrophenyl chloroformate
α	Selectivity factor
AcOH	Acetic acid
APT	Attached proton test
Bn₃SnCH₂Cl	Tributylstannyl chloromethane
CaO	Calcium oxide
CCl₄	Tetrachloromethane
CD₂Br₂	Dibromomethane-d ₂
CE	Cotton Effect
(CF₃CO)₂O	Trifluoroacetic anhydride
CH₂Br₂	Dibromomethane
CH₂N₂	Diazomethane
¹³C-NMR	Carbon-13 nuclear magnetic resonance
CNS	Central Nervous System
CO₂	Carbon dioxide
CSPs	Chiral Stationary Phases
CuAAC	copper(I)-catalyzed alkyne-azide cycloaddition
CuBr	Copper(I) bromide
Cu(OTf)₂	copper(II) triflate
CuSO₄	Copper Sulfate
DCC	<i>N,N'</i> -Dicyclohexylcarbodiimide
DCM	Dichloromethane
DCU	<i>N,N'</i> -Dicyclohexylurea
DEA	Diethylamine
DEPT	Distortionless enhancement by polarization transfer
DIPEA	<i>N,N</i> -Diisopropylethylamine
DMAP	4-Dimethylaminopyridine
DMF	Dimethylformamide
DMSO	Dimethyl sulfoxide
DTG	1,3-di(2-tolyl)guanidine
ECD	Electronic Circular Dichroism
EDG	Electron Donating Group
ER	Endoplasmic Reticulum
Et₃N	Triethylamine
Et₂O	Diethylethere
EtOH	Ethanol
EWG	Electron Withdrawing Group
FACS	Fluorescence-activated cell sorting
FBS	Fetal bovine serum
HCl	Chloride acid
HMBC	Heteronuclear multiple-bond correlation spectroscopy
¹H-NMR	Proton nuclear magnetic resonance
H₂O	Water
HPLC	High Performance Liquid Chromatography
HPMA	Hydroxypropyl methacrylate
HRMS	High Resolution Magic Angle Spinning
HSQC	Heteronuclear single quantum coherence spectroscopy

IARC	International Agency for Research on Cancer
IL-6RE	Interleukin-6 Receptor
InCl₃	Indium(III) chloride
IP3	Inositol trisphosphate
IPA	2-Propanol
<i>i</i>PrMgCl	Isopropylmagnesium chloride
IR	Infrared spectroscopy
IRE1	Inositol Requiring Enzyme 1
<i>k</i>	Retention factor
kbp	kilo base pair
kDa	Kilodalton
Ki	Affinity constant
LDA	Lithium diisopropylamide
LiClO₄	Lithium perchlorate
LiHMDS	Lithium bis(trimethylsilyl)amide
LiOEt	Lithium ethoxide
LNCy₂	Lithium dicyclohexylamide
LTMP	Lithium 2,2,6,6-tetramethylpiperidide
MAM	Mitochondria-associated membrane
MeCN	Acetonitrile
MeLi	Methyl lithium
MeNH₂EtNHMe	<i>N,N'</i> -Dimethylethylenediamine
MeOH	Methanol
mRNA	Messenger RNA
MTS	(3-(4,5-dimethylthiazol-2-yl)-5-(3-carboxymethoxyphenyl)-2-(4-sulfophenyl)-2H-tetrazolium)
NaBH₃CN	Sodium cyanoborohydride
NaH	Sodium hydride
NaHCO₃	Sodium bicarbonate
<i>n</i>-Hep	<i>n</i> -heptane
NaI	Sodium iodide
NaOH	Sodium hydroxide
Na₂SO₄	Sodium sulphate
<i>n</i>-BuLi	<i>n</i> -butyllithium
NCEs	New Chemical Entities
NF-κB	Nuclear Factor kappa-light-chain-enhancer of activated B cells
NGF	Nerve Growth Factor
NH₃	Ammonia
NH₄Cl	Ammonium chloride
NMDA	N-Methyl-D-Aspartate
N₃-PEG₃-NH₂	11-azido-3,6,9-trioxaundecan-1-amine
NOESY	nuclear Overhauser effect spectroscopy
Nrf2	Nuclear factor E2-related factor 2
PEG-400	Polyethylene glycol 400
PET	Positron Emission Tomography
PGRMC1	Progesterone Receptor Membrane Component 1
PhCHO	Benzaldehyde
Ph₂SiClH	Chlorodiphenylsilane
PhSOCH₂Cl	Chloromethyl phenyl sulfoxide
PPh₃	Triphenylphosphine
QSAR	Quantitative structure–activity relationship

ROS	Reactive Oxygen Species
Rs	Resolution factor
rt	Room temperature
RT-PCR	Reverse transcriptase-polymerase chain reaction
SAR	structure–activity relationship
s-BuLi	<i>s</i> -butyllithium
SCX	Strong cation exchange
SFC	Supercritical fluid chromatography
SMVT	Sodium dependent multivitamin transporter
SR	Sigma Receptor
S1R	Sigma 1 Receptor
S2R	Sigma 2 Receptor
SPE	Solid Phase Extraction
TBDMSCI	<i>t</i> -butyldimethylsilyl chloride
<i>t</i>-BuLi	<i>t</i> -butyllithium
TFA	Trifluoroacetic acid
TMS	trimethylsilyl
tR	retention time
UPLC	Ultra performance liquid chromatography
VHA	Vilsmeier-Haack-Arnold

FOREWORD

This Ph.D. thesis is the result of the work carried out at the Department of Drug Sciences, University of Pavia, Italy, and at the Faculty of Life Sciences, University of Vienna, Austria, during the years 2013-2016.

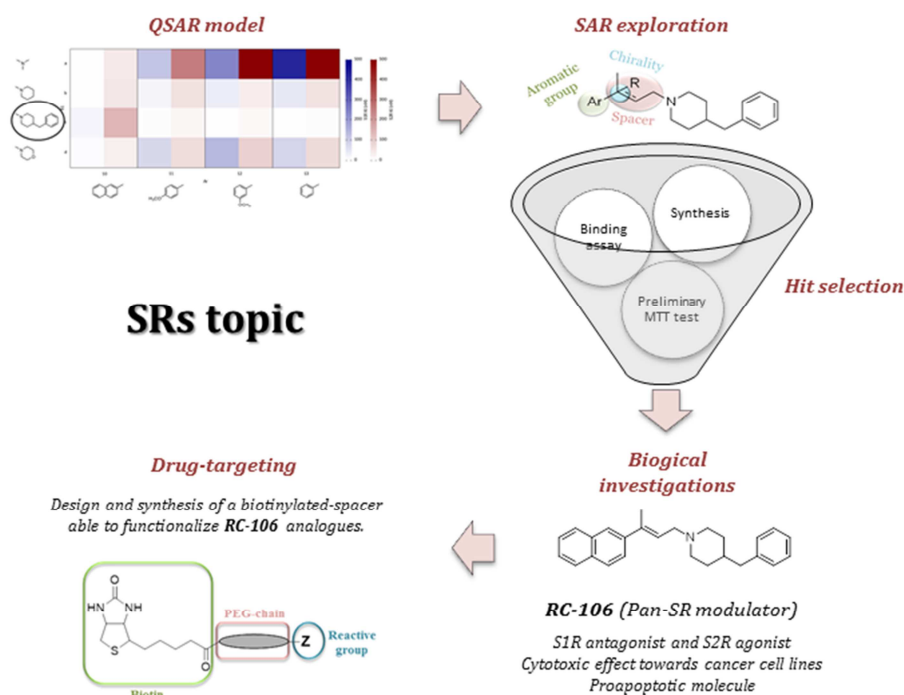
The thesis is structured in two sections, the first is the core of my Medicinal Chemistry project, and the second is focused on the applicability of monohalomethylithium reagents towards enones. In detail, in the first section of this dissertation, the Sigma Receptors (SRs) topic will be deepened, whereas the second section will highlight the versatility of lithium carbenoids in Medicinal Chemistry. These two parts converge in a single goal, which is the possible application of carbenoidic species on a series of SRs modulators.

Medicinal Chemistry is a multifaceted world and encompasses several disciplines. The “trump card” of the Medicinal Chemist’s approach is represented by a motley network of collaborations, which allows a pro and con overview of a project. During my Ph.D. scholarship I had the chance to get in touch with several aspects of this intriguing and fascinating world. In detail, during the last three years I learnt to plan a project, following the classical work flow related to the discovery of novel pharmacological tools.

In this project we took into consideration the SR family as a molecular target, in order to identify New Chemical Entities (NCEs) as promising candidates in the treatment of cancer conditions. In the recent past, SRs have been discovered and two different subtypes have been identified: Sigma 1 and Sigma 2 Receptors (S1R and S2R). They have a diverse anatomical distribution, characterized by distinct pharmacological and pathological activities. The strict relation between S1R and Central Nervous System (CNS) has been widely documented. Indeed, numerous works disclosed the neuroprotective and neuroplastic effects of S1R agonists, therefore SR modulators could be considered as potential molecules in the treatment of neurodegenerative diseases (i.e. Alzheimer and Parkinson diseases, Multiple Sclerosis, Amyotrophic Lateral Sclerosis). Conversely, S1R antagonists deserve to be mentioned in virtue of their beneficial activities against neuropathic pain and cancer.

Differently from S1R, the structure and the pharmacological behaviour of S2R still present enigmatic aspects. However, even though there is the little structural knowledge and the lack of endogenous ligands related to S2R, numerous experimental evidence shows the overexpression of this molecular target in cancer cells. Indeed, the scientific community supports the antiproliferative and the proapoptotic effects associated with S2R modulators.

Accordingly, the driving force of this work is represented by the urgent need of finding “druggable” proteins as new molecular targets to treat cancer conditions. In the discovery of novel anticancer agents, able to guarantee a result with unimportant side effects, SRs modulators are fit for the purpose. Therefore, in this project we present our efforts in designing and synthesizing SR ligands, evaluating their activity through an in depth biological investigation.

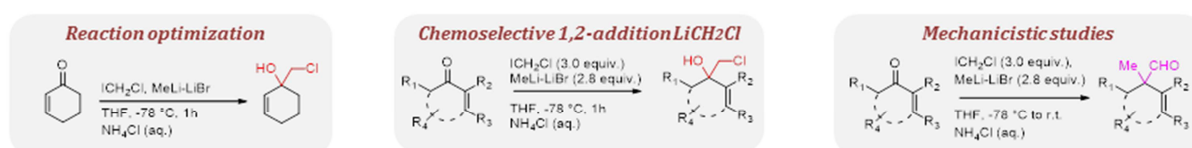


Graphical abstract of SRs topic.

Additionally, I spent a part of my research project at the Organic Laboratory, University of Vienna, in order to improve my skills as an organolithium chemist. Indeed, the main topic of Pace's group is the lithium, as a multitasking element. Lithium reagents present several applications in the synthetic field, in particular lithium carbenoids are useful homologating agents. In fact, in the last sixty years carbenoid-mediated homologations took place as a valuable alternative to the traditional and sometimes hazardous C-C reactions. The high yields and the versatility of carbenoids towards different substrates lead to consider these reagents as an important discovery in organic chemistry. The work presented herein is part of this scenario and it is a pursuance of the prior publication of Pace and co-workers, which developed a strategy to carry out a chemoselective 1,2-addition of LiCH_2Cl to cyclic enones. Once the applicability of the lithium carbenoids towards these ketones has been confirmed, the reactivity/stability of these species was investigated in depth. Therefore, we focused on

the study of the parameters that may influence the behaviour of monohalomethyl lithium reagents, using a syringe pump instrument. Interestingly, from this work unexpected products emerged. Indeed, under particular conditions, a double homologation may occur, furnishing aldehydes. Considering the interest covered by the aldehyde group in synthetic and in medicinal chemistry, we analysed this surprising reaction and disclosed the mechanism that took place.

Lithium carbenoid topic



Graphical abstract of lithium carbenoid topic, LiCH_2Cl

In conclusion, even though several hurdles were envisaged during these three years, we laid the foundation for further studies focused on the discovery of new anticancer agents and a novel application for lithium carbenoids. The success of this multidisciplinary project may be associated with the strict network of collaborations, which is the driving force to reach the main goal in an experimental research. A consistent part of the results reached so far has been already published in international journals. Many people gave a crucial contribution to this work, starting from my supervisors Prof. Simona Collina and Prof. Vittorio Pace to all the co-authors: the groups of Prof. Liedl and Prof. Prici for their support in modelling; Prof. Juza for his contribution to the analytical part; Wuensch's group for the binding assay results; the staff of Prof. Curti, Dr. Tesei and Prof. Paolillo for the biological investigation; Prof. Holzer and Prof. Urban for their technical support in NMR interpretation. They are experts on different disciplines, all essential for conducting a Medicinal Chemistry research project.

List of publication

The Main Text and the Supporting Information related to these papers are reported in the Appendix Section.

- 1) Tripodo, G.#; Mandracchia, D.; Collina, S.*; Rui, M.; Rossi, D.# New perspectives in cancer therapy: the biotin-antitumor molecule conjugates. *Med.Chem.* 2014, DOI: 10.4172/2161.S1-004.
- 2) Rossi, D.#; Marra, A.#; Rui, M.; Laurini, E.; Fermaglia, M.; Pricl, S.; Schepmann, D.; Wuensch, B.; Peviani, M.; Curti, D.; Collina, S.* A step forward in the sigma enigma: A role for chirality in the sigma1 receptor-ligand interaction?. *Med.Chem. Comm.* 2015, 6, 138-146.
- 3) Rossi, D.#; Marra, A.#; Rui, M.; Brambilla, S.; Juza, M.*; Collina, S.* "Fit-for-purpose" development of analytical and (semi-preparative enantioselective high performance liquid and supercritical fluid chromatography for the access to a novel sigma(1) receptor agonist. *Journal of Pharmaceutical and Biomedical Analysis* 2016, 118, 363-369.
- 4) Monticelli, S.; Parisi, G.; Rui, M.; de la Vega Hernandez, K.; Murgia, I.; Urban, E.; Langer, T.; Pace, V.* The Use of the Comins-Meyers Amide in Synthetic Chemistry: an Overview. *Natural Product Communications* 2016, 11, 1729-1732.
- 5) Rui, M.#; Rossi, D.#; Marra, A.; Paolillo, M.; Schinelli, S.; Curti, D.; Tesei, A.; Cortesi, M.; Zamagni, A.; Laurini, E.; Pricl, S.; Schepmann, D.; Wünsch, B.; Urban, E.; Pace, V.; Collina, S.* Synthesis and biological evaluation of new aryl-alkyl(alkenyl)-4-benzylpiperidines, novel Sigma Receptor (SR) modulators, as potential anticancer-agents. *European Journal of Medicinal Chemistry* 2016, 124, 649-665.
- 6) Rui, M.; Marra, A.; Pace, V.; Juza, M.; Rossi, D.; Collina, S.* Novel enantiopure sigma receptor (SR) modulators: quick preparation via (semi)-preparative chiral HPLC and absolute configuration assignment. *Molecules* 2016, 21, 1210-1222.
- 7) Rossi, D.#; Rui, M.; Di Giacomo, M.; Schepmann, D.; Wuensch, B.; Monteleone, S.#; Liedl, K.R.; Collina, S.* Gaining in Pan-Activity Towards Sigma 1 and Sigma 2 Receptors. SAR studies on arylalkylamines. *Bioorganic & Medicinal Chemistry* 2017, 25, 11-19
- 8) Collina, S.*; Bignardi, E.; Rui, M.; Rossi, D.; Gaggeri, R.; Zamagni A.; Cortesi, M.; Tesei, A. Are Sigma modulators an effective opportunity for cancer treatment? A patent overview (1996-2016). *Expert Opinion on Therapeutic Patents.* 2017, DOI: 10.1080/13543776.2017.1276569.
- 9) Pace, V.*; Castoldi, L.; Monticelli, S.; Rui, M.; Collina, S. New Perspectives in Lithium Carbenoids Mediated Homologations. *Synlett* 2017, *Accepted*.

equal contribution; * corresponding author

SIGMA RECEPTORS

1. INTRODUCTION

1. INTRODUCTION

Today cancer is one of the main causes of death worldwide ($\approx 15\%$). Among the over 100 types of neoplasia affecting humans, the most common are lung, breast and prostate tumours [1]. The International Agency for Research on Cancer (IARC) estimated that annually more than 10 million people in the world get cancer and this value is expected to increase over the years [2]. Therefore, there is an urgent need of innovative therapies for this pathology. Despite the enormous advances in the pharmacological oncology field, to date, surgical resection is still the only treatment able to guarantee long-term survival in cancer conditions. Unfortunately, this kind of therapy is reserved only to a small percentage of cases [3] and chemotherapy still remains the first-choice treatment for the majority of patients [4-6]. Today, identifying molecules endowed with unimportant side effects is still a challenge, since chemotherapy shows low selectivity and high toxicity against non-neoplastic tissues [7-8]. A scientific approach, useful to identify new anticancer agents, foresees an in depth comprehension of the molecular basis underlying tumorigenesis. In this context, the discovery of new molecular targets and their signalling cascades may open the door to novel therapeutic strategies. Recent literature data shows the SRs overexpression in several cancer tissues, suggesting the therapeutic potential of SR modulators in tumorous conditions. After a brief overview on SRs, we will focus on the context of oncology, thus introducing my Ph.D. project. The term "Sigma Receptor" was coined in 1976 by Martin et al., in order to identify a new opioid receptor subtype [9]. Despite their capability to interact with the benzomorphan analogue (\pm)-SKF-10,047 (Figure 1), this classification was an erroneous assumption, since the opioid antagonists had no activity toward SRs [10-12]. Subsequently, SRs were proposed as the binding site of phencyclidine (Figure 1), located on the ionic channel associated with the N-methyl-D-aspartate (NMDA) receptor. Also in this case the hypothesis was rejected [13].

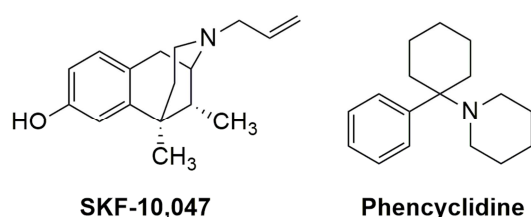


Figure 1. Structures of SKF-10,047 and Phencyclidine.

Despite the SR excursus presents several contradictions and wrong assumptions, the advances in biological and pharmacological fields collimate in defining SR as an orphan receptor family (Figure 2). Currently, two subtypes S1R and S2R are known [14-15]. The

experimental evidence and the literature data collected during the years, suggest that both S1R and S2R are involved in cell proliferation and survival, triggering distinct molecular cascades [16]. In the following sections, the state-of-art knowledge about S1R, S2R and their modulators will be summarized. An in depth description of the proteins and ligands targeting S1R and/or S2R, available so far is reported in the review **MR8**. Furthermore, in this publication we analysed the numerous patents, relating SRs modulators and cancer conditions, disclosed in the last twenty years.

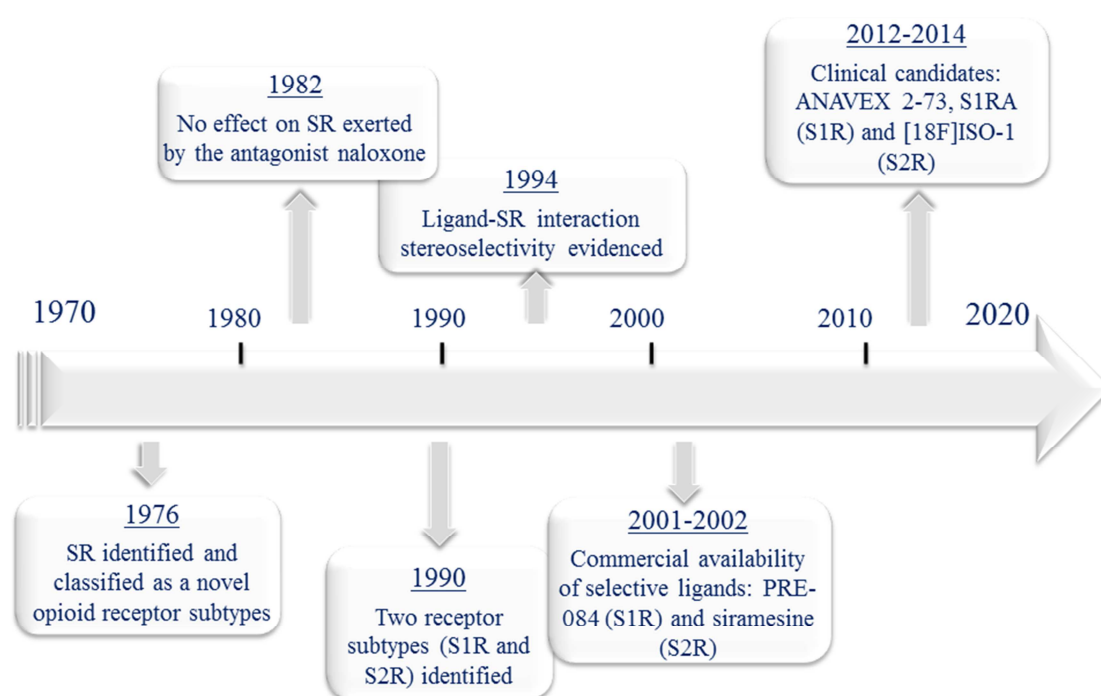


Figure 2. Timeline of key events in the history of SR and their modulators.

1.1. Sigma 1 Receptor (S1R)

The gene encoding S1R has been cloned [17-18] and it expresses an integral membrane protein composed by 223 amino acids, with a molecular weight of 25.3 kDa [19-20]. The isolated S1R gene is 7 kbp long, localized on 13p band of human chromosome 9, which is a region related with psychiatric disorders [17-19, 21, 22]. Several consensus binding sites for transcription factors have been identified on the promoter region of S1R gene. Some of them are implicated in the tumorigenesis, *i.e.* NF- κ B, IL-6RE [19].

For years, the lack of an endogenous ligand as well as the crystal structure of the protein, obliged several research groups to employ a ligand-based drug design approach to identify new molecules targeting S1R. Moreover, in the last ten years, several possible structures of S1R have been postulated. In detail, at the beginning, the analysis of the amino acid sequences

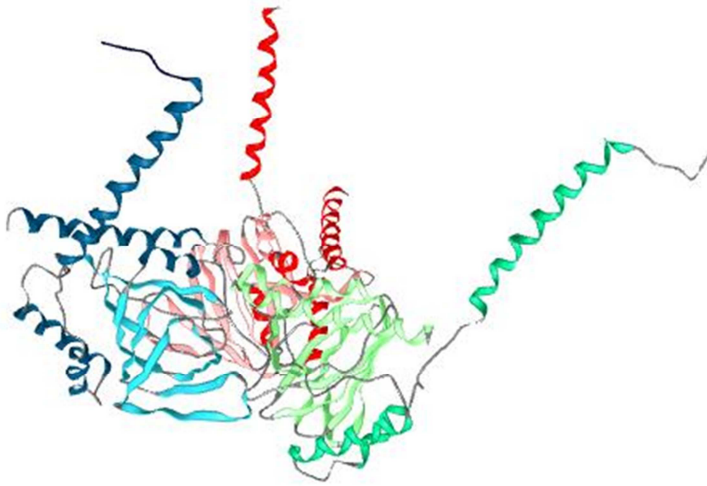


Figure 3. S1R shows a triangular structure comprising three tightly associated protomers, each with a single transmembrane domain at a corner of the oligomeric triangle.

of S1R suggested a single transmembrane segment [17-18, 21]. Subsequently, three hydrophobic domains have been proposed: two transmembrane-spanning domains connected by a *loop*, whereas the third one protrudes from the inner face of the membrane [23-24]. Despite the numerous attempts in elucidating the binding site structure, the advanced proposals about this crucial element mismatched. Only in

2016, the ligand binding pocket has been disclosed, since the three-dimensional structure of S1R has been identified (Figure 3). It is constituted by a trimer, with a single transmembrane helix and a cytosolic domain for each monomer. The ligand binding pocket is placed in the β -barrel region of the cytosolic domain and is constituted mainly by hydrophobic residues. The binding is triggered by an ionic interaction with a highly conserved Glu residue (E172), that is involved in a network of hydrogen bonds with Asp126 and Tyr103. Therefore, only positively charged molecule shows S1R activity. Moreover, ligands form hydrophobic π - π interactions with Tyr103 and other hydrophobic amino acids in the binding site [25]. The previous receptor models present high degree of similarity with the crystal structure. Conversely, the presence of a single transmembrane domain is a structural motif in disagreement with the constructs reported in antecedent studies.

Regarding the localization of S1R, we know that at subcellular level, the receptor is localized at the endoplasmic reticulum/mitochondria interface, in a region called MAM (Mitochondria-associated ER membrane). Only in 2007, the role played by S1R was clarified. It is a molecular chaperone and, during its translocation, it can modulate the activity of different receptors, enzymes and ionic channels [26]. In detail, at the MAM level, it ensures the cell survival through different mechanisms: i) Ca^{2+} homeostasis control, by chaperoning the inositol triphosphate (IP3) receptor; ii) it promotes an increase of antioxidant and antistress proteins, by ensuring the correct transmission of ER stress into the nucleus, through the modulation of Inositol Requiring Enzyme 1 (IRE1); iii) it promotes a decrease of reactive oxygen species (ROS) formation through Nrf2 signalling. Moreover, under stressful conditions or in the case of pharmacological manipulations S1R can translocate from the MAM to other cellular

compartments, affecting other membranous and soluble proteins. This broad network of interactions determines the involvement of S1R in numerous signal transduction pathways, indeed it can be defined a pluripotent modulator in living systems [27]. Macroscopically, S1R is ubiquitously expressed (liver, kidney, heart) above all in the CNS [28], in fact it could be defined as a potential therapeutic target for treating neurodegenerative pathologies (Alzheimer's disease, Parkinson's disease, Amyotrophic Lateral Sclerosis) as well as cocaine addiction, myocardial hypertension and cancer (Figure 4) [16, 29-31].

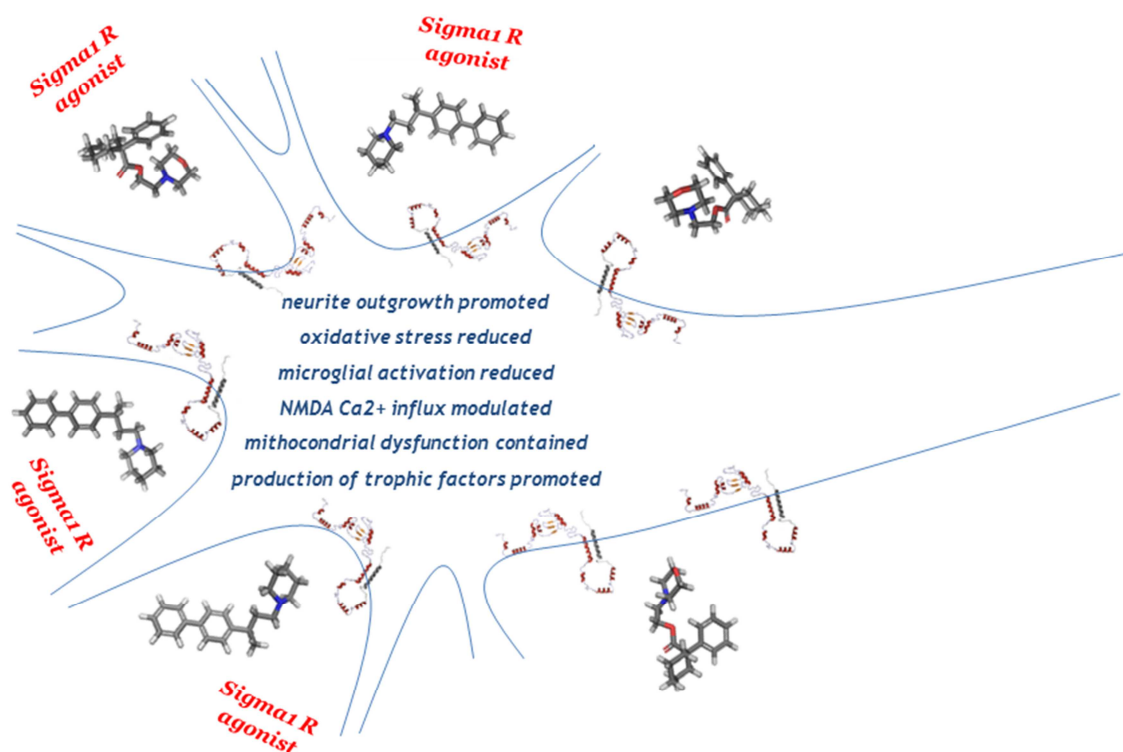


Figure 4. Effects due to the sigma1 receptor activation by agonists on the neurological diseases.

1.2. Sigma 2 Receptor (S2R)

While S1R properties and function have been widely elucidated [27], S2R biological characterization is still to be completely defined, since it has neither been cloned nor its amino acids sequence deciphered. It has been identified through photoaffinity labelling study, using 1,3-di(2-tolyl)guanidine (DTG). The results showed the existence of two protein bands of 25 and 21.5 kDa. The first band was associated to S1R, this assumption was confirmed after cloning the gene encoding S1R, which presented a molecular weight of 25.3 kDa. The second band was assigned to the S2R [32]. In the S2R panorama there are several black holes, nevertheless, Xu *et al.* recently postulated the possible localization of the S2R binding site on the Progesterone Receptor Membrane Component 1 (PGRMC1) [33], which was partially

crystallized (Figure 5) [34]. PGRMC1 is a haem binding protein and its over-expression has been associated to tumour stage and to actively proliferating and invasive cancer cells [35-37]. Despite the evidence of a S2R binding site on PGRMC1, additional experimental data is needed to clarify if S2R and PGRMC1 actually co-exist and to define the exact molecular structure of S2R. It has to be underlined that no firm conclusion about this correlation can be drawn up to the S2R cloning [38]. Several experimental evidence suggests a strict correlation between S2R and cancer conditions. In detail, proliferating breast carcinoma cells express S2R up to ten times more than quiescent cells, and the degree of S2R expression has been correlated with tumour staging and grading [39-41]. It is also relevant that high level of S2R has been detected in pancreatic cancer cell lines (Panc-02, Panc-01, CFPAC-1, AsPC-1) [42]. Remarkably, the pro-apoptotic effects of S2R ligands suggest the involvement of the Caspase family, protease enzymes playing essential roles in programmed cell death. Moreover, in some other cases S2R ligands are able to promote toxic damages, which trigger autophagy or cell-cycle arrest phenomena [43]. The high intracellular Ca^{2+} level could be another implicated mechanism in the cell-death activation. Several organelles and ionic channels are involved in the Ca^{2+} homeostasis control. S2R ligands are able to modulate the activity of these cellular structures, increasing the amount of the ion calcium in the cytosol; thus causing cellular damage and death [44-46]. Lastly, it is noteworthy the S2R modulators ability in increasing the ROS formation, a peculiar event that occurs before apoptosis.

In conclusion, during the abnormal cellular proliferation, S2R subtype is a valid target to take into consideration [47]. Therefore, S2R overexpression could be defined a hallmark in tumorigenesis.

1.3. S1R and S2R modulators

During the years, the interest in SRs has increased. They represent innovative targets with a wide spectra of therapeutic uses. Therefore, design and synthesis of SR modulators acquired an enormous importance. The long road toward the discovery of a novel SR modulator starts with defining the S1R or S2R profile. In this context binding assays are performed, in order to evaluate the affinity constants toward both receptor subtypes. For determining S1R affinity, the highly selective [3H](+)-pentazocine (Figure 5) is commonly used. Instead, for evaluating the S2R binding affinity, [3H]DTG (Figure 5), able to bind both S1R and S2R, is employed, adding unlabeled (+)-pentazocine for masking S1R.

The subsequent step is represented by the comprehension of the agonist/antagonist behaviour. This kind of test is widely accepted for S1R ligands [48-52], conversely the S2R

agonist/antagonist assay has not been validated and today it provides only a functional test towards cancer cell lines (Western Blot - Caspase assay) [53]. Defining a S1R profile contributes to depict the possible pharmacological role of a S1R modulator. S1R agonists are widely known for their neuroprotective and neuroplastic effects. Indeed, they are useful pharmacological tools in treating neurodegenerative diseases [16]. On the contrary, several studies show the involvement of S1R antagonists in the treatment of neuropathic pain. Recently, two molecules in Clinical Trials support this outstanding evidence:

- ANAVEX 2-73 (Figure 5), compound patented by *Anavex Life Sciences Corp.* It has been proposed for the treatment of Alzheimer's Disease [54].
- S1RA (Figure 5), compound patented by *Esteve*. The pharmacological profile includes the treatment of neuropathic pain and opioid analgesia enhancement [55].

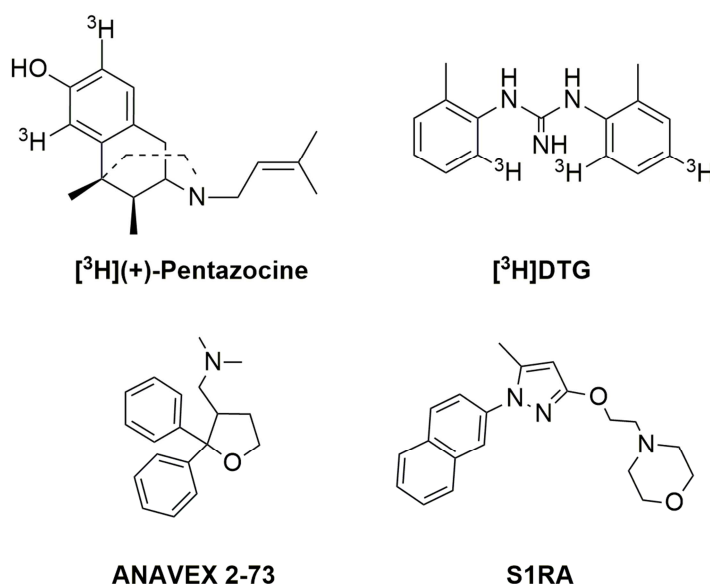


Figure 5. Structures of [³H](+)-pentazocine, [³H]DTG, ANAVEX 2-73 and S1RA.

Although SR has been associated to CNS pathologies, in the last two decades the involvement of this molecular target in cancer manifestations has been described [56-57]. This aspect can be pointed out by the numerous patented molecules, with potential anticancer properties. From Figure 6, it is appreciable the trend of molecules covered by patents, in CNS and in oncology fields. This fact reflects the necessity to find novel targets for cancer therapy and to overcome the major drawbacks of current chemotherapy.

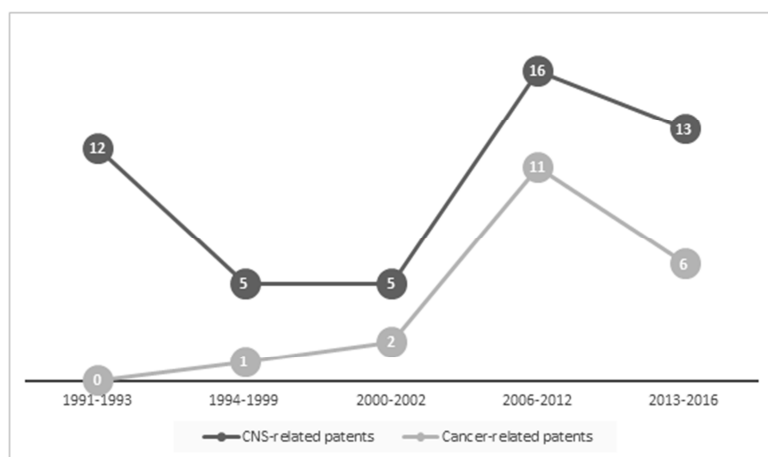


Figure 6. Overview of SRs-related patents from 1986 to 2016.

Numerous studies show a high expression of S1R in lung, breast and prostate cancer cell lines [58-59]. Interestingly, S1R antagonists, including rimcazole, haloperidol, BD-1047 and BD-1063 (Table 1), reduce the proliferation of breast cancer cell lines. Conversely, S1R agonists provide cell proliferation and survival, therefore promote tumor growth.

The signalling pathways triggered by S1R ligands, in causing cell death, have not been clarified yet. A recent study reviews the strict correlation between S1R and ion channels. Therefore, Crottes et al. highlighted the possible involvement of S1R in the electrical remodelling of cancer cell properties. In detail, it is widely documented that cancer cells over-express ion channels and transporters, which guarantee the cell adaption to the metabolic cancer conditions (low pH and pO_2 , poor nutrient supply, etc.). Probably, S1R chaperones can modulate these ion channels, in positive/ negative manner, increasing or decreasing tumour survival and aggressiveness [58]. Other research took into consideration described S1R ligands as carriers of drugs or nanoparticle-delivery systems to the tumour site in melanoma and prostate, lung and breast cancers [60-63].

In conclusion, despite the S1R is over-expressed in several tumour types, some aspects have to be investigated in depth. The scientific community is employing its efforts to disclose the oncology role of S1Rs, in order to define them as diagnostic or prognostic markers or as therapeutic targets.

As aforementioned, design and synthesis of S2R modulators is hard work. Literature data, collected over the years, suggests S2R subtype a promising therapeutic target in cancer manifestations, and thus ligands targeting S2R are important pharmacological tools in this pathology. The recent hypothesis about the possible structure overlapping of S2R and PGRMC1 strengthens the idea that this SR subtype is a marker in tumour genesis. In fact,

PGRMC1 is a protein over expressed in breast tumours and in cancer cell lines from colon, thyroid, ovary lung and cervix. Considering these interesting results, several research groups turned their attention in defining pharmacophoric models, in order to design novel molecules with high affinity and selectivity towards S2R. Recently, Mahfouz T.M. and co-workers proposed a ligand-based pharmacophore model for S2R, taking into consideration 41 ligands. The study elucidated the most important features to gain in affinity toward S2R:

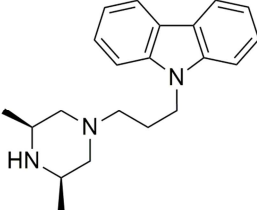
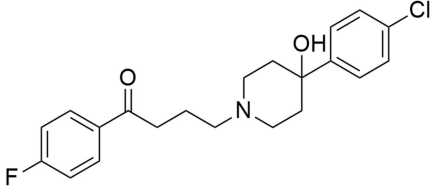
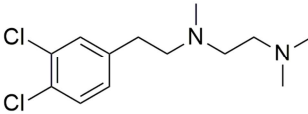
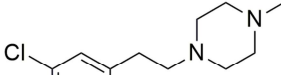
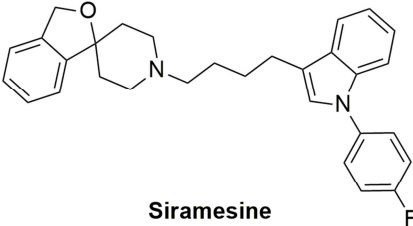
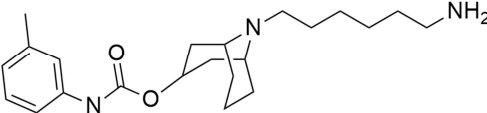
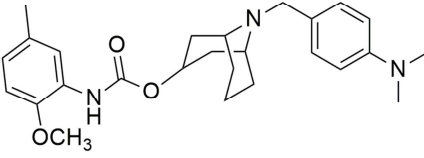
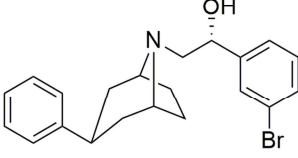
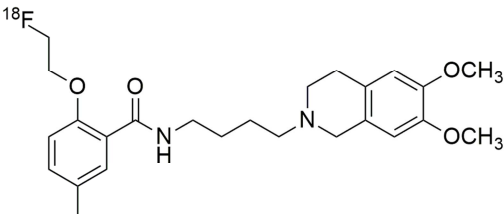
- an hydrophobic/aromatic site and the presence of a group able to generate a hydrogen bond are essential hallmarks
- four hydrogen bond acceptor and two hydrogen bond donor groups as not fundamental elements [64].

Today, the S2R ligands panorama is wide and four main structural classes have been depicted: (i) 6,7-dimethoxytetrahydroisoquinoline derivatives; ii) granatane- or tropane-related bicycle structures; iii) indole derivatives; iv) cyclohexylpiperazine analogues. They share some chemical elements: an aminic portion between two hydrophobic moieties [65-69]. It is noteworthy as some molecules, belonging to different classes, have been extensively investigated in experimental studies. Recent works, carried out on mouse breast cancer, human or murine pancreatic cancer and human melanoma cell lines, show that S2R agonists, i.e. Siramesine, SV119, WC-26 and RHM-138 (Table 1) possess a cytotoxic effect in the micromolar range. The cellular death could be caused by apoptotic phenomena, such as caspase activation, autophagy and impaired cell-cycle progression [42-43].

Although S2R agonists are promising pharmaceutical/therapeutic tools, human use is still at a distance. Only compound [18F]ISO-1, a potential PET marker of cell proliferation, is in phase I clinical trial [70].

In conclusion, over the years, several efforts have been accomplished to find molecules increasingly active toward S1R or S2R. In this context, some of these compounds have shown excellent cytotoxic effects toward cancer cell lines, in the micromolar range.

Table 1. SRs modulators, acting as antiproliferative molecules.

SR behaviour	Examples	
S1R antagonists		
	Rimcazole	Haloperidol
		
	BD-1047	BD-1063
S2R agonists		
	Siramesine	SV119
		
	WC26	RHM-138
		[18F]ISO-1

2. THE RESEARCH

2. THE RESEARCH

In this section, I briefly discuss the results obtained during my Ph.D. thesis research. The activity led to seven papers published in international journals; they are reported as attached documents in the appendix of this thesis. For clarity, the data of the published papers does not reflect the order in which they were carried out. Herein, the results will be presented according to the planning of the research.

2.1. Background

From 2007, the Laboratory of Medicinal Chemistry (LabMedChem) at the University of Pavia worked on the design and synthesis of novel ligands able to bind S1R. Initially, considering the lack of a three-dimensional receptor structure, the LabMedChem adopted a ligand-based drug design approach, in order to discover new molecules. Following a pharmacophoric approach, our research group designed a compound library based on an arylalkyl(alkenyl)aminic scaffold (Figure 9) [71].

Firstly, arylalkylaminic and arylalkenylaminic molecules have been synthesized, with the aim to investigate the Structure-Activity Relationship (SAR) and to obtain compounds with a good affinity toward the S1R binding pocket. Accordingly, other studies, aimed at understanding the role of the spacer bridging the aromatic ring and the aminic groups in the interaction with S1R, provided the synthesis of some compounds characterized by the presence of an alcoholic group. Binding results highlighted that the spacer nature does not influence the binding with the molecular target, instead the aromatic and aminic groups play a crucial role in establishing an interaction network with S1R [71].

From this compound library emerged (*R/S*)-**RC33** (Figure 9), compound endowed with an excellent affinity toward S1R and a high selectivity toward S2R (K_i S1 = 0.70 ± 0.3 nM; K_i S2 = 103 ± 10 nM). Moreover, (*R/S*)-**RC33** showed high metabolic stability in several biological matrices (i.e., mouse and rat blood, rat, dog, and human plasma) [71c-d, 72].

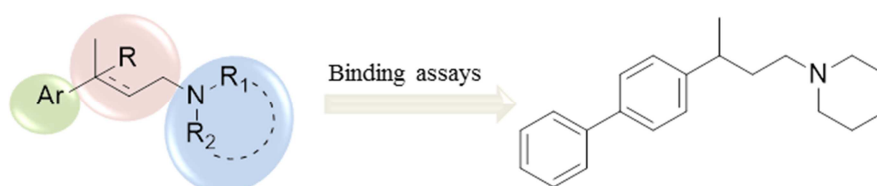


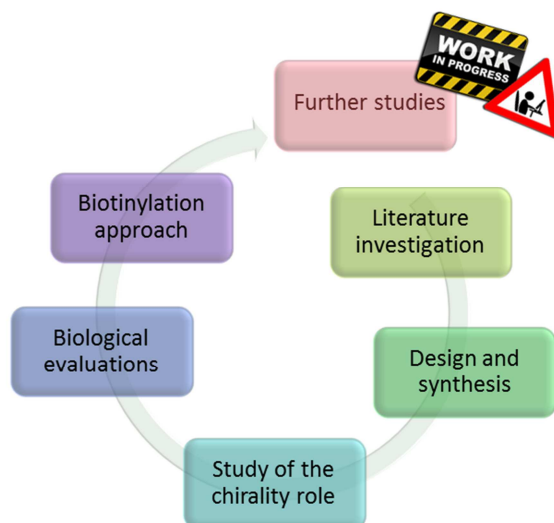
Figure 9. Arylalkyl(alkenyl)aminic scaffold and structure of (*R/S*)-**RC33**.

Firstly, the agonist/antagonist profile of this promising compound was evaluated through Nerve Growth Factor (NGF)-induced neurite outgrowth in neuronal differentiation cell model (PC12 cells) at not cytotoxic dose. Furthermore, the good *in vitro* metabolic stability of (*R/S*)-**RC33** led us to perform further studies, in order to identify a novel S1R agonist of great therapeutic interest for CNS pathologies [30].

My work is part of this scenario and we advanced a strategy to develop anticancer agents, targeting SR subtypes. We hypothesized that pan-modulators could exponentially decrease the cancer cell viability, since these compounds have a combination of effects.

Keeping in mind this goal we planned a work flow:

1. An in depth study of the literature and patents data was required to plan my research activity and to clarify the utility of this project in industrial and academic contexts. As briefly summarized in the “Introduction section” (Paper **MR8**).
2. Design and synthesis of novel compounds, potential pan-SR modulators. (Papers **MR5** and **MR7**).
3. Evaluation of the role of chirality. (Papers **MR2**, **MR3** and **MR6**).
4. Investigation of the pharmacological profile (effect in cancer cell models) of the most interesting compounds. (Paper **MR5**).
5. Individuation of chemical tools able to increase the uptake of the designed molecules in cancer cells. (Paper **MR1**).



SRs project work flow.

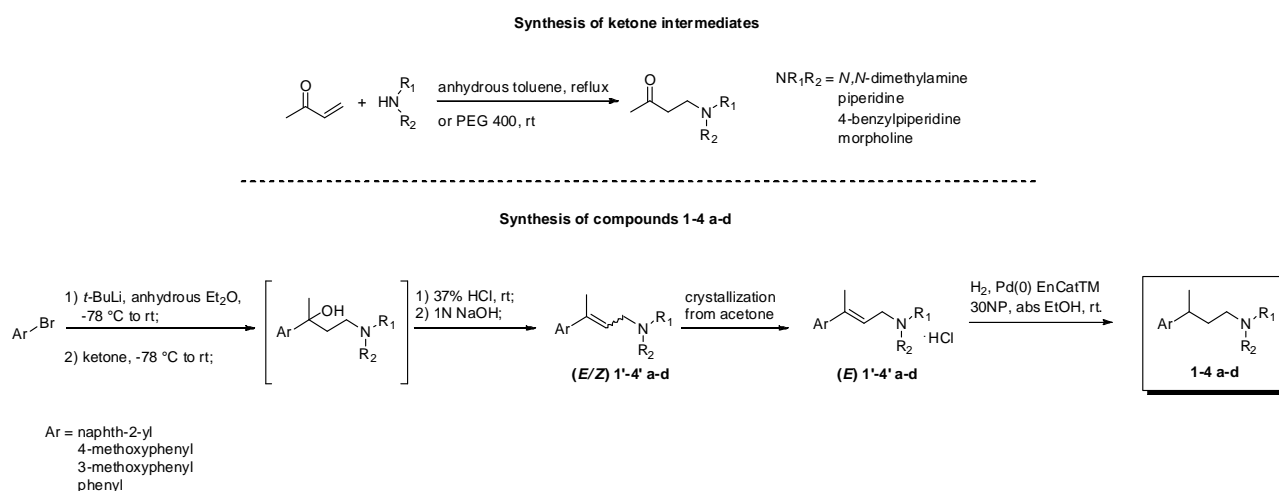
2.2. My Ph.D. Project

Development of a QSAR model for pan-SR modulators

Publication: **MR7**

The discovery of “pan-SR modulators” is of great interest and represents a challenge up to now. Our first strategy provided the design and synthesis of novel arylalkylamines, (*R/S*)-**RC33** analogues (Table 2). The desired compounds **1-4 a-d** were obtained in few synthetic steps, in modest/good yields and in a sufficient amount to perform biological investigations (Scheme 1). In detail, the key step is the C-C bond generation, consisting in the nucleophilic addition of the corresponding aryl-lithium reagents to carbonyl group of the appropriate β -aminoketone **a-d** (Scheme 1). The intermediates **a-d** were prepared *via* Michael addition of the corresponding secondary amine to but-3-en-2-one, according to the methodology reported in our previous works (anhydrous toluene at reflux or PEG 400, rt) [71c]. Once prepared, **a-d** were added to the appropriate aryllithium reagents (generated by aryl bromine through Br/Li exchange using *t*-BuLi at -78 °C) to give the corresponding tertiary aminoalcohols. Without any purification, the alcohols were *in situ* dehydrated under acidic condition (37% HCl, stirring at r.t. for 12 h), thus providing the desired compounds **1'-4' a-d**. The elimination reaction of alcoholic intermediates resulted highly regio- and (*E*)-stereoselective for all alkenylamines synthesized, as confirmed by ¹H-NMR analysis and NOESY experiments of crude compounds, in accordance with our previous experience. Arylalkenylamines **1'-4' a-d** obtained as (*E/Z*)-mixture after chromatographic purification or crystallization could be converted into (*E*)-alkenylamines in satisfactory yields (30-77%). The final step of our synthetic strategy consisted of the conversion of (*E*)-**1'-4' a-d** into the corresponding arylalkylamines **1-4 a-d** by catalytic hydrogenation of C-C double bond under hydrogen atmosphere using Pd(0) EnCat™ 30NP. In this way, arylalkylamines **1-4 a-d**, easily isolated by solid phase extraction (SPE, SCX cartridge), were obtained with acceptable yields (43% - 95%) and in suitable amounts for the biological investigations (Scheme 1). The binding results show that almost all the compounds have a discreet pan-affinity, in the nanomolar range. In detail, with the only exception of compound **4a**, which presents weak affinities toward S1R and S2R, all compounds show from modest to good SR affinities. An important structural feature, to gain affinity toward S1R, is the presence of a bulky aromatic portion, which fits well in the receptor pocket. Conversely, the affinity toward S2R follows *N,N*-dimethylamine < piperidine = morpholine < 4-benzylpiperidine scale, demonstrating that a bulky aminic moiety constitutes the main feature for interacting with the S2R binding site. Lastly, although some piperidine and morpholine derivatives (**2d**, **3b**, **3d**, **4b**) show mixed

affinity toward both molecular targets, only 4-benzylpiperidine compounds (**2-4c**) exhibit the best compromise between affinity and selectivity toward SRs.



Scheme 1. Synthesis of compounds **1-4 a-d**. Reagents and reaction conditions.

Table 2. Binding affinities towards S1R and S2R. Values are expressed as mean \pm SEM of three experiments.

Compound	Ar		K _i S1R (nM) \pm SEM	K _i S2R (nM) \pm SEM	S2R / S1R
1a		<i>N,N</i> -dimethylamine	1.95 \pm 0.2	43.8 \pm 5.2	22
1b	naphth-2-yl	Piperidine	1.5 \pm 0.6	50 \pm 6.4	33.3
1c		4-benzylpiperidine	19 \pm 2.1	144	7.6
1d		Morpholine	5.4 \pm 1.4	33 \pm 2.0	6.1
2a		<i>N,N</i> -dimethylamine	116 \pm 22	255	2.2
2b	4-methoxyphenyl	Piperidine	20 \pm 5.8	58 \pm 9.4	2.9
2c		4-benzylpiperidine	3.5 \pm 0.4	18 \pm 4.4	5.14
2d		Morpholine	76 \pm 7.0	68 \pm 13	0.89
3a	3-methoxyphenyl	<i>N,N</i> -dimethylamine	239	864	3.62
3b		Piperidine	36 \pm 4.1	35 \pm 4.8	0.97
3c		4-benzylpiperidine	2.9 \pm 0.7	14 \pm 1.4	4.83
3d		Morpholine	137 \pm 40	92 \pm 0.2	0.67
4a	phenyl	<i>N,N</i> -dimethylamine	427	> 1000	N.D.
4b		Piperidine	46 \pm 6.2	56 \pm 9.2	1.22
4c		4-benzylpiperidine	2.1 \pm 1.0	6.5 \pm 3.0	3.1
4d		Morpholine	85 \pm 6.3	71 \pm 3.2	1.2

These considerations are in agreement with the results obtained by the generated QSAR model, which is based on the activity data published in literature and our in-house library.

The regression models took into account 7 descriptors (Table 3). Affinity data were converted to pKi (-log₁₀K_i) values in order to normalize the range of data and perform a linear regression. The elaborated QSAR was tested afterwards on our new arylalkylamines **1-4 a-d**. Furthermore, by modelling QSARs, we identified the essential structural features to obtain promising pan-compounds.

Table 3. Molecular descriptors that were used to model quantitative structure activity relationships.

Descriptors	
a_don	Number of H-bond donor atoms
AM1_IP	Ionization potential (kcal/mol)
b_rotN	Number of rotatable bonds
BCUT_SLOGP_3	Atoms connection and contribution to logP
Dipole	Dipole moment calculated from the partial charges of the molecule
E_sol	Solvation energy
Glob	Globularity

QSAR model suggests that, pan-activity is associated to those molecules with some peculiarities. The presence of a nitrogen atom is an essential feature, since it guarantees the formation of an ionic interaction with an acidic amino acid in the binding pocket. Two hydrophobic groups, i.e. an aromatic ring or an aliphatic cycle/long chain, represent the second hallmark. They establish π - π interactions with aromatic residues in the binding site. The lack of one aliphatic element causes a penalty in affinity. This behaviour justifies the absence of activity related to dimethylamine derivatives.

Compounds **1-4b** and **1-4d** are pan-modulators, but they present low binding affinity because of lower hydrophobicity and solvation energy.

In conclusion, we identified highly SR affine ligands in the class of arylalkylamines and our data clearly demonstrates that the driving force to obtain a pan-modulator is represented by the correct choice of the aminic moiety. In detail, the presence of a bulky aminic group, i.e. 4-benzylpiperidine, ameliorates the binding affinity toward both S1R and S2R (Figure 10).

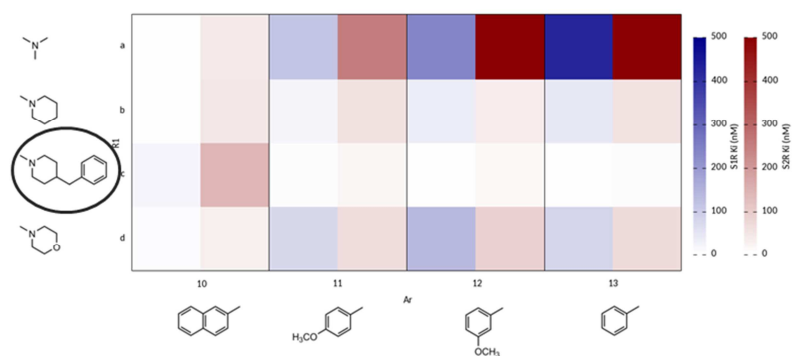


Figure 10. comparison of S1R (blue) and S2R (red) K_i binding affinity values. High affinity towards S1R and S2R is achieved by 4-benzylpiperidine derivatives.

Design and synthesis of novel pan-modulators

Publication: **MR5**

Once the structural features, to design pan-modulators, have been identified, we elaborated a compound series focused on the discovery of potent SR modulators, able to bind both receptor subtypes. Therefore, we proposed a set of 9 4-benzylpiperidine derivatives, reporting a preliminary SAR. Some structural changes have been made, in order to study in depth the SRs/ligand interaction (Figure 11):

- i) the aromatic portion, exploring the naphth-2-yl, 6-hydroxynaphth-2-yl and phenyl groups.
- ii) the spacer bridging the ring system and the aminic moiety, considering alkyl, alkenyl and alcoholic derivatives
- iii) the 4-benzylpiperidine portion has been maintained.

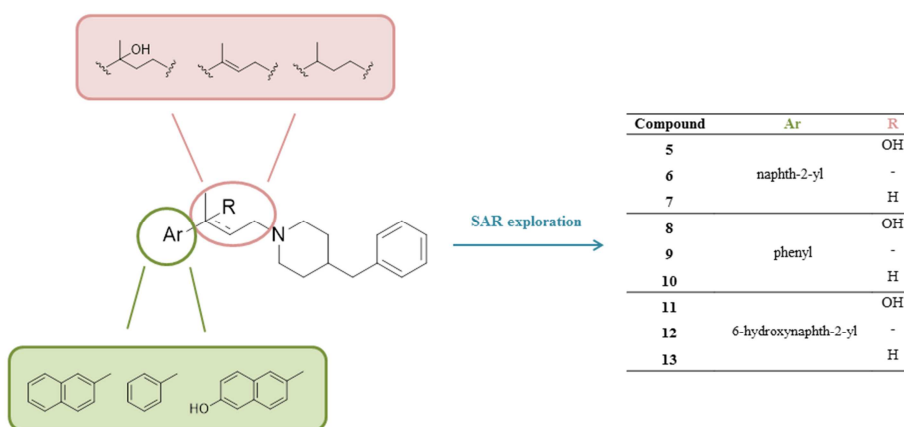
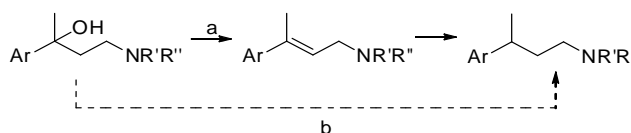


Figure 11. SAR exploration

The final synthetic protocol required an investigation of several reaction methods to obtain the desired compounds in a few steps and in good yields (Scheme 4).

Firstly, the 4-(4-benzylpiperidin-1-yl)butan-2-one, as key intermediate, was prepared *via* a Michael addition reaction. Accordingly, the Li/Br exchange at the appropriate aromatic precursor and thus the addition/substitution of the β -aminoketone, guaranteed access to the desired tertiary alcohols. They represented both our intermediates for the preparation of compound **6** and **9**, as well the final products. Therefore, we decided to apply the strategy depicted in Scheme 2, to prepare the arylalkyl- and the arylalkenyl-4-benzylpiperidines.



Scheme 2. Design of the synthetic protocol.

A dehydration of tertiary carbinol by Martin sulfurane was applied as protocol **a** (Scheme 2), but we obtained as main compound the C3-C4 alkenyl compound, as demonstrated by $^1\text{H-NMR}$ signals (Figure 12). Therefore this strategy was abandoned.

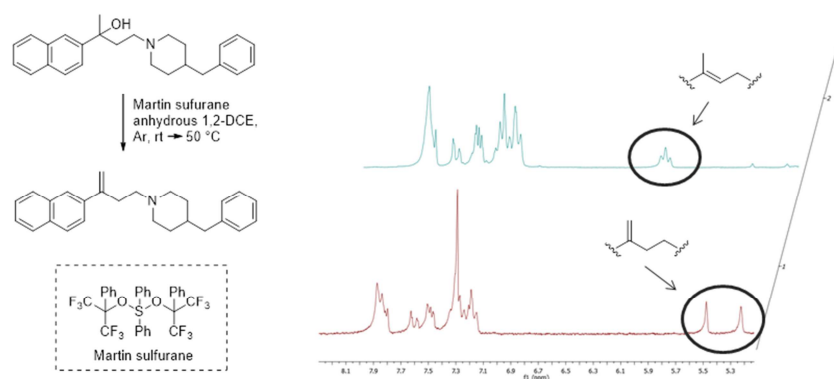


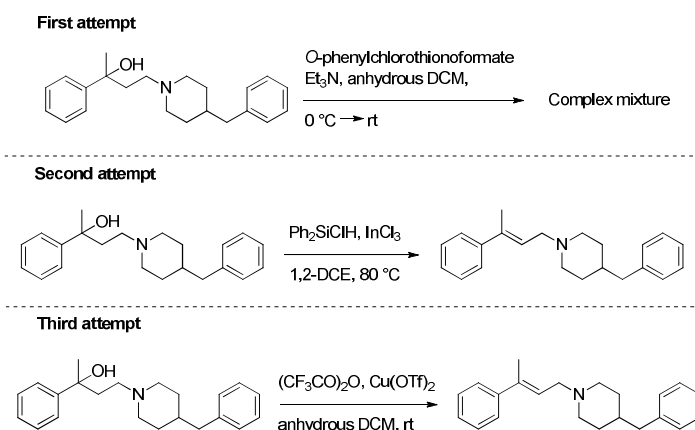
Figure 12. Application of the Martin protocol.

Step **b**, provides the replacement of a hydroxyl functional group with a hydrogen to give an alkyl group. Different reaction conditions have been employed to achieve the arylalkylamines (Scheme 3):

i) Barton-McCombie strategy provides, as first step, the conversion of an alcohol into a reactive carbonthioyl intermediate, which is involved in a radical mechanism. In our case, only a complex mixture was obtained.

ii) Our second attempt provides the employment of a reducing system for tertiary alcohols, using Ph_2SiClH and InCl_3 . The stereoisomer (*E*) was the main product, no traces of the alkyl-compound were present.

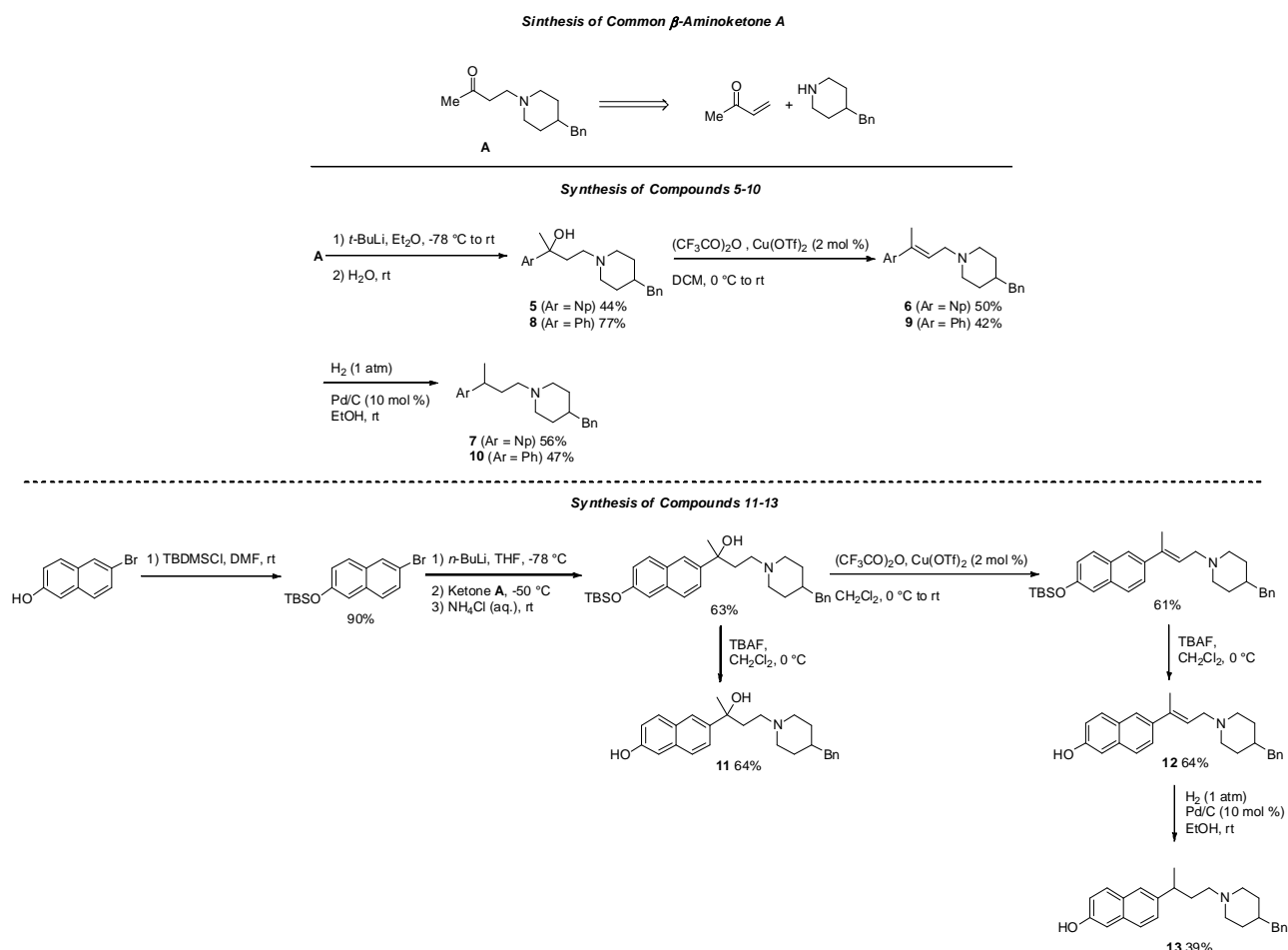
iii) Lastly, we used the radical deoxygenation of tertiary alcohols *via* trifluoroacetates. Surprisingly, we did not obtain the desired ester, probably, an intramolecular mechanism furnished the (*E*)-alkenyl compound, in good yield.



Scheme 3. Experiments performed in order to achieve the desired alkyl compounds.

Considering this lack of success, we decided to adopt a conventional strategy. In other terms, the dehydration of tertiary alcohols with $(\text{CF}_3\text{CO})_2$ under $\text{Cu}(\text{OTf})_2$ catalysis conditions afforded a mixture of olefinic regioisomers C3-C4 and the *E* stereoisomer C2-C3 [73]. After purification, the *trans* olefins were isolated and finally hydrogenated, using H_2 and Pd/C (10% p/p) to access the desired arylalkylamines. The same strategy was applied for accessing 6-hydroxynaphth-2-yl derivatives. However, the protection of the aromatic alcohols as TBS ethers (and their corresponding removal) was required to avoid interference with the lithiation step.

In summary, we identified the synthetic strategy to obtain compounds **5-13** (Scheme 4), as confirmed by ^1H NMR, ^{13}C NMR and UPLC-MS (See the Supporting Information). Their biological evaluation will be deepened in the dedicated section.



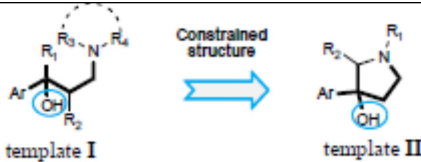
Scheme 4. Synthesis of compounds 5-13. Reagents and reaction conditions.

Chiral role evaluation in the interaction with S1R and S2R

Publications: **MR2**, **MR3** and **MR6**

To investigate the relationship between stereochemistry and receptor affinity, we prepared enantiomerically pure **5**, **7-8**, **10-11** and **13**. Indeed, in Medicinal Chemistry, enantiomers of a chiral compound, have to be considered as two diverse chemical entities, with different pharmacological and/or toxicological behaviors. It is important to define the eutomer in a racemic mixture, in order to obtain a high activity or to avoid toxic effects. Therefore, once the biological activity of racemates has been investigated, studying the enantiomeric profiles in biological assays represents the second issue to disclose. The LabMedChem employed its efforts in studying the role of chirality in the SRs/ligands interaction. SAR studies of chiral SR modulators support the SR ability in discriminating enantiomeric forms and this aspect is strictly dependent on the structural features of ligands. Indeed, our previous experiences showed how the presence or the absence of a pharmacophoric element can affect the stereoselectivity in the interaction with the molecular targets. In detail, we demonstrated that **RC-33** enantiomers (Figure 9) have similar binding affinity toward both S1R and S2R (K_i S1^(S)-

$K_{i(R)-RC-33} = 1.9 \pm 0.2$ nM, $K_{i(S)-RC-33} = 1.8 \pm 0.1$ nM; $K_{i(R)-RC-33} = 98 \pm 64$ nM; $K_{i(S)-RC-33} = 45 \pm 16$ nM), and their pharmacological behaviours can be overlapped. This surprising result is in contrast with the well documented enantioselectivity of SRs/ligands interaction. In order to give an explanation to this unexpected behaviour, in Publication **MR2**, we hypothesized that a pharmacoforic element, such as an electronegative atom, is missing and it causes a loss of stereoselectivity in binding mode of **RC-33** enantiomers. We also evaluated the ability of a series of enantiomerically pure arylalkylaminoalcohols and arylpyrrolidinols, structurally related to **RC-33**, presenting a hydrogen bond centre, in the interaction with S1R. After chiral resolution and absolute configuration assignment of the enantiomers, we performed an in depth analysis, using *in silico* study and binding affinity assays of enantiopure **14-18** compounds (Table 4). From the binding results (Table 4), we deduced that (*S*)-configured compounds present the best S1R binding affinity values respect to their (*R*)-counterparts. This evidence was also highlighted by *in silico* analysis of the binding modes between **14-18** and S1R (data not shown). The presence of a hydroxyl group – missing in **RC-33** structure – allows to establish a hydrogen bond with the carboxyl chain of Glu172 in the binding pocket, which guarantees a mild enantiomeric binding discrimination. Among the series, racemic and enantiomeric **14**, from now on called **RC-34**, was selected for a further biological investigation. We evaluated **RC-34** and its enantiomers on our validated PC12 cell model of neuronal differentiation, in order to investigate their S1R agonistic/antagonistic profile, and thus investigating the role of chirality on NGF-induced neurite outgrowth. The obtained results showed that (*S*)-**RC-34** is the eutomer. Indeed, it enhances NGF-induced neurite outgrowth and its efficacy is greater than (*R/S*)-**RC-34**, while (*R*)-**RC-34** is not effective in promoting NGF induced neurite outgrowth in PC12 cells at the same concentrations. Once we identified (*S*)-**RC-34** as the eutomer and a potent S1R agonist, we developed a rapid and straightforward screening protocol of chiral stationary phases (CSPs) in high performance liquid chromatography (HPLC) and supercritical fluid chromatography (SFC) (Publication **MR3**), aimed at defining methods able to give baseline separation of racemic **RC-34**. The analytical conditions, which give a complete resolution of **RC-34**, with low retention times, were chosen for a scale-up in (semi)-preparative columns.

Table 4. Binding affinities towards S1R and S2R. Values are expressed as mean \pm SEM of three experiments.


Compound	Template	Ar	R ₁	R ₂	NR ₃ R ₄	Ki S1 (nM) \pm SEM	Ki S2 (nM) \pm SEM
(<i>R/S</i>)- 14						6.57 \pm 0.2	34.6 \pm 47
(<i>R</i>)- 14	I	biphenyl-4-yl	CH ₃	H	N(CH ₂) ₅	39 \pm 8	4300 \pm 315
(<i>S</i>)- 14						4.7 \pm 0,3	1800 \pm 288
(<i>R/S</i>)- 15						77 \pm 23	66 \pm 13
(<i>R</i>)- 15	I	naphth-2-yl	CH ₃	H	N(CH ₃) ₂	205 \pm 60	651 \pm 67
(<i>S</i>)- 15						63 \pm 39	75 \pm 5
(<i>R/S</i>)- 16						41 \pm 11	97 \pm 18
(<i>R</i>)- 16	I	6-metoxynaphth-2-yl	CH ₃	H	N(CH ₃) ₂	51 \pm 014	133 \pm 63
(<i>S</i>)- 16						25 \pm 4	1100 \pm 223
(<i>2R/S,3S/R</i>)- 17						65 \pm 18	366 \pm 64
(<i>2R,3S</i>)- 17	II	naphth-2-yl	CH ₃	CH ₃	-	86 \pm 16	94 \pm 23
(<i>2S,3R</i>)- 17						26 \pm 2	432 \pm 53
(<i>2R/S,3S/R</i>)- 18						1900 \pm 304	1500 \pm 219
(<i>2R,3S</i>)- 18	II	6-metoxynaphth-2-yl	CH ₃	CH ₃	-	1500 \pm 226	1200 \pm 212
(<i>2S,3R</i>)- 18						1200 \pm 257	1900 \pm 293

The analytical HPLC screening was carried out using cellulose and amylose derived CSPs. Chiralpak IC, Chiralcel OD-H and Chiralcel OJ-H (all cellulose derivatives) as well as Chiralpak IA and Chiralpak AD-H (amylose derivatives) were selected as the most versatile CSPs available in our laboratory. The analytical protocols involved alcohols (MeOH, EtOH and IPA) and mixtures of *n*-Hep and polar modifiers (EtOH or IPA) as mobile phases (Table 5). Results of the screening protocol are reported in Table 1 of Publication **MR2** as retention (*k*), selectivity (α) and resolution (*R_s*) factors.

Table 5. Mobile phases composition.

Entry	Mobile phase composition (%)			
	MeOH	EtOH	<i>n</i> -Hep	IPA
A	100	-	-	-
B	-	100	-	-
C	-	10	90	-
D	-	5	95	-
E	-	-	98	2

All mobile phases contained 0.1% DEA. In case of Chiralpak IC and IA mobile phase contained also 0.3% TFA.

Considering the obtained results, and keeping in mind that our purpose was to set up an economic and productive preparative enantiomer separation, Chiralcel OJ-H was selected as CSP, using pure methanol as eluent (with 0.1% DEA). This method guaranteed a baseline

separation of **RC-34** with relatively short retention times (3.4 min for the first eluted enantiomer and 4.6 min for the second), high enantioselectivity and good resolution ($\alpha = 1.8$, $R_s = 3.9$ at r.t.) (Figure 13 A).

In the meantime, a SFC screening protocol was performed, in order to identify other conditions for the enantiomeric resolution of **RC-34**. It is well documented that SFC methods promote the separation of racemic compounds in a quick and efficient manner. Therefore, we adopted this methodology to obtain **RC-34** enantiomers with a high enantiomeric excess and in a sufficient amount. At the beginning, we adopted gradient conditions (5% to 45%), using carbon dioxide (CO_2) with polar modifiers (MeOH, EtOH and IPA; all with 0.1% DEA) and two different CSPs (Chiralpak IA and IC). Despite the baseline separation of **RC-34** was achieved, a second screening, using isocratic conditions and polar/apolar solvents, was carried out to optimize selectivity and resolution factors. The best conditions were reported in Figure 13 B, C.

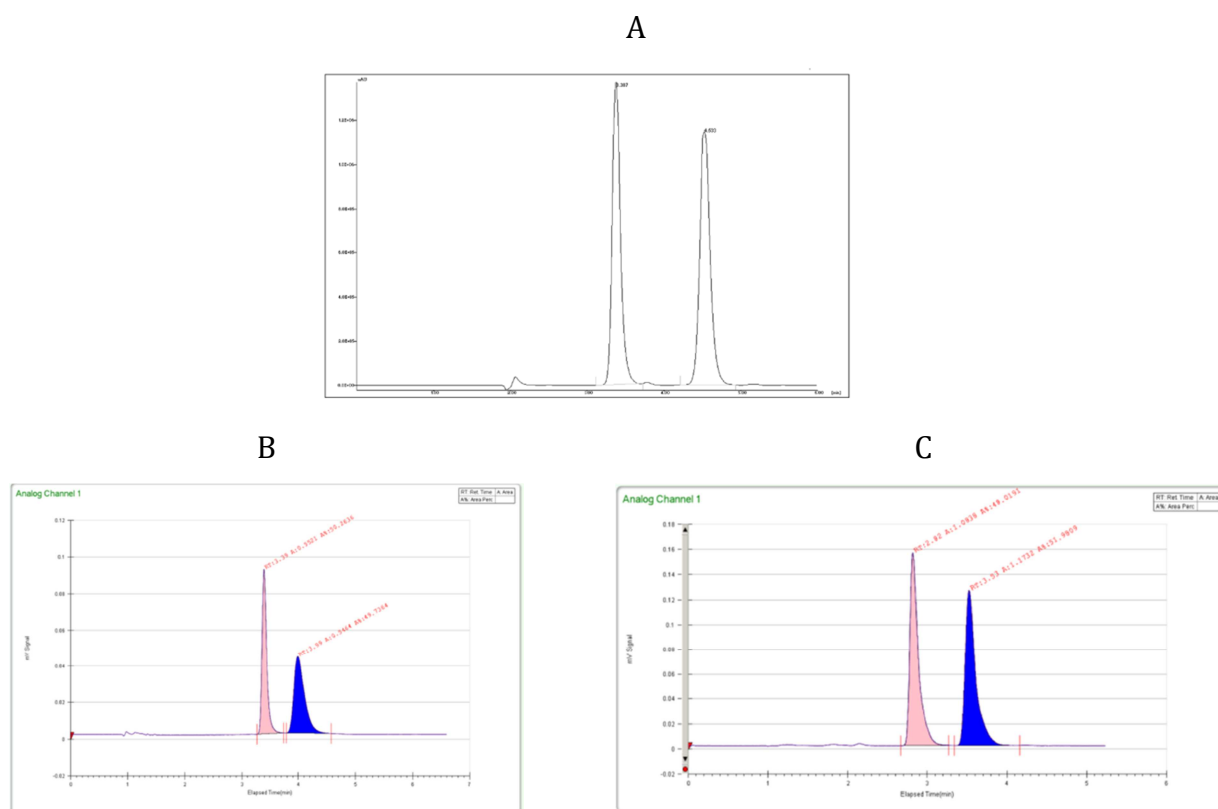


Figure 13. (A) HPLC system: Chiralcel OJ-H. Elution condition: 100% MeOH, DEA 0.1%, flow rate 1.0 mL/min. (B) SFC system: Chiralpak IA. Elution conditions: 70% CO_2 and 30% *n*-Hep/EtOH (90/10 v/v), 0.1% DEA, flow rate 4.0 mL/min. (C) SFC system: Chiralpak IC. Elution conditions: 75% CO_2 and 25% IPA/*n*-Hep (90/10 v/v), 0.1% DEA, flow rate 4.0 mL/min.

The analytical protocols were scaled-up in (semi)-preparative columns, elution conditions and amount of **RC-34** enantiomers were reported in Table 6. In HPLC system, (+)-(*S*)-**RC-34**

enantiomer elutes as the first peak on Chiralcel OJ-H, as well as on Chiralpak IA in SFC system. Conversely, employing Chiralpak IC column, in SFC system, an inversion of elution order was registered. The developed methods proved to be suitable for obtaining a quick access to the desired **RC-34** enantiomers with enantiomeric excess as high as 94.5% and amounts sufficient for preliminary biological assays.

Table 13. (Semi)-preparative resolution of **RC-34** on HPLC and SFC

System	CSP	Processed amount of racemic RC-34 [mg]	n° cycles	Vol. Inj [mL]	Isolated amount [%]	ee [%]	Yield [%]	[α] _D ²⁰ ^a
HPLC	Chiralcel OJ-H	21	7	1.0 ^b	8.7	99.9	43.3	+ 24.0
					9.1	99.9	45.5	- 24.0
SFC	Chiralpak IA	20	40	0.05 ^c	9.1	99.9	45.5	+ 24.0
					8.2	94.5	41.0	- 23.1
	Chiralpak IC	20	40	0.05 ^c	9.6	99.1	48.0	- 23.9
					9.5	98.9	47.5	+ 23.8

^a c = 0.50 % in MeOH

^b c = 3 mg mL⁻¹ in MeOH

^c c = 10 mg mL⁻¹ in IPA

Some compounds of the pan-SR modulator series, which were described in the previous section (Design and synthesis of novel pan-modulators) present a stereogenic centre. Therefore, the chiral compounds were prepared both in racemic and enantiomeric form, with the final aim to address the role of chirality in the SR interaction. HPLC procedures were set up, in order to obtain the enantiomerically pure form of arylalkylaminealcohols (**5**, **8** and **11**) and arylalkylamines (**7**, **10** and **13**). The optimized analytical conditions, able to provide a baseline separation of all compounds, were transferred to (semi)-preparative scale to obtain the enantiomers in a sufficient amount and with an enantiomeric excess higher than 95% to perform the preliminary biological investigations. Lastly, the absolute configuration was empirically assigned to enantiopure compounds, combining the electronic circular dichroism (ECD) technique to the elution order study.

In detail, we performed a first screening using the versatile amylose- and cellulose- based CSPs immobilized on silica gel chiral columns (Chiralpak IC and IA). The elution conditions provided the employment of alcohols (MeOH or/and EtOH), or *n*-Hep in the presence of polar modifiers (EtOH or IPA), DEA 0.1% and TFA 0.3 %.

Chiralpak IC provided a baseline separation of compounds **5**, **7**, **10** and **13**, even if the chromatographic conditions were not suitable for a productive scale-up, since the retention times (t_R) are quite long (t_R of the second eluted enantiomer ranging from 30 to 90 minutes).

Instead, Chiralpak IA gave rise to better results, being effective in resolving compounds **5**, **7-8**, **10-11** and **13**.

Despite the complete resolution of all racemic compounds, using the Chiralpak IA, was achieved, in some compound cases the retention times were not satisfactory to transfer on (semi)-preparative scale. Therefore, we applied a second screening protocol on Chiralcel OJ-H column. This strategy allowed to carry out a baseline separation **5**, **7-8** and **11**, in short retention times. High enantioselectivity and good resolution were achieved eluting only with alcohols (MeOH or EtOH). From the analytical results, we disclosed the optimal conditions to scale up in (semi)-preparative columns. In details, the methods provided the use of Chiralpak IA for achieving enantiomeric resolution of **10** and **13** and of Chiralcel OJ-H, for solving **5**, **7-8** and **11**. In Figure 14, the best conditions to solve compounds **5**, **7-8**, **10-11** and **13** are reported. On (semi)-preparative conditions racemic **5**, **7-8**, **10-11** and **13** were processed in a low number of cycles, leading to enantiopure compounds in satisfactory amounts (6-23 mg) and yields (76-95 %), with an ee \geq 95% (Table 14).

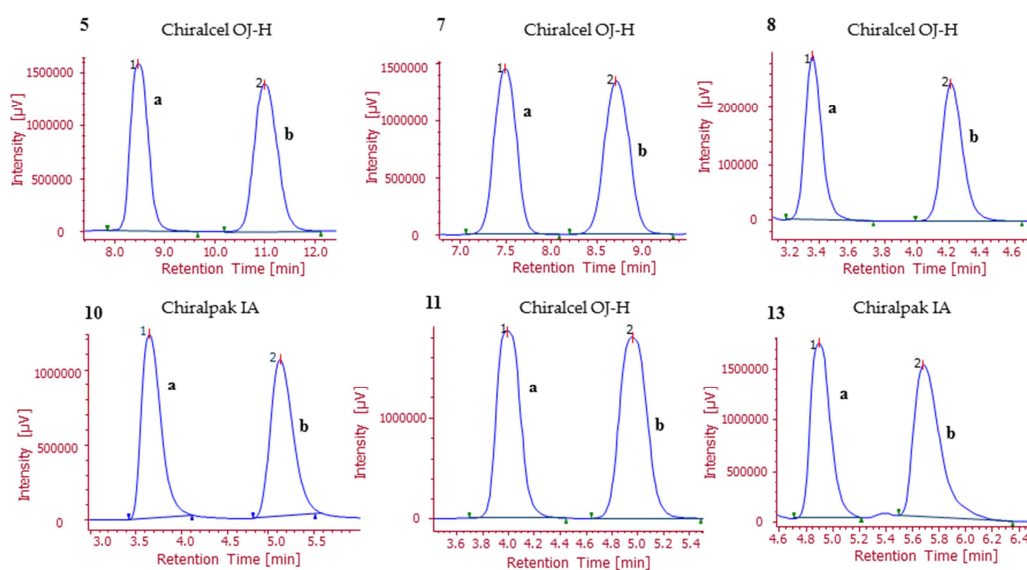


Figure 14. Analytical enantiomer separation of **5**, **7-8** and **11** on Chiralcel OJ-H (4.6 mm \times 150 mm, dp = 5 μ m), and **10** and **13** on Chiralpak IA (4.6 mm \times 250 mm, dp = 5 μ m). **5** elution condition: 100% EtOH, DEA 0.1%, flow rate 0.5 mL/min. **7-8** and **11** elution condition: 100% MeOH, DEA 0.1%, flow rate 1.0 mL/min. **10** and **13** elution condition: 100% MeOH, 0.1% DEA, flow rate 1 mL/min. For all: injection volume 10 μ L.

Table 14. (Semi)-preparative resolution of **5**, **7-8**, and **11** on Chiralcel OJ-H (10 mm × 250 mm, dp = 5 μm), and of **10** and **13** on Chiralpak IA (10 mm × 250 mm, dp = 5 μm). Flow rate: 2.5 mL/min. Detection: 254 nm (compounds **5**, **8**, **11**, **13**) and 220 nm (compounds **7**, **10**). Injection volume: 1.0 mL

Compound	CSP ^a	Processed amount (mg)	No. cycles	Enantiomer	Isolated amount (mg)	ee (%)	Yield (%)	[α] _D ²⁰ (MeOH)
5	Chiralcel OJ-H	30	3	(+)- 5	14.1	96.0	94.0	+ 40.5
				(-)- 5	14.3	97.0	95.3	- 42.3
7	Chiralcel OJ-H	50	4	(+)- 7	22.9	99.9	91.6	+ 10.5
				(-)- 7	23.0	98.0	92.0	- 9.2
8	Chiralcel OJ-H	30	3	(+)- 8	13.8	95.0	92.0	+ 6.1
				(-)- 8	12.5	95.0	83.3	- 6.3
10	Chiralpak IA	16	2	(+)- 10	6.1	99.9	76.3	+ 8.2
				(-)- 10	6.3	99.9	78.8	- 8.3
11	Chiralcel OJ-H	22	4	(+)- 11	9.1	99.9	82.7	+ 24.2
				(-)- 11	8.9	99.9	80.9	- 24.8
13	Chiralpak IA	25	3	(+)- 13	10.5	99.9	84.0	+ 11.8
				(-)- 13	9.8	99.9	78.4	- 12.0

Lastly, electronic circular dichroism (ECD) and chiral HPLC analysis was used, with the aim to establish the absolute configuration at the stereogenic centre of enantiomeric **5**, **7-8**, **10-11** and **13**. For comparative purpose, ECD spectra of the studied compounds were compared to ECD curves of the structural analogues **RC-33** and **RC-34** (known configuration). In detail, the ECD spectra of enantiomeric arylaminoalcohols **5**, **8** and **11** were compared with that of (*S*)-**RC-34** and the ECD spectra of enantiomeric **7**, **10** and **13**, with that of (*S*)-**RC-33**.

Briefly, the (*S*) absolute configuration of (+)-(*S*)-**RC-34** may be proposed also for (+)-**5**, (+)-**8** and (+)-**11**, since they present comparable Cotton effects (CEs). In detail, at 195 and 207 nm there are negative CEs and between 216 and 223 nm there are positive CE, attributable to the electronic transitions of benzene and naphthalene.

The same procedure was adopted to assign the absolute configuration to **7**, **10** and **13**, in this case we considered (*S*)-**RC-33** as reference compound. All the (+)-enantiomeric compounds had the same CE trend of (+)-(*S*)-**RC-33**, since they displayed a negative CE in the wavelength range between 198 and 230 nm and an additional CE between 214 to 255 nm. Therefore, (*S*)-configuration may be proposed for (+)-**7**, (+)-**10** and (+)-**13**.

The study of elution order of chiral HPLC analysis was accomplished to support the configurational assignment. Therefore, (*S*)-**RC-34**, (+)-**5**, (+)-**8** and (+)-**11** were analyzed under the same chromatographic conditions (Chiralcel OJ-H, 50% MeOH and 50% EtOH, 0.1% DEA) and in all cases the (*S*)-configured molecules were the first eluted. Conversely, arylalkylamines (*S*)-**RC-33**, (+)-**7**, (+)-**10** and (+)-**13** profiles were investigated on Chiralpak IC (90/10 *n*-Hep/IPA, 0.1% DEA). All first enantiomers possessed the same absolute

configuration, that is (*S*) configuration. To sum up, the obtained results are in agreement with the data collected through ECD technique.

In conclusion, analytical chiral HPLC screening allows to identify the optimized conditions able to give a complete resolution of racemic compounds. The optimal procedures may be transferred on (semi)-preparative scale, in order to have a quick access to the desired amounts of pure enantiomers even at low specific productivities. Therefore, chiral HPLC remains a straightforward, productive and robust methodology to achieve enantiomeric compounds of interest in medicinal chemistry, since it represents one of the most versatile and cost effective tools for fast isolation of desired enantiomers from a racemic mixture.

The biological investigations of racemic and enantiomeric **5**, **7-8**, **10-11** and **13** will be deepened in the following section.

Pharmacological investigation in cancer cell models

Publication: **MR5**

We evaluated the biological profile of racemic and enantiomeric arylalkylamines **5**, **7-8**, **10-11** and **13** and of arylalkenylamines **6**, **9** and **12**. Keeping in mind that our purpose was the identification of new chemical entities, targeting both SR subtypes as a first work we evaluated the binding affinity of the studied compounds toward S1R and S2R. The assays were performed using guinea pig brain and rat liver membranes, in the presence of radioligands: [³H]-(+)-pentazocine for S1R and [³H]-DTG, for S2R. In Table 15, the binding values were reported. All the tested compounds present a high/good affinity toward S1R, with a *K_i* below 70 nM, as also *in silico* results demonstrate (data reported in Publication **MR5**). S2R affinities have variable values, from 6.5 to 900 nM. In detail, 6-hydroxy naphthyl derivatives possess weak binding constants, probably due to the presence of an aromatic -OH group, which avoid the interaction with the S2R binding site. Conversely, among naphthyl- and phenyl- molecules there are some which show interesting results, i.e. compounds **6**, **7a**, racemic and enantiomeric **10**. Therefore, we selected, from the whole series, compounds with a high affinity toward both receptor subtypes and a low selectivity, close to 1. Pan-SR activity is a feature related to compounds **6** and **10**, thus they were sent for preliminary biological investigation.

Table 15. Binding affinities towards S1R and S2R. Values are expressed as mean \pm SEM of three experiments.

Compound	Ar	R	Ki S1 \pm SEM	Ki S2 \pm SEM
5		OH	6.9 \pm 2	62.5
5a		OH	10 \pm 2	81 \pm 35
5b		OH	11 \pm 1	79 \pm 21
6	2-naphthyl	-	12 \pm 5	22 \pm 3
7		H	5.6 \pm 3	144 ^a
7a		H	6.0 \pm 0.5	26 \pm 9
7b		H	6.9 \pm 1	98
8		OH	9.8 \pm 4	57 \pm 11
8a		OH	27 \pm 9	339 ^a
8b		OH	40 \pm 4	240 ^a
9	phenyl	-	0.7 \pm 1	47 \pm 13
10		H	2.1 \pm 1	6.5 \pm 3
10a		H	2.9 \pm 0.4	8.9 \pm 2.1
10b		H	3.0 \pm 0.3	7.9 \pm 1.9
11		OH	27 \pm 5	118 ^a
11a		OH	70 \pm 21	68 \pm 8
11b		OH	62 \pm 4	905 ^a
12	6-hydroxynaphth-2-yl	-	9.6 \pm 3	305 ^a
13		H	59 \pm 5	314 ^a
13a		H	35 \pm 2	582 ^a
13b		H	13 \pm 4	105 ^a

^a Compounds with high affinity were tested three times. For compounds with low SR affinity (> 100 nM), only one measure was performed.

We evaluated their antiproliferative behaviour, using a MTS test in PaCa3 cells. This cellular line was selected, as consequence of Real Time-Polymerase Chain Reaction (RT-PCR) results on a panel of cancer cell lines (see Publication **MR5**). PaCa3 expresses high levels of both S1R and PGRMC1 (putative S2R binding site) mRNA.

The cytotoxicity assay allowed us to identify the *hit* compound for an in depth biological investigation. The obtained values of compounds **6** and **10** were compared to siramesine (S2R agonist) and NE100 (S1R antagonist). PaCa3, grown in complete medium and in starvation condition, were exposed to increasing concentrations of compounds for 24h. In both mediums, compound **6** caused a cell viability reduction, as well as siramesine, whereas compounds **10** and NE100 showed a poor cytotoxic activity (Figure 15). According to this data, compound **6**, from now on called **RC-106**, was selected for further investigation.

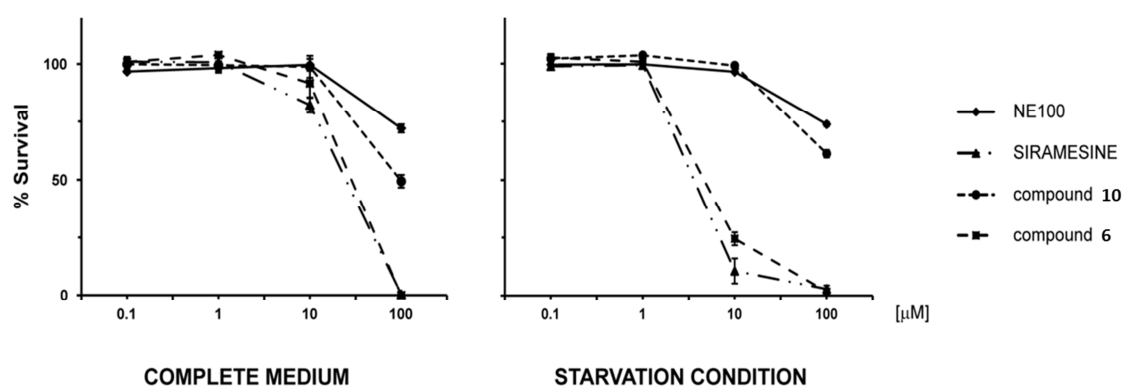


Figure 15. The cells were exposed to compounds NE100, Siramesine, 6 (RC-106) and 10, for 24 hours in the presence or in the absence of 10% FBS. The viability of the cells was determined by MTS assay (mean \pm SD of 3 independent experiments).

As stated in the Introduction, anticancer activity is related to S1R antagonism. Therefore, we evaluated the agonist/antagonist profile of **RC-106**, using NGF-induced neurite outgrowth in PC12 cells model. Experimental evidence shows that S1R agonists are able to potentiate the neurite outgrowth in the presence of NGF. The assay foresees to incubate PC12 cell with increasing concentrations of **RC-106** for 96h. The inhibitory effect of **RC-106** on neurite outgrowth is evident when its concentration is 2.5 μ M (Figure 16 A). Furthermore, in support of this result competition assay was carried out. **RC-106** antagonized the effect of PRE-084 (well documented S1R agonist) at 0.25 μ M concentration (Figure 16 B). All obtained results suggest that **RC-106** is a S1R antagonist.

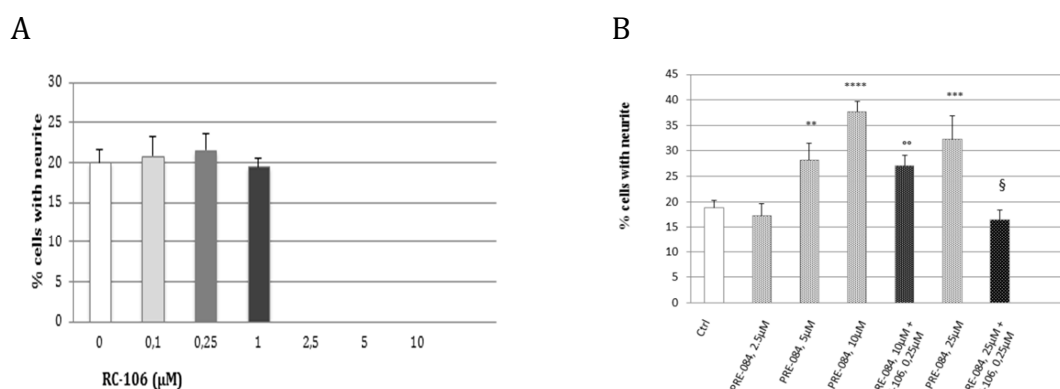


Figure 16. (A) Effect of RC-106 alone in the concentration range 0.1-10 μ M. RC-106 does not affect NGF-induced neurite outgrowth in PC12 cell assay in the concentration range 0.1-1 μ M. Conversely, NGF-induced neurite outgrowth is completely inhibited by in the range 2.5-10 μ M. Histograms represent the mean \pm sem of at least 4 different experiments performed in triplicate. (B) Effect of PRE-084 alone or in combination with **RC-106**, at 0.25 μ M. Histograms represent the mean \pm sem of at least 5 different experiments performed in triplicate. **= p <0.005; ***= p <0.0008; ****= p <0.00004 vs control (0 PRE-084). °= p <0.007; °°= p <0.00004 vs PRE-084 10 μ M and § = p <0.004 vs PRE-084 25 μ M.

Once the S1R agonist/antagonist profile was defined, we evaluated the cytotoxic effect of **RC-106** on a panel of cancer cell lines, through MTS assay. **RC-106** induced a decrease of cell viability in all cell lines starting at 25 μM , with IC_{50} values ranging from 50 μM to 64 μM (Table 16). It is noteworthy that the cytotoxic effect of **RC-106** increases in starvation conditions, at a low compound concentrations (9.6 -10.5 μM) (data not shown).

Table 16. Effect of **RC-106** on cell viability was evaluated on a panel of cancer cell lines with different histotypes. Cells were exposed to the drug for 24 hours in a 10% FBS containing medium. Cell viability was determined by the MTS assay (average of three independent experiments \pm SD).

Cell line	Origin	Tumor source	Morphology	IC_{50}
Capan-2	Pancreas	Primary tumor	Epithelial	52.6 \pm 0.1
Paca3	Pancreas	Primary tumor	Epithelial	49.8 \pm 4.1
SUM 159	Breast	Primary tumor	Epithelial	58.3 \pm 1.8
MDA-MB 231	Breast	Metastatic site	Epithelial	64.9 \pm 8.2
PC3	Prostate	Metastatic site	Epithelial	50.6 \pm 5.6
LNCaP	Prostate	Metastatic site	Epithelial	61.1 \pm 3.0
U87	Glioblastoma	Primary tumor	Epithelial	60.6 \pm 3.4

In summary, **RC-106** shows antiproliferative properties, causing a decrease of the cell viability on a panel of tumorous cell lines. Moreover, TUNEL and Annexin V assays were performed on PaCa3 cell line, to disclose the mechanism involved in the cellular death. Also in these cases the tests envisaged the application of the starvation conditions. The results clearly demonstrated that **RC-106** acts triggering an apoptotic pathway rather than a necrotic one (Figure 17). Furthermore, the Caspase 3 assay was adopted for understanding the pro-apoptotic factors involved by **RC-106** in the antiproliferative activity, as well as the S2R agonist/antagonist profile. Indeed, recently, Zeng *et al.* reported that caspase-dependent cellular death is a hallmark related to S2R agonist. Western Blot assay pointed out that **RC-106** activates Caspase 3 as an apoptotic factor.

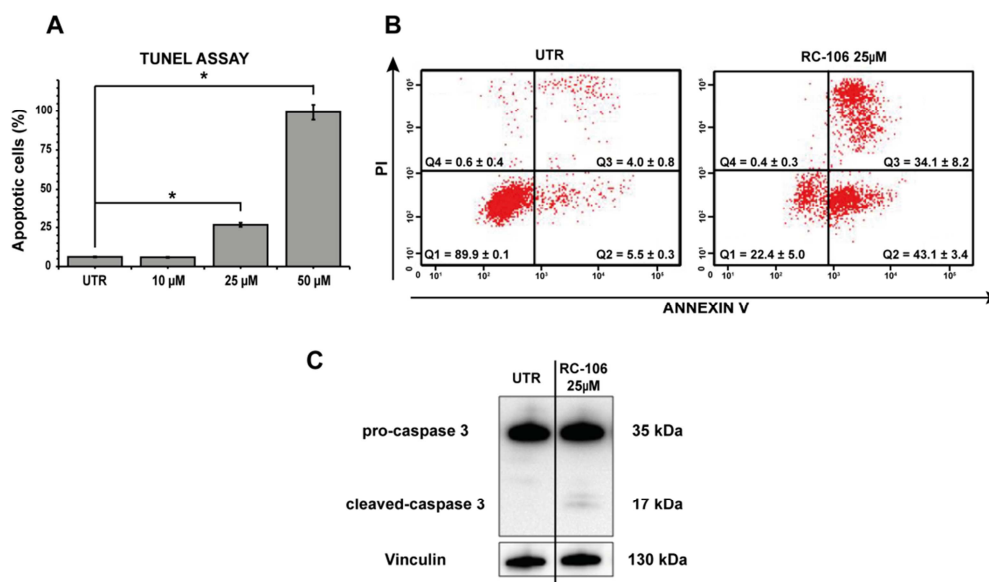


Figure 17. (A) TUNEL assay. Percentage of apoptotic cells after 24 h exposure to compound **3** (RC-106) at 10, 25 and 50 μ M. * p <0.05. (B). Cytofluorimetric (FACS) analysis of apoptosis by Annexin V test. Cells were exposed for 24 h to compound **3** (RC-106) (25 μ M). Q1 area represents viable cells; Q2 early-apoptotic cells; Q3 late-apoptotic cells; Q4 necrotic cells. The images are representative of three experiments. (C) WB analysis of apoptotic-related marker after 24 h exposure to **3** (RC-106) at 25 μ M. Images are representative of two independent experiments.

In conclusion, we identified **RC-106** a pan-SR, S1R antagonist and a S2R agonist, endowed with cytotoxic properties. Furthermore, the molecule activates a caspase-mediated proapoptotic program. Moreover, it is widely documented that S1R antagonists are useful pharmaceutical tools for alleviating neuropathic pain, a pathologic condition that frequently occurs in cancer patients. Accordingly, the design and synthesis of pan-SR modulators may play a key role in developing antitumor and analgesic drugs, and thus they could represent an innovative pharmacological approach for treating cancer patients with advanced disease.

Synthesis of Biotin-derivatives to increase the cancer cell uptake of **RC-106**

Publication: **MR1**

It is widely accepted that chemotherapy presents several drawbacks and side effects, due to its lack of specificity towards cancer cells. Numerous experimental evidence underlined the benefits in targeting SRs, in virtue of their over-expression in different tumorous types. Considering this interesting data, a drug-targeting approach may further enhance the efficacy of SR ligands towards cancer. An in depth literature analysis pointed out the feasibility of this strategy, which may increase the uptake of antiproliferative agents in cancer cells. In detail, vitamin-mediated drug targeting emerged as an attractive method to develop innovative

anticancer drugs [74-78]. In this context, biotin-derivatives took places, according to their high internalization in cells that rapidly divide, such as cancer cell lines [79]. The elevated biotin uptake may be justified by the recent identification of sodium-dependent multivitamin transporter (SMVT) [80-81]. This channel mediates the biotin cell entrance and it is highly expressed in several aggressive tumorous lines, i.e. leukemia (L1210FR), ovarian (OV2008, ID8), colon (Colo-26), mastocytoma (P815), lung (M109), renal (RENCA, RD0995) and breast (4T1, JC, MMT06056) [80-81]. Therefore, different biotin-conjugates have been investigated in order to discover novel anti-neoplastic molecules endowed with poor side effects. Generally, the procedure provides the biotinylation of well-known or new anticancer compounds, as well as antiproliferative peptides. Interestingly, the analysis presented in Publication **MR1** highlights the possibility to enhance the cytotoxic properties of some anticancer drugs commonly used in cancer therapy (taxoids, doxorubicin and gemcitabine) [82-85]. Noteworthy, the toxicity of biotin-conjugates is significantly reduced against normal cells, underlining the great potential of the biotin-mediated drug targeting.

Considering the excellent results obtained *via* biotinylation, our research group focused on the biotin-derivatization of potential pan-SR modulators. Firstly, we designed the biotin-spacer, characterized by three building blocks: i) the biotin; ii) a PEG-chain and iii) a reactive group (Figure 18).

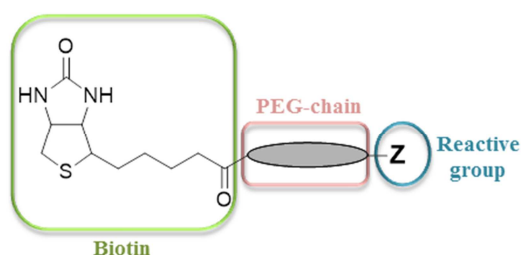
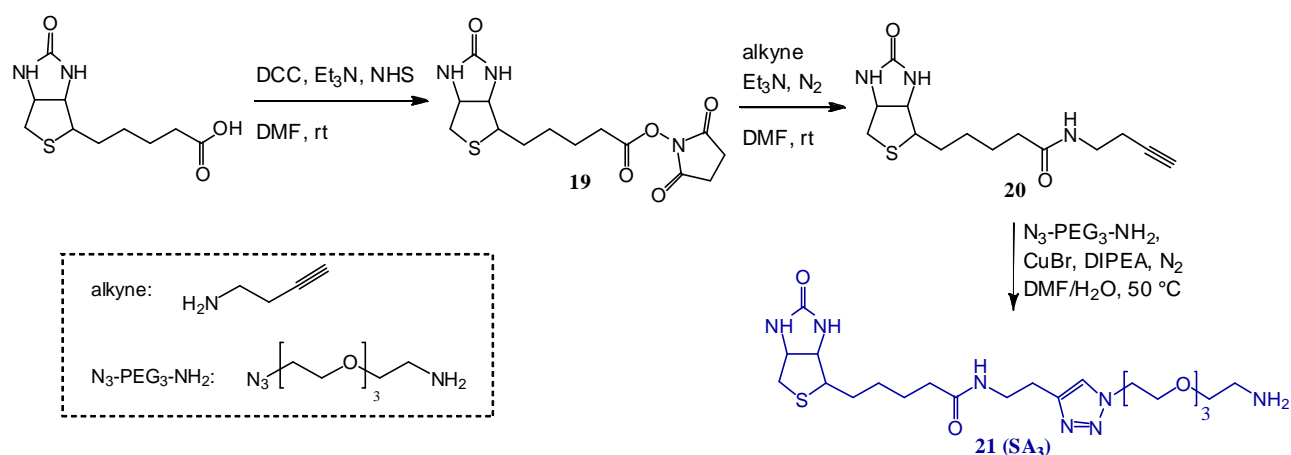


Figure 18. Design of the biotinylated spacer.

A retrosynthetic analysis disclosed the synthetic pathway (Scheme 5) to obtain the desired biotinylated-spacer **21**. The strategy provides the activation of the carboxylic group of biotin, as succinimidyl ester **19**, employing NHS, Et₃N and DCC, as coupling agent. After an amidation was applied to the activated carboxylic acid, using the but-3-yn-1-amine reagent. The amidic intermediate **20**, presenting an alkynyl functionality, reacted with the 11-azido-3,6,9-trioxaundecan-1-amine *via* a 1,3-dipolar cycloaddition, in the presence of a catalytic amount of CuBr. The whole protocol furnished the desired 1,2,3-triazole **SA₃** in good yield, as confirmed by ¹H NMR, ¹³C NMR and HR-MS.



Scheme 5. Synthesis of biotinylated-spacer **21**. Reagents and reaction conditions.

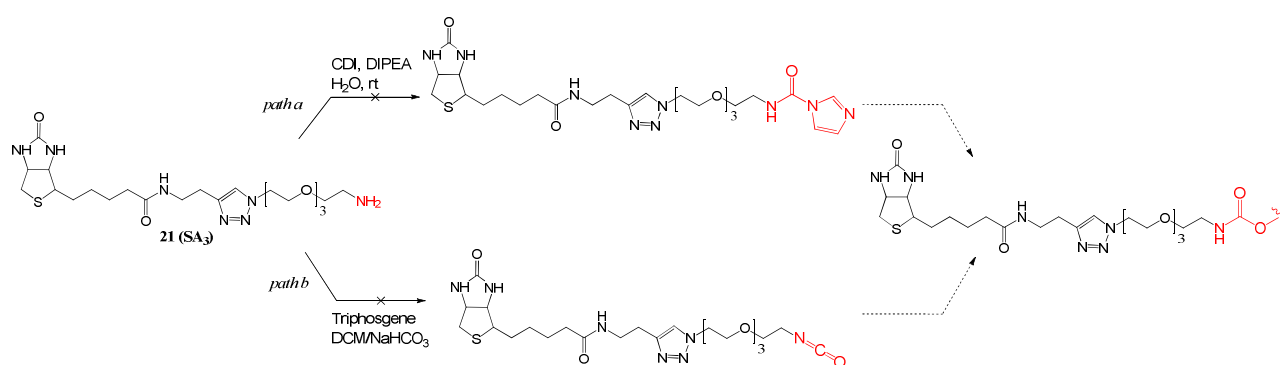
The critical step in this synthetic scheme was represented by the last reaction. In detail, the CuAAC (*Copper(I)-catalyzed Azide-Alkyne Cycloaddition*), also known as “Sharpless-type click reaction” is a variation of the Huisgen 1,3-dipolar cycloaddition. It provides the regioselective formation of a 1,2,3-triazole, starting from an alkyne and an azide. The high yields, the tolerance towards diverse substituents and the employment of solvents with completely different characteristics confer to this reaction an elevated versatility. Moreover, the definition “Click” is related to the time needed to perform the reaction, occurring very quickly. Nevertheless we encountered some difficulties in carrying out the last step. Indeed, we set up different strategies in order to disclose the optimal protocol. In Table 17, the analysed parameters have been reported. From these results, the conditions suitable to obtain the desired biotinylated-spacer **21** in good yield, are described by entry 5. The protocol envisages the employment of the DMF/H₂O mixture as solvent, the CuBr as source of Cu(I) in the presence of DIPEA, under atmosphere of N₂ for three days, at 50 °C.

Table 17. Click chemistry protocols.

Entry	Solvent	Catalyst	Temperature	Time	Yield [%]
1	<i>t</i> -BuOH/H ₂ O	CuSO ₄ ·5H ₂ O/NaAscorbate	rt	24 h	5
2	DMF	CuSO ₄ ·5H ₂ O/NaAscorbate	rt	24h	10
3	DMF	Cu(0)/CuSO ₄ ·5H ₂ O	MW(80°C,100W, 100 Psi)	10min	13
4	DMF/H ₂ O	CuBr/DIPEA	50 °C	48h	38
5	DMF/H ₂ O	CuBr/DIPEA	50 °C	72h	43

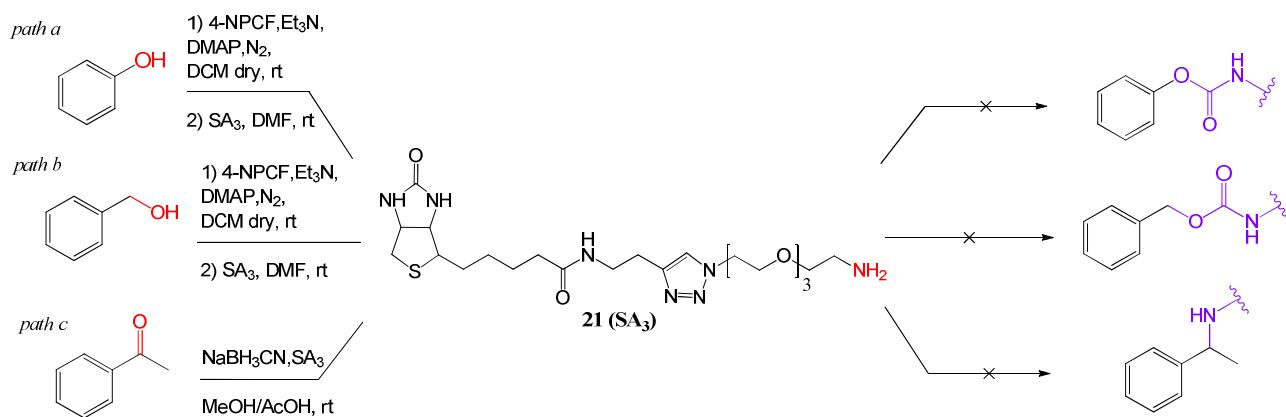
Keeping in mind that our idea was the formation of a biotin-pan-SR conjugate, we performed several attempts to get the desired product. Firstly, we evaluated the synthetic protocol suitable for the biotinylation of compound **12** (selected as model). Considering the presence

of the $-NH_2$, as reactive group in the spacer, and the $-OH$ in molecule **12**, we identified the carbamidic group as the optimal functionality to conjugate the two compounds. Therefore, as the first attempt we applied on **SA₃** a “green” protocol, in order to obtain a carboimidazole derivative, using H_2O as solvent (Scheme 6 – *path a*). The absence of the expected product led us to abandon this strategy and thus, we adopted the dangerous methodology to obtain isocyanates (Scheme 6 – *path b*). Indeed, we used the triphosgene in a $DCM/NaHCO_3$ (5%) mixture, however, also in this case no product has been observed.



Scheme 6. Attempts to obtain the carbamidic derivatives.

These failures were associated to the low reactivity of the aminic group in **SA₃**. According to this speculation, we turned our attention in developing a method useful for the functionalization of compound-derivatives of **12**. In order to avoid the use of **12**, we addressed the investigation toward simple starting materials, presenting functionalities able to react with a $-NH_2$. Accordingly, phenol and benzyl alcohol were selected as substrates, since they present a hydroxyl group suitable to be transformed in a carbamidic functionality, through the “one pot” reaction (Scheme 7 – *path a and b*). In these cases, the use of *p*-nitrophenyl chloroformate provides the formation of the carbonic derivatives, as confirmed by 1H -NMR of the crude, in the presence of a Lewis base (DMAP). Afterwards, **SA₃** was added to the no-purified crude. However, the carbamidic products was not identified. Therefore, we abandoned the synthetic protocols to generate carbamides and we evaluated the potentiality of a reductive amination. Indeed, we treated the acetophenone with acetic acid to activate the carbonyl group. 1 hour later the compound **21** was added to the solution and the mixture was stirred for 3 hours. Lastly, the reductive reagent $NaBH_3CN$ was employed to reduce the putative imine into the desired amine. The 1H -NMR evidenced the absence of the signal related to the desired product.



Scheme 7. Attempts to obtain the biotin-pan-SR conjugates.

We believe that all these negative results could be explained by the low reactivity of the $-NH_2$. The cause may be found in the high flexibility or in the low nucleophilicity of the molecule **21**. Moreover, the polarity of this compound represents an important hurdle to take into consideration, since it may limit the choice towards other reaction strategies that envisage the use of apolar solvents. In conclusion, the biotin-pan-SR conjugates approach is of high interest for the scientific community and therefore this part of the project deserves further investigation.

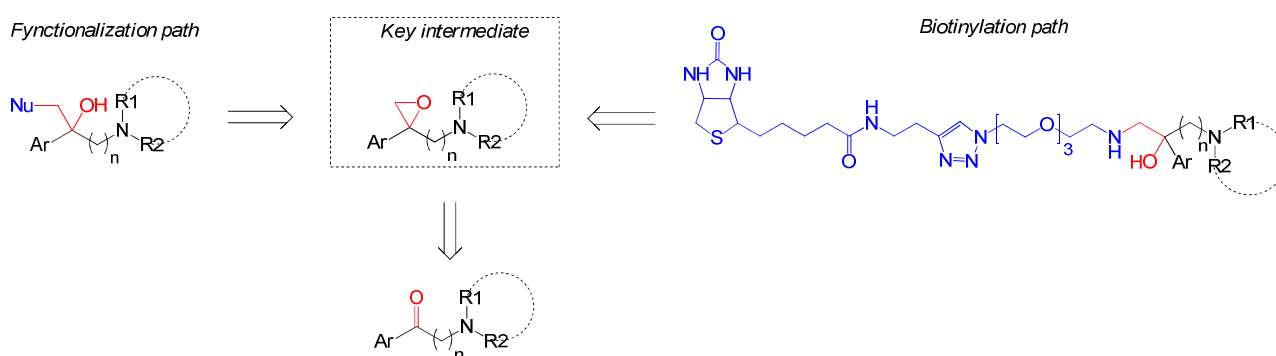
3. CONCLUSION AND OUTLOOK

3. CONCLUSION AND OUTLOOK

The design and synthesis of NCEs are crucial in the drug discovery programs, not only in academia, but also in the pharmaceutical industry. Within the framework of this Ph.D. thesis, we had to deal with the lack of two milestones: the knowledge of the endogenous SR ligands and of the three-dimensional receptor structures. As a consequence, we adopted a ligand-based drug design approach, developing a QSAR model, suitable for designing NCEs potentially able to bind both S1R and S2R. This strategy led to the identification of the main structural feature (a bulky aminic group) suitable to obtain NCEs having affinity for both SR subtypes (pan-affinity). The prepared compounds, belonging to our classical scaffold [arylalkyl(alkenyl)amine] are characterized by the common presence of a 4-benzylpiperidine. Therefore, to acquire more information on SAR of this compound class, we decided to modify the aromatic moiety and the alkyl/alkenyl chaining, and also to study the role of the chirality. Indeed, our previous experience led us to point out that the SRs – ligands interaction may be stereospecific and it is strongly related to the structural elements present in the molecule. Accordingly, a new series of compounds was prepared and characterized. Chiral compounds were subjected to a systematic screening protocol by chiral chromatography and the optimal analytical conditions were transferred to (semi)-preparative scale. In this way, homochiral compounds were obtained and their absolute configurations at the chiral centres were assigned by comparing electronic circular dichroism analysis and chiral HPLC elution order. The whole compound series was then biologically investigated and **RC-106** emerged to possess a pan-SR profile and was selected as a candidate for further biological studies (S1R and S2R agonist/antagonist profile, antiproliferative effect). Obtained results clearly show that **RC-106** has a S1R antagonist and a S2R agonist profile, and is endowed with interesting cytotoxic properties towards a panel of cancer cell lines. Moreover, it exhibited pro-apoptotic effect on PaCa3 cells, triggering the caspase-mediated mechanisms. **RC-106** was selected as a candidate for an in depth pre-clinical evaluation. The kinetic profile of **RC-106**, i.e. the stability studies in different biological matrices and the *in vivo* distribution, is currently under investigation. Another important aspect to disclose is the ability of S1R antagonists in alleviating chronic pain, which is a pathologic condition that frequently occurs in cancer patients. We strongly believe that the identification of potent pan-SR modulators will open new doors for developing drugs with both antitumor and analgesic properties, thus representing an innovative pharmacological approach for the treatment of cancer patients with advanced disease.

Conclusion and Outlook

Noteworthy, our SAR exploration is still open, indeed we would like to identify new SR ligands, with a high degree of structural novelty, with the final aim to design and prepare patentable compounds. In this context, in collaboration with the University of Vienna, we will apply the carbenoids chemistry (described in depth in the following sections) towards our substrates. In detail, we are planning to adopt these reagents on a series of ketones, to obtain oxiranes. These products may represent versatile intermediate compounds suitable for further functionalization as well as for biotinylation (Scheme 8).



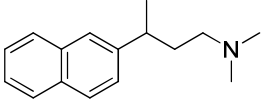
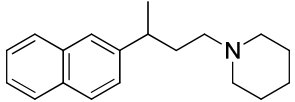
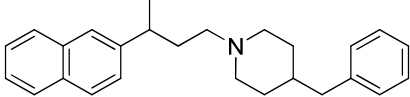
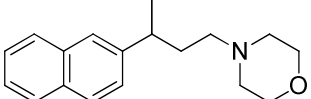
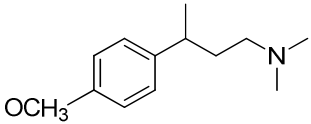
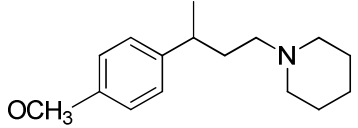
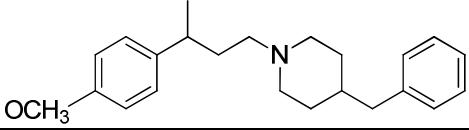
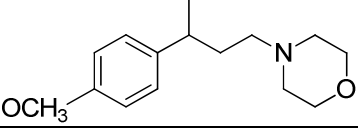
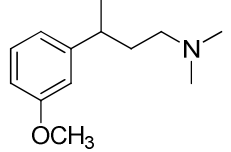
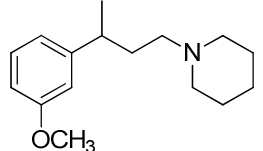
Scheme 8. Retrosynthetic analysis for obtaining functionalized or biotinylated derivatives.

4. EXPERIMENTAL SECTION

4. EXPERIMENTAL SECTION

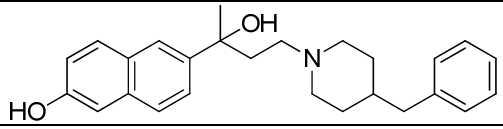
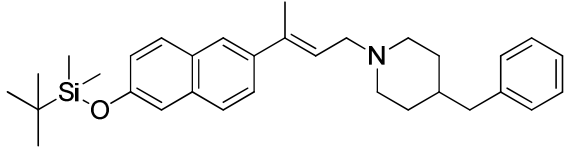
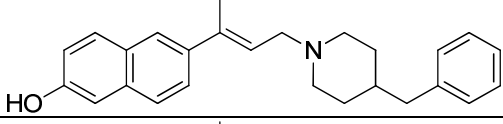
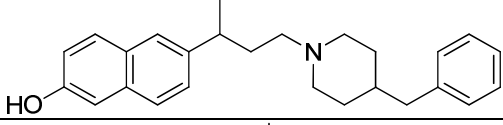
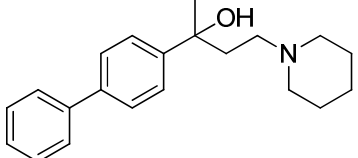
In this section, I will show only the unpublished results. The experimental sections, concerning the data already presented in publications, have been reported as attached file in the Appendix. In detail, all the enclosed Papers (**MR1-MR8**) are followed by their “Supporting Information” file.

4.1. Compounds characterizations and biological evaluations

Name	Compound	Paper	Characterization	Biological assay
1a		MR7 (<i>cmpd 10a</i>)	IR, ¹ H NMR, MS, HPLC	Binding
1b		MR7 (<i>cmpd 10b</i>)	IR, ¹ H NMR, MS, HPLC	Binding
1c		MR7 (<i>cmpd 10c</i>)	IR, ¹ H NMR, MS, HPLC	Binding
1d		MR7 (<i>cmpd 10d</i>)	IR, ¹ H NMR, MS, HPLC	Binding
2a		MR7 (<i>cmpd 11a</i>)	IR, ¹ H NMR, MS, HPLC	Binding
2b		MR7 (<i>cmpd 11b</i>)	IR, ¹ H NMR, MS, HPLC	Binding
2c		MR7 (<i>cmpd 11c</i>)	IR, ¹ H NMR, MS, HPLC	Binding
2d		MR7 (<i>cmpd 11d</i>)	IR, ¹ H NMR, MS, HPLC	Binding
3a		MR7 (<i>cmpd 12a</i>)	IR, ¹ H NMR, MS, HPLC	Binding
3b		MR7 (<i>cmpd 12b</i>)	IR, ¹ H NMR, MS, HPLC	Binding

Experimental Section

3c		MR7 (<i>cmpd 12c</i>)	IR, ¹ H NMR, MS, HPLC	Binding
3d		MR7 (<i>cmpd 12d</i>)	IR, ¹ H NMR, MS, HPLC	Binding
4a		MR7 (<i>cmpd 13a</i>)	IR, ¹ H NMR, MS, HPLC	Binding
4b		MR7 (<i>cmpd 13b</i>)	IR, ¹ H NMR, MS, HPLC	Binding
4c		MR7 (<i>cmpd 13c</i>)	IR, ¹ H NMR, MS, HPLC	Binding
4d		MR7 (<i>cmpd 13d</i>)	IR, ¹ H NMR, MS, HPLC	Binding
5		MR5 (<i>cmpd 1</i>)	IR, ¹ H NMR, ¹³ C NMR, UPLC-MS	Binding
6 RC-106		MR5 (<i>cmpd 3</i>)	IR, ¹ H NMR, ¹³ C NMR, UPLC-MS	Binding PC12 test, MTT, TUNEL, AnnexinV, WB
7		MR5 (<i>cmpd 5</i>)	IR, ¹ H NMR, ¹³ C NMR, UPLC-MS	Binding
8		MR5 (<i>cmpd 2</i>)	IR, ¹ H NMR, ¹³ C NMR, UPLC-MS	Binding
9		MR5 (<i>cmpd 4</i>)	IR, ¹ H NMR, ¹³ C NMR, UPLC-MS	Binding MTT
10		MR5 (<i>cmpd 6</i>)	IR, ¹ H NMR, ¹³ C NMR, UPLC-MS	Binding
-		MR5 (<i>cmpd 7</i>)	IR, ¹ H NMR, ¹³ C NMR, MS	-
-		MR5 (<i>cmpd 8</i>)	IR, ¹ H NMR, ¹³ C NMR, MS	-

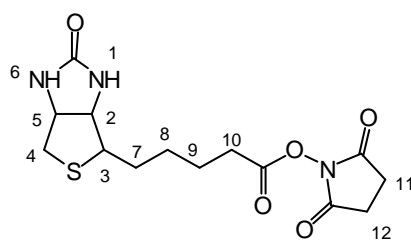
11		MR5 (<i>compd 9</i>)	IR, ¹ H NMR, ¹³ C NMR, UPLC-MS	Binding
-		MR5 (<i>compd 10</i>)	IR, ¹ H NMR, ¹³ C NMR, MS	-
12		MR5 (<i>compd 11</i>)	IR, ¹ H NMR, ¹³ C NMR, UPLC-MS	Binding
13		MR5 (<i>compd 12</i>)	IR, ¹ H NMR, ¹³ C NMR, UPLC-MS	Binding
RC-34		MR2 (<i>compd 1</i>)	¹ H NMR, HPLC	Binding PC12 test

4.2. Materials and methods

Reagents and solvents for synthesis were obtained from Aldrich (Italy). Solvents were purified according to the guidelines in Purification of Laboratory Chemicals. Melting points were measured on SMP3 Stuart Scientific apparatus and are uncorrected. Analytical thin-layer-chromatography (TLC) was carried out on silica gel precoated glass-backed plates (Fluka Kieselgel 60 F254, Merck) and on aluminiumoxid precoated aluminium-backed plates (DC-Alufolien Aluminiumoxid 60 F254 neutral, Merck); visualized by ultra-violet (UV) radiation, acidic ammonium molybdate (IV), or potassium permanganate. Flash chromatography (FC) was performed with Silica Gel 60 (particle size 230–400 mesh) purchased from NovaChimica and neutral aluminium oxide (particle size 0.05-0.15 mm) purchased from Fluka. Bond Elute SCX cartridges were purchased from Varian. IR spectra were recorded on a Jasco FT/IR-4100 spectrophotometer; only noteworthy absorptions are given. ¹H NMR spectra were measured with an AVANCE 400 spectrometer Bruker, Germany at rt. Chemical shifts (δ) are given in ppm, coupling constants (*J*) are in Hertz (Hz) and signals are designated as follows: (s) singlet, (br s) broad singlet, (d) doublet, (t) triplet, (q) quartet, and (m) multiplet. TMS was used as internal standard. MS spectra were recorded on a Finnigan LCQ Fleet system (Thermo Finnigan, San Jose, CA, USA), using an ESI source operating in positive ion mode. The purities of target compounds were determined on a Jasco HPLC system equipped with a Jasco autosampler (model AS-2055 plus), a quaternary gradient pump (model PU-2089 plus), and a multiwavelength detector (model MD-2010 plus). The HPLC method for the arylalkenylamines was as follows: column XBridge™ Phenyl, 4.6 mm x 150 mm, 5 μm; column temperature, ambient; flow rate, 1 mL/min; gradient elution, 10% methanol in phosphate buffer (5 mM, pH 7.6) to 90% methanol in phosphate buffer (5 mM, pH 7.6) in 10 min, followed by isocratic elution, 90% methanol in phosphate buffer (5 mM, pH 7.6) for 10 min.

4.3. Synthesis of biotin derivative 21 (SA₃)

4.3.1. Preparation of compound 19



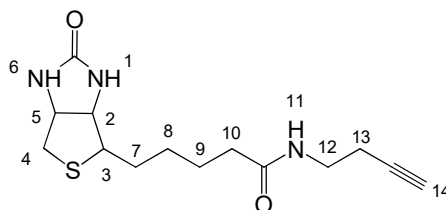
NHS (2.0 mmol) and DCC (2.0 mmol) were added to a solution of Biotin (1.0 mmol) in DMF (8.0 mL), at 45 °C. The reaction mixture was stirred for 24 h, at rt. Afterwards, the mixture was filtered through sintered glass funnel, in order to eliminate the DCU. The obtained solution was evaporated under reduced pressure. The solid crude was washed with cold Et₂O and thus, white solid compound **19** was obtained.

2,5-dioxopyrrolidin-1-yl 5-(2-oxohexahydro-1*H*-thieno[3,4-*d*]imidazol-4-yl)pentanoate

Yield: 98%, white solid, mp: 202-205 °C. IR (cm⁻¹) 3014, 2967, 1748, 1718, 1362, 1230, 1214.

¹H NMR (400 MHz, DMSO) δ (ppm): 6.45-6.39 (d, 2H, H-1,6), 4.31 (t, 1H, H-5), 4.15 (t, 1 H, H-2), 3.11 (m, 1H, H-3), 2.79-2.87 (d e m, 5H, H-4,11,12), 2.68 (t, 2H, H-10), 2.57 (d, 1H, H-4); 1.35-1.67 (m, 6H, H-7,8,9).

4.3.2. Preparation of compound 20

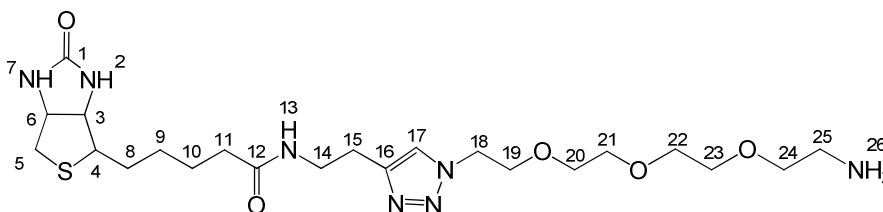


A solution of compound **2** (1.0 mmol) in DMF (11.0 mL) was added dropwise to a solution of but-3-yn-1-amine (1.2 mmol) and Et₃N (1.5 mmol) in DMF (2.3 mL), under N₂ atmosphere. The reaction mixture was stirred for 24 h, at rt. Afterwards, the solvents were evaporated under reduced pressure and the so-obtained crude was washed with cold Et₂O (3x20 mL). Pure compound **20** was synthesized as white solid.

N-(but-3-yn-1-yl)-5-(2-oxohexahydro-1*H*-thieno[3,4-*d*]imidazol-4-yl)pentanamide

Yield: 88%, white solid, mp: 147-149 °C. IR (cm⁻¹) 3629, 3450, 2967, 2139, 1733, 1553. ¹H NMR (400 MHz, DMSO) δ (ppm): 7.97 (t, 1H, H-11), 6.44-6.37 (d, 2H, H-1,6), 4.30 (t, 1H, H-5), 4.13 (t, 1H, H-2), 3.15-3.09 (m, 3H, H-3,12), 2.82 (m, 2H, H-4,14), 2.58 (d, 1H, H-4), 2.27 (t, 2H, H-13), 2.06 (t, 2H, H-10), 1.60-1.31 (m, 6H, H-7,8,9).

4.3.3. Preparation of compound 21 (SA₃)



Experimental Section

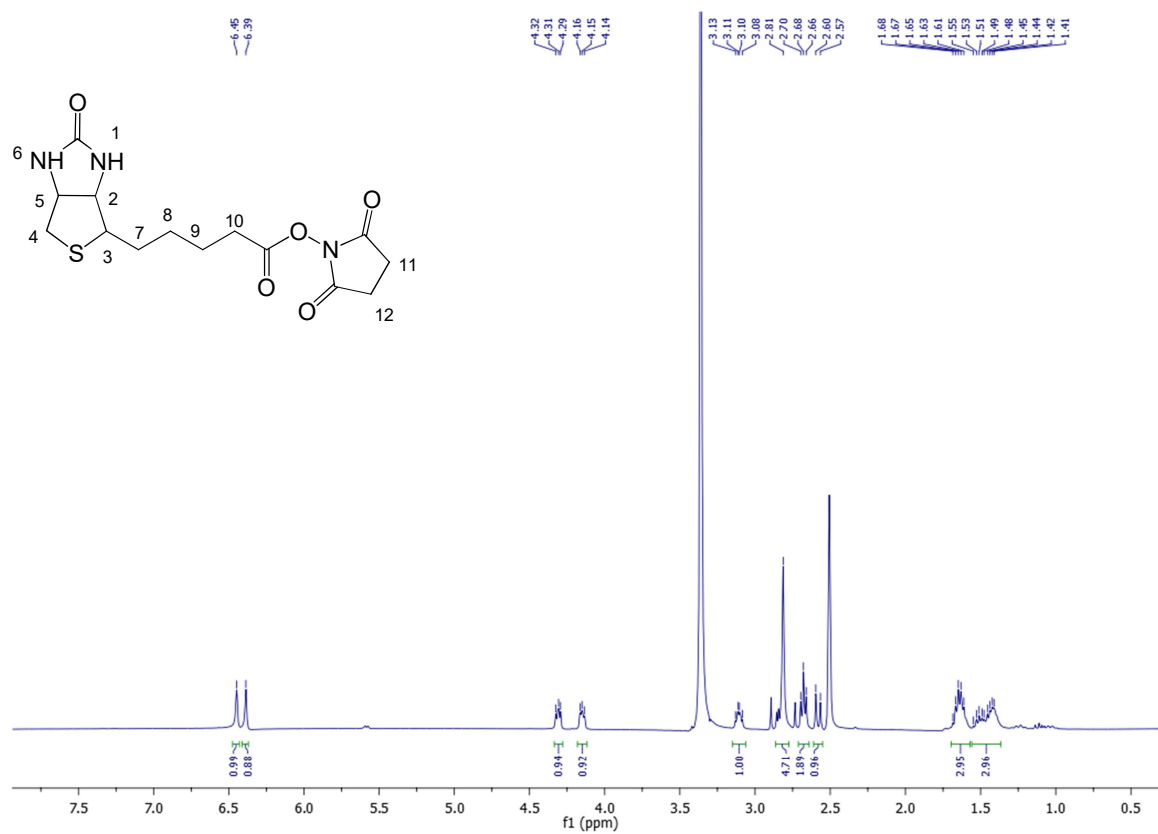
A solution of compound **20** (1.0 mmol) in DMF (5.0 mL) and degassed H₂O (5.0 mL) was added to a solution of N₃-PEG₃-NH₂ (1.0 mmol) and DIPEA (6.0 mmol) in DMF (1.0 mL) and degassed water (1.0 mL). Lastly, CuBr (0.2 mmol) was added to the mixture, under N₂ atmosphere. The reaction was stirred for 72 h, at 50 °C. The mixture was filtered on a silica pad, eluting with DCM:MeOH, 50:50, v/v + 2,5% NH₃ in MeOH as mobile phase. Afterwards, the reaction was evaporated under reduced pressure, obtaining a yellow oil. The crude was purified through flash chromatography (mobile phase: DCM:MeOH, 50:50, v/v + 2,5% NH₃ in MeOH). Compound **21** was obtained as yellow oil, as confirmed by ¹H NMR and HPLC-MS.

***N*-(2-(1-(2-(2-(2-(2-aminoethoxy)ethoxy)ethoxy)ethyl)-1*H*-1,2,3-triazol-4-yl)ethyl)-5-(2-oxohexahydro-1*H*-thieno[3,4-*d*]imidazol-4-yl)pentanamide**

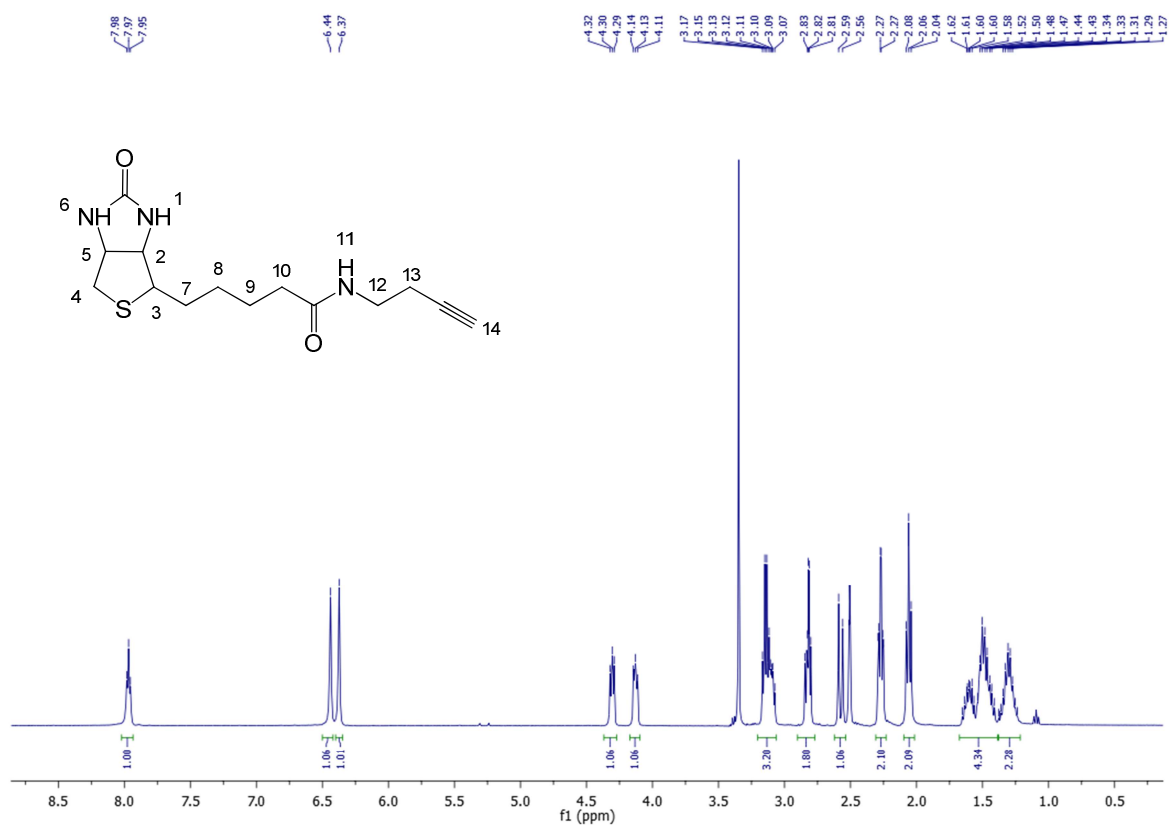
Yield: 43%, yellow oil. **IR** (cm⁻¹) 3435, 2988, 2869, 1818, 1676, 1392, 1293, 1142, 999. **¹H NMR** (400 MHz, DMSO) δ (ppm): 8.05 (t, 1H, H-17), 7.87 (d, 1H, H-13), 6.45-6.41 (d, 2H, H-2,7), 4.46 (t, 2H, H-18), 4.30 (t, 1H, H-5), 4.13 (t, 1H, H-3), 3.79 (t, 2H, H-15); 3,50 (m, 10H, H-20-24), 3.27-3.21 (m, 3H, H-4,25), 3.10 (m, 2H, H-19), 2.84-2.81 (dd, 1H, H-5), 2.74 (t, 2H, H-14), 2.60-2.57 (d, 1H, H-5), 2.06 (t, 2H, H-11), 1.61-1.29 (m, 6H, H-8,9,10). **¹³C NMR** (100 MHz, DMSO) δ (ppm): 172.09 (C-12), 162.76 (C-1), 144.26 (C-16), 122.60 (C-17), 69.69, 69.63 and 69.59 (C-20-24), 68.79 (C-19), 61.05 (C-3), 59.21 (C-6), 55.45 (C-4), 49.26 (C-18), 40.07 (C-5), 38.38 (C-14), 35.21 (C-11), 28.22 (C-9), 28.05 (C-8), 25.61 (C-15), 25.28 (C-10). **HPLC-MS** tR = 5.29 min (m/z = 514 [M+H]⁺, m/z = 536 [M+Na]⁺, m/z = 1027 [2M+H]⁺; m/z = 1049 [2M+Na]⁺).

4.3.4. ¹H and ¹³C NMR Spectra of Compounds 19-21

Compound 19



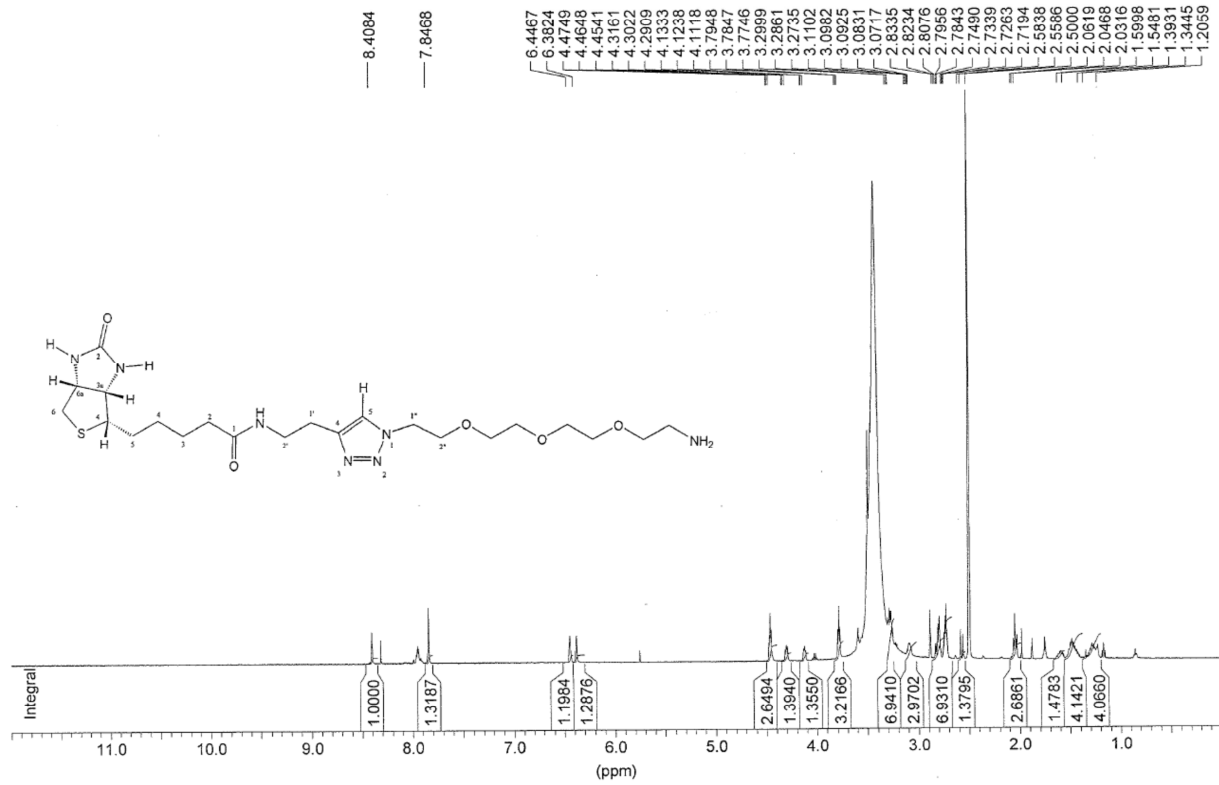
Compound 20



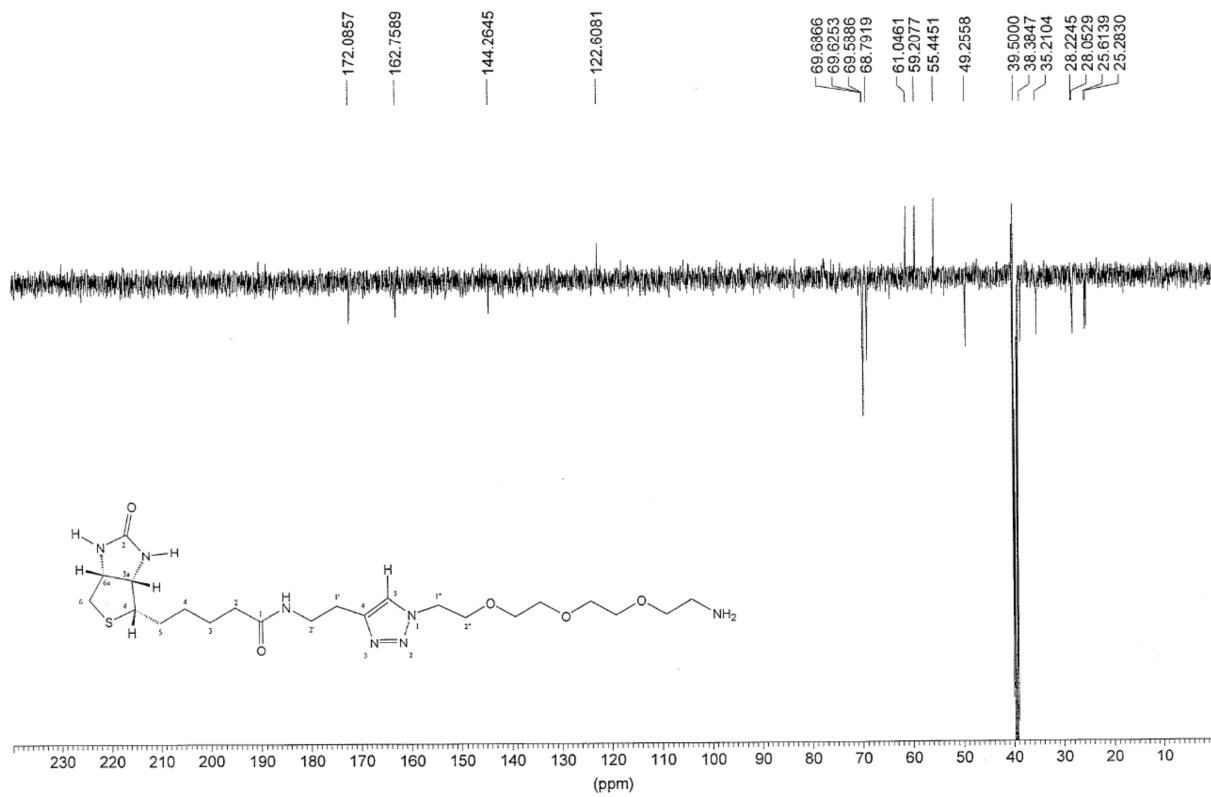
Experimental Section

Compound 21 (SA₃)

MR_SA3 in d6DMSO (Proton), 3.3.2015



MR_SA3 in d6DMSO (APT), 3.3.2015



5. REFERENCES

5. REFERENCES

1. World Health Organization, *World Cancer Report 2014*. **2014**. Chapter 1.1.
2. Torre, L.A.; Siegel, R.L.; Ward, E.M.; Jemal, A. *Cancer Epidemiol. Biomarkers Prev.* **2016**, *25*, 16.
3. Lionetto, R.; Pugliese, V.; Bruzzi, P.; Rosso, R. *Eur. J. Cancer.* **1995**, *31A*, 882.
4. Tripodo, G.; Mandracchia, D.; Collina, S.; Rui, M.; Rossi, D. *Med. Chem.* **2014**, S(1).
5. Chimento, A.; Sala, M.; Gomez-Monterrey I.M.; Musella, S.; Bertamino, A.; Caruso, A.; Sinicropi, M.S.; Sirianni, R.; Puoci, F.; Parisi, O.I.; Campana, C.; Martire, E.; Novellino, E.; Saturnino, C.; Campiglia, P.; Pezzi, V. *Bioorg. Med. Chem. Lett.* **2013**, *23*, 6401.
6. Saturnino, C.; Buonerba, M.; Boatto, G.; Pascale, M.; Moltedo, O.; de Napoli, L.; Montesarchio, D.; Lancelot, J.C.; de Caprariis, P. *Chem. Pharm. Bulletin.* **2003**, *51*, 971.
7. Timmers, L.; Boons, C.C.; Kropff, F.; van de Ven, P.M.; Swart, E.L.; Smit, E.F.; Zweegman, S.; Kroep, J.R.; Timmer-Bonte, J.N.; Boven, E.; Hugtenburg, J.G. *Acta Oncol.* **2014**, *53*, 259.
8. Cavaletti, G.; Marmioli, P. *Curr. Opin. Neurol.* **2015**, *28*, 500.
9. Martin, W.R.; Eades, C.G.; Thompson, J.A.; Huppler, R.E.; Gilbert, P.E. *J. Pharmacol. Exp. Ther.* **1976**, *197*, 517.
10. Su, T.P. *J. Pharmacol. Experimental Therap.* **1982**, *223*, 284.
11. Maurice, T.; Lockhart, B.P. *Prog. Neuro-Psychoph.* **1997**, *21*, 69.
12. Vaupel, D.B. *Eur. J. Pharmacol.* **1983**, *92*, 269.
13. Skuza G. *Pol. J. Pharmacol.* **2003**, *55*, 923.
14. Quirion, R.; Bowen, W.D.; Itzhak, Y.; Junien, J.L.; Musacchio, J.M.; Rothman, R.B.; Su, T.P.; Tam, S.W.; Taylor, D.P. *Trends Pharmacol. Sciences.* **1992**, *13*, 85.
15. Hellewell, S.B.; Bruce, A.; Feinstein, G.; Orringer, J.; Williams, W.; Bowen, W.D. *Eur. J. Pharmacol.* **1994**, *268*, 9.
16. Collina, S.; Gaggeri, R.; Marra, A.; Bassi, A.; Negrinotti, S.; Negri, F.; Rossi, D. *Expert Opin Ther Pat.* **2013**, *23*, 597.
17. Hanner, M.; Moebius, F.F.; Flandorfer, A.; Knaus, H.G.; Striessnig, J.; Kempner, E.; Glossmann, H. *Proc. Natl. Acad. Sci. U S A.* **1996**, *93*, 8072.
18. Seth, P.; Fei, Y.J.; Li, H.W.; Huang, W.; Leibach, F.H.; Ganapathy, V. *J. Neurochem.* **1998**, *70*, 922.
19. Prasad, P.D. Fei, Y.J.; Li, H.W.; Huang, W.; Leibach, F.H.; Ganapathy, V. *J. Neurochem.* **1998**, *70*, 443.
20. Walker, J. *Washington DC: Ltd TF.* **1993**, 91.

References

21. Kekuda, R.; Prasad, P.D.; Fei, Y.J.; Leibach, F.H.; Ganapathy, V. *Biochem. Biophys. Research Comm.* **1996**, *229*, 553.
22. Mei, J.; Pasternak, G.W. *Biochem. Pharmacol.* **2001**, *62*, 349.
23. Laurini, E.; Col, V.D.; Mamolo, M.G.; Zampieri, D.; Posocco, P.; Fermeglia, M.; Vio, L.; Prici, S. *Acs Med. Chem. Lett.* **2011**, *2*, 834.
24. Ortega-Roldan, J.L.; Ossa, F.; Amin, N.T.; Schnell, J.R. *FEBS Lett.* **2016**, *589*, 659.
25. Schmidt, H.R.; Zheng, S.; Gurpinar, E.; Koehl, A.; Manglik, A.; Kruse, A.C. *Nature.* **2016**, *532*, 527.
26. Hayashi, T.; Su, T.P. *Cell.* **2007**, *131*, 596.
27. Su, T.P.; Su, T.C.; Nakamura, Y.; Tsai, S.Y. *Trends Pharmacol. Sci.* **2016**, *37*, 262.
28. Maurice, T.; Su, T.P. *Pharmacol. Ther.* **2009**, *124*, 195.
29. Peviani, M.; Salvaneschi, E.; Bontempi, L.; Petese, A.; Manzo, A.; Rossi, D.; Salmona, M.; Collina, S.; Bigini, P.; Curti, D. *Neurobiol. Dis.* **2014**, *62*, 218.
30. Marra, A.; Rossi, D.; Pignataro, L.; Bigogno, C.; Canta, A.; Oggioni, N.; Malacrida, A.; Corbo, M.; Cavaletti, G.; Peviani, M.; Curti, D.; Dondio, G.; Collina, S. *Future Med. Chem.* **2016**, *8*, 287.
31. Kourrich, S.; Su, T.P.; Fujimoto, M.; Bonci, A. *Trends Neurosci.* **2012**, *35*, 762.
32. Hellewell, S.B.; Bowen, W.D. *Brain Research.* **1990**, *527*, 244.
33. Xu, J.; Zeng, C.; Chu, W.; Pan, F.; Rothfuss, J.M.; Zhang, F.; Tu, Z.; Zhou, D.; Zeng, D.; Vangveravong, S.; Johnston, F.; Spitzer, D.; Chang, K.C.; Hotchkiss, R.S.; Hawkins, W.G.; Wheeler, K.T.; Mach, R.H. *Nature Comm.* **2011**, *2*, 380.
34. Kabe, Y.; Nakane, T.; Koike, I.; Yamamoto, T.; Sugiura, Y.; Harada, E.; Sugase, K.; Shimamura, T.; Ohmura, M.; Muraoka, K.; Yamamoto, A.; Uchida, T.; Iwata, S.; Yamaguchi, Y.; Krayukhina, E.; Noda, M.; Handa, H.; Ishimori, K.; Uchiyama, S.; Kobayashi, T.; Suematsu, M. *Nature Commun.* **2016**, *7*, 11030.
35. Cahill, M.A. *J. Steroid Biochem. Mol. Biol.* **2007**, *105*, 16.
36. Ahmed, I.S.; Rohe, H.J.; Twist, K.E.; Craven, R.J. *J. Biol. Chem.* **2010**, *285*, 24775.
37. Ahmed, I. S.; Rohe, H.J.; Twist, K.E.; Mattingly, M.N.; Craven, R.J. *J. Pharmacol. Exper. Therap.* **2010**, *333*, 564.
38. Chu, U.B.; Mavlyutov, T.A.; Chu, M.L.; Yang, H.; Schulman, A.; Mesangeau, C.; McCurdy, C.R.; Guo, L.W.; Ruoho, A.E. *E. Bio. Medicine.* **2015**, *2*, 1806.
39. Mach, R.H.; Smith, C.R.; al-Nabulsi, I.; Whirrett, B.R.; Childers, S.R.; Wheeler, K.T. *Cancer Res.* **1997**, *57*, 156.
40. Wheeler, K.T.; Wang, L.M.; Wallen, C.A.; Childers, S.R.; Cline, J.M.; Keng, P.C.; Mach, R.H. *Br. J. Cancer* **2000**, *82*, 1223.

41. Colabufo, N.A.; Berardi, F.; Contino, M.; Ferorelli, S.; Niso, M.; Perrone, R.; Pagliarulo, A.; Saponaro, P.; Pagliarulo, V. *Cancer Lett.* **2006**, *237*, 83.
42. Kashivagi, H.; McDunn, J.E.; Simon, P.O. Jr; Goedegebuure, P.S.; Xu, J.; Jones, L.; Chang, K.; Johnston, F.; Trinkaus, K.; Hotchkiss, R.S.; Mach, R.H.; Hawkins, W.G. *Mol. Cancer.* **2007**, *6*, 48.
43. Zeng, C.; Rothfuss, J.; Zhang, J.; Chu, W.; Vangveravong, S.; Tu, Z.; Pan, F.; Chang, K.C.; Hotchkiss, R.; Mach, R.H. *Br. J. Cancer* **2012**, *106*, 693.
44. Vilner, B.J.; Rothfuss, J.; Zhang, J.; Chu, W.; Vangveravong, S.; Tu, Z.; Pan, F.; Chang, K.C.; Hotchkiss, R.; Mach, R.H. *J. Pharmacol. and Exper. Therap.* **2000**, *292*, 900.
45. Cassano, G.; Gasparre, G.; Niso, M.; Contino, M.; Scalera, V.; Colabufo, N.A. *Cell Calcium.* **2009**, *45*, 340.
46. Cassano, G.; Gasparre, G.; Contino, M.; Niso, M.; Berardi, F.; Perrone, R.; Colabufo, N.A. *Cell Calcium.* **2006**, *40*, 23.
47. Hornick, J.R.; Xu, J.; Vangveravong, S.; Tu, Z.; Mitchem, J.B.; Spitzer, D.; Goedegebuure, P.; Mach, R.H.; Hawkins, W.G. *Molecular Cancer.* **2010**, *298*, 1.
48. Takebayashi, M.; Hayashi, T.; Su, T.P. *J. Pharmacol. Exp. Ther.* **2002**, *303*, 1227.
49. Nishimura, T.; Ishima, T.; Iyo, M.; Hashimoto, K. *PLoS One* **2008**, *3*, e2558.
50. Ishima, T.; Hashimoto, K. *PLoS One* **2012**, *7*, e37989.
51. Robson, M.J.; Noorbakhsh, B.; Seminerio, M.J.; Matsumoto, R.R. *Curr. Pharm. Des.* **2012**, *18*, 902.
52. Ishima, T.; Fujita, Y.; Hashimoto, K. *Eur. J. Pharmacol.* **2014**, *727*, 167.
53. Zeng, C.; Rothfuss, J.M.; Zhang, J.; Vangveravong, S.; Chu, W.; Li, S.; Tu, Z.; Xu, J.; Mach, R.H. *Anal. Biochem.* **2014**, *448*, 68.
54. Macfarlane, S. et al. New Alzheimer's Drug ANAVEX 2-73: A Phase 2a Study, Clinical Safety, Tolerability and Maximum tolerated dose finding in mild-to-moderate Alzheimer's patients. 2016.
55. Abadias, M.; Escriche, M.; Vaqué, A.; Sust, M.; Encina, G. *Br. J. Clin. Pharmacol.* **2013**, *75*, 103.
56. Aydar, E.; Palmer, C.P.; Djamgoz, M.B. *Cancer Res.* **2004**, *64*, 5029.
57. Huang, Y.S.; Lu, H.L.; Zhang, L.J.; Wu, Z. *Med. Res. Rev.* **2014**, *34*, 532.
58. Crottès, D.; Guizouarn, H.; Martin, P.; Borgese, F.; Soriani, O. *Front. Physiol.* **2013**, *4*.
59. Happy, M.; Dejoie, J.; Zajac, C.K.; Cortez, B.; Chakraborty, K.; Aderemi, J.; Sauane, M. *Biochem. Biophys. Res. Commun.* **2015**, *456*, 683.
60. Li, S.D.; Dejoie, J.; Zajac, C.K.; Cortez, B.; Chakraborty, K.; Aderemi, J.; Sauane, M. *Molecular Pharmacology* **2006**, *3*, 579.

References

61. Chen, Y.; Bathula, S.R.; Yang, Q.; Huang, L. *J. Invest. Dermatol.* **2010**, *130*, 2790.
62. Guo, J.; Ogier, J.R.; Desgranges, S.; Darcy, R.; O'Driscoll, C. *Biomaterials.* **2012**, *33*, 7775.
63. Kim, S.K.; Huang, L. *J. Control. Release.* **2012**, *157*, 279.
64. Rhoades, D.J.; Kinder, D.H.; Mahfouz, T.M. *Med. Chem.* **2014**, *10*, 98.
65. Tu, Z.; Xu, J.; Jones, L.A.; Li, S.; Zeng, D.; Kung, M.P.; Kung, H.F.; Mach, R.H. *Applied Radiation and Isotopes.* **2010**, *68*, 2268.
66. Chu, W.; Xu, J.; Zhou, D.; Zhang, F.; Jones, L.A.; Wheeler, K.T.; Mach, R.H. *Bioorg. Med. Chem.* **2009**, *17*, 1222.
67. Ostefeld, M.S.; Fehrenbacher, N.; Høyer-Hansen, M.; Thomsen, C.; Farkas, T.; Jäättelä, M. *Cancer Res.* **2005**, *65*, 8975.
68. Groth-Pedersen, L.; Ostefeld, M.S.; Høyer-Hansen, M.; Nylandsted, J.; Jäättelä, M. *Cancer Res.* **2007**, *67*, 2217.
69. Petersen, N. H.; Olsen, O.D.; Groth-Pedersen, L.; Ellegaard, A.M.; Bilgin, M.; Redmer, S.; Ostefeld, M.S.; Ulanet, D.; Dovmark, T.H.; Lønborg, A.; Vindeløv, S.D.; Hanahan, D.; Arenz, C.; Ejsing, C.S.; Kirkegaard, T.; Rohde, M.; Nylandsted, J.; Jäättelä, M. *Cancer Cell.* **2013**, *24*, 379.
70. Dehdashti, F.; Laforest, R.; Gao, F.; Shoghi, K.I.; Aft, R.L.; Nussenbaum, B.; Kreisel, F.H.; Bartlett, N.L.; Cashen, A.; Wagner-Johnston, N.; Mach, R.H. *J. Nucl. Med.* **2013**, *54*, 350.
71. (a) Collina, S.; Loddo, G.; Urbano, M.; Linati, L.; Callegari, A.; Ortuso, F.; Alcaro, S.; Laggner, C.; Langer, T.; Prezzavento, O.; Ronsisvalle, G.; Azzolina, O. *Bioorg. Med. Chem.* **2007**, *15*, 771; (b) Rossi, D.; Urbano, M.; Pedrali, A.; Serra, M.; Zampieri, D.; Mamolo, M.G.; Laggner, C.; Zanette, C.; Florio, C.; Schepmann, D.; Wuensch, B.; Azzolina, O.; Collina, S. *Bioorg. Med. Chem.* **2010**, *18*, 1204; (c) Rossi, D.; Pedrali, A.; Urbano, M.; Gaggeri, R.; Serra, M.; Fernández, L.; Fernández, M.; Caballero, J.; Ronsisvalle, S.; Prezzavento, O.; Schepmann, D.; Wuensch, B.; Peviani, M.; Curti, D.; Azzolina, O.; Collina, S. *Bioorg. Med. Chem.* **2011**, *19*, 6210; (d) Rossi, D.; Marra, A.; Picconi, P.; Serra, M.; Catenacci, L.; Sorrenti, M.; Laurini, E.; Fermeglia, M.; Pricl, S.; Brambilla, S.; Almirante, N.; Peviani, M.; Curti, D.; Collina, S. *Bioorg. Med. Chem.* **2013**, *21*, 2577.
72. Rossi, D.; Pedrali, A.; Gaggeri, R.; Marra, A.; Pignataro, L.; Laurini, E.; Dal Col, V.; Fermeglia, M.; Pricl, S.; Schepmann, D.; Wunsch, B.; Peviani, M.; Curti, D.; Collina, S. *Chem. Med. Chem.* **2013**, *8*, 1514.
73. Pace, V.; Martínez, F.; Fernández, M.; Sinisterra, J.V.; Alcántara, A.R. *Advanced Synthesis & Catalysis.* **2009**, *351*, 3199.
74. Mahato, R.; Tai, W.; Cheng, K. *Adv. Drug Deliv. Rev.* **2011**, *63*, 659.

-
75. Fortin, S.; Bérubé, G. *Expert Opin. Drug Discov.* **2013**, *8*, 1029.
76. Jaracz, S.; Chen, J.; Kuznetsova, L.V.; Ojima, I. *Bioorg. Med. Chem.* **2005**, *13*, 5043.
77. Bildstein, L.; Dubernet, C.; Couvreur, P. *Adv. Drug Deliv. Rev.* **2011**, *63*, 3.
78. Russell-Jones, G.; McTavish, K.; McEwan, J.; Rice, J.; Nowotnik, D. *J. Inorg. Biochem.* **2008**, *98*, 1625.
79. Rodriguez-Melendez, R.; Zempleni, J. *J. Nutr. Biochem.* **2003**, *14*, 680.
80. Chen, S.; Zhao, X.; Chen, J.; Chen, J.; Kuznetsova, L.; Wong, S.S.; Ojima, I. *Bioconjug. Chem.* **2010**, *21*, 979.
81. Shi, J.F.; Wu, P.; Jiang, Z.H.; Wei, X.Y. *Eur. J. Med. Chem.* **2014**, *71*, 219.
82. Lis, L.G.; Smart, M.A.; Luchniak, A.; Gupta, M.L. Jr; Gurvich, V.J. *ACS Med. Chem. Lett.* **2012**, *3*, 745.
83. Ibsen, S.; Zahavy, E.; Wrasdilo, W.; Berns, M.; Chan, M.; Esener, S. *Pharm. Res.* **2010**, *27*, 1848.
84. Maiti, S.; Park, N.; Han, J.H.; Jeon, H.M.; Lee, J.H.; Bhuniya, S.; Kang, C.; Kim, J.S. *J. Am. Chem. Soc.* **2013**, *135*, 4567.
85. Fahrner, J.; Schweitzer, B.; Fiedler, K.; Langer, T.; Gierschik, P.; Barth, H. *Bioconjugate Chem.* **2013**, *24*, 595.

LITHIUM CARBENOIDS

1. INTRODUCTION

1. INTRODUCTION

In a homologous series, compounds differ in a constant unit, generally a methylene group (-CH₂-) [1]. In Medicinal Chemistry, homologations represent important synthetic steps, useful to obtain pharmacologically active molecules. One of the most intriguing aspects to mention in the systematic introduction of methylene groups is the possibility to modify the bioactive properties related to a drug. Indeed, the examples in literature are numerous (Figure 1), i.e. nicotinic ligands hexamethonium and decamethonium possess a completely distinct effect (antagonist and agonist respectively) towards the receptor; another case is represented by superior homologues of Enalaprilat, which exhibit significantly lower IC₅₀.

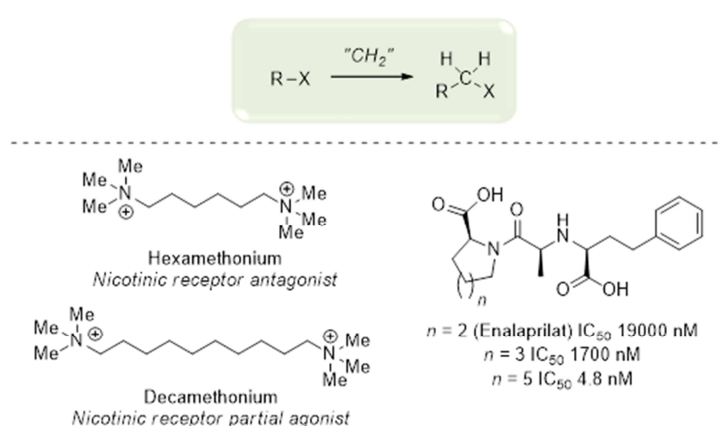
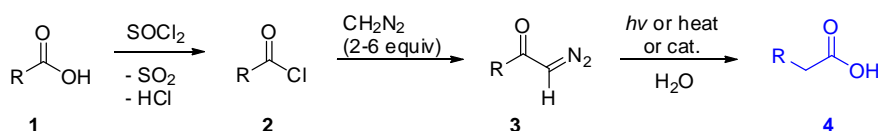


Figure 1. Examples of pharmacologically active molecules.

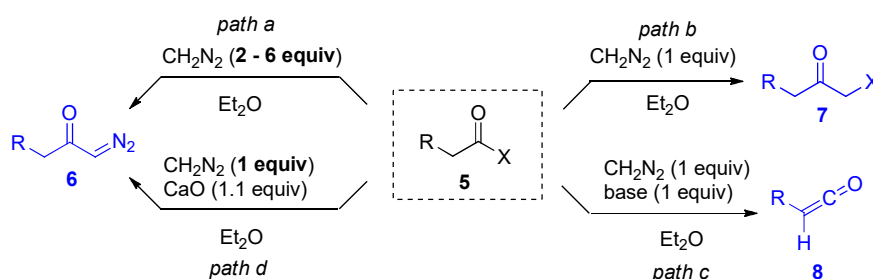
From an organic point of view, several homologation protocols have been developed in order to insert a CH₂ group into the molecules [2]. Among them, it is noteworthy the Arndt-Eistert reaction, which provides the conversion of a carboxylic acid **1** to its homologue **4**, through the formation of the key intermediate diazomethylketone **3** (Scheme 1) [3].



Scheme 1. The Arndt-Eistert homologation.

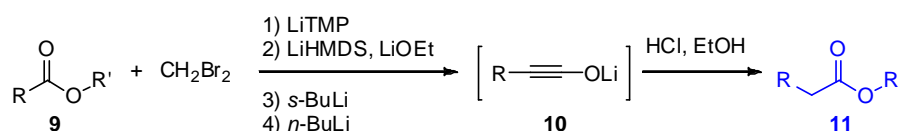
A considerable issue to disclose is the formation of side products, i.e. chloroketone **7**, due to the presence of HCl, as by-product (Scheme 2 – *path b*). Two or more equivalents of diazomethane may be used to overcome this drawback. (Scheme 2 – *path a*) [4]. Another strategy to consider is the employment of triethylamine, which reacts with the released HCl

[5]. The protocol efficacy is arguable, since the experimental conditions might produce a ketene when the acid chlorides bear acidic protons (Scheme 2 – *path c*) [6]. Lastly, an innovative and practical strategy, proposed by Pace and De Kimpe, suggests the use of calcium oxide as acid scavenger (Scheme 2 – *path d*) [3d].



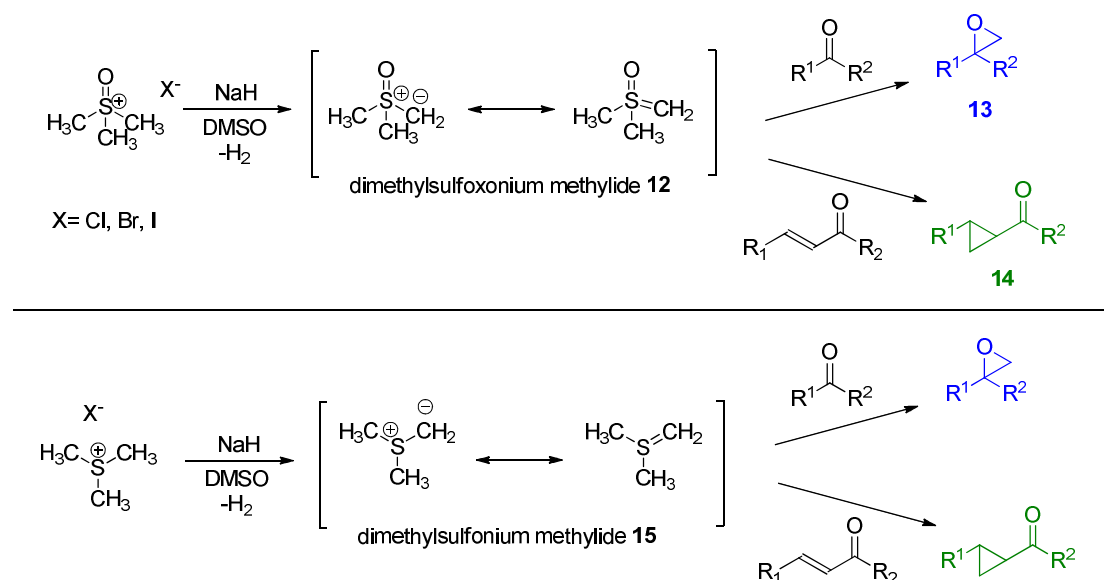
Scheme 2. Alternative protocols for the Arndt-Eistert homologation.

Although these solutions have been proposed to reduce the formation of by-products, the hazard of the diazomethane remains an important hurdle to take into consideration. Therefore, Conrad J. Kowalski designed a chemical reaction for the homologation of esters as a safer alternative to the Arndt–Eistert synthesis, since it avoids the use of diazomethane. The reaction provides the formation of the alkynolate anion **10**, which is converted into the homologous ester **11**, through a still undisclosed mechanism (Scheme 3) [7].



Scheme 3. Kowalsky homologation for ester compounds.

The Corey-Chaykovsky homologation is a valuable reaction to carry out for obtaining epoxides from aldehyde or ketone [8]. The reactive species is a sulfur ylide, a dimethylsulfoxonium methyllide **12** or a dimethylsulfonium methyllide **15**, prepared through the deprotonation of the corresponding sulfonium salts [9]. Two main drawbacks have to be considered: i) the treatment of an α,β -unsaturated carbonyl compound with **12** produces as major product the cyclopropane; ii) sulfur ylide **15** is more reactive and less stable than **12**, so it is usually generated and used at low temperatures (Scheme 4).



Scheme 4. Corey-Chaykovsky homologation.

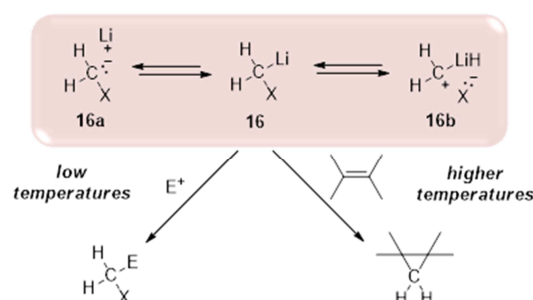
In this scenario, carbenoidic reagents took place as homologating agents [10]. The term *carbenoid* was coined by Closs and Moss [11], and it defines organometallic compounds containing a carbon bridging a metal atom (e.g. Li, Mg) and an electronegative element (e.g. halogen). This definition takes into consideration the carbene-like features (Scheme 5), which are analogous to those of carbenes without necessarily being free divalent carbon species. The pioneer in this synthetic panorama was G. Köbrich, who published, in the sixties, different seminal works [12]. He described the relevance of carbenoids as versatile synthetic tools.

1.1. Lithium carbenoids

Carbenoids are characterised by the presence of an electron-donating and an electron-withdrawing substituent; these elements confer to the carbon centre an ambiphilic activity. Indeed, carbenoids possess a dual reactivity, since they may act as nucleophiles or as electrophiles, depending on the experimental conditions. At low temperatures the nucleophilicity prevails; conversely, electrophilic behaviour is shown at higher temperatures (Scheme 5). The mesomeric structures explain the ambivalent character of carbenoid reagents. In fact, carbenoids present two different ionization forms: negative charge located on the carbon or a positive charge associated to the carbon, nucleophilic **16a** and electrophilic **16b** behaviour, respectively. Considering their characteristics, carbenoids may be involved into two different reaction categories: i) nucleophilic additions (eventually followed by elimination – i.e. acyl nucleophilic substitutions); ii) cyclopropanation-type processes. Moreover, the reaction trend is conditioned by the metal bonded to the carbon atom. In

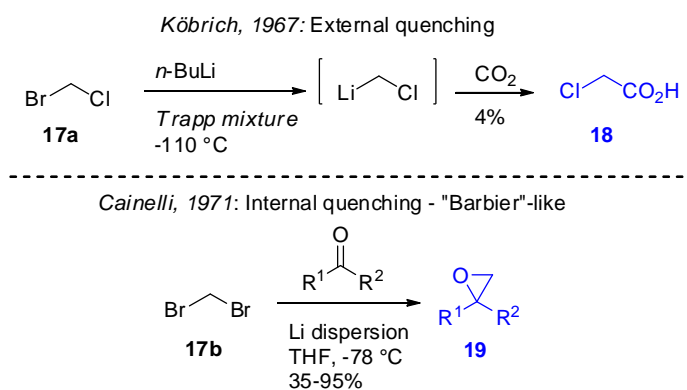
particular, lithium and magnesium carbenoids exhibit carbanionic-like reaction [10d], whereas zinc and rhodium carbenoids operate as carbocation molecules [10c, 13].

To conclude, the ambiphilicity of these reagents leads to consider carbenoids as versatile agents to carry out C-C reactions.



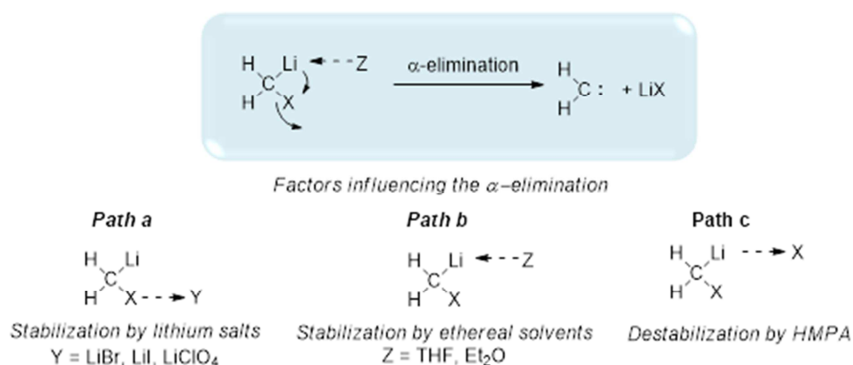
Scheme 5. Nucleophilic or electrophilic behaviour of carbenoids.

Nevertheless, there is an important hurdle to highlight: the thermolability of carbenoids. Several works examine in depth this aspect in order to identify the optimal conditions to achieve a compromise between stability and reactivity of these species. Köbrich proposed to generate chloromethylithium (LiCH_2Cl) from bromochloromethane and *n*-BuLi, at $-110\text{ }^\circ\text{C}$, followed by carbonation [12, 14]. This protocol provided the chloroacetic acid in only 4% yield (Scheme 6). In a second seminal work, Cainelli generated the monohalomethylithium at $-78\text{ }^\circ\text{C}$ in the presence of the electrophile ("Barbier"-like manner) [15]. Therefore, the carbenoid species was immediately involved in the homologation of a ketone into the corresponding halohydrin, followed by the cyclization into the final epoxide (Scheme 6). Furthermore, Köbrich disclosed that dihalomethyl- and trihalomethylithiums reagents are significantly more stable than the monohalocarbenoids [16].



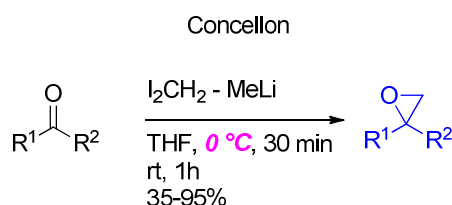
Scheme 6. Initial studies about temperature.

Cainelli was the first to establish that an internal quenching allows carrying out the homologation reactions mediated by carbenoids at $-78\text{ }^{\circ}\text{C}$ [15]. Nevertheless, this approach may provide the α -elimination by-product (carbene). Accordingly, a subsequent study performed by Villieras and coworkers highlighted the requirement of temperatures below $-115\text{ }^{\circ}\text{C}$, which avoid the undesired α -elimination reaction [17]. Besides, this study disclosed the importance of lithium halides as stabilizing agents, which coordinate the halogen atom of the carbenoid [18]. These salts interfere with the internal Li-X interaction responsible for α -elimination, which promotes decomposition of the carbenoid to the free carbene (Scheme 7 – *path a*). Additionally, Lewis basic ethereal-type solvents constitute meaningful stabilizing elements for carbenoids, in virtue of their ability to coordinate the metal atom of the carbenoidic reagents (Scheme 7 – *path b*). Conversely, destabilization of monohalolithium carbenoids can be achieved using polar solvents like hexamethylphosphoramide (HMPA) (Scheme 7 – *path c*). They strongly coordinate – through the oxygen atom – the lithium atom of the carbenoid, thus promoting the breaking of the carbon-lithium bond. Therefore, this kind of solvent determines the activation of the degradative α -elimination process. A noteworthy case is that of dihalolithium carbenoids, which maintain the nucleophilic behaviour even if polar solvent is added.



Scheme 7. Pathways that promote stabilization or destabilization of carbenoids.

Later, Matteson and Barluenga carried out the reactions at $-78\text{ }^{\circ}\text{C}$, suggesting this temperature as the optimal one [19-20]. Indeed, it guarantees a good compromise between thermal stability and reactivity of chloromethyl lithium and bromomethyl lithium. Notably, in the early 2000s, Concellón reported the employment of $0\text{ }^{\circ}\text{C}$ for generating iodomethyl lithium to accomplish a homologation towards ketone compounds (Scheme 8) [21].



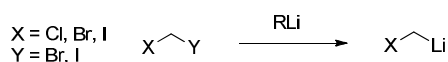
Scheme 8. Concellón procedure.

To conclude, a certain shrewdness must be taken into consideration in order to elude the activation of degradation pathways. Firstly, the adoption of an internal quenching guarantees high yields. Moreover, lithium carbenoids require low temperatures, suggesting -78°C as the optimal one, since it permits to combine stability and reactivity of these species. Lithium salts are valuable reagents, which allow the stabilization of lithium carbenoids.

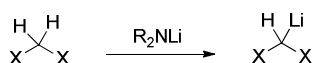
1.2. Generation of monohalolithium carbenoids

The literature suggests four main methods to prepare organolithium reagents [22]: 1) lithiation *via* lithium-halogen exchange; 2) lithiation *via* lithium-hydrogen exchange (i.e. deprotonation); 3) lithiation *via* lithium-sulfoxide exchange; 4) lithiation *via* lithium-tin exchange (Scheme 9).

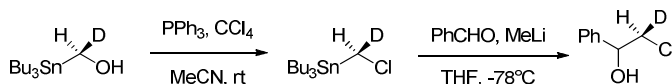
1) *Lithium-halogen exchange (most common method)*



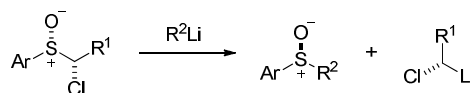
2) *Deprotonation*



3) *Lithium-tin exchange*



4) *Lithium-sulfoxide exchange*



Scheme 9. Lithium halocarbenoids preparation.

Lithiation via Lithium-Halogen Exchange

The lithium-halogen exchange represents the prototypical approach to be employed for carbenoid formation (Scheme 9 – *path 1*). Indeed, it presents some advantages: i) the easy operational details required and ii) the availability of dihalomethane precursors [22a]. Over the years several experimental conditions have been proposed. At the beginning, Villieras [17] accomplished the exchange reaction using *s*-BuLi in Trapp mixture (THF–Et₂O–*n*-pentane, 75:15:10 *v/v*) at -115°C [23]. Some studies have recently shown that this lithium base is advisable to perform deprotonations rather than exchange reactions [24]. Accordingly, MeLi and *n*-BuLi arose as the optimal lithium sources [20b]. Moreover, Matteson and Pace

employed the commercially available MeLi-LiBr complex in Et₂O to synthesize carbenoids. Lithium bromide causes the stabilization of the carbenoid and furthermore avoids the competing attack of MeLi to the electrophile present in the reaction medium under Barbier conditions [25].

In conclusion, the homologation reaction provides the *in situ* generation of carbenoid, which reacts immediately with the electrophile present therein. In this experimental condition, LiBr facilitates the attack of the formed carbenoid to the electrophile counterpart, since it coordinates the oxygen carbonyl lone pairs of the electrophilic species, exerting a mild Lewis acid effect. Considering the easy and fast exchange between iodine and lithium, the selected 1,1-dihalomethane as carbenoid precursor is usually the iodochloromethane. Another aspect to analyse is the stoichiometric ratio between dihalomethane and organolithium reagent. The kinetic suggests that a 1:1 ratio is sufficient to achieve a quantitative exchange. However, it is advisable to employ a small excess of dihalomethane to avoid the possibility of competing attack of the lithium species to the electrophile. Additionally, as reported above the instability of lithium carbenoids is a considerable issue, for this reason it is wise to add slowly and at low temperatures the alkyllithium to a solution containing the electrophile and the dihalomethane.

Lithiation via Lithium-Hydrogen Exchange

An alternative method to generate lithium carbenoids is the lithium-hydrogen exchange (Scheme 9 – *path 2*). This approach presents a significant hurdle, indeed basic *s*-BuLi may be involved in a halogen/lithium exchange, as reported by Villieras [17]. Consequently, deprotonation reaction became the protocol of choice for obtaining dihalomethylcarbenoids (*e.g.* LiCHCl₂, LiCHBr₂ and LiCHI₂) from the corresponding dihalomethanes, using lithium amide base such as LTMP, LNCy₂, LDA or LiHDMS.

Although different studies, reported by Nozaki, suggested to carry out the reaction with an internal quenching [26], recently, Bull demonstrated that this requirement may be eluded. Indeed, LiCHI₂ could be easily formed prior to the reaction with the electrophile [27]. Furthermore, Molinski applied deprotonation for obtaining trichloromethylithium from chloroform and *n*-BuLi at -100 °C [28]. The presence of these three halogens in the carbenoid makes it a soft nucleophile, which can react in a Michael manner with an unsaturated sultam. In this case Barluenga conditions are not necessary either.

Lithiation via Lithium-Sulfoxide Exchange

As reported by Hoffmann magnesium carbenoids can be generated through magnesium-sulfoxide exchange (Scheme 9 – path 3) [29]. These reactions are accomplished treating sulfoxide with Grignard reagents, above all *i*-PrMgCl. In this case as well, -80 °C is required as optimal temperature. It is noteworthy that these reactants present configurational stability, thus they are useful for asymmetric synthesis [30-31]. In the early 2000s, this attractive strategy has been employed by Blackemore and co-workers for obtaining lithium carbenoids, starting from a halogenated arylsulfoxide [32]. *p*-tolyl substituent is generally the aromatic ring attached to the sulfoxide; the R² group replaces the non-aromatic group on the sulfoxide R¹ (Scheme 9 – path 3). From a stereochemical point of view, the inversion of configuration at sulfur is registered. In the case of the generated carbenoid, the stereochemistry is not predictable.

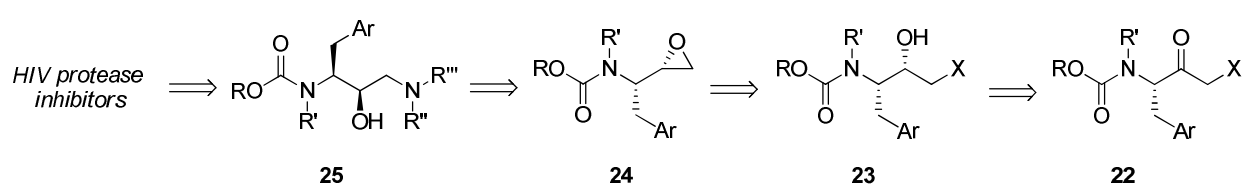
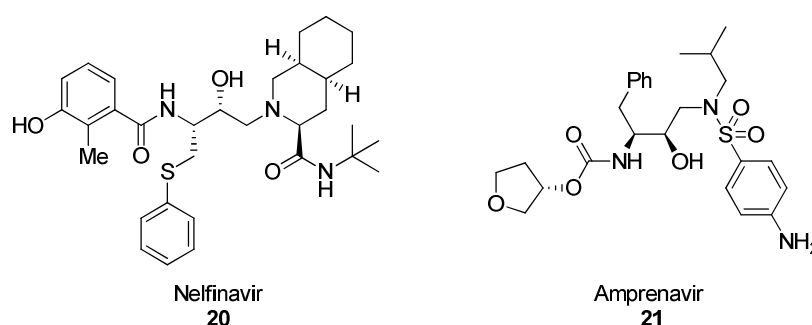
Lithiation via Lithium-Tin Exchange

This protocol, introduced by Hammerschmidt and co-workers, may be useful in asymmetric chemistry (Scheme 9 – path 4). More specifically, chiral stannane, reacting with MeLi, promotes the synthesis of configurationally stable chloromethylolithiums, which easily reacts with the electrophile at -78 °C [33]. The desired product can be obtained using the homochiral tributylstannyl-[*D*₁]-methanol, as precursor. Alcohol-derivative is converted into enantiopure chloromethylstannane-[*D*₁] applying Appel conditions [34]. Notably, the formation of side-products is strictly related to the employed arylalkyllithium reagents. In particular, MeLi provides highly satisfactory results in the tin-lithium exchange compared to *n*-BuLi, which produces less clean reactions with a considerable formation of undesired impurities. A possible explanation of MeLi behaviour is its lower basicity compared to *n*-BuLi. The seminal Hammerschmidt's work laid the foundations in chiral organolithium chemistry. Indeed, he depicted the first example of chiral carbenoid, operating at -95 °C; this reaction trend is maintained up to -78 °C, and above this temperature carbenoid decomposes.

1.3. Carbon electrophiles for carbenoids

Recently, lithium carbenoids have found application in the Medicinal Chemistry field, for the preparation of HIV protease inhibitors (e.g. nelfinavir **20**, amprenavir **21**) (Scheme 10) [35, 36]. The retrosynthetic analysis highlights the importance associated to the α -haloketones **22**, as intermediate, which are easily obtained using carbenoids. This precursor is stereoselectively reduced into the homochiral aminohalohydrin **23** [37], the direct precursor

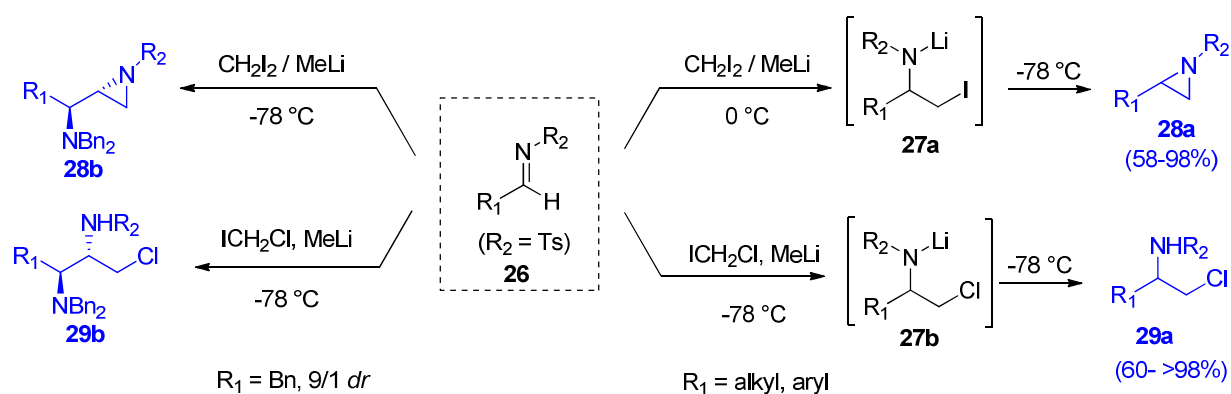
of the enantiopure epoxide **24**. This oxirane reacts with a nucleophilic amine leading to the 1,3-diaminopropan-2-ol fragment **25**, which represents the common building block of such class of inhibitors (Scheme 10) [35, 38-39]. This example demonstrates the importance of carbenoids and, in particular, their potential usefulness in obtaining final and intermediate compounds, worthwhile as pharmaceutical tools. Therefore, in this section, as well in the review **MR9**, the potentiality of lithium carbenoids towards different electrophiles will be investigated in depth.



Scheme 10. Retrosynthetic pathway to obtain HIV protease inhibitors.

Imines

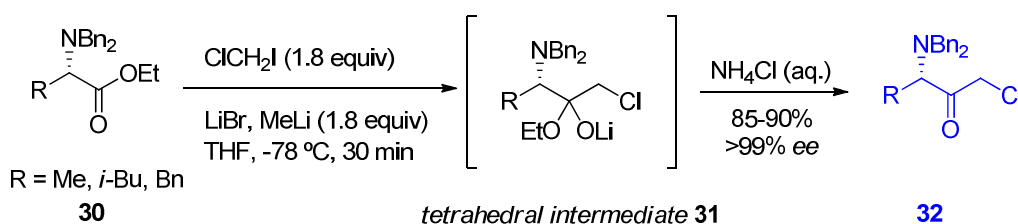
Imines are attractive species, since they can be easily converted in other molecules, i.e. β -haloamines or aziridines, useful as final or intermediate compounds. In 2008, Concellón published the addition of iodomethylithium to sulfonyl-protected imines (Scheme 11), demonstrating that the protective group enhances the electrophilicity of the azomethinic carbon through an electron-withdrawing effect [40]. Moreover, it is important to underline that *N*-tosylaziridines **28a-b** are easily prepared in short reaction times. However, harsh conditions are required to remove the tosyl-type protecting groups. To date, the use of SmI_2 could be a considerable alternative to overcome this problem [41]. Subsequently, the same protocol has been applied on *N*-sulfonyl protected imines, adding chloromethylithium [42]. The method afforded β -chloroamines **29a-b** upon simple acidic work-up.



Scheme 11. Reactions of sulfonyl-protected imines with iodomethyl lithium.

Esters and Weinreb amides

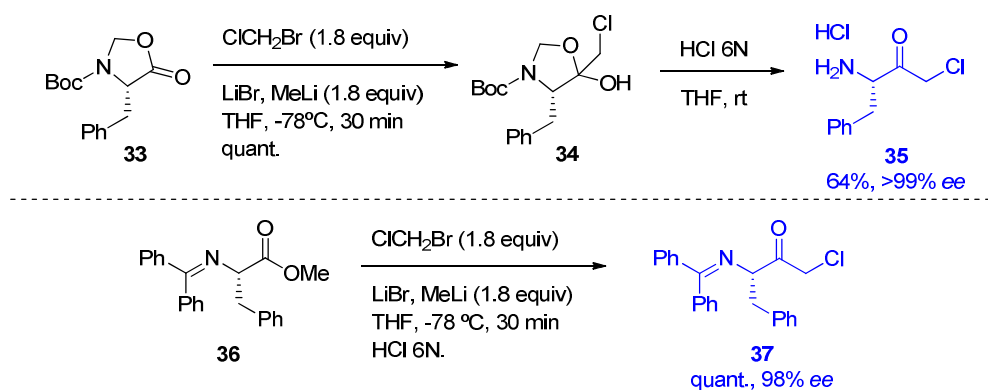
As mentioned before, α -haloketones are interesting prochiral building blocks in organic and in pharmaceutical chemistry. This kind of compounds could be achieved using as precursors esters or Weinreb amides. In particular, the pioneer in homologation of esters was Barluenga, who reported the conversion of ester compounds (general formula **30**) into α -haloketones **32** by a single addition of carbenoids at $-78\text{ }^\circ\text{C}$ (Scheme 12) [20b,c]. Usually, these electrophiles react with organometallic reagent to produce carbinols through the double addition of the nucleophile [20b,c]. In this case, the reaction mechanism evidences the formation of the tetrahedral intermediate **31**, which is stable and thus it avoids the double addition of the organometallic species [43]. The stability of this intermediate is guaranteed by the presence of the halogen and oxygen substituents which avert the elimination of the alkoxyde group.



Scheme 12. Barluenga's condition: homologation of esters.

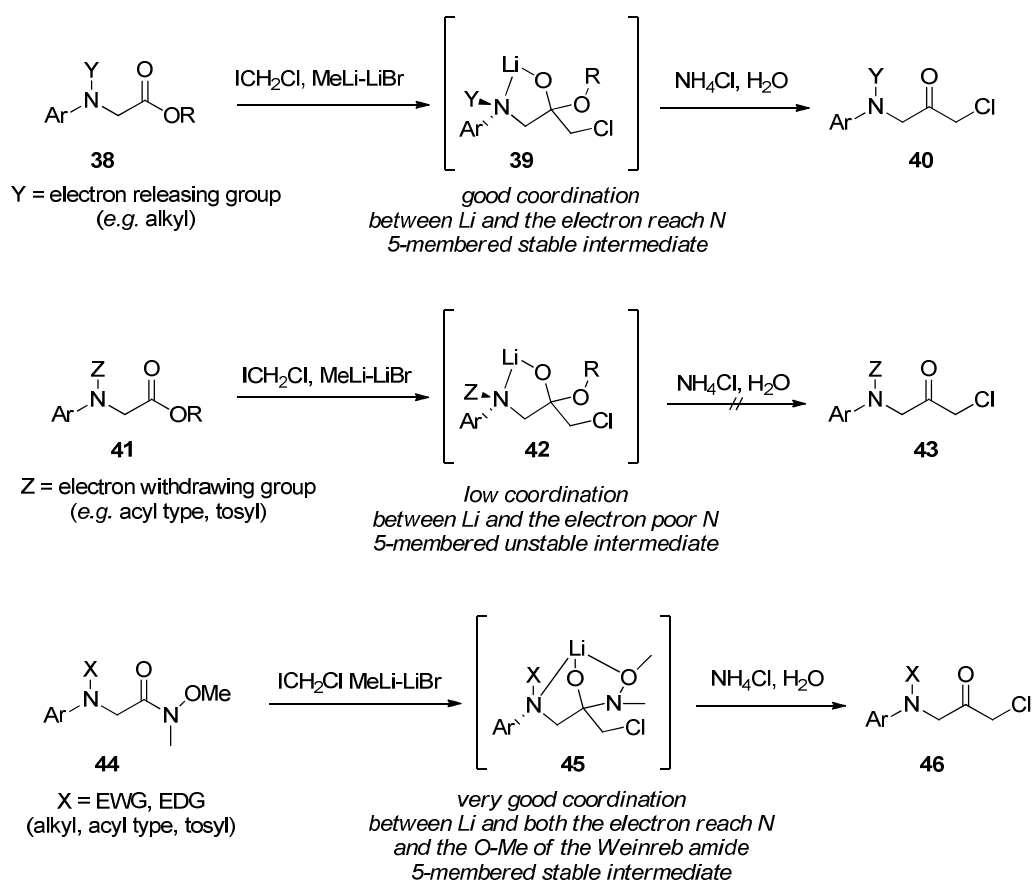
Interestingly, this homologation is prevented by the presence of amino or amido groups, since the nitrogen bears a hydrogen atom, which can be abstracted by carbinoid. Nevertheless, the industrial team Ajinomoto Co., led by K. Izawa, proposed a solution to overcome this hurdle [44]. Indeed, they introduced the employment of *N*-protected 3-oxazolidin-5-ones **33** which can be easily chloromethylated to generate the intermediate **34**, followed by its transformation into the desired chloroketone **35** upon acidic treatment (Scheme 13). An alternative to prevent this drawback was proposed by Hilpert, who applied the temporary

protection of a (secondary) amide moiety with the trimethylsilyl (TMS) group prior to homologation [45]. Furthermore, Izawa's group reported that the chemoselective chloromethylation of *N*-imine protected amino acids esters **36** [44b]. The bulkiness of the acetophenone derivative thwarts the addition of the carbinoid to the azomethinic position.



Scheme 13. Homologation of lactones and imino-esters using Izawa conditions.

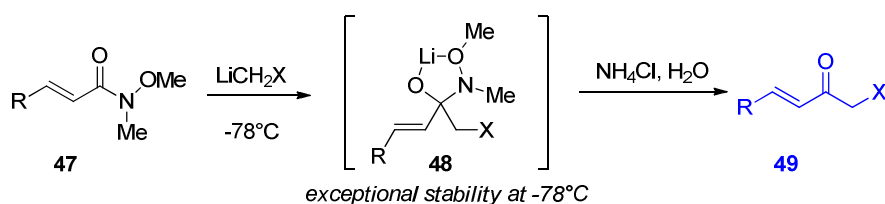
In this panorama, Pace *et al.* gave their contribution to explain the behaviour of carbenoids in the homologation of carboxylic acid derivatives [25c]. Specifically, a comparative study between esters and Weinreb amides remarked that the driving force for the success of these reactions is the formation of a stable putative tetrahedral intermediate (Scheme 14) [46]. The work, conducted on *N*-arylamino acetic acid derivatives, suggests that in the case of an ester the homologation happens when an additional EDG is present on the nitrogen. In fact, the relative basicity of the nitrogen can stabilize the intermediate **39**, and thus the reaction proceeds. Conversely, an EWG diminishes the basicity of the nitrogen and destabilizes the intermediate **42**, thus the transformation does not happen. Instead, in the case of *N*-methoxy-*N*-methyl amides, the reaction takes place regardless the nature of the substituent on the nitrogen. The stability of the chelated 5-membered tetrahedral intermediate **45** represents the explanation to this unexpected result. Indeed, the basicity of the nitrogen does not influence the stability of the intermediate, since it is involved in the chelate with the methoxy group of the Weinreb amide.



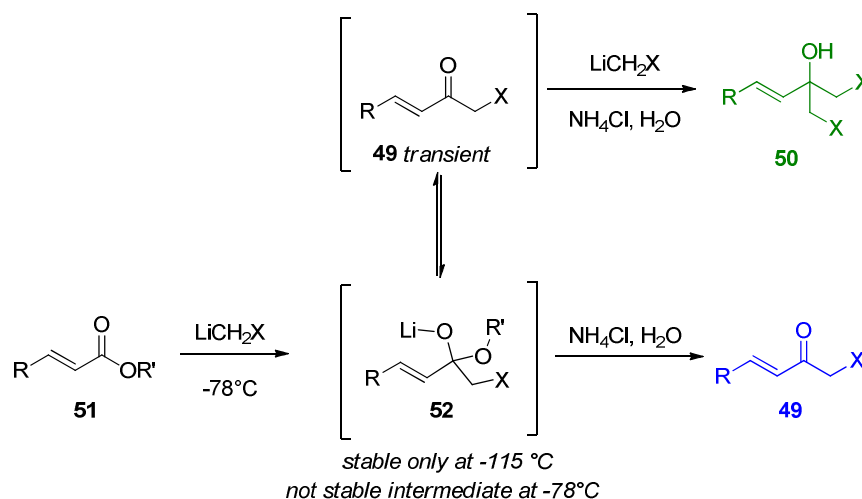
Scheme 14. Different behaviour of esters and Weinreb amides, after treatment with lithium carbenoids. Mechanistic explanation.

Pace *et al.* reported another interesting comparative study on homologation of α,β -unsaturated Weinreb amides and esters (**47** and **51** respectively) [25a]. This work was accomplished in order to rationalize the different chemoselectivity of these reactions. They assumed the peculiar stability at $-78\text{ }^\circ\text{C}$ of the intermediate **48** offered by the *N*-methoxy group of the Weinreb amide, which hinders a second addition of LiCH_2X (Scheme 15, *path a*). Accordingly, the transformation stops to the desired α -halo ketone **49**. Instead, tetrahedral intermediate **52** (not stable at $-78\text{ }^\circ\text{C}$), resulting from the addition of carbenoid to ester **51**, is more susceptible to a second attack of the carbenoid, and thus providing the carbinol **50** (Scheme 15, *path b*). Moreover, the α -halo ketone is the major product when the reaction on esters is performed at $-115\text{ }^\circ\text{C}$. Hence, it is conceivable that the tetrahedral intermediate **52** - generated through mono addition to an ester - is only stable at very low temperature, thwarting the second addition.

Path a: Chemoselective monoaddition of LiCH_2X to Weinreb amides at -78°C



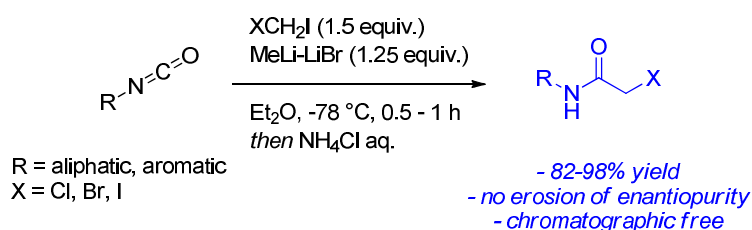
Path b: Temperature depending addition of LiCH_2X to esters



Scheme 15. Different behaviour towards halomethylithium reagents of Weinreb amides (path a) and esters (path b). Temperature-based mechanistic explanation.

Isocyanates

In 2013, Pace *et al.* defined a new method to synthesize α -haloamides, through the addition of lithium carbenoids to isocyanates (Scheme 16) [25b]. The protocol guarantees high-yields and no purification. The advantages of this synthetic protocol are numerous compared to the classical procedures used to prepare the α -haloamides. As a matter of fact, the success of the reaction is independent from the nucleophilicity of the amine and the steric hindrance on the isocyanate does not influence the transformation.



Scheme 16. Homologation of isocyanates.

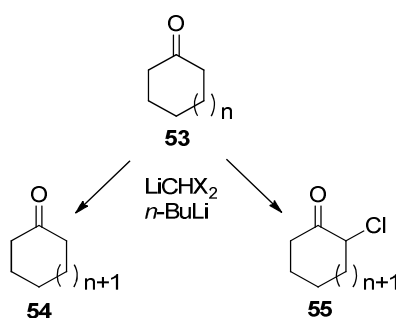
2. THE RESEARCH

2. THE RESEARCH

2.1. Background

As already extensively reported in the “Introduction”, lithium halomethylcarbenoids acquired an enormous interest both in academic and industrial environment. These reagents are synthetically versatile tools for accomplishing homologation reactions towards several electrophiles. The carbon species are the main carbenoid counterparts, however, the electrophilic panorama has been recently extended to boron, zirconium, germanium/silicon, sulfur-containing substrates [32a, 47-51].

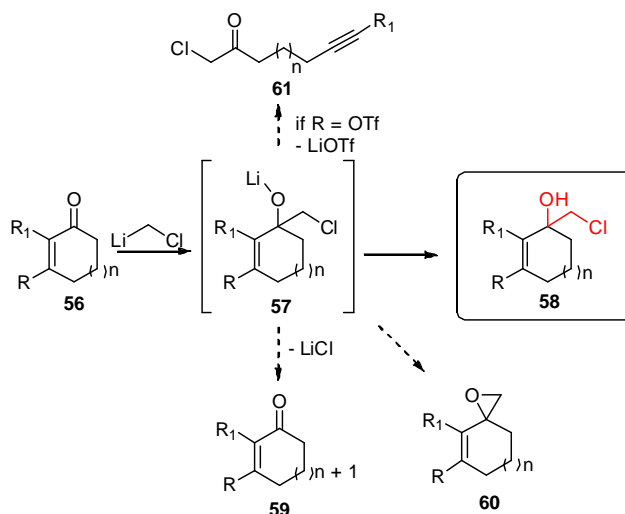
The applicability of carbenoid chemistry towards carbonyl compounds, i.e. ketone or aldehyde, is widely documented. Indeed, over the years, several studies highlighted the feasibility of the reaction between carbenoids and carbonyl compounds, which easily provides halohydrins [15, 17, 19, 20b, 21, 52, 53]. Moreover, the obtained products are versatile building blocks in a synthetic pathway and they may be susceptible to other transformations, i.e. epoxidation or cyclic enlargement [54-56]. In this context, the forefather Nozaki developed a series of protocols, involving cyclic ketone (general formula **53**) and dihalomethyl lithium reagents (e.g., LiCHCl_2 or LiCHBr_2), in order to access the homologated saturated structures. The process provides a β -oxido carbenoid rearrangement in the presence of a lithium base, giving a simple homologated ketone **54** or a homologated α -chloro ketone **55** (Scheme 17) [57-59].



Scheme 17. Nozaki's protocols.

As regards the monohalomethyl lithium carbenoids, their applications have been limited to the formation of oxiranes, starting from saturated cyclic ketone. Therefore, Pace *et al.* employed their efforts to examine in depth the carbenoid behaviour towards cyclic ketone compounds, presenting another functionalization, such as an α,β -unsaturation, in order to strengthen the versatility of these reagents [60]. The double bond in the starting material **56** may interfere with the reaction success. Indeed, several by-products may contaminate the desired

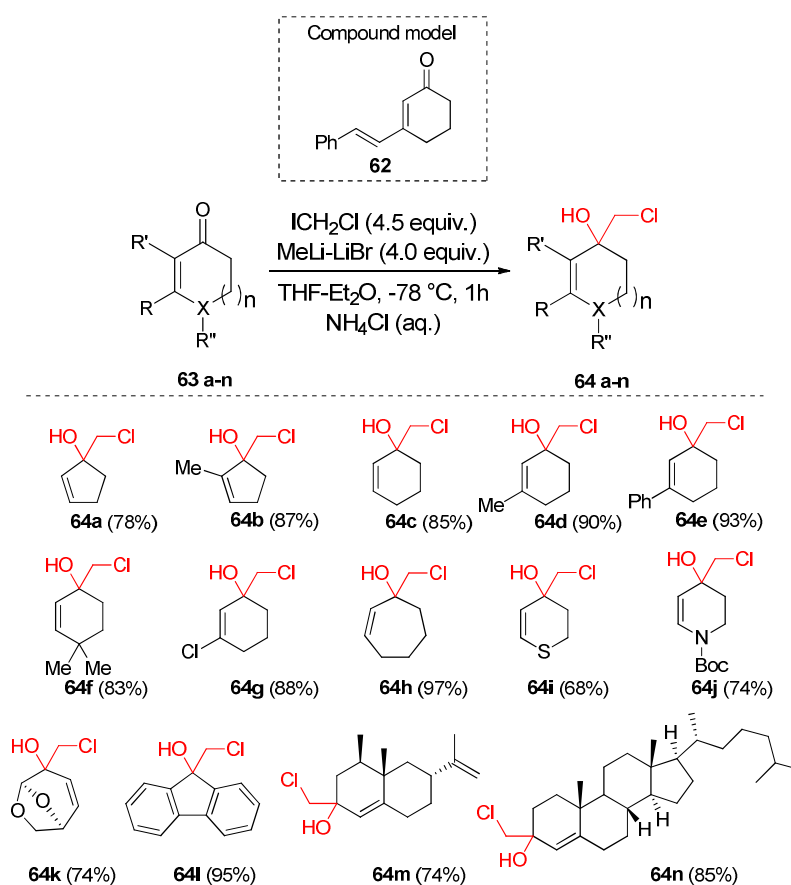
halohydrin **58** (Scheme 18). In particular, Tiffeneau-Demjanov-like tetrahedral intermediate **57** could expel the halogen atom and, through a transposition, access the homologated ketone **59** [61]. The same intermediate could be involved into an internal displacement, which guarantees the epoxide **60** formation [56b, 62-63]. Lastly, enones like vinylogous carboxylic acid triflates may promote tandem nucleophilic addition-fragmentation reactions, providing alkynyl ketones **61** [64-65].



Scheme 18. Possible side reactions, in the chemoselective 1,2-addition of LiCH₂Cl to cyclic enones.

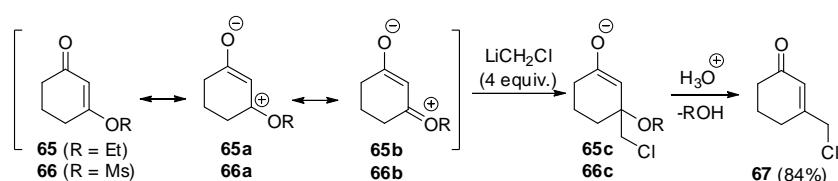
In 2014, Pace and co-workers disclosed a chemoselective 1,2-addition of LiCH₂Cl to cyclic enones (Scheme 19) [60]. The study provided an optimization of the conditions in order to define the best protocol to perform the reactions and to maximize the yields. The enone **62** (Scheme 19) has been selected as model precursor, bearing two conjugated olefinic moieties and thus, susceptible to cyclopropanation as well as to 1,4- or 1,6-conjugate additions. Several conditions have been explored, firstly the equivalents of reactants to generate carbenoid at -78 °C have been selected: MeLi-LiBr (4.0 equiv.) with ICH₂Cl (4.5 equiv.). Once the ratio between reagents was identified, the effect of solvents was analysed: the mixture THF-Et₂O provided the optimal results. The LiBr action as a mild Lewis acid is noteworthy; its coordinating effect prevents the decomposition of carbenoid into carbene, accordingly the yields exponentially increased. The optimised protocol was adopted in order to pursue the goal of the work, which is validating the feasibility of this method to different α,β-unsaturated ketone substrates. The results highlighted that the reaction mechanism provides the addition of carbenoid to the most activated carbon, obtaining the tertiary cyclic allylic alcohols. From the high yields of the desired alcohols emerged that side products, such as epoxides or

homologated ketones, are present in small traces. Moreover, this protocol was successfully applied to five-, six- and seven-membered enones including fused natural products structures. The reaction is tolerant to sensitive olefins and/or other functionalities susceptible to carbenoids. Particularly, the results showed that this strategy yields halohydrins in several cases: different sized ring systems, such as clopente (**64a-b**), cyclohexene (**64c-f**) and cycloheptene (**64h**) derivatives bearing different substituents across the cyclic core. The method tolerates functionalities sensitive to organolithiums, i.e. a chlorine atom (**64g**) or even the bicyclic acetal-type system of levoglucosenone (**64k**). Furthermore, the success of the homologation is not influenced by the presence of heteroatoms in the starting enones (**64i-j**). Notably, the reaction might be carried out with complex enone systems incorporated into natural products such as nootkatone (**64m**), a sesquiterpene derived from grapefruit with insecticide-repellent properties towards deer ticks. The same methodology was efficiently applied to prepare the medicinally relevant scaffold (**64n**) from cholest-4-en-3-one (**63n**) in high yield.



Scheme 19. Pace's addition of chloromethyl lithium to cyclic enones.

A relevant case was described in this work, regarding the effect exerted by an electron-releasing oxygen atom at the β -position of the olefinic bond (Scheme 20). From a structural point of view, this kind of enones can be considered as 1,3-dicarbonyl-like derivatives; indeed, the mesomeric effect provides structures **65a/65b** and **66a/66b**, which are subject to the attack of the carbenoid, providing the intermediates **65c** and **66c**, respectively. The nature of the group linked to the enol-type oxygen atom plays a key role in determining the mechanism for the collapse of the addition intermediates of type **c**. Thus, in the presence of nucleofugal leaving groups (e.g., EtO or MsO) which could be easily eliminated, upon quenching the enone system is re-established providing compound **67** as the only product.



Scheme 20. β -Activating effect of an RO group: the case of 3-alkoxy systems.

Considering the excellent results gained in this study, my project took place in this context. A work flow was planned, in order to further investigate the carbenoid behaviour towards this electrophilic compound class:

1. We evaluated how the slowly addition of lithium reagents might influence the success of homologation reactions.
2. The optimal conditions was applied on a set of α,β -unsaturated ketones.
3. We disclosed a new rearrangement mechanism, which provides a double homologation, producing an aldehyde.



Lithium carbenoids project workflow.

2.2. My Ph.D. Project

Identification of the optimal conditions

As mentioned before, Pace et al. reported a strategy to identify the optimal conditions to carry out the chemoselective 1,2-addition of LiCH₂Cl on α,β -unsaturated ketones. My project has been focused on the reactivity/stability study of monohalomethylithium carbenoids, when the syringe pump is employed to perform the addition of lithium base. This work was conducted in order to demonstrate how a slowly introduction of lithium reagents may positively influence the trend of a homologation reaction. We used cyclohex-2-en-1-one (**68**), as compound model, to perform these reactions. Barbier-like conditions were employed and thus, lithium base (flow: 0.200 mL/min) was added to a solution of ketone and chloriodomethane, cooled at -78 °C. In Table 1, the results related to the screening of solvents and equivalents were reported.

Table 1. Screening protocol to individuate the correct solvent and equivalents to perform the chemoselective 1,2-addition of LiCH₂Cl to compound **68**.

Entry	ICH ₂ Cl (equiv.)	RLi (equiv.)	Solvent	Yield [%]
1	4.5	MeLi-LiI (4.0)	THF	90
2	4.5	MeLi (4.0)	THF	99
3	4.5	MeLi-LiBr (4.0)	THF	99
4	3.0	MeLi-LiBr (2.8)	THF	99
5	2.0	MeLi-LiBr (1.8)	THF	82
6	1.3	MeLi-LiBr (1.1)	THF	66
7	3.0	MeLi-LiBr (2.8)	MeTHF	61
8	3.0	MeLi-LiBr (2.8)	CPME	39
9	3.0	MeLi-LiBr (2.8)	TRAPP mixture	57
10	3.0	MeLi-LiBr (2.8)	Et2O	67
11	3.0	MeLi-LiBr (2.8)	Toluene	47

From this first analysis we can assert that the use of syringe pump allows to decrease the reagent equivalents for generating carbenoids. Indeed, in the previous work, Pace showed that the correct ratio between starting material: ICH₂Cl:RLi is 1:4.5:4.0; whereas from this experimental evidence a lower ratio promotes in any case a quantitative reaction. Moreover, the solvents screening disclosed THF as the best means to access the product.

Once the first parameters were identified, we applied other methodologies to generate carbenoids. Lithium-sulfoxide and lithium-tin exchanges are not advisable to perform the reactions with this electrophile, since the only obtained product is starting material (Table 2).

Table 2. Other methodologies to generate carbenoids and their application.

Entry	XCH ₂ Y (equiv.)	RLi (equiv.)	Solvent	Yield [%]
12	PhSOCH ₂ Cl (2.0)	MeLi (1.8)	THF	NR
13	PhSOCH ₂ Cl (2.0)	<i>t</i> -BuLi (1.8)	THF	NR
14	PhSOCH ₂ Cl (2.0)	PhLi (1.8)	THF	NR
15	PhSOCH ₂ Cl (2.0)	MeLi-LiBr (1.8)	THF	NR
16	Bn ₃ SnCH ₂ Cl (3.0)	MeLi-LiBr (2.8)	THF	NR

Another parameter to take into consideration is the temperature. It is widely accepted that the thermolability is a big drawback associated to lithium carbenoids. Therefore, we examined in depth this aspect performing a temperature dependence study, in order to identify the optimal degrees, which guarantee a good compromise between stability and reactivity (Figure 2). For comparative purpose, we applied the temperature screening protocol to a Weinreb amide.

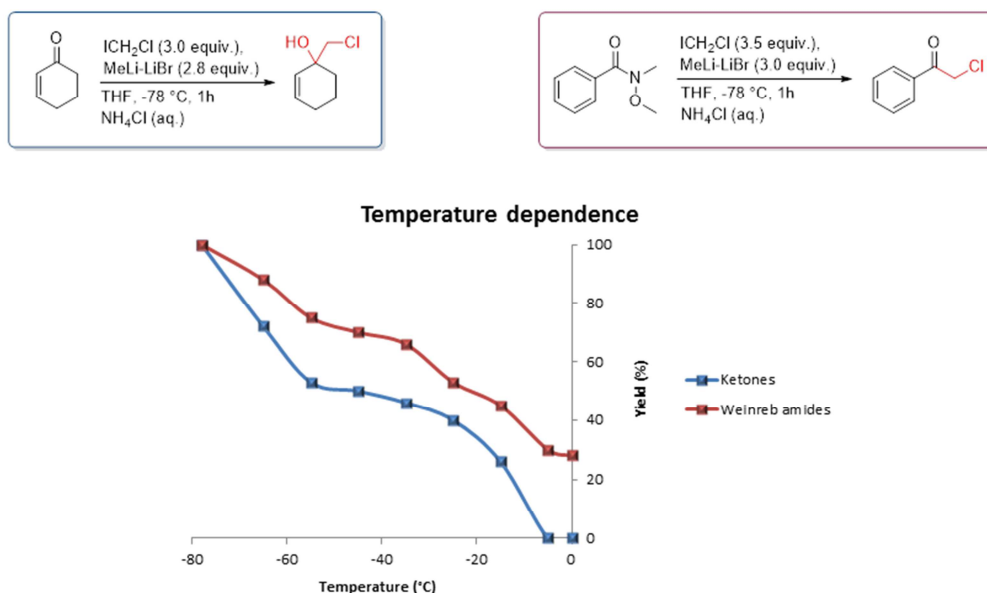


Figure 2. Temperature dependence study. A comparison between the reaction trend of α,β -unsaturated ketone (blue) and Weinreb amide (red).

The histogram highlights that the stability and reactivity of carbenoids are strictly related to the selected temperature. High yields were obtained at -78 °C. In case of ketone, the curve

trend exponentially collapses when the temperature range was between -78 °C and -55 °C; afterwards a plateau was reached and the yields varied among 53% and 40%. Lastly, warming the reaction until 0 °C, the carbenoid lost its effect and no reaction was registered.

On the bases of this experimental evidence, we may conclude affirming that the slowly addition of lithium base, through syringe pump, exerts no effect on the temperature selection. Therefore, the use of additional salts (3.0 equiv.) has been implemented, in order to achieve even higher conversion rates at higher temperatures. In Table 3, the results were reported and we compared them with the conversion rate of REF, which indicates the reaction performed in absence of additives.

Table 3. Use of additive/salts.

Reaction scheme showing the conversion of cyclohex-2-en-1-one (**68**) to 2-(chloromethyl)cyclohex-2-en-1-ol (**69**) and 2-(chloromethyl)cyclohex-2-enal (**70**). Reagents: ICH₂Cl (3.0 equiv.), MeLi-LiBr (2.8 equiv.), Additive (3.0 equiv.), THF, -35 °C, 1h, NH₄Cl (aq.).

Entry	Additive	68 [%]	69 [%]	70 [%]
REF	REF	62	46	2
1	LiCl	81	18	1
2	LiBr	68	17	5
3	Ti(O <i>i</i> Pr) ₄	56	44	0
4	MnCl ₄ Li ₂	32	68	0
5	TMEDA	92	7	1
6	LaCl ₃	86	11	3
7	CeCl ₃	83	17	0
8	FeCl ₃	53	47	0
9	CoCl ₂	78	22	0
10	NiCl ₂	73	26	1
11	PbCl ₂	83	16	1
12	InCl ₃	80	20	0
13	LiClO ₄	0	>99	0
14	CuCl	79	19	2
15	CuI	58	37	5
16	SbCl ₃	57	43	0
17	CdCl ₂	85	15	0
18	MeNH <i>Et</i> NHMe	54	38	8
19	HMPA	51	20	2
20	DMPU	81	17	2

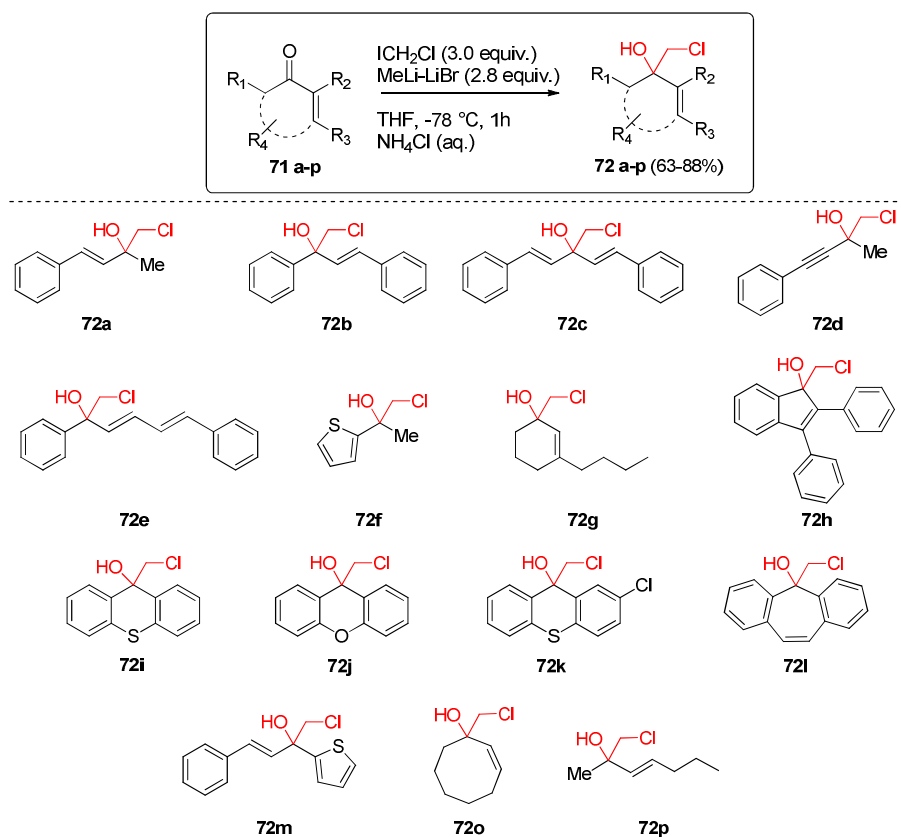
Conversions (%) of **68** to **69** and **70** based on ¹H-NMR

Considering the tabulated values, the addition of salts has almost no beneficial effect on the conversion towards **69**. Nevertheless, few cases deserve to be mentioned, i.e. entries **2**, **15** and **18**. Although the additives LiBr, CuI and MeNH*Et*NHMe do not promote the complete

conversion of **68**, they provide the formation of aldehyde **70** in small traces. Moreover, lithium perchlorate (LiClO_4 , entry **13**) is the only salt which allows to access quantitatively the desired halohydrin **69** (> 99 %). Probably, this additive exerts a strong coordinating effect, guaranteeing a high yield.

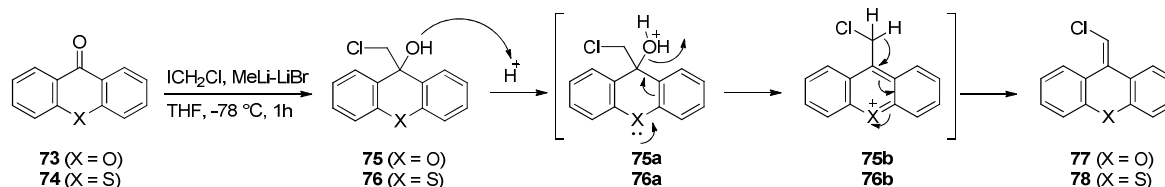
Application of the optimal conditions

The optimal conditions were applied on a set of cyclic and non-cyclic α,β -unsaturated ketones. The desired halohydrins were obtained in good yields, ranging between 63 % and 88 %. Phenyl allyl ketones are worth mentioning, since they represent useful scaffolds to design and synthesize compounds of pharmaceutical interest. Indeed, chalconoids are widely known as central core for various biological molecules endowed with antibacterial, antifungal, antitumor and anti-inflammatory properties. Another example to take into consideration is the xanthone, which was introduced as an insecticide. Therefore, these starting materials are important building blocks to manipulate and the proposed protocol may have different application in academic and industrial environments (Scheme 21).



Scheme 21. New protocol applied on cyclic and acyclic enones.

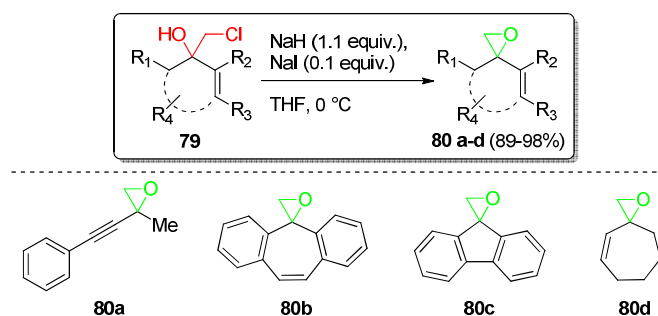
This work is a pursuance of the aforementioned Communication reported by Pace *et al.* In this context, the carbenoid chemistry was successfully applied to other sized ring systems, i.e. cyclooctenone or to alkynyl compound. It is of great interest, the tolerance demonstrated by olefinic ketones, which are included into an aromatic system. Notably, the monohalomethylithium does not display any electrophilic reactivity towards the aromatic rings. Moreover, this protocol could be efficiently used towards molecules presenting heteroatoms. Interestingly, unexpected products were obtained, treating xanthone and thioxanthone with chloromethylithium. In particular, as side-product of the reaction, chlorovinyl derivatives (**77-78**) were produced. Furthermore, compounds **77-78** represent the major products, when the quenching of the reaction is carried out using H₂SO₄ (2 M), rather than with NH₄Cl (aq.). The explanation of this fact may be found into the tandem elimination-rearrangement mechanism, which takes place (Scheme 22). The desired halohydrins (**75-76**), in presence of an acidic proton, provide the formation of a water molecule, which is easily eliminated, as a consequence of the electron pair shift at the oxygen (**75a-76a**). The subsequent transposition of the H, in β-position to the chlorine and the aromatic ring reconstitution (**75b-76b**) offer the chlorovinyl derivatives **77-78**.



Scheme 22. The heteroatom effect: the case of xanthone derivatives.

Accordingly, these results disclose the benefit in employing the chloromethylithium reagents as homologating agents. Despite the temperature hurdle, the protocol provides the expected product in good/high yields.

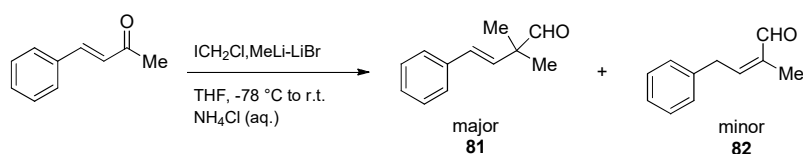
Considering the high versatility of halohydrins **79** in synthetic process, we evaluated their reactivity in a classical ring enclosure (epoxidation). After a meticulous investigation among several in-house alkaline reagents, we set up the optimal protocol that led to the desired oxiranes (**80**). The methodology required the use of hard and hazardous conditions, such as NaH in the presence of a catalytic amount of NaI (Scheme 23).



Scheme 23. Epoxidations.

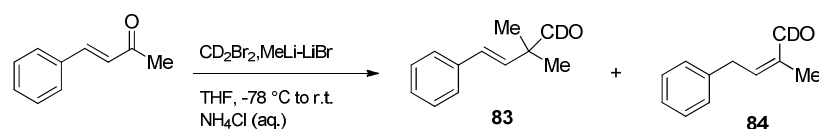
Pace/Holzer rearrangement

During the optimization of the reaction between carbenoids and α,β -unsaturated ketones, the aldehyde **70** was obtained as by-product, at high temperature. Therefore, we investigated this unexpected outcome, in order to elucidate the possible side mechanisms involved in the chemoselective 1,2-addition of LiCH_2Cl to enones. The optimal reaction conditions were set up, performing various attempts on (*E*)-4-phenylbut-3-en-2-one, which was selected as model. The protocol envisaged the classical conditions to get halohydrins; some temperature and time parameters were modified. Specifically, after adding the lithium base (MeLi-LiBr) to the starting material and chloriodomethane solubilized in THF, at -78 °C, the reaction was stirred for 1h and subsequently warmed overnight up to rt (Scheme 24). Once the quenching with aqueous saturated solution of NH_4Cl was carried out, two aldehydes were identified (8.5-9 ppm $^1\text{H-NMR}$) in the crude. However, no trace of halohydrin was recognized. The purification step, through silica gel column, revealed that the compound **81** was the main product, whereas **82** was the minor one.



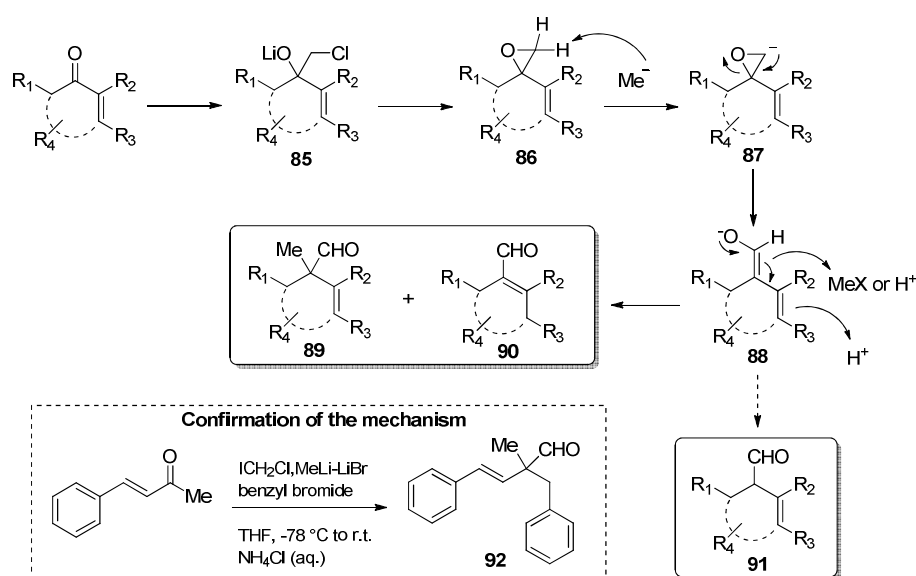
Scheme 24. Optimal experimental conditions.

Considering this experimental evidence, we focused on investigating the mechanism occurring between the reagents. Firstly, we studied the role of temperature by carrying out the reaction at -78 °C, for 8h. The lack of aldehyde in the crude disclosed a thermodynamic mechanism. Furthermore, we employed the deuterated-reagent, CD_2Br_2 , aiming at the deeply comprehension of the reaction mechanism (Scheme 25). The products **83-84** were obtained, as confirmed by $^1\text{H-NMR}$ and $^{13}\text{C-NMR}$ analysis.



Scheme 25. Experiments performed using deuterated-reagents, CD_2Br_2 and D_2O .

With this data in the hand, we postulated the potential mechanism (Scheme 26). The high temperature may promote the formation of oxirane **86** and thus, the epoxide-aldehyde rearrangement **87** takes place. The electrophilic species in the reaction environment (MeX and H^+) may be attacked by the nucleophilic double bond **88**, leading to compounds **89** and **90**. In certain cases, the product **91** also emerged in traces, as third aldehyde. This assumption was confirmed by performing the same reaction in the presence of a hard electrophile, the benzyl bromide. The resulting compound **92**, as well as the previous experiments, guarantees the reliability of the proposed mechanism.

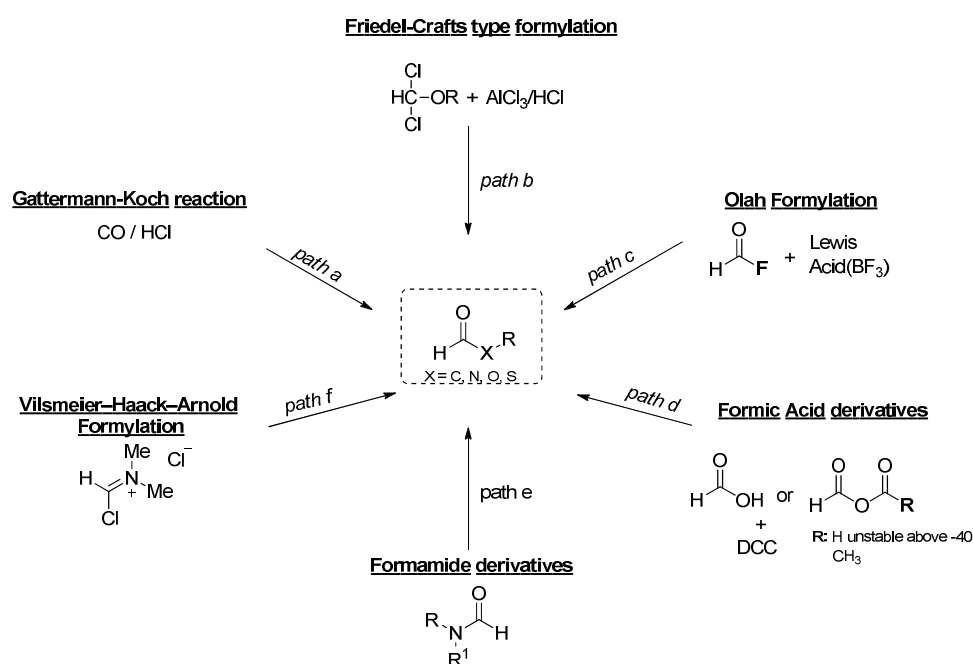


Scheme 26. Reaction mechanism.

As reported in Publication **MR4**, the ubiquity of formyl motif in natural and synthetic molecules of pharmaceutical interest is broadly documented. Furthermore, the formyl group may be susceptible to other organic transformations, due to its particular reactivity. The polarizability of carbonyl bond, due to the hard donor oxygen and to the fairly hard acceptor carbon behaviours, leads to consider formyl moiety as electrophile. Considering the high interest in formylation, several protocols and reagents were proposed in order to introduce formyl functionality (Scheme 27). Firstly, the formylating agents may be grouped in two

distinct classes: i) those working under acid catalysis conditions and, ii) those delivering the CHO to polarized species [66].

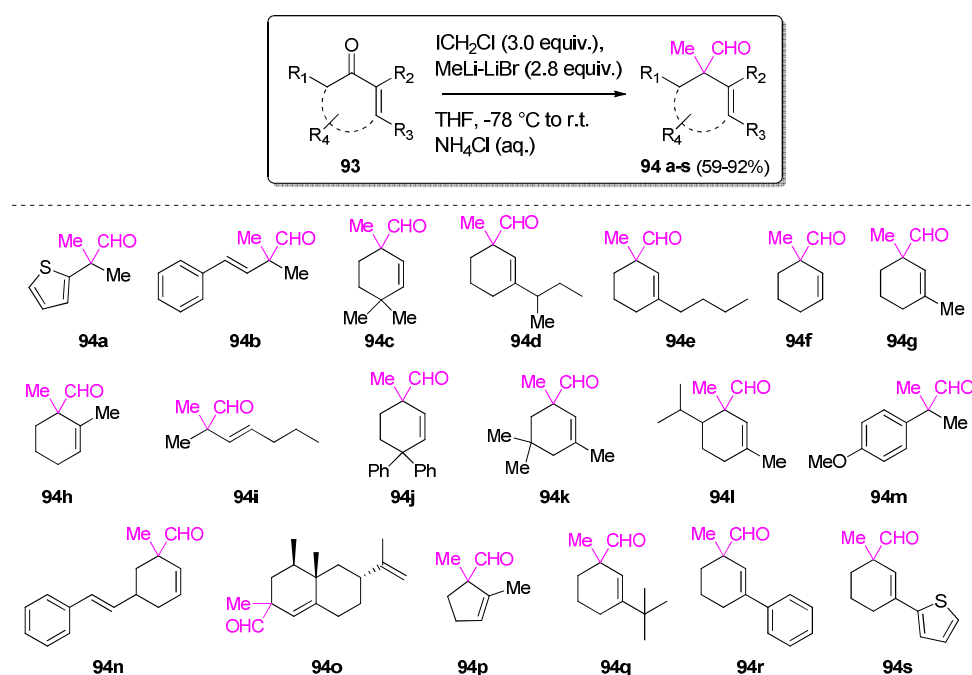
To the first group belongs the oldest Gattermann-Koch reaction, which provides a formylation *via* addition of carbon monoxide under superacidic conditions (Scheme 27 - *path a*) [67]. The introduction of the formyl group may be achieved through Friedel-Crafts-like chemistry, using dichloromethyl ethers or dichloromethyl amines (Scheme 27 - *path b*) [68-69]. Olah proposed formyl fluoride, in the presence of a Lewis acid, as formylating agent (Scheme 27 - *path c*) [70]. In order to achieve formyl derivatives, the relatively inert formic acid may be employed; however, in this case it is advisable to introduce anhydride to improve the efficiency of the processes (Scheme 27 - *path d*) [71-72]. The second class of formylating agents includes the Comins-Meyers amides and Vilsmeier-Haack-Arnold (VHA) reagent (*N*-chloromethylene-*N,N*-dimethylammonium chloride), useful tools for adding a CHO group (Scheme 27 - *path e and f*) [73-74].



Scheme 27. Methodologies useful to introduce the formyl group on substrates.

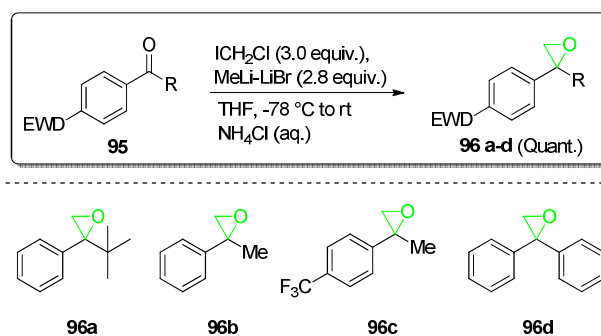
Despite the conceptually distinct approach achieved *via* formylating reagents, our study as well envisaged the “introduction” of a CHO, using the homologating reagent lithiumcarbenoid. Moreover, the procedure reported herein enables to obtain an aldehyde bearing a quaternary stereocenter, which is a challenge in several cases [75]. In order to verify the feasibility of our protocol, we adopted the method on a series of cyclic and acyclic enones (Scheme 28). The methodology may be used towards different starting materials with various substituents and

functionalities, such as ethers and sulphur. Moreover, despite the high temperature employed, no trace of cyclopropyl by-product has been observed.



Scheme 28. New protocol applied on cyclic and acyclic enones.

Interestingly, acetophenone derivatives, under the same conditions, arrested the reaction to the corresponding epoxide, which is obtained in a quantitative amount (Scheme 29). This experimental data demonstrates that the presence of an electron-withdrawing or a bulky group stabilized the oxirane, avoiding the rearrangement into the aldehyde.



Scheme 29. The acetophenone-derivatives case.

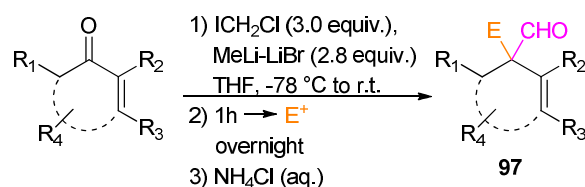
To conclude, a rearrangement-nucleophilic addition mechanism was disclosed. In particular, the chemoselective addition of carbenoids to enones promotes, in “one pot”, the access to β,γ -unsaturated aldehydes in high/good yields.

3. CONCLUSION AND OUTLOOK

3. CONCLUSION AND OUTLOOK

In the “Overview Section”, we investigated the reactivity/stability of carbenoids towards the α,β -unsaturated ketones. The employment of a syringe pump, as an instrument to add the lithium reagents, is of great importance. Indeed, it may contribute in reducing the equivalents of reactants to generate carbenoidic species. Moreover, an in depth analysis promoted the identification of the optimal conditions to carry out the chemoselective 1,2-addition of LiCH_2Cl to cyclic/acyclic ketones. The desired halohydrins have been obtained in high yield, demonstrating the applicability of this procedure. Notably, the so-obtained products may be involved in an epoxidation reaction under harsh conditions, for accessing to oxiranes, which represent interesting intermediates in medicinal chemistry. These results led us to postulate that the syringe pump may increase the yields and decrease the equivalents of reagents in other synthesis, involving different starting electrophiles (e.g. isocyanates, Weinreb amides). Taking into account these considerations, we are applying the “Syringe pump” protocol on different substrates to verify this assumption.

Remarkably, an innovative mechanism to form aldehydes was depicted. The simple variation of the temperature guarantees the generation of formylating derivatives. It is noteworthy that in the case of acetophenone, presenting an electron-withdrawing group or a bulky substituent, the reaction arrests at the corresponding oxirane, avoiding the subsequent rearrangement into the aldehyde. This behaviour may be explained by the high stability shown by these species. Considering the results described in the previous section, this tandem rearrangement-nucleophilic addition mechanism (Pace/Holzer rearrangement) deserves further investigations. In particular, we would like to demonstrate that this procedure may be applied in the presence of other electrophiles, i.e. benzyl bromide, allyl bromide, crotyl bromide, propargyl bromide and tert-butyl bromoacetate, in order to obtain **97** compound-like (Scheme 30), instead of the methyl addition product.



Scheme 30. Reaction with different electrophiles.

Lastly, as highlighted in the prior Chapter, the optimised conditions will be adopted to functionalise **RC-106** derivatives, in order to obtain key intermediates, suitable for further functionalizations and/or biotinylations. The results will be described in due the course.

4. EXPERIMENTAL SECTION

4. EXPERIMENTAL SECTION

4.1. Materials and methods

All ^1H NMR and ^{13}C NMR spectra were recorded on Bruker Avance spectrometers operating at 200, 300, 400 or 500 MHz and at 50, 75, 100, or 125 MHz, respectively, from CDCl_3 solutions. The (residual) solvent signal was used as an internal standard which was related to TMS with δ 7.26 ppm (^1H) and δ 77.0 ppm (^{13}C). Spin-spin coupling constants (J) are given in Hz. In some cases, full and unambiguous assignment of all ^1H , ^{13}C , resonances was performed by combined application of standard NMR techniques, such as APT, DEPT, HSQC, HMBC and NOESY experiments.

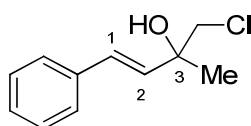
All melting points are uncorrected. Column chromatography purifications were conducted on silica gel 60 (40-63 μm). TLC was carried out on aluminum sheets pre-coated with silica gel 60F254; the spots were visualized under UV light ($\lambda = 254$ nm) and/or KMnO_4 (aq.) was used as revealing system.

Starting enone-type materials were supplied from commercial sources otherwise indicated.

4.2. General Procedure for the Chemoselective Addition of LiCH_2Cl to Ketones, to obtain halohydrins

To a cooled (-78 °C) solution of enone (1.0 equiv) in dry THF was added chloriodomethane (3.0 equiv). After 2 min, an ethereal solution of MeLi-LiBr (2.8 equiv, 1.5 M) was added dropwise, using a syringe pump (flow: 0.200 mL/min). The resulting solution was stirred for 1 h, at that temperature. Saturated aq NH_4Cl was added (2 mL/mmol substrate) and the cooling bath was removed, the mixture was stirred till it reached r.t., and then, it was extracted with Et_2O (2 x 5 mL) and washed with water (5 mL) and brine (10 mL). The organic phase was dried (anhydrous Na_2SO_4), filtered and, after removal of the solvent under reduced pressure, the so-obtained crude mixture was subjected to chromatography (silica gel) to afford pure compounds.

(3E)-1-chloro-2-methyl-4-phenyl-3-buten-2-ol (72a)



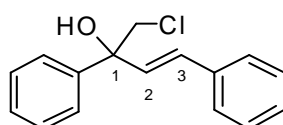
By following the General Procedure, starting from (*E*)-4-phenylbut-3-en-2-one (146 mg, 1.00 mmol, 1.0 equiv), ICH_2Cl (529 mg, 0.22 mL, 3.0 mmol, 3.0 equiv), MeLi-LiBr complex (1.5 M,

Experimental Section

1.87 mL, 2.8 mmol, 2.8 equiv) and THF (2 mL), the desired product was obtained in 76% (149 mg) as a colorless oil after chromatography on silica gel (90:10 hexane:ethylacetate).

¹H NMR (400 MHz, CDCl₃) δ: 7.40 (m, 2H, Ph H-2,6), 7.33 (m, 2H, Ph H-3,5), 7.26 (m, 1H, Ph H-4), 6.73 (d, *J* = 16.0 Hz, 1H, H-1), 6.26 (d, *J* = 16.0 Hz, 1H, H-2), 3.65 and 3.62 (AB-system, ²*J* = 11.0 Hz, 2H, CH₂Cl), 2.35 (s, 1H, OH), 1.49 (s, 1H, Me). **¹³C NMR** (100 MHz, CDCl₃) δ: 136.3 (Ph C-1), 132.3 (C-2), 129.8 (C-1), 128.6 (Ph C-3,5), 127.9 (Ph C-4), 126.6 (Ph C-2,6), 72.5 (C-3), 54.4 (CH₂Cl), 25.8 (Me). **ESI-HRMS** *m/z*: 197.82 [M+H]⁺

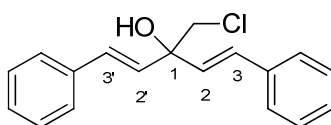
(3E)-1-chloro-2,4-diphenyl-3-buten-2-ol (72b)



By following the General Procedure, starting from (*E*)-chalcone (208 mg, 1.00 mmol, 1.0 equiv), ICH₂Cl (529 mg, 0.22 mL, 3.0 mmol, 3.0 equiv), MeLi-LiBr complex (1.5 M, 1.87 mL, 2.8 mmol, 2.8 equiv) and THF (2 mL), the desired product was obtained in 75% (194 mg) as a white solid after chromatography on silica gel (90:10 hexane:ethylacetate).

¹H NMR (400 MHz, CDCl₃) δ: 7.56 (m, 2H, 2-Ph H-2,6), 7.42 (m, 4H, 2-Ph H-3,5; 4-Ph H-2,6), 7.34 (m, 3H, 2-Ph H-4; 4-Ph H-3,5), 7.27 (m, 1H, 4-Ph H-4), 6.71 (d, *J* = 16.0 Hz, 1H, H-3), 6.52 (d, *J* = 16.0 Hz, 1H, H-2), 3.99 and 3.98 (AB-system, ²*J* = 11.4 Hz, 2H, CH₂Cl), 2.94 (s, 1H). **¹³C NMR** (100 MHz, CDCl₃) δ: 142.3 (2-Ph C-1), 136.2 (4-Ph C-1), 131.5 (Ph C-4), 131.5 (C-2), 131.0 (C-3), 128.6 (2-Ph C-3,5), 128.5 (4-Ph C-3,5), 128.0 (4-Ph C-4), 127.8 (2-Ph C-4), 126.7 (4-Ph C-2,6), 125.7 (2-Ph C-2,6), 76.2 (C-1), 53.8 (CH₂Cl). **ESI-HRMS** *m/z*: 281.07 [M+Na]⁺

(1E, 4E)-3-(chloromethyl)-1,5-diphenyl-1,4-pentadien-3-ol (72c)

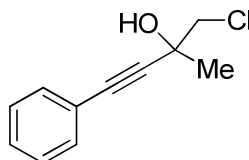


By following the General Procedure, starting from (1*E*, 4*E*)-1,5-diphenylpenta-1,4-dien-3-one (285 mg, 1.00 mmol, 1.0 equiv), ICH₂Cl (529 mg, 0.22 mL, 3.0 mmol, 3.0 equiv), MeLi-LiBr complex (1.5 M, 1.87 mL, 2.8 mmol, 2.8 equiv) and THF (2 mL), the desired product was obtained in 72% (205 mg) as a white solid after chromatography on silica gel (90:10 hexane:ethylacetate).

¹H NMR (400 MHz, CDCl₃) δ: 7.43 (m, 4H, Ph H-2,6,2',6'), 7.34 (m, 4H, Ph H-3,5,3',5'), 7.27 (m, 2H, Ph H-4,4'), 6.81 (d, *J* = 16.0 Hz, 2H, H-3,3'), 6.35 (d, *J* = 16.0 Hz, 2H, H-2,2'), 3.79 (s, 2H, CH₂Cl), 2.64 (s, 1H, OH). **¹³C NMR** (100 MHz, CDCl₃) δ: 136.2 (Ph C-1,1'), 131.2 (C-3,3'), 130.1

(C-2,2'), 128.6 (Ph C-3,5,3',5'), 128.0 (Ph C-4,4'), 126.7 (Ph C-2,6,2',6'), 75.0, 53.1 (CH₂Cl). **ESI-HRMS** m/z: 285.23 [M+H]⁺

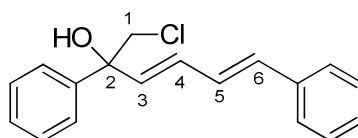
1-chloro-2-methyl-4-phenyl-3-butyn-2-ol (72d)



By following the General Procedure, starting from 4-phenylbut-3-yn-2-one (144 mg, 1.00 mmol, 1.0 equiv), ICH₂Cl (529 mg, 0.22 mL, 3.0 mmol, 3.0 equiv), MeLi-LiBr complex (1.5 M, 1.87 mL, 2.8 mmol, 2.8 equiv) and THF (2 mL), the desired product was obtained in 67% (130 mg) as a bright yellow oil after chromatography on silica gel (80:20 hexane:ethylacetate).

¹H NMR (400 MHz, CDCl₃) δ: 7.45 (m, 2H, Ph H-2,6), 7.32 (m, 3H, Ph H-3,4,5), 3.78 and 3.69 (AB-system, ²J = 10.9 Hz, 2H, CH₂Cl), 2.86 (s, 1H, OH), 1.68 (s, 3H, Me). **¹³C NMR** (100 MHz, CDCl₃) δ: 131.8 (Ph C-2,6), 128.6 (Ph C-4), 128.2 (Ph C-3,5), 122.0 (Ph C-1), 89.5 (C-alkyne), 84.5 (C-alkyne), 68.0, 54.1 (CH₂Cl), 26.9 (Me). **ESI-HRMS** m/z: 217.04 [M+Na]⁺

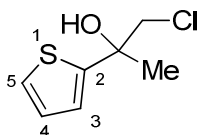
(3E,5E)-1-chloro-2,6-diphenyl-3,5-hexadien-2-ol (72e)



By following the General Procedure, starting from (2E,4E)-1,5-diphenylpenta-2,4-dien-1-one (234 mg, 1.00 mmol, 1.0 equiv), ICH₂Cl (529 mg, 0.22 mL, 3.0 mmol, 3.0 equiv), MeLi-LiBr complex (1.5 M, 1.87 mL, 2.8 mmol, 2.8 equiv) and THF (2 mL), the desired product was obtained in 83% (236 mg) as a bright yellow solid after chromatography on silica gel (90:10 hexane:ethylacetate).

¹H NMR (400 MHz, CDCl₃) δ: 7.50 (m, 2H, 2-Ph H-2,6), 7.40 (m, 2H, 2-Ph H-3,5), 7.38 (m, 2H, 6-Ph H-2,6), 7.31 (m, 3H, 2-Ph H-4, 6-Ph H-3,5), 7.23 (m, 1H, 6-Ph H-4), 6.80 (dd, J = 15.7 and 10.5 Hz, 1H), 6.58 (d, J = 15.7 Hz, 1H), 6.52 (dd, J = 15.3 and 10.5 Hz, 1H), 6.10 (d, J = 15.3 Hz, 1H), 3.94 and 3.92 (AB-system, ²J = 11.2 Hz, 2H, CH₂Cl), 2.83 (s, 1H, OH). **¹³C NMR** (100 MHz, CDCl₃) δ: 142.3 (2-Ph C-1), 136.9 (6-Ph C-1), 135.3 (C-3), 133.9 (C-6), 131.5 (C-4), 128.6 (2-Ph C-3,5), 128.5 (6-Ph C-3,5), 127.8 (2-Ph C-4), 127.7 (C-5), 127.0 (6-Ph C-4), 126.4 (6-Ph C-2,6), 125.6 (2-Ph C-2,6), 76.2 (C-2), 53.7 (CH₂Cl). **APCI-HRMS** m/z: 267.09 [M-H₂O]⁺

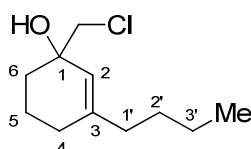
1-chloro-2-(2-thiophenyl)-2-propanol (72f)



By following the General Procedure, starting from 1-(thiophen-2-yl)ethanone (126 mg, 1.00 mmol, 1.0 equiv), ICH₂Cl (529 mg, 0.22 mL, 3.0 mmol, 3.0 equiv), MeLi-LiBr complex (1.5 M, 1.87 mL, 2.8 mmol, 2.8 equiv) and THF (2 mL), the desired product was obtained in 68% (120 mg) as a yellow oil after chromatography on silica gel (80:20 hexane:ethylacetate).

¹H NMR (400 MHz, CDCl₃) δ: 7.24 (dd, *J* = 4.6 and 1.8 Hz, 1H, H-5), 6.99 (m, 1H, H-3), 6.98 (m, 1H, H-4), 3.82 and 3.73 (AB-system, ²*J* = 11.2 Hz, 2H, CH₂Cl), 3.12 (br s, 1H, OH), 1.72 (s, 3H, Me). **¹³C NMR** (100 MHz, CDCl₃) δ: 148.7 (C-2), 126.7 (C-4), 124.6 (C-5), 123.3 (C-3), 72.9, 54.9 (CH₂Cl), 27.5 (CH₃). **ESI-HRMS** *m/z*: 199.00 [M+Na]⁺

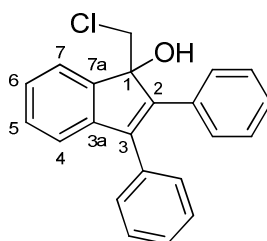
3-butyl-1-(chloromethyl)-2-cyclohexen-1-ol (72g)



By following the General Procedure, starting from 3-butyl-cyclohex-2-enone (152 mg, 1.00 mmol, 1.0 equiv), ICH₂Cl (529 mg, 0.22 mL, 3.0 mmol, 3.0 equiv), MeLi-LiBr complex (1.5 M, 1.87 mL, 2.8 mmol, 2.8 equiv) and THF (2 mL), the desired product was obtained in 81% (164 mg) as a bright yellow oil after chromatography on silica gel (70:30 hexane:ethylacetate).

¹H NMR (400 MHz, C₆D₆) δ: 5.30 (s, 1H, H-2), 3.29 (s, 2H, CH₂Cl), 1.87 (br s, 1H, OH), 1.80 (m, 2H, H-1'), 1.72-1.57 (m, 4H, H-4,5,6), 1.50 (m, 1H, H-6), 1.34-1.14 (m, 5H, H-5,2',3'), 0.86 (t, *J* = 7.1 Hz, 3H, Me). **¹³C NMR** (100 MHz, C₆D₆) δ: 143.8 (C-3), 123.6 (C-2), 69.7, 54.4 (CH₂Cl), 37.6 (C-1'), 33.5 (C-6), 29.9 (C-2'), 28.9 (C-4), 22.7 (C-3'), 19.6 (C-5), 14.2 (Me). **ESI-HRMS** *m/z*: 225.10 [M+Na]⁺

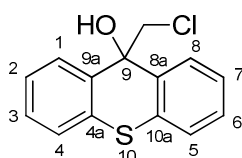
1-(chloromethyl)-2,3-diphenyl-1*H*-inden-1-ol (72h)



By following the General Procedure, starting from 2,3-diphenyl-inden-1-one (282 mg, 1.00 mmol, 1.0 equiv), ICH₂Cl (529 mg, 0.22 mL, 3.0 mmol, 3.0 equiv), MeLi-LiBr complex (1.5 M, 1.87 mL, 2.8 mmol, 2.8 equiv) and THF (2 mL), the desired product was obtained in 70% (232 mg) as a yellow solid after chromatography on silica gel (90:10 hexane:ethylacetate).

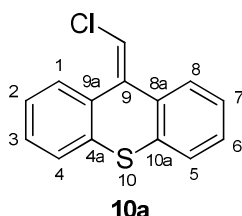
¹H NMR (400 MHz, CDCl₃) δ: 7.70 (m, 1H, H-7), 7.45 (m, 2H, 2-Ph H-2,6), 7.35 (m, 5H, 3-Ph H-2,3,4,5,6) 7.34 (m, 1H, H-5), 7.29 (m, 1H, H-4), 7.27 (m, 4H, 2-Ph H-3,4,5 and H-6), 3.98 and 3.66 (AB-system, ²J = 11.0 Hz, 2H, CH₂Cl), 2.75 (s, 1H, OH). **¹³C NMR** (100 MHz, CDCl₃) δ: 145.6 (C-7a), 143.0 (C-2), 142.9 (C-3a), 141.9 (C-3), 134.0 (3-Ph C-1), 133.9 (2-Ph C-1), 129.4 (2-Ph C-2,6), 129.2 (3-Ph C-2,6), 129.1 (C-5), 128.5 (3-Ph C-3,5), 128.2 (2-Ph C-3,5), 127.8 (3-Ph C-4), 127.7 (2-Ph C-4), 126.7 (C-6), 122.9 (C-7), 121.0 (C-4), 84.3, 49.1 (CH₂Cl). **ESI-HRMS** m/z: 355.09 [M+Na]⁺

9-(chloromethyl)-9H-thioxanthen-9-ol (72i)



By following the General Procedure, starting from thioxanthen-9-one (212 mg, 1.00 mmol, 1.0 equiv), ICH₂Cl (529 mg, 0.22 mL, 3.0 mmol, 3.0 equiv), MeLi-LiBr complex (1.5 M, 1.87 mL, 2.8 mmol, 2.8 equiv) and THF (2 mL), the desired product was obtained in 63% (166 mg) as a yellow oil after chromatography on silica gel (90:10 hexane:ethylacetate).

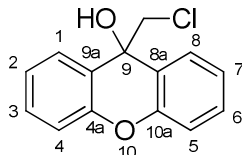
¹H NMR (400 MHz, C₆D₆) δ: 7.71 (m, 2H, H-1,8), 7.17 (m, 2H, H-4,5), 7.04 (m, 2H, H-2,7), 6.89 (m, 2H, H-3,6), 3.55 (s, 2H, CH₂Cl), 2.75 (s, 1H, OH). **¹³C NMR** (100 MHz, C₆D₆) δ: 137.1 (C-8a,9a), 130.6 (C-4a,10a), 128.0 (C-3,6), 126.9 (C-1,8), 126.7 (C-2,4,5,7), 74.6 (C-9), 49.1 (CH₂Cl). **ESI-HRMS** m/z: 263.92 [M+H]⁺



9-(chloromethylene)-9H-thioxanthen-9-ol (78) **¹H NMR** (400 MHz, CDCl₃) δ: 8.00 (m, 1H, H-1), 7.51 (m, 1H, H-4), 7.47 (m, 1H, H-8), 7.45 (m, 1H, H-5), 7.37 (m, 1H, H-2), 7.31 (m, 1H, H-3), 7.30 (m, 2H, H-6,7), 6.55 (s, 1H, CH). **¹³C NMR** (100 MHz, CDCl₃) δ: 136.4 (C-9), 134.9 (C-8a),

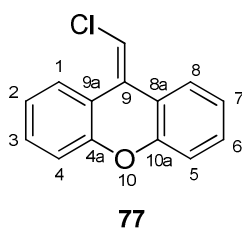
133.1 (C-4a), 131.9 (C-10a), 130.9 (C-9a), 129.2 (C-1), 127.9 (C-3), 127.6 (C-6), 126.9 (C-7), 126.5 (C-4), 126.0 (C-5), 125.7 (C-2,8), 117.1(CH).

9-(chloromethyl)-9H-xanthen-9-ol (72j)



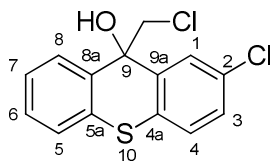
By following the General Procedure, starting from thioxanthen-9-one (196 mg, 1.00 mmol, 1.0 equiv), ICH₂Cl (529 mg, 0.22 mL, 3.0 mmol, 3.0 equiv), MeLi-LiBr complex (1.5 M, 1.87 mL, 2.8 mmol, 2.8 equiv) and THF (2 mL), the desired product was obtained in 68% (168 mg) as a yellow oil after chromatography on silica gel (90:10 hexane:ethylacetate).

¹H NMR (400 MHz, C₆D₆) δ: 7.47 (m, 2H, H-1,8), 7.07 (m, 2H, H-4,5), 7.02 (m, 2H, H-3,6), 6.91 (m, 2H, H-2,7), 3.43 (s, 2H, CH₂Cl), 2.21 (s, 1H, OH). **¹³C NMR** (100 MHz, C₆D₆) δ: 151.2 (C-4a,10a), 129.7 (C-3,6), 127.1 (C-1,8), 124.6 (C-8a,9a), 123.5 (C-2,7), 116.4 (C-4,5), 68.9 (C-9), 54.8 (CH₂Cl). **ESI-HRMS** m/z: 247.96 [M+H]⁺



9-(chloromethylene)-9H-xanthen-9-ol (77) **¹H NMR** (400 MHz, C₆D₆) δ: 8.45 (m, 1H, H-1), 7.05 (m, 1H, H-4), 7.00 (m, 1H, H-5), 6.96 (m, 1H, H-3), 6.93 (m, 1H, H-8), 6.92 (m, 1H, H-6), 6.90 (m, 1H, H-2), 6.73 (m, 1H, H-7) 6.10 (s, 1H, CH). **¹³C NMR** (100 MHz, C₆D₆) δ: 152.6 (C-4a), 151.1 (C-10a), 130.1 (C-3), 129.4 (C-6), 128.4 (C-1), 127.6 (C-9), 124.0 (C-7), 128.3 (C-8), 123.0 (C-2), 122.7 (C-8a), 120.2 (C-9a), 117.1 (C-4,5), 111.7 (CH).

2-chloro-9-(chloromethyl)-9H-thioxanthen-9-ol (72k)

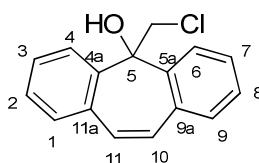


By following the General Procedure, starting from 2-chloro-9H-thioxanthen-9-one (247 mg, 1.00 mmol, 1.0 equiv), ICH₂Cl (529 mg, 0.22 mL, 3.0 mmol, 3.0 equiv), MeLi-LiBr complex (1.5

M, 1.87 mL, 2.8 mmol, 2.8 equiv) and THF (2 mL), the desired product was obtained in 71% (211 mg) as a yellow oil after chromatography on silica gel (90:10 hexane:ethylacetate).

¹H NMR (400 MHz, C₆D₆) δ: 7.78 (dd, 1H, *J* = 2.2 and 0.5 Hz, H-1), 7.62 (dd, 1H, *J* = 7.9 and 1.4 Hz, H-8), 7.11 (ddd, 1H, *J* = 7.7, 1.3 and 0.5 Hz, H-5), 7.02 (m, 1H, H-7), 6.87 (m, 1H, H-6), 6.85 (dd, 1H, *J* = 8.3 and 2.2 Hz, H-3), 6.81 (dd, 1H, *J* = 8.3 and 0.5 Hz, H-4), 3.40 and 3.37 (AB-system, ²*J* = 11.0 Hz, 2H, CH₂Cl), 2.47 (s, 1H, OH). **¹³C NMR** (100 MHz, C₆D₆) δ: 138.9 (C-9a), 136.5 (C-8a), 133.1 (C-4a), 130.2 (C-5a), 129.1 (C-2), 128.2 (C-6), 128.1 (C-3), 127.8 (C-4), 127.2 (C-1), 126.9 (C-8), 126.8 (C-7), 12.6 (C-5), 74.5 (C-9), 48.5 (CH₂Cl). **ESI-HRMS** *m/z*: 298.32 [M+H]⁺

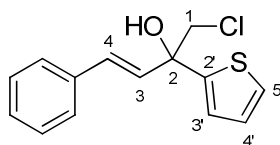
5-(chloromethyl)-5*H*-dibenzo[*a,d*][7]annulen-5-ol (72l)



By following the General Procedure, starting from 5*H*-dibenzo[*a,d*][7]annulen-5-one (206 mg, 1.00 mmol, 1.0 equiv), ICH₂Cl (529 mg, 0.22 mL, 3.0 mmol, 3.0 equiv), MeLi-LiBr complex (1.5 M, 1.87 mL, 2.8 mmol, 2.8 equiv) and THF (2 mL), the desired product was obtained in 74% (190 mg) as a colourless oil after chromatography on silica gel (90:10 hexane:ethylacetate).

¹H NMR (400 MHz, C₆D₆) δ: 8.03 (m, 2H, H-4,6), 7.21 (m, 2H, H-3,7), 7.04 (m, 4H, H-1,2,8,9), 6.59 (s, 2H, H-10,11), 3.81 (s, 2H, CH₂Cl), 3.19 (s, 1H, OH). **¹³C NMR** (100 MHz, C₆D₆) δ: 139.4 (C-4a,5a), 132.7 (C-9a,10a), 131.5 (C-10,11), 129.8 (C-1,9), 129.2 (C-3,7), 127.4 (C-2,8), 125.6 (C-4,6), 76.1 (C-5), 49.7 (CH₂Cl). **ESI-HRMS** *m/z*: 257.07 [M+H]⁺

(3*E*)-1-chloro-4-phenyl-2-(2-thienyl)-3-buten-2-ol (72m)

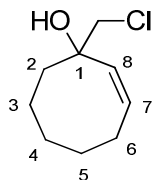


By following the General Procedure, starting from (*E*)-3-phenyl-1-(thiophen-2-yl)prop-2-en-1-one (214 mg, 1.00 mmol, 1.0 equiv), ICH₂Cl (529 mg, 0.22 mL, 3.0 mmol, 3.0 equiv), MeLi-LiBr complex (1.5 M, 1.87 mL, 2.8 mmol, 2.8 equiv) and THF (2 mL), the desired product was obtained in 80% (212 mg) as a colourless oil after chromatography on silica gel (90:10 hexane:ethylacetate).

¹H NMR (400 MHz, CDCl₃) δ: 7.17 (m, 2H, Ph H-2,6), 7.08 (m, 2H, Ph H-3,5), 7.04 (m, 1H, Ph H-4), 6.83 (dd, *J* = 5.0 and 1.1 Hz, 1H, H-5'), 6.75 (d, *J* = 15.9 Hz, 1H, H-4), 6.74 (dd, *J* = 3.6 and 1.1

Hz, 1H, H-3'), 6.69 (dd, $J = 5.0$ and 3.6 Hz, 1H, H-4'), 6.32 (d, $J = 15.9$ Hz, 1H, H-3), 3.61 and 3.51 (AB-system, $^2J = 11.1$ Hz, 2H, CH₂Cl), 2.67 (s, 1H). **¹³C NMR** (100 MHz, CDCl₃) δ : 147.6 (C-2'), 136.6 (Ph C-1), 131.4 (C-3), 131.3 (C-4), 128.8 (Ph C-3,5), 128.2 (Ph C-4), 127.0 (Ph C-2,6, C-4'), 125.5 (C-5'), 124.7 (C-3'), 75.4 (C-2), 56.0 (C-1). **ESI-HRMS** m/z : 265.05 [M+H]⁺

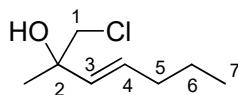
(2Z)-1-(chloromethyl)-2-cycloocten-1-ol (72n)



By following the General Procedure, starting from (*Z*)-cyclooct-2-enone (124 mg, 1.00 mmol, 1.0 equiv), ICH₂Cl (529 mg, 0.22 mL, 3.0 mmol, 3.0 equiv), MeLi-LiBr complex (1.5 M, 1.87 mL, 2.8 mmol, 2.8 equiv) and THF (2 mL), the desired product was obtained in 79% (138 mg) as a colourless oil after chromatography on silica gel (70:30 pentane:diethylether).

¹H NMR (400 MHz, CDCl₃) δ : 5.42 (m, 1H, H-8), 5.41 (m, 1H, H-7), 3.12 and 3.09 (AB-system, $^2J = 10.7$ Hz, 2H, CH₂Cl), 2.58 (m, 1H, H-6), 1.87 (m, 1H, H-6), 1.70 (s, 1H, OH), 1.67 (m, 1H, H-3), 1.64 (m, 1H, H-4), 1.63 (m, 1H, H-2), 1.41 (m, 2H, H-2, 3), 1.36 (m, 2H, H-5), 1.25 (m, 1H, H-4). **¹³C NMR** (100 MHz, CDCl₃) δ : 133.6 (C-8), 131.5 (C-7), 74.3 (C-1), 56.2 (CH₂Cl), 38.2 (C-2), 27.7 (C-5), 25.1 (C-4), 24.8 (C-6), 22.2 (C-3). **ESI-HRMS** m/z : 175.95 [M+H]⁺

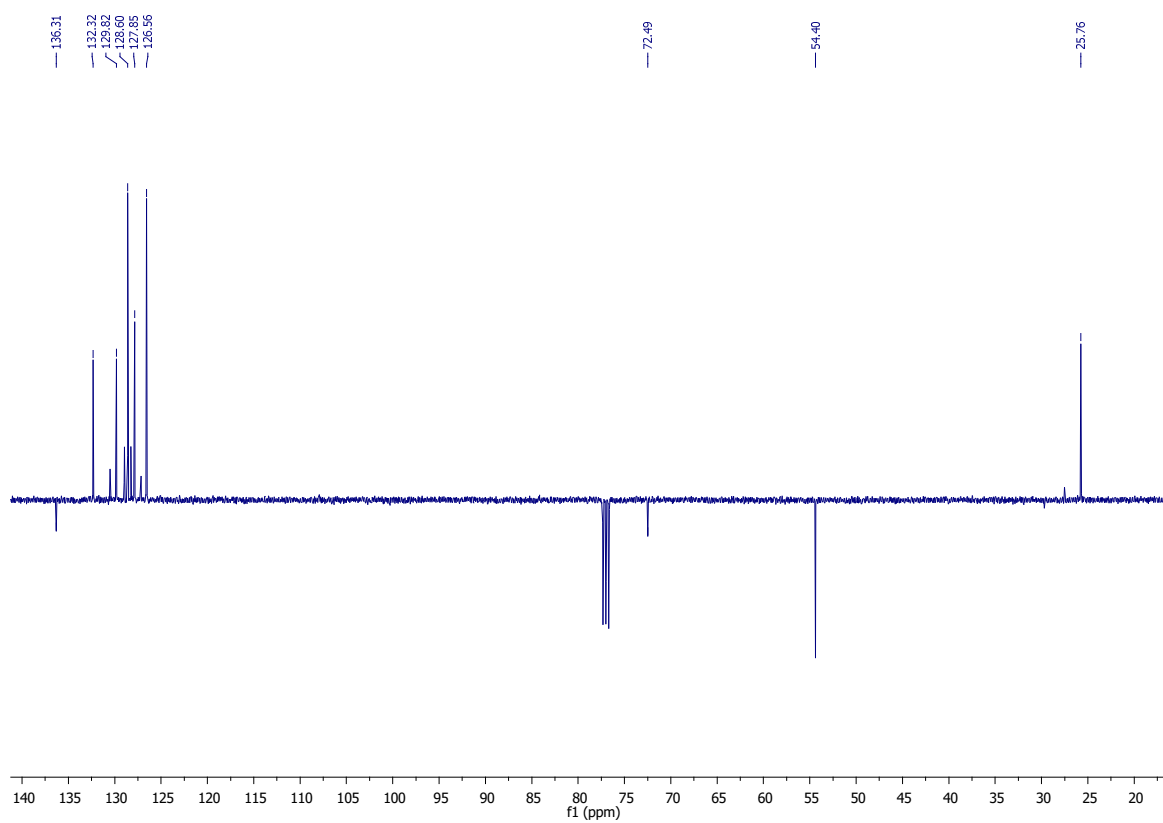
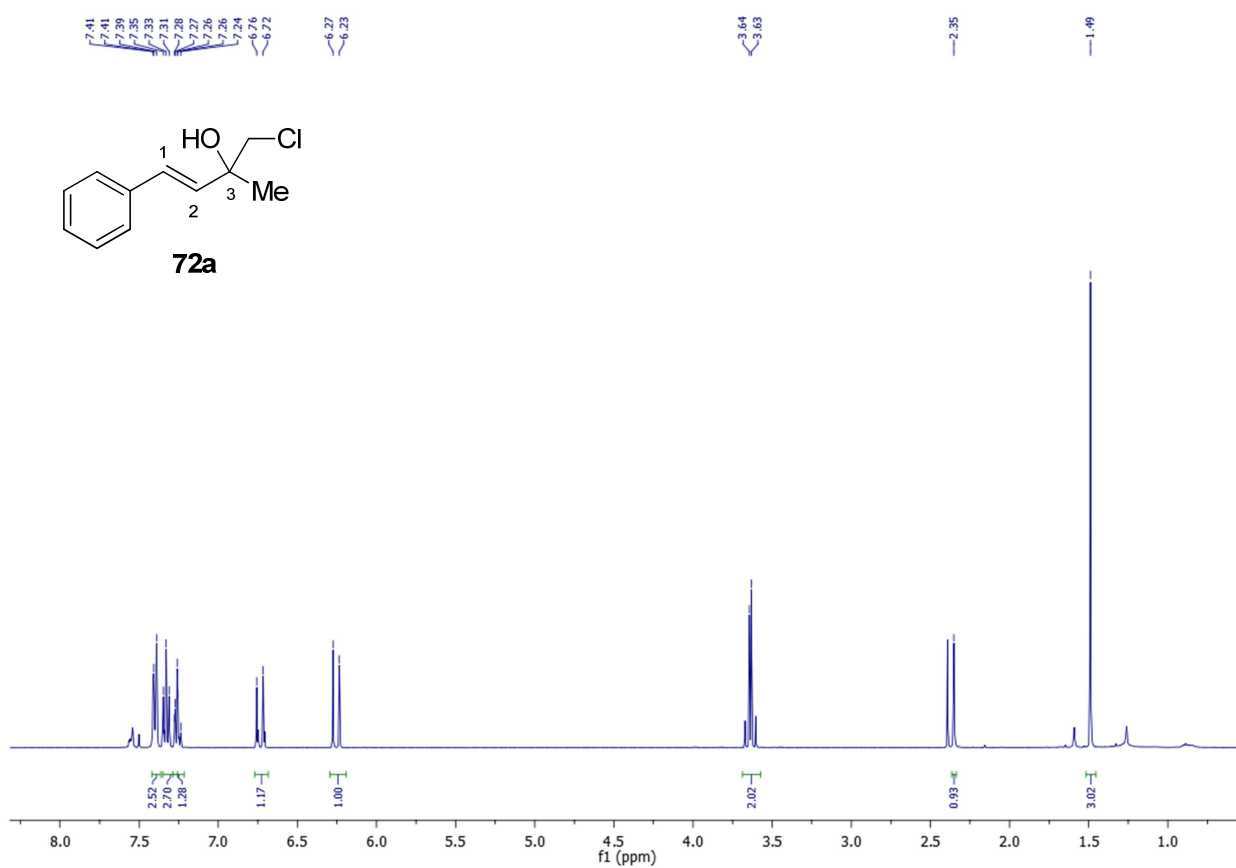
(3E)-1-chloro-2-methyl-3-hepten-2-ol (72o)

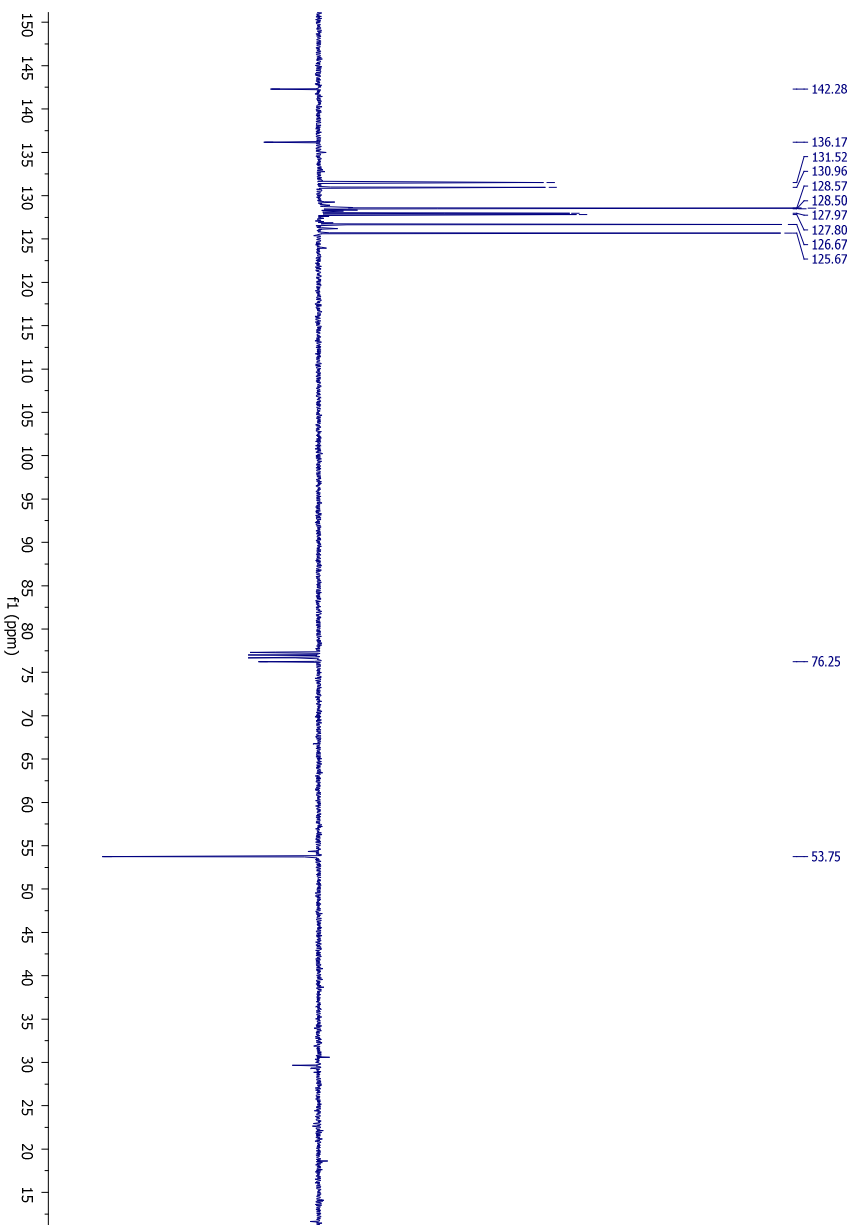
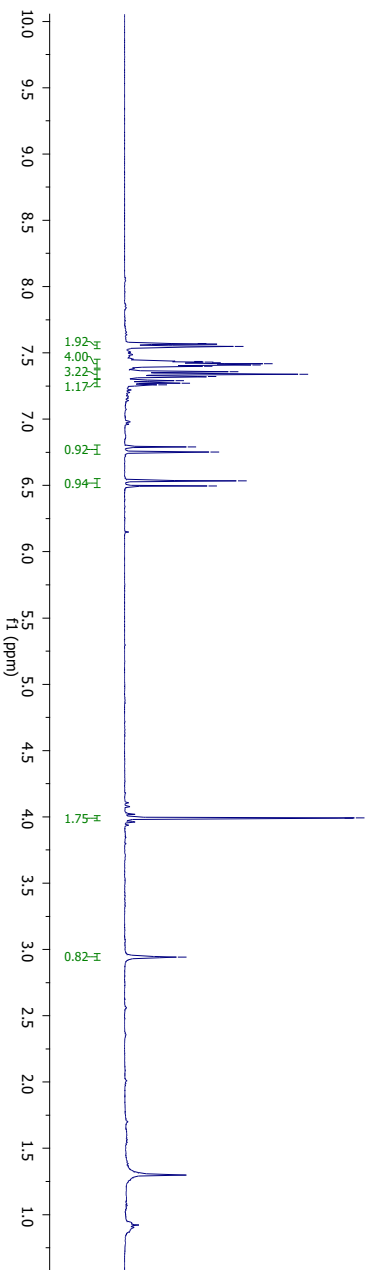
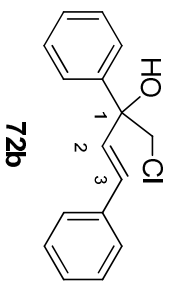


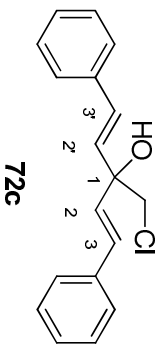
By following the General Procedure, starting from (*3E*)-hept-3-en-2-one (112 mg, 1.00 mmol, 1.0 equiv), ICH₂Cl (529 mg, 0.22 mL, 3.0 mmol, 3.0 equiv), MeLi-LiBr complex (1.5 M, 1.87 mL, 2.8 mmol, 2.8 equiv) and THF (2 mL), the desired product was obtained in 88% (143 mg) as a bright yellow oil after chromatography on silica gel (70:30 pentane:diethylether).

¹H NMR (400 MHz, C₆D₆) δ : 5.64 (td, $J = 15.5$ Hz, 6.9 Hz, 1H, H-4), 5.30 (td, $J = 15.5$ Hz, 1.5 Hz, 1H, H-5), 3.18 and 3.14 (AB-system, $^2J = 10.8$ Hz, 2H, H-1), 1.88 (s, 1H, OH) 1.87 (m, 2H, H-5), 1.28 (m, 2H, H-6), 1.13 (s, 3H, CH₃), 0.82 (t, $J = 7.3$ Hz, 3H, H-7). **¹³C NMR** (100 MHz, C₆D₆) δ : 133.9 (C-5), 130.4 (C-4), 71.9 (C-2), 54.7 (C-1), 34.5 (C-5), 25.7 (CH₃), 22.6 (C-6), 13.7 (C-7). **ESI-HRMS** m/z : 163.13 [M+H]⁺

Copies of NMR spectra

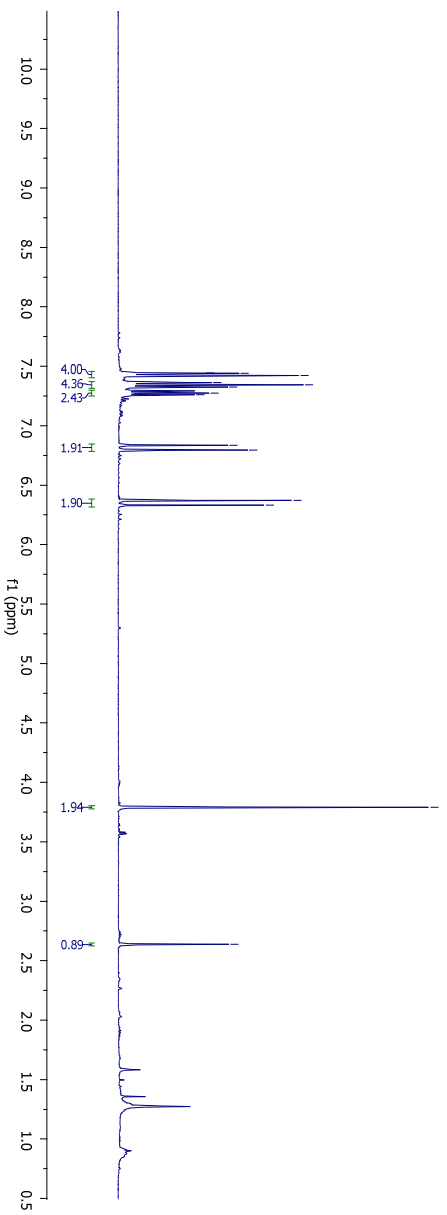






3.79

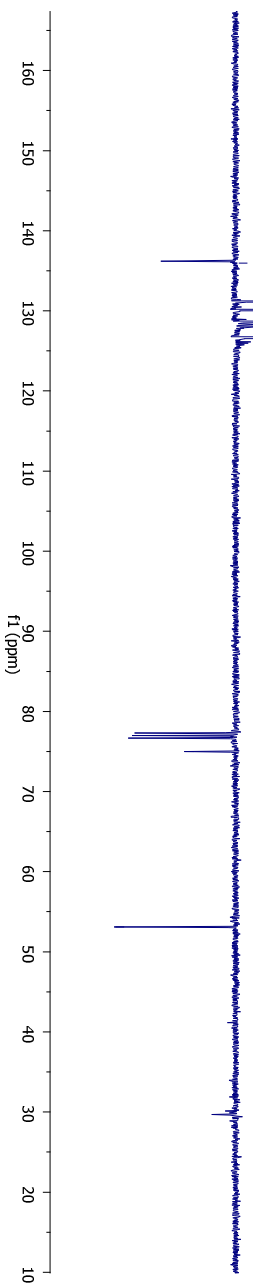
2.64

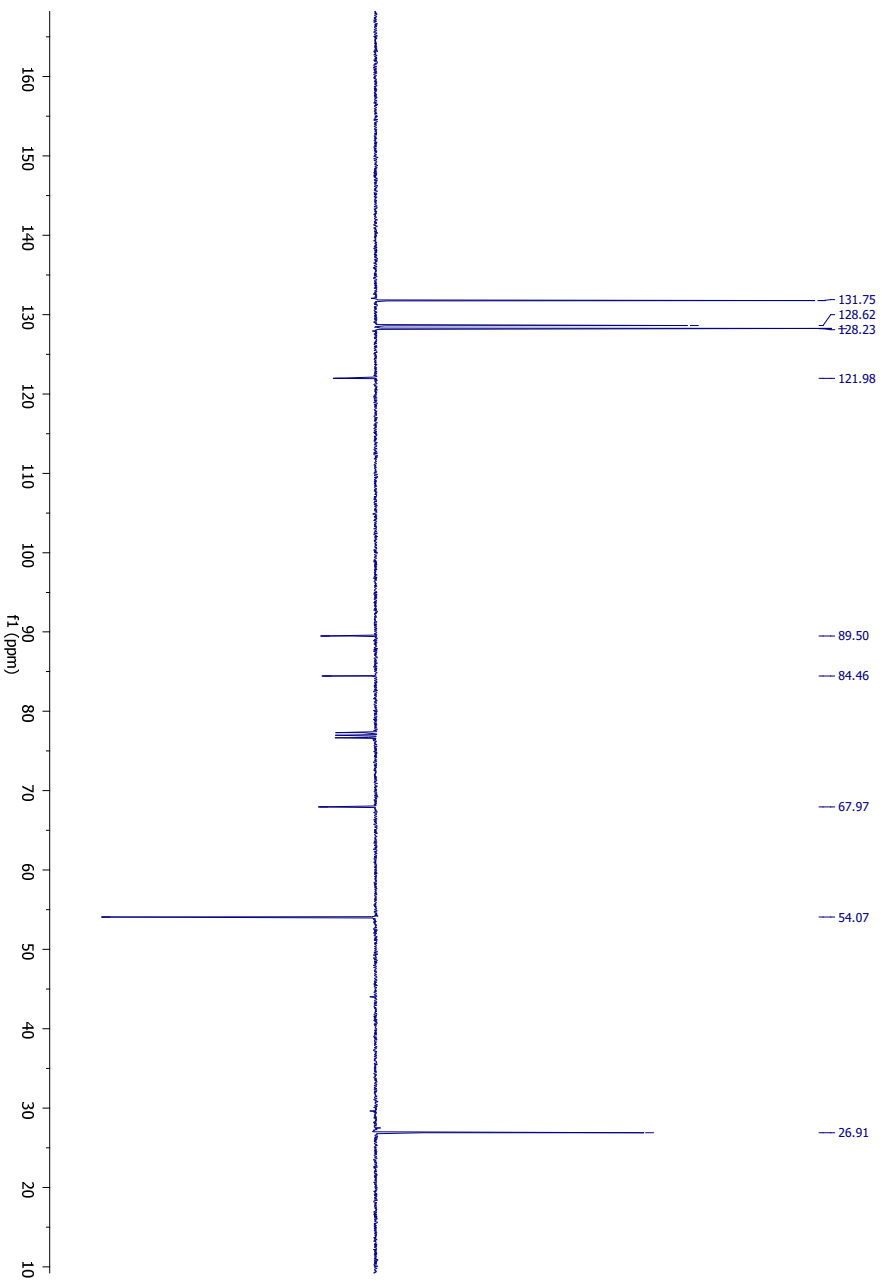
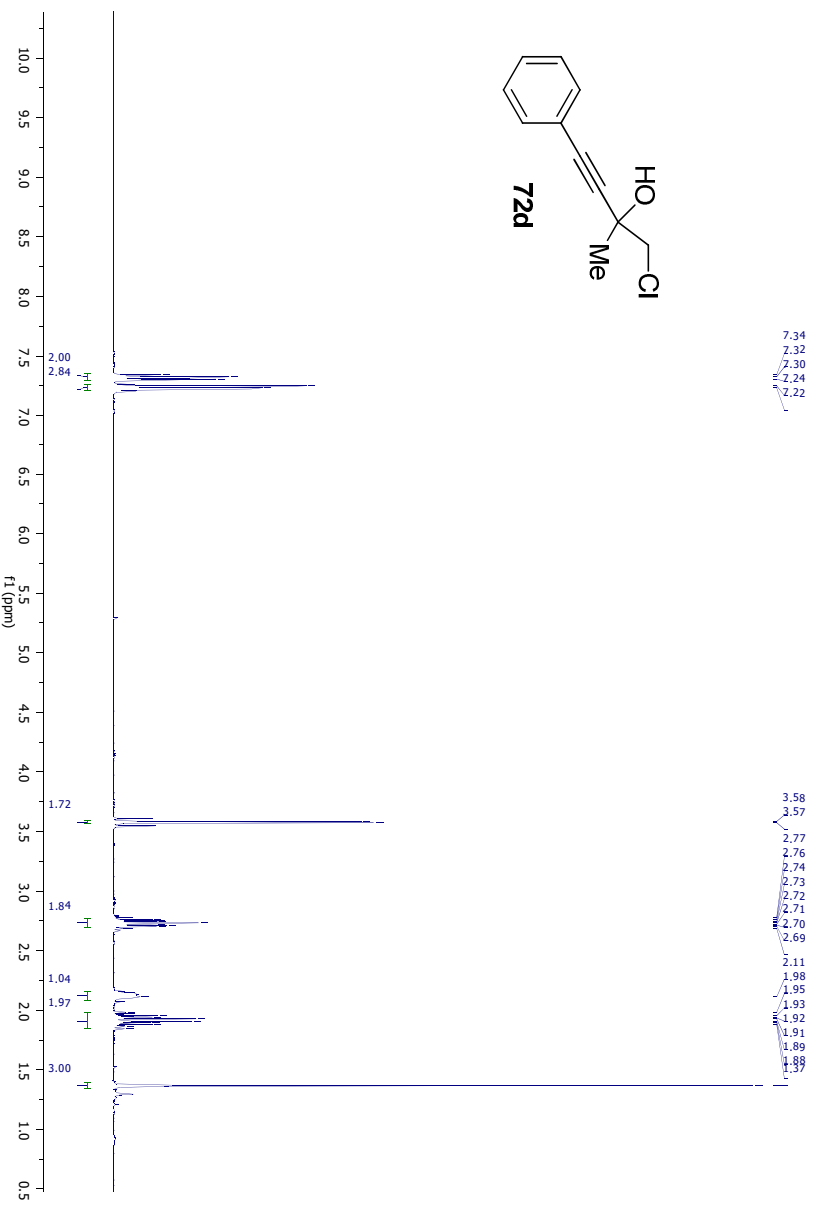
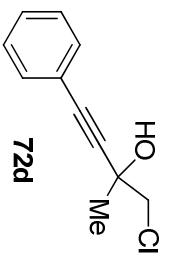


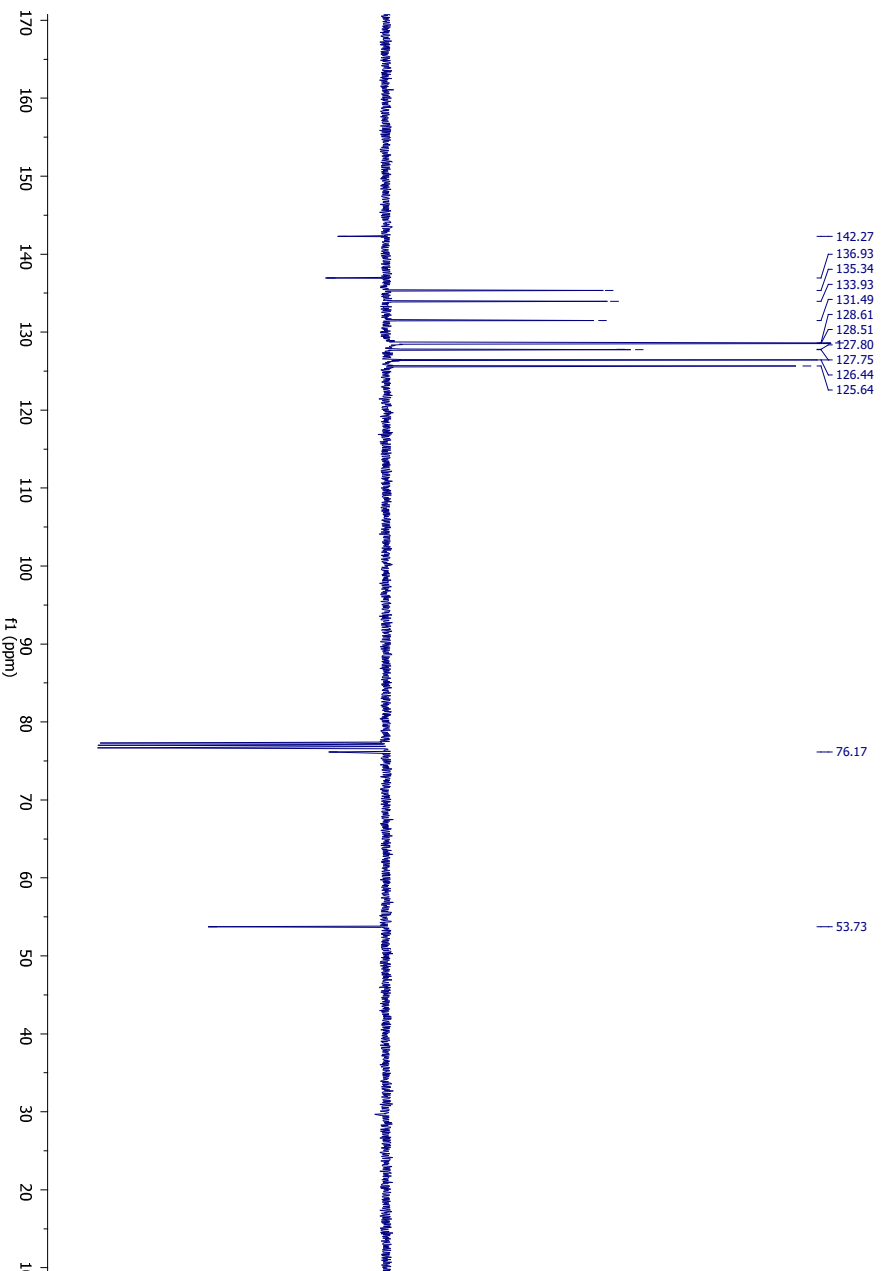
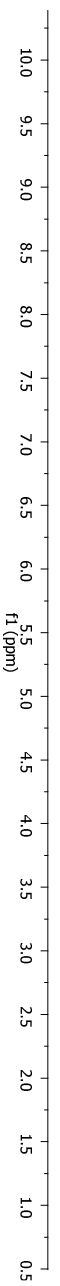
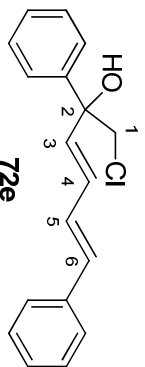
135.96
131.15
130.07
128.62
128.04
126.68

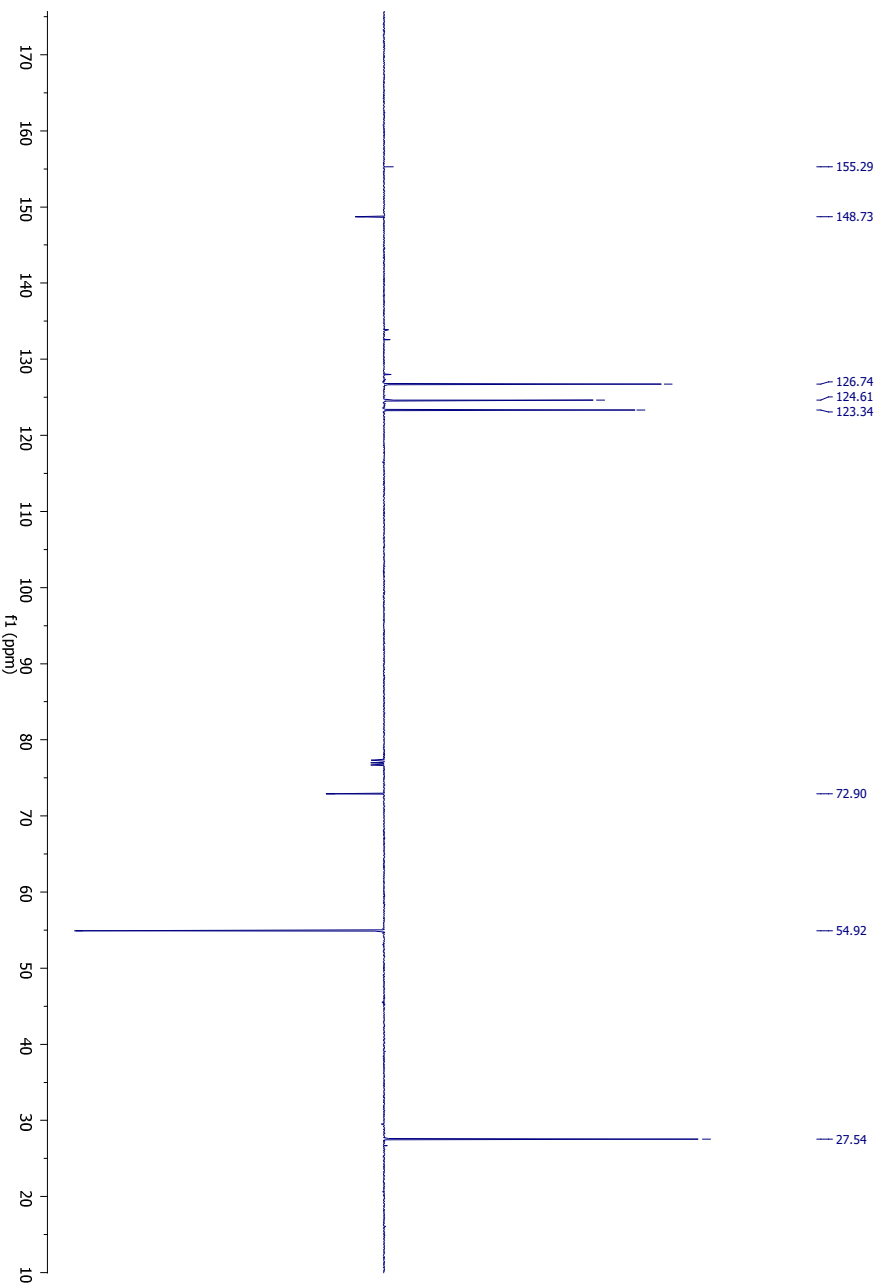
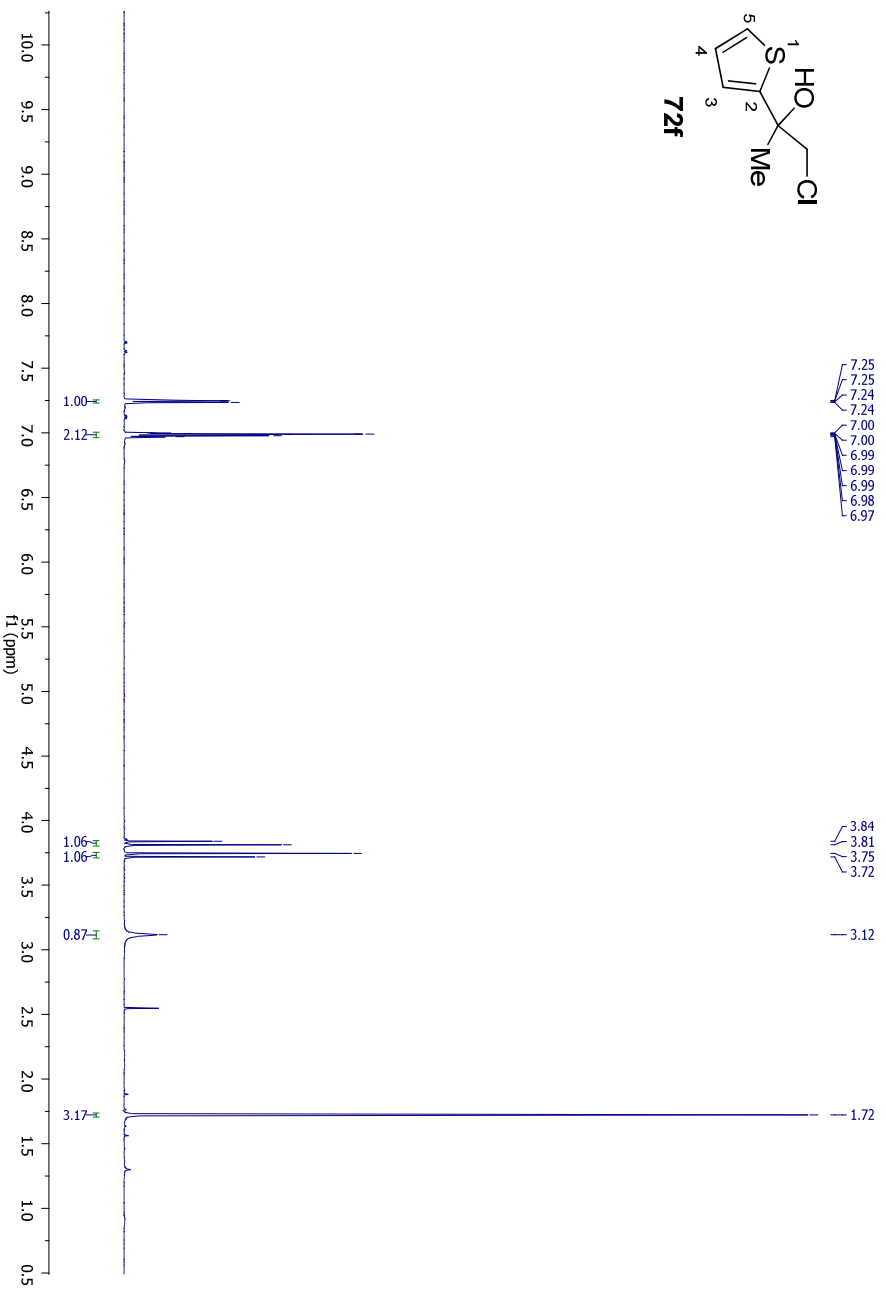
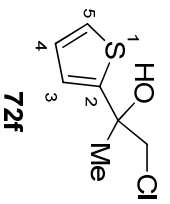
75.01

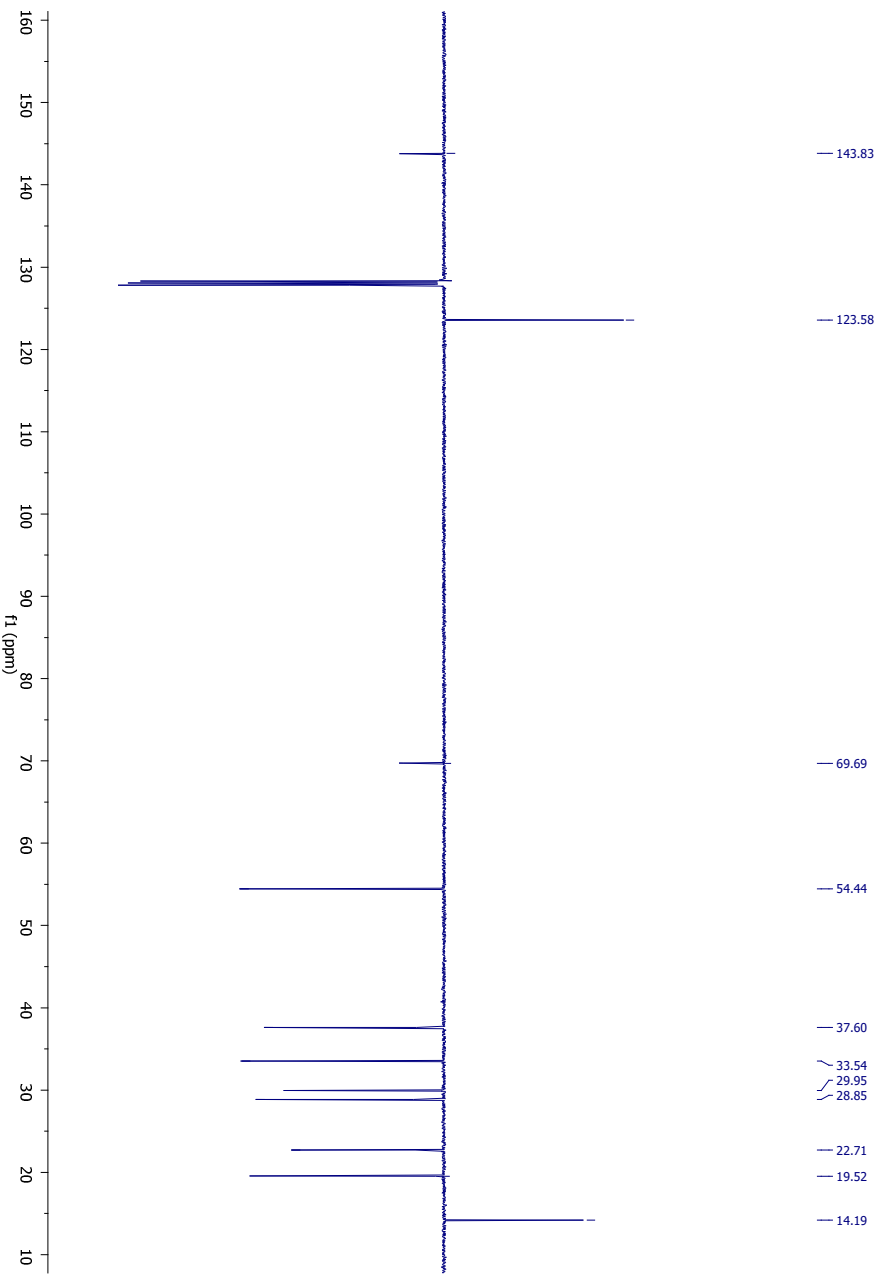
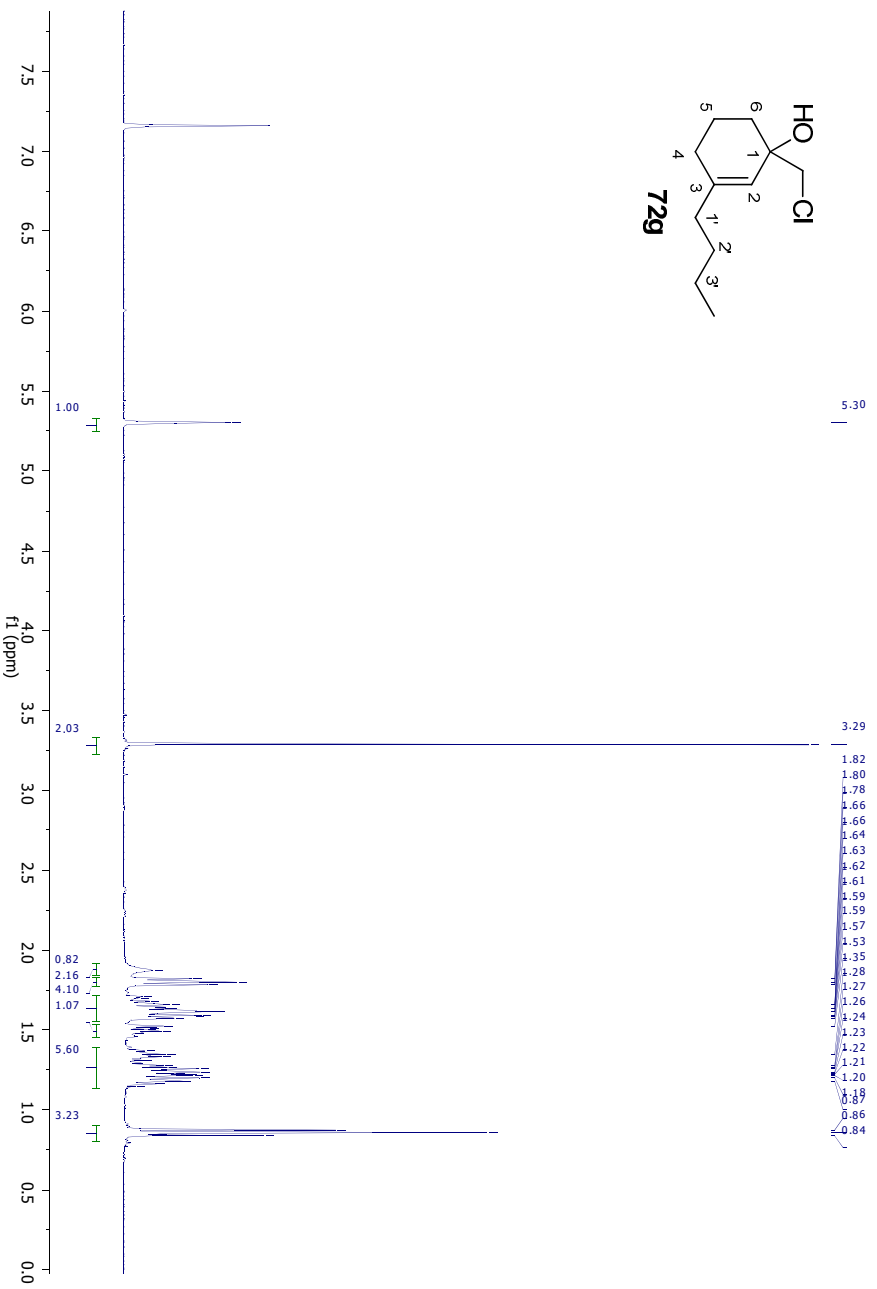
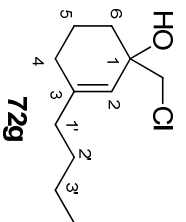
53.09

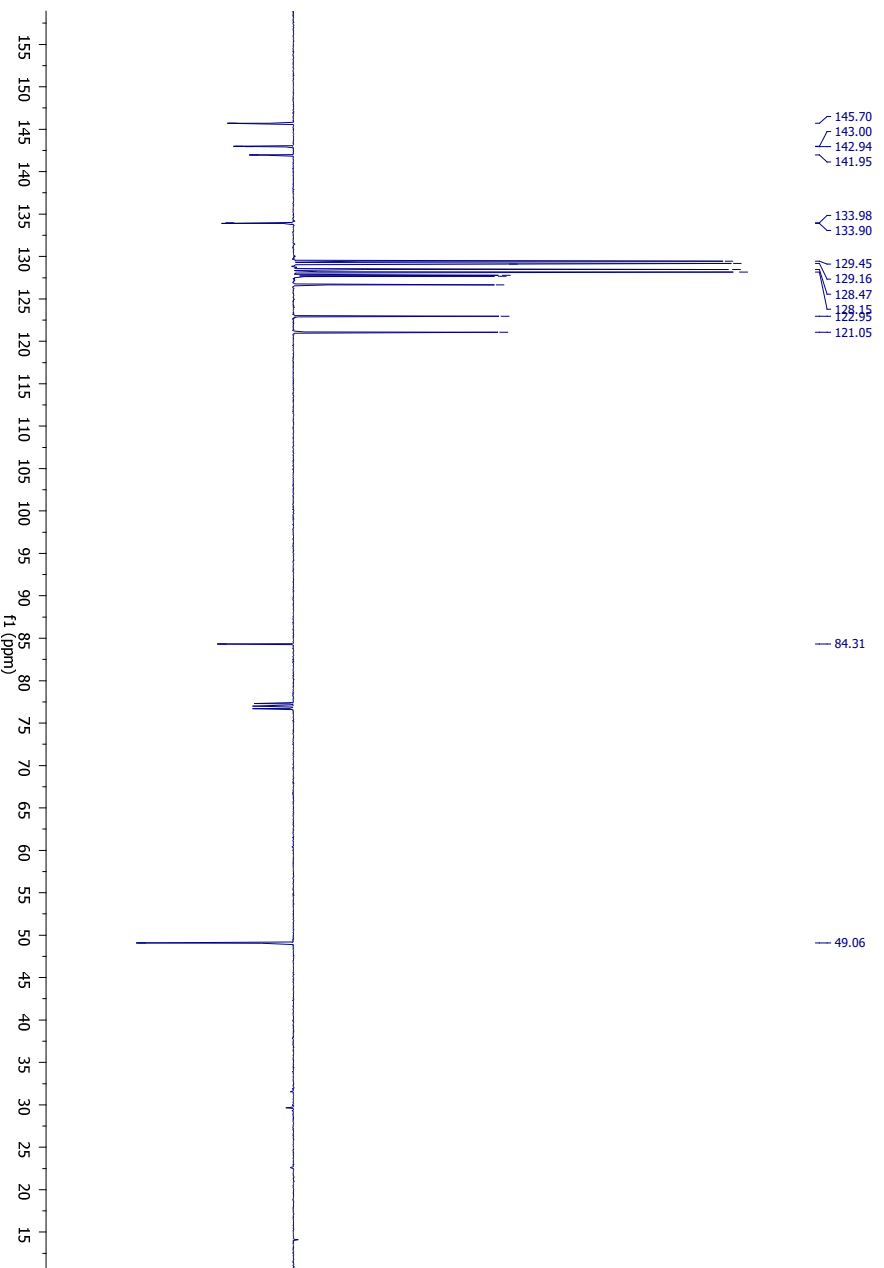
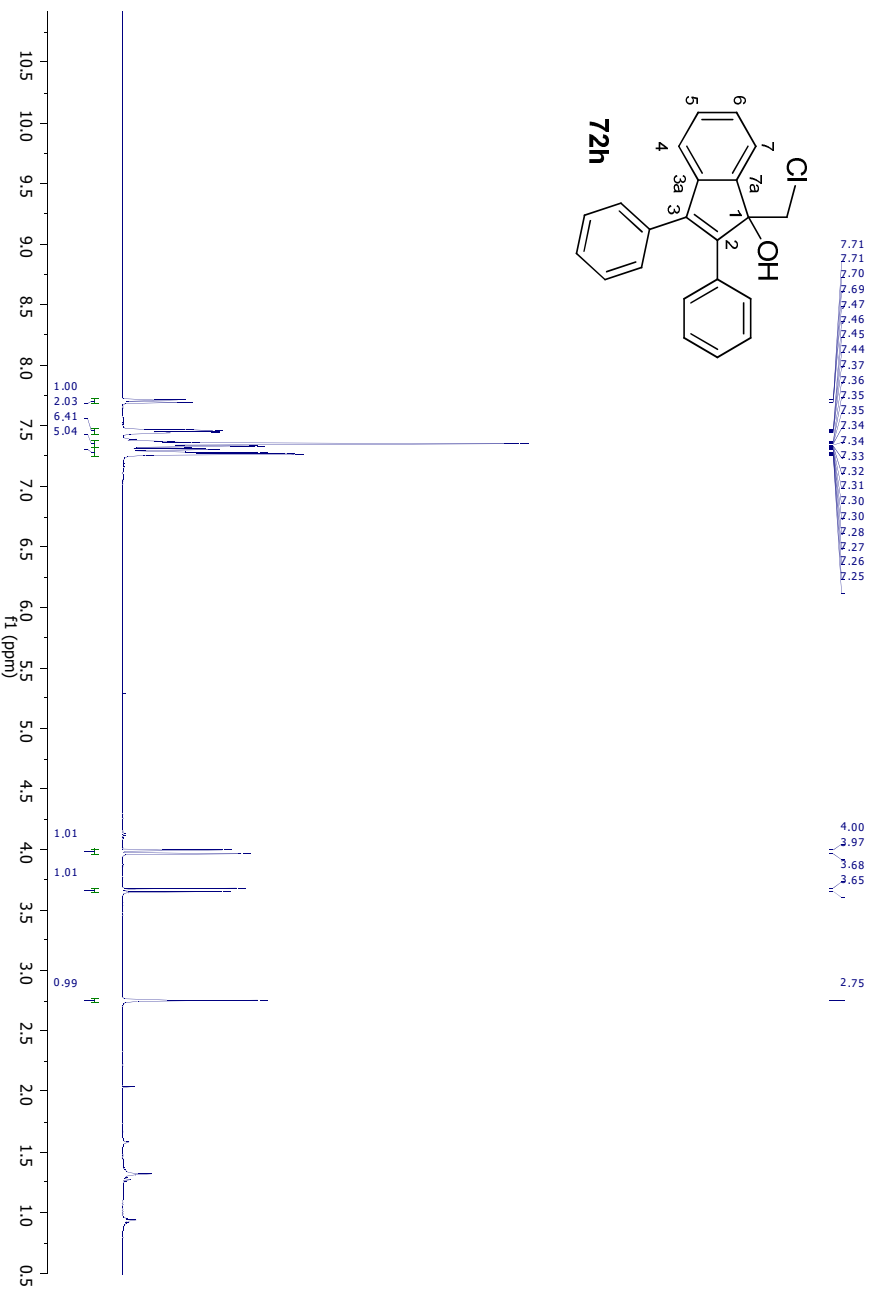
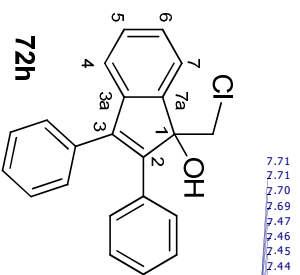


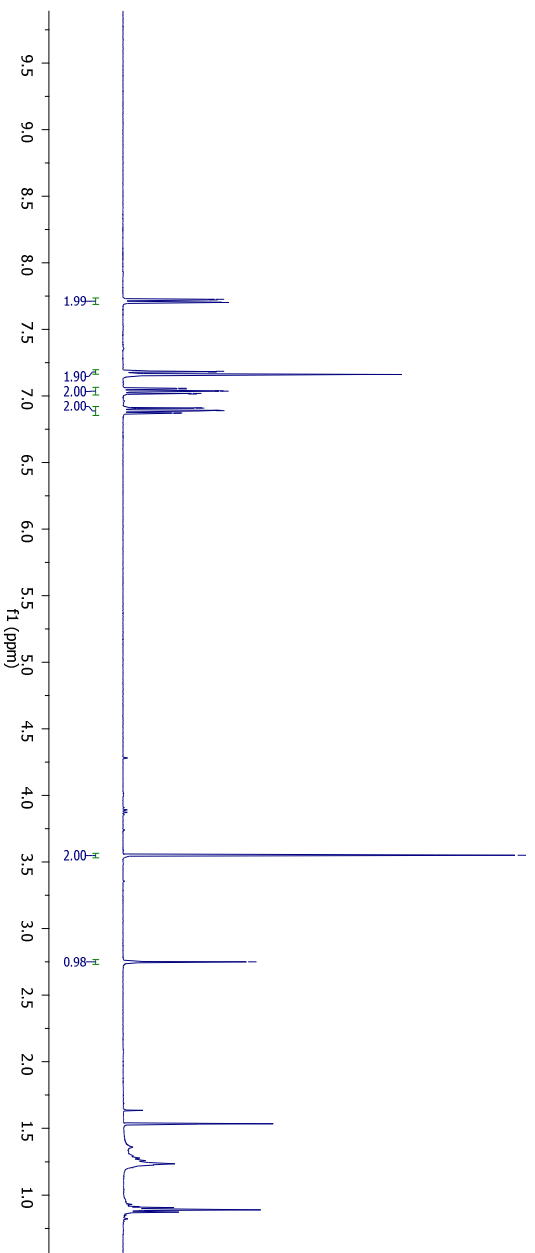
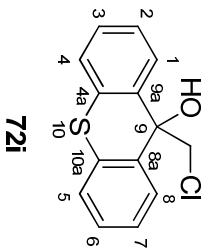








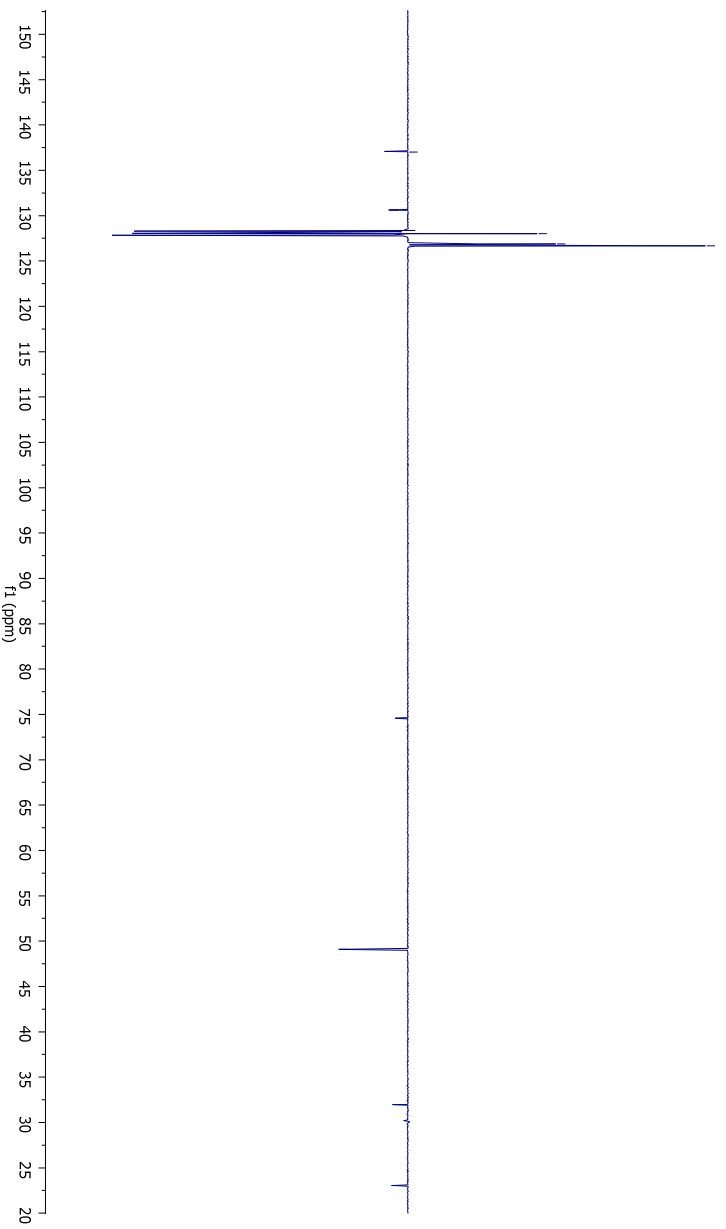




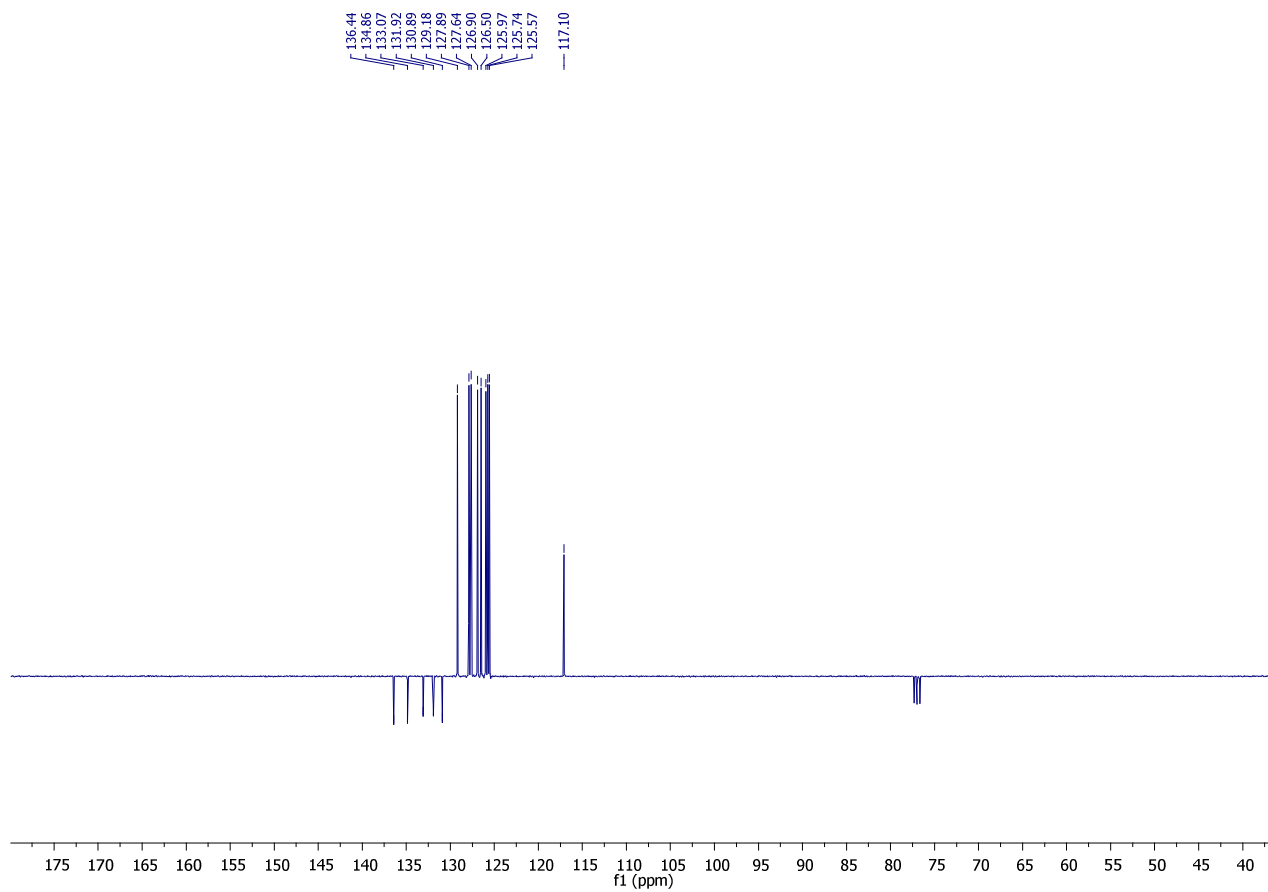
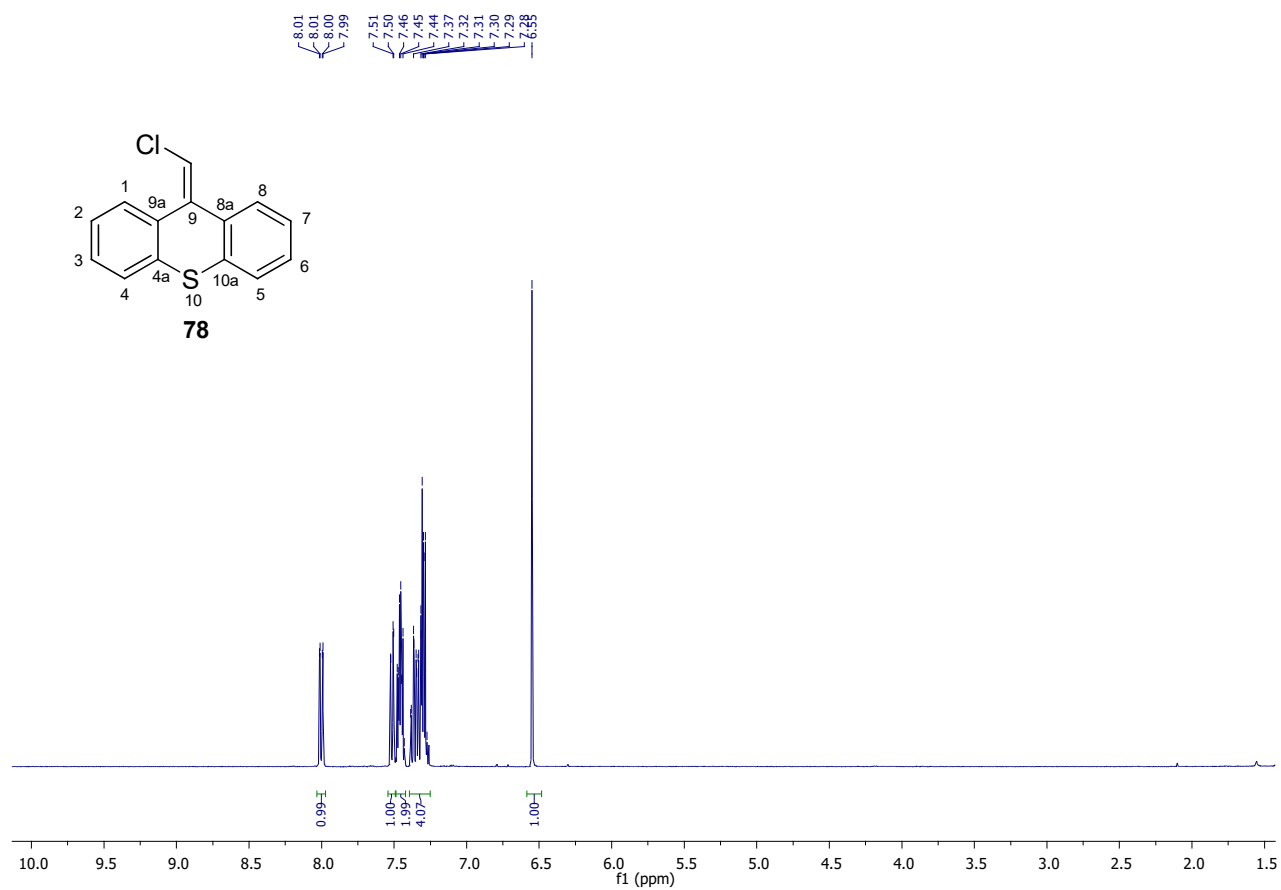
137.01
130.63
128.02
126.88
126.67

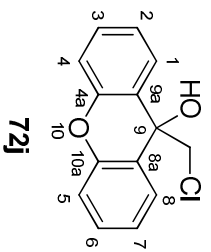
74.57

49.10



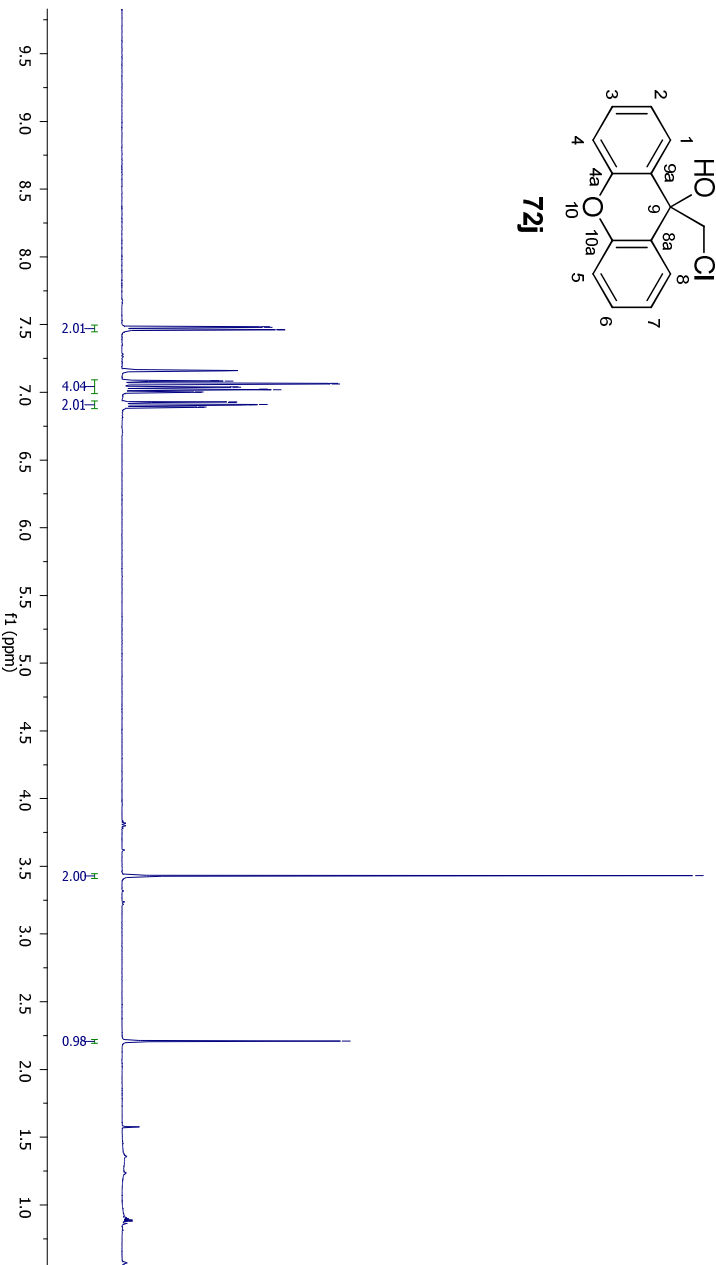
Experimental Section





3.43

2.21



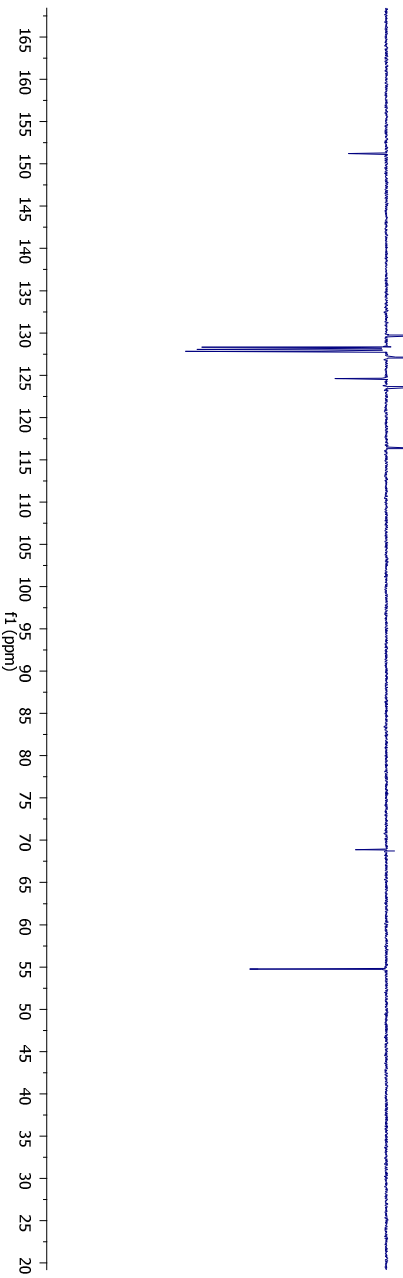
151.21

129.68
127.11
124.62
123.54

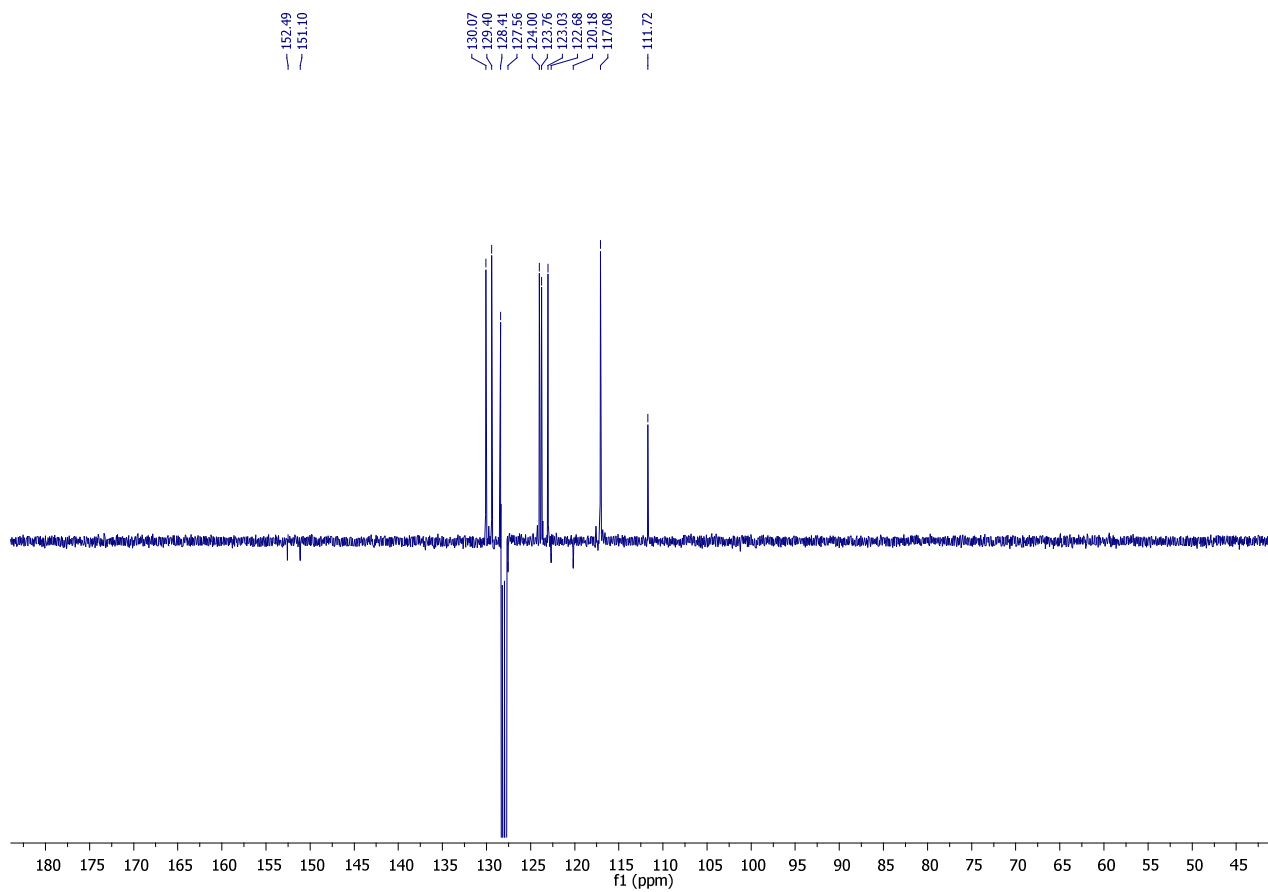
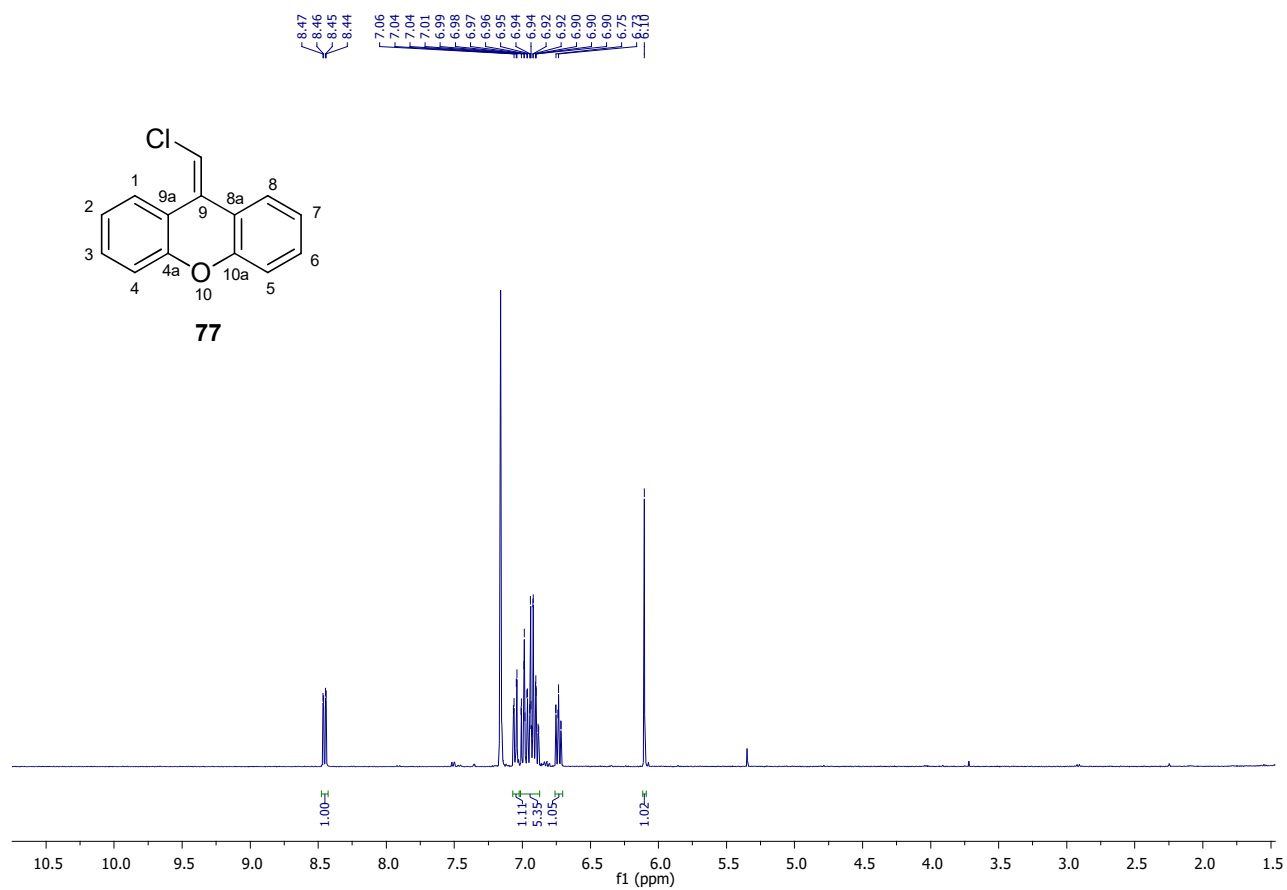
116.38

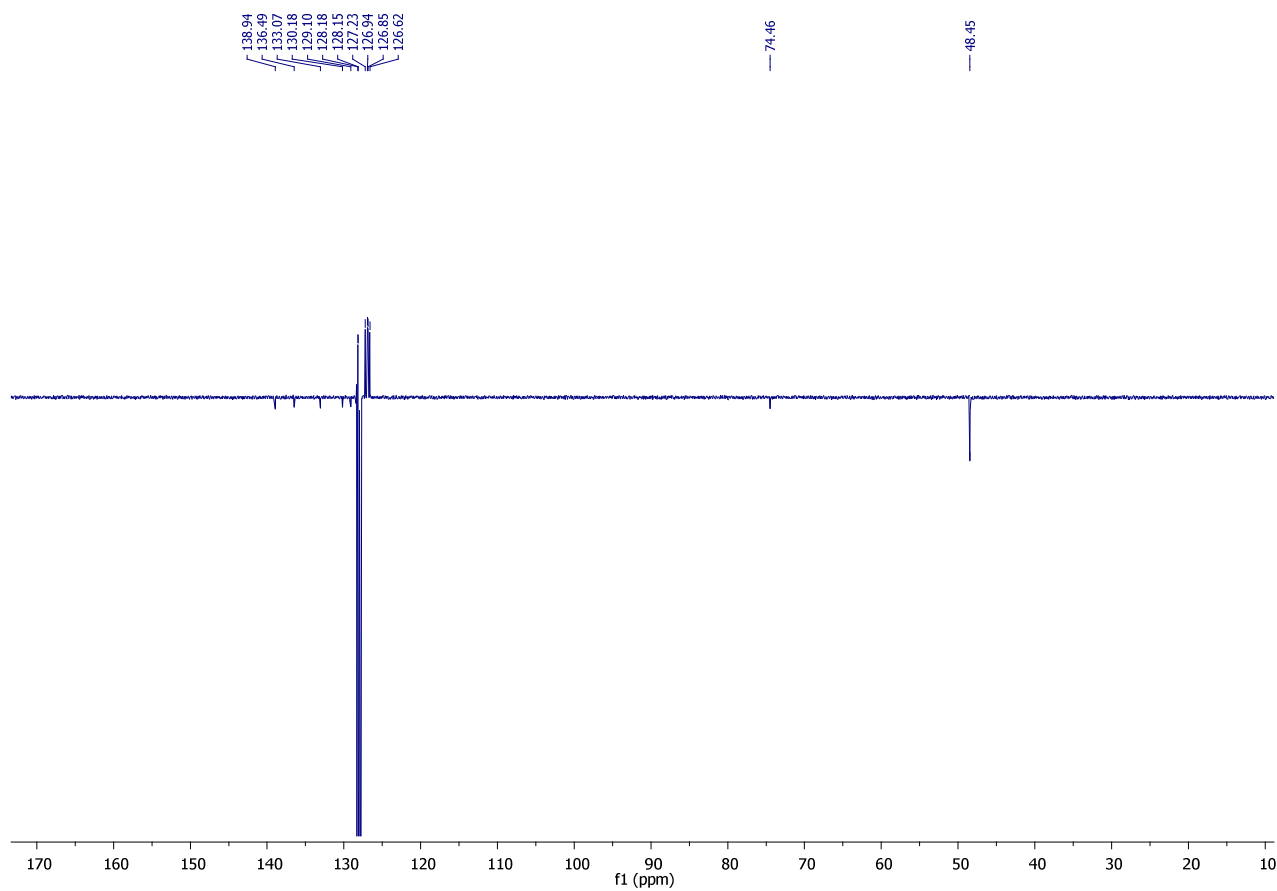
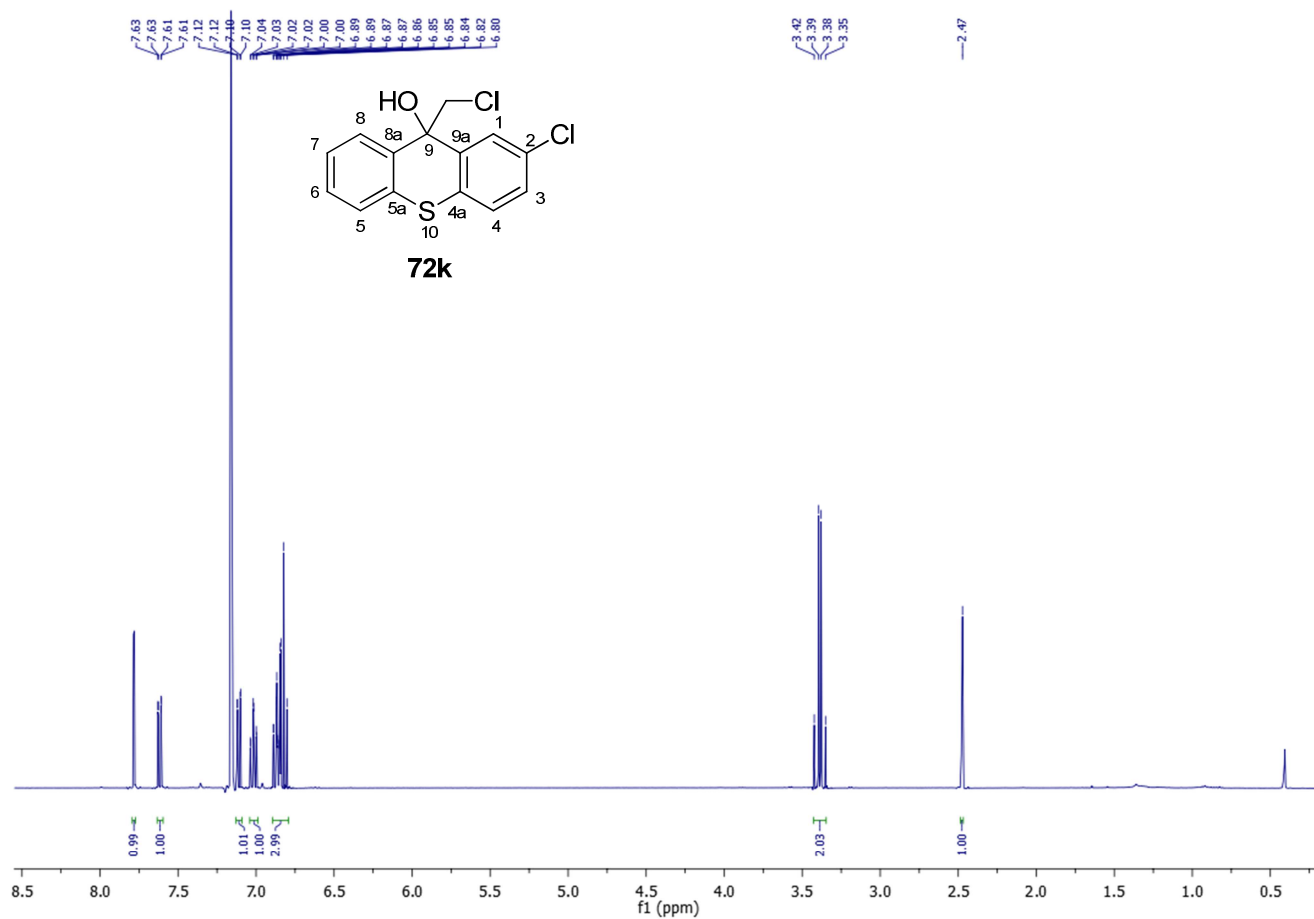
68.74

54.75

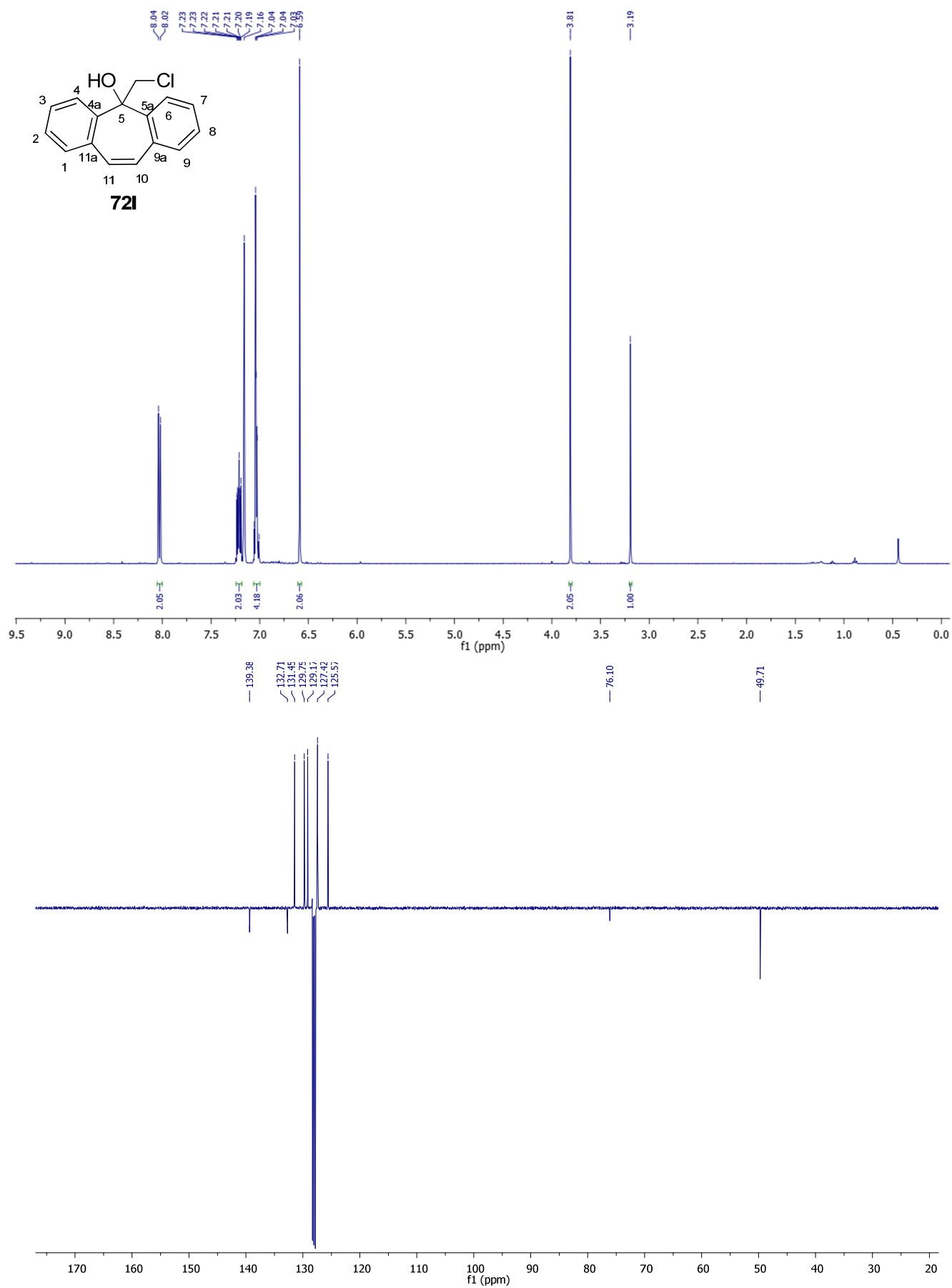


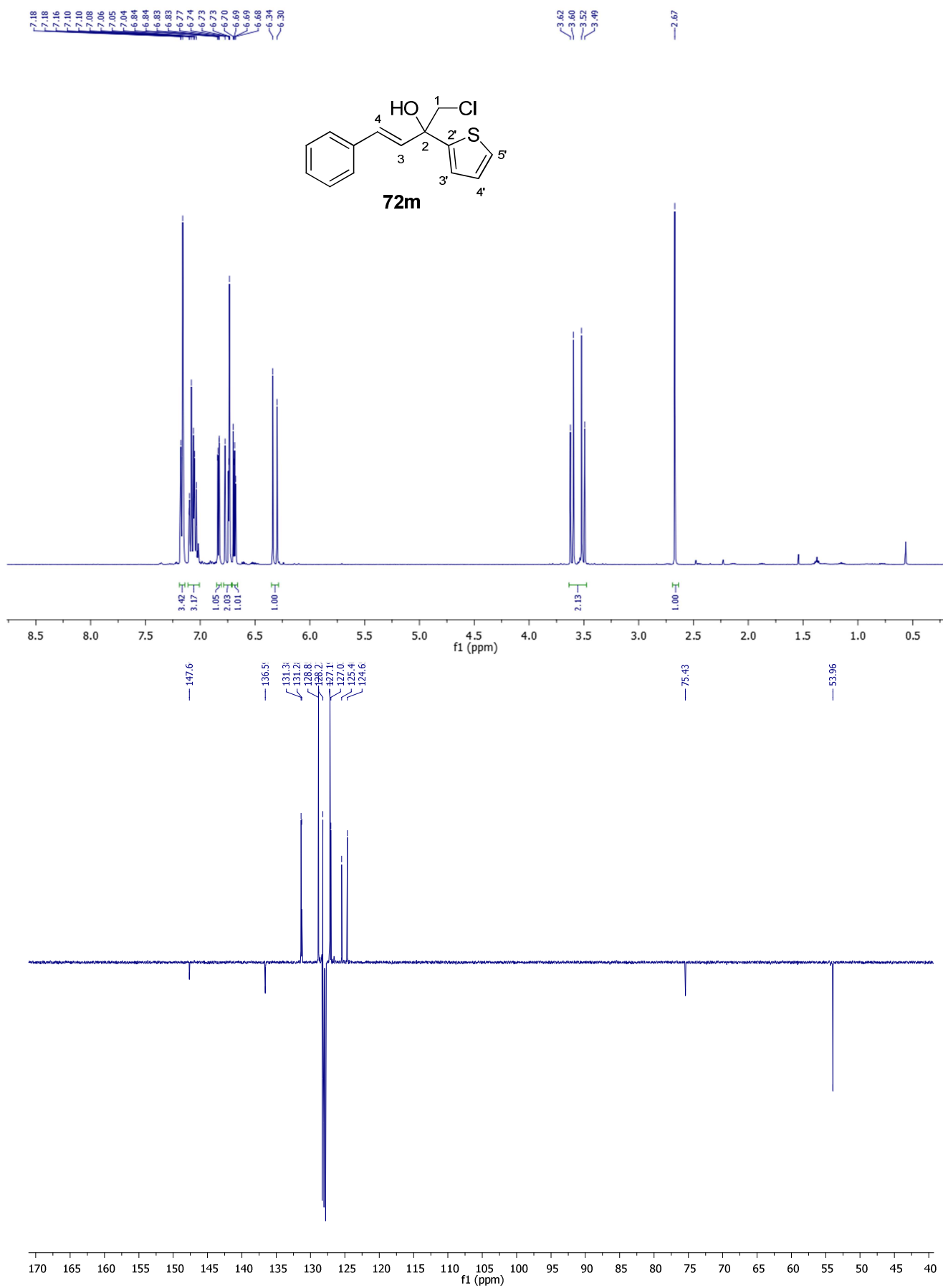
Experimental Section



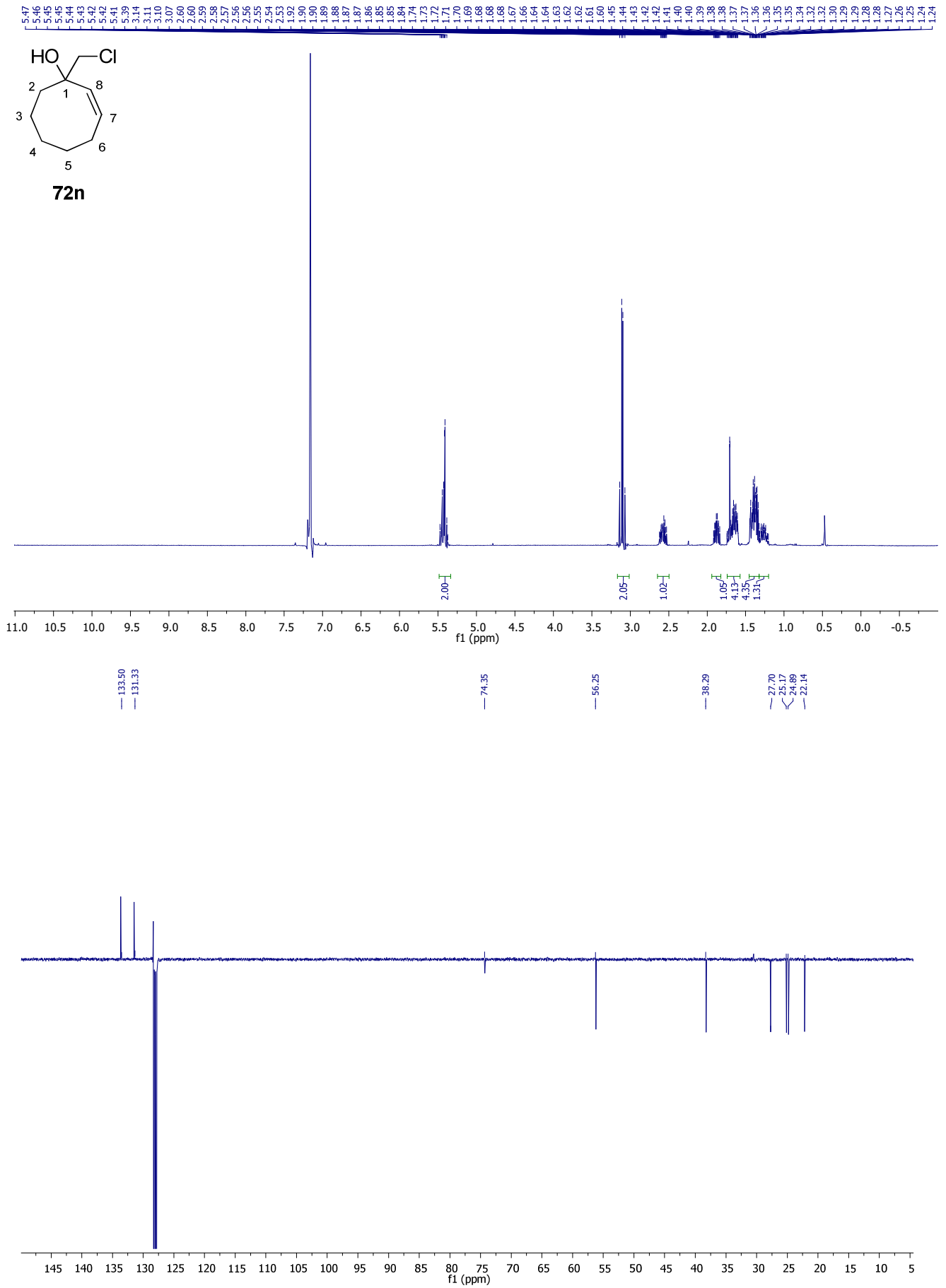


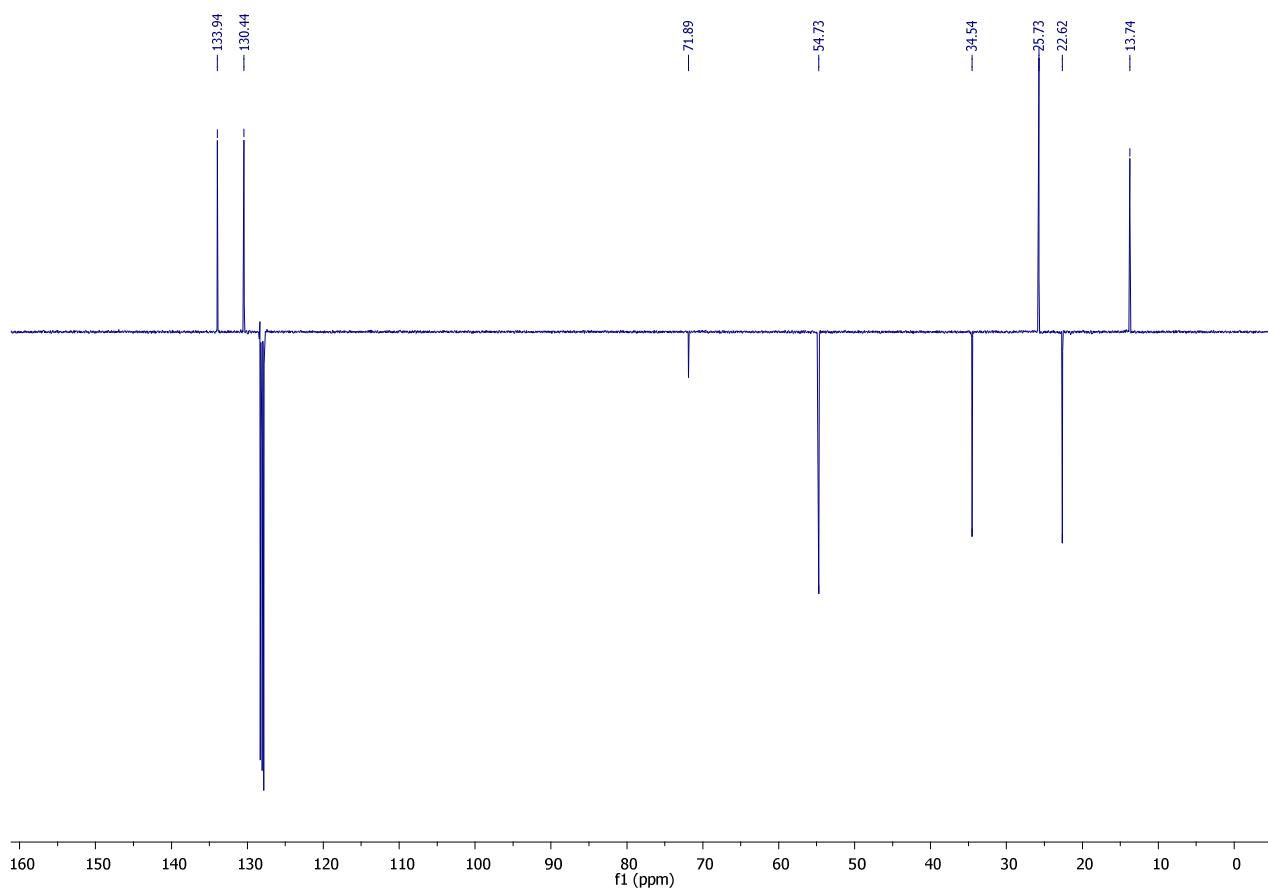
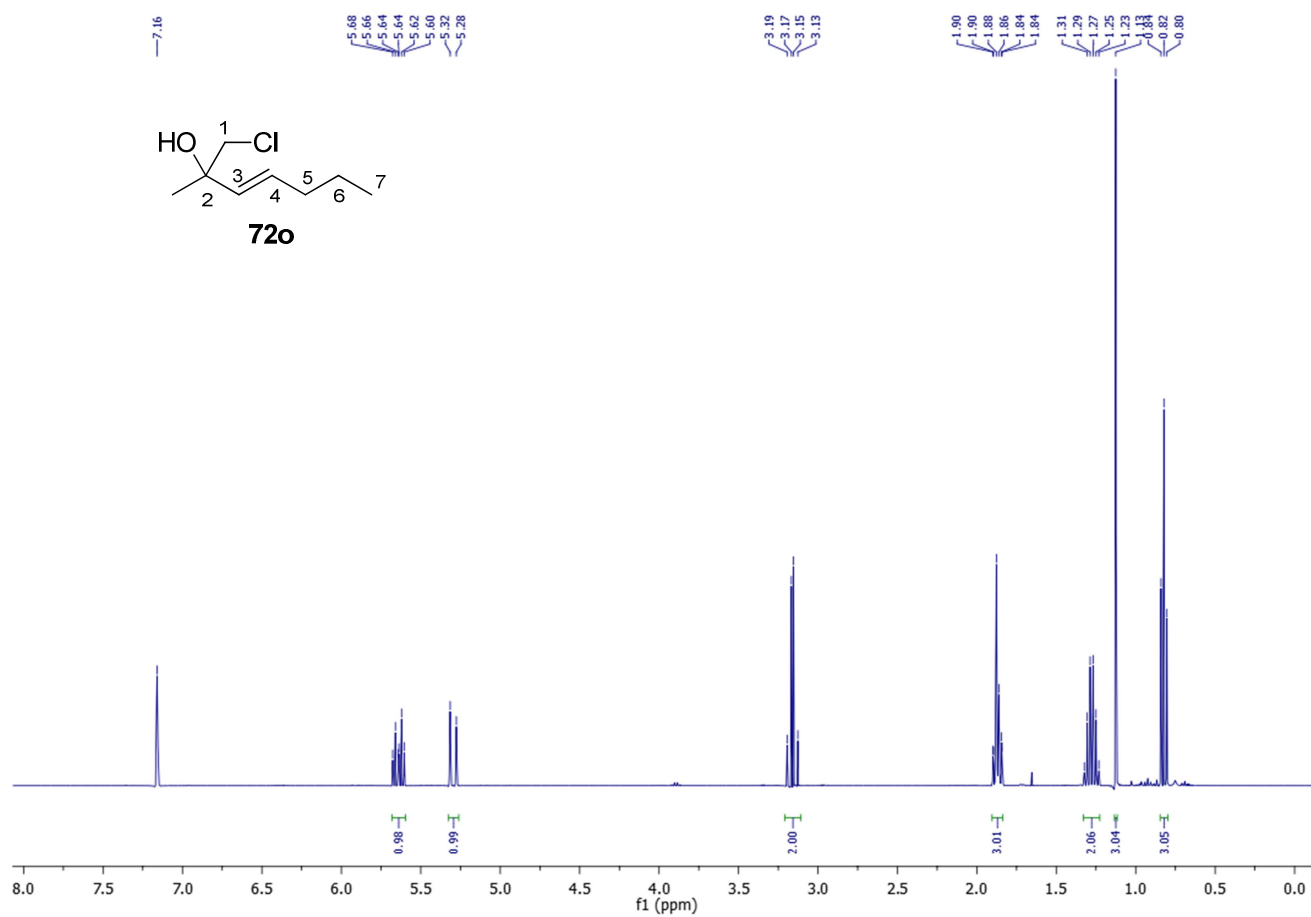
Experimental Section





Experimental Section

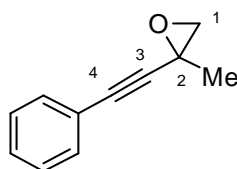




4.3. General Procedure for the conversion of the halohydrins into epoxides

A round bottom flask was torched under a stream of argon and charged with THF (1 M). The reaction vessel was cooled to 0 °C in an ice bath and NaH (95%, 1.1 eq) and NaI (10 mol%) were added. The heterogenous mixture was stirred for 5 minutes then halohydrin (1.0 equiv) dissolved in an equal volume of THF, was added slowly over 30 minutes. When the addition was complete the reaction was maintained at 0 °C and the reaction progress followed by TLC. When the starting material was consumed the reaction was quenched with saturated aq. NH₄Cl (2 mL) and extracted with Et₂O (3 x 5 mL). The organic layer was washed with brine (5 mL), dried over Na₂SO₄, filtered and after removing the solvent under reduced pressure (bath 20 °C), the pure epoxide was obtained.

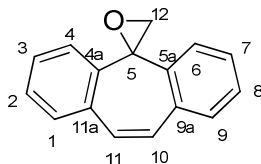
2-methyl-2-(phenylethynyl)oxirane (80a)



By following the General Procedure, starting 1-chloro-2-methyl-4-phenyl-3-butyn-2-ol (194 mg, 1.00 mmol, 1.0 equiv.), NaH (95%, 1.1 equiv), NaI (10% mol) and THF (1 M), the desired product was obtained in 98% (155 mg) as a a bright yellow oil.

¹H NMR (400 MHz, C₆D₆) δ: 7.37 (m, 2H, Ph H-2,6), 6.93 (m, 3H, Ph H-3,4,5), 2.80 (d, *J* = 5.7 Hz, 1H, H-1), 2.26 (d, *J* = 5.7 Hz, 1H, H-1), 1.37 (s, 3H, Me). **¹³C NMR** (100 MHz, CDCl₃) δ: 132.1 (Ph C-2,6), 128.7 (Ph C-4), 128.6 (Ph C-3,5), 122.9 (Ph C-1), 89.7 (C-3), 82.3 (C-4), 55.1 (C-1), 47.4 (C-2), 23.1 (Me). **ESI-HRMS** *m/z*: 159.67 [M+H]⁺

Spiro[dibenzo[a,d][7]annulene-5,2'-oxirane (80b)

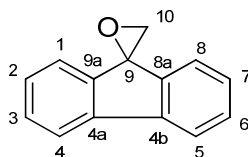


By following the General Procedure, starting 5-(chloromethyl)-5*H*-dibenzo[a,d][7]annulene-5-ol (256 mg, 1.00 mmol, 1.0 equiv.), NaH (95%, 1.1 equiv), NaI (10% mol) and THF (1 M), the desired product was obtained in 89% (196 mg) as a a bright yellow oil.

¹H NMR (400 MHz, C₆D₆) δ: 7.83 (m, 2H, H-4,6), 7.12 (m, 2H, H-3,7), 7.05 (m, 2H, H-1,9), 7.03(m, 2H, H-2,8), 6.77 (s, 2H, H-10,11), 2.41 (s, 2H, H-12). **¹³C NMR** (100 MHz, C₆D₆) δ: 138.8

(C-4a,5a), 134.6 (C-9a,10a), 131.5 (C-10,11), 128.9 (C-3,7), 128.4 (C-1,9), 127.5 (C-2,8), 124.4 (C-4,6), 60.6 (C-5), 57.7 (C-12). **ESI-HRMS** m/z : 221.14 [M+H]⁺

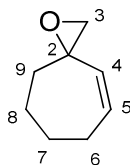
spiro[fluorene-9,2'-oxirane] (80c)



By following the General Procedure, starting 9-(chloromethyl)-9H-fluoren-9-ol (231 mg, 1.00 mmol, 1.0 equiv.), NaH (95%, 1.1 equiv), NaI (10% mol) and THF (1 M), the desired product was obtained in 92% (179 mg) as a bright yellow oil.

¹H NMR (400 MHz, C₆D₆) δ : 7.41 (m, 2H, H-4,5), 7.13 (m, 2H, H-3,6), 7.03 (m, 2H, H-1,8), 7.01 (m, 2H, H-2,7), 3.14 (s, 2H, H-10). **¹³C NMR** (100 MHz, C₆D₆) δ : 141.7 (C-8a,9a), 141.5 (C-4a,4b), 129.3 (C-3,6), 127.7 (C-2,7), 122.1 (C-1,8), 120.5 (C-4,5), 62.3 (C-9), 54.5 (C-10). **ESI-HRMS** m/z : 195.11 [M+H]⁺

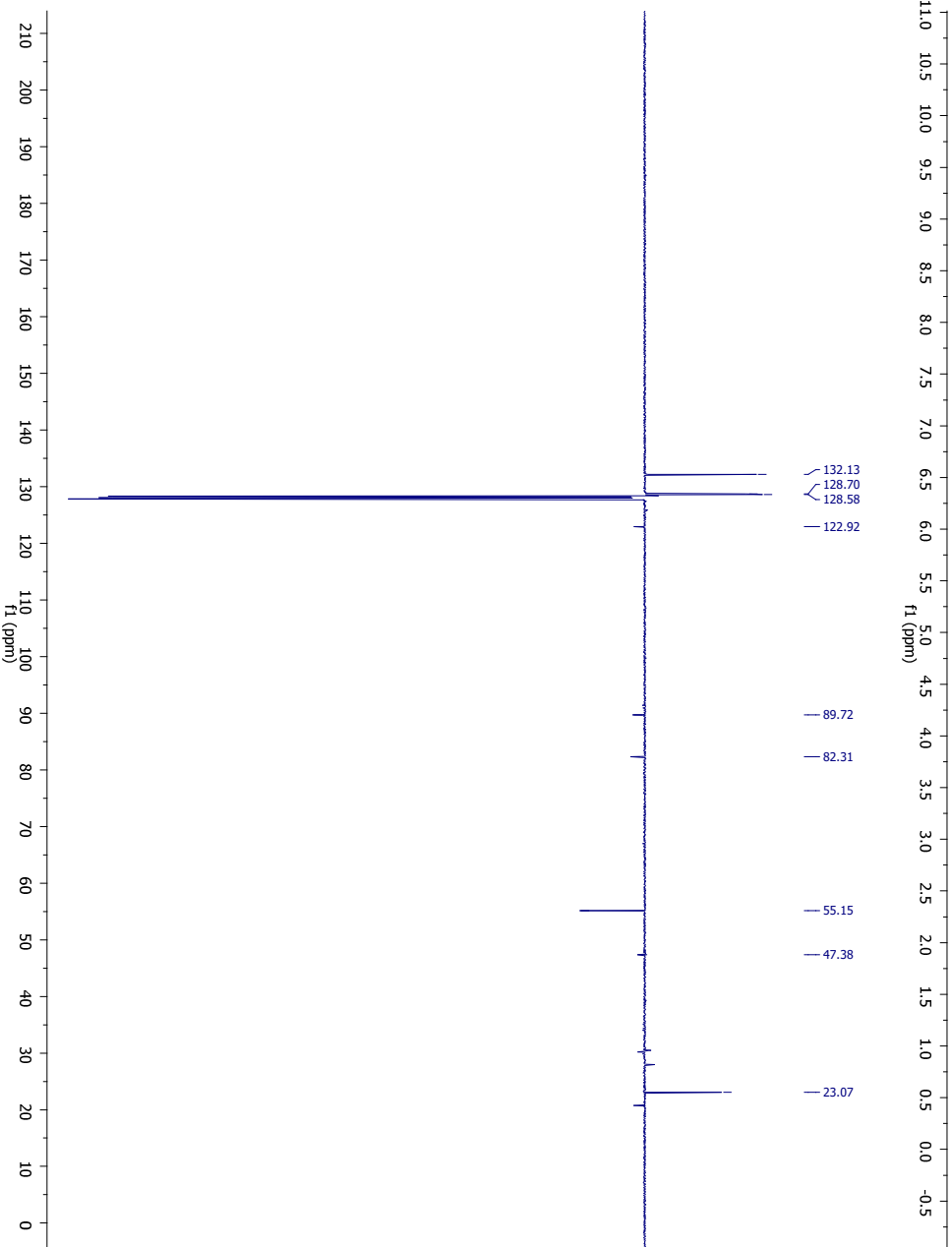
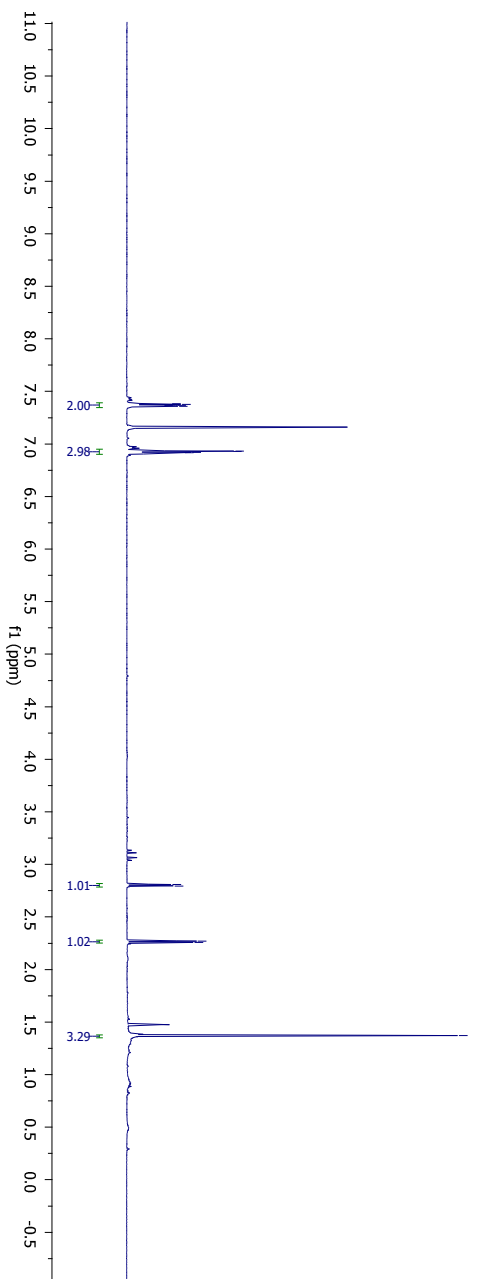
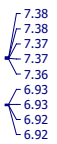
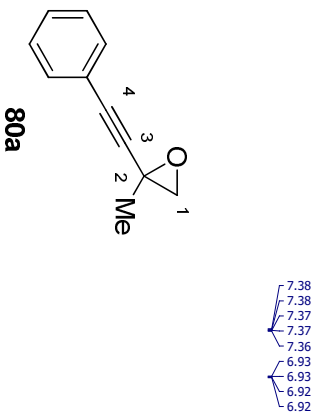
1-oxaspiro[2.6]non-4-ene (80d)

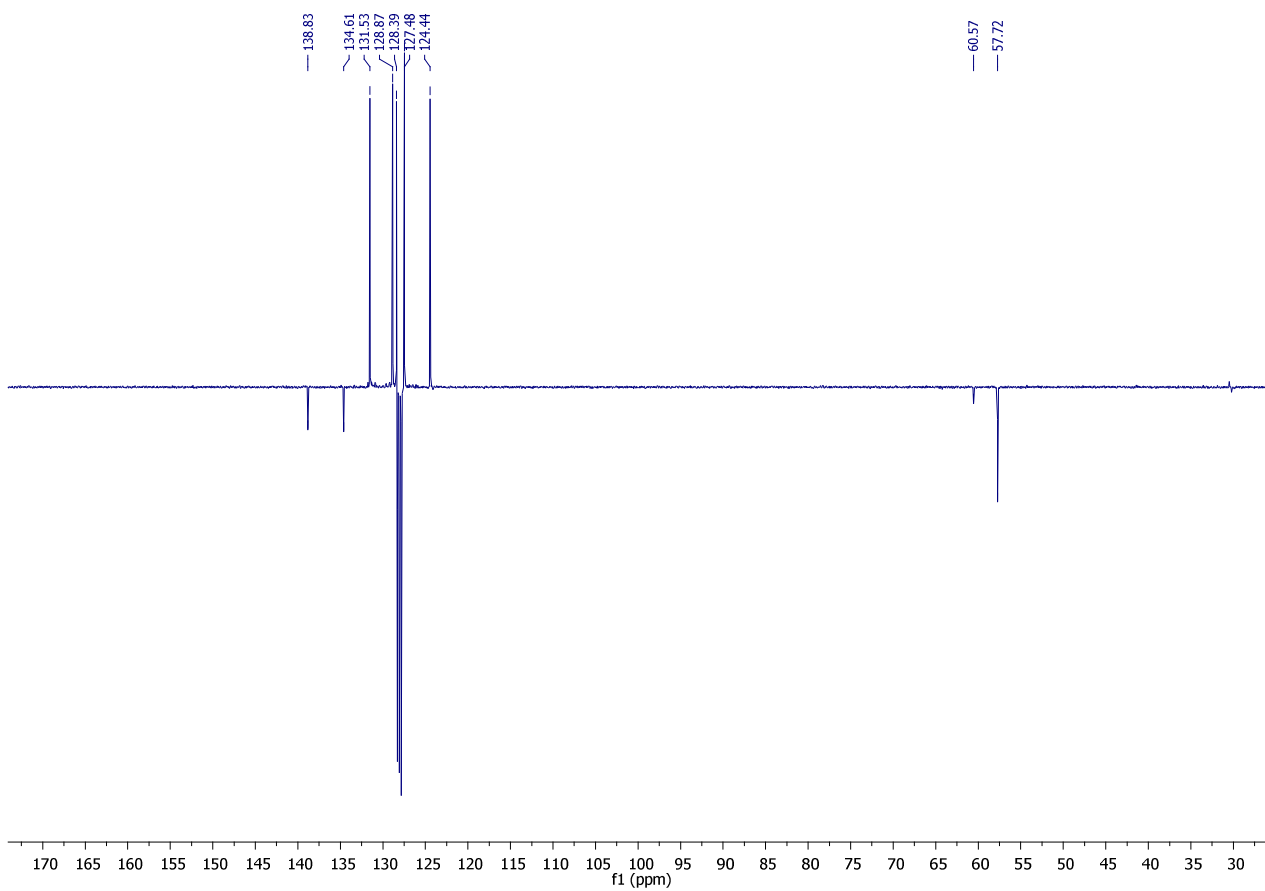
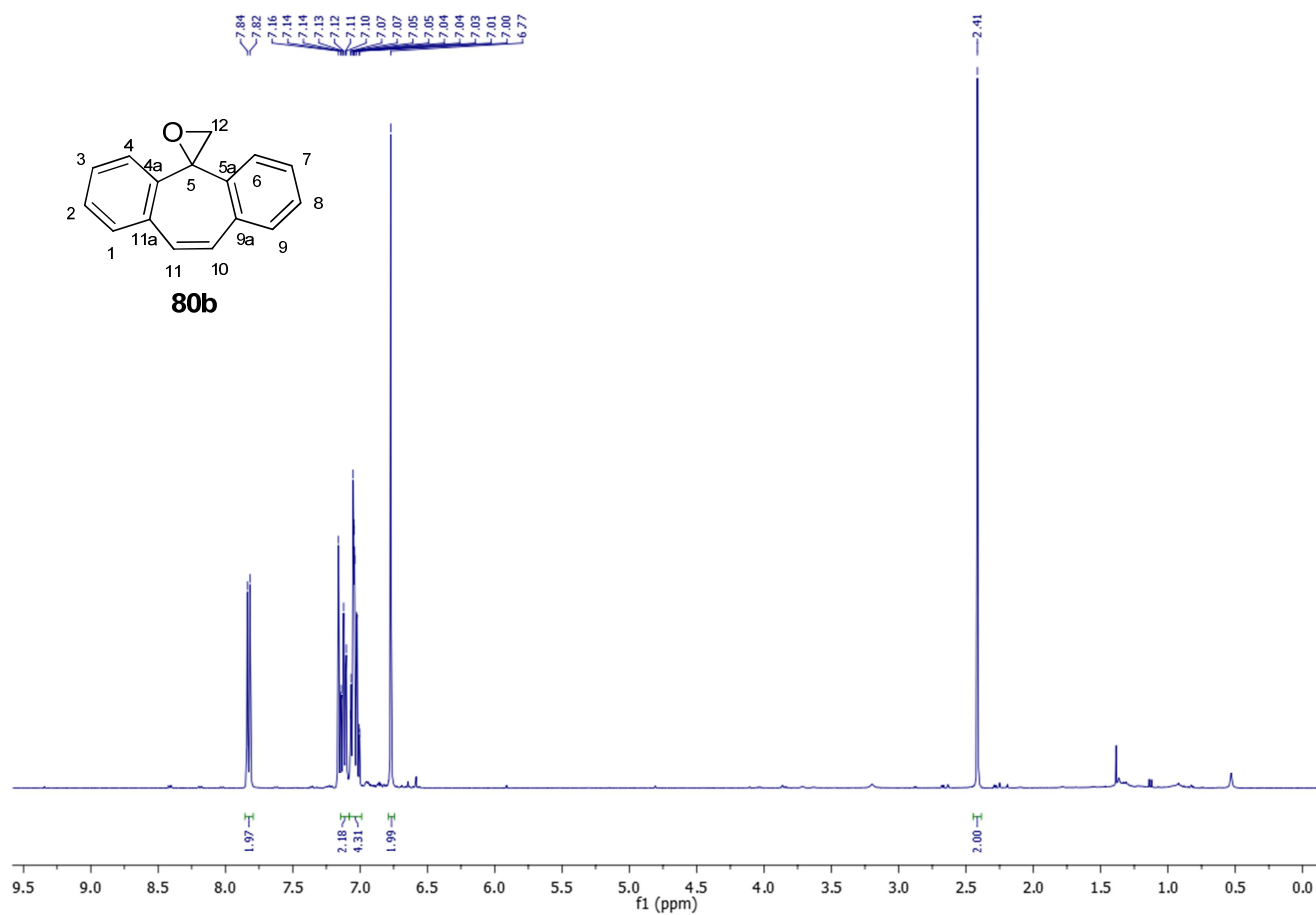


By following the General Procedure, starting 1-(chloromethyl)cyclohept-2-enol (161 mg, 1.00 mmol, 1.0 equiv.), NaH (95%, 1.1 equiv), NaI (10% mol) and THF (1 M), the desired product was obtained in 91% (113 mg) as a bright yellow oil.

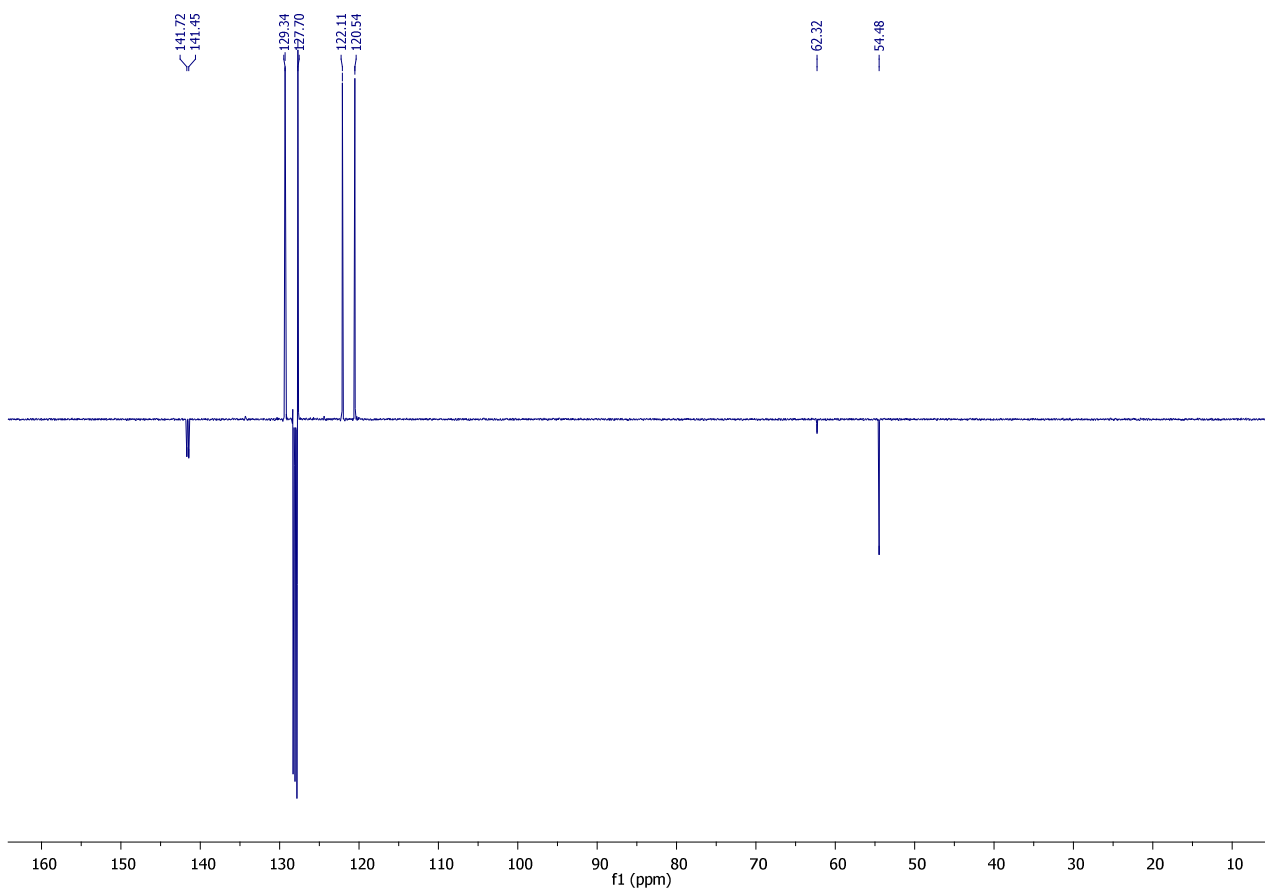
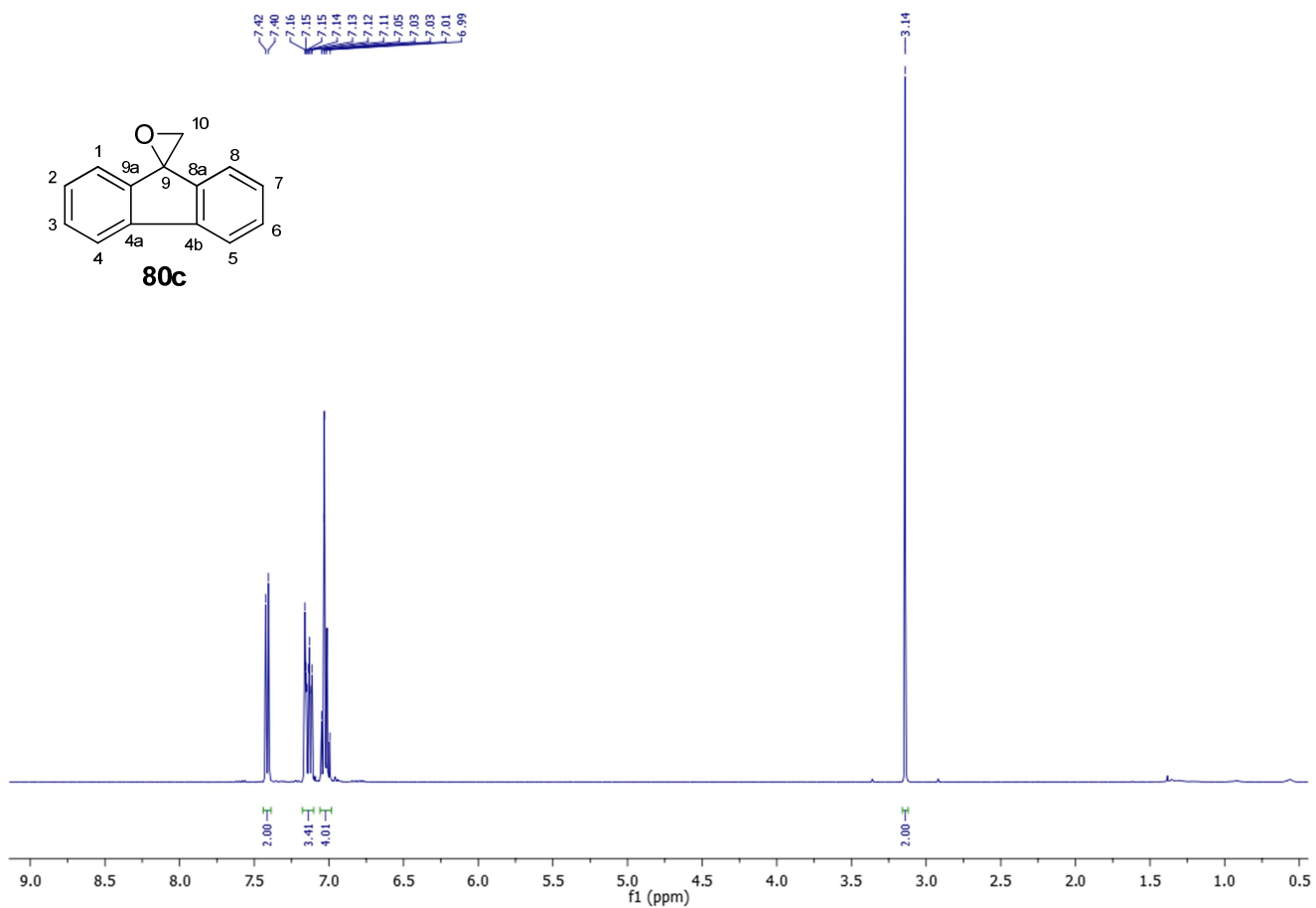
¹H NMR (400 MHz, CDCl₃) δ : 5.71 (d, J = 11.7 Hz, 1H, H-5), 5.41 (d, J = 11.7 Hz, 1H, H-4), 2.44 (dd, J = 5.5 and 1.3 Hz, 1H, H-3), 2.41 (d, J = 5.5 Hz, 1H, H-3), 1.97 (m, 1H, H-6), 1.93 (m, 1H, H-6), 1.86 (m, 1H, H-9), 1.61 (m, 1H, H-8), 1.48 (m, 1H, H-7), 1.44 (m, 1H, H-7), 1.42 (m, 2H, H-9), 1.36 (m, 2H, H-8). **¹³C NMR** (100 MHz, CDCl₃) δ : 133.9 (C-4), 134.0 (C-5), 58.4 (C-2), 54.2 (C-3), 35.7 (C-9), 28.6 (C-6), 27.3 (C-7), 25.4 (C-8). **ESI-HRMS** m/z : 125.16 [M+H]⁺

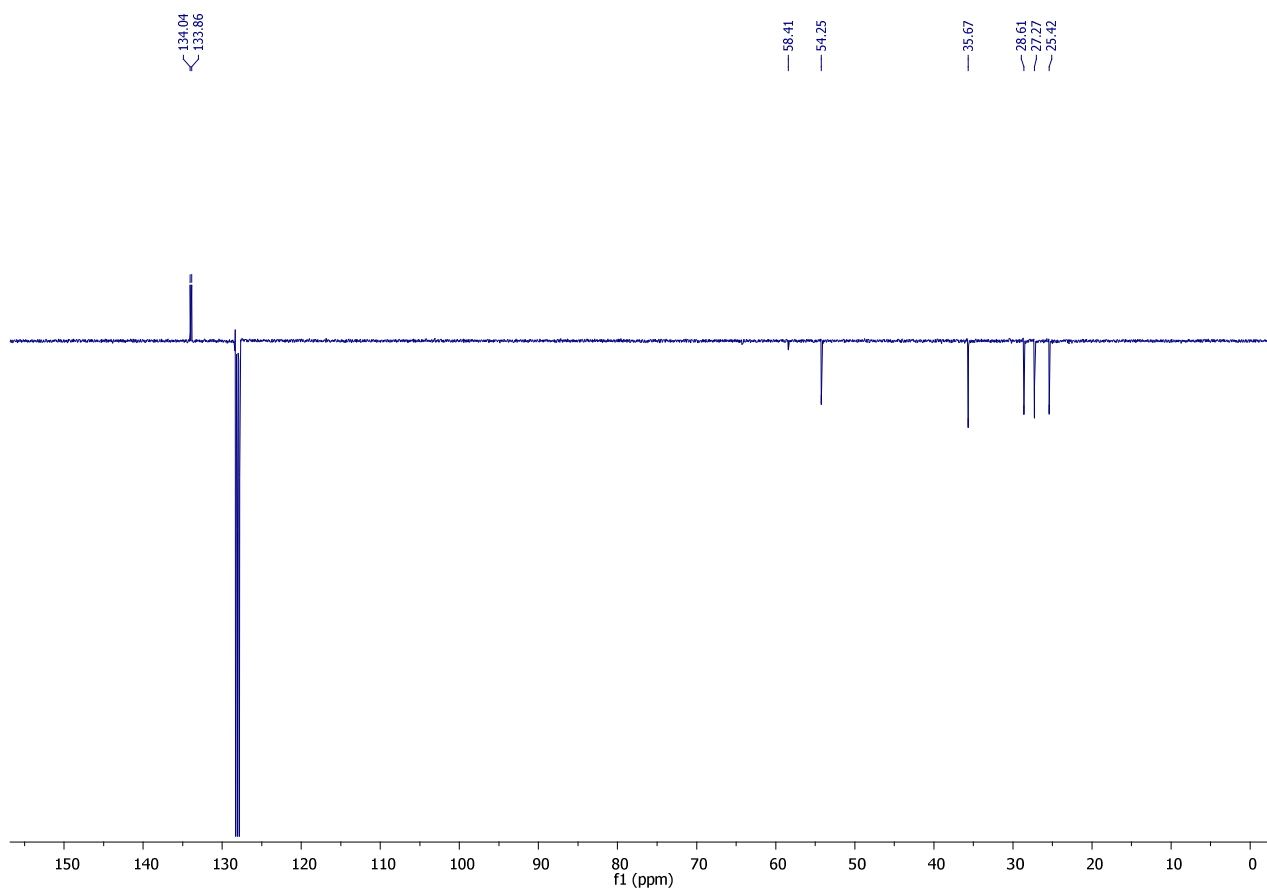
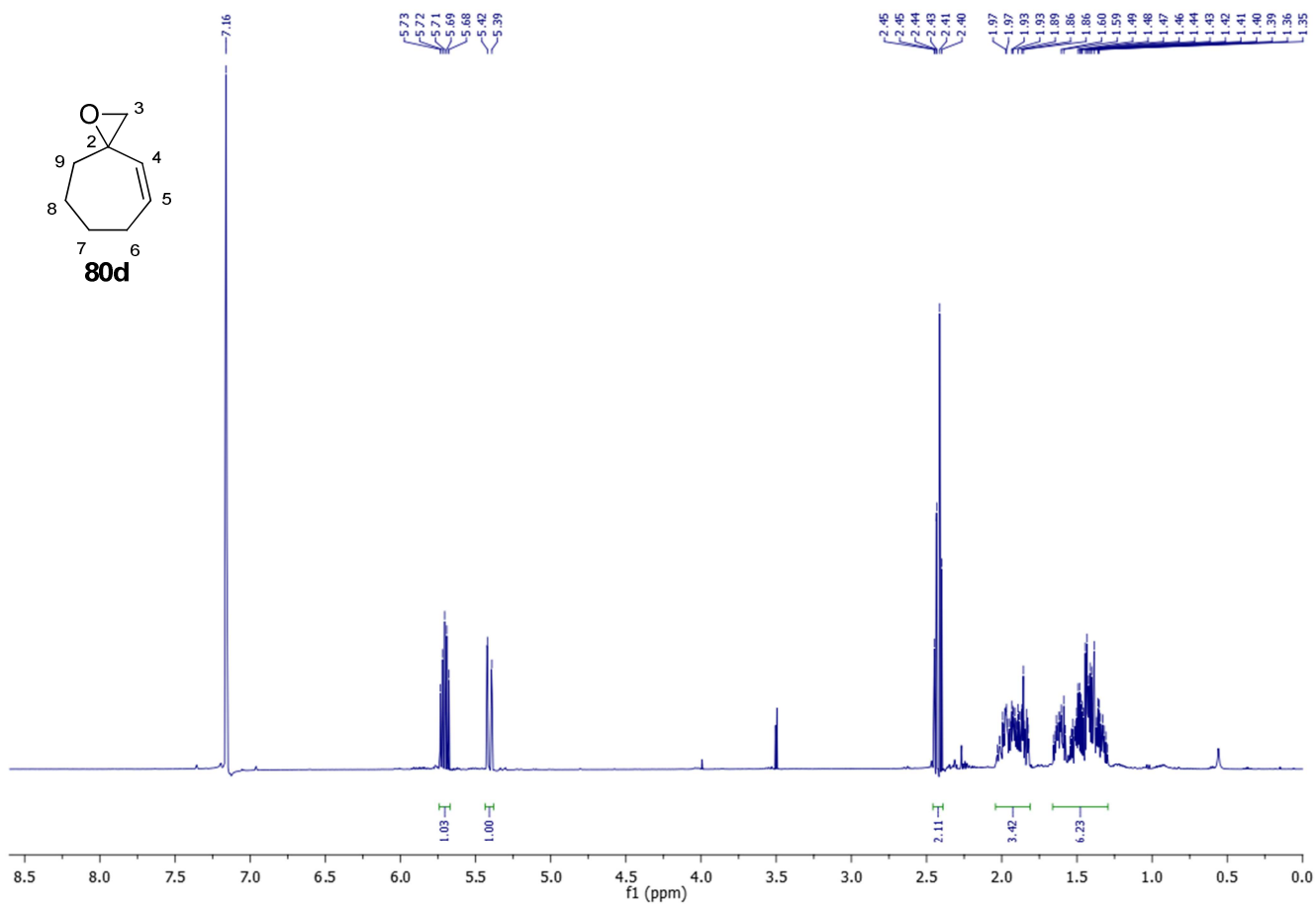
Copies of NMR spectra





Experimental Section

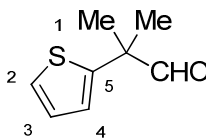




4.4. General Procedure for the Chemoselective Addition of LiCH₂Cl to Ketones to obtain aldehydes

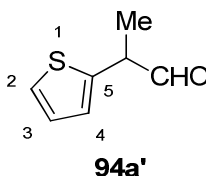
To a cooled (-78 °C) solution of enone (1.0 equiv) in dry THF was added chloriodomethane (3.0 equiv). After 2 min, an ethereal solution of MeLi-LiBr (2.8 equiv, 1.5 M) was added dropwise, using a syringe pump (flow: 0.200 mL/min). The resulting solution was stirred overnight until the room temperature was reached. Saturated aq NH₄Cl was added (2 mL/mmol substrate) and then, it was extracted with Et₂O (2 x 5 mL) and washed with water (5 mL) and brine (10 mL). The organic phase was dried (anhydrous Na₂SO₄), filtered and, after removal of the solvent under reduced pressure, the so-obtained crude mixture was subjected to chromatography (silica gel) to afford pure compounds.

2-methyl-2-(2-thienyl)propanal (94a)

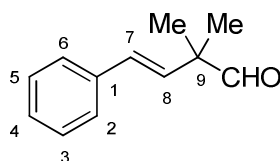


By following the General Procedure, starting from 1-(thiophen-2-yl)ethanone (126 mg, 1.00 mmol, 1.0 equiv), ICH₂Cl (529 mg, 0.22 mL, 3.0 mmol, 3.0 equiv), MeLi-LiBr complex (1.5 M, 1.87 mL, 2.8 mmol, 2.8 equiv) and THF (2 mL), the desired product was obtained in 73% (113 mg) as a bright yellow oil after chromatography on silica gel (90:10 hexane:ethylacetate).

¹H NMR (400 MHz, C₆D₆) δ: 9.10 (s, 1H, CHO), 6.80 (dd, *J* = 5.1 and 1.2 Hz, 1H, H-2), 6.67 (dd, *J* = 5.1 and 3.6 Hz, 1H, H-3), 6.54 (dd, *J* = 3.6 and 1.2 Hz, 1H, H-4), 1.20 (s, 6H, Me). ¹³C NMR (100 MHz, C₆D₆) δ: 198.6 (CHO), 146.3 (C-5), 127.5 (C-3), 125.2 (C-2), 124.8 (C-4), 48.7, 23.4 (Me). ESI-HRMS *m/z*: 155.57 [M+H]⁺

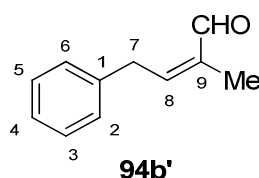


2-(2-thionyl)propanal (94a') ¹H NMR (400 MHz, C₆D₆) δ: 9.24 (d, *J* = 1.5 Hz, 1H, CHO), 6.78 (dd, *J* = 5.1 and 1.2 Hz, 1H, H-2), 6.67 (dd, *J* = 5.1 and 3.5 Hz, 1H, H-3), 6.49 (ddd, *J* = 3.6, 1.2 and 0.8 Hz, 1H, H-4), 3.19 (m, 1H, CH), 1.14 (d, *J* = 7.1 Hz, 3H, Me). ¹³C NMR (100 MHz, C₆D₆) δ: 197.0 (CHO), 140.7 (C-5), 127.5 (C-3), 125.5 (C-4), 125.1 (C-2), 47.8, 15.3 (Me).

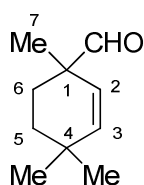
(3E)-2,2-dimethyl-4-phenyl-3-butenal (94b)

By following the General Procedure, starting from (E)-4-phenylbut-3-en-2-one (146 mg, 1.00 mmol, 1.0 equiv), ICH₂Cl (529 mg, 0.22 mL, 3.0 mmol, 3.0 equiv), MeLi-LiBr complex (1.5 M, 1.87 mL, 2.8 mmol, 2.8 equiv) and THF (2 mL), the desired product was obtained in 81% (141 mg) as a bright yellow oil after chromatography on silica gel (90:10 hexane:ethylacetate).

¹H NMR (400 MHz, C₆D₆) δ: 9.18 (s, 1H, CHO), 7.13 (m, 2H, H-2, 6), 7.11 (m, 2H, H-3, 5), 7.06 (m, 1H, H-4), 6.25 (d, *J* = 16.3 Hz, 1H, H-7), 5.93 (d, *J* = 16.3 Hz, 1H, H-8), 0.99 (s, 6H, Me). ¹³C NMR (100 MHz, C₆D₆) δ: 200.7 (CHO), 137.2 (C-1), 131.6 (C-8), 131.2 (C-7), 128.8 (C-3, 5), 128.0 (C-4), 126.8 (C-2, 6), 48.6 (C-9), 21.5 (Me). ESI-HRMS *m/z*: 175.86 [M+H]⁺



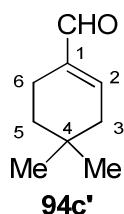
(Z)-2-methyl-4-phenyl-2-butenal (94b') ¹H NMR (400 MHz, C₆D₆) δ: 9.20 (s, 1H, CHO), 7.14-7.01 (m, 3H, H-2, 6, 4), 6.89-6.84 (m, 2H, H-3, 5), 5.98-5.93 (m, 1H, H-8), 3.08 (d, *J* = 4.0 Hz, 2H, H-7), 1.64 (s, 3H, Me). ¹³C NMR (100 MHz, C₆D₆) δ: 193.9 (CHO), 150.8 (C-8), 139.7 (C-1), 138.7 (C-9), 128.9 (C-2, 6), 128.7 (C-3, 5), 126.8 (C-4), 34.9 (C-7), 9.25 (Me).

1,4,4-trimethyl-2-cyclohexene-1-carbaldehyde (94c)

By following the General Procedure, starting from 4,4-dimethylcyclohex-2-enone (124 mg, 1.00 mmol, 1.0 equiv), ICH₂Cl (529 mg, 0.22 mL, 3.0 mmol, 3.0 equiv), MeLi-LiBr complex (1.5 M, 1.87 mL, 2.8 mmol, 2.8 equiv) and THF (2 mL), the desired product was obtained in 89% (136 mg) as a bright yellow oil after chromatography on silica gel (96:4 pentane:diethylether).

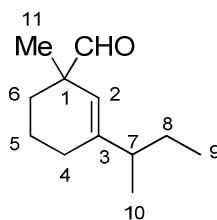
¹H NMR (400 MHz, C₆D₆) δ: 9.23 (s, 1H, CHO), 5.45 (d, *J* = 10.0 Hz, 1H, H-3), 5.14 (d, *J* = 10.0 Hz, 1H, H-2), 1.79 (m, 1H, H-6), 1.32 (m, 1H, H-5), 1.24 (m, 1H, H-5), 1.18 (m, 1H, H-6), 0.87 (s, 3H, H-7), 0.82 (s, 6H, Me). ¹³C NMR (100 MHz, C₆D₆) δ: 201.5 (CHO), 141.1 (C-3), 125.7 (C-2),

47.6 (C-1), 33.7 (C-5), 31.5 (C-4), 29.5 (Me), 29.1 (Me), 27.1 (C-6), 22.0 (C-7). **ESI-HRMS** m/z: 153.79 [M+H]⁺

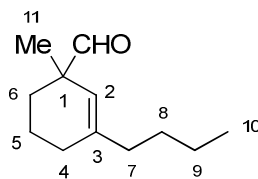


4,4-dimethyl-1-cyclohexene-1-carbaldehyde (94c') ¹H NMR (400 MHz, C₆D₆) δ: 9.31 (s, 1H, CHO), 6.00 (m, 1H, H-2), 2.20 (m, 2H, H-6), 1.58 (m, 2H, H-3), 1.05 (t, *J* = 6.5 Hz, 2H, H-5), 0.66 (s, 6H, Me). ¹³C NMR (100 MHz, C₆D₆) δ: 192.7 (CHO), 148.7 (C-2), 140.6 (C-1), 40.1 (C-3), 34.3 (C-5), 29.1 (C-4), 28.0 (Me), 19.6 (C-6).

3-sec-butyl-1-methyl-2-cyclohexene-1-carbaldehyde (94d)

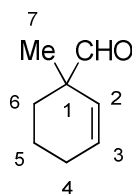


By following the General Procedure, starting from 3-(sec-butyl)cyclohex-2-enone (152 mg, 1.00 mmol, 1.0 equiv), ICH₂Cl (529 mg, 0.22 mL, 3.0 mmol, 3.0 equiv), MeLi-LiBr complex (1.5 M, 1.87 mL, 2.8 mmol, 2.8 equiv) and THF (2 mL), the desired product was obtained in 80% (144 mg) as a bright yellow oil after chromatography on silica gel (96:4 pentane:diethylether). ¹H NMR (400 MHz, C₆D₆) δ: 9.293 (s, 1H, CHO), 9.290 (s, 1H, CHO), 5.04 (s, 1H, H-2), 1.82 (m, 1H, H-7), 1.78 (m, 1H, H-6), 1.53 – 1.70 (m, 2H, H-4), 1.32 – 1.51 (m, 2H, H-5), 1.15 – 1.30 (m, 2H, H-8), 1.09 (m, 1H, H-6), 0.95 (s, 3H, H-11), 0.94 (s, 3H, H-11), 0.89 (d, *J* = 6.9 Hz, 3H, H-10), 0.76 (t, *J* = 7.4 Hz, 3H, H-9), 0.75 (t, *J* = 7.4 Hz, 3H, H-9). ¹³C NMR (100 MHz, C₆D₆) δ: 201.83 (CHO), 201.74 (CHO), 146.40 (C-3), 146.39 (C-3), 121.71 (C-2), 121.67 (C-2), 47.73 (C-1), 47.68 (C-1), 43.43 (C-7), 43.37 (C-7), 30.28 (C-6), 30.17 (C-6), 27.86 (C-8), 24.91 (C-4), 24.87 (C-4), 22.54 (C-11), 22.52 (C-11) 19.81 (C-5), 19.71 (C-5), 19.41 (C-10), 19.29 (C-10), 12.14 (C-9), 12.13 (C-9). **ESI-HRMS** m/z: 181.53 [M+H]⁺

3-butyl-1-methyl-2-cyclohexene-1-carbaldehyde (94e)

By following the General Procedure, starting from 3-butylcyclohex-2-enone (152 mg, 1.00 mmol, 1.0 equiv), ICH_2Cl (529 mg, 0.22 mL, 3.0 mmol, 3.0 equiv), MeLi-LiBr complex (1.5 M, 1.87 mL, 2.8 mmol, 2.8 equiv) and THF (2 mL), the desired product was obtained in 92% (166 mg) as a bright yellow oil after chromatography on silica gel (96:4 pentane:diethylether).

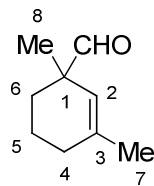
$^1\text{H NMR}$ (400 MHz, C_6D_6) δ : 9.29 (s, 1H, CHO), 5.04 (s, 1H, H-2), 1.83 (t, $J = 6.9$ Hz, 2H, H-7), 1.77 (m, 1H, H-6), 1.65 (m, 2H, H-4), 1.35 – 1.52 (m, 2H, H-5), 1.25 (m, 2H, H-8), 1.21 (m, 2H, H-9), 1.09 (m, 1H, H-6), 0.94 (s, 3H, H-11), 0.86 (t, $J = 7.0$ Hz, 3H, H-10). **$^{13}\text{C NMR}$** (100 MHz, C_6D_6) δ : 201.8 (CHO), 142.5 (C-3), 121.9 (C-2), 47.7 (C-1), 38.0 (C-7), 30.1 (C-8), 30.0 (C-6), 28.3 (C-4), 22.7 (C-9), 19.7 (C-5), 14.2 (C-10). **ESI-HRMS** m/z : 181.78 $[\text{M}+\text{H}]^+$

1-methyl-2-cyclohexene-1-carbaldehyde (94f)

By following the General Procedure, starting from cyclohex-2-enone (96 mg, 1.00 mmol, 1.0 equiv), ICH_2Cl (529 mg, 0.22 mL, 3.0 mmol, 3.0 equiv), MeLi-LiBr complex (1.5 M, 1.87 mL, 2.8 mmol, 2.8 equiv) and THF (2 mL), the desired product was obtained in 70% (87 mg) as a bright yellow oil after chromatography on silica gel (96:4 pentane:diethylether).

$^1\text{H NMR}$ (400 MHz, C_6D_6) δ : 9.24 (s, 1H, CHO), 5.67 (td, $J = 10.0$ Hz, 3.8 Hz, 1H, H-3), 5.26 (td, $J = 10.0$ Hz, 2.1 Hz, 1H, H-2), 1.74 (m, 1H, H-6), 1.63 – 1.68 (m, 2H, H-4), 1.26 – 1.44 (m, 2H, H-5), 1.07 (m, 1H, H-6), 0.87 (s, 3H, H-7). **$^{13}\text{C NMR}$** (100 MHz, C_6D_6) δ : 201.7 (CHO), 130.7 (C-3), 128.2 (C-2), 47.5 (C-1), 30.0 (C-6), 24.9 (C-4), 22.1 (C-7), 19.1 (C-5). **ESI-HRMS** m/z : 125.43 $[\text{M}+\text{H}]^+$

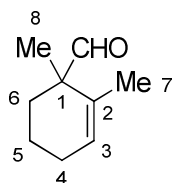
1,3-dimethylcyclohex-2-enecarbaldehyde (94g)



By following the General Procedure, starting from 3-methylcyclohex-2-enone (110 mg, 1.00 mmol, 1.0 equiv), ICH_2Cl (529 mg, 0.22 mL, 3.0 mmol, 3.0 equiv), MeLi-LiBr complex (1.5 M, 1.87 mL, 2.8 mmol, 2.8 equiv) and THF (2 mL), the desired product was obtained in 65% (90 mg) as a bright yellow oil after chromatography on silica gel (96:4 pentane:diethylether).

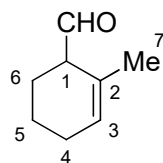
$^1\text{H NMR}$ (400 MHz, C_6D_6) δ : 9.27 (s, 1H, CHO), 4.99 (m, 1H, H-2), 1.74 (m, 1H, H-6), 1.58 (m, 2H, H-4), 1.49 (m, 3H, H-7), 1.31-1.49 (m, 2H, H-5), 1.05 (m, 1H, H-6), 0.90 (s, 3H, H-8). **$^{13}\text{C NMR}$** (100 MHz, C_6D_6) δ : 201.8 (CHO), 138.4 (C-3), 122.5 (C-2), 47.7 (C-1), 29.8 (C-4), 29.7 (C-6), 24.1 (C-7), 22.3 (C-8), 19.6 (C-5). **ESI-HRMS** m/z : 139.61 $[\text{M}+\text{H}]^+$

1,2-dimethyl-2-cyclohexene-1-carbaldehyde (94h)



By following the General Procedure, starting from 2-methylcyclohex-2-enone (110 mg, 1.00 mmol, 1.0 equiv), ICH_2Cl (529 mg, 0.22 mL, 3.0 mmol, 3.0 equiv), MeLi-LiBr complex (1.5 M, 1.87 mL, 2.8 mmol, 2.8 equiv) and THF (2 mL), the desired product was obtained in 59% (82 mg) as a bright yellow oil after chromatography on silica gel (96:4 pentane:diethylether).

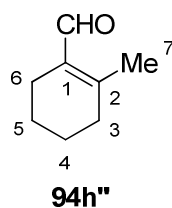
$^1\text{H NMR}$ (400 MHz, C_6D_6) δ : 9.26 (s, 1H, CHO), 5.45 (m, 1H, H-3), 1.70 – 1.76 (m, 2H, H-4), 1.54 (m, 1H, H-6), 1.47 (m, 3H, H-7), 1.37 (m, 1H, H-5), 1.28 (m, 1H, H-5), 1.08 (m, 1H, H-6), 1.00 (s, 3H, H-8). **$^{13}\text{C NMR}$** (100 MHz, C_6D_6) δ : 202.4 (CHO), 132.7 (C-2), 127.0 (C-3), 50.5 (C-1), 31.7 (C-6), 25.6 (C-4), 19.9 (C-7), 19.5 (C-8), 18.7 (C-5). **ESI-HRMS** m/z : 139.80 $[\text{M}+\text{H}]^+$



94h'

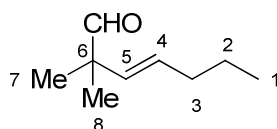
2-methyl-2-cyclohexene-1-carbaldehyde (94h') **$^1\text{H NMR}$** (400 MHz, C_6D_6) δ : 9.32 (d, $J = 2.3$ Hz, 1H, CHO), 5.43 (m, 1H, H-3), 2.38 (m, 1H, H-1), 1.72 (m, 2H, H-4), 1.68 (m, 1H, H-6), 1.56

(m, 3H, H-7), 1.28 (m, 1H, H-6), 1.20-1.32 (m, 2H, H-5). ^{13}C NMR (100 MHz, C_6D_6) δ : 200.6 (CHO), 129.1 (C-2), 126.1 (C-3), 52.6 (C-1), 25.1 (C-4), 23.0 (C-6), 22.8 (C-7), 19.5 (C-5).



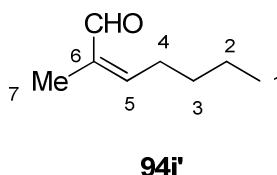
2-methyl-2-cyclohexene-1-carbaldehyde (94h'') ^1H NMR (400 MHz, C_6D_6) δ : 10.04 (s, 1H, CHO), 2.24 (m, 2H, H-5), 1.61 (m, 2H, H-3), 1.49 (m, 3H, H-7), 1.29 (m, 2H, H-6), 1.22 (m, 2H, H-4). ^{13}C NMR (100 MHz, C_6D_6) δ : 189.7 (CHO), 153.6 (C-2), 133.9 (C-1), 22.7 (C-5), 22.3 (C-4), 22.0 (C-6).

(3E)-2,2-dimethyl-3-heptenal (94i)



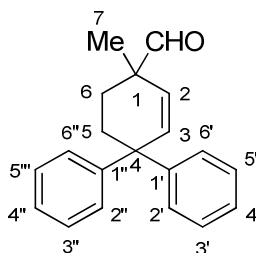
By following the General Procedure, starting from (3E)-hept-3-en-2-one (112 mg, 1.00 mmol, 1.0 equiv), ICH_2Cl (529 mg, 0.22 mL, 3.0 mmol, 3.0 equiv), MeLi-LiBr complex (1.5 M, 1.87 mL, 2.8 mmol, 2.8 equiv) and THF (2 mL), the desired product was obtained in 69% (97 mg) as a bright yellow oil after chromatography on silica gel (96:4 pentane:diethylether).

^1H NMR (400 MHz, C_6D_6) δ : 9.19 (s, 1H, CHO), 5.29 (td, $J = 15.8$ Hz, 6.6 Hz, 1H, H-4), 5.18 (td, $J = 15.8$ Hz, 1.2 Hz, 1H, H-5), 1.82 (m, 2H, H-3), 1.22 (m, 2H, H-2), 0.95 (s, 6H, H-7, H-8), 0.79 (t, $J = 7.4$ Hz, 3H, H-1). ^{13}C NMR (100 MHz, C_6D_6) δ : 201.2 (CHO), 132.3 (C-5), 131.9 (C-4), 48.3 (C-6), 35.1 (C-3), 22.7 (C-2), 21.6 (C-7, C-8), 13.7 (C-1). **ESI-HRMS** m/z : 141.45 $[\text{M}+\text{H}]^+$



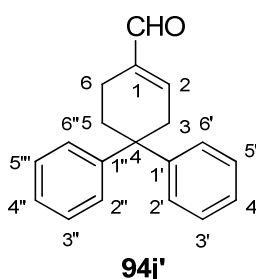
(2Z)-2-methyl-2-heptenal (94i') ^1H NMR (400 MHz, C_6D_6) δ : 9.29 (s, 1H, CHO), 5.84 (m, 1H, H-5), 1.83 (m, 2H, H-4), 1.63 (m, 3H, H-7), 1.07 (m, 4H, H-2, H-3), 0.78 (m, 3H, H-1). ^{13}C NMR (100 MHz, C_6D_6) δ : 194.0 (CHO), 139.6 (C-6), 153.1 (C-5), 30.6 (C-3), 28.5 (C-4), 22.5 (C-2), 14.0 (C-1), 9.2 (C-7).

1-methyl-4,4-diphenyl-2-cyclohexene-1-carbaldehyde (94j)

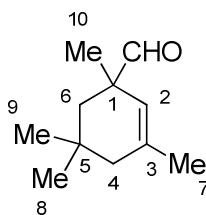


By following the General Procedure, starting 4,4-diphenyl-2-cyclohexen-1-one (248 mg, 1.00 mmol, 1.0 equiv), ICH_2Cl (529 mg, 0.22 mL, 3.0 mmol, 3.0 equiv), MeLi-LiBr complex (1.5 M, 1.87 mL, 2.8 mmol, 2.8 equiv) and THF (2 mL), the desired product was obtained in 81% (225 mg) as a colourless solid after chromatography on silica gel (96:4 pentane:diethylether).

$^1\text{H NMR}$ (400 MHz, C_6D_6) δ : 9.19 (s, 1H, CHO), 7.14 (m, 2H, H-6', H-6''), 7.12 (m, 2H, H-2', H-2''), 7.09 (m, 2H, H-3', H-3''), 7.03 (m, 1H, H-4'), 7.01 (m, 1H, H-4''), 6.11 (d, $J = 10.1$ Hz, 1H, H-3), 5.41 (d, $J = 10.1$ Hz, H-2), 2.07 – 2.21 (m, 2H, H-5), 1.77 (m, 1H, H-6), 1.16 (m, 1H, H-6). **$^{13}\text{C NMR}$** (100 MHz, C_6D_6) δ : 201.1 (CHO), 148.7 (C-1'), 148.2 (C-1''), 138.2 (C-3), 128.53 (C-3', C-3''), 128.47 (C-5', C-5''), 128.40 (C-2', C-2''), 128.4 (C-2), 128.09 (C-6', C-6''), 126.35 (C-4'), 126.31 (C-4''), 48.8 (C-4), 47.7 (C-1), 33.0 (C-5), 26.6 (C-6), 26.1 (C-7). **ESI-HRMS** m/z : 277.65 $[\text{M}+\text{H}]^+$

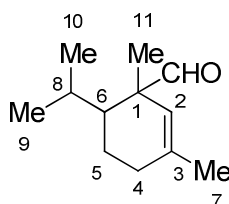


4,4-diphenyl-1-cyclohexene-1-carbaldehyde (94j') **$^1\text{H NMR}$** (400 MHz, C_6D_6) δ : 9.25 (s, 1H, CHO), 7.06 (m, 4H, H-3', H-3'', H-5', H-5''), 7.00 (m, 2H, H-4', H-4''), 6.95 (4H, H-2', H-2'', H-6', H-6''), 6.12 (m, 1H, H-2), 2.41 (m, 2H, H-3), 1.99 (m, 2H, H-6), 1.96 (m, 2H, H-5). **$^{13}\text{C NMR}$** (100 MHz, C_6D_6) δ : 192.0 (CHO), 148.2 (C-1', C-1''), 147.7 (C-2), 141.7 (C-1), 128.4 (C-3', C-3'', C-5', C-5''), 127.2 (C-2', C-2'', C-6', C-6''), 126.3 (C-4', C-4''), 45.9 (C-4), 39.2 (C-3), 32.2 (C-5), 19.5 (C-6).

1,3,5,5-tetramethyl-2-cyclohexene-1-carbaldehyde (94k)

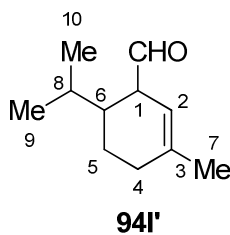
By following the General Procedure, starting 3,5,5-trimethylcyclohex-2-enone (138 mg, 1.00 mmol, 1.0 equiv), ICH_2Cl (529 mg, 0.22 mL, 3.0 mmol, 3.0 equiv), MeLi-LiBr complex (1.5 M, 1.87 mL, 2.8 mmol, 2.8 equiv) and THF (2 mL), the desired product was obtained in 63% (105 mg) as a colourless solid after chromatography on silica gel (96:4 pentane:diethylether).

$^1\text{H NMR}$ (400 MHz, C_6D_6) δ : 9.30 (s, 1H, CHO), 5.18 (m, 1H, H-2), 1.79 (ddd, $J = 13.7$ Hz, 1.7 Hz, 1.0 Hz, H-6), 1.54 (m, 3H, H-7), 1.51 (m, 1H, H-4), 1.38 (m, 1H, H-4), 0.92 (d, $J = 13.7$ Hz, 1H, H-6), 0.87 (s, 3H, H-10), 0.81 (s, 3H, H-9), 0.72 (s, 3H, H-8). **$^{13}\text{C NMR}$** (100 MHz, C_6D_6) δ : 202.5 (CHO), 135.9 (C-3), 121.9 (C-2), 48.2 (C-1), 44.1 (C-4), 43.0 (C-6), 30.7 (C-9), 30.0 (C-5), 28.0 (C-8), 24.3 (C-7), 24.0 (C-10). **ESI-HRMS** m/z : 167.83 $[\text{M}+\text{H}]^+$

6-isopropyl-1,3-dimethyl-2-cyclohexene-1-carbaldehyde (94l)

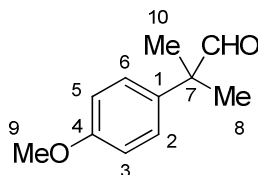
By following the General Procedure, starting 6-isopropyl-3-methylcyclohex-2-enone (152 mg, 1.00 mmol, 1.0 equiv), ICH_2Cl (529 mg, 0.22 mL, 3.0 mmol, 3.0 equiv), MeLi-LiBr complex (1.5 M, 1.87 mL, 2.8 mmol, 2.8 equiv) and THF (2 mL), a mixture of two aldehydes (which are inseparable) was obtained in 61% (110 mg) as a bright yellow oil after chromatography on silica gel (96:4 pentane:diethylether).

$^1\text{H NMR}$ (400 MHz, C_6D_6) δ : 9.70 (s, 1H, CHO), 4.71 (m, 1H, H-2), 1.88 (m, 1H, H-8), 1.77 (m, 2H, H-4), 1.52 (m, 3H, H-7), 1.50 (m, 1H, H-5), 1.37 (m, 1H, H-5), 1.18 (m, 1H, H-6), 1.16 (s, 3H, H-11), 0.77 (d, $J = 6.9$ Hz, 3H, H-10), 0.65 (d, $J = 6.9$ Hz, 3H, H-9). **$^{13}\text{C NMR}$** (100 MHz, C_6D_6) δ : 201.0 (CHO), 139.3 (C-3), 124.1 (C-2), 52.2 (C-1), 49.6 (C-6), 31.0 (C-4), 26.5 (C-8), 23.7 (C-7), 23.6 (C-10), 21.3 (C-11), 19.4 (C-5), 18.27 (C-9). **ESI-HRMS** m/z : 181.92 $[\text{M}+\text{H}]^+$



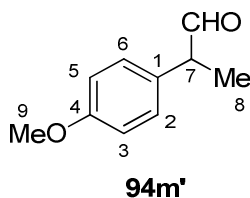
6-isopropyl-3-methyl-2-cyclohexene-1-carbaldehyde (94l') $^1\text{H NMR}$ (400 MHz, C_6D_6) δ : 9.26 (d, $J = 3.2$ Hz, 1H, CHO), 5.08 (m, 1H, H-2), 2.72 (m, 1H, H-1), 1.65 (m, 2H, H-4), 1.52 (m, 5H, H-6, H-8, H-7), 1.43 (m, 1H, H-5), 1.10 (m, 1H, H-5), 0.70 (d, $J = 6.6$ Hz, 3H, H-9). $^{13}\text{C NMR}$ (100 MHz, C_6D_6) δ : 201.3 (CHO), 139.2 (C-3), 116.1 (C-2), 53.4 (C-1), 38.9 (C-6), 29.4 (C-4), 29.3 (C-8), 23.8 (C-7), 22.1 (C-5), 21.1 (C-10), 18.24 (C-9).

2-(4-methoxyphenyl)-2-methylpropanal (94m)

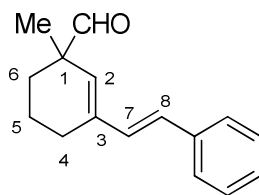


By following the General Procedure, starting 4-methoxy-acetophenone (150 mg, 1.00 mmol, 1.0 equiv), ICH_2Cl (529 mg, 0.22 mL, 3.0 mmol, 3.0 equiv), MeLi-LiBr complex (1.5 M, 1.87 mL, 2.8 mmol, 2.8 equiv) and THF (2 mL the desired product was obtained in 62% (111 mg) as a colourless solid after chromatography on silica gel (96:4 pentane:diethylether).

$^1\text{H NMR}$ (400 MHz, C_6D_6) δ : 9.28 (s, 1H, CHO), 6.96 (m, 2H, H-2, H-6), 6.72 (m, 2H, H-3, H-5), 3.30 (s, 3H, H-9), 1.19 (s, 6H, H-7, H-8). $^{13}\text{C NMR}$ (100 MHz, C_6D_6) δ : 200.9 (CHO), 159.2 (C-4), 133.5 (C-1), 128.1 (C-2, C-6), 114.5 (C-3, C-5), 54.8 (C-9), 49.6 (C-7), 22.5 (C-8, C-10). **ESI-HRMS** m/z : 179.73 $[\text{M}+\text{H}]^+$

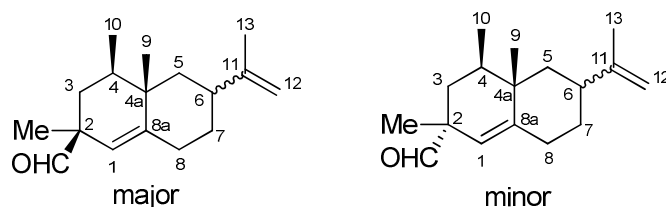


2-(4-methoxyphenyl)propanal (94m') $^1\text{H NMR}$ (400 MHz, C_6D_6) δ : 9.38 (d, $J = 1.4$ Hz, 1H, CHO), 6.80 (m, 2H, H-2, H-6), 6.71 (m, 2H, H-3, H-5), 3.27 (s, 3H, H-9), 3.03 (m, 1H, H-7), 1.18 (d, $J = 7.1$ Hz, 3H, H-8). $^{13}\text{C NMR}$ (100 MHz, C_6D_6) δ : 199.6 (CHO), 159.5 (C-4), 130.1 (C-1), 129.6 (C-2, C-6), 114.8 (C-5), 54.8 (C-9), 52.3 (C-7), 14.8 (C-8).

(E)-1-methyl-3-styryl-2-cyclohexene-1-carbaldehyde (94n)

By following the General Procedure, starting (*E*)-3-styryl-2-cyclohexen-1-one (198 mg, 1.00 mmol, 1.0 equiv), ICH_2Cl (529 mg, 0.22 mL, 3.0 mmol, 3.0 equiv), MeLi-LiBr complex (1.5 M, 1.87 mL, 2.8 mmol, 2.8 equiv) and THF (2 mL), the desired product was obtained in 72% (163 mg) as a colourless solid after chromatography on silica gel (96:4 pentane:diethylether).

$^1\text{H NMR}$ (400 MHz, CDCl_3) δ : 9.41 (s, 1H, CHO), 7.34 (d, $J = 8.0$ Hz, 2H, Ph-2, Ph-6), 7.24 (t, $J = 8.0$ Hz, 2H, H-3, H-5), 7.14 (t, $J = 8.0$ Hz, 1H, H-4), 6.72 (d, $J = 12.0$ Hz, 1H, H-7), 6.49 (d, $J = 12.0$ Hz, 1H, H-8), 5.53 (s, 1H, H-2), 2.28-2.17 (m, 2H, H-4), 1.97-1.92 (m, 1H, H-6), 1.77-1.62 (m, 2H, H-5, H-6), 1.41-1.36 (m, 1H, H-5), 1.11 (s, 3H, Me). $^{13}\text{C NMR}$ (100 MHz, CDCl_3) δ : 202.7 (CHO), 138.3 (Ph-1), 137.4 (C-3), 131.4 (C-7), 129.3 (C-2), 128.6 (Ph-3, Ph-5), 127.4 (Ph-2, Ph-6), 127.3 (Ph-4), 126.4 (C-8), 48.6 (C-1), 29.9 (C-6), 24.3 (C-4), 22.2 (Me), 19.0 (C-5). **ESI-HRMS** m/z : 227.81 $[\text{M}+\text{H}]^+$

6-isopropenyl-2,4,4a-trimethyl-2,3,4,4a,5,6,7,8-octahydro-2-naphthalenecarbaldehyde (94o)

By following the General Procedure, starting 4,4a-dimethyl-6-(prop-1-en-2-yl)-4,4a,5,6,7,8-hexahydronaphthalen-2(3H)-one (218 mg, 1.00 mmol, 1.0 equiv), ICH_2Cl (529 mg, 0.22 mL, 3.0 mmol, 3.0 equiv), MeLi-LiBr complex (1.5 M, 1.87 mL, 2.8 mmol, 2.8 equiv) and THF (2 mL) the desired product was obtained in 63% (155 mg) as a colourless oil after chromatography on silica gel (96:4 pentane:diethylether).

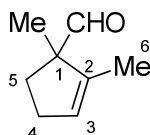
Major $^1\text{H NMR}$ (400 MHz, C_6D_6): δ 9.18 (s, 1H, CHO), 4.94 (m, 1H, H-1), 4.80-4.76 (m, 2H, H-12), 2.14 (m, 1H, Hax-8), 2.11 (m, 1H, Hax-6), 1.98 (m, 1H, Hax-8), 1.83 (m, 1H, Heq-5), 1.67 (m, 1H, Heq-7), 1.63 (m, 3H, H-13), 1.57 (m, 1H, Heq-3), 1.44 (m, 1H, Hax-4), 1.12 (m, 1H, Hax-7), 1.05 (s, 3H, CH_3), 0.95 (m, 1H, Hax-3), 0.90 (m, 1H, Hax-5), 0.75 (s, 3H, H-9), 0.72 (d, $J = 6.7$ Hz, 3H, H-10). $^{13}\text{C NMR}$ (100 MHz, C_6D_6): δ 201.97 (CHO), 149.93 (C-6), 147.21 (C-8a), 120.69

Experimental Section

(C-1), 109.1 (C-12), 49.03 (C-2), 45.07 (C-5), 40.98 (C-11), 38.29 (C-4a), 36.60 (C-4), 33.45 (C-3), 33.16 (C-7), 33.02 (C-8), 21.51 (CH₃), 20.97 (C-13), 18.12 (C-9), 15.44 (C-10).

Minor ¹H NMR (400 MHz, C₆D₆): δ 9.34 (d, *J* = 0.8 Hz, 1H, CHO), 4.98 (m, 1H, H-1), 4.80-4.76 (m, 2H, H-12), 2.14 (m, 1H, Hax-8), 2.11 (m, 1H, Hax-6), 1.98 (m, 1H, Hax-8), 1.83 (m, 1H, Heq-5), 1.69 (m, 1H, Heq-3), 1.67 (m, 1H, Heq-7), 1.61 (m, 3H, H-13), 1.50 (m, 1H, Hax-4), 1.12 (m, 1H, Hax-7), 1.07 (m, 1H, Hax-3), 0.84 (s, 3H, CH₃), 0.90 (m, 1H, Hax-5), 0.77 (s, 3H, H-9), 0.73 (d, *J* = 6.8 Hz, 3H, H-10). ¹³C NMR (100 MHz, C₆D₆): δ 201.33 (CHO), 149.90 (C-11), 147.83 (C-8a), 121.69 (C-1), 109.2 (C-12), 47.98 (C-2), 44.81 (C-5), 41.09 (C-6), 37.95 (C-4a), 38.28 (C-4), 35.21 (C-3), 33.17 (C-7), 33.02 (C-8), 23.07 (CH₃), 20.90 (C-13), 18.22 (C-9), 15.50 (C-10).

1,2-dimethyl-2-cyclopentene-1-carbaldehyde (94p)

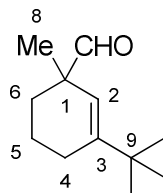


By following the General Procedure, starting 2-methylcyclopent-2-enone (96 mg, 1.00 mmol, 1.0 equiv), ICH₂Cl (529 mg, 0.22 mL, 3.0 mmol, 3.0 equiv), MeLi-LiBr complex (1.5 M, 1.87 mL, 2.8 mmol, 2.8 equiv) and THF (2 mL the desired product was obtained in 70% (87 mg) as a colourless oil after chromatography on silica gel (96:4 pentane:diethylether).

¹H NMR (400 MHz, C₆D₆): δ 9.26 (s, 1H, CHO), 5.29 (m, 1H, H-3), 2.03 (m, 2H, H-4), 1.98 (m, 1H, H-5), 1.38 (m, 3H, H-6), 1.36 (m, 1H, H-5), 1.02 (s, 3H, CH₃). ¹³C NMR (100 MHz, C₆D₆): δ 201.3 (CHO), 140.1 (C-2), 129.4 (C-3), 61.8 (C-1), 33.7 (C-5), 30.4 (C-4), 17.9 (CH₃), 13.0 (C-6).

ESI-HRMS *m/z*: 125.32 [M+H]⁺

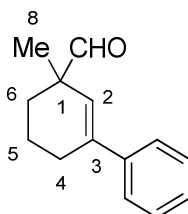
1-methyl-3-(2-methyl-2-propanyl)-2-cyclohexene-1-carbaldehyde (94q)



By following the General Procedure, starting 3-(*t*-butyl)cyclohex-2-enone (152 mg, 1.00 mmol, 1.0 equiv), ICH₂Cl (529 mg, 0.22 mL, 3.0 mmol, 3.0 equiv), MeLi-LiBr complex (1.5 M, 1.87 mL, 2.8 mmol, 2.8 equiv) and THF (2 mL the desired product was obtained in 85% (153 mg) as a colourless oil after chromatography on silica gel (96:4 pentane:diethylether).

¹H NMR (400 MHz, C₆D₆): δ 9.29 (s, 1H, CHO), 5.18 (t, *J* = 1.6 Hz, 1H, H-2), 1.78 (m, 1H, H-6), 1.75 (m, 2H, H-4), 1.38 (m, 9H, CH₃), 1.51 (m, 1H, H-5), 1.02 (s, 3H, H-8). **¹³C NMR** (100 MHz, C₆D₆): δ 201.6 (CHO), 150.2 (C-3), 118.7 (C-2), 47.5 (C-1), 35.5 (C-6), 29.6 (C-9), 28.8 (CH₃), 24.4 (C-4), 22.5 (C-8), 20 (C-5).

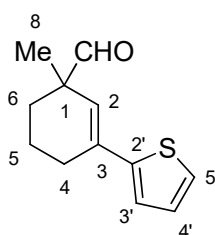
1-methyl-3-phenyl-2-cyclohexene-1-carbaldehyde (94r)



By following the General Procedure, starting 5,6-dihydro-[1,1'-biphenyl]-3(4H)-one (172 mg, 1.00 mmol, 1.0 equiv), ICH₂Cl (529 mg, 0.22 mL, 3.0 mmol, 3.0 equiv), MeLi-LiBr complex (1.5 M, 1.87 mL, 2.8 mmol, 2.8 equiv) and THF (2 mL the desired product was obtained in 79% (158 mg) as a colourless oil after chromatography on silica gel (96:4 pentane:diethylether).

¹H NMR (400 MHz, C₆D₆): δ 9.28 (s, 1H, CHO), 7.23 (m, 2H, Ph-H 2,6), 7.15 (m, 2H, Ph H-3,5), 7.10 (m, 1H, Ph H-4), 5.68 (t, *J* = 1.6 Hz, 1H, H-2), 2.10-2.06 (m, 2H, H-4), 1.79 (m, 1H, H-6), 1.56-1.39 (m, 2H, H-5), 1.10 (m, 1H, H-6), 0.94 (s, 3H, H-8). **¹³C NMR** (100 MHz, C₆D₆): δ 201.4 (CHO), 142.1 (Ph C-1), 142.0 (C-3), 128.6 (Ph C-3,5), 127.6 (Ph C-4), 125.8 (Ph C-2,6), 125.0 (C-2), 48.2 (C-1), 29.6 (C-6), 27.4 (C-4), 22.3 (C-8), 19.7 (C-5).

1-methyl-3-(2-thienyl)-2-cyclohexene-1-carbaldehyde (94s)

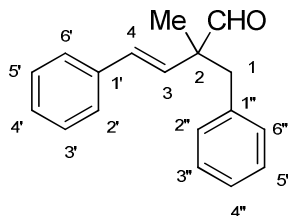


By following the General Procedure, starting 3-(thiophen-2-yl)cyclohex-2-enone (178 mg, 1.00 mmol, 1.0 equiv), ICH₂Cl (529 mg, 0.22 mL, 3.0 mmol, 3.0 equiv), MeLi-LiBr complex (1.5 M, 1.87 mL, 2.8 mmol, 2.8 equiv) and THF (2 mL the desired product was obtained in 74% (153 mg) as a colourless oil after chromatography on silica gel (96:4 pentane:diethylether).

¹H NMR (400 MHz, C₆D₆): δ 9.18 (s, 1H, CHO), 6.79 (dd, *J* = 4.9 Hz and 1.2 Hz, 1H, H-5'), 6.78 (dd, *J* = 3.7 and 1.2 Hz, 1H, H-3'), 6.73 (dd, *J* = 4.9 Hz and 3.7 Hz, 1H, H-4'), 5.88 (t, *J* = 1.7 Hz, 1H, H-2), 2.14-2.00 (m, 2H, H-4), 1.73 (m, 1H, H-6), 1.50-1.32 (m, 2H, H-5), 1.03 (m, 1H, H-6), 0.87 (s, 3H, H-8). **¹³C NMR** (100 MHz, C₆D₆): δ 200.9 (CHO), 146.0 (C-2'), 135.0 (C-3), 127.4 (C-

4'), 124.0 (C-5'), 123.6 (C-2), 122.9 (C-3'), 48.1 (C-1), 29.6 (C-6), 27.5 (C-4), 22.1 (C-8), 19.4 (C-5).

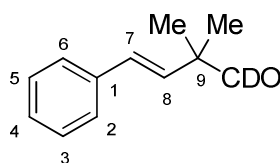
(3E)-2-benzyl-2-methyl-4-phenyl-3-butenal (92)



By following the General Procedure, starting (*E*)-4-phenylbut-3-en-2-one (256 mg, 1.00 mmol, 1.0 equiv), ICH_2Cl (529 mg, 0.22 mL, 3.0 mmol, 3.0 equiv), MeLi-LiBr complex (1.5 M, 1.87 mL, 2.8 mmol, 2.8 equiv), benzylbromine (833 μL , 7.0 equiv) and THF (2 mL), the desired product was obtained in 82% (205 mg) as a colourless solid after chromatography on silica gel (90:10 hexane:diethylether).

$^1\text{H NMR}$ (400 MHz, C_6D_6) δ : 9.31 (s, 1H, CHO), 7.12 (m, 2H, H-2', H-6'), 7.11 (m, 2H, H-3', H-5'), 7.05 (m, 3H, H-4', H-3'', H-5''), 7.03 (m, 1H, H-4''), 6.95 (m, 2H, H-2'', H-6''), 6.19 (d, $J = 16.4$ Hz, 1H, H-4), 6.02 (d, $J = 16.4$ Hz, 1H, H-3), 2.79-2.73 (AB-system, $^2J_{\text{AB}} = 13.4$ Hz, 2H, H-1), 0.98 (s, 3H, H-5). **$^{13}\text{C NMR}$** (100 MHz, C_6D_6) δ : 200.8 (CHO), 137.2 (C-1'), 137.0 (C-1''), 132.0 (C-4), 130.8 (C-2'', C-6''), 130.5 (C-3), 128.9 (C-3', C-5'), 128.3 (C-3'', C-5''), 128.0 (C-4'), 126.8 (C-4''), 126.75 (C-2', C-6'), 53.3 (C-2), 42.6 (C-1), 18.3 (C-5). **ESI-HRMS** m/z : 251.76 [M+H]⁺

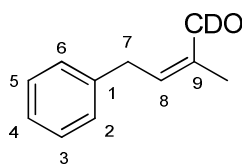
(3E)-2,2-dimethyl-4-phenyl(1- ^2H)-3-butenal (83)



By following the General Procedure, starting (*E*)-4-phenylbut-3-en-2-one (256 mg, 1.00 mmol, 1.0 equiv), CD_2Br_2 (528 mg, 0.22 mL, 3.0 mmol, 3.0 equiv), MeLi-LiBr complex (1.5 M, 1.87 mL, 2.8 mmol, 2.8 equiv), benzylbromine (and THF (2 mL), the desired product was obtained in 31% (54 mg) as a colourless solid after chromatography on silica gel (90:10 hexane:diethylether).

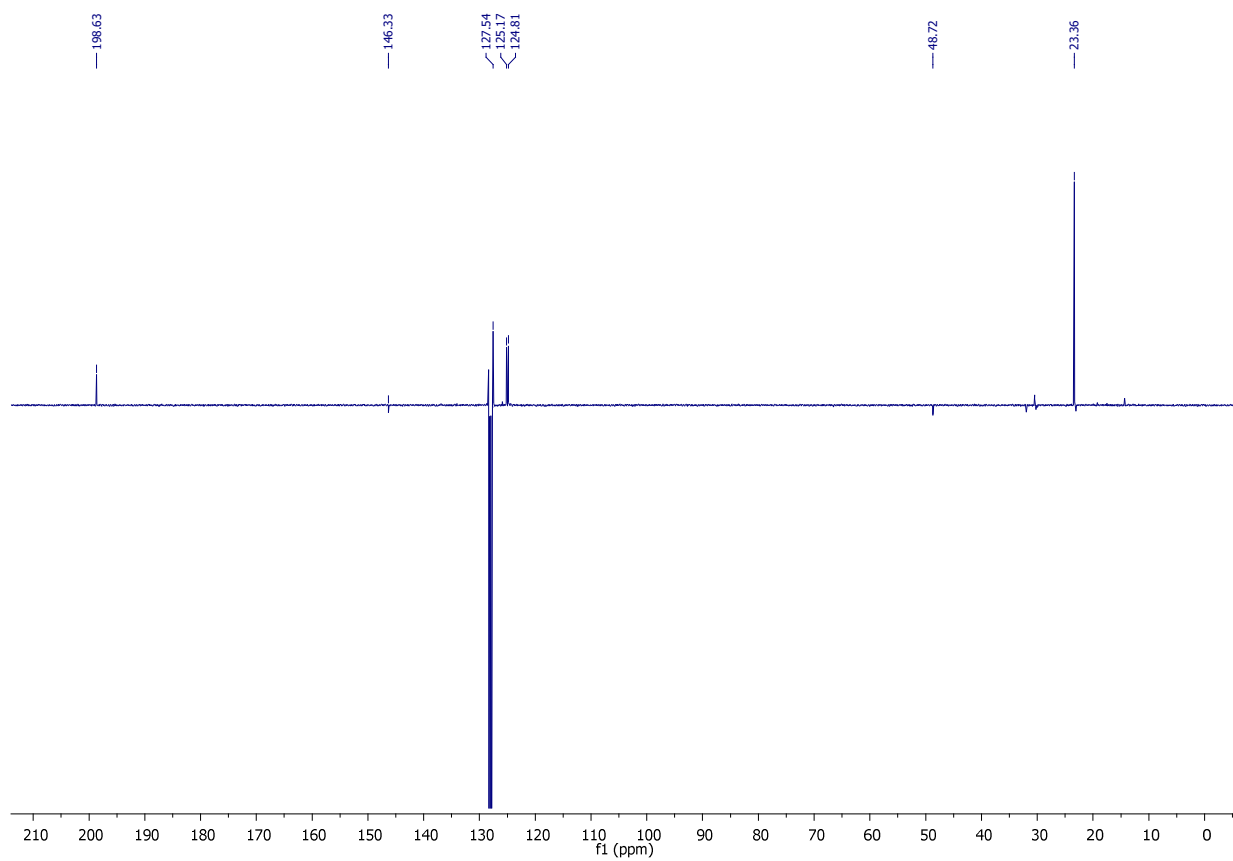
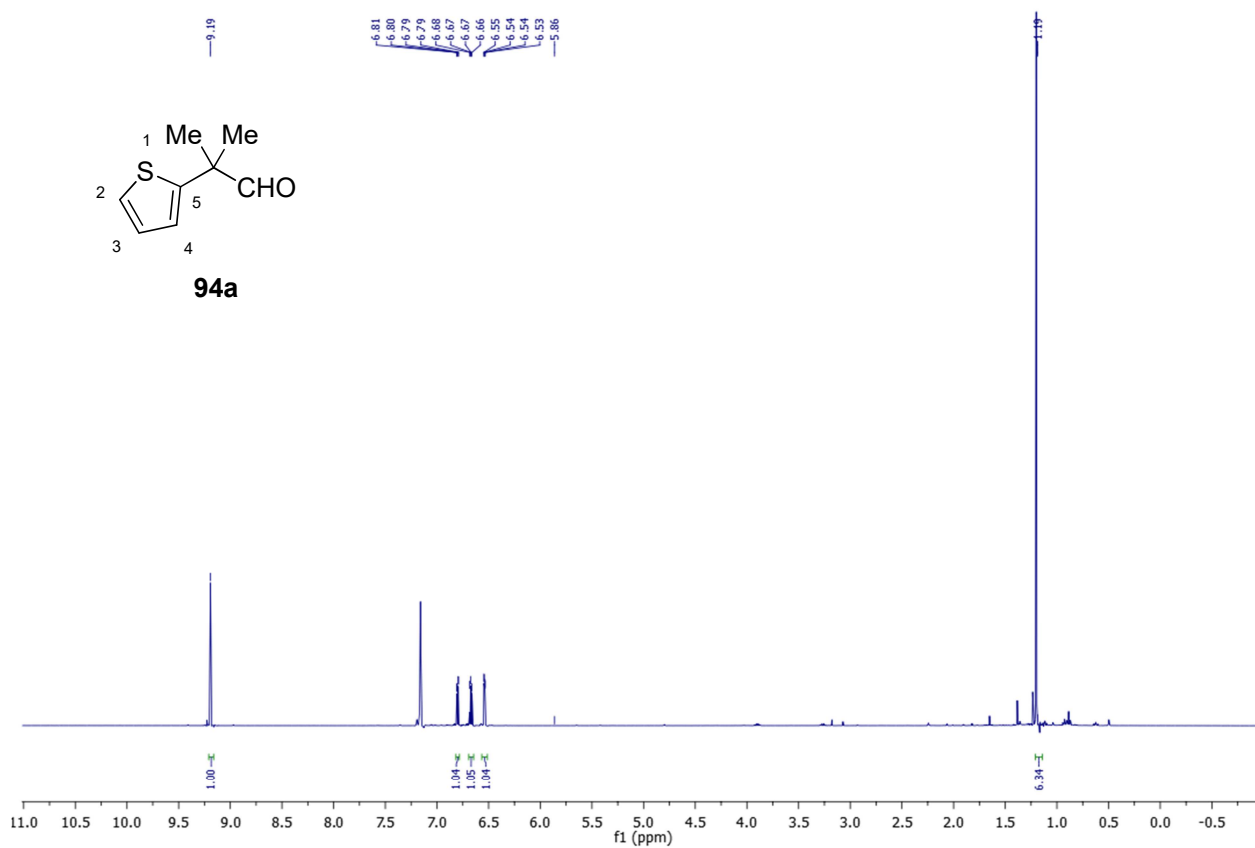
$^1\text{H NMR}$ (400 MHz, C_6D_6) δ : 7.13 (m, 2H, H-2, H-6), 7.10 (m, 2H, H-3, H-5), 7.07 (m, 1H, H-4), 6.25 (d, $J = 16.3$ Hz, 1H, H-7), 5.93 (d, $J = 16.3$ Hz, 1H, H-8), 0.98 (s, 6H, Me). **$^{13}\text{C NMR}$** (100 MHz, C_6D_6) δ : 200.4 (t, 1:1:1, $J = 26.6$ Hz, C=O), 137.2 (C-1), 131.6 (C-8), 131.2 (C-7), 128.8 (C-

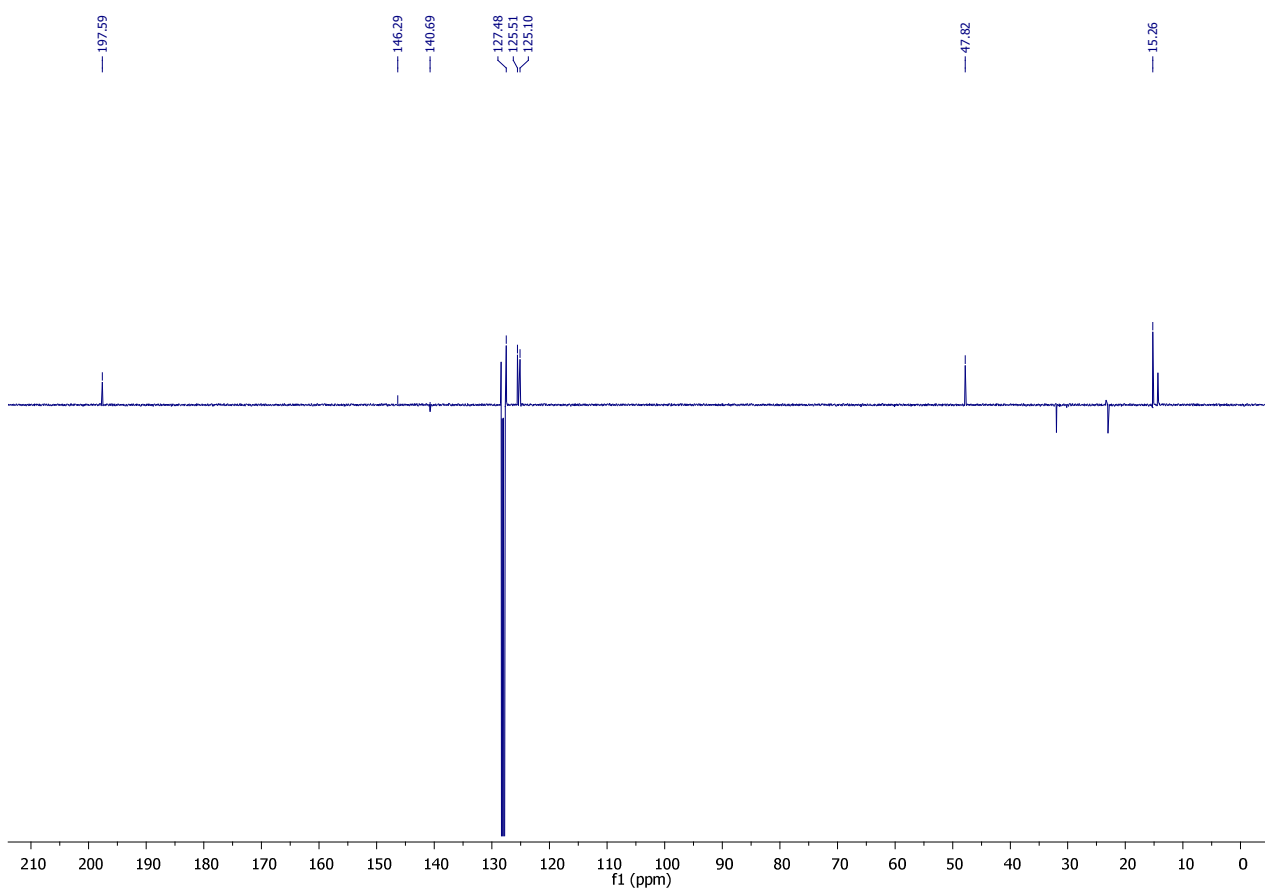
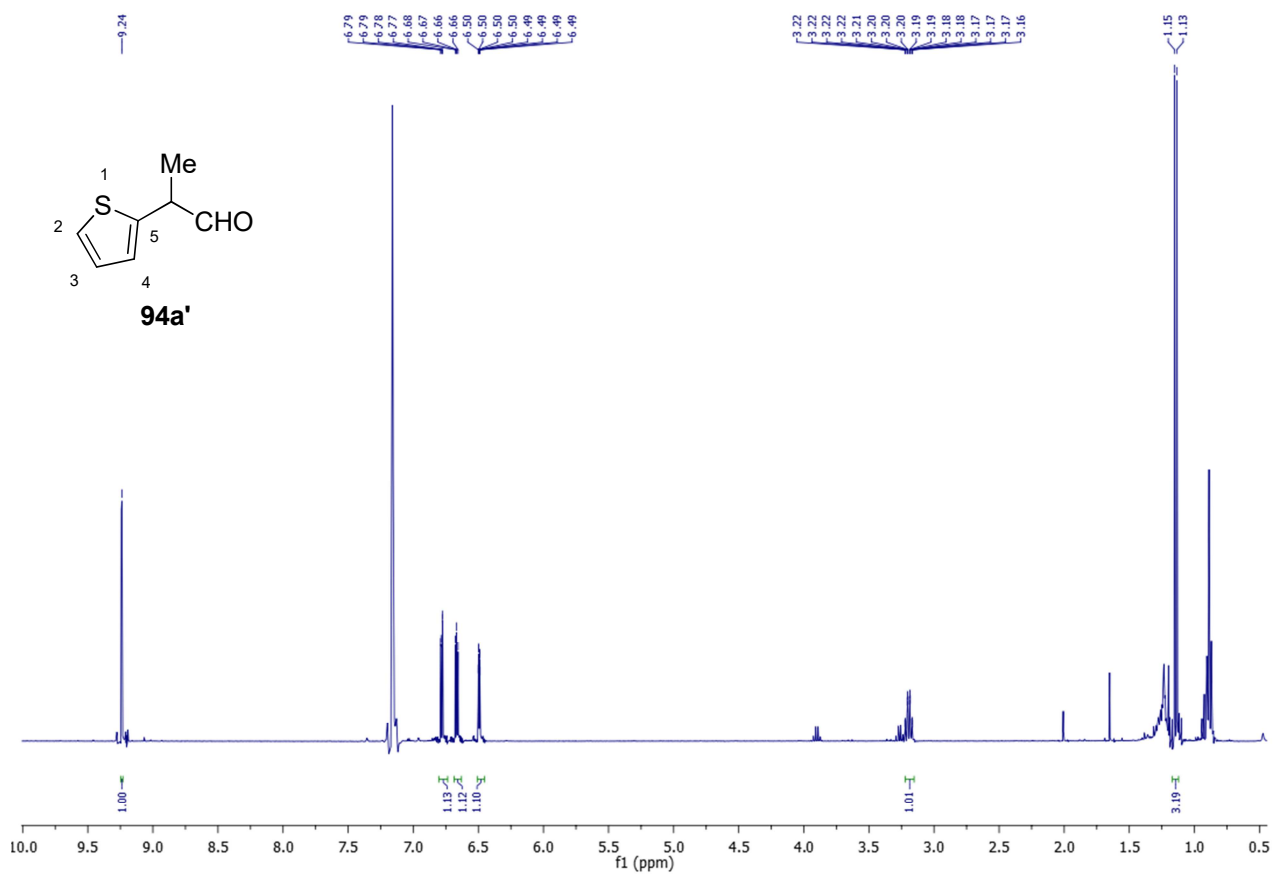
3, C-5), 128.0 (C-4), 126.8 (C-2,6), 48.5 (t, 1:1:1, $J = 3.3$ Hz, C-9), 21.5 (Me). **ESI-HRMS** m/z : 176.48 [M+H]⁺



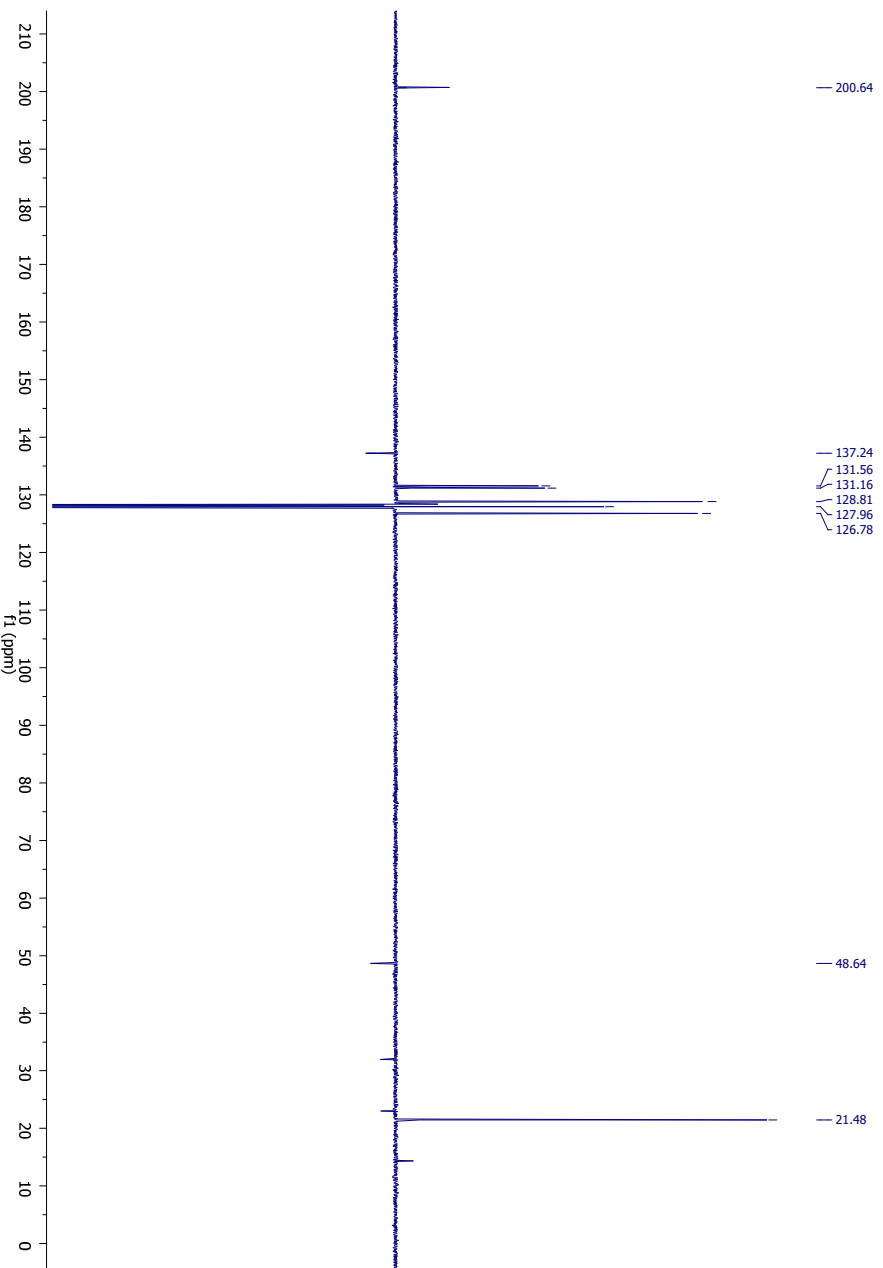
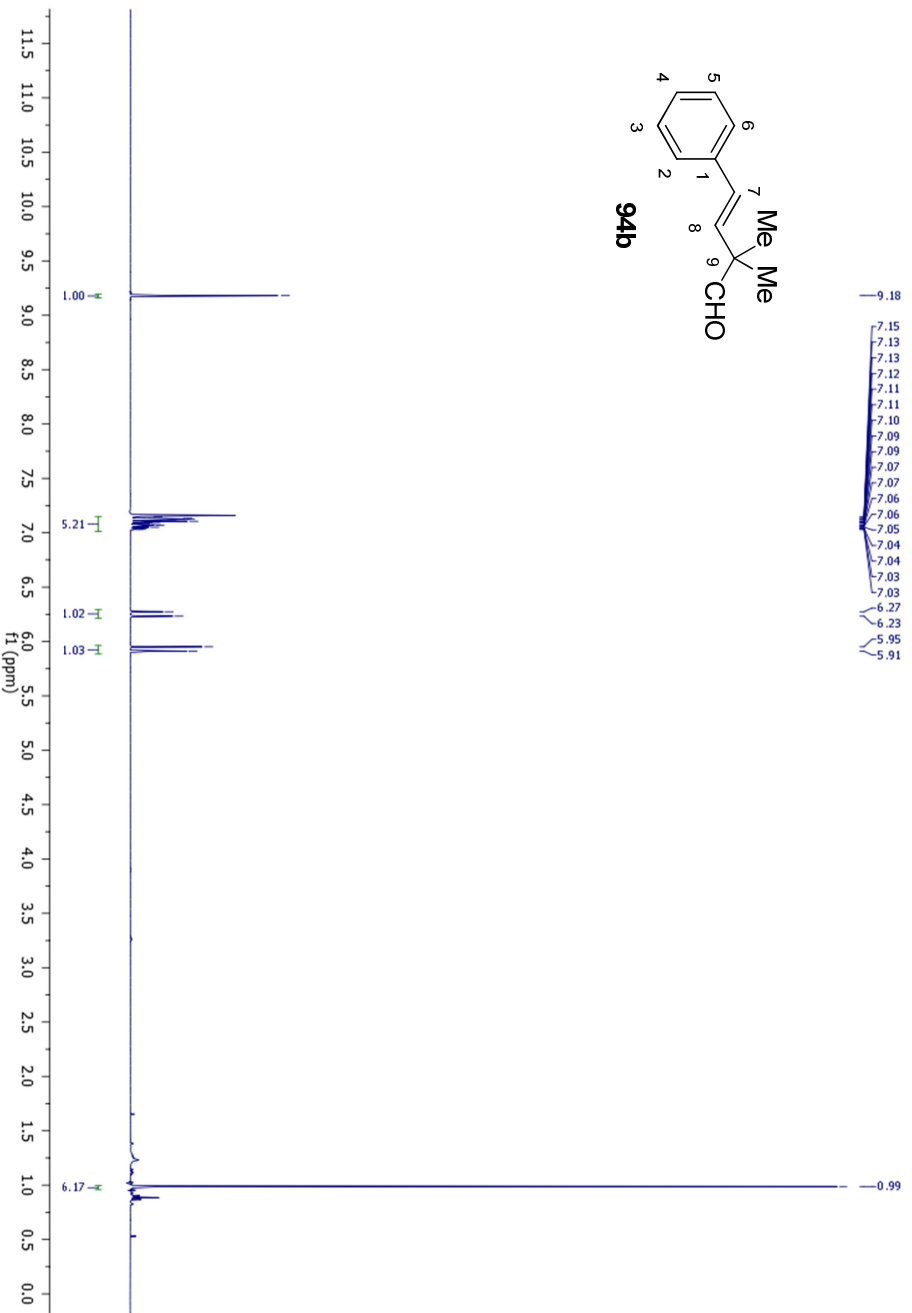
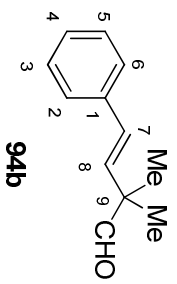
1-methyl-3-phenyl-2-cyclohexene-1-carbaldehyde (84) ¹H NMR (400 MHz, C₆D₆): 7.12 (m, 2H, H-3,5), 7.06 (m, 1H, H-4), 6.85 (m, 2H, H-2,6), 5.95 (qt, $J = 7.4$ and 1.4 Hz, 1H, H-8), 3.09 (d, $J = 7.4$ Hz, 2H, H-7), 1.64 (td, $J = 1.4$ and 0.9 Hz, 3H, CH₃). ¹³C NMR (100 MHz, C₆D₆): δ 193.5 (t 1:1:1, $J = 26.4$ Hz, CDO), 150.7 (C-8), 139.6 (t 1:1:1, $J = 3.7$ Hz, C-9), 138.7 (C-1), 129.0 (C-3,5), 128.7 (C-2,6), 126.8 (C-4), 35.0 (C-7), 9.21 (CH₃).

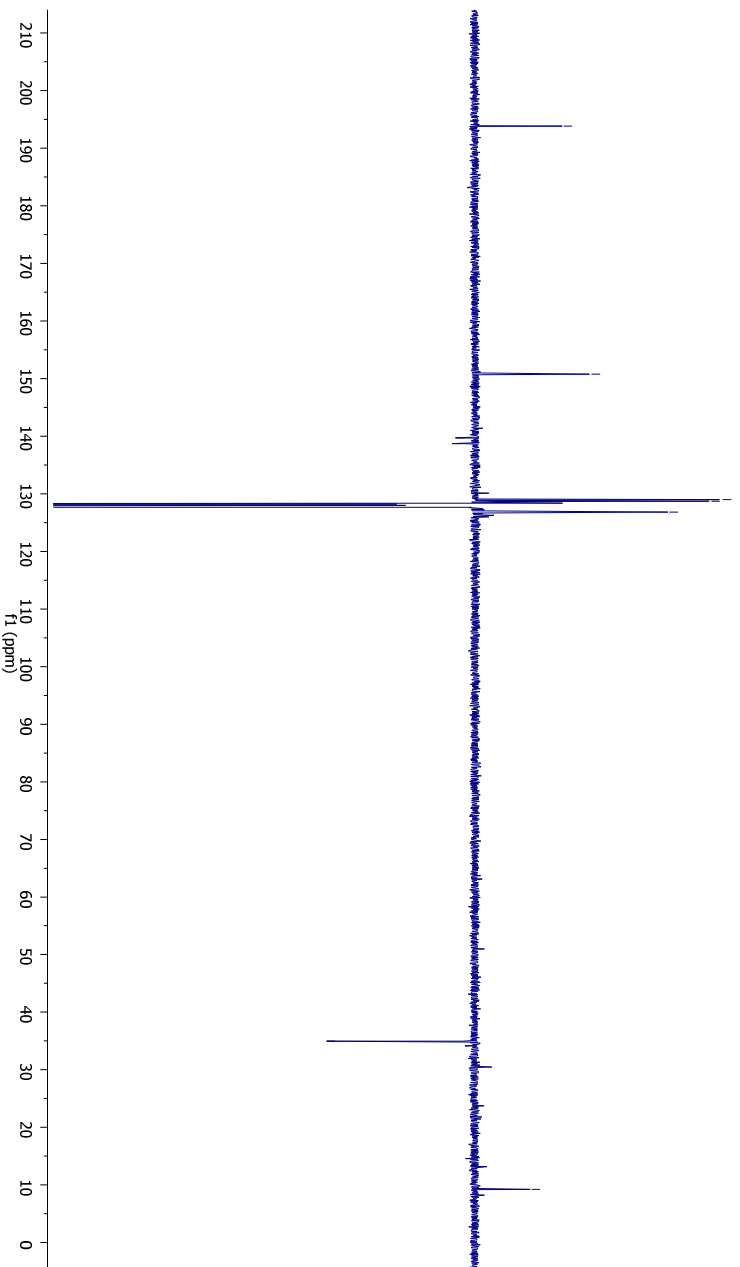
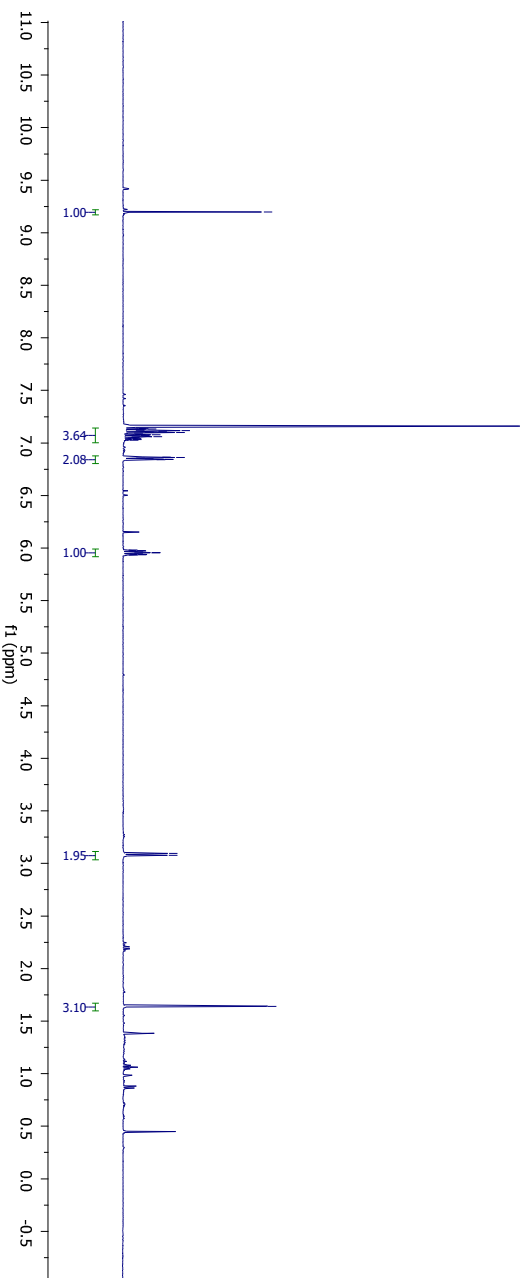
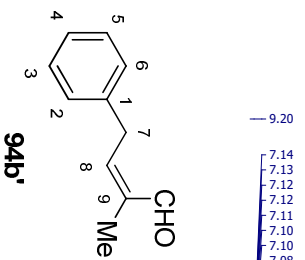
Copies of NMR spectra



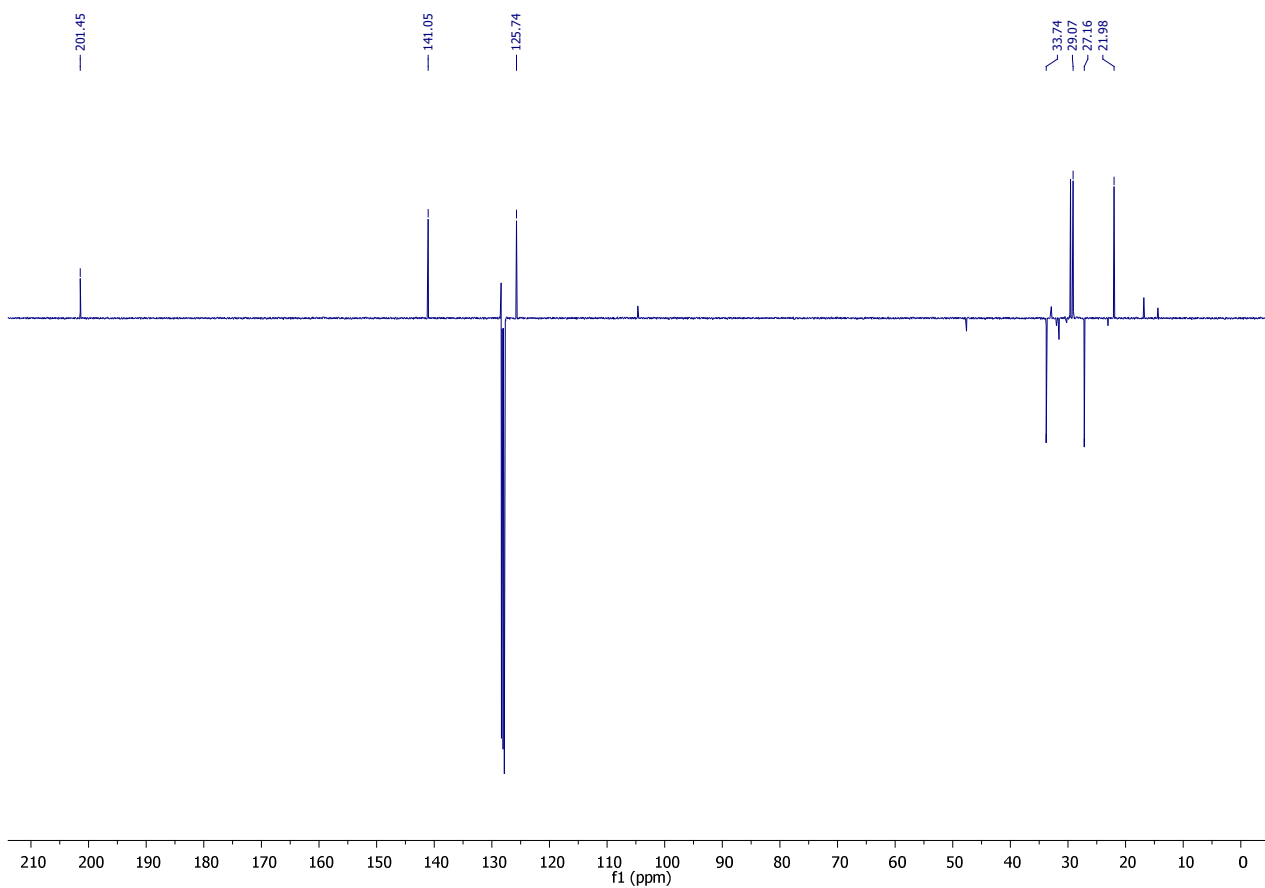
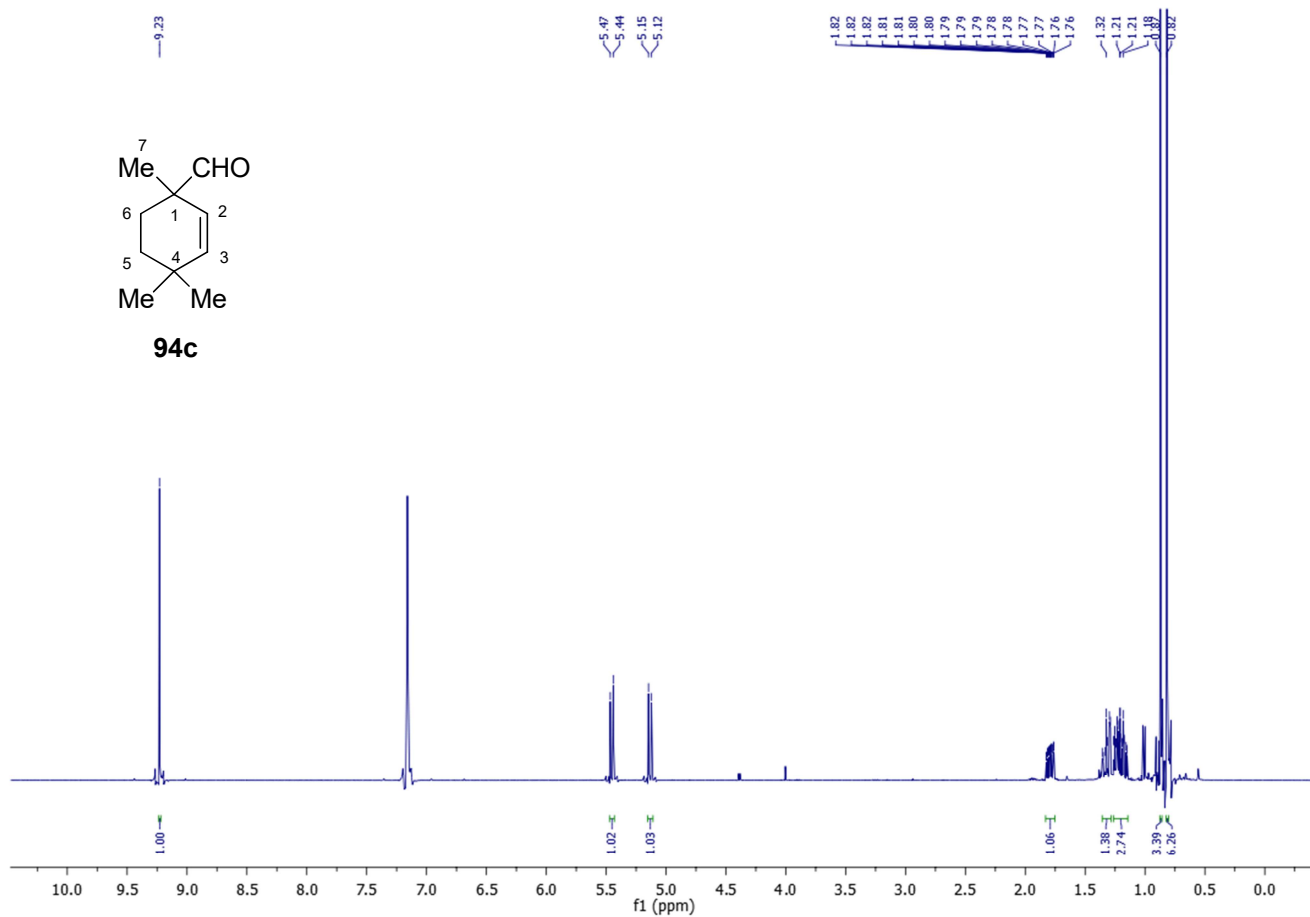


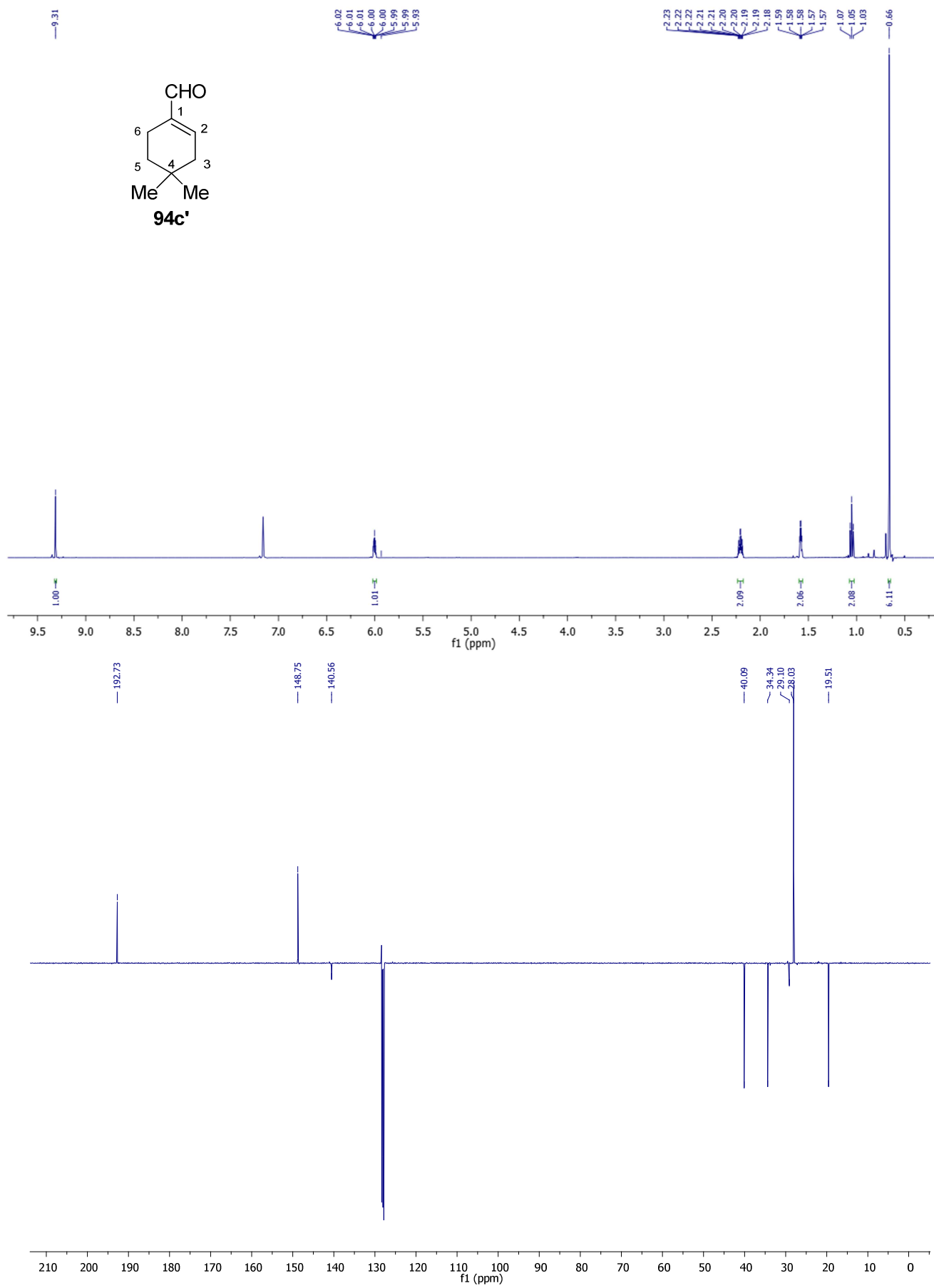
Experimental Section

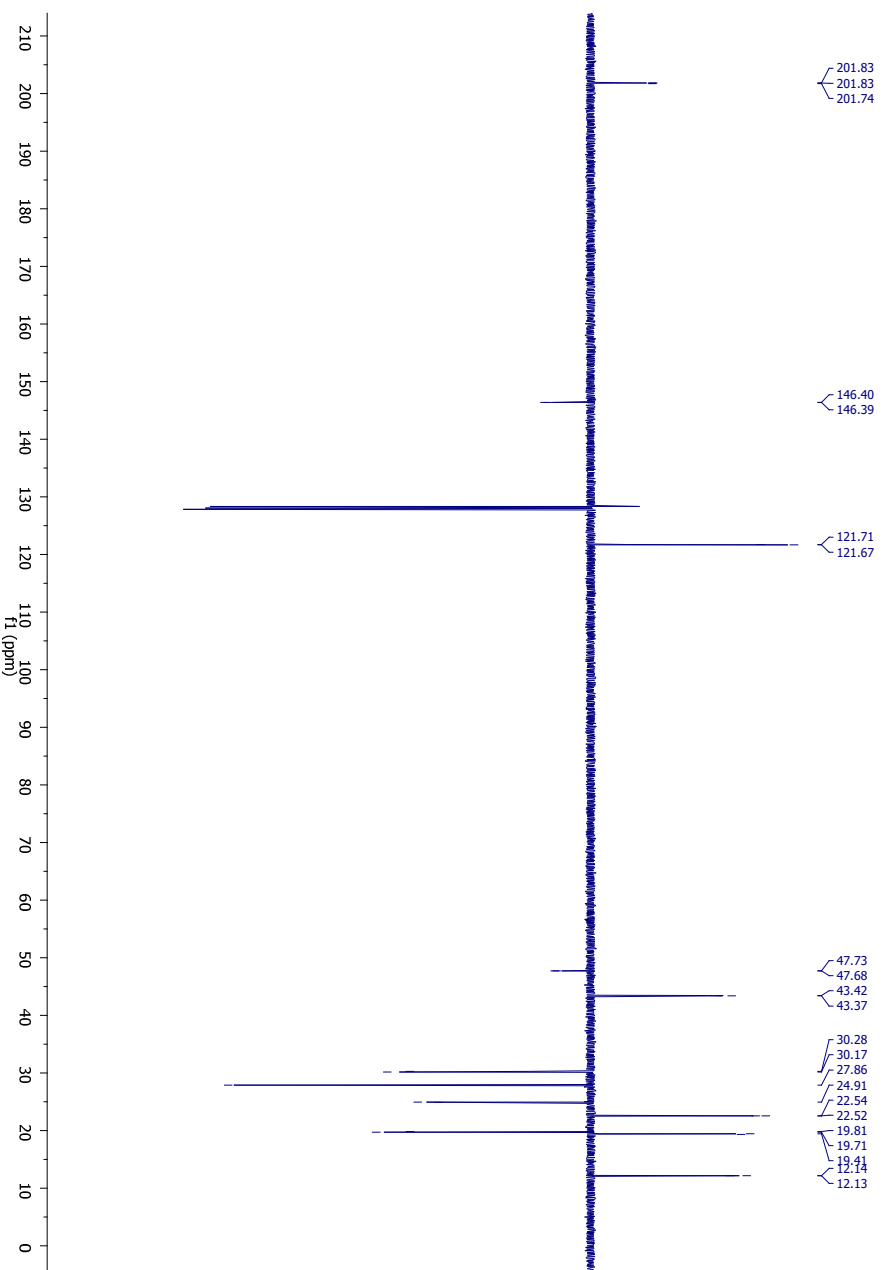
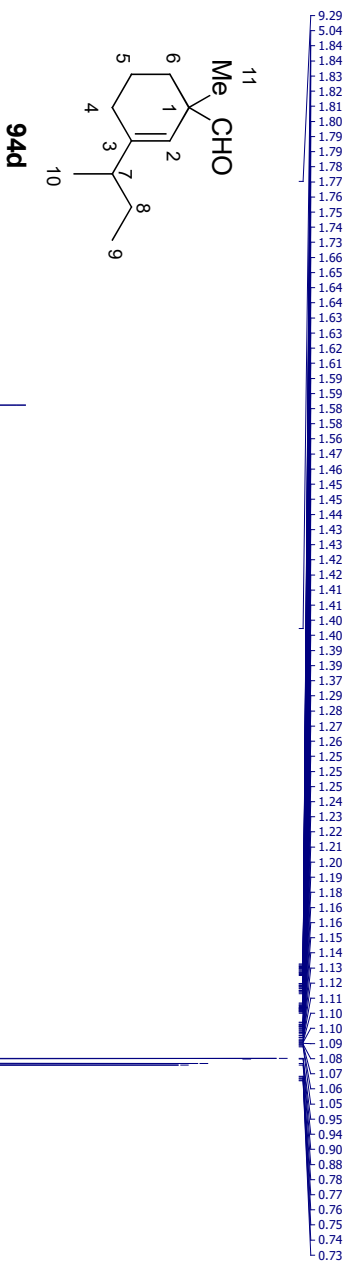


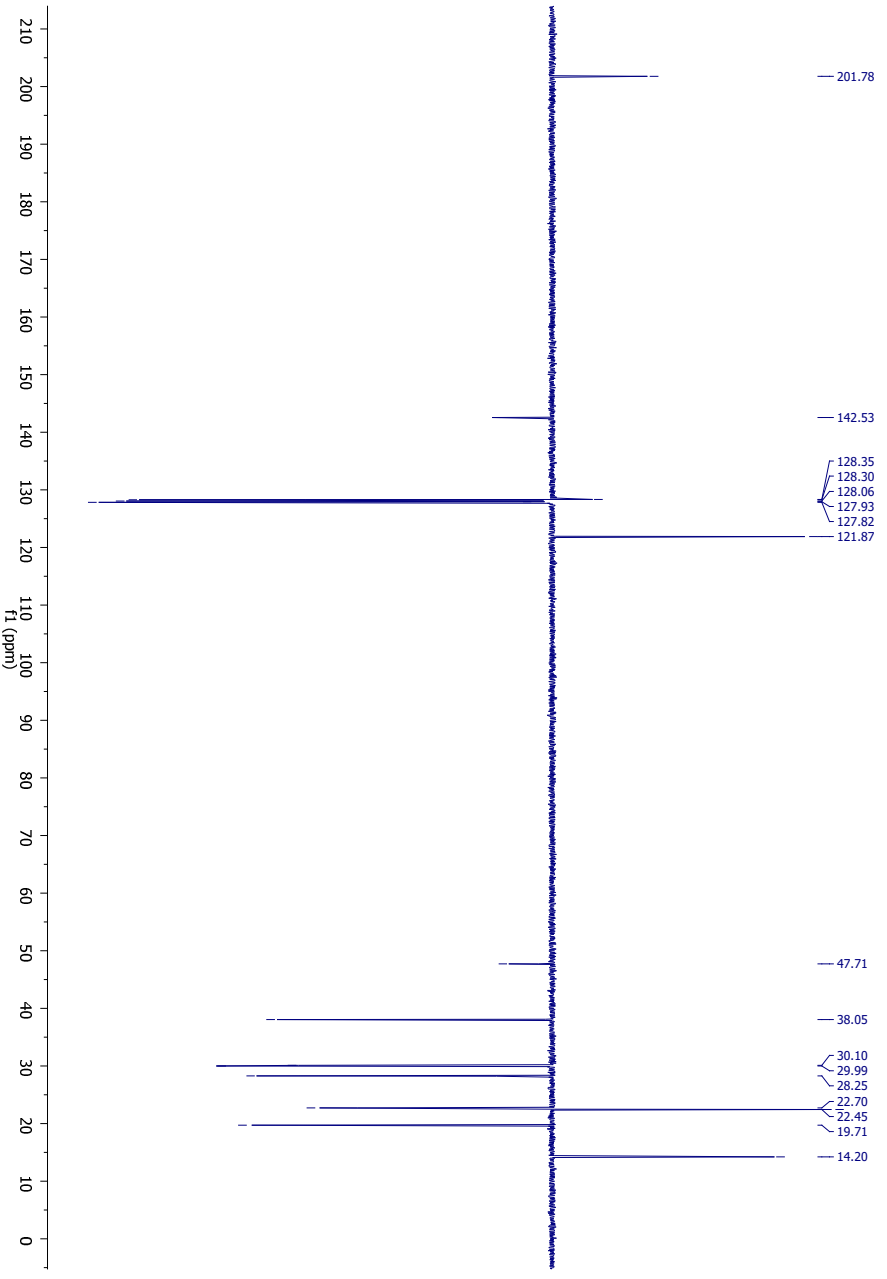
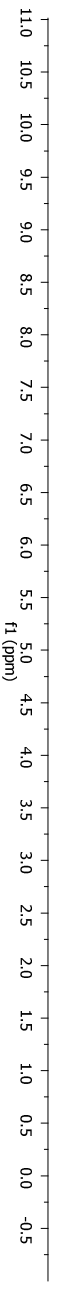


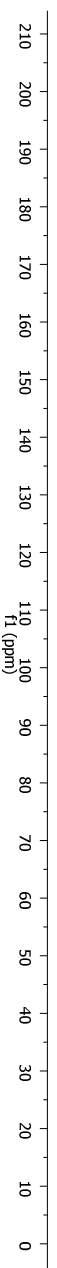
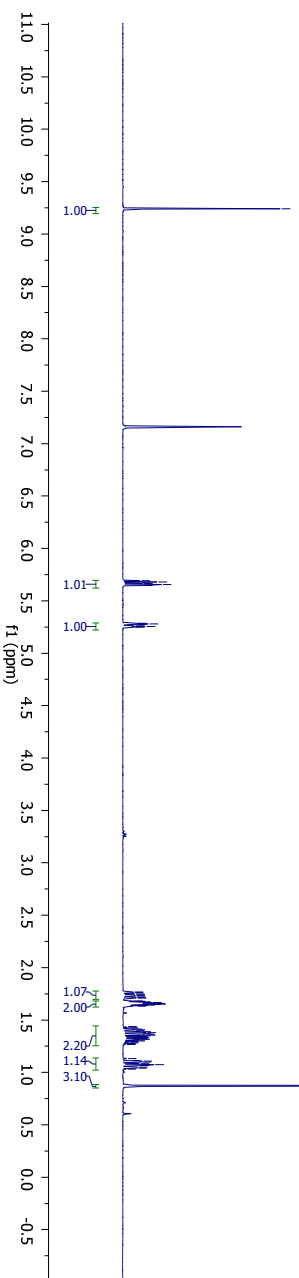
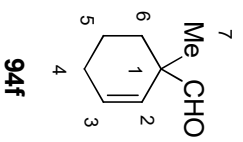
Experimental Section

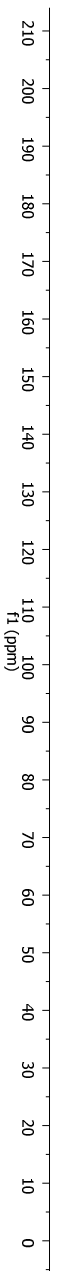
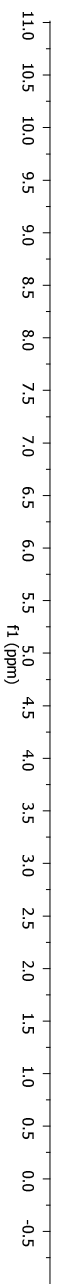
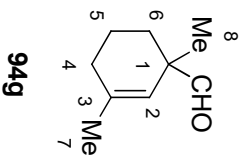




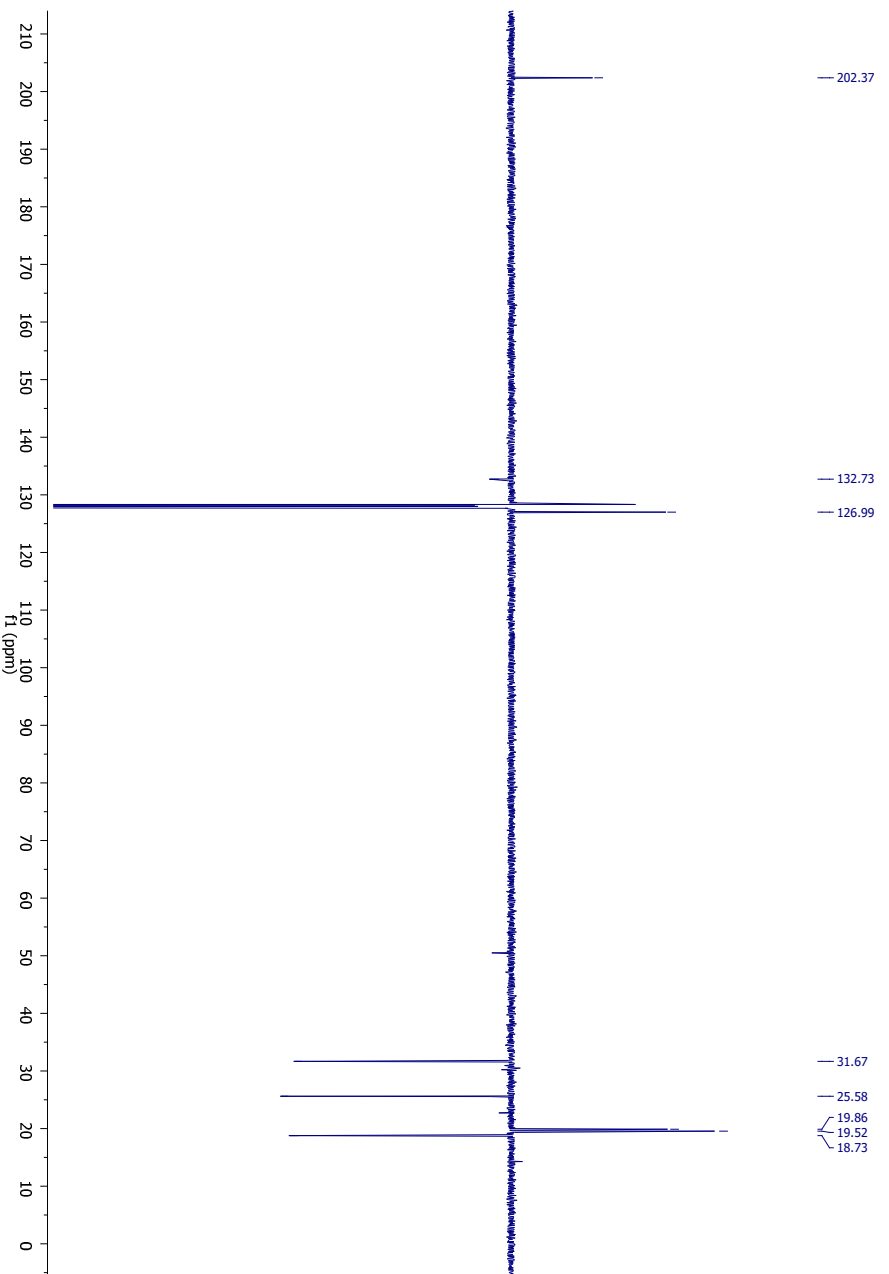
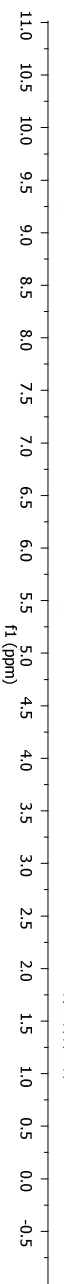
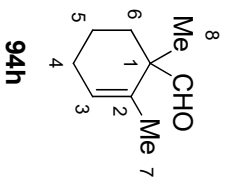


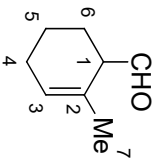






Experimental Section

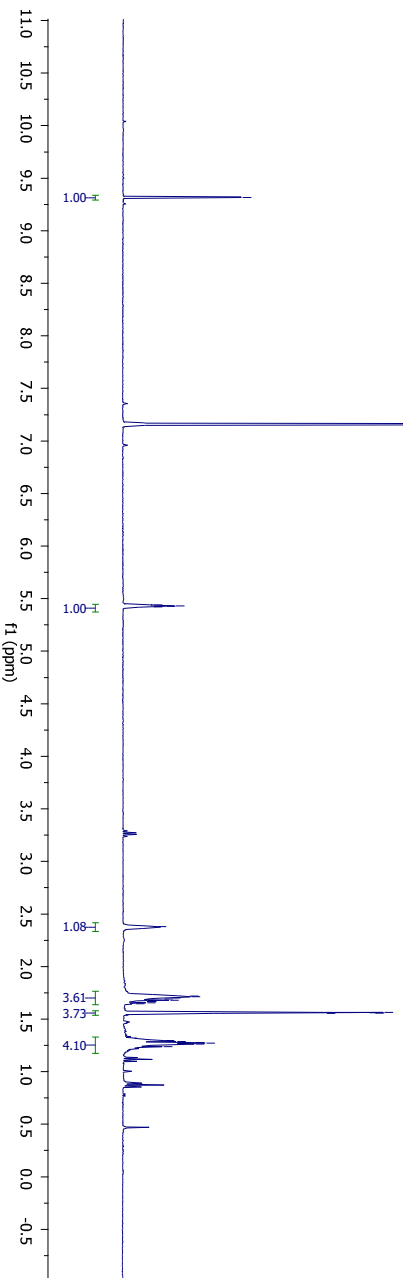




9.32

5.44
5.43
5.43
5.42

2.38
1.72
1.71
1.70
1.69
1.68
1.67
1.67
1.66
1.65
1.56
1.56
1.56
1.29
1.29
1.28
1.27
1.26
1.24

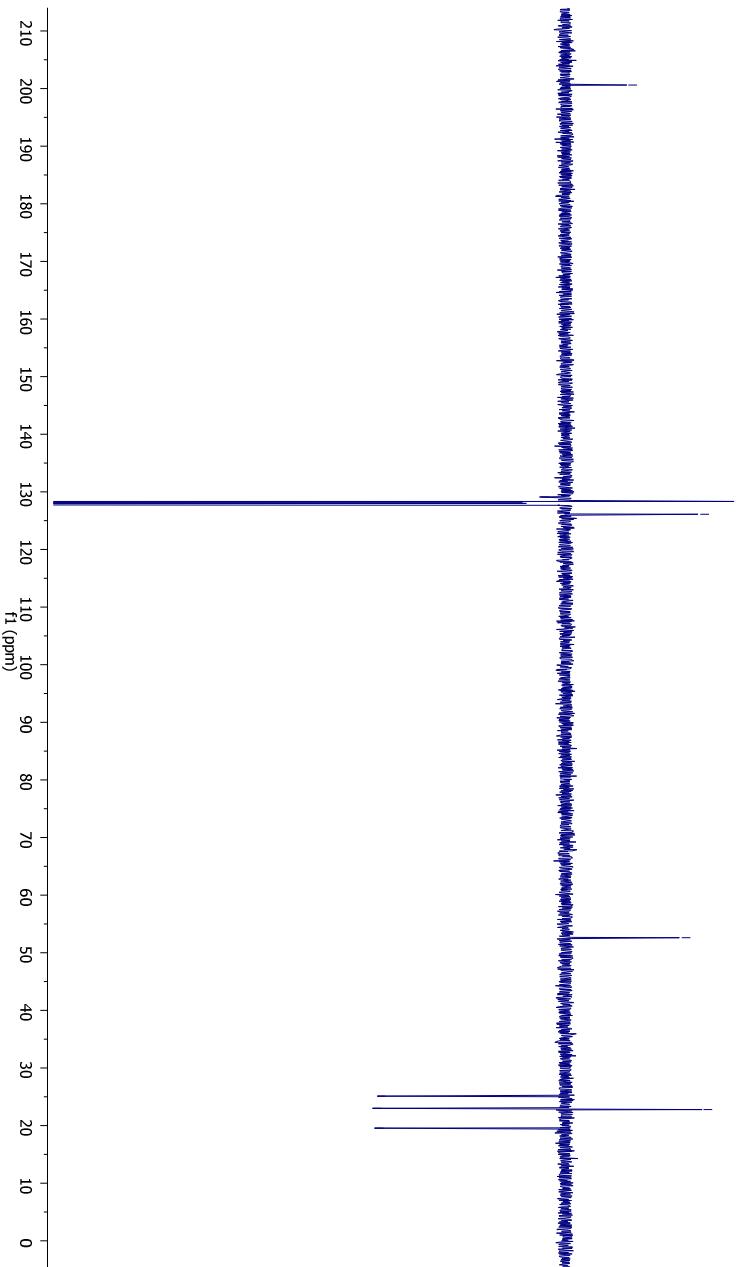


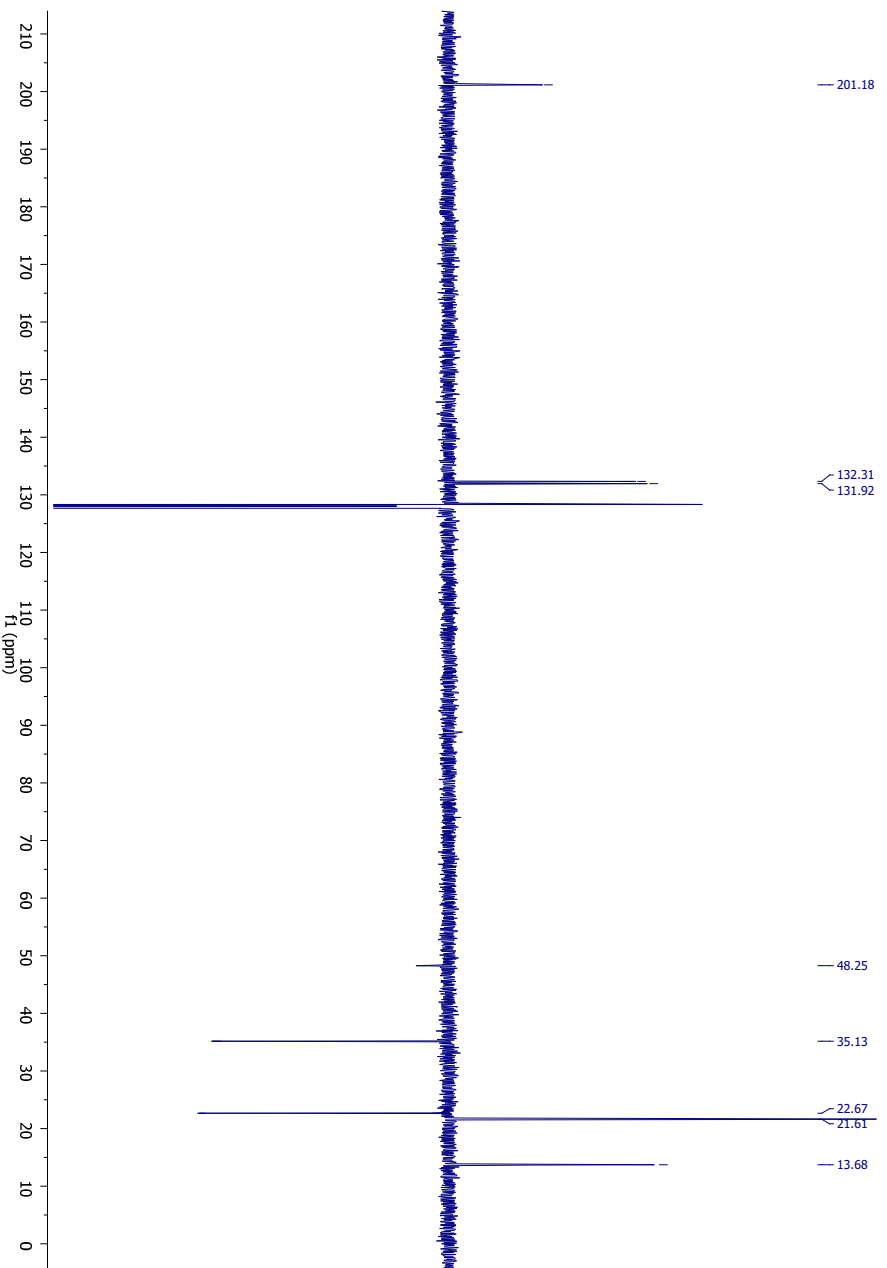
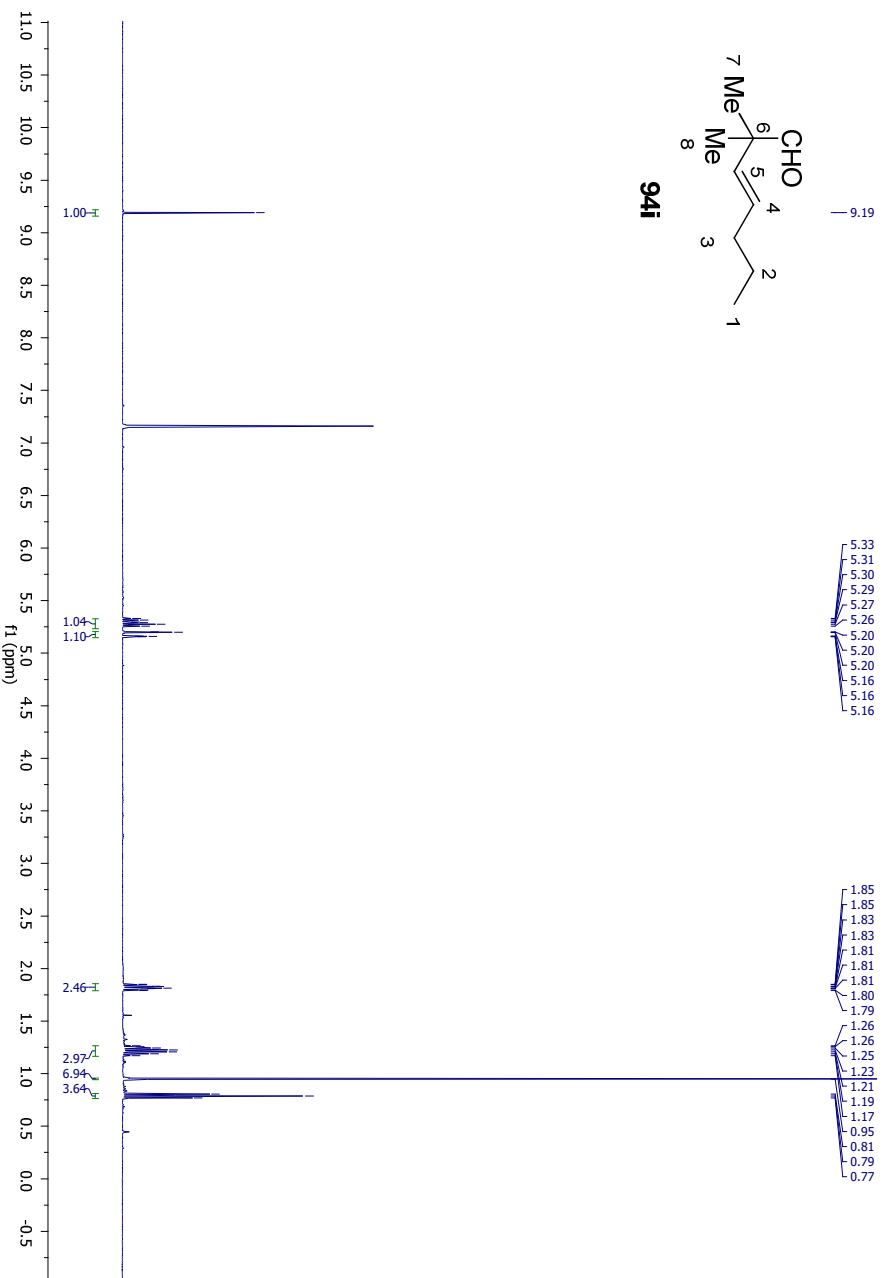
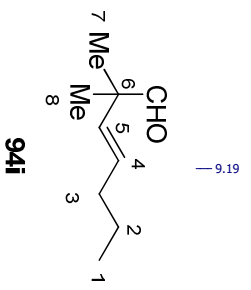
200.59

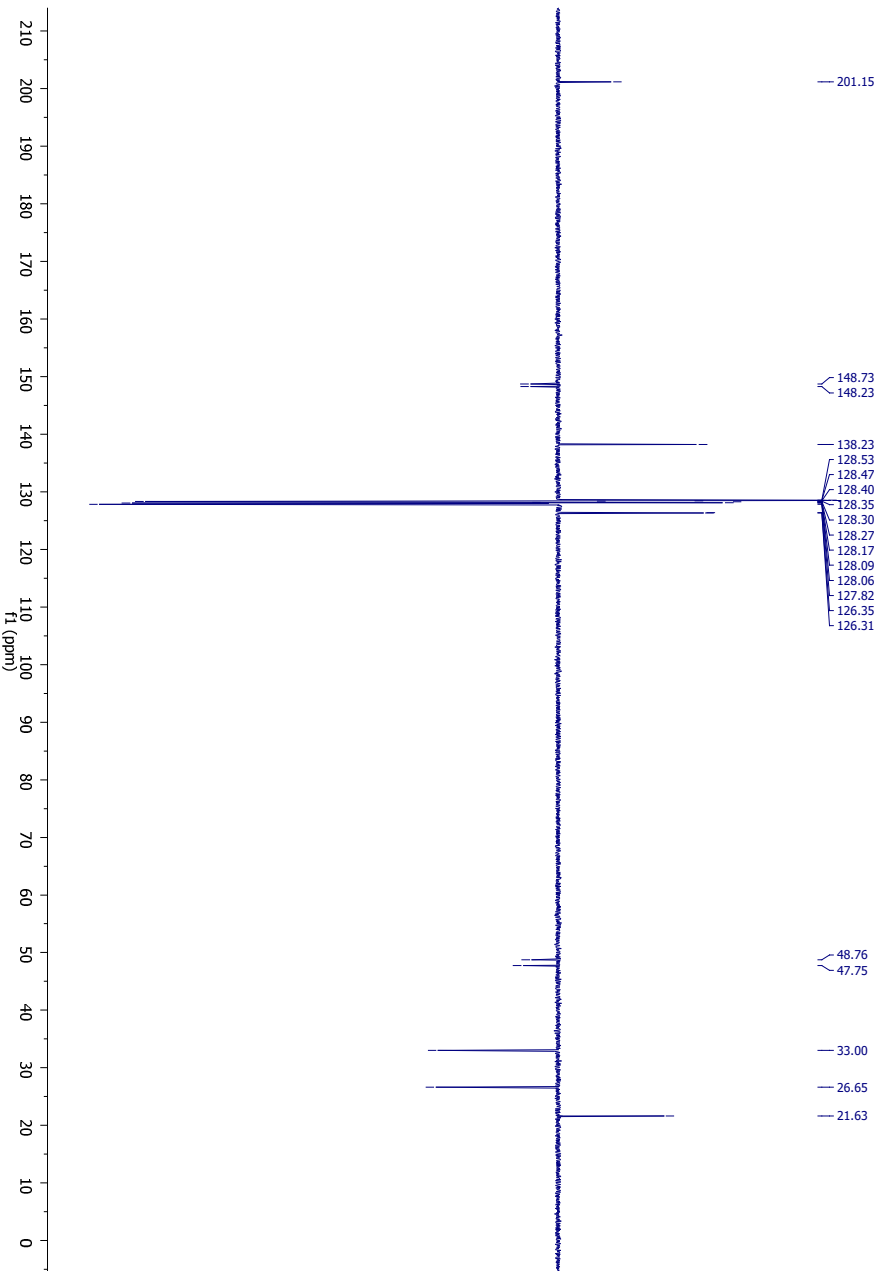
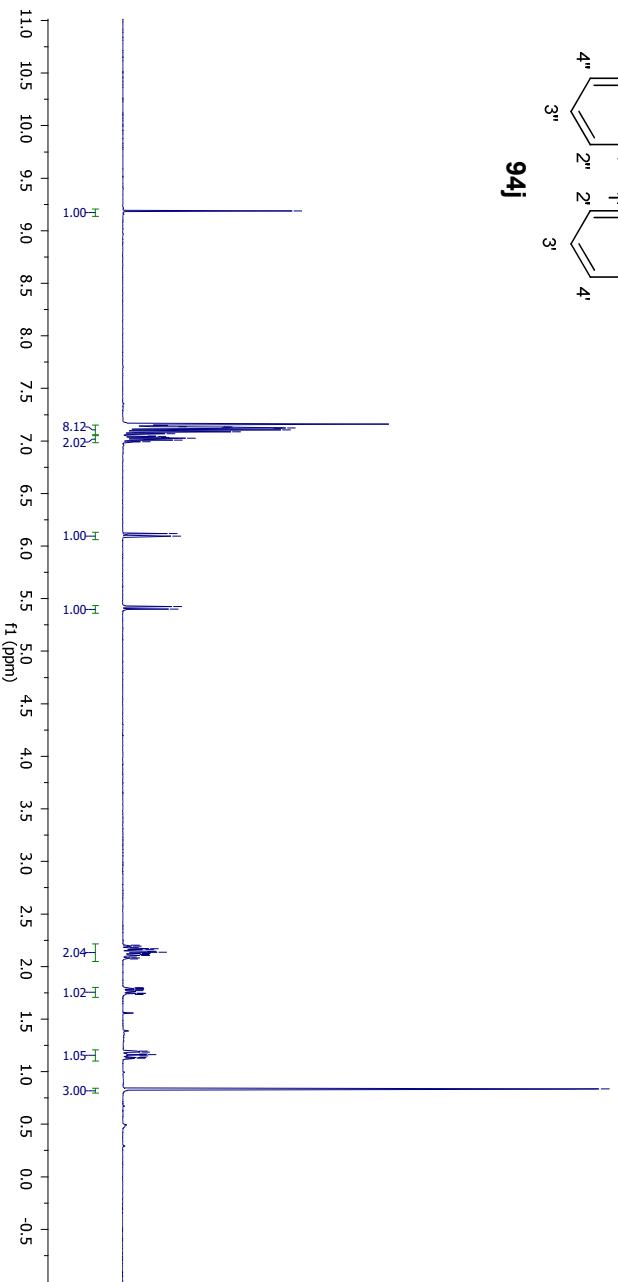
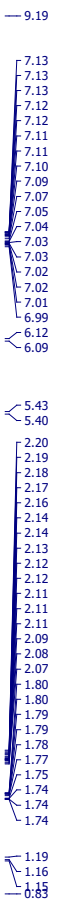
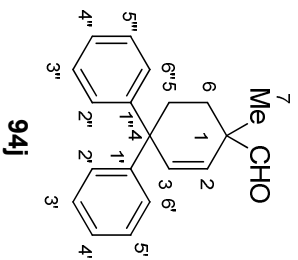
129.08
126.11

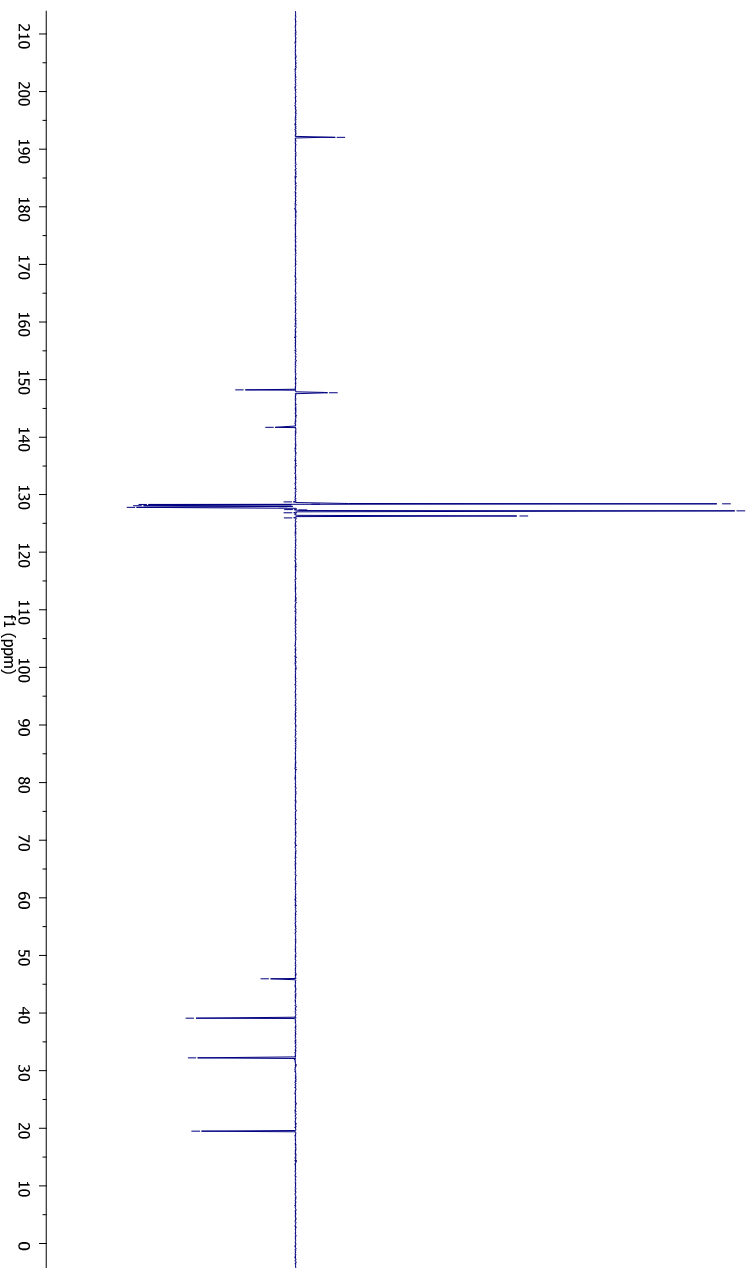
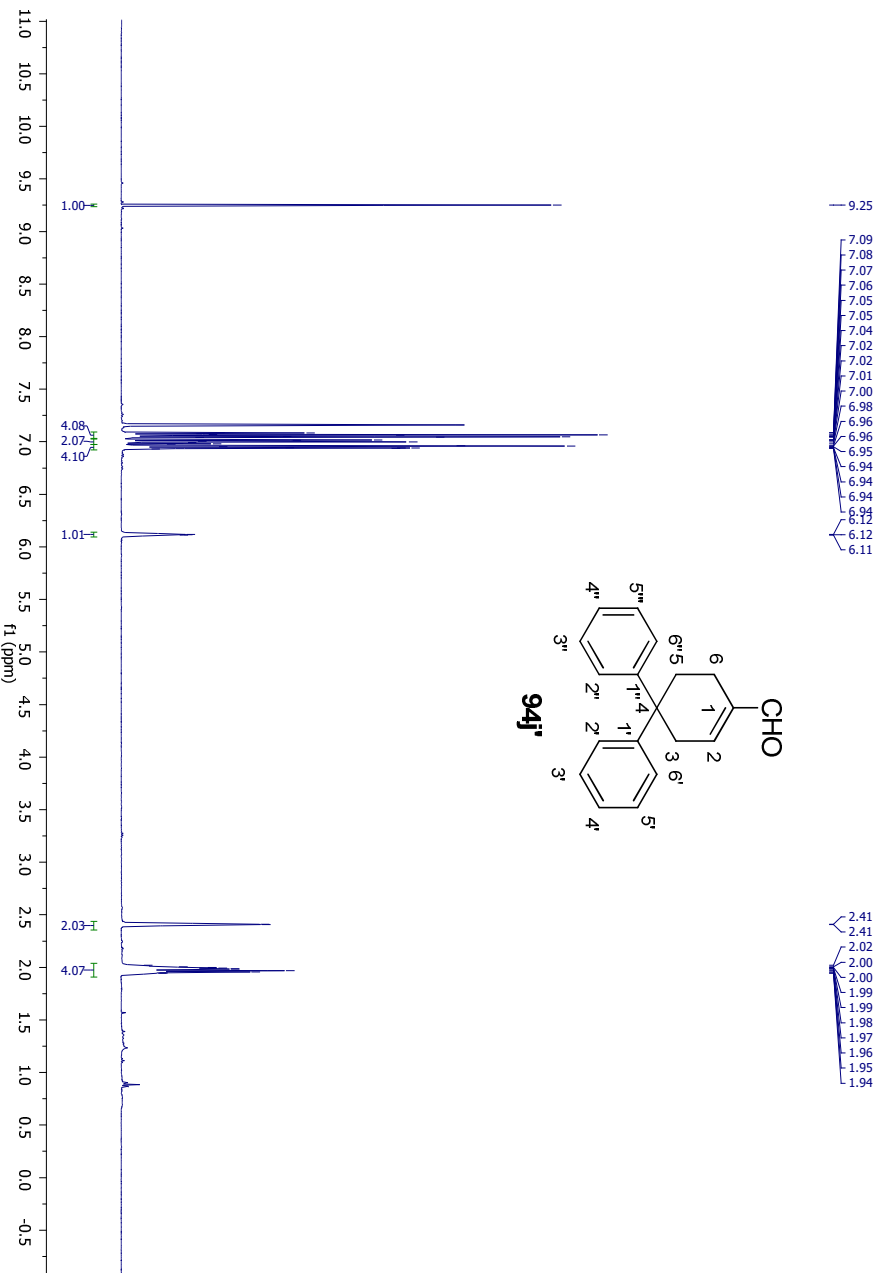
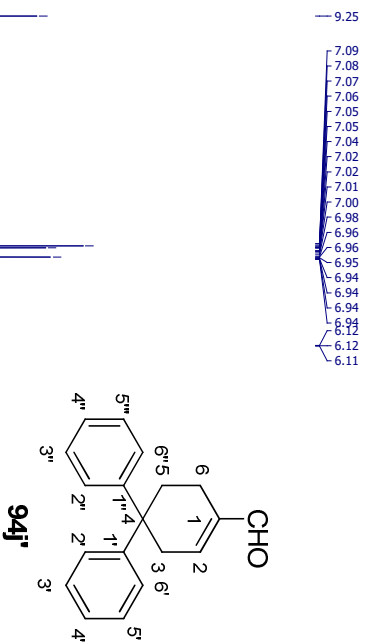
52.58

25.11
23.00
22.77
19.51

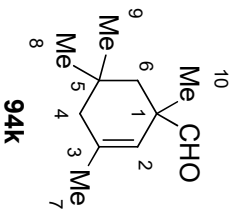








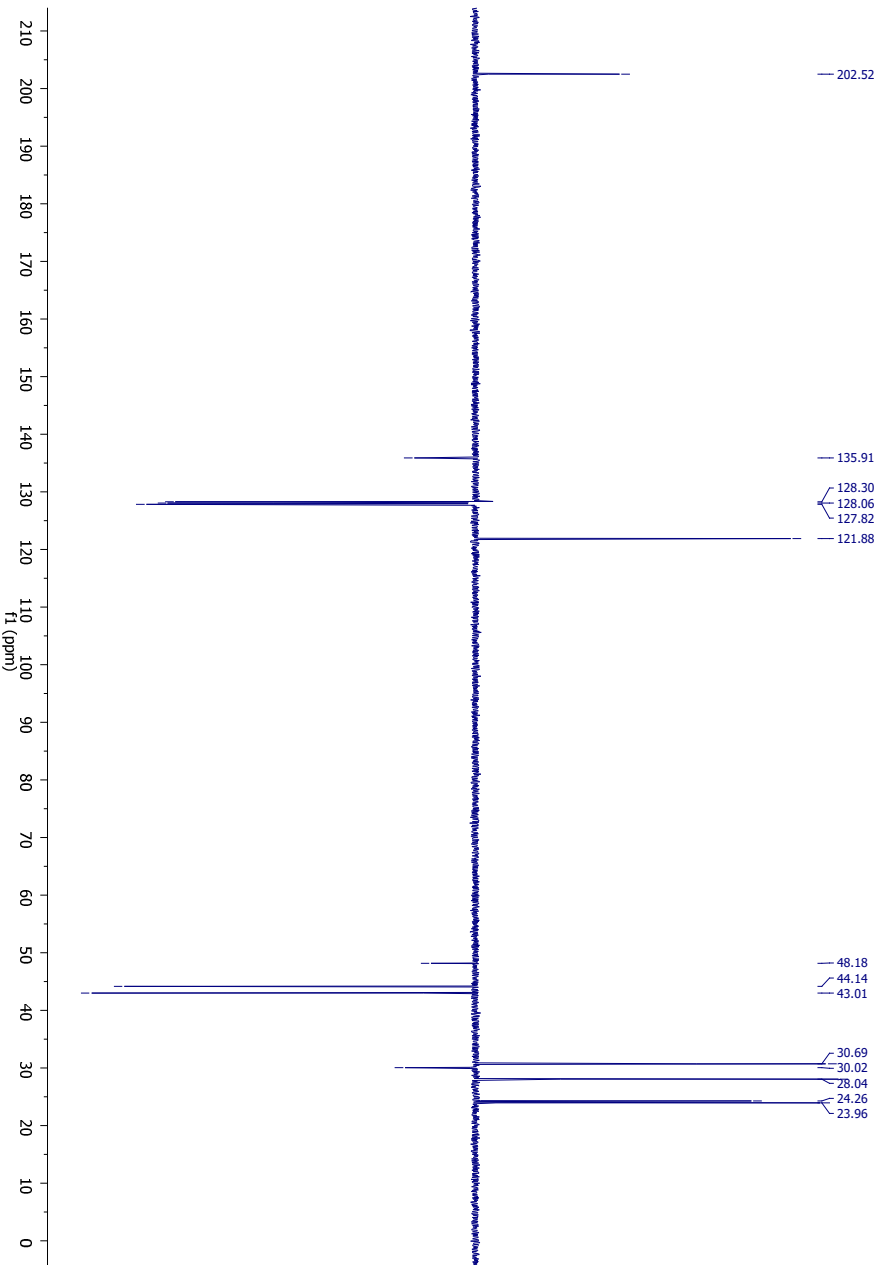
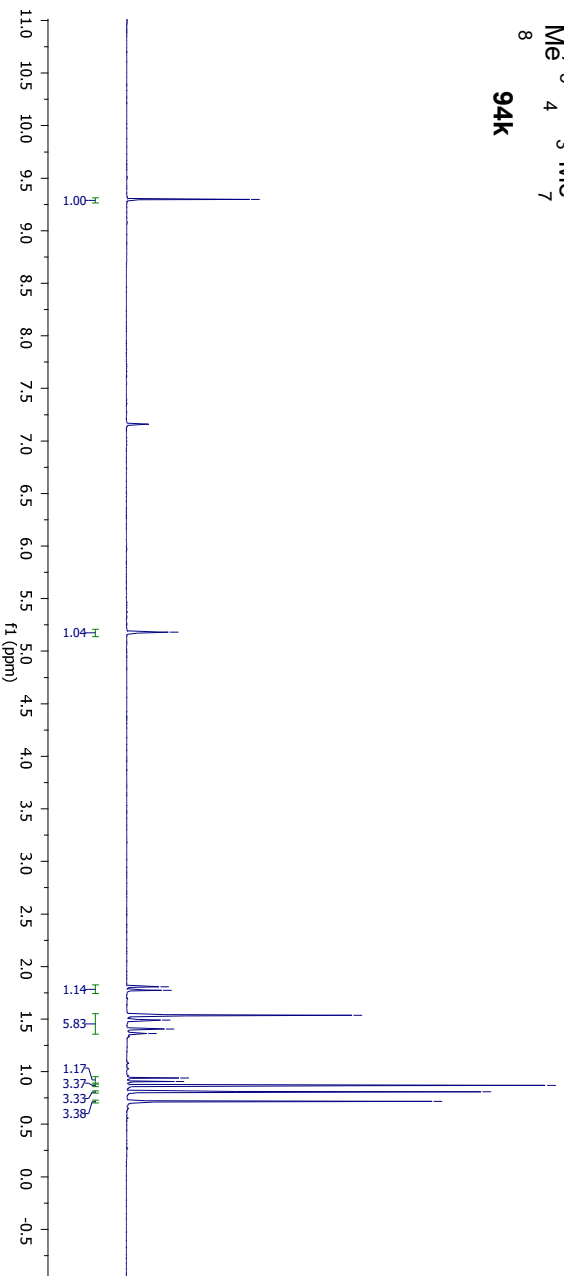
Experimental Section

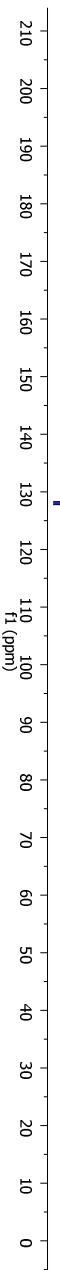
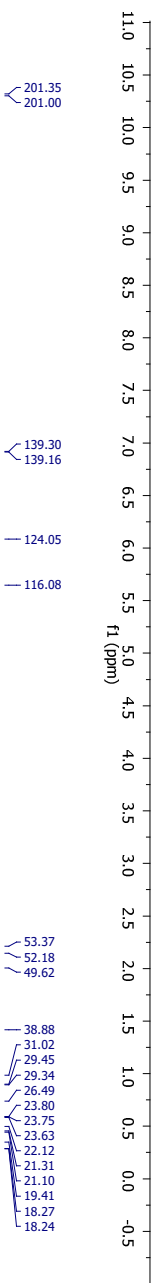
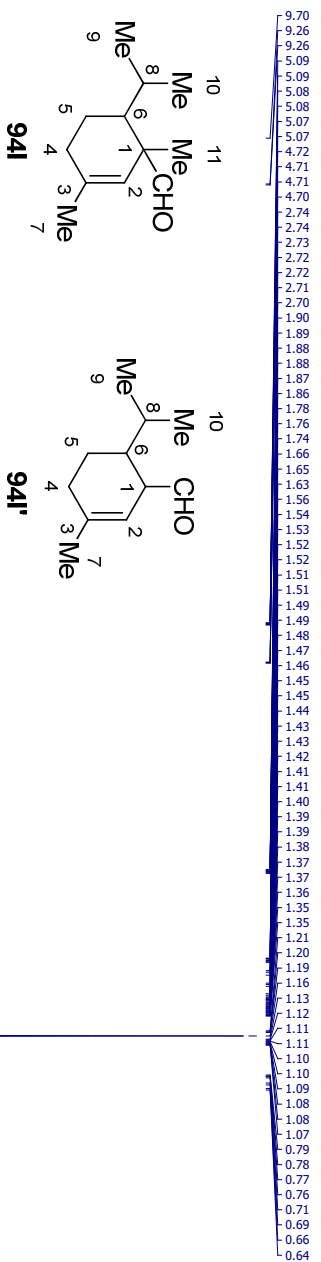


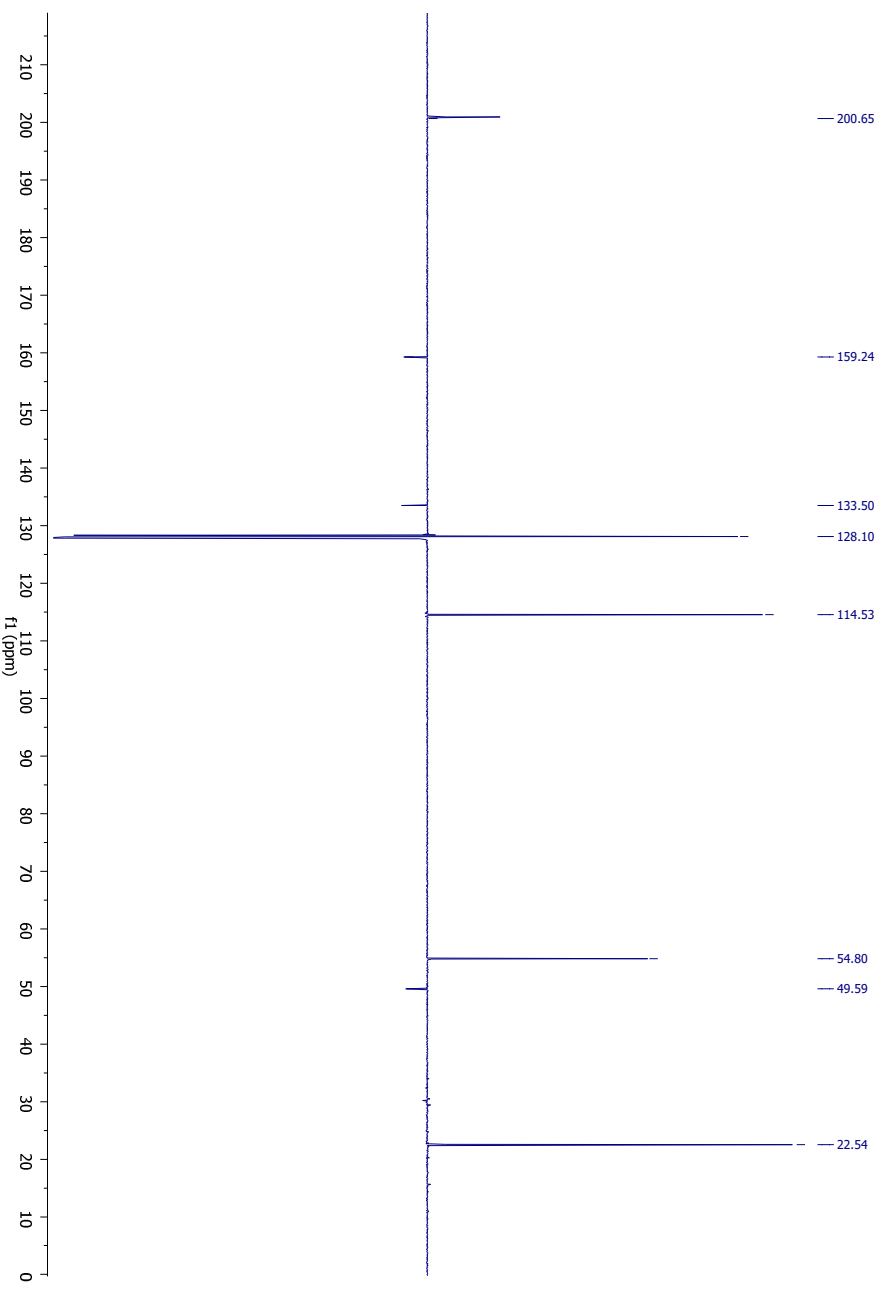
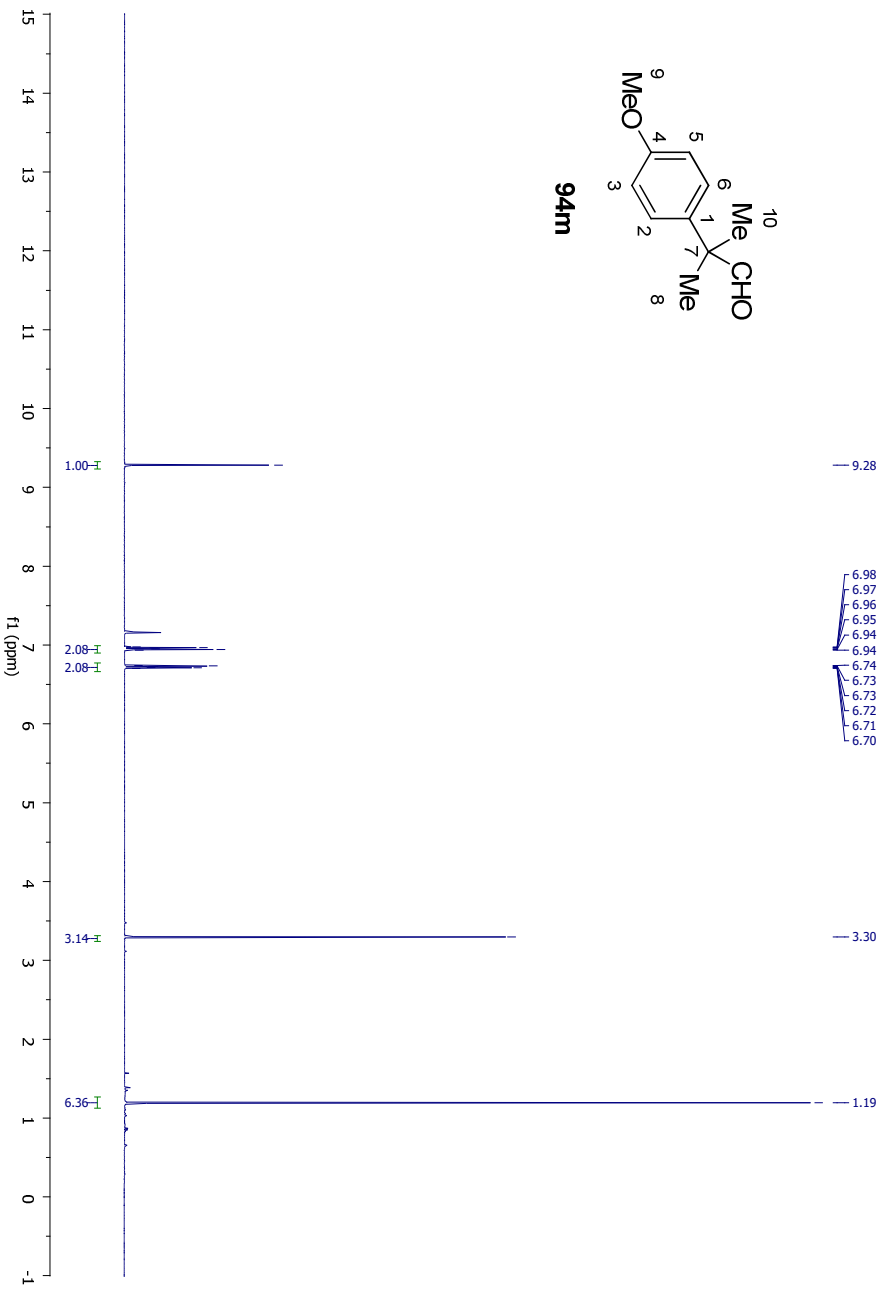
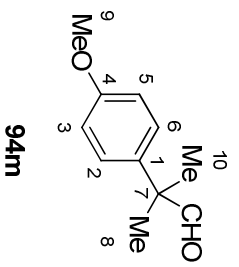
9.30

5.18

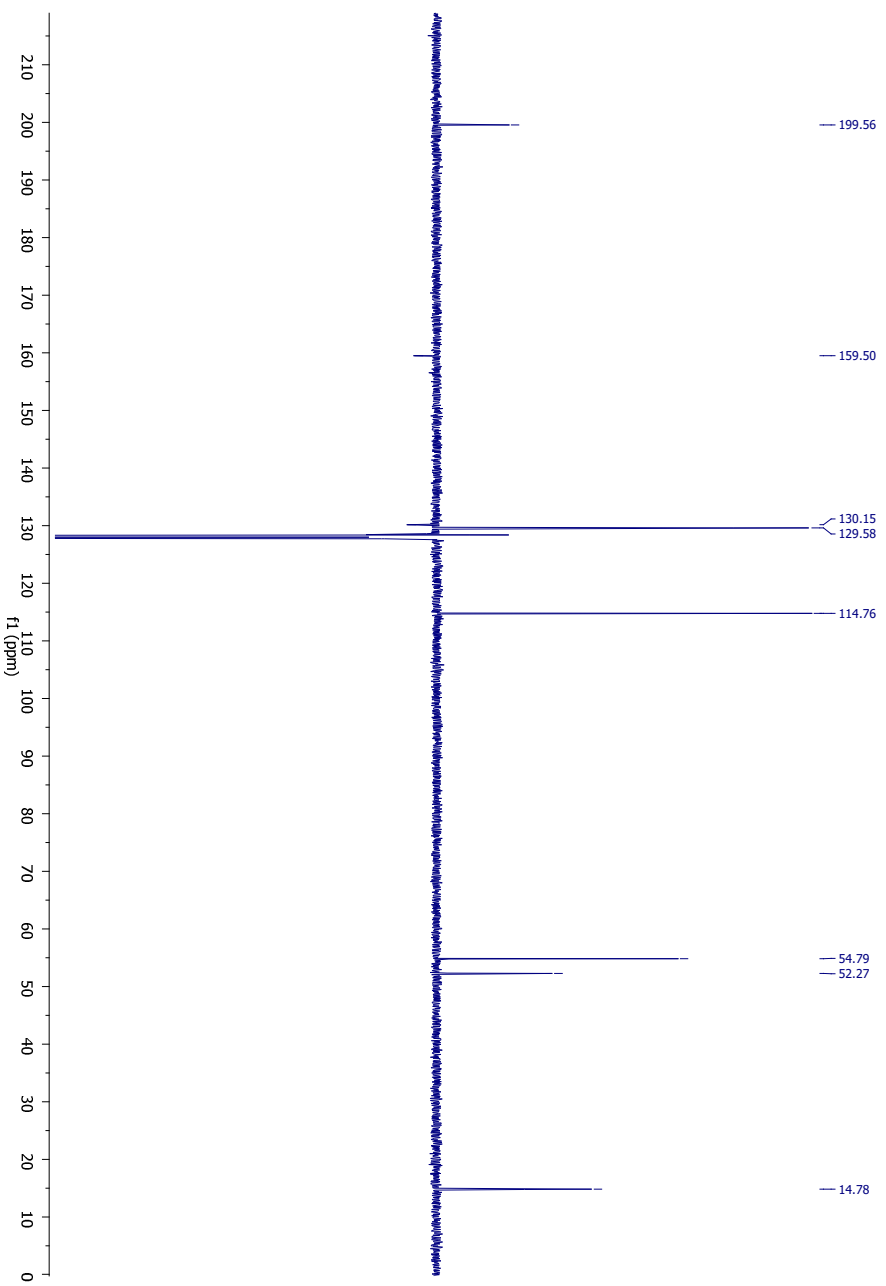
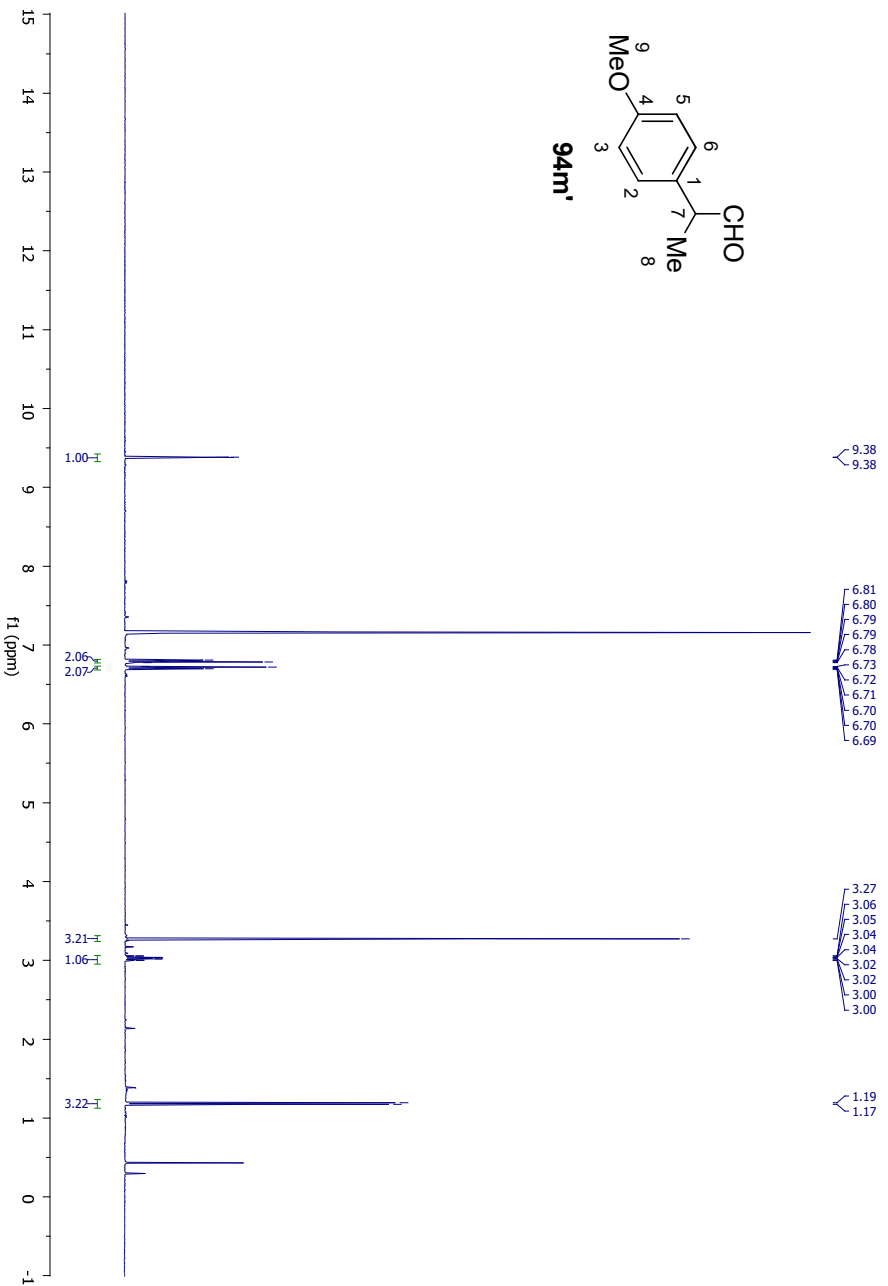
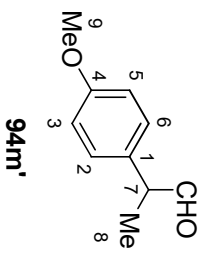
1.81
1.77
1.54
1.49
1.41
1.36
0.94
0.91
0.87
0.81
0.72

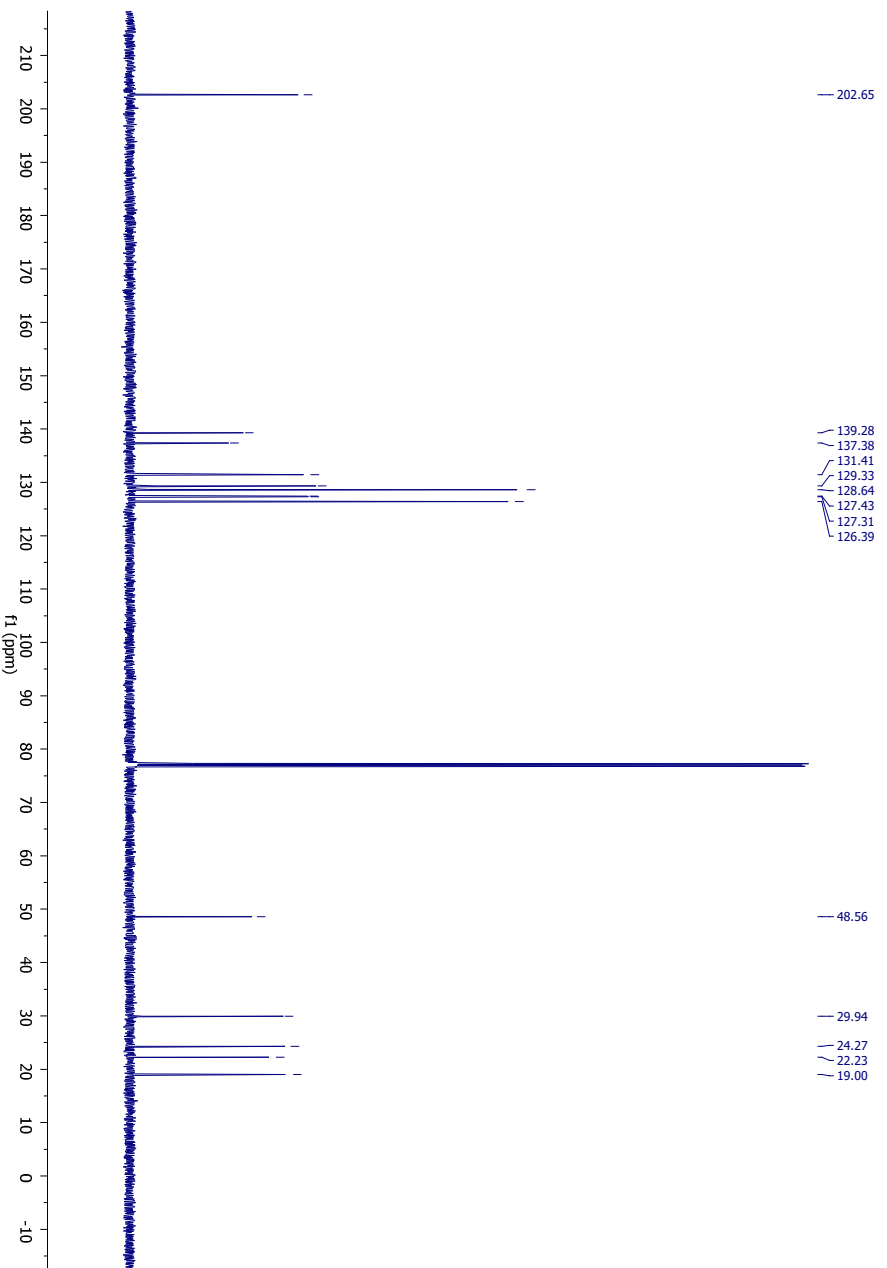
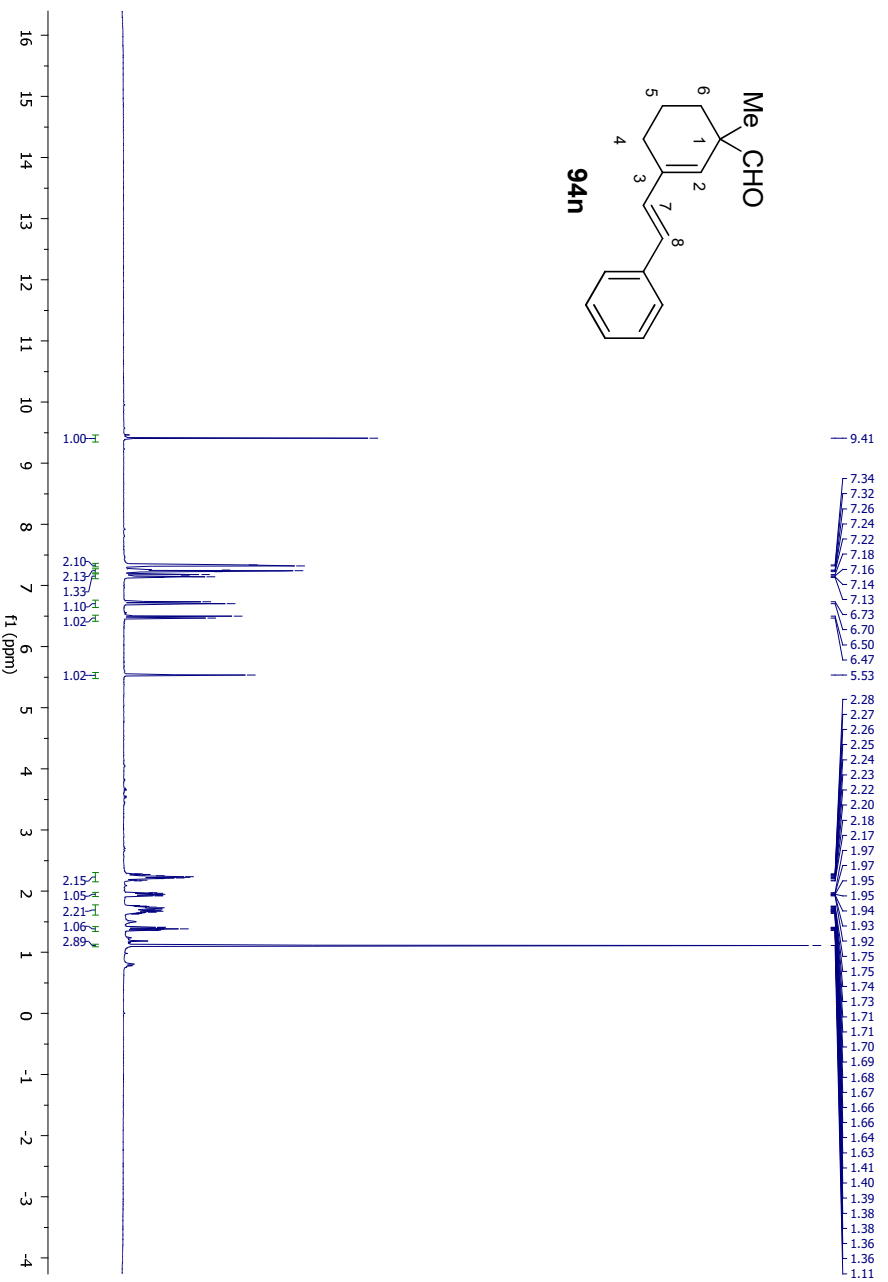
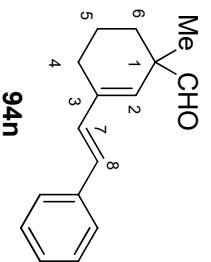




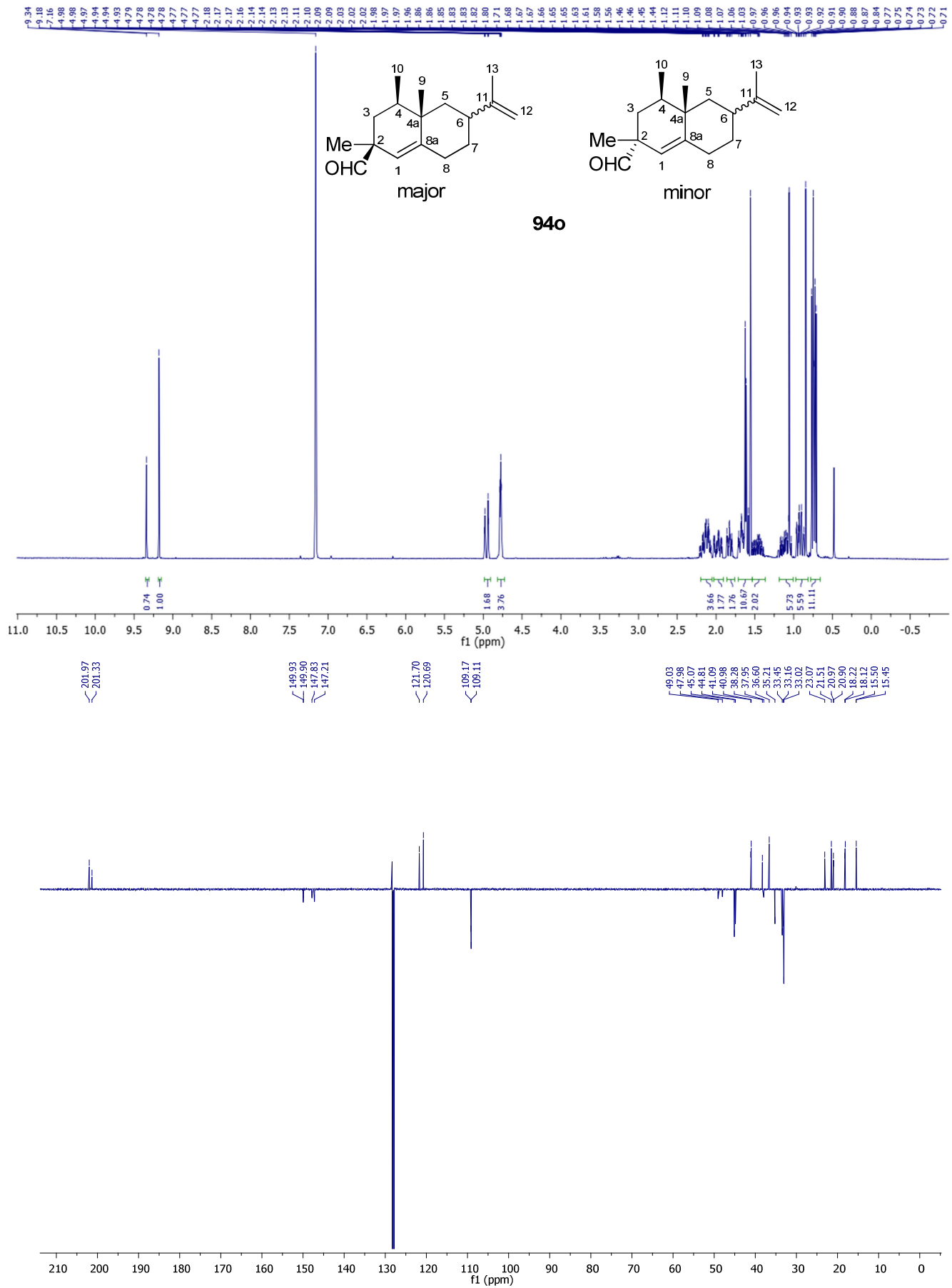


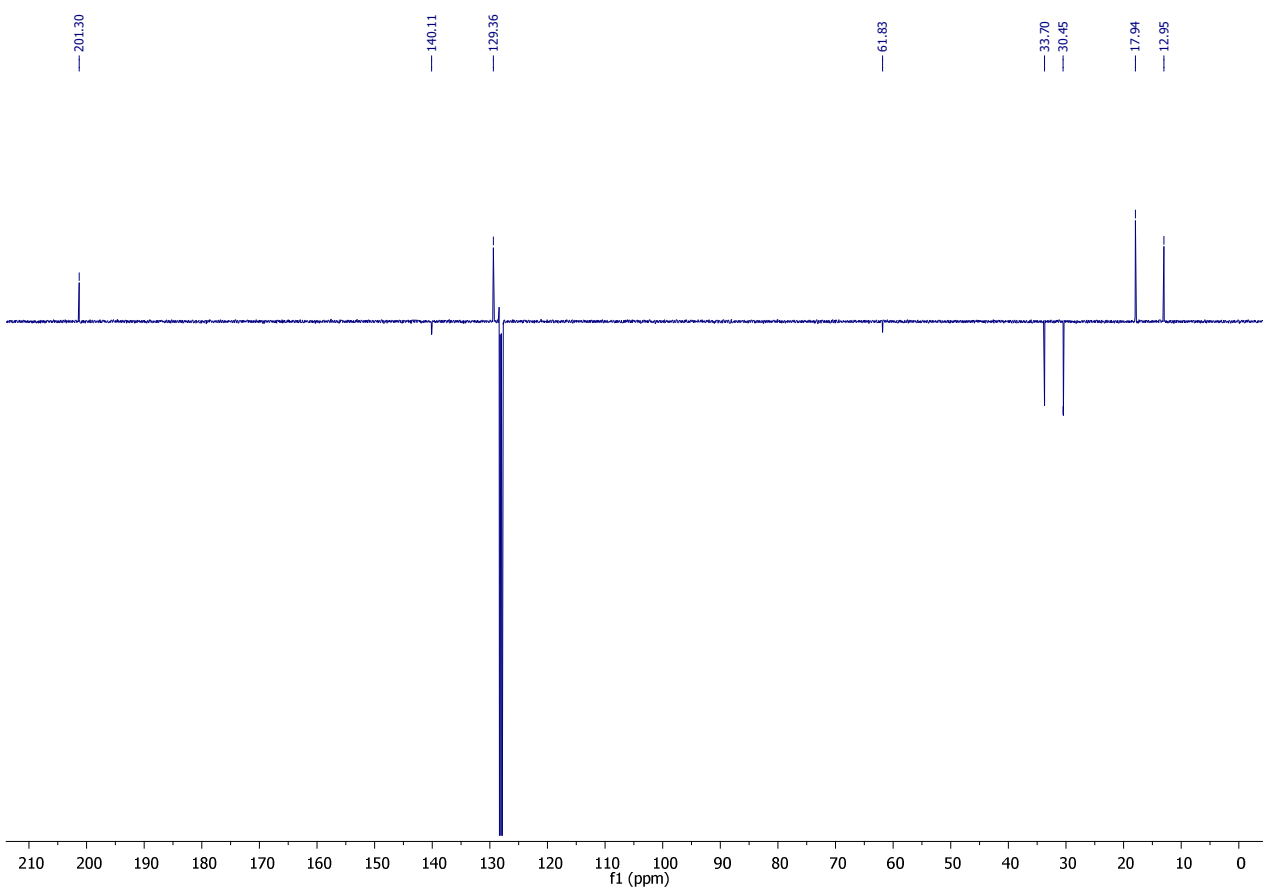
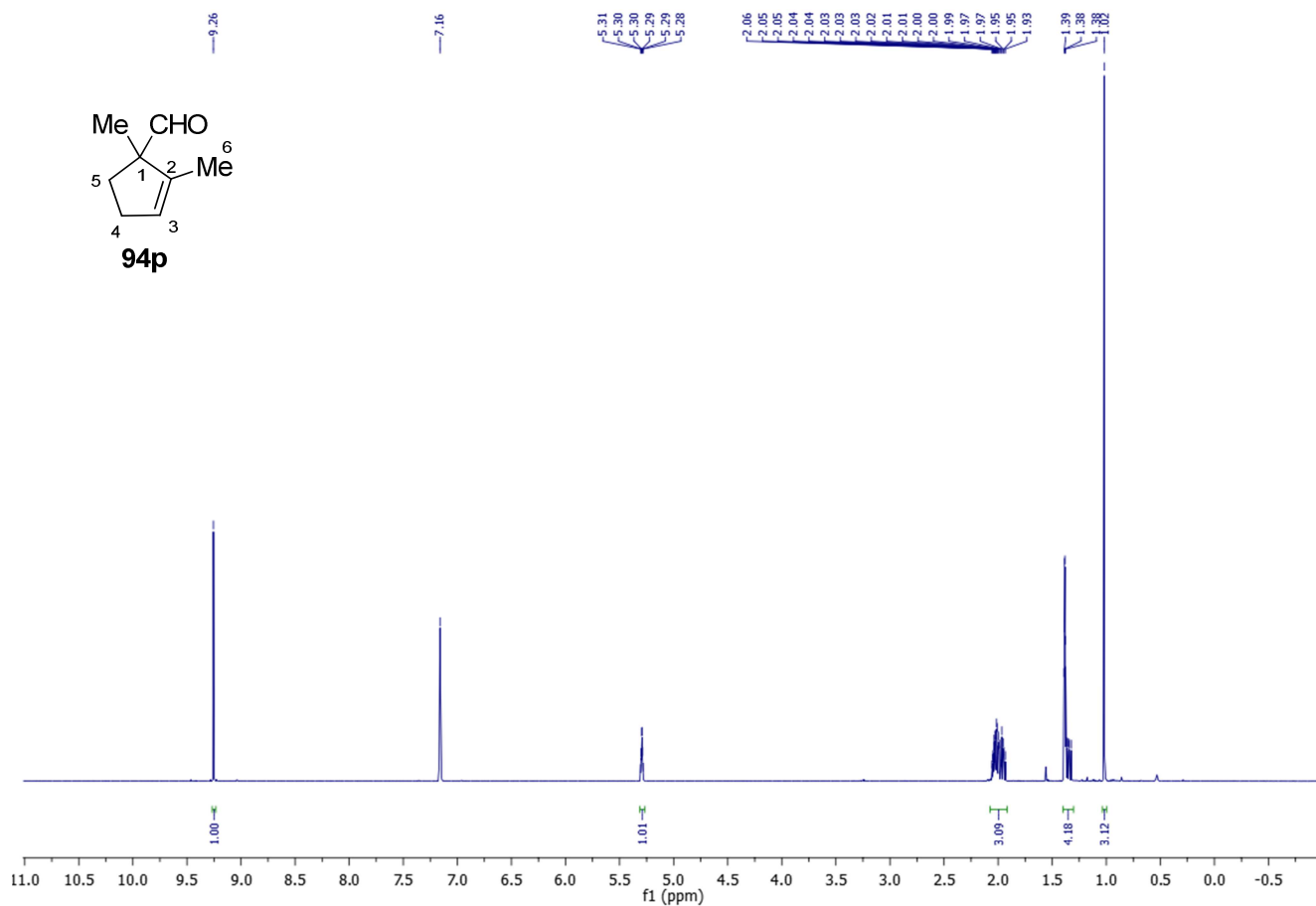
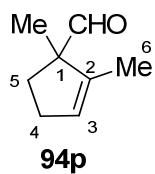
Experimental Section



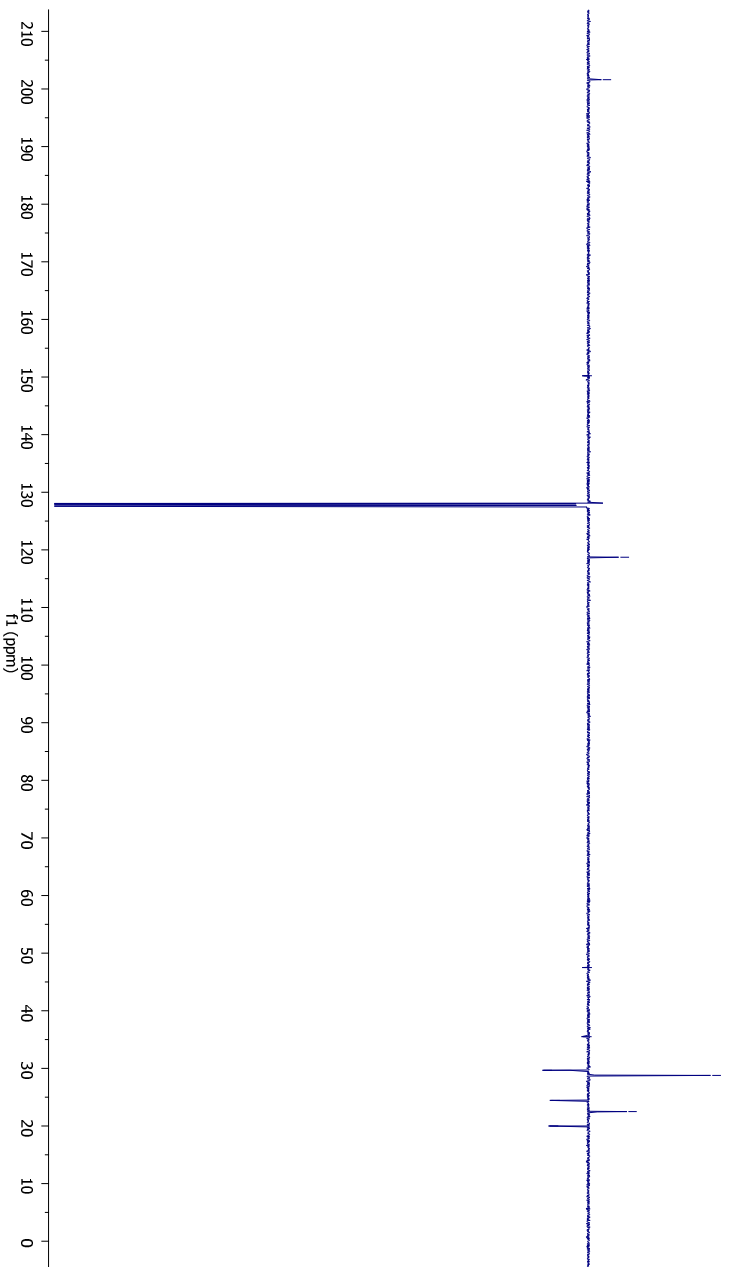
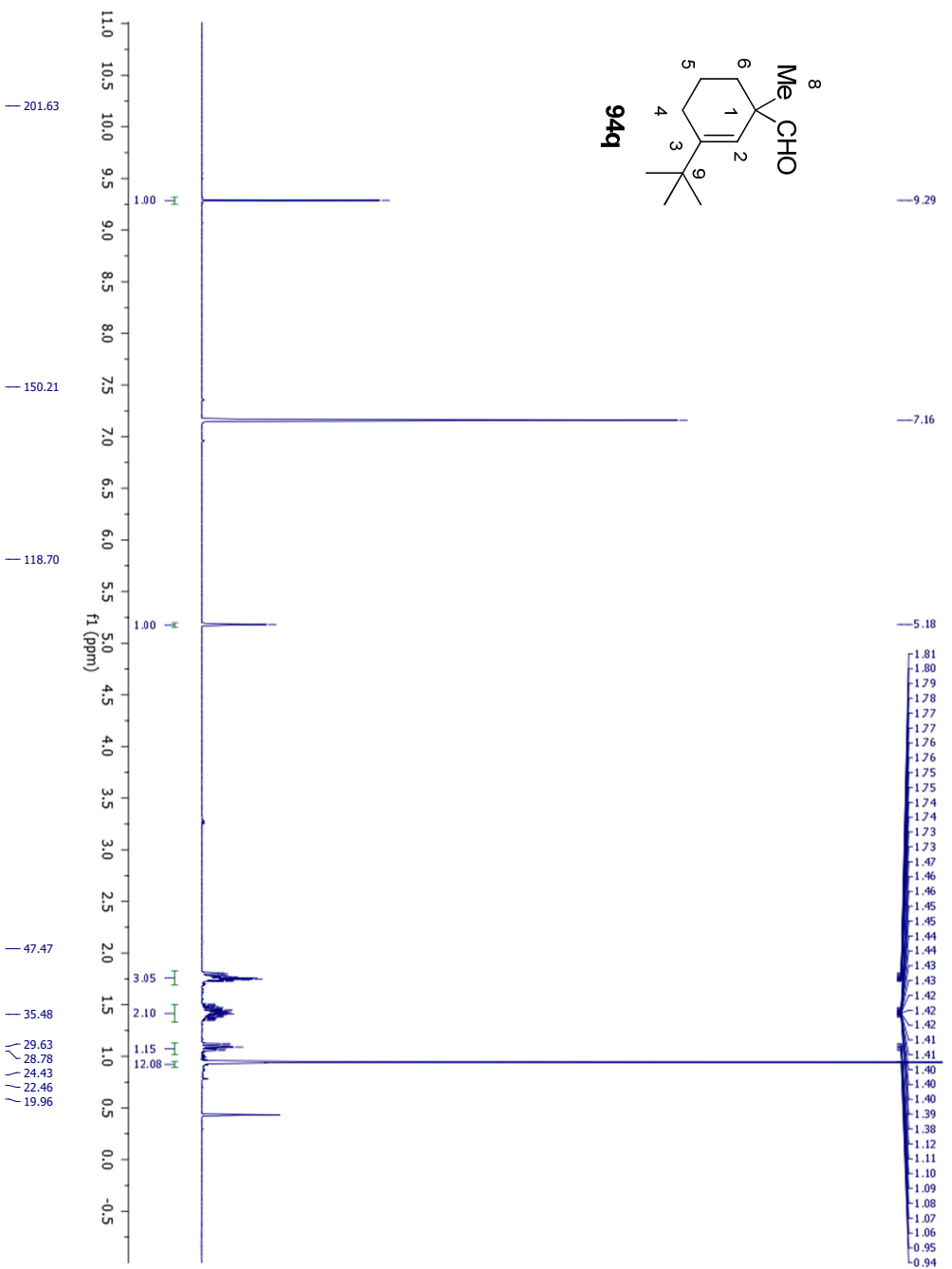
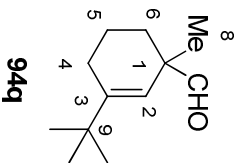


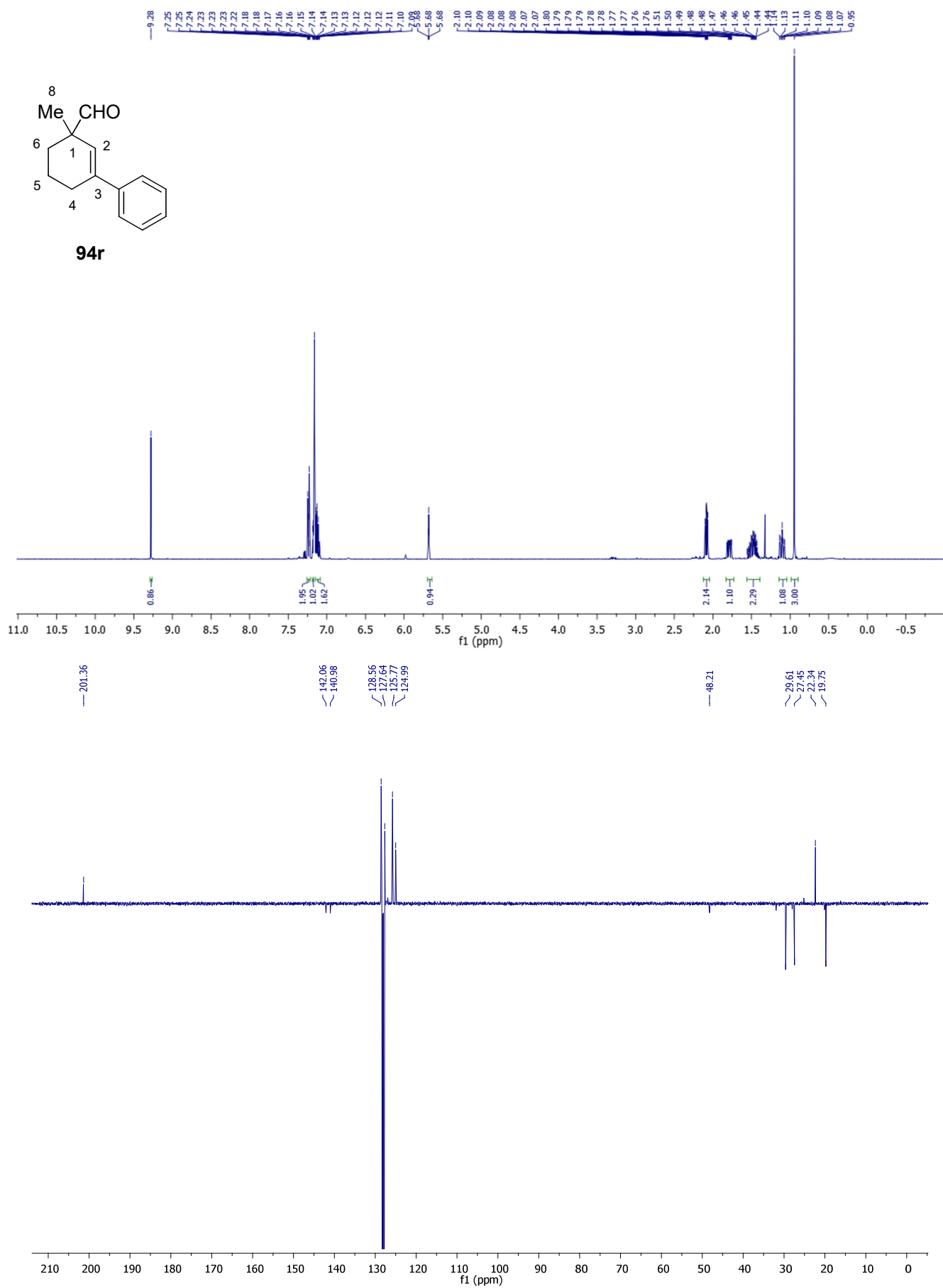
Experimental Section



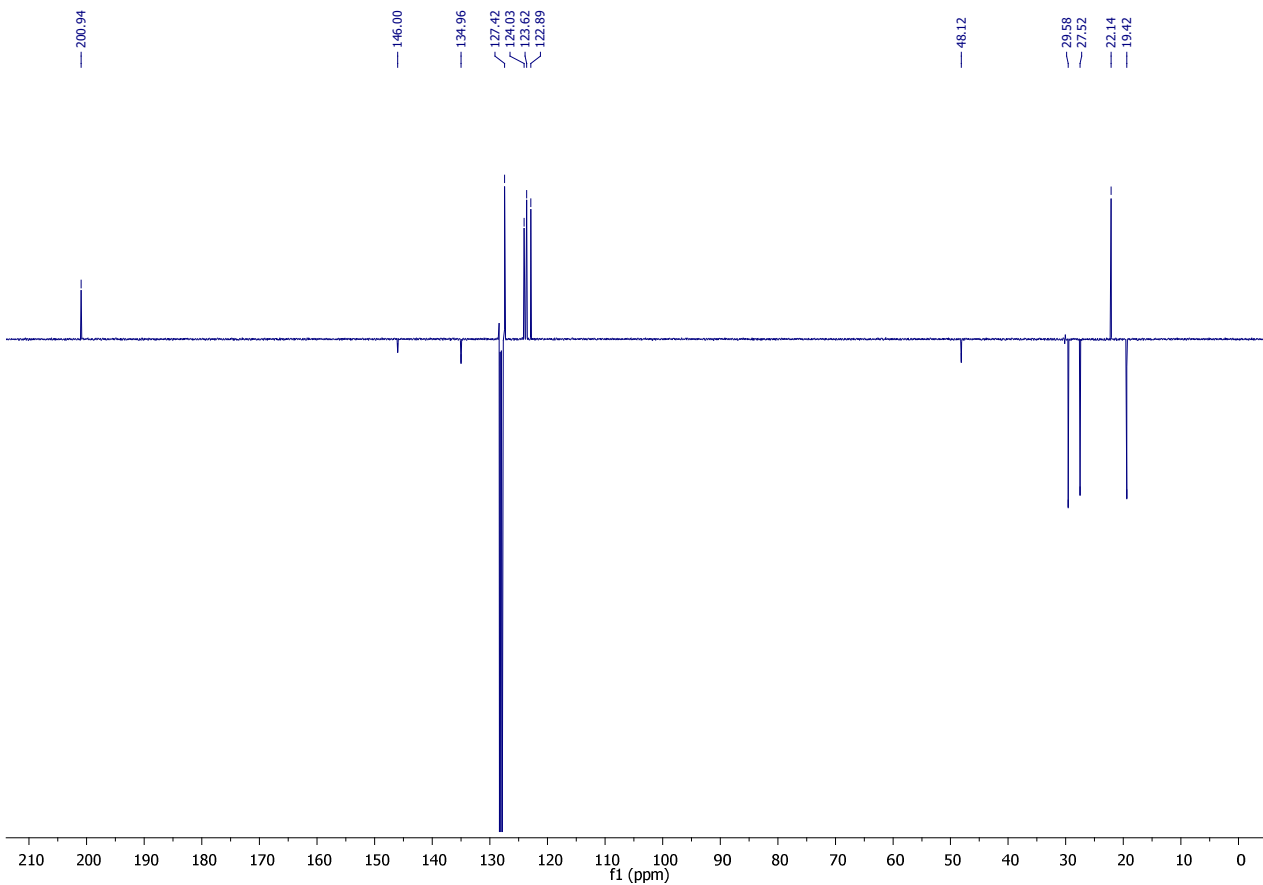
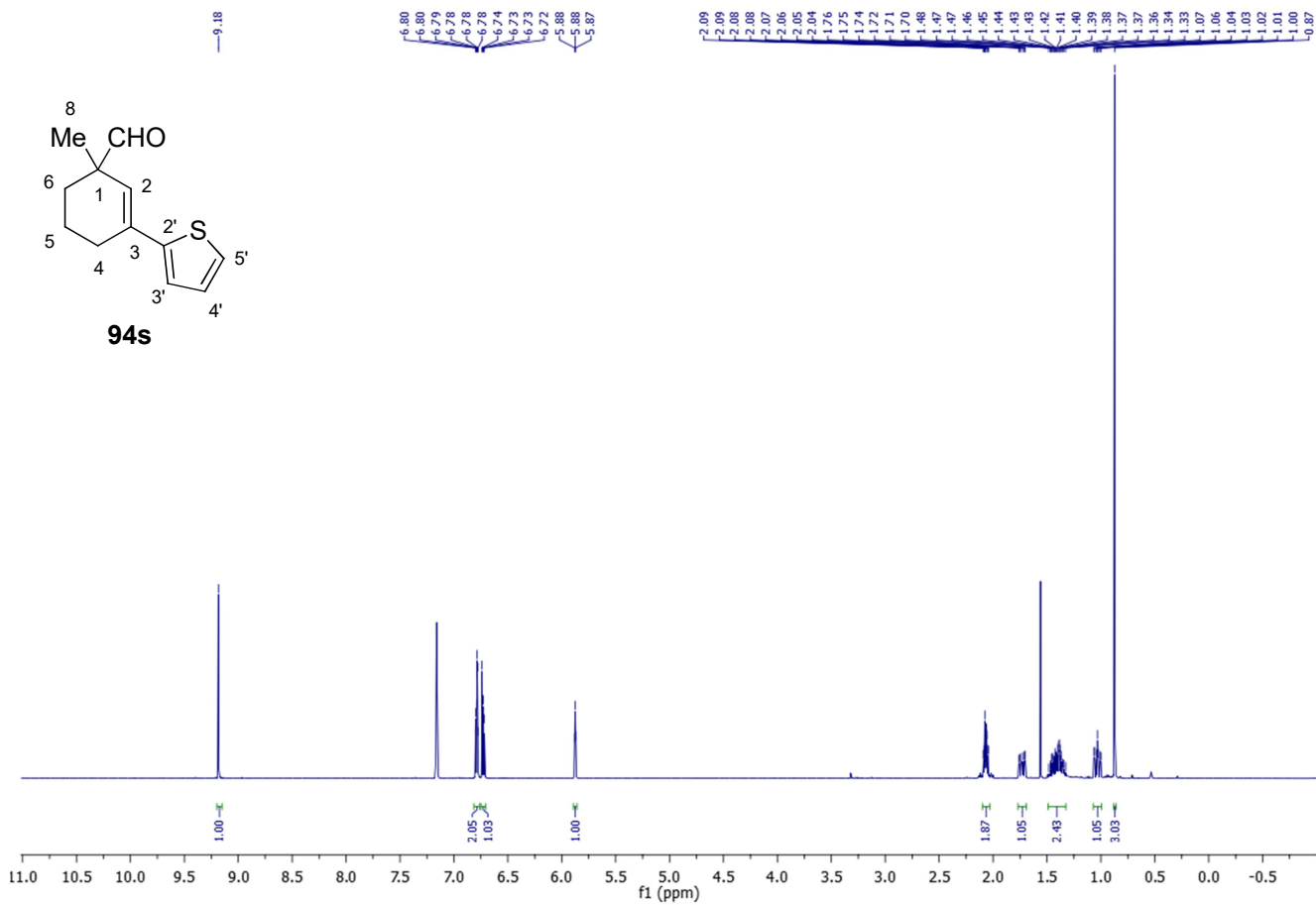


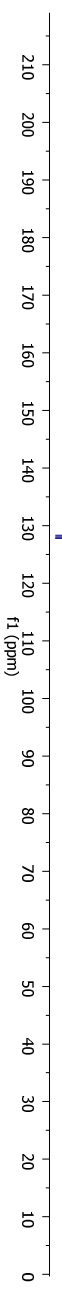
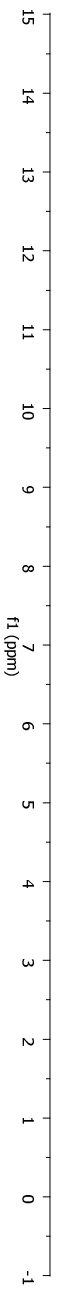
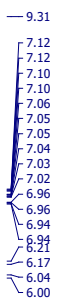
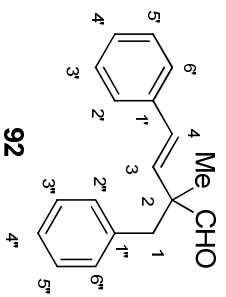
Experimental Section



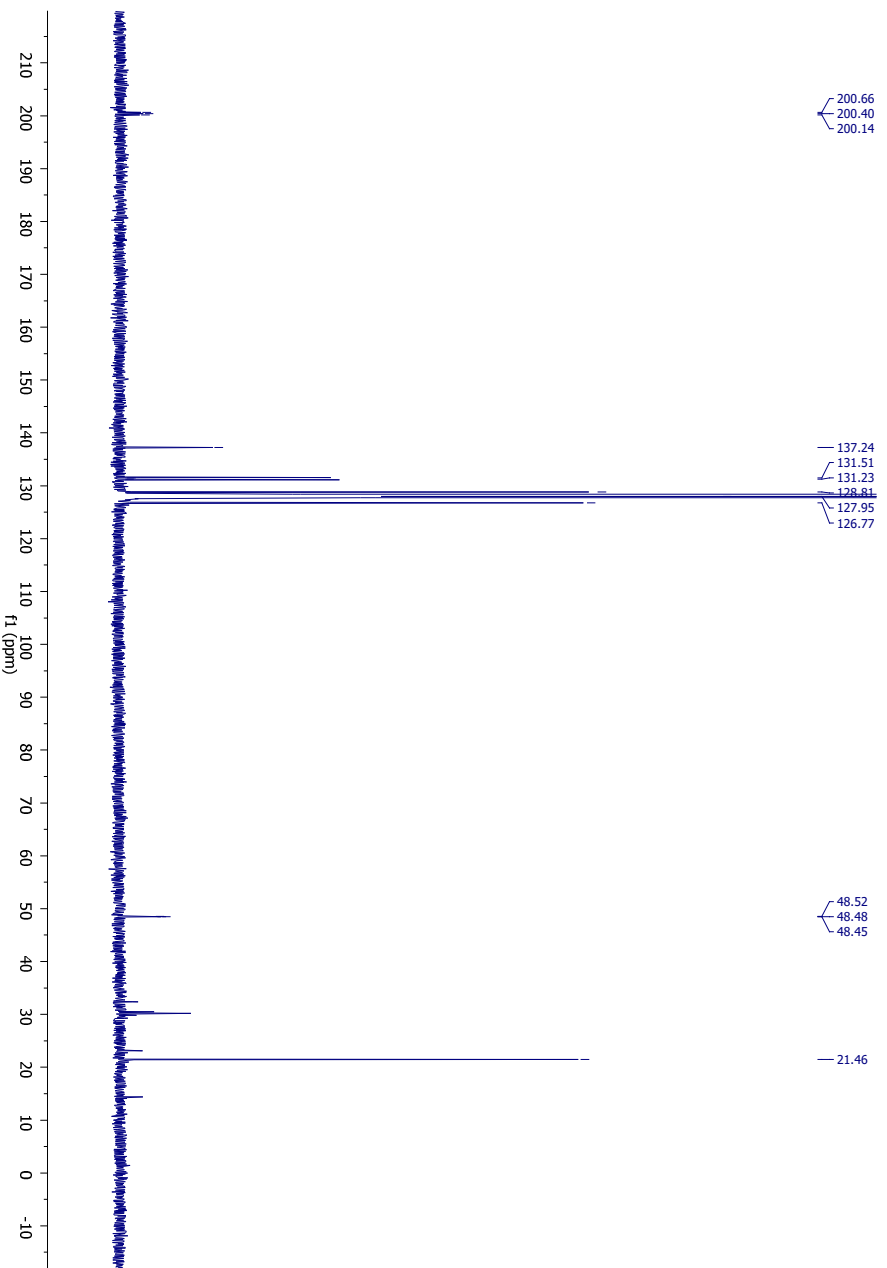
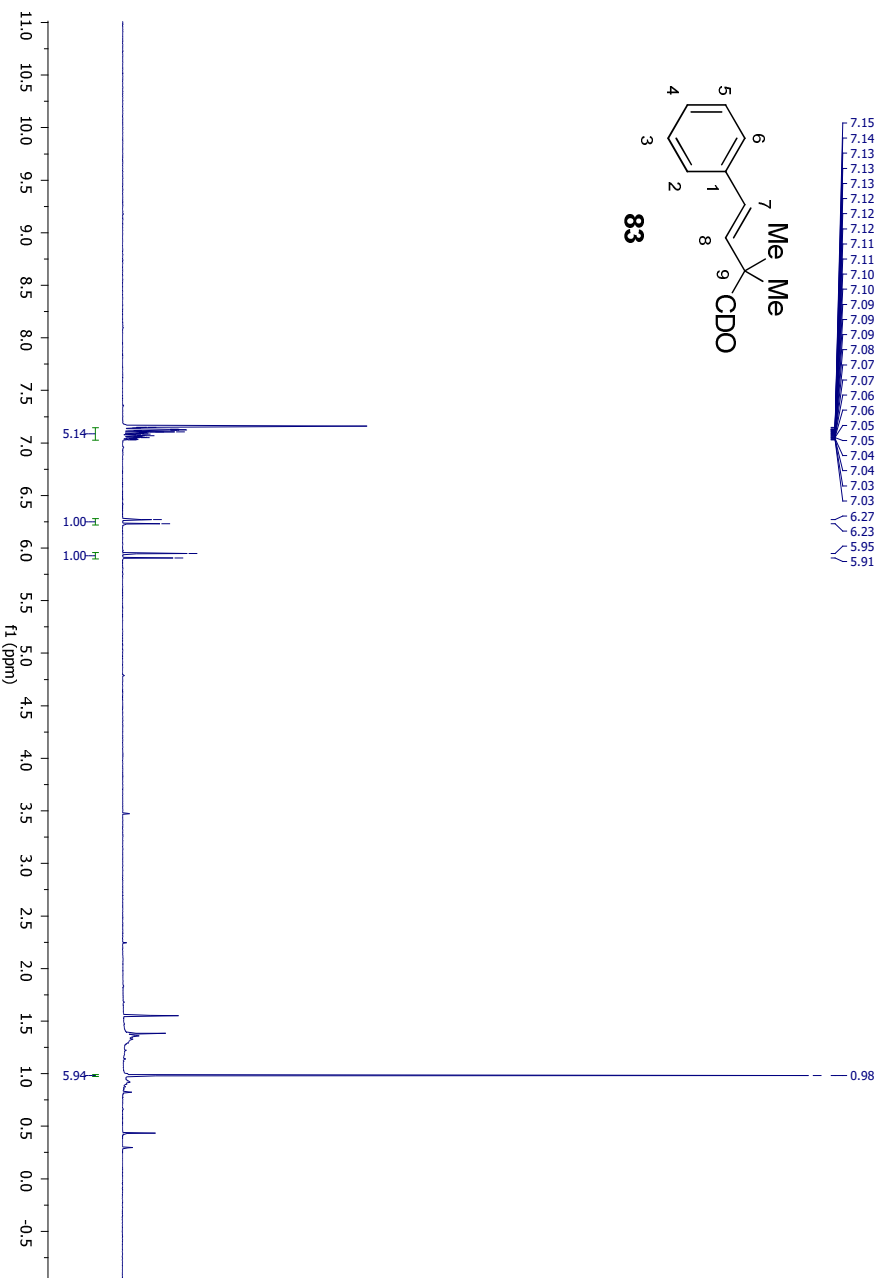
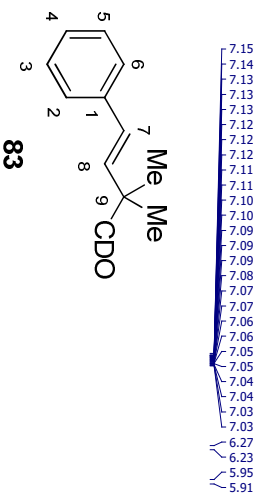


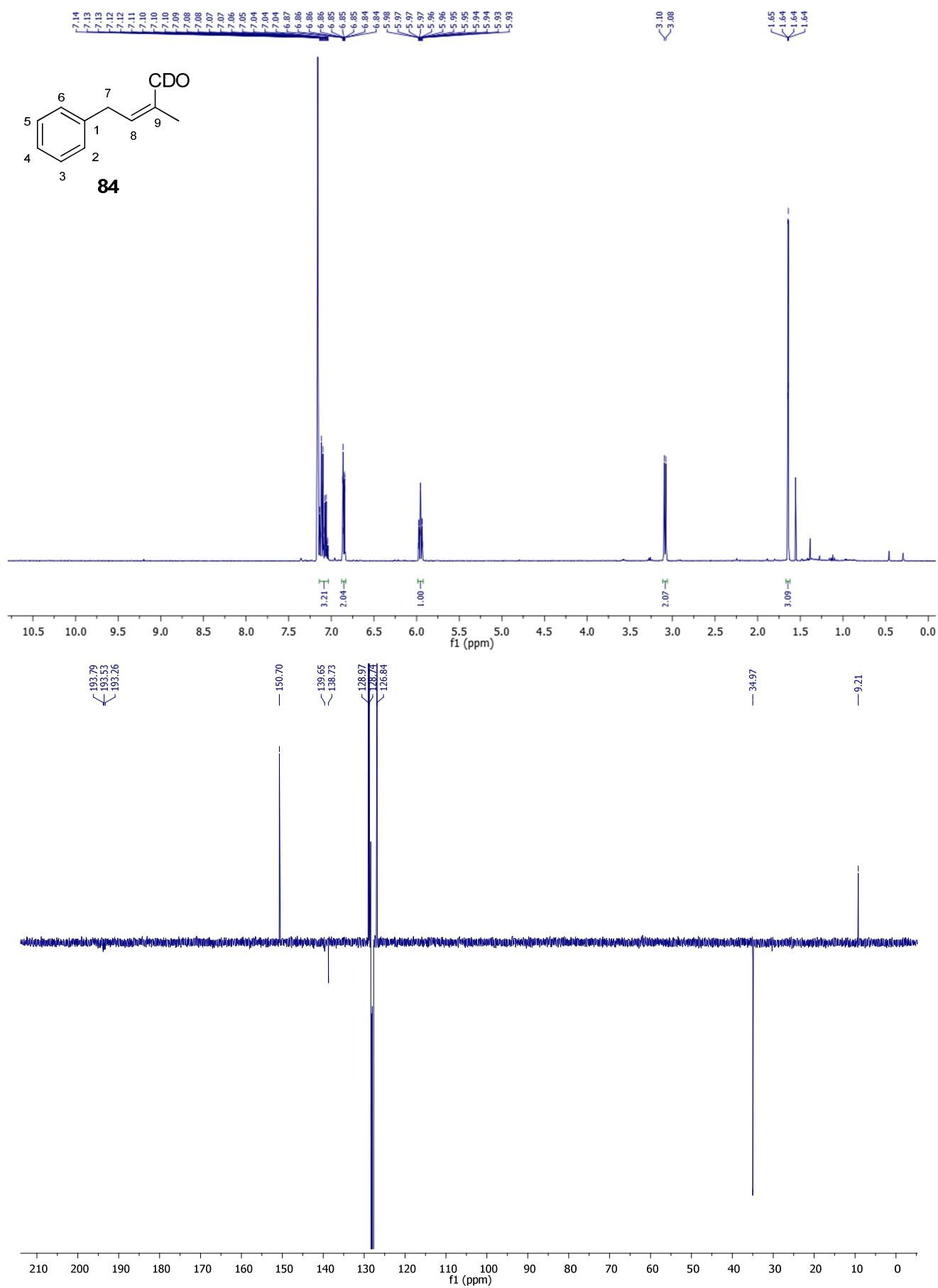
Experimental Section





Experimental Section

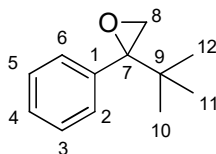




4.5. General Procedure for the Chemoselective Addition of LiCH₂Cl to Ketones to obtain epoxides

To a cooled (-78 °C) solution of enone (1.0 equiv) in dry THF was added chloriodomethane (3.0 equiv). After 2 min, an ethereal solution of MeLi-LiBr (2.8 equiv, 1.5 M) was added dropwise, using a syringe pump (flow: 0.200 mL/min). The resulting solution was stirred overnight until the room temperature was reached. Saturated aq NH₄Cl was added (2 mL/mmol substrate) and then, it was extracted with Et₂O (2 x 5 mL) and washed with water (5 mL) and brine (10 mL). The organic phase was dried (anhydrous Na₂SO₄), filtered and, after removal of the solvent under reduced pressure, pure compounds were obtained.

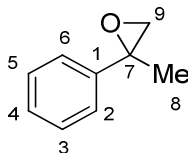
2-(2-methyl-2-propanyl)-2-phenyloxirane (96a)



By following the General Procedure, starting 2,2-dimethyl-1-phenylpropan-1-one (162 mg, 1.00 mmol, 1.0 equiv), ICH₂Cl (529 mg, 0.22 mL, 3.0 mmol, 3.0 equiv), MeLi-LiBr complex (1.5 M, 1.87 mL, 2.8 mmol, 2.8 equiv) and THF (2 mL), the desired product was obtained in 99% (174 mg) as a bright yellow oil.

¹H NMR (400 MHz, CDCl₃) δ: 7.35 (m, 2H, H-2, H-6), 7.30 (m, 2H, H-3, H-5), 7.28 (m, 1H, H-4), 3.11 (d, ²J = 5.1 Hz, 1H, H-8), 2.65 (d, ²J = 5.1 Hz, 1H, H-8), 0.98 (s, 9H, H-10, H-11, H-12). ¹³C NMR (100 MHz, CDCl₃) δ: 139.5 (C-1), 128.8 (C-2, C-6), 127.3 (C-3, C-5), 127.2 (C-4), 66.8 (C-7), 50.8 (C-8), 33.7 (C-9), 26.3 (C-10, C-11, C-12). APCI-HRMS m/z: 177.12 [M+H]⁺

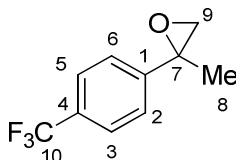
2-methyl-2-phenyloxirane (96b)



By following the General Procedure, starting acetophenone (120 mg, 1.00 mmol, 1.0 equiv), ICH₂Cl (529 mg, 0.22 mL, 3.0 mmol, 3.0 equiv), MeLi-LiBr complex (1.5 M, 1.87 mL, 2.8 mmol, 2.8 equiv) and THF (2 mL), the desired product was obtained in 99% (133 mg) as a bright yellow oil.

¹H NMR (400 MHz, CDCl₃) δ: 7.37 (m, 2H, H-2, H-6), 7.34 (m, 2H, H-3, H-5), 7.28 (m, 1H, 4), 2.98 (d, *J* = 5.4 Hz, 1H, H-9), 2.81 (qd, *q* = 0.7, *d* = 5.4, 1H, H-9), 1.73 (d, *J* = 0.7 Hz, 3H, H-8). **¹³C NMR** (100 MHz, CDCl₃) δ: 141.2 (C-1), 128.3 (C-3, C-5), 127.4 (C-4), 125.3 (C-2, C-6), 57.0 (C-9), 56.7 (C-7), 21.8 (C-8). **ESI-HRMS** *m/z*: 135.39 [M+H]⁺

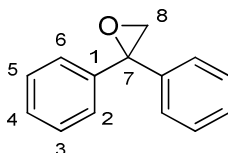
2-methyl-2-[4-(trifluoromethyl)phenyl]oxirane (96c)



By following the General Procedure, starting 4'-(trifluoromethyl)acetophenone (188 mg, 1.00 mmol, 1.0 equiv), ICH₂Cl (529 mg, 0.22 mL, 3.0 mmol, 3.0 equiv), MeLi-LiBr complex (1.5 M, 1.87 mL, 2.8 mmol, 2.8 equiv) and THF (2 mL), the desired product was obtained in 99% (200 mg) as a red oil.

¹H NMR (400 MHz, C₆D₆) δ: 7.30 (m, 2H, H-3, H-5), 7.05 (m, 2H, H-2, H-6), 2.40 (d, *J* = 5.5 Hz, 1H, H-9), 2.21 (dq, *d* = 5.5, *q* = 0.7, 1H, H-9), 1.26 (d, *J* = 0.7 Hz, 3H, H-8). **¹³C NMR** (100 MHz, C₆D₆) δ: 145.9 (C-1), 129.7 (g, *J* = 32.2 Hz, C-4), 126.0 (C-2, C-5), 125.5 (g, *J* = 3.9 Hz, C-3, C-5), 124.9 (g, *J* = 271.7 Hz, C-10), 56.6 (C-9), 55.9 (C-7), 21.2 (C-8). **¹⁹F NMR (376 MHz, C₆D₆)** δ: -62.2 (CF₃). **ESI-HRMS** *m/z*: 203.47 [M+H]⁺

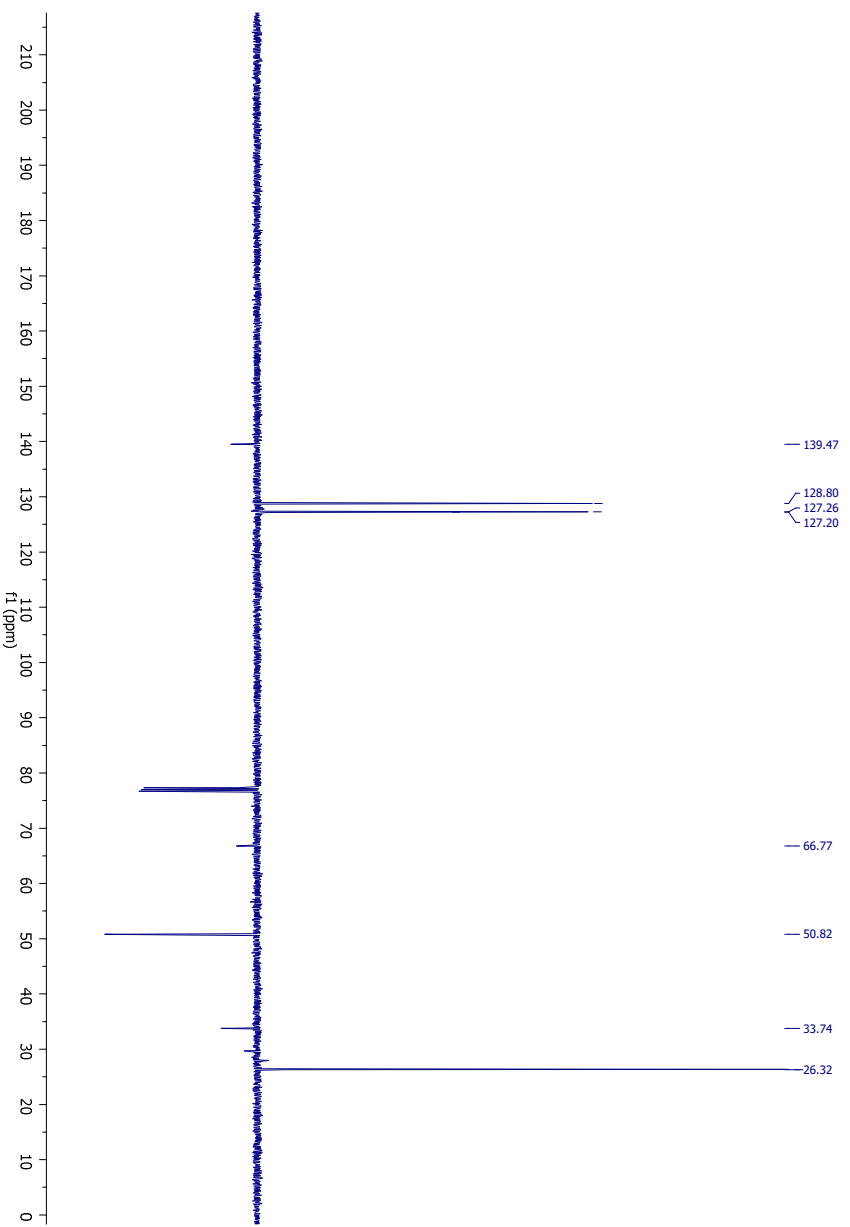
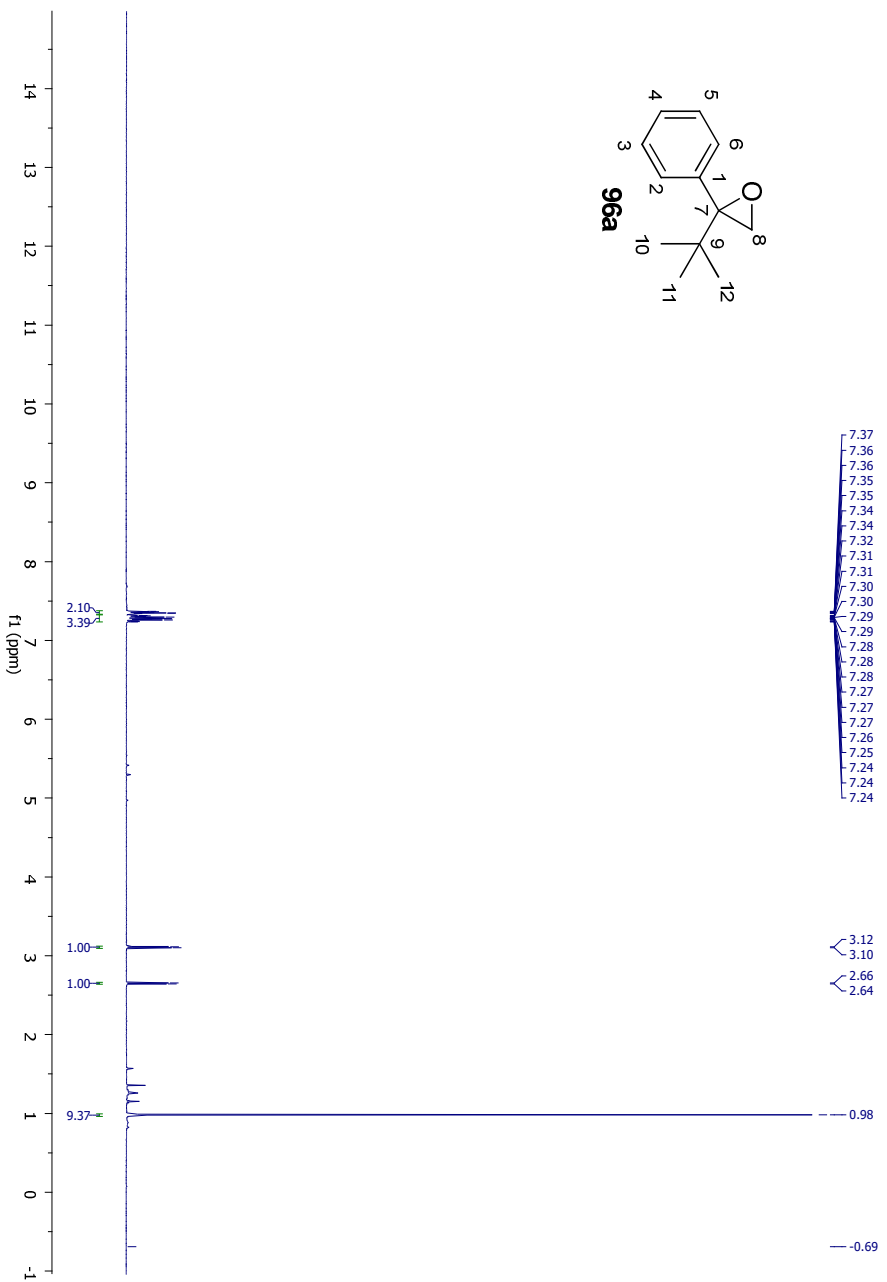
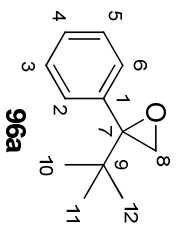
2,2-diphenyloxirane (96d)

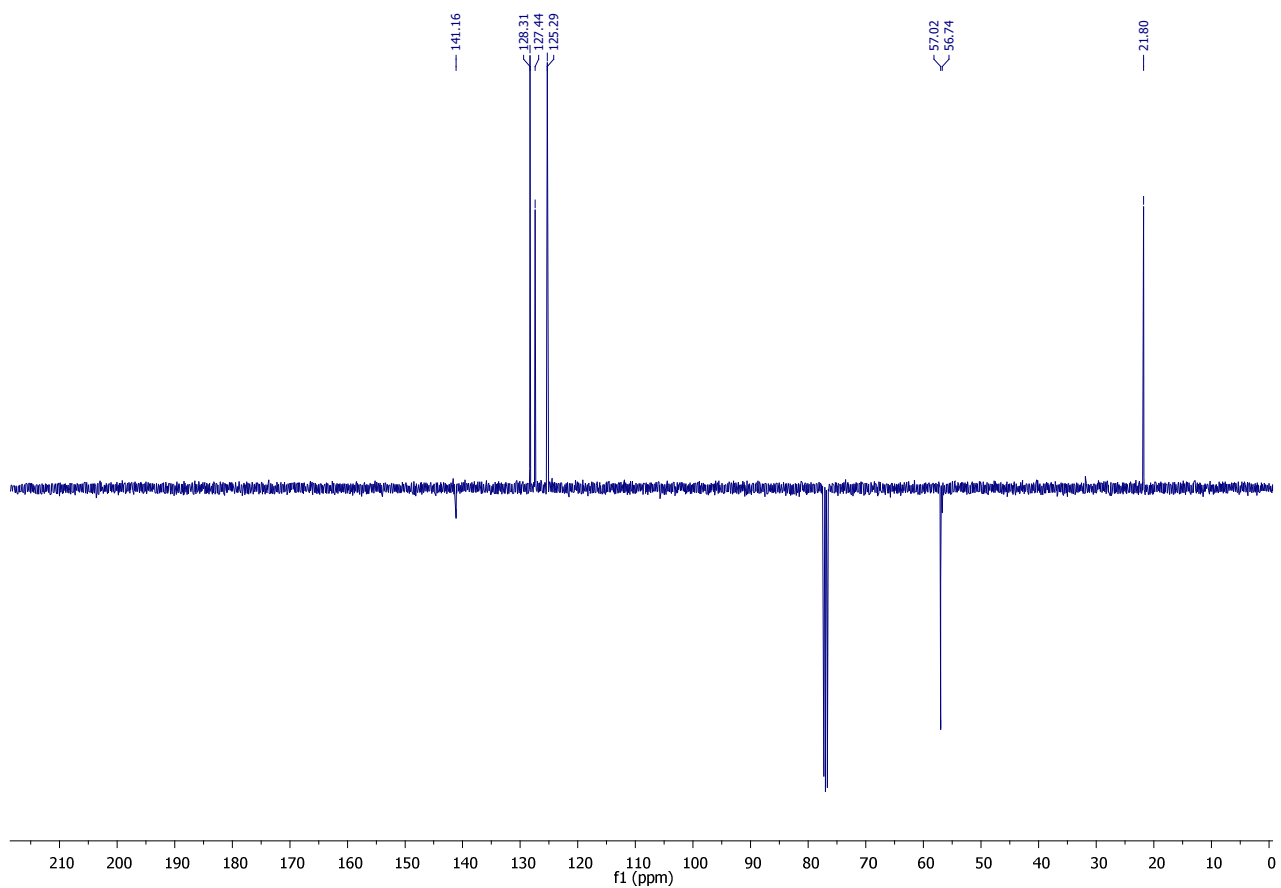
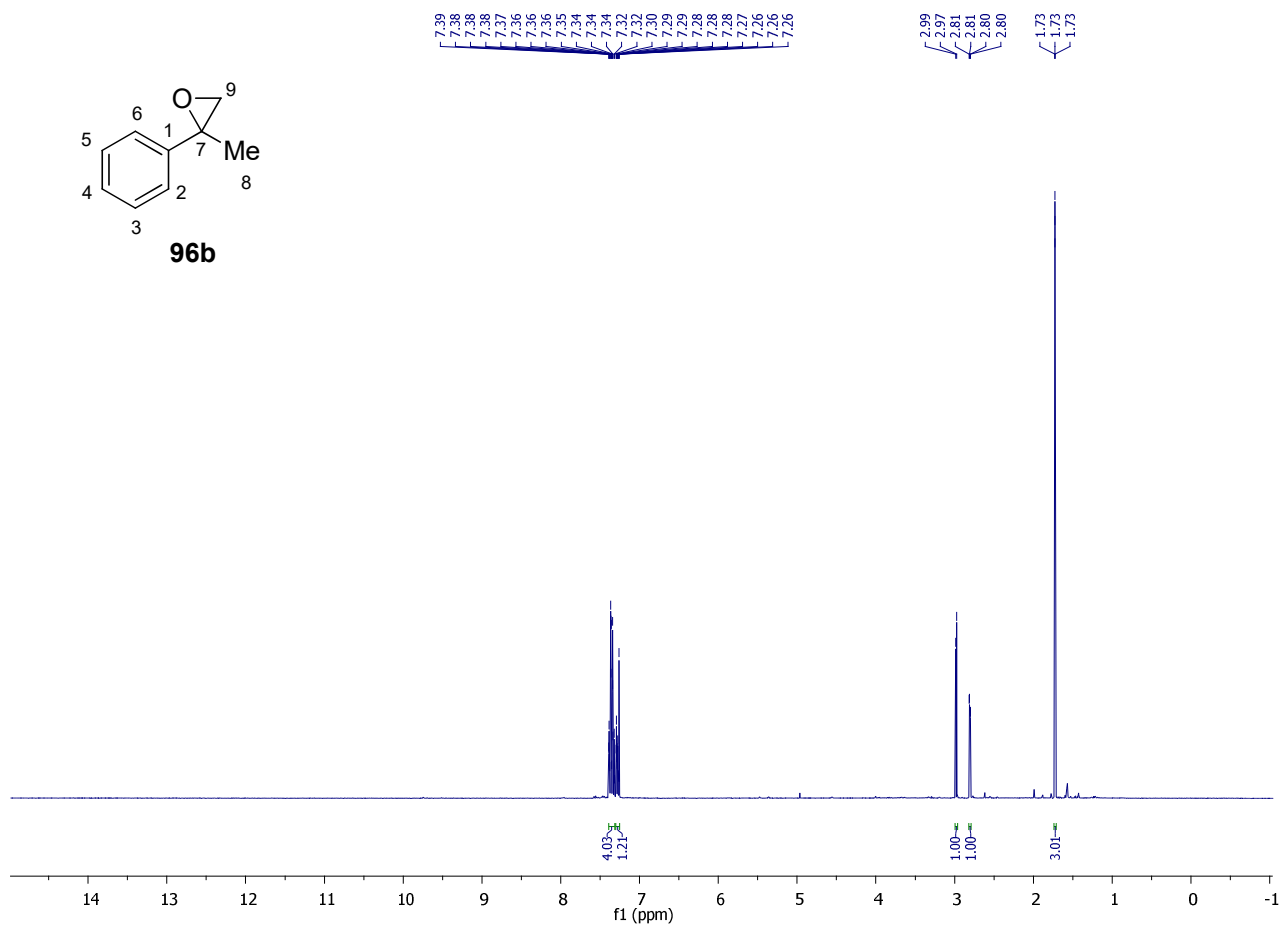
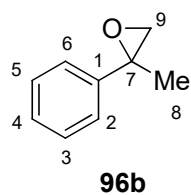


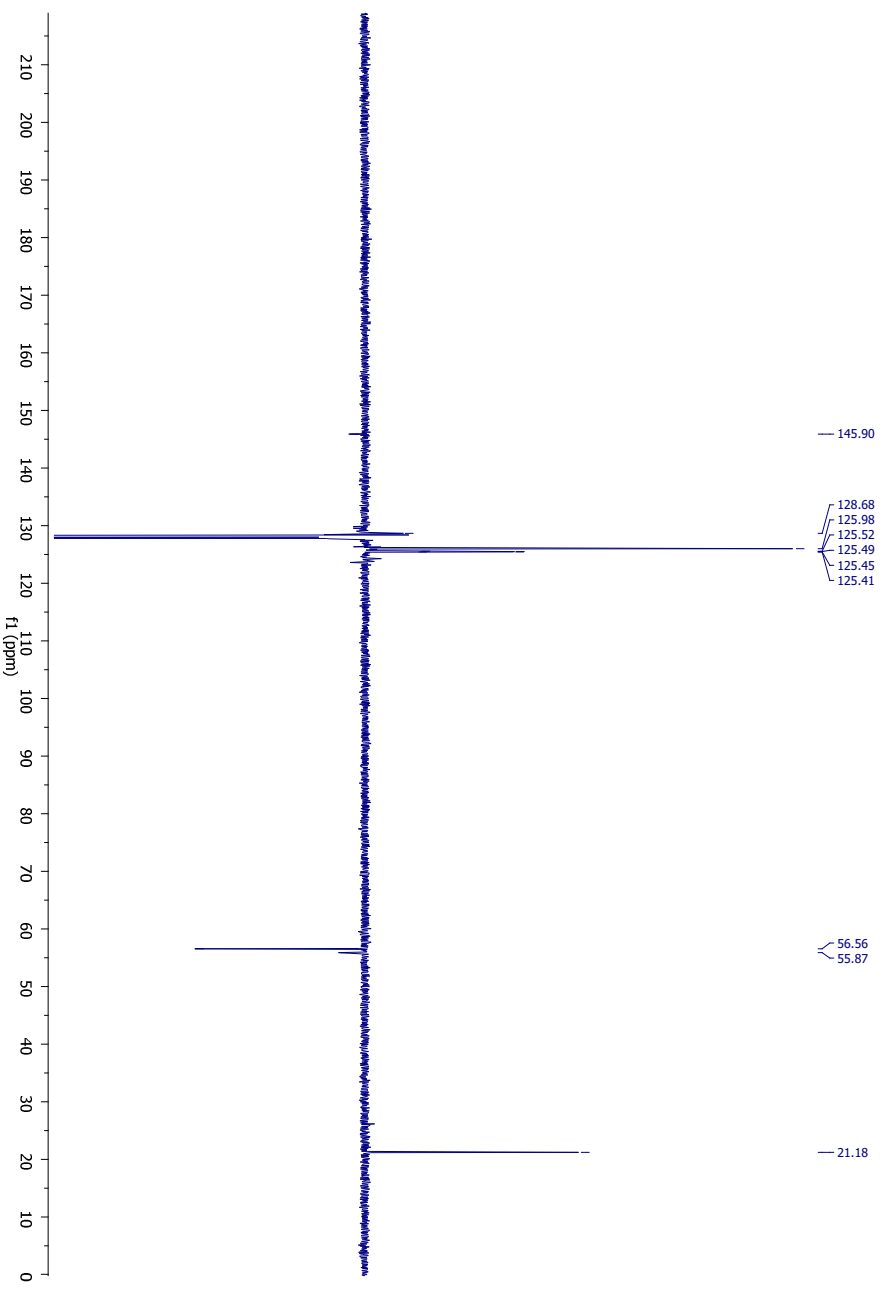
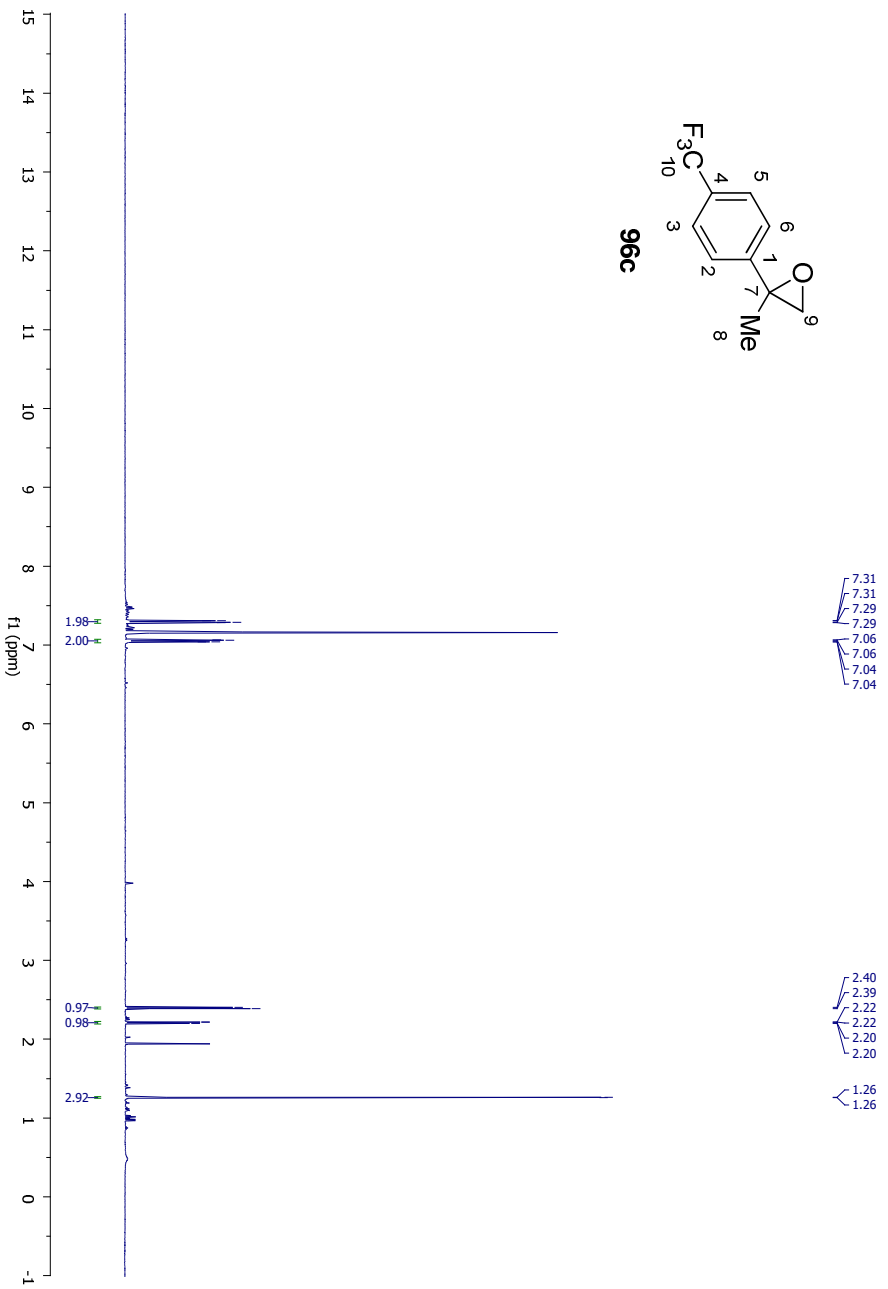
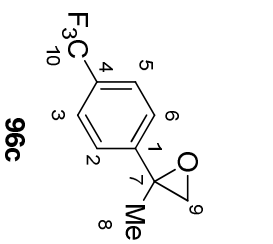
By following the General Procedure, starting benzophenone (182 mg, 1.00 mmol, 1.0 equiv), ICH₂Cl (529 mg, 0.22 mL, 3.0 mmol, 3.0 equiv), MeLi-LiBr complex (1.5 M, 1.87 mL, 2.8 mmol, 2.8 equiv) and THF (2 mL), the desired product was obtained in 99% (194 mg) as a red oil.

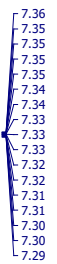
¹H NMR (400 MHz, CD₂Cl₂) δ: 7.30-7.36 (m, 5H, Ph1, Ph2), 3.26 (s, 2H, H-8). **¹³C NMR** (100 MHz, CD₂Cl₂) δ: 140.2 (C-1), 128.6 (C-3, C-5), 128.3 (C-4), 127.8 (C-2, C-6), 62.0 (C-7), 57.1 (C-8). **ESI-HRMS** *m/z*: 197.69 [M+H]⁺

Copies of NMR spectra

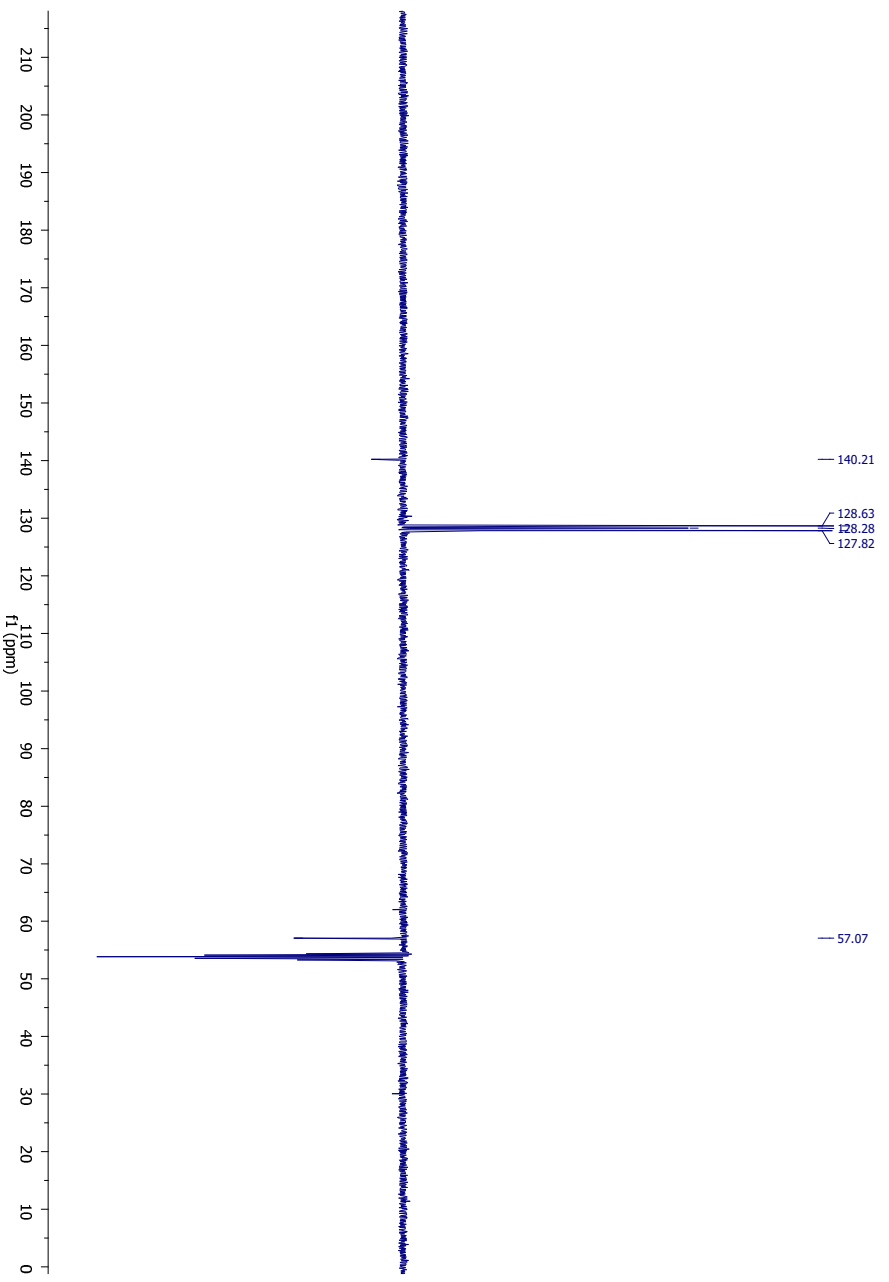
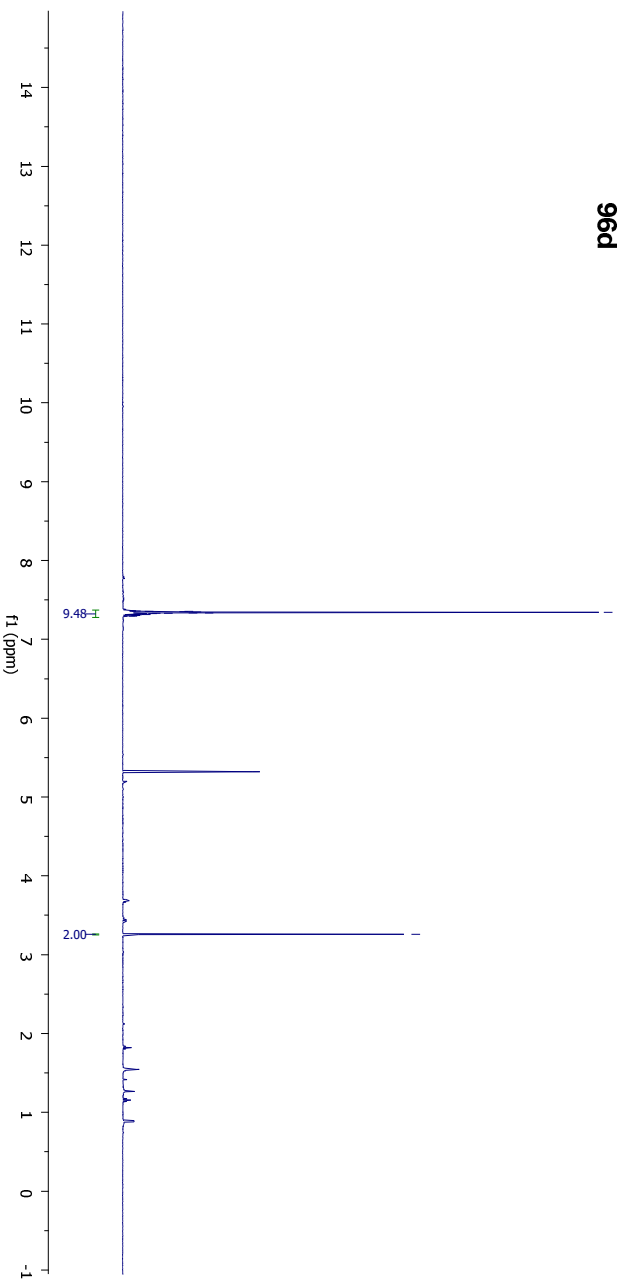
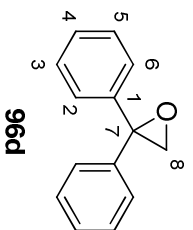








3.26



5. REFERENCES

5. REFERENCES

1. Li, J. J. *Name Reactions for Homologation*; Wiley: Hoboken, **2009**.
2. (a) Trost, B.M. *Acc. Chem. Res.* **2002**, *35*, 695. (b) Afagh, N.A.; Yudin, A.K. *Angew. Chem. Int. Ed.* **2010**, *49*, 262.
3. (a) Arndt, F.; Eistert, B.; Ender, W. *J. Chem. Ber.* **1929**, *62*, 44. (b) Arndt, F.; Eistert, B. *Ber. Dtsch. Chem. Ges.* **1935**, *68*, 200. (c) Podlech, J.; Seebach, D. *Angew. Chem. Int. Ed.* **1995**, *34*, 471. (d) Pace, V.; Verniest, G.; Sinisterra, J.V.; Alcántara, A.R.; De Kimpe, N. *J. Org. Chem.* **2010**, *75*, 5760.
4. Proctor, L.D.; Warr, A.J. *J. Org. Proc. Res. Dev.* **2002**, *6*, 884.
5. Scott, L.T.; Minton, M.A. *J. Org. Chem.* **1977**, *42*, 3757.
6. Taggi, A.E.; Hafez, A.M.; Wack, H.; Young, B.; Ferraris, D.; Lectka, T. *J. Am. Chem. Soc.* **2002**, *124*, 6626.
7. Kowalski, C.J.; Haque, M.S.; Fields, K.W. *J. Am. Chem. Soc.* **1985**, *107*, 1429.
8. Corey, E.J.; Chaykovsky, M. *J. Am. Chem. Soc.* **1962**, *84*, 867.
9. (a) Corey, E.J.; Chaykovsky, M. *J. Am. Chem. Soc.* **1964**, *86*, 1640. (b) Gololobov, Y.G.; Nesmeyanov, A.N.; Lysenko, V.P.; Boldeskul, I.E. *Tetrahedron* **1987**, *43*, 2609. (c) Ciaccio, J.A.; Drahus, A.L.; Meis, R.M.; Tingle, C.T.; Smrtka, M.; Geneste, R. *Synth. Commun.* **2003**, *33*, 2135. (d) Szostak, M.; Aubé, J. *J. Am. Chem. Soc.* **2009**, *131*, 13246. (e) Kavanagh, S.A.; Piccinini, A.; Connon S. *J. Adv. Synth. Catal.* **2010**, *352*, 2089.
10. (a) Capriati, V.; Florio, S. *Chem. Eur. J.* **2010**, *16*, 4152. (b) Capriati, V. *Modern Lithium Carbenoid Chemistry*. In *Contemporary Carbene Chemistry*; John Wiley & Sons, Inc: 2013; pp. 325-362. (c) Boche, G.; Lohrenz, J.C.W. *Chem. Rev.* **2001**, *101*, 697. (d) Braun, M. *Lithium carbenoids*. In *The Chemistry of Organolithium Compounds*; Rappoport, Z., Marek, I., Eds.; John Wiley and Sons: Chichester, 2004; 1; pp. 829-900.
11. Closs, G. L.; Moss, R. A. *J. Am. Chem. Soc.* **1964**, *86*, 4042.
12. Köbrich, G. *Angew. Chem. Int. Ed.* **1967**, *6*, 41.
13. Charette, A. B.; Beauchemin, A. *Simmons-Smith Cyclopropanation Reaction*. In *Organic Reactions*; John Wiley & Sons, Inc.: 2004.
14. Pace, V. *Aust. J. Chem.* **2014**, *67*, 311.
15. Cainelli, G.; Tangari, N.; Umani-Ronchi, A. *Tetrahedron* **1972**, *28*, 3009.
16. Köbrich, G. *Angew. Chem. Int. Ed.* **1972**, *11*, 473.
17. Tarhouni, R.; Kirschleger, B.; Rambaud, M.; Villieras, J. *Tetrahedron Lett.* **1984**, *25*, 835.
18. Loupy, A. et al. *Salt Effects in Organic and Organometallic Chemistry*; VCH: Weinheim, 1992.

References

19. (a) Sadhu, K.M.; Matteson, D.S. *Tetrahedron Lett.* **1986**, *27*, 795. (b) Michnick, T.J.; Matteson, D.S. *Synlett* **1991**, *9*, 631.
20. (a) Barluenga, J.; Llavona, L.; Yus, M.; Concellon, J.M. *Tetrahedron* **1991**, *47*, 7875. (b) Barluenga, J.; Baragana, B.; Alonso, A.; Concellon, J.M. *J. Chem. Soc., Chem. Commun.* **1994**, 969. (c) Barluenga, J.; Baragana, B.; Concellon, J.M. *J. Org. Chem.* **1995**, *60*, 6696.
21. Concellón, J.M.; Cuervo, H.; Fernandez-Fano, R. *Tetrahedron* **2001**, *57*, 8983.
22. (a) Clayden, J. *Organolithiums: Selectivity for Synthesis*; Pergamon: Oxford, 2002. (b) Pace, V.; Luisi, R. *ChemCatChem* **2014**, *6*, 1516. (c) *Lithium Compounds in Organic Synthesis: From Fundamentals to Applications*; Luisi, R.; Capriati, V., Eds.; Wiley-VCH: Weinheim, 2014; Vol. in press. (d) Wu, G. G.; Huang, M. Organolithium in Asymmetric Processes. In *Topics in Organometallic Chemistry*; Springer Berlin / Heidelberg, 2004; *6*; pp. 1-35.
23. Köbrich, G.; Trapp, H. *Chem. Ber.* **1966**, *99*, 670.
24. (a) Stymiest, J.L.; Dutheuil, G.; Mahmood, A.; Aggarwal, V.K. *Angew. Chem. Int. Ed.* **2007**, *46*, 7491. (b) Dearden, M.J.; Firkin, C.R.; Hermet, J.P.R.; O'Brien, P. *J. Am. Chem. Soc.* **2002**, *124*, 11870. (c) Hoppe, D.; Hense, T. *Angew. Chem. Int. Ed.* **1997**, *36*, 2282.
25. (a) Pace, V.; Castoldi, L.; Holzer, W. *J. Org. Chem.* **2013**, *78*, 7764. (b) Pace, V.; Castoldi, L.; Holzer, W. *Chem. Commun.* **2013**, *49*, 8383. (c) Pace, V.; Holzer, W.; Verniest, G.; Alcántara, A.R.; De Kimpe, N. *Adv. Synth. Catal.* **2013**, *355*, 919.
26. (a) Taguchi, H.; Yamamoto, H.; Nozaki, H. *Bull. Chem. Soc. Jpn.* **1977**, *50*, 1588. (b) Taguchi, H.; Yamamoto, H.; Nozaki, H. *J. Am. Chem. Soc.* **1974**, *96*, 6510.
27. Bull, J.A.; Boulwood, T.; Taylor, T.A. *Chem. Commun.* **2012**, *48*, 12246.
28. Brantley, S.E.; Molinski, T.F. *Org. Lett.* **1999**, *1*, 2165.
29. Hoffmann, R. W. *Chem. Soc. Rev.* **2003**, *32*, 225.
30. Satoh, T. *Chem. Soc. Rev.* **2007**, *36*, 1561.
31. Satoh, T.; Mizu, Y.; Kawashima T.; Yamakawa K. *Tetrahedron* **1995**, *51*, 703.
32. (a) Blakemore, P.R.; Burge, M.S. *J. Am. Chem. Soc.* **2007**, *129*, 3068. (b) Blakemore, P.R.; Marsden, S.P.; Vater, H.D. *Org. Lett.* **2006**, *8*, 773. (c) Barsamian, A.L.; Blakemore, P.R. *Organometallics* **2011**, *31*, 19.
33. Kapeller, D.C.; Hammerschmidt, F. *J. Am. Chem. Soc.* **2008**, *130*, 2329.
34. Appel, R. *Angew. Chem. Int. Ed.* **1975**, *14*, 801.
35. Honda, Y.; Katayama, S.; Kojima, M.; Suzuki, T.; Kishibata, N.; Izawa, K. *Org. Biomol. Chem.* **2004**, *2*, 2061.
36. (a) Hamada, T.; Torii, T.; Onishi, T.; Izawa, K.; Ikariya, T. *J. Org. Chem.* **2004**, *69*, 7391. (b) Reeder, M.R.; Anderson, R.M. *Chem. Rev.* **2006**, *106*, 2828.

37. Pace, V.; Cabrera, A.C.; Ferrario, V.; Sinisterra, J.V.; Ebert, C.; Gardossi, L.; Braiuca, P.; Alcántara, A.R. *J. Mol. Catal. B: Enzym.* **2011**, *70*, 23.
38. Kaldor, S.W.; Kalish, V.J.; Davies, J.F. 2nd; Shetty, B.V.; Fritz, J.E.; Appelt, K.; Burgess, J.A.; Campanale, K.M.; Chirgadze, N.Y.; Clawson, D.K.; Dressman, B.A.; Hatch, S.D.; Khalil, D.A.; Kosa, M.B.; Lubbehusen, P.P.; Muesing, M.A.; Patick, A.K.; Reich, S.H.; Su, K.S.; Tatlock, J.H. *J. Med. Chem.* **1997**, *40*, 3979.
39. (a) Ng, J.S.; Przybyla, C.A.; Liu, C.; Yen, J.C.; Muellner, F.W.; Weyker, C.L. *Tetrahedron* **1995**, *51*, 6397. (b) Patel, R.N.; Banerjee, A.; Szarka, L.J. *Tetrahedron: Asymmetry* **1997**, *8*, 2547. (c) Kempf, D.J.; Sham, H.L.; Marsh, K.C.; Flentge, C.A.; Betebenner, D.; Green, B.E.; McDonald, E.; Vasavanonda, S.; Saldivar, A.; Wideburg, N.E.; Kati, W.M.; Ruiz, L.; Zhao, C.; Fino, L.; Patterson, J.; Molla, A.; Plattner, J.J.; Norbeck, D.W. *J. Med. Chem.* **1998**, *41*, 602.
40. Concellón, J.M.; Rodríguez-Solla, H.; Simal, C. *Org. Lett.* **2008**, *10*, 4457.
41. Pace, V.; Rae, J.P.; Procter, D.J. *Org. Lett.* **2014**, *16*, 476.
42. Concellón, J.M.; Rodríguez-Solla, H.; Bernad, P.L.; Simal, C. *J. Org. Chem.* **2009**, *74*, 2452.
43. Adler, M.; Boche, G. *J. Phys. Org. Chem.* **2005**, *18*, 193.
44. (a) Onishi, T.; Hirose, N.; Nakano, T.; Nakazawa, M.; Izawa, K. *Tetrahedron Lett.* **2001**, *42*, 5887.
45. Goehring, W.; Gokhale, S.; Hilpert, H.; Roessler, F.; Schlageter, M.; Vogt, P. *Chimia* **1996**, *50*, 532.
46. (a) Nahm, S.; Weinreb, S.M. *Tetrahedron Lett.* **1981**, *22*, 3815. (b) Balasubramaniam, S.; Aidhen, I.S. *Synthesis* **2008**, 3707. (c) Pace, V.; Castoldi, L.; Alcántara, A.R.; Holzer, W. *RSC Adv.* **2013**, *3*, 10158.
47. Brown, C. A. *Chem. Eur. J.* **2015**, *21*, 1390.
48. Emerson, C. R.; Zakharov, L. N.; Blakemore, P. R. *Chem. Eur. J.* **2013**, *19*, 16342.
49. (a) Matteson, D.S.; Ray, R. *J. Am. Chem. Soc.* **1980**, *102*, 7588; (b) Matteson, D.S. *Organometallics*. **1983**, *2*, 1529; (c) Matteson, D.S. *J. Org. Chem.* **2013**, *78*, 10009; (d) Sonawane, R.P.; Jheengut, V.; Rabalakos, C.; Larouche-Gauthier, R.; Scott, H.K.; Aggarwal, V.K. *Angew. Chem. Int. Ed.* **2011**, *50*, 3760; (e) Burns, M.; Essafi, S.; Bame, J.R.; Bull, S.P.; Webster, M.P.; Balieu, S.; Dale, J.W.; Butts, C.P.; Harvey, J.N.; Aggarwal, V.K. *Nature* **2014**, *513*, 183; (f) Balieu, S.J.; Hallett, G.E.; Burns, M.; Bootwicha, T.; Studley, J.; Aggarwal, V.K. *Am. Chem. Soc.* **2015**, *137*, 4398; (g) Hoyt, A.L.; Blakemore, P.R. *Tetrahedron Lett.* **2015**, *56*, 2980.
50. Boddaert, T.; François, C.; Mistico, L.; Querolle, O.; Meerpoel, L.; Angibaud, P.; Durandetti, M.; Maddaluno, J. *Chem. Eur. J.* **2014**, *20*, 10131.

References

51. Pace, V.; Pelosi, A.; Antermite, D.; Rosati, O.; Curini, M.; Holzer, W. *Chem. Commun.* **2016**, *52*, 2639.
52. Cainelli, G.; Ronchi, A.U.; Bertini, F.; Grasselli, P.; Zubiani, G. *Tetrahedron* **1971**, *27*, 6109.
53. Lautens, M.; Maddess, M.L.; Sauer, E.L.O.; Ouellet, S.G. *Org. Lett.* **2001**, *4*, 83.
54. (a) Newman, D.J. *J. Nat. Prod.* **2007**, *70*, 461; (b) Otera, J. *Modern Carbonyl Chemistry*, Wiley-VCH, Weinheim, 2000.
55. (a) Yang, D. *Acc. Chem. Res.* **2004**, *37*, 497; (b) Sello, G.; Fumagalli, T.; Orsini, F. *Curr. Org. Synth.* **2006**, *3*, 457; (c) Yudin, A.K. *Aziridines and Epoxides in Organic Synthesis* Wiley-VCH, Weinheim, 2006; (d) Singh, G.S.; Mollet, K.; D'hooghe, M.; De Kimpe, N. *Chem. Rev.* **2013**, *113*, 1441.
56. (a) Hesse, M. *Ring Enlargement in Organic Chemistry*, Wiley-VCH, Weinheim, 1991; (b) Krow, G.R. *Tetrahedron* **1987**, *43*, 3.
57. Boche, G. J.; Lohrenz, C.W. *Chem. Rev.* **2001**, *101*, 697.
58. (a) Taguchi, H.; Yamamoto, H.; Nozaki, H. *Bull. Chem. Soc. Jpn.* **1977**, *50*, 1592; (b) Taguchi, H.; Yamamoto, H.; Nozaki, H. *J. Am. Chem. Soc.* **1974**, *96*, 6510; (c) Villieras, J.; Baquet, C.; Normant, J.F. *J. Organomet. Chem.* **1975**, *97*, 355.
59. Nozaki, H. *Synlett.* **1990**, 441.
60. Pace, V.; Castoldi, L.; Holzer, W. *Adv. Synth. Catal.* **2014**, *356*, 1761.
61. (a) Hashimoto, T.; Naganawa, Y.; Maruoka, K. *J. Am. Chem. Soc.* **2009**, *131*, 6614; (b) Liu, H.; O'Connor, M.J.; Sun, C.; Wink, D.J.; Lee, D. *Org. Lett.* **2013**, *15*, 2974; (c) Liu, H.; Sun, C.; Lee, N.K.; Henry, R.F.; Lee, D. *Chem. Eur. J.* **2012**, *18*, 11889; (d) Alcaide, B.; Almendros, P.; Quirós, M.T.; Fernández, I. *Chem. Plus Chem* **2012**, *77*, 563; (e) Rendina, V.L.; Moebius, D.C.; Kingsbury, J.S. *Org. Lett.* **2011**, *13*, 2004; (f) Dabrowski, J.A.; Moebius, D.C.; Wommack, A.J.; Kornahrens, A.F.; Kingsbury, J.S. *Org. Lett.* **2010**, *12*, 3598; (g) Moebius, D.C.; Kingsbury, J.S. *J. Am. Chem. Soc.* **2009**, *131*, 878.
62. Corey, E.J.; Chaykovsky, M. *J. Am. Chem. Soc.* **1962**, *84*, 867.
63. Gololobov, Y.G.; Nesmeyanov, A.N.; Lysenko, V.P.; Boldeskul, I.E. *Tetrahedron* **1987**, *43*, 2609.
64. (a) Kamijo, S.; Dudley, G.B. *J. Am. Chem. Soc.* **2005**, *127*, 5028; (b) Kamijo, S.; Dudley, G.B. *J. Am. Chem. Soc.* **2006**, *128*, 6499; (c) Kamijo, S.; Dudley, G.B. *Org. Lett.* **2006**, *8*, 175.
65. (a) Eschenmoser, A. *Helv. Chim. Acta* **1967**, *50*, 708; (b) Tanabe, M.; Crowe, D.F.; Dehn, R.L. *Tetrahedron Lett.* **1967**, *8*, 3943.
66. Olah, G.A.; Ohannesian, L.; Arvanaghi, M. *Chem. Rev.* **1987**, *87*, 671.
67. Gattermann, L.; Koch, J.A. *Chem. Ber.* **1897**, *30*, 1622.

68. Rieche, A.; Gross, H.; Hoft, E. *Chem. Ber.* **1960**, *93*, 88.
69. DeHaan, F.P.; Covey, W.D.; Delker, G.L.; Baker, N.J.; Feigon, J.F.; Ono, D.; Miller, K.D.; Stelter, E.D. *J. Org. Chem.* **1984**, *49*, 3963.
70. Olah, G.A.; Kuhn, S.J. *J. Am. Chem. Soc.* **1960**, *82*, 2380.
71. Olah, G.A.; Narang, S.C.; Gupta, B.G.B.; Malhotra, R. *Angew. Chem. Int. Ed. Engl.* **1979**, *18*, 614.
72. Huffman, C.W. *J. Org. Chem.* **1958**, *23*, 727.
73. Böhme, H.W.; Viehe, H.G. (Eds.). *Iminium salts in organic chemistry*. John Wiley & Sons, New York. 1976
74. Bredereck, H.; Effenberger, F.; Hofmann, A. *Chem. Ber.* **1963**, *96*, 3260.
75. Alba, A.N.; Viciano, M.; Rios, R. *Chem. Cat. Chem.* **2009**, *1*, 437.

ACKNOWLEDGEMENTS

I express my great appreciation to my supervisor Prof. Simona Collina (University of Pavia) for welcoming me into her group. Her guidance, knowledge, support, constant encouragement, advice throughout the years were essential for the completion of this work. I have been lucky to have a supervisor who cared so much about me and my project and who responded to my questions and queries so promptly, despite her busy schedule.

I am grateful to my supervisor Prof. Vittorio Pace (University of Vienna) for his exceptional guidance, his support and advice. I learned so much from him and his enthusiasm in chemistry has been the best example I could have asked for. He has not only helped to develop my skills as organolithium chemist but he was also able to encourage me to do always the best in laboratory. I also value for his friendship and all the discussions we had during my stay in Vienna.

I thank the reviewers of my thesis, Prof. Anna K. H. Hirsch (University of Groningen) and Prof. Diego Muñoz-Torrero (University of Barcelona), for devoting their time to review the manuscript and for their valuable comments and suggestions.

I wish to thank the members of the LabMedChem group: my friend and Ph.D. colleague Rita Nasti for her immense support during these years, for her unequivocal skill sharing in laboratory and advice regarding everything. You were always by my side, both in dismal and joyful moments, we laughed and cried. Thank you very much and *Ad maiora*

Dr. Emanuela Martino for her enormous help in providing information, guidance and her funny jokes throughout the day.

Dr. Daniela Rossi and Dr. Annamaria Marra for sharing me their laboratory skills and kind suggestions. I warmly acknowledge their support throughout the project.

I am truly thankful to Emanuele Bignardi for sharing his expertise in biology, his perfect English and his friendship. I wish you all the best.

I am grateful to all my friends and colleagues from the University of Vienna: Vanna Parisi, Serena Monticelli, Laura Castoldi, Azzurra Pelosi for their countless encouragement and support during my stay abroad. Your enthusiasm in science has been an inspiration to me. I will never forget the nice period that I spent with you in Vienna. All the best my dears.

Acknowledgements

I am deeply indebted to all the M.Sc. Students: Sara Bigiotti, Chiara Bongio, Ilaria Rocchio, Caterina Mazzeo, Giovanni Crippa, Nicolò Di Natale, Silvia Del Pra, Chiara Ghezza, Tatiana Bruniera, Elena Lupo, Selina Rusconi, Michela Culanti, Giuseppe Afflitto, Marilù Tarantino, Miriana Moretto, Francesco Moretti, Veronica Castelluccio, Eugenia Mazzeo. The visiting Ph.D. student Bédís Amri. The greenhorns: Giacomo Rossino, Serena Della Volpe, Licia Campo, Erica Gelsomino, Valeria Cavalloro, Simone D'Amato, Paolo Schena. Your precious help was indispensable to achieve the success of this project.

Among my other collaborators and coauthors, I thank Ph.D. Student Stefania Monteleone, Prof. Klaus Liedl (University of Innsbruck) and Prof. Sabrina Pricl (University of Trieste) for sharing their expertise in computational modelling, as well as my collaborators at the University of Pavia – Prof. Daniela Curti and Prof. Mayra Paolillo, for the collaboration on the biological experiments. Dr. Anna Tesei (IRST) for her essential contribute on the biological assays. Prof. Bernhard Wuensch (University of Muenster) for his undoubted support in binding results. Prof. Juza for his help in the analytical part. Prof Wolfgang Holzer and Prof Ernest Urban (University of Vienna) for their advice and help during NMR sample record and interpretation.

I am thankful to all my friends outside the University from the South to the North of Italy. In particular all my best friends Sara, Mirco, Flo, Eli, Angi, Fede, Rita, Chiara, Ilaria, Ari, Sandro and Floriana. They trust in me, support me. Their presence in my life was/is and will be essential.

I am forever grateful to my family Mariagrazia, Francesco e Mattia who have been the constant source of love, concern, strength and support throughout my life. I obviously wouldn't be where I am today without the everlasting guidance of my family.

My loving thanks are for you Paolo. During these years you have been my lighthouse and an inspiration. You have the ability to make me laugh and you taught me that there is always a solution for every problem. You have always gone along with my choices without hindering. We shared unforgettable moments and despite the distance we were always close. Thank you for your patience, support and confidence. This work would not have been completed without you.

APPENDIX

New Perspectives in Cancer Therapy: The Biotin-Antitumor Molecule Conjugates

Giuseppe Tripodo^{1#}, Delia Mandracchia², Simona Collina^{1*}, Marta Rui¹ and Daniela Rossi^{1#}

¹Department of Drug Sciences, University of Pavia, Viale Taramelli 12, 27100 Pavia, Italy

²Department of Pharmacy, University of Bari "Aldo Moro", Via Orabona 4, 70125 Bari, Italy

[#]Giuseppe Tripodo and Daniela Rossi contributed equally to this work

Abstract

Chemotherapy is still the first-line treatment of cancer, even if drugs currently used in therapy generally possess high toxicity and poor selectivity. In the last two decades several efforts have been made to overcome these drawbacks by specifically carrying anticancer drugs to the tumors. Among the different approaches, the so called vitamin-mediated drug targeting has recently emerged as a novel and valuable strategy. Indeed, the linkage of cytotoxic drugs to selected vitamins, leading to vitamin-drug conjugates, would result in specifically delivering great amounts of the targeted drug at high doses to cancer cells. Among vitamins, biotin seems to be the most promising targeting agent. The aim of this review is to get an overview on recent success in the conjugation of biotin with molecules endowed with anticancer properties.

Keywords: Anticancer drugs; Biotin; Doxorubicin; Drug targeting; Gemcitabine; Taxol

Introduction

Chemotherapy is still the first-line treatment of cancer, even if the drugs currently used in therapy, generally possess high toxicity and poor selectivity. Drugs commonly used in cancer therapy are characterized by different mechanisms of action i.e. i) toxicity to specific cancer cells, ii) anti-proliferative activity or iii) capability of modifying the cell cycle at specific phases [1-5]. As a direct consequence of the cellular activity of anti-cancer drugs, in particular with respect to rapidly proliferating and dividing cells, they show low selectivity towards not-cancerous cells like red blood cells, gut epithelia, bone marrow or hair follicles [6]. On the other side, due to the slow proliferation typical of certain tumors, several anticancer drugs used so far result ineffective against such tumors, thus leading to the need of high dose therapies to limit the cancer growing. These high doses could destroy part of the cancer cells but also result in a hard damage to the adjacent normal-proliferating cells. Due to these drawbacks, the cancer therapy has to be discontinued and sometimes stopped before the tumor mass has been reduced or eliminated [7,8]. Thus, reaching a real selectivity of anti-cancer drugs is a milestone and still a challenge in cancer research. To this aim, different approaches could be applied. One of the most common consists in providing the drug with a suitable carrier. The polymeric drug carriers emerged as the most effective ones because of their versatility of use as well as their straightforward chemical modification [9-17]. These systems usually bring to a passive drug targeting due to their ability to accumulate in a specific organ as a result of their route of elimination or for particular organotropism. A more specific drug targeting could be attained by providing the carrier with specific targeting agent, such as antibodies, vitamins, magnetic particles, hormones or peptides [18-24]. Another widely applied approach for drug targeting is the direct linking of the targeting molecule to the drug to form a new chemical entity pharmacologically active per se or a prodrug [7,25-27]. In this context, the so called vitamin-mediated drug targeting has recently emerged as a novel concept in specifically carrying anticancer drugs to the tumors [7,28-31]. As known, for their survival living cells need to consume vitamins during their life cycle. This is particularly true for those cells that rapidly divide, such as cancer cells. Indeed, the intense metabolic activity of cancer cell arises from their fast growth and is accompanied by a strong use of essential vitamins; consequently the receptors involved in vitamin internalization are overexpressed on

the cell surface. This concept is essential from a therapeutic point of view. In fact, it has been argued that the linkage of cytotoxic drug to selected vitamins, leading to vitamin-drug conjugates, would result in specifically delivering great amounts of the targeted drug at high doses to cancer cells, and thus, represents an attractive and valuable approach for targeting tumor cells. In this context, biotin, folic acid, vitamin B12 and riboflavin, that are essential for the division of all cells and in particular for tumor cells, have been recently experimented as targeting agents [20,32-35]. Interestingly, among these vitamins, biotin seems to be the most promising targeting agent. It is well known that the uptake of biotin by mammalian cells is receptor-mediated [36]. Among the first insights on cell surface biotin receptors there are the studies from SM Grassl in 1992 and Janos Zempleni and Donald M. Mock in 1998. Studying the biotin uptake by human peripheral blood mononuclear cells (PBMC) Zempleni and Mock found that "...in the presence of ouabain, biotin uptake into PBMC is dependent on normal function of Na-K-ATPase. It seems likely that biotin is co-transported with sodium, because biotin uptake into PBMC was reduced when extracellular sodium was replaced by choline, lithium, or ammonium. Likewise, as observed by others, the biotin uptake into rat hepatocytes, rat intestinal cells, or Hep G2 cells was reduced by ouabain and by sodium-free media." [37-39]. In a subsequent study, they also found that PBMC accumulate biotin by a transporter that is specific for biotin. These studies provided evidence that another, less specific transporter in mammalian cells may bind biotin, pantothenic acid, and similar compounds. However, the contribution of this transporter to biotin uptake into PBMC is quantitatively minor [38]. The main transporter for biotin has been found in the sodium-dependent multivitamin transporter (SMVT), which has been found to be overexpressed in several aggressive cancer lines such as leukemia (L1210FR), ovarian

***Corresponding author:** Simona Collina, Department of Drug Sciences, University of Pavia, Viale Taramelli 12, 27100 Pavia, Italy, Tel: +39 (0) 382987379; E-mail: simona.collina@unipv.it

Received March 18, 2014; Accepted April 21, 2014; Published April 23, 2014

Citation: Tripodo G, Mandracchia D, Collina S, Rui M, Rossi D (2014) New Perspectives in Cancer Therapy: The Biotin-Antitumor Molecule Conjugates. Med chem S1: 004. doi:[10.4172/2161-0444.S1-004](https://doi.org/10.4172/2161-0444.S1-004)

Copyright: © 2014 Tripodo G, et al. This is an open-access article distributed under the terms of the Creative Commons Attribution License, which permits unrestricted use, distribution, and reproduction in any medium, provided the original author and source are credited.

(OV 2008, ID8), colon (Colo-26), mastocytoma (P815), lung (M109), renal (RENCA, RD0995), and breast (4T1, JC, MMT06056) cancer cell lines [40,41]. Additionally, its overexpression was found superior to that of folate receptor [30]. This is not surprising because biotin belongs to a particular category of (exogenous) micronutrients required for cellular functions and, in particular, for cell growth [42,43]. For this reason, the biotin demand in tumors, especially in the rapidly growing tumors, is higher than normal tissues.

One of the first papers dealing with the evaluation of the effectiveness of folate, vitamin B12 or biotin-functionalized polymeric materials as active drug targeting agents to tumor cells was published in 2004 by Russell-Jones et al. Particularly, by examining *in vitro* several tumor cell lines, they reported "cell types appeared to cluster in three categories. Category one, represented by 0157, BW5147, B16, LL-2 and HCT-116, were shown to have no enhancement of uptake with any of the targeting agent. Category two, represented by L1210FR, Ov2008, ID8, and OvcAR, showed enhanced uptake of folate and biotin-targeted polymers, but not vitamin B12 (Cbl). Category three, tumors represented by Colo-26, P815, M109, RENCA, RD995, 4T1, JC and MMT060562, showed enhanced uptake of vitamin B12 and biotin-labeled polymers" [31]. They also reported that the cells overexpressing the receptors for folate or vitamin B12, also overexpress receptors for biotin. Furthermore, an *in vivo* study revealed that a rhodamine-labeled polyacrylate reached relatively high level in the mice tumor cells only when targeted by biotin or folate, but not by vitamin B12. Moreover, although the relative increase in uptake of targeted polymer is varying between different cell lines, as a tendency, the biotin labeled polymer showed the highest level of uptake. The same trend has been observed when the cytotoxic drug methotrexate has been conjugated to the vitamin targeted polymer. Indeed, the biotin targeted systems resulted more cytotoxic than the folate or vitamin B12-targeted ones. They also found that the treatment of Colo-26-bearing mice with vitamin-doxorubicin- polymer conjugates resulted in greatly enhanced killing, with respect to the control, when using the biotin targeted drug-polymer complex. However, the same effect was not seen when either folate or vitamin B12 were used as targeting agents [31]. These results are clearly addressing biotin as the most promising targeting agent.

As we will report in this review, the biotin-mediated drug targeting of anti-tumor drugs emerges as an attractive approach to both improve efficiency and efficacy and reduce cytotoxicity of anti-cancer therapy. It is worth noting that the application of biotin-anticancer drug conjugates in drug development is still at its early stage, and translation in clinical research is being done progressively. The purpose of this review is to bring an objective view on the antitumor potential of biotin conjugates showing recent works, with particular emphasis on the last 4 years. A focus will be made on conjugates in which biotin is linked to i) drugs used in cancer therapy or their derivatives, ii) anticancer drug candidates and iii) protein with antitumor effect.

Biotinylation of Drugs used in Cancer Therapy or their Derivatives

Biotin conjugated to taxoids

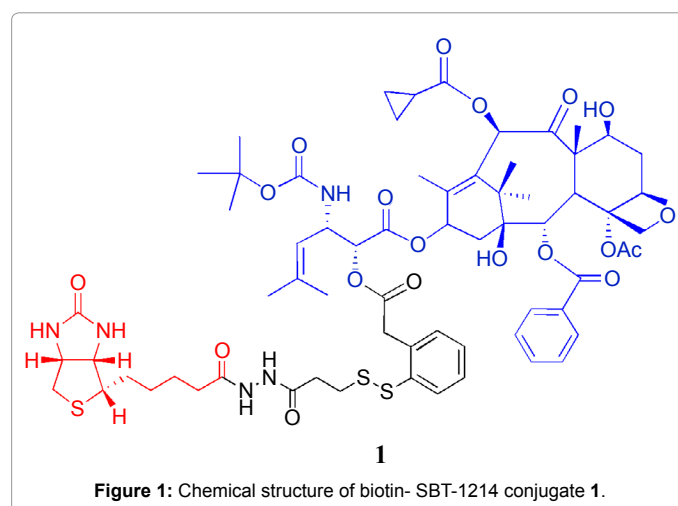
The microtubules, which are formed by α - and β -tubulin heterodimers, are the main components of the cytoskeleton and possess a variety of functions in intracellular processes, i.e. in maintaining cell shape and structure or in regulating the receptors moving inside the cell [44]. To date, numerous antimicrotubule agents with antimitotic properties and anticancer potential have been discovered and developed [3,45,46]. Among these agents, Paclitaxel is a natural highly oxygenated

diterpenoid that was first isolated in 1971 from the stem bark of the western yew, *Taxus brevifolia*. It is widely used to treat a variety of solid tumors such as breast, ovarian, non-small cell lung, head and neck cancers [47,48]. Since Paclitaxel was discovered, its structure has been extensively studied and modified yielding the so called taxoids, a class of proven anticancer drugs which promote microtubule assembly and suppress microtubule dynamics, thus causing the block of mitotic activity and subsequent cellular apoptosis [3,5].

In 2010, Chen et al., applied what they called "an efficient mechanism-based tumor-targeting drug delivery system, based on tumor-specific vitamin-receptor mediated endocytosis...". The Authors prepared a biotin conjugates with one of the new-generation taxoids, SBT-1214 [40]. The approach of this work is clear: to use the biotin- SBT-1214 conjugate 1 (Figure 1), which is characterized by an intracellularly labile disulfide linkage, to target the cancer cell by exploiting the overexpression of biotin receptor on the tumor cell surface.

In order to follow the entire process involved in the tumor targeting of the conjugate, the Authors synthesized three fluorescent biotin conjugates (Figure 2): i) the biotin-fluorescein conjugate 2, to observe the receptor-mediated endocytosis by tracking the fluorescent biotin in its route, ii) the biotin-coumarin conjugate 3, as a fluorogenic probe to evaluate the intracellular degradation of the disulfide linkage between the linker and coumarin, which becomes fluorescent only when it is released as a free molecule via disulfide cleavage of the spacer and iii) the biotin- SBT-1214 -fluorescein conjugate 4, to validate the whole internalization by receptor-mediated endocytosis and drug release processes, wherein the released fluorescent taxoid should bind to microtubules in the cancer cells.

In details, conjugates 2, 3 and 4 have been tested on L1210FR murine leukemia cell line, which overexpress receptors for biotin on their cell surface. Firstly, the Authors proved the internalization of the biotin-fluorescein conjugate 2 into the leukemia cells, by evaluating the intracellular fluorescence after incubation with the probe. Furthermore, they confirmed that the internalization was receptor-mediated by pre-incubation of the same cells with an excess of free biotin. They found that in these conditions the fluorescence of the biotin-fluorescein conjugate 2 decreased about 4.5 times, thus confirming that the biotin-fluorescein internalization is receptor-mediated. Secondly, the Authors confirmed the effectiveness of the fluorogenic biotin- coumarin conjugate 3 by incubating the chosen cell line with conjugate 3. Differently from



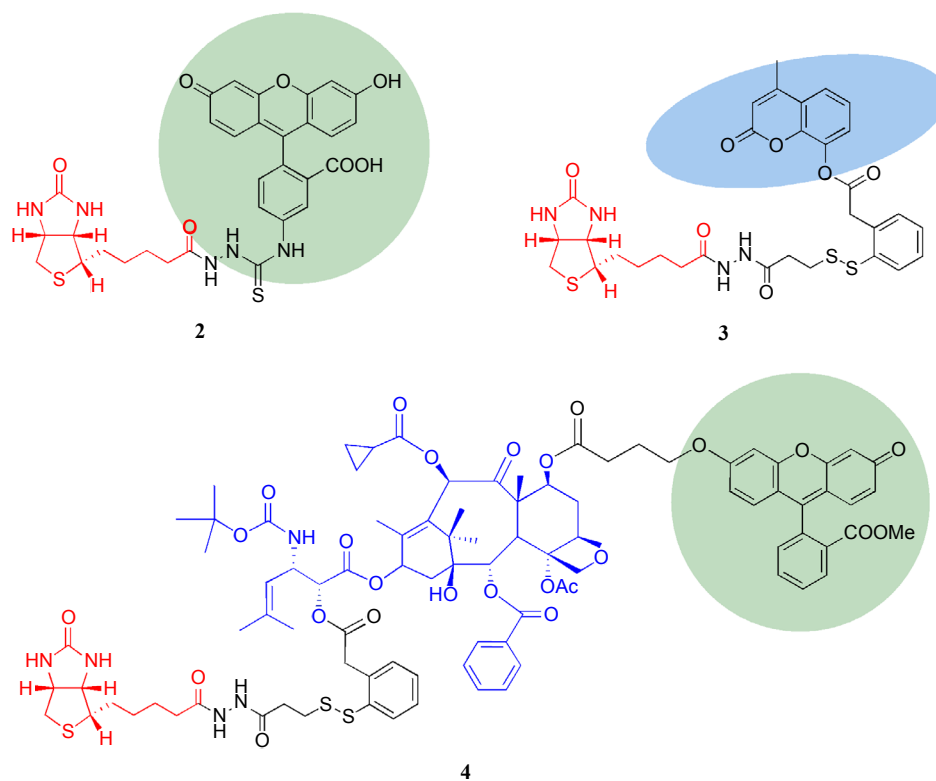


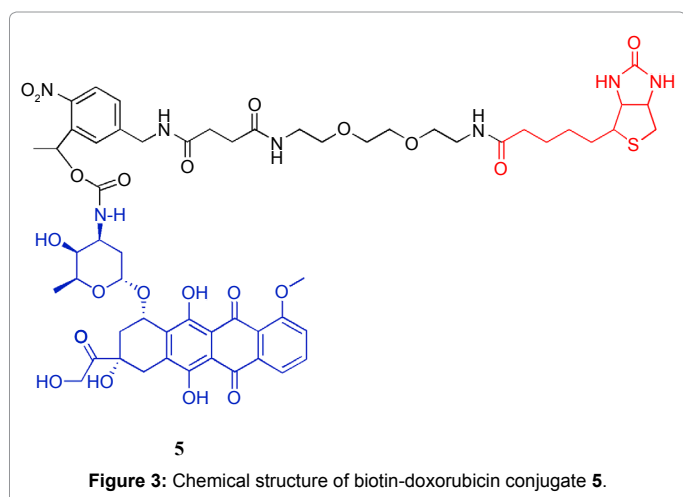
Figure 2: Chemical structure of biotin-fluorescein conjugate 2, biotin-coumarin conjugate 3 and biotin-SBT-1214-fluorescein conjugate 4.

conjugate 2, the intracellular fluorescence for conjugate 3 could be only evidenced after reductive cleavage of the spacer. Due to the visualized intracellular fluorescence, this study clearly demonstrated that the intracellular release of coumarin *via* cleavage of the disulfide linkage by GSH followed by thiolactonization took place as designed. Successively, they tested the biotin-SBT-1214-fluorescein conjugate 4. These results confirmed the internalization of the conjugate and also clearly proved that the released fluorescent taxoid binds to the microtubules. A cross-confirmation of the previous data has been performed by testing conjugate 4 using two more cell lines, L1210 murine leukemia cell line and WI38 noncancerous human lung fibroblast cell line, which do not overexpress receptors for biotin on their cell surfaces. This experiment resulted in a much stronger (about 12-13 times) fluorescence in L1210FR cells (with biotin receptors overexpressed) as compared to that in L1210 cells or WI38 cells, so confirming the biotin-mediated drug targeting. Finally, the Authors evaluated the cytotoxicity of the compound 1 against L1210FR, L1210 and WI38 cell lines by using the MTT assays. The conjugate 1 resulted high cytotoxic against L1210FR (IC_{50} 8.8 nM), while the cytotoxicity against L1210 (IC_{50} 522 nM) and WI38 (IC_{50} 570 nM) cell lines were 59 times and 65 times lower, respectively, as a further confirmation of the receptor mediated endocytosis. A fundamental consideration arises from the last results: the low toxicity that these conjugates showed against not-cancerous cells demonstrates that these systems could differentiate cancer cells from normal ones so reducing the side effects related to the use of cytotoxic drugs. These results are of paramount importance in the field of biotin targeted drugs because clearly demonstrated that: i) the biotin-drug conjugates are preferentially internalized into cancer cells, ii) the toxicity against normal cell is significantly reduced, and iii) the intracellular cleavage of the employed spacer allows a better systemic stability and a lower interaction with non-cancerous cells.

Biotin conjugated to doxorubicin

The antibiotic doxorubicin is extensively used against different human cancers, such as breast cancer, soft tissue sarcomas, and Hodgkin's and non-Hodgkin's lymphomas. The anticancer activity of doxorubicin has been addressed to several mechanisms of action: i) inhibition of DNA synthesis in the tumor cell, ii) generation of free radicals, iii) DNA adduct formation and DNA cross-linking, iv) interference with DNA strand separation and DNA helicase, v) interaction with cell membranes, vi) induction of DNA damage through interference with topoisomerase II, vii) induction of apoptosis and viii) growth arrest of tumor cells [49]. Nevertheless, the clinical use of doxorubicin is affected by several harmful side effects, among them, the cardiotoxicity is the most important one, leading to cardiomyopathy and congestive heart failure. Indeed, doxorubicin is known to cause cardiotoxicity through multiple routes, including the build-up of reactive oxygen species and disruption of the calcium homeostasis in cardiac myocytes. Several approaches have been proposed to limit its cardiotoxic effects, i.e. incorporation of the drug inside liposomes, formation of prodrugs proteolytically activated in the tumor cells, or the formation of polymeric prodrugs bearing specific drug-targeting moieties. Although these approaches are valuable, they are still not resolving the drawbacks connected to doxorubicin side effects [50]. Aiming at limiting the adverse side effects of doxorubicin, in 2010 Ibsen S. *et al.* designed and synthesized the biotin-doxorubicin conjugate 5 (Figure 3), in which the amine group of doxorubicin was derivatized with a photocleavable biotinylated spacer [51].

They demonstrated that the active drug is released only after the internalization of the conjugates in cancer cells and the subsequent activation of the photocleavable group *via* exposure to UV at 350 nm, thus minimizing the cytotoxic effects on non-cancerous cells.



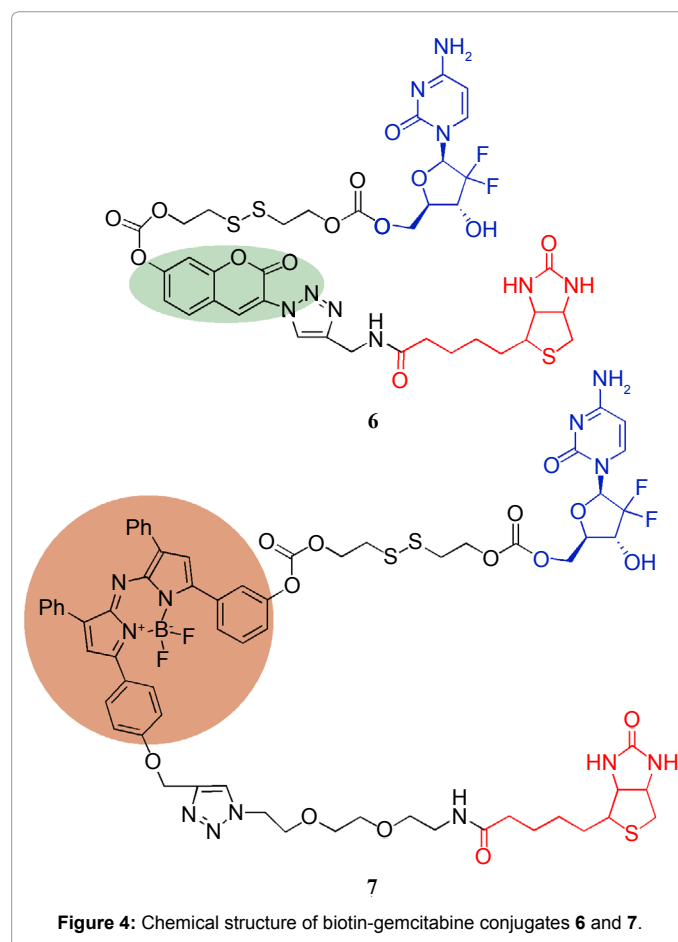
The Authors affirmed that the UV irradiation of deep tissues could be performed by implanting optic fibers or UV light-emitting diodes into the tumor mass and that light with 350 nm wavelength has significant penetration through tissue that does not contain melanin with minimal absorption also by DNA [52]. The Authors also studied the cell uptake and cellular localization in PTK2 epithelial cells, which are sensitive to doxorubicin and capable to remain flat during cell division, allowing the mitotic spindle and chromosomes to be readily visible. Interestingly, they found that the intracellular localization of doxorubicin was distinct from that of biotin-doxorubicin conjugate. In details, doxorubicin was found into the cell and concentrated almost exclusively in the nucleus, where it was associated with the chromatin most likely through a DNA intercalation mechanism. As a consequence, the nuclear membrane was degraded and doxorubicin strongly localized to the exposed chromosomes. On the contrary, the biotin-doxorubicin conjugate 5 showed a quick internalization and did not concentrate in the nucleus, but around it. The biotin-doxorubicin conjugate was thus excluded from the mitotic spindle and the associated chromosomes. Moreover, its intracellular concentration resulted 10 times higher than that of doxorubicin and the cells much healthier, appearing to be undergoing normal mitosis. After one hour of UV exposition, the photocleavage of the spacer allowed the release of the naturally fluorescent doxorubicin, which, in turn, accumulated into the nucleus, as proved by the intense fluorescence observed. The Authors also evaluated the cytotoxicity of both doxorubicin and its conjugate 5 on the human lung cancer cell line A549. The results of the cell proliferation assay clearly evidenced a significantly lower cytotoxicity of conjugate 5 with respect to that of free doxorubicin, being the IC_{50} value equal to 1.2 μM and 250 μM for doxorubicin and the biotin-doxorubicin conjugate, respectively. As expected, after UV exposure of the treated cells, the IC_{50} values for conjugate 5 resulted comparable to that of free doxorubicin. Another important consideration that emerges from this study is that the incorporation of the biotin moiety might help to increase the clearance rate of the freely circulating biotinylated doxorubicin, because it has been demonstrated that the elimination of biotinylated molecules from the human body could be higher than the corresponding non-biotinylated ones [25,53]. Summarizing, this approach allowed to obtain a system able to spare non-cancer cell from the drug cytotoxicity so targeting the conjugate to tumor cells, where the drug could be "activated" by *in-situ* UV irradiation. Overall, result obtained so far strongly suggest that the biotin-doxorubicin conjugate 5 could be a good drug candidate to reduce the undesirable systemic side effects of doxorubicin.

Biotin conjugated to gemcitabine

Gemcitabine is an anti-metabolite used to control non-small cell lung, pancreatic, metastatic breast and current ovarian cancers [54,55]. After cellular uptake, gemcitabine is phosphorylated to gemcitabine monophosphate (dFdCMP) which, in turn, is converted to gemcitabine di- and triphosphate (dFdCDP and dFdCTP, respectively) that are the active drug metabolites. The triphosphate analogue of gemcitabine acts i) replacing one cytidine during DNA replication and ii) inhibiting the DNA polymerase [56]. Some characteristic of gemcitabine, i.e. its short plasma half-life (9-13 min in human) due to its rapid renal clearance, and its myelosuppression side effect, contribute to decrease the gemcitabine chemotherapeutic index [57].

In their efforts to overcome the side effects of gemcitabine, in two recent papers Maiti et al. and Bhuniya et al. synthesized two new theranostic anticancer targeted prodrugs of gemcitabine (conjugates 6 and 7, Figure 4), which are characterized by a disulfide cleavable linker containing a fluorescent probe (coumarin for 6 and IR fluorescent BODIPY fluorophore for 7) [55,58]. A theranostic is a special type of Drug Delivery System (DDS) useful for therapeutic and diagnostic applications, which is able to provide not only a specific cellular drug release, but also a real time monitoring of the drug released in tissue [59].

The Authors studied the behavior of 6 and 7 in the presence of glutathione (GSH), which is the most abundant thiol in cells, or dithiothreitol (DTT) and demonstrated that gemcitabine release is due to cleavage of the sulfide bond upon GSH or DTT treatment,



followed by an intramolecular nucleophilic substitution of the thiol at the carbamate moiety. This mechanism of gemcitabine release is supported by further studies carried out in the presence of different biologically relevant analyte containing or not thiol groups, such as cysteine, homocysteine, non-thiol amino acids or metal ions. Results clearly evidenced that conjugates 6 and 7 undergo only a thiol-mediated cleavage, with no significant interference from other molecules present in biological environment. To investigate whether the biotin moiety can guide 6 and 7 to biotin receptor-positive or biotin receptor-negative tumor cells, Authors evaluated the fluorescence by confocal microscopy in A549 (biotin receptor-positive) and WI38 (biotin receptor-negative) cells pre-incubated with 6 and 7. A strong fluorescence intensity was only observed in the A549 cells, thus confirming that biotin acts as targeting agent to cancer cells. Additionally, to investigate the intracellular location of gemcitabine release, Authors performed colocalization experiments using fluorescent endoplasmic reticulum (ER) and lysosome-selective markers. They found that biotin-gemcitabine conjugate 7, containing the near IR BODIPY fluorophore, localized to the ER, while biotin-gemcitabine conjugate 6, containing coumarin, localized to the lysosome, probably by receptor mediated endocytosis. The subsequent thiol-induced disulfide cleavage released gemcitabine which, in turn, diffused to the cell nucleus. Finally, MTT assay performed on A549 cells clearly evidenced a stronger anticancer effect for the biotin conjugates 6 and 7 with respect to their analogues without the biotin moiety, further confirming the biotin-mediated targeting to tumor cells. In summary, also in these studies the conjugation of anticancer drugs with biotin emerged as a successful approach to spare cancer and non-cancer cells, thus increasing the cell specificity of the drug.

Biotinylation of Potential Anti-tumor Drug Candidates

Biotin conjugated to Annonaceous Acetogenin derivatives

Squamocin (compound 8, Figure 5) and bullatacin (compound 9, Figure 5) are annonaceous acetogenins (ACGs) belonging to adjacent bis-THF type of acetogenins [41,60,61]. ACGs are secondary metabolites occurring in some plants of Annonaceae family. They are derivatives of long-chain fatty acid (C32 or C34) bearing a terminal γ -lactone ring and have been reported to potently inhibit the activity of NADH-ubiquinone oxidoreductase (respiratory complex I). These long-chain fatty acid derivatives display impressive cytotoxicity against various tumor cell lines (IC_{50} value ranging from 10^{-6} M to 10^{-14} M) as well as *in vivo* antitumor effect [41,62-64].

In a just-published research paper, Shi et al. report on the synthesis of nineteen biotinylated derivatives of 8 and 9 as well as on their cytotoxicity against three cancer cell lines: 4T1 (breast cancer), P815 (mastocytoma) and L1210 (leukemia). The first two cell lines overexpress the receptor for biotin, while the third one is not overexpressing the receptor [41]. Generally, they found that the cytotoxic activity of the biotin-ACG conjugates against L1210 cell

line is almost the same as that of the parent 8 and 9. This datum is fundamental to assess that biotinylation of 8 and 9 does not adversely affect their cytotoxic potential. On the other side, the biotin-ACG conjugates showed significantly higher cytotoxicity than 8 and 9 against 4T1 and P815 cell lines. In particular, the biotin-squamocin conjugate 10 (Figure 6) resulted ten and twenty six times more active than 8 against 4T1 and P815 cells, respectively. Similarly, the biotin-bullatacin conjugate 11 (Figure 6), resulted three and eight times more potent than 9 against 4T1 and P815 cells, respectively. Taken together, the results clearly demonstrate that biotin targeted derivatives of 8 and 9 are still active against different cancer cell lines and that cytotoxicity is significantly increased by biotin conjugation.

Concerning the influence of the number of biotinyl residues on the cytotoxic activity, the Authors found that the addition of a second biotinyl residue does not generally result in further improvement of the potency of the biotin-ACG conjugate, with the only exception of the already mentioned biotin-squamocin conjugate 10. Indeed, this conjugate, which is characterized by two biotinyl moieties, resulted up to three times more potent and two times more selective than the corresponding mono-biotinylated derivative 12 (Figure 6). Interestingly, the Authors also noticed that the optimal site of attachment of biotin strongly depend on whether or not the 6-aminocaproic acid residue is present as a linker between the ACG scaffold and the biotinyl residue. Particularly, concerning biotin-squamocin conjugates, the preferred site of attachment of biotin is the C-28 hydroxyl group when biotin is directly attached to the scaffold, and become the C-15 hydroxyl group when the linker between biotin and squamocin is present. In the case of biotin-bullatacin conjugates, the optimal site for biotinyl derivatization is the C-15 hydroxyl group in the absence of the linker, which changes to the C-4 and C-24 hydroxyl groups in the presence of the linker. Moreover, regarding the effect of the linker on the biological activity, Authors showed that biotin-ACG conjugates bearing the linker are generally more potent than the analogues which lack such linker, thus proving that the presence of the linking spacer positively affect the anticancer potential of the conjugates. Indeed, the biotin-squamocin conjugate 12 (Figure 6), biotinylated at C-15 and bearing the linker between squamocin and biotin, is almost four and ten times more potent against 4T1 cells and P815 cells, respectively, than the analogue without the linker. Similarly, conjugates 11 and 13 (Figure 6), biotinylated at C-24 and C-4, respectively, and both bearing the linker between bullatacin and biotin, are twelve to forty nine times more active against 4T1 cells and P815 cells, respectively, than the corresponding analogues without the linker. In summary, in this study a broad investigation of the effect of biotin conjugation on the anticancer activity of two ACGs has been described. The results clearly proved that biotin conjugation significantly increases the anticancer potential ACGs, which, in turn, is significantly affected by i) the number of biotinyl residues included in the conjugates, ii) the point of attachment of the biotinyl residue, as well as iii) the presence or not of a spacer between ACG and biotin.

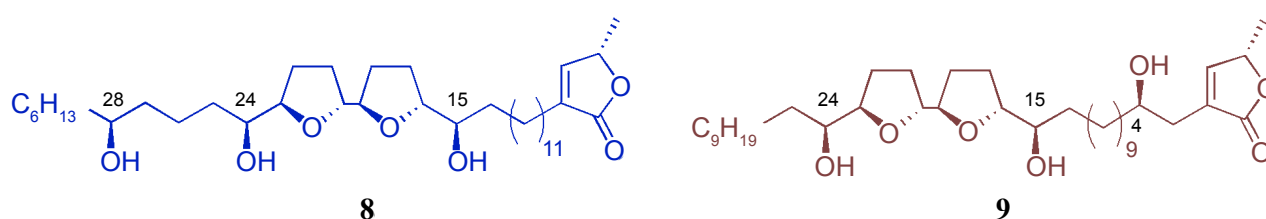


Figure 5: Chemical structure of Squamocin 8 and Bullatacin 9.

Biotinylation of Protein with Antitumor Effect

Biotin conjugated to p53 protein

p53 is a transcription factor involved in various cellular functions, such as cell-cycle regulation, initiation of apoptotic cell death and DNA repair. Mutated or otherwise deactivated p53 is observed in the majority of human cancers [65]. Several mechanisms, i.e. mutations in p53 DNA binding domain and enhanced proteasomal degradation upon ubiquitination, are responsible for p53 inactivation. Due to its vital functions, p53 has attracted a great attention, and several approaches have been pursued to deliver p53 into tumor cells [66]. In this context, in 2013 Fahrner et al. demonstrated that biotinylation of p53 represents a successful strategy to target and deliver the protein to cancer cells [67]. In this study the Authors take advantage of the already developed C2-streptavidin transporter [68,69] to introduce the biotin-p53 conjugate into various mammalian cell lines. Briefly, as reported in Figure 7, the nontoxic moiety of Clostridium botulinum C2 toxin of the recombinant C2-streptavidin fusion protein mediates the cellular uptake by a cascade of events that bring to the internalization of the toxin by a clathrin-dependent endocytosis and, on the other side, the streptavidin unit serves as a binding platform for biotin-labeled cargo molecules. Firstly, recombinant human p53 was produced in insect cells infected with p53 baculovirus [70] and then, it was properly biotinylated, yielding a biotin-p53 conjugate in which the protein was modified with 2.2 biotin groups per molecule. Next, the Authors clearly demonstrated that the biotinylation of p53 does not affect its DNA-binding activity. Indeed the DNA-binding of biotin-p53 conjugate was comparable to that of unmodified p53. Furthermore, the addition

of the biotin-p53 conjugate to specific DNA sequences resulted in the formation of DNA-p53 complexes in a concentration-dependent manner. Finally, the Authors assessed the C2-streptavidin-mediated internalization of biotin-p53 conjugate in both Vero cells (monkey kidney epithelial cells) and HeLa (cervix carcinoma) cells. Interestingly, an efficient internalization of biotin-p53 conjugate in a C2-streptavidin-dependent manner was observed in both cases. Summarizing, these data demonstrate that biotin conjugation to p53 is a successful approach to promote the C2-streptavidin mediated internalization of the transcription factor into cultured tumor cells, where the biotin-p53 conjugate resulted stable over 24 h and not underwent proteasomal degradation. It should be noted that the mild chemistry adopted by the Authors for the biotin conjugation to p53 could be used for wide number of labile proteins or peptides of pharmaceutical interest.

Conclusions

This review gives a highlight on recent progresses on the so-called biotin-mediated drug targeting of molecules endowed with anticancer properties. Particularly, the review has been organized in three different sections in which we have examined recent success in the conjugation of biotin with i) anticancer drugs commonly used in cancer therapy (toxoids, doxorubicin and gemcitabine) or their derivatives, as well as ii) anticancer drug candidates or iii) protein with antitumor effect, furnishing biotin conjugates able to preferentially deliver the anticancer molecules to cancer cells.

In summary, from the analysis of the literature on this topic clearly emerged that the conjugation of biotin with anticancer molecules represents an attractive and highly innovative approach to improve efficiency and efficacy and reduce cytotoxicity of anti-cancer therapy.

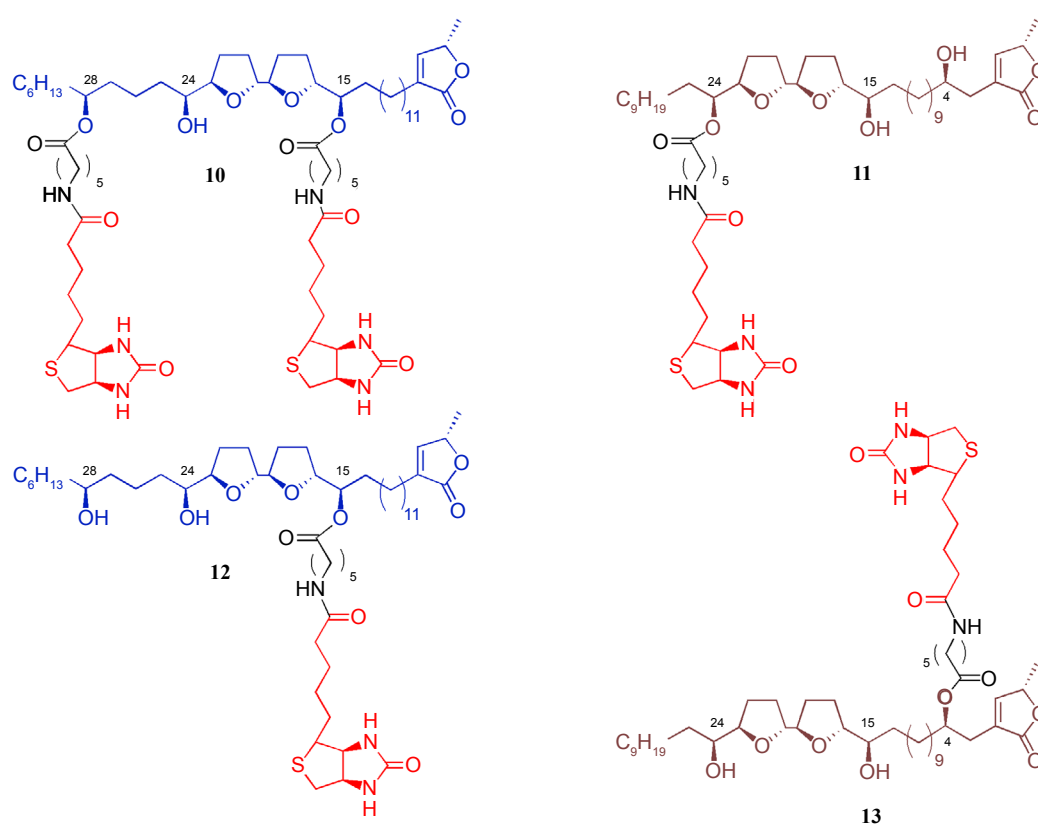


Figure 6: Chemical structure of biotin-squamocin conjugates 10 and 12; chemical structure of biotin-bullatacin conjugates 11 and 13.

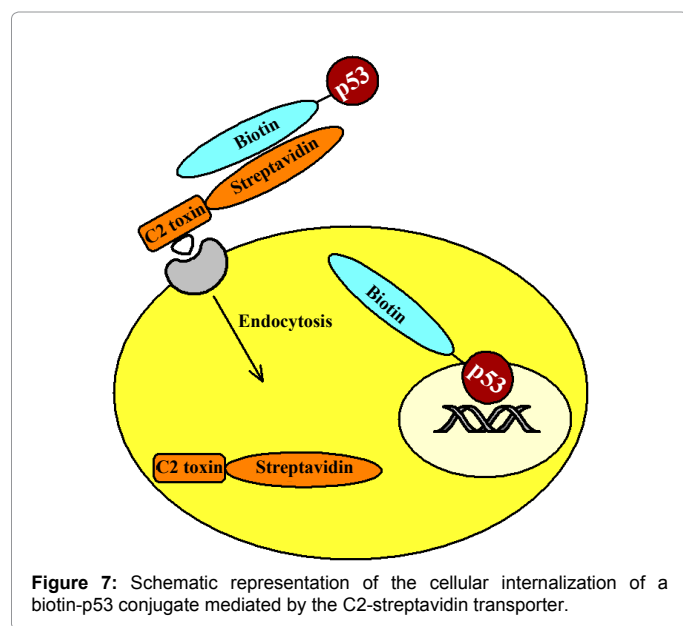


Figure 7: Schematic representation of the cellular internalization of a biotin-p53 conjugate mediated by the C2-streptavidin transporter.

Although only few targeted drugs have been developed so far, this area is in constant growth and we strongly believe that this approach could give an added value to cancer therapy.

References

1. Bolden JE, Peart MJ, Johnstone RW (2006) Anticancer activities of histone deacetylase inhibitors. *Nat Rev Drug Discov* 5: 769-784.
2. Jamieson ER, Lippard SJ (1999) Structure, Recognition, and Processing of Cisplatin-DNA Adducts. *Chem Rev* 99: 2467-2498.
3. Dumontet C, Jordan MA (2010) Microtubule-binding agents: a dynamic field of cancer therapeutics. *Nat Rev Drug Discov* 9: 790-803.
4. Jordan MA, Wilson L (2004) Microtubules as a target for anticancer drugs. *Nat Rev Cancer* 4: 253-265.
5. Jordan MA (2002) Mechanism of action of antitumor drugs that interact with microtubules and tubulin. *Curr Med Chem Anticancer Agents* 2: 1-17.
6. Timmers L, Boons CC, Kropff F, van de Ven PM, Swart EL, et al. (2014) Adherence and patients' experiences with the use of oral anticancer agents. *Acta Oncol* 53: 259-267.
7. Mahato R, Tai W, Cheng K (2011) Prodrugs for improving tumor targetability and efficiency. *Adv Drug Deliv Rev* 63: 659-670.
8. Couffignal AL, Lapeyre-Mestre M, Bonhomme C, Bugat R, Montastruc JL (2000) [Adverse effects of anticancer drugs: apropos of a pharmacovigilance study at a specialized oncology institution]. *Therapie* 55: 635-641.
9. Mandracchia D, Tripodo G, Latrofa A, Dorati R (2014) Amphiphilic inulin-D- α -tocopherol succinate (INVITE) bioconjugates for biomedical applications. *Carbohydr Polym* 103: 46-54.
10. Tripodo G, Mandracchia D, Dorati R, Latrofa A, Genta I, et al. (2013) Nanostructured Polymeric Functional Micelles for Drug Delivery Applications. *Macromol Symp* 334: 17-23.
11. LoPresti C, Vetri V, Ricca M, Fodera V, Tripodo G, et al. (2011) Pulsatile protein release and protection using radiation-crosslinked polypeptide hydrogel delivery devices. *React Funct Polym* 71: 155-167.
12. Tripodo G, Pitarresi G, Cavallaro G, Palumbo FS, Giammona G (2009) Controlled release of IgG by novel UV induced polysaccharide/poly(amino acid) hydrogels. *Macromol Biosci* 9: 393-401.
13. Pitarresi G, Palumbo FS, Tripodo G, Cavallaro G, Giammona G (2007) Preparation and characterization of new hydrogels based on hyaluronic acid and alpha,beta-polyaspartylhydrazide. *Eur Polym J* 43: 3953-3962.
14. Pitarresi G, Pierro P, Tripodo G, Mandracchia D, Giammona G (2005) Drug delivery from mucoadhesive disks based on a photo-cross-linkable polyaspartamide derivative. *J Drug Deliv Sci Technol* 15: 377-382.
15. Mandracchia D, Denora N, Franco M, Pitarresi G, Giammona G, et al. (2010) New Biodegradable Hydrogels Based on Inulin and alpha,beta-Polyaspartylhydrazide Designed for Colonic Drug Delivery: In Vitro Release of Glutathione and Oxytocin. *J Biomater Sci Polym Ed*.
16. Mandracchia D, Piccionello AP, Pitarresi G, Pace A, Buscemi S, et al. (2007) Fluoropolymer based on a polyaspartamide containing 1,2,4-oxadiazole units: a potential artificial oxygen (O₂) carrier. *Macromol Biosci* 7: 836-845.
17. Giammona G, Pitarresi G, Cavallaro G, Carlisi B, Craparo EF, et al. (2006) pH-sensitive hydrogel based on a polyaspartamide derivative. *J Drug Deliv Sci Technol* 16: 77-84.
18. Gibiansky L, Gibiansky E (2014) Target-mediated drug disposition model and its approximations for antibody-drug conjugates. *J Pharmacokinet Pharmacodyn* 41: 35-47.
19. Lammers T, Kiessling F, Hennink WE, Storm G (2012) Drug targeting to tumors: principles, pitfalls and (pre-) clinical progress. *J Control Release* 161: 175-187.
20. Bareford LM, Avaritt BR, Ghandehari H, Nan A, Swaan PW (2013) Riboflavin-targeted polymer conjugates for breast tumor delivery. *Pharm Res* 30: 1799-1812.
21. Nan A, Ghandehari H, Hebert C, Siavash H, Nikitakis N, et al. (2005) Water-soluble polymers for targeted drug delivery to human squamous carcinoma of head and neck. *J Drug Target* 13: 189-197.
22. Licciardi M, Craparo EF, Giammona G, Armes SP, Tang Y, et al. (2008) in vitro biological evaluation of folate-functionalized block copolymer micelles for selective anti-cancer drug delivery. *Macromol Biosci* 8: 615-626.
23. Cavallaro G, Maniscalco L, Campisi M, Schillaci D, Giammona G (2007) Synthesis, characterization and in vitro cytotoxicity studies of a macromolecular conjugate of paclitaxel bearing oxytocin as targeting moiety. *Eur J Pharm Biopharm* 66: 182-192.
24. Akdemir ZS, Akçakaya H, Kahraman MV, Ceyhan T, Kayaman-Apohan N, et al. (2008) Photopolymerized injectable RGD-modified fumarated poly(ethylene glycol) diglycidyl ether hydrogels for cell growth. *Macromol Biosci* 8: 852-862.
25. Axworthy DB, Reno JM, Hylarides MD, Mallett RW, Theodore LJ, et al. (2000) Cure of human carcinoma xenografts by a single dose of pretargeted yttrium-90 with negligible toxicity. *Proc Natl Acad Sci U S A* 97: 1802-1807.
26. Altaner C, Altanero V, Cihova M, Ondicova K, Rychly B, et al. (2014) Complete regression of glioblastoma by mesenchymal stem cells mediated prodrug gene therapy simulating clinical therapeutic scenario. *Int J Cancer* 134: 1458-1465.
27. Elsadek B, Graeser R, Esser N, Schäfer-Obodozie C, Abu Ajaj K, et al. (2010) Development of a novel prodrug of paclitaxel that is cleaved by prostate-specific antigen: an in vitro and in vivo evaluation study. *Eur J Cancer* 46: 3434-3444.
28. Fortin S, Berube (2013) Advances in the development of hybrid anticancer drugs. *Expert Opin Drug Discov* 8: 1029-1047.
29. Jaracz S, Chen J, Kuznetsova LV, Ojima I (2005) Recent advances in tumor-targeting anticancer drug conjugates. *Bioorg Med Chem* 13: 5043-5054.
30. Bildstein L, Dubernet C, Couvreur P (2011) Prodrug-based intracellular delivery of anticancer agents. *Adv Drug Deliv Rev* 63: 3-23.
31. Russell-Jones G, McTavish K, McEwan J, Rice J, Nowotnik D (2004) Vitamin-mediated targeting as a potential mechanism to increase drug uptake by tumours. *J Inorg Biochem* 98: 1625-1633.
32. Kozyraki R, Cases O (2013) Vitamin B12 absorption: mammalian physiology and acquired and inherited disorders. *Biochimie* 95: 1002-1007.
33. Gupta Y, Kohli DV, Jain SK (2008) Vitamin B12-mediated transport: a potential tool for tumor targeting of antineoplastic drugs and imaging agents. *Crit Rev Ther Drug Carrier Syst* 25: 347-379.
34. Reddy JA, Low PS (1998) Folate-mediated targeting of therapeutic and imaging agents to cancers. *Crit Rev Ther Drug Carrier Syst* 15: 587-627.
35. Kolhatkar R, Lote A, Khambati H (2011) Active tumor targeting of nanomaterials using folic acid, transferrin and integrin receptors. *Curr Drug Discov Technol* 8: 197-206.
36. Rodriguez-Melendez R, Zemleni J (2003) Regulation of gene expression by biotin (review). *J Nutr Biochem* 14: 680-690.
37. Zemleni J, Mock DM (1998) Uptake and metabolism of biotin by human peripheral blood mononuclear cells. *Am J Physiol* 275: C382-388.

38. Zempleni J, Mock DM (1999) Human peripheral blood mononuclear cells; Inhibition of biotin transport by reversible competition with pantothenic acid is quantitatively minor. *J Nutr Biochem* 10: 427-432.
39. Grassl SM (1992) Human placental brush-border membrane Na⁺-biotin cotransport. *J Biol Chem* 267: 17760-17765.
40. Chen S, Zhao X, Chen J, Chen J, Kuznetsova L, et al. (2010) Mechanism-based tumor-targeting drug delivery system. Validation of efficient vitamin receptor-mediated endocytosis and drug release. *Bioconjug Chem* 21: 979-987.
41. Shi JF, Wu P, Jiang ZH, Wei XY (2014) Synthesis and tumor cell growth inhibitory activity of biotinylated annonaceous acetogenins. *Eur J Med Chem* 71: 219-228.
42. Vadlapudi AD, Vadlapatla RK, Pal D, Mitra AK (2012) Functional and molecular aspects of biotin uptake via SMVT in human corneal epithelial (HCEC) and retinal pigment epithelial (D407) cells. *AAPS J* 14: 832-842.
43. Luo S, Kansara VS, Zhu X, Mandava NK, Pal D, et al. (2006) Functional characterization of sodium-dependent multivitamin transporter in MDCK-MDR1 cells and its utilization as a target for drug delivery. *Mol Pharm* 3: 329-339.
44. Vale RD (2003) The molecular motor toolbox for intracellular transport. *Cell* 112: 467-480.
45. Pitarresi G, Tripodo G, Calabrese R, Craparo EF, Licciardi M, et al. (2008) Hydrogels for potential colon drug release by thiol-ene conjugate addition of a new inulin derivative. *Macromol Biosci* 8: 891-902.
46. Wang Y, O'Brate A, Zhou W, Giannakakou P (2005) Resistance to microtubule-stabilizing drugs involves two events: beta-tubulin mutation in one allele followed by loss of the second allele. *Cell Cycle* 4: 1847-1853.
47. Lis LG, Smart MA, Luchniak A, Gupta ML Jr, Gurvich VJ (2012) Synthesis and Biological Evaluation of a Biotinylated Paclitaxel With an Extra-Long Chain Spacer Arm. *ACS Med Chem Lett* 3: 745-748.
48. Nicolaou KC, Dai WM, Guy RK (1994) Chemistry and Biology of Taxol. *Angew Chem-Int Edit* 33: 15-44.
49. Gewirtz DA (1999) A critical evaluation of the mechanisms of action proposed for the antitumor effects of the anthracycline antibiotics adriamycin and daunorubicin. *Biochem Pharmacol* 57: 727-741.
50. Minotti G, Menna P, Salvatorelli E, Cairo G, Gianni L (2004) Anthracyclines: molecular advances and pharmacologic developments in antitumor activity and cardiotoxicity. *Pharmacol Rev* 56: 185-229.
51. Ibsen S, Zahavy E, Wrasdilo W, Berns M, Chan M, et al. (2010) A novel Doxorubicin prodrug with controllable photolysis activation for cancer chemotherapy. *Pharm Res* 27: 1848-1860.
52. Sutherland JC, Griffin KP (1981) Absorption spectrum of DNA for wavelengths greater than 300 nm. *Radiat Res* 86: 399-409.
53. Weiden PL, Breitz HB (2001) Pretargeted radioimmunotherapy (PRIT) for treatment of non-Hodgkin's lymphoma (NHL). *Crit Rev Oncol Hematol* 40: 37-51.
54. Friberg G, Kindler HL (2005) Chemotherapy for advanced pancreatic cancer: past, present, and future. *Curr Oncol Rep* 7: 186-195.
55. Maiti S, Park N, Han JH, Jeon HM, Lee JH, et al. (2013) Gemcitabine-coumarin-biotin conjugates: a target specific theranostic anticancer prodrug. *J Am Chem Soc* 135: 4567-4572.
56. Mini E, Nobili S, Caciagli B, Landini I, Mazzei T (2006) Cellular pharmacology of gemcitabine. *Ann Oncol* 17 Suppl 5: v7-12.
57. Noble S, Goa KL (1997) Gemcitabine. A review of its pharmacology and clinical potential in non-small cell lung cancer and pancreatic cancer. *Drugs* 54: 447-472.
58. Bhuniya S, Lee MH, Jeon HM, Han JH, Lee JH, et al. (2013) A fluorescence off-on reporter for real time monitoring of gemcitabine delivery to the cancer cells. *Chem Commun (Camb)* 49: 7141-7143.
59. Lee MH, Kim JY, Han JH, Bhuniya S, Sessler JL, et al. (2012) Direct fluorescence monitoring of the delivery and cellular uptake of a cancer-targeted RGD peptide-appended naphthalimide theragnostic prodrug. *J Am Chem Soc* 134: 12668-12674.
60. Degli Esposti M, Ghelli A, Ratta M, Cortes D, Estornell E (1994) Natural substances (acetogenins) from the family Annonaceae are powerful inhibitors of mitochondrial NADH dehydrogenase (Complex I). *Biochem J* 301: 161-167.
61. Londershausen M, Leicht W, Lieb F, Moeschler H, Weiss H (1991) Molecular-mode of action of annonins. *Pestic Sci* 33: 427-438.
62. Duval R, Lewin G, Hocquemiller R (2003) Semisynthesis of heterocyclic analogues of squamocin, a cytotoxic annonaceous acetogenin, by an unusual oxidative decarboxylation reaction. *Bioorg Med Chem* 11: 3439-3446.
63. Derbre S, Roue G, Poupon E, Susin SA, Hocquemiller R (2005) Annonaceous acetogenins: The hydroxyl groups and THF rings are crucial structural elements for targeting the mitochondria, demonstration with the synthesis of fluorescent squamocin analogues. *Chem Bio Chem* 6: 979-982.
64. McLaughlin JL (2008) Paw paw and cancer: annonaceous acetogenins from discovery to commercial products. *J Nat Prod* 71: 1311-1321.
65. Romer L, Klein C, Dehner A, Kessler H, Buchner J (2006) p53--a natural cancer killer: structural insights and therapeutic concepts. *Angew Chem Int Ed Engl* 45: 6440-6460.
66. Horn HF, Vousden KH (2007) Coping with stress: multiple ways to activate p53. *Oncogene* 26: 1306-1316.
67. Fahrer J, Schweitzer B, Fiedler K, Langer T, Gierschik P, et al. (2013) C2-Streptavidin Mediates the Delivery of Biotin-Conjugated Tumor Suppressor Protein p53 into Tumor Cells. *Bioconjugate Chem* 24: 595-603.
68. Fahrer J, Plunien R, Binder U, Langer T, Seliger H, et al. (2010) Genetically engineered clostridial C2 toxin as a novel delivery system for living mammalian cells. *Bioconjug Chem* 21: 130-139.
69. Fahrer J, Rieger J, van Zandbergen G, Barth H (2010) The C2-streptavidin delivery system promotes the uptake of biotinylated molecules in macrophages and T-leukemia cells. *Biol Chem* 391: 1315-1325.
70. Fahrer J, Kranaster R, Altmeyer M, Marx A, Burkle A (2007) Quantitative analysis of the binding affinity of poly(ADP-ribose) to specific binding proteins as a function of chain length. *Nucleic Acids Res* 35: e143.

This article was originally published in a special issue, **Cancer Prevention and Therapy** handled by Editor(s). Dr. Dong Xiao, University of Pittsburgh School of Medicine, USA

Citation: Tripodo G, Mandracchia D, Collina S, Rui M, Rossi D (2014) New Perspectives in Cancer Therapy: The Biotin-Antitumor Molecule Conjugates. *Med chem S1*: 004. doi:[10.4172/2161-0444.S1-004](https://doi.org/10.4172/2161-0444.S1-004)

Submit your next manuscript and get advantages of OMICS Group submissions

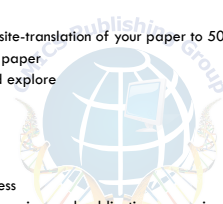
Unique features:

- User friendly/feasible website-translation of your paper to 50 world's leading languages
- Audio Version of published paper
- Digital articles to share and explore

Special features:

- 350 Open Access Journals
- 30,000 editorial team
- 21 days rapid review process
- Quality and quick editorial, review and publication processing
- Indexing at PubMed (partial), Scopus, EBSCO, Index Copernicus and Google Scholar etc
- Sharing Option: Social Networking Enabled
- Authors, Reviewers and Editors rewarded with online Scientific Credits
- Better discount for your subsequent articles

Submit your manuscript at: <http://omicsgroup.info/editorialtracking/medicinalchemistry/>



CrossMark
click for updatesCite this: *Med. Chem. Commun.*, 2015, 6, 138

A step forward in the sigma enigma: a role for chirality in the sigma₁ receptor–ligand interaction?†

Daniela Rossi,^{‡a} Annamaria Marra,^{‡a} Marta Rui,^a Erik Laurini,^b Maurizio Fermeglia,^b Sabrina Pricl,^{bc} Dirk Schepmann,^d Bernhard Wuensch,^d Marco Peviani,^e Daniela Curti^e and Simona Collina^{*a}

In our recent research racemic RC-33 was identified as a potent and highly promising σ_1 receptor agonist, showing excellent σ_1 receptor affinity and promoting NGF-induced neurite outgrowth in PC12 cells at very low concentrations. Surprisingly, both its interaction with the biological target and its effect on neurite sprouting proved to be non-stereoselective. Starting from the observation that a hydrogen bond center in the scaffold of a σ_1 ligand is an important pharmacophoric element for receptor/ligand interaction, we hypothesized that the absence of such pharmacophoric feature in the structure of RC-33 could be also responsible for the lack of enantioselectivity in its interaction with the target receptor. To verify our hypothesis, in this paper we evaluated – both *in silico* and *in vitro* – the ability of a series of enantiomeric arylalkylaminoalcohols and arylpyrrolidinols 1–5 to interact with the receptor. All these compounds are structurally related to RC-33 and are characterized by the presence of an –OH group as the additional pharmacophore feature. Interestingly, the results of our study show that the σ_1 receptor exhibits enantiopreference toward compounds characterized by (S)-configuration at the stereogenic center bearing the aromatic moiety only when the alcoholic group is also present at that chiral center, thus supporting our original hypothesis.

Received 13th August 2014
Accepted 17th September 2014

DOI: 10.1039/c4md00349g

www.rsc.org/medchemcomm

Introduction

The sigma (σ) binding sites were originally defined and classified as opioid receptor subtypes.¹ Later investigations demonstrated that σ receptors were distinct from opioid and phencyclidine analogues, and since then at least two distinct σ receptor subtypes, designated σ_1 and σ_2 ,² have been pharmacologically characterized.^{3–5} In particular, the σ_1 receptor subtype has been purified and cloned from several animal species and humans.^{6,7}

σ_1 receptors are ubiquitously expressed in mammalian tissues and highly distributed in the central nervous system (CNS),^{8–10} with the highest density found in the spinal cord, cerebellum, hippocampus, hypothalamus, midbrain, cerebral cortex, and pineal gland. Strong pharmacological evidence indicates that σ_1 receptors are involved in the pathophysiology of all major CNS disorders,¹¹ including mood disorders (anxiety¹² and depression¹³), psychosis and schizophrenia,¹⁴ as well as drug addiction, pain,¹⁵ and neurodegenerative diseases such as Parkinson's, Alzheimer's, and amyotrophic lateral sclerosis.¹⁶ Moreover, from a biological perspective, the σ_1 receptors reside in the endoplasmic reticulum (ER) at the ER-mitochondria interface,¹⁷ and they are unique ligand-regulated molecular chaperones^{18–20} that can translocate to the plasma membrane or to other subcellular compartments under stressful conditions and/or pharmacological manipulation.

Ligands displaying preferential affinity for the σ_1 receptor subtype are (+)-benzomorphans such as (+)-pentazocine and (+)-N-allylnormetazocine (NANM, SKF-10047), whereas haloperidol and 1,3-di-(2-tolyl)guanidine (DTG) exhibit high affinity for both receptor subtypes.²¹ Since (+)-pentazocine shows a very low affinity for the σ_2 receptors, it represents the prototypical selective agonist used in its tritiated form to label σ_1 receptors. Several compounds endowed with σ_1 affinity and selectivity, characterized by different scaffolds, have been identified, e.g.,

^aDepartment of Drug Sciences, Medicinal Chemistry and Pharmaceutical Technology section, University of Pavia, Viale Taramelli 12, 27100 Pavia, Italy. E-mail: simona.collina@unipv.it; Fax: +39 0382-422975; Tel: +39 0382 987379

^bMOSE – DEA-University of Trieste, Via Valerio 10, 34127 Trieste, Italy

^cNational Interuniversity Consortium for Material Science and Technology (INSTM), Research Unit MOSE-DEA University of Trieste, Trieste, Italy

^dInstitute of Pharmaceutical and Medicinal Chemistry, University of Muenster, Correnstrasse 48, 48149 Muenster, Germany

^eDepartment of Biology and Biotechnology “L. Spallanzani”, Laboratory of Cellular and Molecular Neuropharmacology, University of Pavia, Via Ferrata 9, 27100 Pavia, Italy

† Electronic supplementary information (ESI) available: Details of chemical synthesis, chiral resolution and absolute configuration assignment of compound 1, and all details of the molecular modeling study and biological investigation. See DOI: 10.1039/c4md00349g

‡ These authors contributed equally to this work.

arylalkylamines,^{22a-f} benzooxazolones,²³ and spirocyclic pyranopyrazoles,²⁴ and different pharmacophore models for σ_1 receptor ligands have been published. All these models share the common features of a basic amino group and at least two hydrophobic substituents at the basic nitrogen atom.^{25a-f} However, the last-generation, three-dimensional (3D) pharmacophore models^{25c-f} are characterized by an additional pharmacophore requirement: a heterogroup in the scaffold of the molecule that is able to form hydrogen bond interactions with the receptor counterpart. Actually, heteroatoms such as O or S are frequently present in very potent σ_1 ligands, bridging the aromatic component and the classic alkyl or cycloalkyl intermediate spacer linked to the basic nitrogen atom.^{26,27}

In this scenario, our group designed and synthesized a large number of very interesting σ_1 receptor ligands.^{22a-c} Among these, the most promising molecule is 1-[3-(1,1'-biphen)-4-yl]butylpiperidine (**RC-33**, Fig. 1), showing excellent σ_1 receptor affinity and agonistic profile in its racemic form, as testified by its $K_i\sigma_1$ value of 0.70 ± 0.3 nM and by the potentiation of the NGF-induced neurite outgrowth in the PC12 cell at very low concentrations.^{22c,d}

Racemic resolution of **RC-33** and isolation of the enantiomers revealed that (i) the interaction with the biological target is non-stereoselective ($K_i\sigma_1^{(S)\text{-RC-33}} = 1.9 \pm 0.2$ nM, $K_i\sigma_1^{(R)\text{-RC-33}} = 1.8 \pm 0.1$ nM) and (ii) the pharmacological activity is not dependent on the absolute configuration.^{22e,f} The behavior of **RC-33** is particularly surprising, since the enantioselectivity of the σ_1 receptor is well documented.²⁰ Starting from the observation that an important pharmacophoric element is missing in the **RC-33** structure (*i.e.*, a hydrogen bond donor or acceptor),^{25c-e} we first hypothesized that the absence of such pharmacophoric feature could be responsible for the lack of enantioselectivity in the interaction with the biological target. Then, we verified our hypothesis by evaluating the ability of a series of enantiomeric arylalkylaminoalcohols and arylpyrrolidinols, structurally related to **RC-33**, to interact with σ_1 receptors. Specifically, here we report and discuss in detail the results of the *in silico* study, synthesis, chiral resolution and biological evaluation of the arylalkylaminoalcohol **1** (Table 1), analogue of **RC-33**, complemented by the *in silico* and *in vitro* studies of other enantiomeric arylalkylaminoalcohol and arylpyrrolidinol derivatives (Table 1). These molecules were selected from a compound cohort previously prepared and characterized by us as analgesic agents with effects similar or higher than morphine but never evaluated as σ_1 receptor ligands.^{28a-d}

The final aim of our work is to understand how chirality may affect the σ_1 receptor-ligand interaction and activity, thus

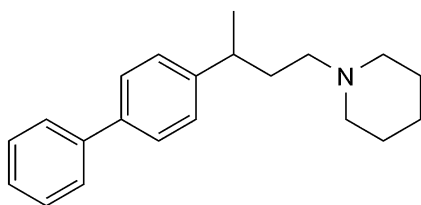


Fig. 1 (*R,S*)-**RC-33**.

Table 1 Alcoholic compounds structurally related to **RC-33**

Compound	Template	Ar	R ₁	R ₂	NR ₃ R ₄
(<i>R,S</i>)- 1 (<i>R</i>)- 1 (<i>S</i>)- 1	I	biphenyl-4yl	CH ₃	H	N(CH ₂) ₅
(<i>R,S</i>)- 2 (<i>R</i>)- 2 (<i>S</i>)- 2	I	naphth-2-yl	CH ₃	H	N(CH ₃) ₂
(<i>R,S</i>)- 3 (<i>R</i>)- 3 (<i>S</i>)- 3	I	6-methoxy-naphth-2-yl	CH ₃	H	N(CH ₃) ₂
(2 <i>R,S</i> ,3 <i>S/R</i>)- 4 (2 <i>R</i> ,3 <i>S</i>)- 4 (2 <i>S</i> ,3 <i>R</i>)- 4	II	naphth-2-yl	CH ₃	CH ₃	
(2 <i>R,S</i> ,3 <i>S/R</i>)- 5 (2 <i>R</i> ,3 <i>S</i>)- 5 (2 <i>S</i> ,3 <i>R</i>)- 5	II	6-methoxy-naphth-2-yl	CH ₃	CH ₃	

contributing a step forward in unveiling the sigma-enigma. Indeed, even although our knowledge of the sigma receptors has evolved over the past 20 years, several aspects in the sigma field still remain rather obscure.

Results and discussion

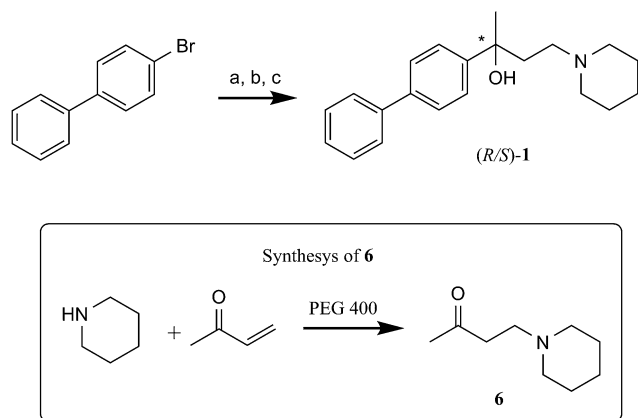
Compound selection

With the aim of evaluating the role of a hydrogen bond center as an additional pharmacophore element in the stereoselective interaction with the σ_1 receptor we designed compound **1**, featuring an alcoholic function on the alkyl spacer bridging the aromatic ring to the basic nitrogen atom, as an analogue of the arylalkylamino derivative **RC-33** (Table 1).

For the purpose of comparison and discussion, we selected other structurally related alcoholic compounds from our library of chiral molecules synthesized over the years. Among these, we chose molecules **2** and **3** (template **I**, Table 1) as structurally related to **1**, and the constrained arylpyrrolidinols **4** and **5** (template **II**, Table 1), being characterized by less conformational freedom.^{28a,c,d}

Synthesis, chiral resolution and configurational assignment

For the synthesis of (*R,S*)-**1** we planned to follow the methodology described in our previous work, with suitable modifications (Scheme 1).^{28a} We started our synthetic approach with the synthesis of 4-piperidinyl butan-2-one (**6**), obtained *via* Michael addition from a solution of piperidine and but-3-en-2-one in PEG 400 in good yield (62%). Concerning the synthesis of (*R,S*)-**1**, β -aminoketone **6** was added to the biphenyl anion, obtained



Scheme 1 Synthesis of *(R,S)*-1. Reagents and conditions: (a) *t*-BuLi, anhydrous Et₂O, -40 °C to rt; (b) 4-piperidinyl butan-2-one (**6**), -78 °C to 0 °C; (c) H₂O rt.

by halogen-metal exchange between the aromatic substrate and *tert*-butyllithium (*tert*-BuLi) in anhydrous ethyl ether (Et₂O) at -40 °C. After an acid-base work-up and purification by crystallization from methanol/water, *(R,S)*-1 was obtained as a white solid in good yield (68%). The final compound was characterized by ¹H-NMR.

In order to make *(R,S)*-1 suitable for biological assays, a small amount of this compound was obtained in its salt form as *(R,S)*-1·*dl*-tartrate.

Chiral resolution of *(R,S)*-1 was achieved using chiral high performance liquid chromatography (HPLC). To identify the

best experimental condition for the subsequent scaling-up, a standard screening protocol for cellulose and amylose derived chiral stationary phases (CSPs) was applied to the Chiralcel OJ-H (4.6 mm diameter × 150 mm length, 5 μm), Chiralpak AS-H (4.6 mm diameter × 250 mm length, 5 μm) and Chiralpak IC (4.6 mm diameter × 250 mm length, 5 μm) columns, whose chiral selectors are cellulose tris-(4-methylbenzoate) (Chiralcel OJ-H) and amylose tris [(*S*)- α -methylbenzylcarbamate] (Chiralpak AS-H) coated on a silica gel substrate and cellulose tris (3,5-dichlorophenylcarbamate) immobilized on silica gel (Chiralpak IC). Elution conditions adopted included mixtures of *n*-heptane and polar modifiers (EtOH or 2-propanol), alcohols (MeOH, EtOH, and 2-propanol), and acetonitrile; in all cases 0.1% of diethylamine was added to the mobile phase; in the analysis with Chiralpak IC 0.3% of trifluoroacetic acid was also added. The best result, in terms of enantioselectivity (α) and resolution factor (R_S), was obtained with Chiralcel OJ-H, eluting with MeOH/diethylamine (100/0.1, v/v), as clearly illustrated in Fig. 2 (t_{r1} = 6.99 min; t_{r2} = 9.59 min; α = 1.98; R_S = 6.93).

These experimental conditions are characterized by the most important prerequisites for an economic and productive enantiomeric separation on a semi-preparative scale, such as high solubility of racemate and enantiomers in the eluent solvent, shortest retention times, and the use of a mobile phase consisting of a pure low-cost solvent, which ultimately facilitates workup and re-use of the mobile phase. Therefore, the analytical method was suitably transferred to the semi-preparative scale employing a Chiralcel OJ-H column (10 mm × 250 mm, 5 μm). In 17 cycles, 51 mg of *(R,S)*-1 were processed, yielding 22.1 mg of the first eluted

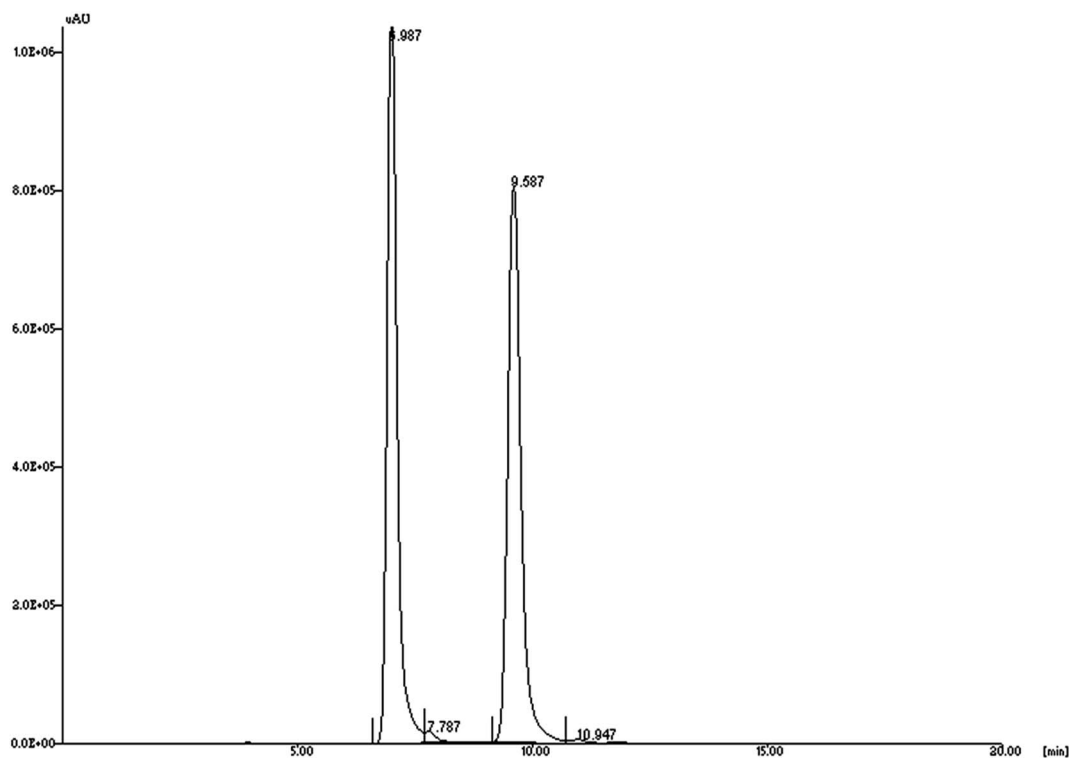


Fig. 2 Analytical separation of *(R,S)*-1. Chromatographic conditions: Chiralcel OJ-H (4.6 mm × 150 mm, 5 μm), MeOH/diethylamine 100/0.1 (v/v), flow rate: 0.5 mL min⁻¹, UV detector at 254 nm.

enantiomer and 23.2 mg of the second eluted one, characterized by $[\alpha]_D^{20}$ values of +24.1 and -24.2 , respectively (c: 0.5 in MeOH), along with 5.7 mg of an intermediate fraction as a mixture of the two enantiomers. Both enantiomers of **1** were obtained with a yield of about 87% and ee \geq 99.9%, as evidenced by analytical control of the collected fractions.

The configuration assignment study of the resolved enantiomers of compound **1** was then performed comparing the electronic circular dichroism (ECD) curves of (+)-**1** with that of (S)-(-)-**2**, whose absolute configuration was already assigned.^{28a} The ECD spectra (reported in the ESI†) of both (+)-**1** and (S)-(-)-**2** evidenced a similar profile in the range of wavelength between 200 and 300 nm. In detail, both compounds show a negative Cotton Effect (CE) at about 210 nm [(+)-**1**: λ_{\max} 206.5 nm, Mol. CD -6.61 ; (S)-(-)-**2**: λ_{\max} 209.0 nm, Mol. CD -6.21] and a positive CE in the range 220–260 nm [(+)-**1**: λ_{\max} 253.5 nm, Mol. CD $+2.60$; (S)-(-)-**2**: λ_{\max} 224.0 nm, Mol. CD $+16.80$]. Based on these considerations, the absolute configuration (S) was assigned to (+)-**1**. Both enantiomers of **1** were finally converted into the corresponding tartrates [(R)-**1**·l-tartrate and (S)-**1**·d-tartrate, respectively], suitable for biological investigation.

Molecular modeling studies

Molecular Dynamics (MD) simulations were carried out to predict binding mode, affinity, and eventual stereoselective binding features of the selected compounds towards the σ_1 receptors. To the purpose, both (R) and (S) enantiomers of compounds **1**–**5** were modeled and the relevant free energy of binding (ΔG_{bind}) with the protein was estimated *via* MM/PBSA calculations^{29a,b} using the optimized structure of the compounds in complex with our validated homology model of the σ_1 receptor.^{30a,b}

Taking compounds (R)-**1** and (S)-**1** as a proof-of-concept, the analysis of the corresponding MD trajectories revealed that four

major types of interactions are involved in the binding mode of both (R)-**1** and (S)-**1** to the σ_1 receptor, as shown in Fig. 3A and B: (i) a permanent salt bridge is detected between the $-\text{NH}^+$ moiety of the ligand piperidine ring and the COO^- group of Asp126; (ii) the side chains of Arg119 and Trp121 are engaged in stabilizing π interactions with the biphenyl group of the ligands; (iii) several further hydrophobic interactions concur to stabilize compound/receptor binding, mainly *via* the side chains of the σ_1 residues belonging to the hydrophobic pocket Ile128, Phe133, and Tyr173; and (iv) a hydrogen bond (HB) between the hydroxyl group of the compounds and the carboxylic chain of Glu172 conclusively anchors the ligand to the protein binding cavity.

The results of our modeling investigation predict that both enantiomers of **1** can be aptly accommodated within the σ_1 binding site and establish similar networks of stabilizing interactions with the receptor.

To quantify the overall effect of these interactions, binding free energy calculations were applied and, according to our simulations, both molecules are endowed with similar affinities towards the biological target, with a slight preference of the receptor for the (S) enantiomer, as $\Delta G_{\text{bind}} = -10.81 \pm 0.22$ kcal mol⁻¹ for (R)-**1** and $\Delta G_{\text{bind}} = -11.09 \pm 0.23$ kcal mol⁻¹ for (S)-**1**. The same trend was obtained for all other protein/ligand complexes considered, although compounds **2**–**5** showed lower affinities towards the σ_1 receptor with respect to the biphenyl derivatives, as seen from the ΔG_{bind} values listed in Table 2.

To investigate in detail the reason for this behavior, deconvolution of the enthalpic component (ΔH_{bind}) of the binding free energy into contributions from each protein residue was carried out. As shown in Fig. 4 for compounds (R)-**1** and (S)-**1**, the stable salt bridge involving Asp126 is responsible for comparable stabilizing contribution of -2.15 kcal mol⁻¹ and -2.19 kcal mol⁻¹, respectively (average dynamic length (ADL) = 4.11 ± 0.05 Å for (R)-**1** and ADL = 4.08 ± 0.06 Å for (S)-**1**).

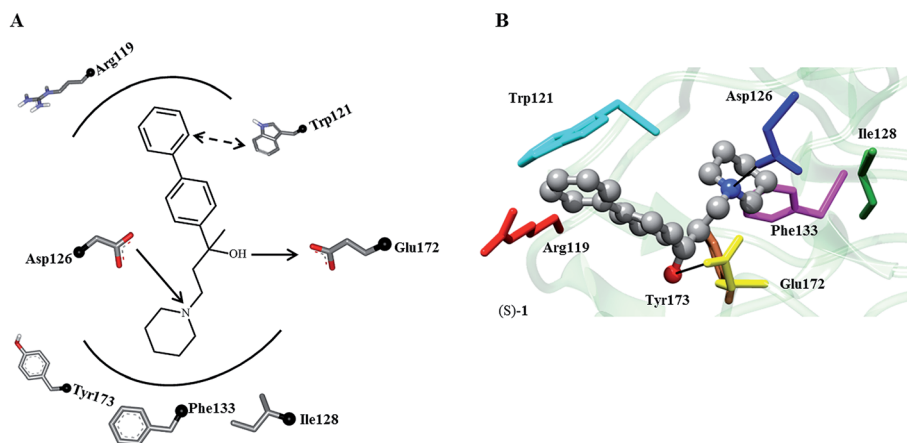


Fig. 3 (A) Two dimensional schematic representation of postulated interactions between the σ_1 receptor and **1**, established by direct affinity measurements. The lines/arrows indicate proposed key interaction between the receptor and its ligand. (B) Modeled complex of the σ_1 receptor with (S)-**1** showing the key interactions proposed in the topographical interaction model depicted in part A. The main protein residues involved in these interactions are Arg119 (red), Trp121 (cyan), Asp126 (blue), Ile128 (forest green), Glu172 (yellow), and Tyr173 (magenta). The ligand is portrayed in sticks and balls and colored by element, while the protein residues mainly involved in the interaction with (S)-**1** are highlighted as colored sticks and labeled. Salt bridge and H-bond interactions are shown as black lines. Water, ions, and counterions are not shown for clarity.

Table 2 Binding free energies ΔG_{bind} (kcal mol⁻¹) and $K_{\text{i}\sigma_1(\text{calcd})}$ values for the tested compounds in the complex with the σ_1 receptor. *The calculated $K_{\text{i}\sigma_1}$ values were estimated from the corresponding ΔG_{bind} values using the relationship $\Delta G_{\text{bind}} = -RT \ln(1/K_{\text{i}\sigma_1(\text{calcd})})$

Compounds	ΔH_{bind} kcal mol ⁻¹	$-T\Delta S$ kcal mol ⁻¹	ΔG_{bind} kcal mol ⁻¹	$K_{\text{i}\sigma_1(\text{calcd})}^*$
(<i>R</i>)-1	-23.89 ± 0.09	-13.08 ± 0.20	-10.81 ± 0.22	12 nM
(<i>S</i>)-1	-24.20 ± 0.08	-13.11 ± 0.22	-11.09 ± 0.23	7.5 nM
(<i>R</i>)-2	-22.55 ± 0.11	-12.83 ± 0.21	-9.72 ± 0.24	76 nM
(<i>S</i>)-2	-22.71 ± 0.12	-12.79 ± 0.20	-9.92 ± 0.23	54 nM
(<i>R</i>)-3	-22.51 ± 0.13	-12.81 ± 0.23	-9.70 ± 0.26	78 nM
(<i>S</i>)-3	-22.74 ± 0.10	-12.86 ± 0.19	-9.88 ± 0.21	57 nM
(2 <i>R</i> ,3 <i>S</i>)-4	-20.97 ± 0.08	-11.88 ± 0.22	-9.09 ± 0.23	219 nM
(2 <i>S</i> ,3 <i>R</i>)-4	-21.46 ± 0.09	-11.93 ± 0.24	-9.53 ± 0.26	104 nM
(2 <i>R</i> ,3 <i>S</i>)-5	-19.90 ± 0.10	-11.79 ± 0.21	-8.11 ± 0.23	1.1 μM
(2 <i>S</i> ,3 <i>R</i>)-5	-19.89 ± 0.12	-11.70 ± 0.18	-8.19 ± 0.22	998 nM

Furthermore, the substantial van der Waals and electrostatic interactions contributed, *via* the aforementioned π interaction, by Arg119 (-0.82 kcal mol⁻¹ for (*R*)-1 and -0.88 kcal mol⁻¹ for (*S*)-1) and Trp121 (-1.01 kcal mol⁻¹ for (*R*)-1 and -0.98 kcal mol⁻¹ for (*S*)-1), and by the residues belonging to the hydrophobic pocket Ile128, Phe133, and Tyr173 (with a clustered contribution of -3.08 kcal mol⁻¹ for (*R*)-1 and -3.04 kcal mol⁻¹ for (*S*)-1), also did not discriminate the affinity of the enantiomers for the receptor. In contrast, the stabilizing effects provided by the permanent hydrogen bond through interactions with Glu172 are dissimilar, as confirmed by the corresponding ADL (2.08 ± 0.06 Å for (*R*)-1 and 1.92 ± 0.04 Å for (*S*)-1, Fig. 4A) and, more importantly, the specific ΔH_{bind} values (-1.01 kcal mol⁻¹ for (*R*)-1 and -1.59 kcal mol⁻¹ for (*S*)-1, Fig. 4B). This structural and energetical evidence explains the slightly higher affinity of the enantiomer with (*S*) configuration toward the σ_1 receptor.

This per residue-based analysis allowed us to better understand and quantitatively explain the differences in affinity among all compounds of the series. As shown in Table 2, the derivatives 2 and 3 show a decrease in ΔG_{bind} of about 1 kcal mol⁻¹ compared to the best ligand 1. Based on the results of our computational approach both molecules are able to preserve all key interactions with the main σ_1 residues involved in the binding site (Fig. S3A and B†). Nevertheless, taking the (*S*) enantiomers as reference for our considerations, the

replacement of the piperidine portion of (*S*)-1 with a less bulky *N,N*-dimethyl group leads to a substantial reduction of the stabilizing contribution afforded by the σ_1 amino acids Ile128, Phe133, and Tyr172 which constitute the typical hydrophobic pocket of the σ_1 binding site (Fig. S4†). Actually, if the contribution of the other residues remained comparable to that of (*S*)-1, the clustered ΔH_{bind} of these three residues (-1.36 kcal mol⁻¹ for (*S*)-2 and -1.45 kcal mol⁻¹ for (*S*)-3, respectively) would become significantly lower in comparison with the value of the piperidine derivative (-3.04 kcal mol⁻¹).

Regarding the constrained derivatives (2*S*,3*R*)-4 and (2*S*,3*R*)-5, the increased structural rigidity leads to a different binding pose with respect to the compounds discussed above. As already shown in other studies on σ_1 ligands,^{25f,30} to comply with the pharmacophoric requirements upon target binding these molecules must adopt a reverse orientation into the hydrophobic binding pocket (Fig. S3C and D†). Therefore, the aryl-pyrrolidinol derivative (2*S*,3*R*)-4 exhibits a moderate binding affinity ($K_{\text{i}\sigma_1(\text{calcd})} = 104$ nM, Table 2) since its naphthyl moiety can still be encased in the binding pocket by establishing favorable interactions with the involved σ_1 residues. As a result of this binding pose, the interaction profile of Ile128, Phe133, and Tyr172 with (2*S*,3*R*)-4 is very similar to that of compound (*S*)-1 (Fig. S4†). However, the structure of this compound prevents it to establish other stabilizing interactions: indeed, we detected a drastic loss in the stabilization effect of the salt

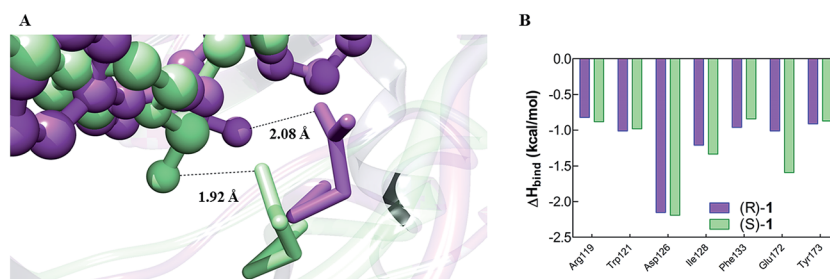


Fig. 4 (A) Comparison between the zoomed view of a MD representative snapshot of the hydrogen bond interaction between (*R*)-1 (purple) and (*S*)-1 (green) with the σ_1 receptor residue Glu172. The compounds are portrayed as ball-and-stick, while the amino acid is depicted as stick and colored accordingly. (B) Per residue energy decomposition for the σ_1 receptor in complex with (*R*)-1 (purple) and (*S*)-1 (green), showing those residues for which $|\Delta H_{\text{bind}}| > 0.60$ kcal mol⁻¹.

Table 3 Binding affinity of the compounds toward the σ_1 receptor. Values are means \pm SEM of three experiments

Compound	$K_{i\sigma_1}$ (nM) \pm SEM	$K_{i\sigma_2}$ (nM) \pm SEM
(<i>R,S</i>)-RC-33	0.9 \pm 0.3	103 \pm 10
(<i>R</i>)-RC-33	1.8 \pm 0.1	45 \pm 16
(<i>S</i>)-RC-33	1.9 \pm 0.2	98 \pm 64
(<i>R,S</i>)-1	6.57 \pm 0.2	34.6 \pm 47
(<i>R</i>)-1	39 \pm 8	4.3 μ M \pm 315
(<i>S</i>)-1	4.7 \pm 0.3	1.8 μ M \pm 288
(<i>R,S</i>)-2	77 \pm 23	66 \pm 13
(<i>R</i>)-2	205 \pm 60	651 \pm 67
(<i>S</i>)-2	63 \pm 39	75 \pm 5
(<i>R,S</i>)-3	41 \pm 11	97 \pm 18
(<i>R</i>)-3	51 \pm 14	133 \pm 63
(<i>S</i>)-3	25 \pm 4	1.1 μ M \pm 223
(2 <i>R,S</i> /3 <i>S,R</i>)-4	65 \pm 18	366 \pm 64
(2 <i>R</i> ,3 <i>S</i>)-4	86 \pm 16	94 \pm 23
(2 <i>S</i> ,3 <i>R</i>)-4	26 \pm 2	432 \pm 53
(2 <i>R,S</i> /3 <i>S,R</i>)-5	1.9 μ M \pm 304	1.5 μ M \pm 219
(2 <i>R,S</i>)-5	1.5 μ M \pm 226	1.2 μ M \pm 212
(2 <i>S</i> ,3 <i>R</i>)-5	1.2 μ M \pm 257	1.9 μ M \pm 293

bridge with Asp126 and of the hydrogen bond with Glu172 (Fig. S4†). In addition, the contribution of the π interaction with Arg119 and Trp121 was completely abolished (Fig. S3†). Finally, the 6-OCH₃ substituted compound (2*S*,3*R*)-5 ranks as the weakest σ_1 binder of the series, with an estimated affinity in the μ M range (Table 2). In fact, the steric hindrance of its methoxyl group prevents the molecule to penetrate deeply in the receptor binding pocket, (Fig. S3D†) with a consequent overall decrease of all binding stabilizing interactions (Fig. S4†).

Taken together, our *in silico* studies support our original hypothesis: actually, the presence of an extra pharmacophoric feature in compounds 1–5, missing in the original compound RC-

33, leads to an additional interaction of the ligands with the σ_1 receptor. Importantly, however, the presence of this feature does not afford a meaningful contribution in differentiating binding affinity of enantiomeric ligands. But, at the same time, it seems to be a potential key-requirement for the stereoselective compound interaction with the σ_1 receptor. In fact, notwithstanding the interaction spectra of (*R*)- and (*S*)-1 reported in Fig. 4B differ, both qualitatively and quantitatively, from those obtained for (*R*)- and (*S*)-RC-33,^{22e} the contribution afforded by each residue involved in ligand binding is somewhat lower in the case of 1 with respect to RC-33, ultimately resulting in an only slightly lower affinity of 1 for the receptor. Hence, the presence of the additional pharmacophore feature detected for the present series of compounds seems to play an orientational, rather than an energetic role, in the selectivity of σ_1 for their (*S*) enantiomers.

Pharmacological evaluation

The affinities of (*R,S*)-1–3, (2*R/S*,3*S/R*)-4–5, (*R*)-1–3, (2*R*,3*S*)-4–5, (*S*)-1–3, and (2*S*,3*R*)-4–5 towards the σ_1 and σ_2 receptors were experimentally determined in radioligand receptor binding studies.

In σ_1 receptor binding assay the test compounds compete with a potent and selective radioligand (*i.e.* [³H]-(+)-pentazocine) for the respective binding site. Nonspecific binding was recorded in the presence of cold non-radiolabeled (+)-pentazocine in large excess. Membrane preparations from guinea pig cerebral cortex homogenates served as the receptor source. In the σ_2 assay, membrane preparations of the rat liver served as the source for σ_2 receptors. The nonselective radioligand [³H]DTG was employed in the σ_2 assay because no σ_2 -selective radioligands are commercially available yet. To mask the σ_1 receptors, an excess of non-tritiated (+)-pentazocine was added to the assay solution, while a high concentration of non-tritiated DTG was used to determine nonspecific binding. In Table 3 the

Effect of (*R,S*)-1-DL tartrate and corresponding pure enantiomers on NGF-induced neurite outgrowth in PC12

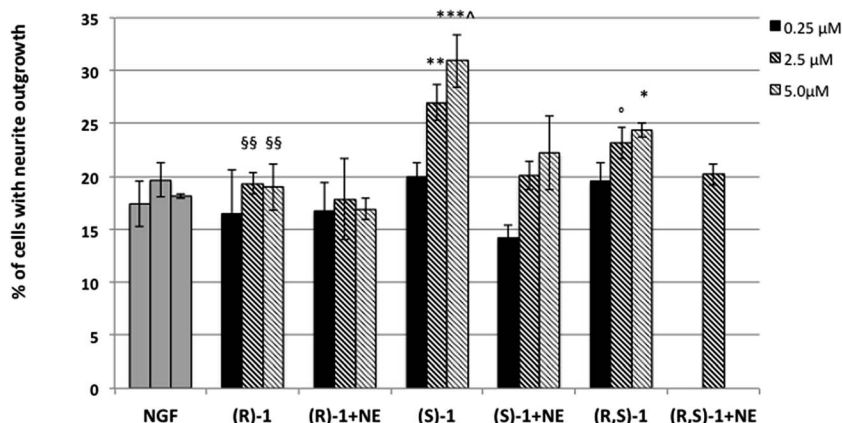


Fig. 5 Effect of σ_1 receptor ligands (*R,S*)-1-dl-tartrate and corresponding enantiomers on NGF-induced neurite outgrowth. Co-administration of NE-100 selective σ_1 receptor antagonist totally blocked the potentiating effect of (*R,S*)-1 and (*S*)-1 compounds. Histograms represent the mean \pm SEM of at least three different experiments performed in duplicate. *** = $p < 0.005$; ** = $p < 0.01$; * = $p < 0.05$; ° = $p = 0.05$ vs. NGF alone. ^ = $p < 0.01$ vs. (*R,S*)-1; §§ = $p < 0.01$ vs. (*S*)-1.

σ_1 and σ_2 receptor affinities of all tested compounds are summarized and compared with affinities of racemic and enantiomeric **RC-33**^{22c} as reference compounds. With the only exception of arylpyrrolidinol **5**, which is a weak σ_1 receptor binder, all compounds generally showed an interesting σ_1 affinity, in accordance with our *in silico* predictions (Table 2). Most importantly, the (*S*)-configured enantiomers at the stereogenic center directly linked to the aromatic moiety exhibit a preferential interaction with the target protein, thus suggesting that the interaction with the receptor is stereoselective. This is particularly evident for (*S*)-**1**, which shows a eudismic ratio of about 8 and represents the compound with both the highest affinity and selectivity toward σ_2 receptors among all molecules investigated ($K_1\sigma_1 = 4.7 \pm 0.3$ nM, $K_1\sigma_2/K_1\sigma_1 = 382$, Table 3).

Racemic and enantiomeric **1** were then selected for further investigation in our validated PC12 cell model of neuronal differentiation with the purpose of determining their agonistic/antagonistic profile and investigating the role of chirality and their effect on NGF-induced neurite outgrowth. The range of concentrations for racemic and enantiomeric **1** was chosen according to our previous assays^{22c} performed on **RC-33**. Both (*S*)-**1**·**d-tartrate** and (*R,S*)-**1**·**dl-tartrate** displayed a σ_1 agonistic profile, consistently and significantly potentiating NGF-induced neurite outgrowth at concentrations of 2.5 and 5 μ M ($p = 0.05$ and $p < 0.05$, respectively, *vs.* NGF alone for (*R,S*)-**1**; $p < 0.01$ and $p < 0.005$, respectively, *vs.* NGF alone for (*S*)-**1**, Fig. 5). Consistently, the effect of these compounds was totally blocked by co-administration of the selective σ_1 antagonist NE-100. In contrast, (*R*)-**1**·**l-tartrate** did not affect the percentage of cells with neurite outgrowth with respect to NGF alone (Fig. 5). Importantly, (*S*)-**1**·**dl-tartrate** was more effective than the corresponding racemate in promoting NGF induced neurite outgrowth ($p < 0.01$ *vs.* (*R,S*)-**1**, Fig. 5).

Taken together, these results show that (*S*)-**1**·**d-tartrate** is the eutomer. Indeed it enhances NGF-induced neurite outgrowth and its efficacy is greater than (*R,S*)-**1**·**dl-tartrate**, while (*R*)-**1**·**l-tartrate** is not effective in promoting NGF induced neurite outgrowth in PC12 cells at the same concentrations.

Conclusions

The stereoselectivity of the ligand binding to σ_1 receptor remains one of the obscure yet intriguing aspects of the activity of this enigmatic transmembrane protein. In this paper, to enrich our knowledge of the structural origins of the enantioselective interaction of σ_1 ligands we studied the enantiomeric compounds **1–5** structurally related to the potent σ_1 agonist **RC-33**. According to the latest and more specific σ_1 receptor 3D pharmacophore models and with respect to the reference ligand **RC-33** (for which the interaction with its target receptor is not dependent on the absolute configuration), compounds **1–5** present an additional pharmacophoric feature: a hydrogen bond center. Our *in silico* analysis of the binding modes and interactions between compounds **1–5** and the σ_1 receptor revealed that, for these molecules, four major intermolecular interactions are involved in stabilizing ligand binding within the receptor binding pocket. Among those, the extra hydrogen

bond interaction – missing in the **RC-33**/ σ_1 receptor complex – plays a role in mild enantiomeric binding discrimination. Interestingly, the mechanism of enantiomer recognition is typically described assuming that three³¹ or four³² key interactions are necessary to distinguish one enantiomer from the other. Thus, our results seem to be in line with this view. Accordingly, for all studied compounds, a weak (about two) to moderate (about eight) stereoselectivity in the interaction with the σ_1 receptor was observed and (*S*)-**1** was found to be the most active compound of the entire series ($K_1\sigma_1 = 4.7$ nM, eudismic ratio = 8). In summary, we showed that the σ_1 receptor exhibits enantioselectivity toward compounds characterized by (*S*)-configuration at the stereogenic center bearing the aromatic moiety only when the alcoholic group is present at the chiral center. Although a more robust and populated dataset of compounds is undoubtedly needed to verify our hypothesis, we postulate that a heterogroup at the chiral center is required for a σ_1 -ligand interaction to be stereoselective. An effort to corroborate this claim is ongoing in our laboratories.

Regarding the effect in promoting neurite outgrowth, the results of the functional assays related to **1** demonstrated that the chirality of the molecule affects the biological activity; indeed (*S*)-**1** enhances NGF-induced neurite outgrowth and, also, its efficacy is greater than (*R,S*)-**1**. Most importantly (*R*)-**1** is not effective in potentiating NGF-induced neurite outgrowth at the tested concentrations.

Altogether our observations provide further insights into the role of chirality in the σ_1 receptor–ligand interaction and represent a step-forward in future development of more specific and effective σ_1 agonists.

Author contribution

Simona Collina, Sabrina Priel and Daniela Curti conceived the work and contributed in reviewing the whole manuscript. S.C. was also responsible for the correctness of the whole studies. Daniela Rossi was responsible for the design of the experimental work and for data analysis of the whole study and wrote the manuscript. Annamaria Marra and Marta Rui performed the synthesis and chiral resolution of compounds (A.M. also contributed to the writing of the manuscript). Erik Laurini, Maurizio Fermeglia and Sabrina Priel were responsible for the *in silico* studies (E.L. also contributed the writing of molecular modeling section). Dirk Schepmann, Bernhard Wuensch Marco Peviani and Daniela Curti were responsible for biological investigations (D.S. and B.W.: binding assays; D.C. and M. P.: NGF-induced neurite outgrowth investigations) and contributed to the writing of the biological section.

Acknowledgements

D.R., S.C., M.P., and D.C. gratefully acknowledge financial support from ARISLA (Grant SaNet-ALS). E.L., M.F., and S.P. gratefully acknowledge financial support from ESTECO s.r.l. (Gran DDOS). Access to the CINECA supercomputing facility was granted through the sponsored Italian Super Computing

Resource Allocation (ISCRA), projects INSIDER and SIMBIOSY (to E.L. and S.P.).

References

- 1 W. R. Martin, C. E. Eades, J. A. Thompson, R. E. Huppler and P. E. Gilbert, *J. Pharmacol. Exp. Ther.*, 1976, **197**, 517–532.
- 2 W. D. Bowen, *Pharm. Acta Helv.*, 2000, **74**, 211–218.
- 3 S. B. Hellewell and W. D. Bowen, *Brain Res.*, 1990, **527**, 235–236.
- 4 Y. Itzhak and I. Stein, *Brain Res.*, 1991, **566**, 166–172.
- 5 R. Quirion, W. D. Bowen, Y. Itzhak, J. L. Junien, J. M. Mustacchio, R. B. Rothman, T. P. Su, S. W. Tam and D. P. Taylor, *Trends Pharmacol. Sci.*, 1992, **13**, 85–86.
- 6 S. McLean and E. Weber, *Neuroscience*, 1988, **25**, 259–269.
- 7 R. R. Matsumoto, M. K. Hemstreet, N. L. Lai, A. Thurkauf, B. R. De Costa, K. C. Rice, S. B. Helleweel, W. D. Bowen and J. M. Walker, *Pharmacol., Biochem. Behav.*, 1990, **36**, 151–155.
- 8 G. Alonso, V. L. Phan, I. Guillemain, M. Saunier, A. Legrand, M. Anoa and T. Maurice, *Neuroscience*, 2000, **97**, 155–170.
- 9 V. L. Phan, G. Alonso, F. Sandillon, A. Privat and T. Maurice, *Soc. Neurosci. Abstr.*, 2000, **26**, 2172.
- 10 S. Collina, R. Gaggeri, A. Marra, A. Bassi, S. Negrinotti, F. Negri and D. Rossi, *Expert Opin. Ther. Pat.*, 2013, **23**(5), 597–613.
- 11 T. Maurice and T. P. Su, *Pharmacol. Ther.*, 2009, **124**, 195–206.
- 12 S. K. Kulkarni and A. Dhir, *Expert Rev. Neurother.*, 2009, **9**, 1021–1034.
- 13 J. E. Bermack and G. J. Debonnel, *Pharmacol. Sci.*, 2005, **97**, 317–336.
- 14 S. H. Snyder and B. L. Largent, *J. Neuropsychiatry Clin. Neurosci.*, 1989, **1**(1), 7–15.
- 15 A. A. Luty, J. B. Kwok, C. Dobson-Stone, C. T. Loy, K. G. Coupland, H. Karlstrom, T. Sobow, J. Tchorzewska, A. Maruszak, M. Barcikowska, P. K. Panegyres, C. Zekanowski, W. S. Brooks, K. L. Williams, I. P. Blair, K. A. Mather, P. S. Sachdev, G. M. Halliday and P. R. Schofield, *Ann. Neurol.*, 2010, **68**, 639–649.
- 16 M. Peviani, E. Salvaneschi, L. Bontempi, A. Petese, A. Manzo, D. Rossi, M. Salmona, S. Collina, P. Bigini and D. Curti, *Neurobiol. Dis.*, 2014, **62**, 218–232.
- 17 T. Hayashi, R. Rizzuto, G. Hajnoczky and T. P. Su, *Trends Cell Biol.*, 2009, **19**, 81–88.
- 18 T. Hayashi, Z. Justinova, E. Hayashi, G. Cormaci, T. Mori, S. Y. Tsai, C. Barnes, S. R. Goldberg and T. P. Su, *J. Pharmacol. Exp. Ther.*, 2010, **332**, 1054–1063.
- 19 T. Hayashi and T. P. Su, *J. Pharmacol. Exp. Ther.*, 2003, **306**, 726–733.
- 20 T. Hayashi, S. Y. Tsai, T. Mori, M. Fujimoto and T. P. Su, *Expert Opin. Ther. Targets*, 2011, **15**, 557–577.
- 21 J. M. Walker, W. D. Bowen, F. O. Walker, R. R. Matsumoto, B. De Costa and K. C. Rice, *Pharmacol. Rev.*, 1990, **42**, 355–402.
- 22 (a) S. Collina, G. Loddo, M. Urbano, L. Linati, A. Callegari, F. Ortuso, S. Alcaro, C. Laggner, T. Langer, O. Prezzavento, G. Ronsisvalle and O. Azzolina, *Bioorg. Med. Chem.*, 2007, **15**, 771–783; (b) D. Rossi, M. Urbano, A. Pedrali, M. Serra, D. Zampieri, M. G. Mamolo, C. Laggner, C. Zanette, C. Florio, D. Shepmann, B. Wünsch, O. Azzolina and S. Collina, *Bioorg. Med. Chem.*, 2010, **18**, 1204–1212; (c) D. Rossi, A. Pedrali, M. Urbano, R. Gaggeri, M. Serra, L. Fernandez, M. Fernandez, J. Caballero, S. Rosinsvalle, O. Prezzavento, D. Shepmann, B. Wünsch, M. Peviani, D. Curti, O. Azzolina and S. Collina, *Bioorg. Med. Chem.*, 2011, **19**, 6210–6224; (d) D. Rossi, A. Marra, P. Picconi, M. Serra, L. Catenacci, M. Sorrenti, E. Laurini, M. Fermeglia, S. Pricl, S. Brambilla, N. Almirante, M. Peviani, D. Curti and S. Collina, *Bioorg. Med. Chem.*, 2013, **21**, 2577–2586; (e) D. Rossi, A. Pedrali, R. Gaggeri, A. Marra, L. Pignataro, E. Laurini, V. DalCol, M. Fermeglia, S. Pricl, D. Schepmann, B. Wünsch, M. Peviani, D. Curti and S. Collina, *ChemMedChem*, 2013, **8**, 1514–1527; (f) D. Rossi, A. Pedrali, A. Marra, L. Pignataro, D. Schepmann, B. Wünsch, L. Ye, K. Leuner, M. Peviani, D. Curti, O. Azzolina and S. Collina, *Chirality*, 2013, **25**, 814–822.
- 23 D. Zampieri, M. G. Mamolo, E. Laurini, C. Zanette, C. Florio, S. Collina, D. Rossi, O. Azzolina and L. Vio, *Eur. J. Med. Chem.*, 2009, **44**, 124–130.
- 24 T. Schläger, D. Shepmann, K. Lehmkuhl, J. Holenz, J. M. Vela, H. Buschmann and B. Wünsch, *J. Med. Chem.*, 2011, **54**(19), 6704–6713.
- 25 (a) R. A. Glennon, S. Y. Ablordeppey, A. M. Ismaiel, M. B. El-Ashmawy, J. B. Fischer and K. B. Howie, *J. Med. Chem.*, 1994, **37**, 1214–1219; (b) T. M. Gund, J. Floyd and D. J. Jung, *J. Mol. Graphics Modell.*, 2004, **22**, 221–230; (c) C. Laggner, C. Schieferer, B. Fiechtner, G. Poles, R. D. Hoffmann, H. Glossmann, T. Langer and F. F. Moebius, *J. Med. Chem.*, 2005, **48**, 4754–4764; (d) D. Zampieri, M. G. Mamolo, E. Laurini, C. Florio, C. Zanette, M. Fermeglia, P. Posocco, M. S. Paneni, S. Pricl and L. Vio, *J. Med. Chem.*, 2009, **52**, 5380–5393; (e) C. Oberdorf, T. J. Schmidt and B. Wünsch, *Eur. J. Med. Chem.*, 2010, **45**(7), 3116–3124; (f) C. Meyer, D. Schepmann, S. Yanagisawa, J. Yamaguchi, V. Dal Col, E. Laurini, K. Itami, S. Pricl and B. Wuensch, *J. Med. Chem.*, 2012, **55**, 8047–8065.
- 26 R. Kekuda, P. D. Prasad, J. Y. Fei, F. H. Leibach and V. Ganapathy, *Biochem. Biophys. Res. Commun.*, 1996, **229**, 553–558.
- 27 R. A. Glennon, *Mini-Rev. Med. Chem.*, 2005, **5**, 927–940.
- 28 (a) O. Azzolina, S. Collina, G. Brusotti, D. Rossi, A. Callegari, L. Linati, A. Barbieri and V. Ghislandi, *Tetrahedron: Asymmetry*, 2002, **13**, 1073–1081; (b) S. Collina, O. Azzolina, D. Vercesi, M. Sbacchi, M. A. Scheideler, A. Barbieri, E. Lanzac and V. Ghislandi, *Bioorg. Med. Chem.*, 2000, **8**, 1925–1930; (c) S. Collina, O. Azzolina, D. Vercesi, G. Brusotti, D. Rossi, A. Barbieri, E. Lanza, L. Mennuni, S. Alcaro, D. Battaglia, L. Linati and V. Ghislandi, *Il Farmaco*, 2003, **58**, 939–946; (d) S. Collina, D. Rossi, G. Loddo, A. Barbieri, E. Lanza, L. Linati, S. Alcaro, A. Gallelli and O. Azzolina, *Bioorg. Med. Chem.*, 2005, **13**, 3117–3126.

- 29 (a) J. Srinivasan, T. E. Cheatham, P. Cieplak, P. A. Kollman and D. A. Case, *J. Am. Chem. Soc.*, 1998, **120**, 9401–9409; (b) P. A. Kollman, I. Massova, C. Reyes, B. Kuhn, S. Huo, L. Chong, M. Lee, T. Lee, Y. Duan, W. Wang, O. Donini, P. Cieplak, J. Srinivasan, D. A. Case and T. E. Cheatham, *Acc. Chem. Res.*, 2000, **33**, 889–897.
- 30 (a) E. Laurini, V. Dal Col, M. G. Mamolo, D. Zampieri, P. Posocco, M. Fermeglia, V. Vio and S. Pricl, *ACS Med. Chem. Lett.*, 2011, **2**, 834–839; (b) E. Laurini, D. Marson, V. Dal Col, M. Fermeglia, M. G. Mamolo, D. Zampieri, L. Vio and S. Pricl, *Mol. Pharmaceutics*, 2012, **9**, 3107–3126.
- 31 D. W. Armstrong, T. J. Ward, R. D. Armstrong and T. E. Beesley, Separation of drug stereoisomers by the formation of beta-cyclodextrin inclusion complexes, *Science*, 1986, **232**(4754), 1132–1135.
- 32 A. D. Mesecar and D. E. Koshland Jr, A new model for protein stereospecificity, *Nature*, 2000, **403**(6770), 614–615.

Supporting Information

A step forward in the sigma enigma: a role for chirality in the sigma1 receptor-ligand interaction?

Daniela Rossi,¹ Annamaria Marra,¹ Marta Rui,¹ Erik Laurini,² Maurizio Fermeglia,² Sabrina Priel,^{2,3}
Dirk Schepmann,⁴ Bernhard Wuensch,⁴ Marco Peviani,⁵ Daniela Curti,⁵ Simona Collina ^{1*}

¹*Department of Drug Sciences, Medicinal Chemistry and Pharmaceutical Technology section, University of Pavia, Viale Taramelli 12, 27100 Pavia (Italy)*

² *MOSE – DEA- University of Trieste Via Valerio 10, 34127 Trieste (Italy)*

³ *National Interuniversity Consortium for Material Science and Technology (INSTM), Research Unit MOSE-DEA University of Trieste, Trieste, Italy*

⁴*Institute of Pharmaceutical and Medicinal Chemistry, University of Muenster, Correnstrasse 48, 48149 Muenster (Germany)*

⁵*Department of Biology and Biotechnology “L. Spallanzani”, **Laboratory** of Cellular and Molecular Neuropharmacology, University of Pavia, Via Ferrata 9, 27100 Pavia (Italy)*

Table of contents

1. Chemistry	S2
1.1 General	S2
1.2 Synthesis of (<i>R,S</i>)- 1	S2
2. Chiral Resolution of (<i>R,S</i>)- 1	S3
3. Electronic Circular Dichroism	S4
4. Molecular Modeling	S4
5. Biological Investigation	S6
5.1 Binding Assays	S6
5.2 NGF-induced neurite outgrowth in PC12 cells	S8
6. References	S9

1. Chemistry

1.1 General

All reagents and solvents were purchased from commercial suppliers and used without any further purification. All reactions involving air-sensitive reagents were performed under nitrogen atmosphere. Anhydrous solvents were obtained according to standard procedures. All solvents were evaporated under reduced pressure using a Heidolph Laborota 4000. Melting points were determined in open capillaries on SMP3 Stuart Scientific apparatus and are uncorrected. Proton nuclear magnetic resonance (NMR) spectra were recorded on a Bruker Avance 400 spectrometer operating at 400.13 MHz. Proton chemical shifts (δ) are reported in ppm with the solvent reference relative to tetramethylsilane (TMS) employed as the internal standard (CDCl_3 , $\delta = 7.26$ ppm; CD_2Cl_2 , $\delta = 5.32$ ppm; $[\text{D}_6]\text{acetone}$, $\delta = 2.05$ ppm). The following abbreviations are used to describe spin multiplicity: s = singlet, d = doublet, t = triplet, q = quartet, m = multiplet, br = broad signal, dd = doublet-doublet, td = triplet-doublet. Reaction courses were checked by thin layer chromatography (TLC) on silica gel (Fluka Kieselgel 60 F254, Merck) pre-coated glass-backed plates purchased from Fluka and the chromatograms were detected by UV radiations, potassium permanganate and acidic ammonium molybdate (IV). Intermediates and final compounds were purified by flash chromatography using Silica Gel 60 (particle size 230–400 mesh) purchased from Nova Chimica (Cinisello Balsamo, Italy).

Optical rotation values were measured on the Jasco photoelectric polarimeter DIP 1000 with a 1 dm cell at the sodium D line ($\lambda = 589$ nm); sample concentration values c are given in $\text{g } 10^{-2} \text{ mL}^{-1}$. Circular dichroism spectra were recorded on a Jasco J-710 dichrograph.

1.2 Synthesis of (R,S)-1

Synthesis of 4-Piperidin-1-yl-butan-2-one (6).

A solution of piperidine (0.1 mL, 1 mmol) and but-3-en-2-one (0.12 mL, 1.5 mmol) in PEG 400 (2.5 g) was stirred at rt for 35 min. Subsequently, 10% HCl was added to the mixture until pH 2 was reached and an acid-basic work-up was performed. Initially, the aqueous phase was washed with dichloromethane (CH_2Cl_2), then made alkaline with 1 N NaOH solution (pH 10) and extracted with CH_2Cl_2 . The combined organic layers were dried over anhydrous Na_2SO_4 and concentrated under reduced pressure affording the desired product as yellow oil (96 mg, 62%).

Synthesis of 2-([1,1'-biphenyl]-4-yl)-4-(piperidin-1-yl)butan-2-ol [(R,S)-1].

To a solution of 4-bromo-1,1'-biphenyl (12.5 mmol) in anhydrous diethyl ether (Et_2O , 50 mL), cooled to -40°C , *tert*-BuLi (25 mmol, 1.7 M in pentane) was added with stirring under nitrogen atmosphere (N_2), keeping the temperature for 20 min. The reaction mixture was then slowly

allowed to warm to room temperature. After 1 h stirring, a solution of 4-(piperidin-1-yl)butan-2-one (10 mmol) in dry Et₂O (15 mL) was added dropwise at -78°C. The reaction mixture was slowly allowed to warm to 0°C and stirring was continued for 3 h; then the reaction mixture was treated with water (30 mL). The aqueous phase was extracted with Et₂O and the combined organic phases were extracted with 5% DL-tartaric acid aqueous solution until pH 4. The acid aqueous layer was made alkaline with 1 N NaHCO₃ to pH 8, extracted with CH₂Cl₂ and concentrated in vacuum, yielding a white solid. The crude product was further purified by crystallization from methanol/water (8/2, v/v) and transformed into the salts **(R,S)-1·DL-tartrate** (molar ratio 1/1).

[(R,S)-1] 2-([1,1'-biphenyl]-4-yl)-4-(piperidin-1-yl)butan-2-ol: white solid (105 mg, 68%). Mp: 110 – 111°C. R_f: 0,46 (TLC: AcOEt/NH₃, 100/0,1, v/v); ¹H-NMR δ_H(400 MHz; DMSO) 1,40 (2H, bs, N(CH₂CH₂)CH₃), 1,44 (3H, s, CCH₃), 1,51 (4H, m, N(CH₂CH₂)₂CH₂), 1,98 (2H, m, CH₂CH₂N), 2,25 (4H, m, N(CH₂CH₂)₂CH₂), 2,41 (2H, m, ArCCH₂CH₂), 6,23 (1H, bs, OH), 7,38 (1H, m, aromatic), 7,54 (4H, m, aromatics), 7,69 (4H, m, aromatics).

2. Chiral Resolution of **(R,S)-1**

Analytical chiral resolution of **1** was performed via chiral high performance liquid chromatography (HPLC) using a Jasco (Cremella, LC, Italy) system equipped with a Jasco AS-2055 plus autosampler, a PU-2089 plus quaternary gradient pump, and a MD-2010 plus multiwavelength detector, and using the following columns: Chiralcel OJ-H (4.6 mm diameter x 150 mm length, 5µm), Chiralpak AS-H (4.6 mm diameter x 250 mm length, 5µm) and Chiralpak IC (4.6 mm diameter x 250 mm length, 5µm). Experimental data were acquired and processed by Jasco Borwin PDA and Borwin Chromatograph Software. Solvents used for enantioselective chromatography were HPLC grade and supplied by Carlo Erba (Milan, Italy). All HPLC analyses were performed at room temperature (rt). Sample solutions were prepared dissolving analyte in MeOH (c: 0.5 mg/mL) and filtering the solution through 0.45 µm PTFE membranes before analysis. The injection volume was 10 µL, the flow rate of 0.5 mL/min and the analysis were carried out by UV detector at 254 nm. The retention factor (*k*) was calculated using the equation $k = (t_R - t_0) / t_0$, where *t_R* is the retention time and *t₀* the dead time (*t₀* was considered to be equal to the peak of the solvent front and was taken from each particular run). The enantioselectivity (*α*) and the resolution factor (*R_s*) were calculated as follows: $\alpha = k_2 / k_1$ and $R_s = 2 (t_{R2} - t_{R1}) / (w_1 + w_2)$ where *t_{R2}* and *t_{R1}* are the retention times of the second and the first eluted enantiomers, and *w₁* and *w₂* are the corresponding base peak widths.

Pure enantiomers of **1** were obtained by a semi-preparative process using a Chiralcel OJ-H column (10 mm diameter \times 250 mm length, 5 μ m), eluting with MeOH/diethylamine 100/0.1 (v/v) at rt with a flow rate of 3 mL/min (UV detector: 254 nm). Sample solutions were prepared dissolving analyte in MeOH (c: 3 mg/mL), filtered through 0.45 μ m PTFE membranes before analysis, and the injection volume was 1 mL. The fractions were collected as reported in Figure S1. Analytical control of collected fractions was performed on Chiralcel OJ-H eluting with MeOH/diethylamine 100/0.1 (v/v), at a flow rate 0.5 mL/min, UV detector at 254 nm. The fractions obtained containing the enantiomers were evaporated at reduced pressure.

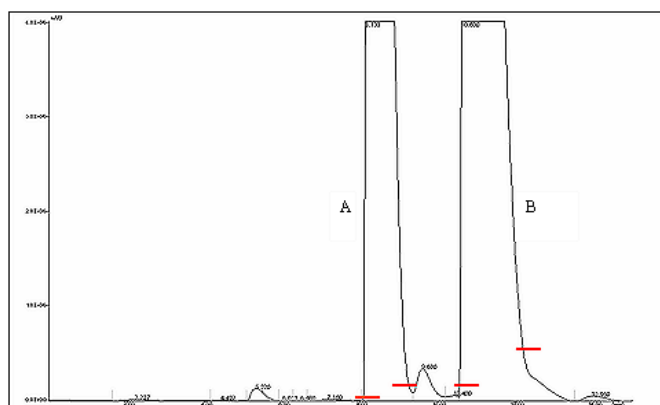


Fig. S1. Semi-preparative enantiomer separation of (*R,S*)-**1**. Chromatographic conditions: Chiralcel OJ-H (10 mm \times 250 mm, 5 μ m), MeOH/diethylamine 100/0.1 (v/v), flow rate: 3 mL/min, UV detector at 254 nm, injected amount 3 mg, cut points given by dashes (—).

3. Electronic Circular Dichroism

The solutions of (+)-**1** (c: 2.02×10^{-5} M in n-hexane, optical pathway 1 cm) and (-)-(*S*)-**2** (c: 2.5×10^{-5} M in n-hexane, optical pathway 1 cm) were analyzed in nitrogen atmosphere. ECD spectra were scanned at 50 nm/min with a spectral band width of 2 nm and data resolution of 0.5 nm (Fig.S2).

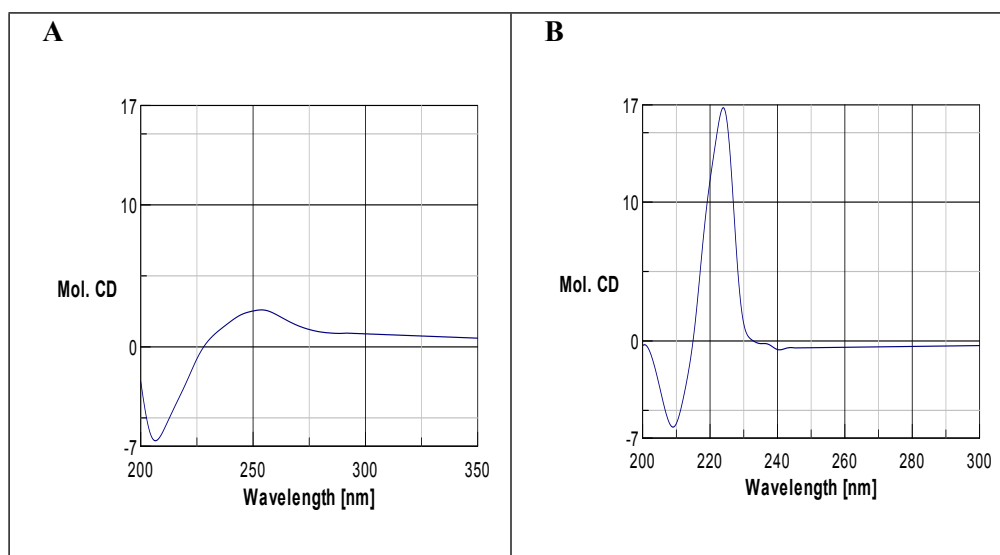


Fig. S2 CD curves of (+)-**1** (c: $2.02 \times 10^{-5} \text{M}$ in n-hexane) (A), and (-)-(*S*)-**2** (c: $2.5 \times 10^{-5} \text{M}$ in n-hexane) (B).

4. Molecular Modeling

The model structures of compounds **1-5** were sketched and geometrically optimized using Discovery Studio (DS, version 2.5, Accelrys, San Diego, CA). A conformational search was then carried out using a well-validated, ad hoc developed combined molecular mechanics/molecular dynamics simulated annealing (MDSA) protocol^{S1a-b, S2, S3a-b} using Amber 12^{S4} and the ff03 force field.^{S5} The optimized compound structures were then docked into the σ_1 putative binding pocket by applying a consolidated procedure performed with Autodock 4.3/Autodock Tools 1.4.6^{S6} on a win64 platform. For each compound only the molecular conformation satisfying the combined criteria of having the lowest (i.e., more favorable) Autodock energy and belonging to a highly populated cluster was selected to carry for further modeling.

Each ligand/receptor complex obtained from the docking procedure was further refined in Amber 12 using the quenched molecular dynamics (QMD) method. According to QMD, 1 ns MD simulations at 300 K were employed to sample the conformational space of each ligand/receptor complex in the GB/SA continuum solvation environment.^{S7a-b} The integration step was equal to 1 fs. After each picosecond, each system was cooled to 0 K, and the structure was extensively minimized and stored. To prevent global conformational changes of the protein, the backbone atoms of the protein binding site were constrained by a harmonic force constant of 100 kcal/Å, whereas the amino acid side chains and the ligands were allowed to move without any constraint. The best energy configuration of each complex resulting from the previous step was subsequently solvated by a cubic box of TIP3P^{S7} water molecules extending at least 10 Å in each direction from the solute. Each system was then neutralized and, furthermore, the solution ionic strength was adjusted to the physiological value of 0.15 M by adding the required amounts of Na⁺ and Cl⁻ ions. Each solvated system was relaxed by 500 steps of steepest descent followed by 500 other conjugate-gradient minimization steps and then gradually heated to a temperature of 300 K in intervals of 50 ps of NVT MD, using a Verlet integration time step of 1.0 fs. The Langevin thermostat was used to control temperature, with a collision frequency of 2.0 ps⁻¹. The SHAKE method^{S8} was used to constrain all of the covalently bound hydrogen atoms, while long-range nonbonded van der Waals interactions were truncated by using dual cutoffs 6 and 12 Å. The particle mesh Ewald (PME)^{S9} was applied to treat long-range electrostatic interactions. The protein was restrained with a force constant of 2.0 kcal/(mol Å), and all simulations were carried out with periodic boundary conditions.

The density of the system was subsequently equilibrated via MD runs in the isothermal – isobaric (NPT) ensemble (with isotropic position scaling and a pressure relaxation time of 1.0 ps), for 50 ps with a time step of 1 fs. Each system was further equilibrated using NPT MD runs at 300 K, with a pressure relaxation time of 2.0 ps. Five equilibration steps were performed, each 2 ns long and with a time step of 2.0 fs. To check the system stability, the fluctuations of the root-mean-square deviation (rmsd) of the simulated position of the backbone atoms of the σ_1 receptor with respect to those of the initial protein were monitored. All chemico-physical parameters and rmsd values showed very low fluctuations at the end of the equilibration process, indicating that the systems reached a true equilibrium condition.

The equilibration phase was followed by a data production run consisting of 20 ns of MD simulations in the canonical (NVT) ensemble. Only the last 10 ns of each equilibrated MD trajectory were considered for statistical data collections.

The binding free energy, ΔG_{bind} , between all ligands and the σ_1 receptor was estimated by resorting to the MM/PBSA approach. According to this well-validated methodology^{S3, S10a-b, S11a-e} the free energy was calculated for each molecular species (complex, receptor, and ligand), and the binding free energy was computed as the difference:

$$\Delta G_{\text{bind}} = G_{\text{complex}} - (G_{\text{receptor}} + G_{\text{ligand}}) = \Delta E_{\text{MM}} + \Delta G_{\text{sol}} - T\Delta S \quad (\text{Eq.1})$$

The molecular mechanics energy ΔE_{MM} was calculated as the sum of the van der Waals and electrostatic interactions:

$$\Delta E_{\text{MM}} = \Delta E_{\text{VDW}} + \Delta E_{\text{ELE}} \quad (\text{Eq.2})$$

The solvation free energy term ΔG_{sol} was composed of the polar and nonpolar contributions:

$$\Delta G_{\text{sol}} = \Delta G_{\text{PB}} + \Delta G_{\text{NP}} \quad (\text{Eq.3})$$

ΔG_{PB} was estimated using DelPhi,^{S12} which solves the Poisson–Boltzmann equations numerically and calculates the electrostatic energy according to the electrostatic potential. Dielectric constants of 1 and 80 were used for solute and solvent, respectively. A grid spacing of 0.5 per angstrom, extending 20% beyond the dimensions of the solute, was employed in these calculations.

The nonpolar solvation contribution was determined using the following relationship:^{S13}

$$\Delta G_{\text{NP}} = \gamma \times SA + \beta \quad (\text{Eq.4})$$

in which $\gamma = 0.00542 \text{ kcal}/(\text{mol } \text{\AA}^2)$, $\beta = 0.92 \text{ kcal}/\text{mol}$, and SA is the molecular surface area estimated by means of the MSMS software.^{S14}

The conformational entropy (translation, rotation, and vibration) upon ligand binding ($-T\Delta S$ in Eq. (1)) was estimated using normal-mode analysis^{S15} with the Nmode module of Amber 12. Prior to normal-mode calculations, each MD snapshot of each receptor/ligand complex was energy minimized using a distance-dependent

dielectric constant $\epsilon = 4r_{ij}$ until the root-mean-square of the elements of the gradient vector was less than 10^{-4} kcal/mol Å. To minimize the effects due to different conformations adopted by individual snapshots, and due to the high computational demand of this approach, we averaged the estimation of entropy over MD 100 snapshots for each molecular complex that were evenly extracted from the last 10 ns of each corresponding MD trajectory.

The per residue binding free energy decomposition was performed exploiting the MD trajectory of each given compound/receptor complex, with the aim of identifying the key residues involved in the ligand-receptor interaction. This analysis was carried out using the MM/GBSA approach^{S16} and was based on the same snapshots used in the binding free energy calculation.

All simulations were carried out using the Sander and Pmemd modules of Amber 12, running on the EURORA-CPU/GPU calculation cluster of the CINECA supercomputer facility (Bologna, Italy). The entire MD simulation and data analysis procedure was optimized by integrating Amber 12 in modeFRONTIER, a multidisciplinary and multiobjective optimization and design environment.^{S17}

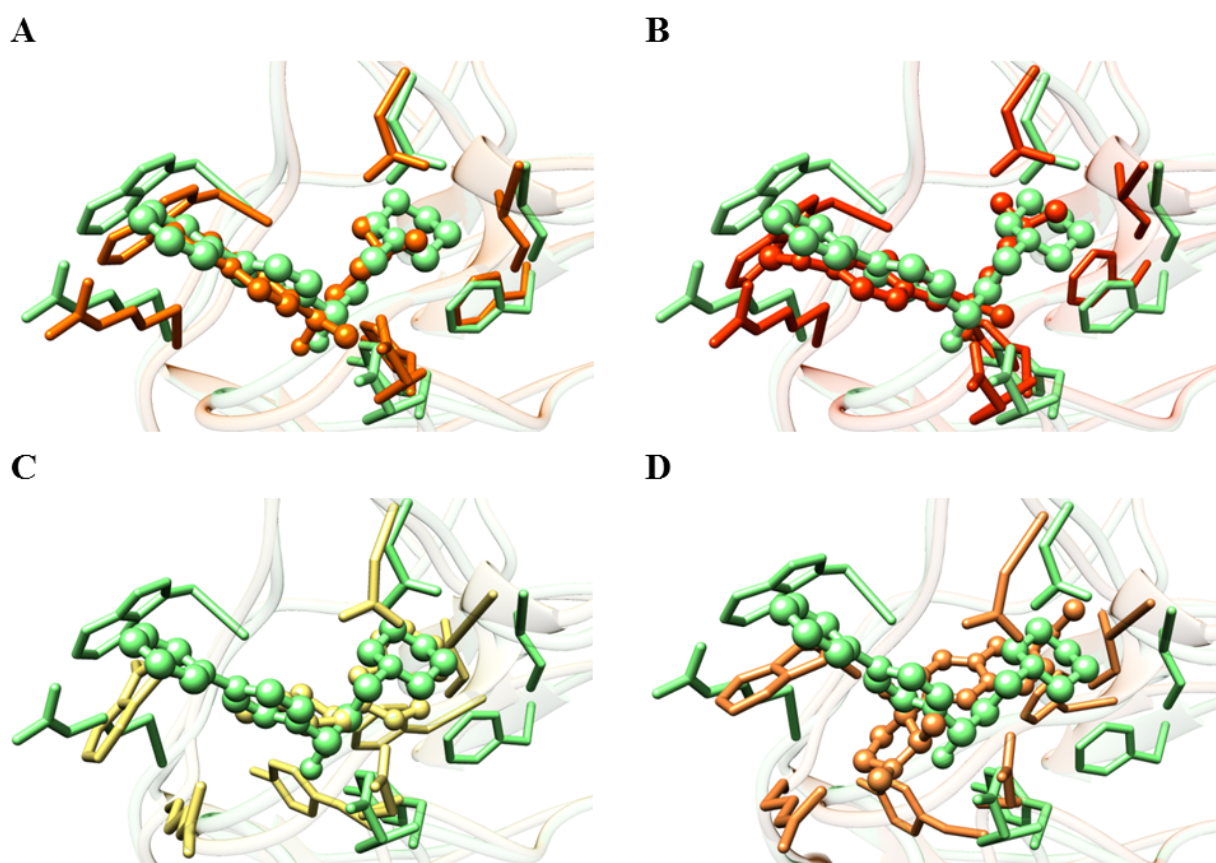


Fig. S3. Superposition of equilibrated MD snapshots of the s_1 receptor in complex with (S)-1 (green) in comparison with (S)-2 (A, orange), (S)-3 (B, orange red), (2S,3R)-4 (C, khaki) and (2S,3R)-5 (D, sandy brown). Hydrogen atoms, water molecules, ions and counterions are omitted for clarity.

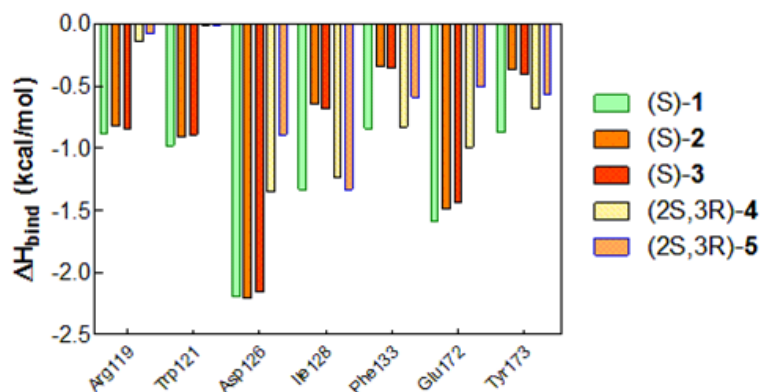


Fig. S4. Per residue energy decomposition for σ_1 receptor in complex with (S)-1 (green), (S)-2 (orange), (S)-3 (orange red), (2S,3R)-4 (khaki) and (2S,3R)-5 (sandy brown) showing those residues involved in key binding interactions.

5. Biological investigation

5.1 Binding Assays

Materials: Guinea pig brains for the σ_1 receptor binding assays were commercially available (Harlan–Winkelmann, Borcheln, Germany). Homogenizer: Elvehjem Potter (B. Braun Biotech International, Melsungen, Germany) and Soniprep 150, MSE, London, UK). Centrifuges: Cooling centrifuge model Rotina 35R (Hettich, Tuttlingen, Germany) and High-speed cooling centrifuge model Sorvall RC-5C plus (Thermo Fisher Scientific, Langenselbold, Germany). Multiplates: standard 96-well multiplates (Diagonal, Muenster, Germany). Shaker: self-made device with adjustable temperature and tumbling speed (scientific workshop of the institute). Vortexer: Vortex Genie 2 (Thermo Fisher Scientific, Langenselbold, Germany). Harvester: MicroBeta FilterMate-96 Harvester. Filter: Printed Filtermat Type A and B. Scintillator: Meltilex (Type A or B) solid-state scintillator. Scintillation analyzer: MicroBeta Trilux (all PerkinElmer LAS, Rodgau-Jügesheim, Germany). Chemicals and reagents were purchased from various commercial sources and were of analytical grade.

Preparation of membrane homogenates from rat liver : Two rat livers (Sprague–Dawley rats) were cut into small pieces and homogenized with the potter (500–800 rpm, 10 up-and-down strokes) in six volumes of cold 0.32m sucrose. The suspension was centrifuged at 1200 g for 10 min at 4 °C. The supernatant was separated and centrifuged at 31 000 g for 20 min at 4 °C. The pellet was re-suspended in 5–6 volumes of buffer (50 mm Tris, pH 8.0) and incubated at RT for 30 min. After incubation, the suspension was centrifuged again at 31000 g for 20 min at 4 °C. The final pellet was re-suspended in 5–6 volumes of buffer and stored at - 80 °C in 1.5 mL portions containing ~2 (mg protein)mL⁻¹

Preparation of membrane homogenates from guinea pig brain cortex: Five guinea pig brains were homogenized with the potter (500–800 rpm, 10 up-and-down strokes) in six volumes of cold 0.32M sucrose. The suspension was centrifuged at 1200 g for 10 min at 4°C. The supernatant was separated and centrifuged at 23500 g for 20 min at 4°C. The pellet was re-suspended in 5–6 volumes of buffer (50 mM Tris, pH 7.4) and centrifuged again at 23500 g (20 min, 4 °C). This procedure was repeated twice. The final pellet was resuspended in 5–6 volumes of buffer and frozen (-80°C) in 1.5 mL portions containing ~1.5 (mg protein)mL⁻¹.

Protein determination: The protein concentration was determined by the method of Bradford^{S18} modified by Stoscheck.^{S19} The Bradford solution was prepared by dissolving 5 mg of Coomassie Brilliant Blue G 250 in 2.5 mL EtOH (95% v/v). Deionized H₂O (10 mL) and phosphoric acid (85% w/v, 5 mL) were added to this solution, and the mixture was stirred and filled to a total volume of 50 mL with deionized water. Calibration was carried out using bovine serum albumin as a standard in nine concentrations (0.1, 0.2, 0.4, 0.6, 0.8, 1.0, 1.5, 2.0, and 4.0 mg mL⁻¹). In a 96-well standard multiplate, 10 mL of the calibration solution or 10 mL of the membrane receptor preparation were mixed with 190 mL of the Bradford solution. After 5 min, the UV absorption of the protein–dye complex at $\lambda=595$ nm was measured with a plate reader (Tecan Genios, Tecan, Crailsheim, Germany).

General protocol for binding assays: The test compound solutions were prepared by dissolving ~10 mmol (usually 2–4 mg) of test compound in DMSO so that a 10 μ M stock solution was obtained. To obtain the required test solutions for the assay, the DMSO stock solution was diluted with the respective assay buffer. The filtermats were presoaked in 0.5% aqueous polyethylenimine solution for 2 h at RT before use. All binding experiments were carried out in duplicate in 96-well multiplates. The concentrations given are the final concentrations in the assay. Generally, the assays were performed by addition of 50 μ L of the respective assay buffer, 50 μ L test compound solution at various concentrations (10^{-5} , 10^{-6} , 10^{-7} , 10^{-8} , 10^{-9} and 10^{-10} M), 50 μ L of corresponding radioligand solution, and 50 μ L of the respective receptor preparation into each well of the multiplate (total volume 200 μ L). The receptor preparation was always added last. During the incubation, the multiplates were shaken at a speed of 500–600 rpm at the specified temperature. Unless otherwise noted, the assays were terminated after 120 min by rapid filtration using the harvester. During the filtration each well was washed five times with 300 mL of water. Subsequently, the filtermats were dried at 95°C. The solid scintillator was melted on the dried filtermats at 95°C for 5 min. After solidifying of the scintillator at RT, the trapped radioactivity in the filtermats was measured with the scintillation analyzer. Each position on the filtermat corresponding to one well of the multiplate was measured for 5 min with the [³H]-counting

protocol. The overall counting efficiency was 20%. The IC₅₀ values were calculated with GraphPad Prism 3.0 (GraphPad Software, San Diego, CA, USA) by nonlinear regression analysis. The IC₅₀ values were subsequently transformed into K_i values using the equation of Cheng and Prusoff.^{S20} The K_i values are given as mean value ±SEM from three independent experiments.

σ₁ receptor binding assay: The assay was performed with the radioligand [³H](+)-pentazocine (22.0 Ci mmol⁻¹; PerkinElmer). The thawed membrane preparation of guinea pig brain cortex (~100 mg protein) was incubated with various concentrations of test compounds, 2 nM [³H](+)-pentazocine, and Tris buffer (50 mM, pH 7.4) at 37°C. The nonspecific binding was determined with 10 mM unlabeled (+)-pentazocine. The K_d value of (+)-pentazocine is 2.9 nM.

σ₁ receptor binding assay: The assays were performed with the radioligand [³H]DTG (specific activity 50 Ci mmol⁻¹; ARC, St. Louis, MO, USA). The thawed membrane preparation of rat liver (~100 mg protein) was incubated with various concentrations of the test compound, 3 nM [³H]DTG, and buffer containing (+)-pentazocine (500 nM (+)-pentazocine in 50 mM Tris, pH 8.0) at RT. The non-specific binding was determined with 10 mM unlabeled DTG. The K_d value of [³H]DTG is 17.9 nM.

5.2 NGF-induced neurite outgrowth in PC12 cells.

Cell culture: PC12 cells were cultured at 37°C, under 5% CO₂ in RPMI 1640 medium supplemented with 5% heat-inactivated fetal bovine serum (FBS), 10% heat-inactivated horse serum (HS), 1% Glutamax, 1% Zell (Biochrom). The medium was changed two or three times a week. When NGF with or without the test compounds had to be added, cells were detached from the culture dishes, centrifuged at 150 g for 5 min, re-suspended in RPMI 1640 medium containing 0.5% HS, 1% Glutamax, 1% Zell and plated at 8000 cells mL⁻¹ in 24-well tissue culture plates coated with poly-D-lysine; 24 h after plating, the medium was replaced and NGF (2.5 ng mL⁻¹) was added with or without drugs. Stock solutions (10 mM) of compounds (*R,S*)-1·DL-tartrate, (*R*)-1·L-tartrate and (*S*)-1·D-tartrate were dissolved with apyrogenic H₂O to 1 mM solution and added to the cell medium to reach the selected final concentrations (0.25 μM, 2.5 μM, 5 μM). In some experiments, the well-characterized σ₁ receptor antagonist NE-100 was co-administered with (*R,S*)-1·DL-tartrate, (*R*)-1·L-tartrate or (*S*)-1·D-tartrate at a final concentration of 3 μM.

Quantification of neurite outgrowth: five days after incubation with NGF (2.5 ng mL⁻¹) with or without drugs, PC12 cells were fixed at RT for 30 min in phosphate-buffered saline (PBS) containing 4% (w/v) paraformaldehyde. Morphometric analysis was performed on digitized images of fixed cells taken under phase-contrast illumination with a microscope (Optika) linked to a digital camera. Images of at least six fields per well were taken at 20 x magnification in order to count an

average of 300 cells. At least three independent experiments were performed for each condition, using different batches of PC12 cells. Neurite outgrowth was scored by measuring the percentage of differentiated cells bearing at least one neurite longer than the cell body diameter. Cell counting and neurite length measurements were performed in a blind manner by two independent observers using NeuronJ plugin^{S21} of ImageJ public domain software.

Statistical analysis: Data are expressed as the mean \pm standard error of the mean (SEM). Statistical analysis was performed by two-way analysis of variance (ANOVA) followed by post hoc Bonferroni-Dunnett's test. Values of $p < 0.05$ were considered statistically significant.

6. References

- (S1) (a) D. Rossi, A. Marra, P. Picconi, M. Serra, L. Catenacci, M. Sorrenti, E. Laurini, M. Fermeglia, S. Pricl, S. Brambilla, N. Almirante, M. Peviani, D. Curti, S. Collina, *Bioorg. Med. Chem.*, 2013, **21**, 2577-2586; (b) D. Rossi, A. Pedrali, R. Gaggeri, A. Marra, L. Pignataro, E. Laurini, V. DalCol, M. Fermeglia, S. Pricl, D. Schepmann, B. Wünsch, M. Peviani, D. Curti, S. Collina, *Chem. Med. Chem.*, 2013, **8**, 1514-1527.
- (S2) C. Meyer, D. Schepmann, S. Yanagisawa, J. Yamaguchi, V. Dal Col, E. Laurini, K. Itami, S. Pricl, B. Wuensch, *J. Med. Chem.*, 2012, **55**, 8047-8065.
- (S3) (a) J. Srinivasan, T.E. Cheatham, P. Cieplak, P.A. Kollman, D.A. Case, *J Am Chem Soc.*, 1998; **120**, 9401-9409. (b) P.A. Kollman, I. Massova, C. Reyes, B. Kuhn, S. Huo, L. Chong, M. Lee, T. Lee, Y. Duan, W. Wang, O. Donini, P. Cieplak, J. Srinivasan, D.A. Case, T.E. Cheatham, *Acc Chem Res.*, 2000, **33**, 889-897.
- (S4) Case, D. A. et al. AMBER 12; University of California: San Francisco, CA, 2012.
- (S5) Duan, Y. et al. *J. Comput. Chem.*, 2003, **24**, 1999-2012.
- (S6) Morris, G. M.; Huey, R.; Lindstrom, W.; Sanner, M. F.; Belew, R. K.;Goodsell, D. S.; Olson, A. J. *J Comput Chem.*, 2009, **30**, 2785-2791.
- (S7) (a) Onufriev, A.; Bashford, D.; Case, D.A. *J. Phys. Chem. B*, 2000, **104**, 3712-3720. (b) Feig, M.; Onufriev, A.; Lee, M. S.; Im, W.; Case, D. A.; Brooks III, C. L. *J. Comput. Chem.*, 2004, **25**, 265-284.
- (S8) Jorgensen, W. L.; Chandrasekhar, J.; Madura, J. D.; Impey, R. W.; Klein, M. L. *J. Chem. Phys.*, 1983, **79**, 926-935.
- (S9) Ryckaert, J.-P.; Ciccotti, G.; Berendsen, H. J. C. *J. Comput. Phys.*, 1977, **23**, 327-341.
- (S10) (a) Laurini, E.; Dal Col, V.; Mamolo, M. G.; Zampieri, D.; Posocco, P.; Fermeglia, M.; Vio, V.; Pricl, S. *ACS Med. Chem. Lett.*, 2011, **2**, 834-839. (b) Laurini, E.; Marson, D.; Dal

Col, V.; Fermeglia, M.; Mamolo, M. G.; Zampieri, D.; Vio, L.; Pricl, S. *Mol. Pharmaceutics*, 2012, **9**, 3107-3126.

- (S11) For a list of recent, successful applications of the MM/PBSA methodology in related topics from our group see, for instance: (a) D.L. Gibbons, S. Pricl, P. Posocco, E. Laurini, M. Fermeglia, H. Sun, M. Talpaz, N. Donato, A. Quintás-Cardama, *Proc Natl Acad Sci U S A*, 2014, **111**, 3550-3555. (b) Bozzi, F.; E. Conca, E. Laurini, P. Posocco, A. Lo Sardo, G. Jocollè, R. Sanfilippo, A. Gronchi, F. Perrone, E. Tamborini, G. Pelosi, M.A. Pierotti, R. Maestro, S. Pricl, S. Pilotti, *Lab Invest.*, 2013, **93**, 1232-1240. (c) E. Laurini, P. Posocco, M. Fermeglia, D.L. Gibbons, A. Quintás-Cardama, S. Pricl, *Mol Oncol.*, 2013, **7**, 968-975. (d) E. Conca, C. Miranda, V. Dal Col, E. Fumagalli, G. Pelosi, M. Mazzoni, M. Fermeglia, E. Laurini, M.A. Pierotti, S. Pilotti, A. Greco, S. Pricl, E. Tamborini, *Mol Oncol.*, 2013, **7**, 756-762. (e) P. Dileo, S. Pricl, E. Tamborini, T. Negri, S. Stacchiotti, A. Gronchi, P. Posocco, E. Laurini, P. Coco, E. Fumagalli, P.G. Casali, S. Pilotti, *Int J Cancer* , 2011, **128**, 983-990.
- (S12) M. Gilson, K.A. Sharp, B. Honig, *J. Comput. Chem.*, 1987, **9**, 327-335.
- (S13) D. Sitkoff, K. A. Sharp, B. Honig, *J. Phys. Chem.*, 1994, **98**, 1978-1988.
- (S14) M. F. Sanner, A.J. Olson, J.C. Spehner, *Biopolymers*, 1996, **38**, 305-320.
- (S15) E.B. Wilson, J.C. Decius, P.C. Cross, *Molecular Vibrations*, New York, NY: McGraw-Hill; 1995.
- (S16) A. Onufriev, D. Bashford, D.A. Case, *J. Phys. Chem. B*, 2000, **104**, 3712-3720. (b) M. Feig, A. Onufriev, M.S. Lee, W. Im, D.A. Case, C.L. Brooks, *J. Comput. Chem.*, 2004, **25**, 265-284.
- (S17) www.esteco.com/home/mode_frontier/mode_frontier.html
- (S18) M.M. Bradford, *Anal. Biochem.*, 1976, **72**, 248 –254.
- (S19) C.M. Stoscheck, *Methods Enzymol.*, 1990, **182**, 50–68.
- (S20) Y. Cheng, W.H. Prusoff, *Biochem. Pharmacol.*, 1973, **22**, 3099 – 3108.
- (S21) E. Meijering, M. Jacob, J.C.F. Sarria, P. Steiner, H. Hirling, M. Unser, *Cytometry Part A*, 2004, **58A**, 167 –176.



“Fit-for-purpose” development of analytical and (semi)preparative enantioselective high performance liquid and supercritical fluid chromatography for the access to a novel σ_1 receptor agonist

Daniela Rossi^{a,1}, Annamaria Marra^{b,1}, Marta Rui^a, Stefania Brambilla^b, Markus Juza^{c,*}, Simona Collina^{a,**}

^a Department of Drug Sciences, Medicinal Chemistry and Pharmaceutical Technology Section, University of Pavia, Viale Taramelli 12, 27100 Pavia, Italy

^b NicOx Research Institute, Via Ariosto 21, 20091 Bresso (MI), Italy

^c Corden Pharma Switzerland LLC, Eichenweg 1, 4410 Liestal, Switzerland

ARTICLE INFO

Article history:

Received 29 July 2015

Received in revised form 30 October 2015

Accepted 31 October 2015

Available online 4 November 2015

Keywords:

Amylose and cellulose derived CSPs

Chiral resolution

Elution order

Enantioselective HPLC and SFC

Sigma 1 (σ_1) receptor agonist

ABSTRACT

A rapid and straightforward screening protocol of chiral stationary phases (CSPs) in HPLC and SFC resulted in three different methods “fit-for-purpose”, i.e. analysis and scale-up to semi-preparative enantioselective chromatography. The efficient use of these three methods allowed expedited preparation of an important drug discovery target, (*R/S*)-**1**, a potent new sigma 1 (σ_1) receptor agonist. The approach taken resulted in significant savings of both time and labor for the isolation of enantiomers compared to the development of a stereo-selective synthesis.

The enantiomers of **1** have been isolated allowing studies of their chiroptical properties and an in-deep comparative examination of the pharmacological profile for the individual enantiomers.

© 2015 Elsevier B.V. All rights reserved.

1. Introduction

The sigma 1 receptor (σ_1R) has been intensively studied in an attempt to investigate its role as a therapeutic target in several pathologies [1], including neurodegenerative diseases, such as Parkinson's, Alzheimer's and amyotrophic lateral sclerosis [2], mood disorders [3,4] and pain [5]. In the last decade, our group designed and synthesized a large number of σ_1R ligands [6–8]. Among these, (*R/S*)-2-(4-phenylphenyl)-4-(1-piperidyl)butan-2-ol, (*R/S*)-**1** (Table 1) was recently identified as a potent σ_1R agonist [9]. Given that the stereoselectivity of the ligand binding to σ_1R remains one of the obscure, yet intriguing aspects of the activity of this protein, (*R*)- and (*S*)-**1** were prepared in amount suitable for evaluating their interaction with the biological target and their effect in promoting neurite outgrowth. As a result, (*S*)-**1** was found to be the best σ_1R ligand ($K_i\sigma_1 = 4.7$ nM, eudismic ratio = 8) and the only enantiomer effective in enhancing NGF-induced neurite outgrowth at the tested concentrations [9]. Unfortunately, during this

study both enantiomers of **1** were obtained in minute amounts, only sufficient to support a preliminary in vitro biological investigation.

The work here presented is as a part of our ongoing efforts focused on the development of rapid and easy to use methods suitable for obtaining a quick access to the enantiomers of medicinal chemistry interest with high enantiomeric excess and amounts sufficient for biological investigations [10]. In the light of the above considerations, the aim of the present work was to develop a productive and robust system “fit-for-purpose” [11] suitable for isolating pure enantiomers of **1** in amounts sufficient to support an exhaustive biological investigation. It should be stressed that in medicinal chemistry and early phases of drug development high throughput of candidates rather than sophisticated analytical methods suitable for validation or fully optimized separations dedicated to production under GMP are the main focus. Therefore, a general applicable set of experimental conditions was developed and tested employing racemic **1**, for which neither a stereoselective synthesis, nor any other method for isolating the enantiomers had been described before.

Among the different approaches for the preparation of enantiopure compounds, (semi)-preparative enantioselective high performance liquid chromatography (HPLC) and (semi)-preparative enantioselective supercritical fluid chromatography using chiral stationary phases (CSPs) have been successfully employed for the

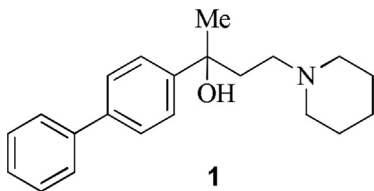
* Corresponding author.

** Corresponding author. Fax: +39 0382422975.

E-mail addresses: Markus.Juza@cordenpharma.com, maju24@sunrise.ch (M. Juza), simona.collina@unipv.it (S. Collina).

¹ These authors contributed equally to this work.

Table 1
Screening results for enantiomer separation of (*R/S*)-2-(4-phenylphenyl)-4-(1-piperidyl)butan-2-ol, (*R/S*)-**1**, via HPLC.



Eluent ^a	Cellulose based CSPs											
	Chiralpak IC ^b				Chiralcel OD-H				Chiralcel OJ-H			
	k_A	k_B	α	R_s	k_A	k_B	α	R_s	k_A	k_B	α	R_s
A		0.36	1	n.a.	0.34		1	n.a.	0.69	1.27	1.83	4.89
B		1.05	1	n.a.	0.19		1	n.a.	0.37	0.69	1.84	2.99
C	5.22	7.06	1.35	3.37	0.26		1	n.a.	0.69	1.05	1.52	2.95
D	4.22	5.02	1.19	2.54	0.25		1	n.a.	0.94	1.5	1.6	3.75
E			n.a.		0.44	0.71	1.59	1.61			n.a.	
Eluent ^a	Amylose based CSPs											
	Chiralpak IA ^b				Chiralpak AD-H							
	k_A	k_B	α	R_s	k_A	k_B	α	R_s				
A		1.18	1	n.a.	0.69		0.89	1.29				1.69
B		1.1	1	n.a.		0.9		1				n.a.
C	2.38		2.88	1.2	0.76		0.97	1.28				2
D	5.63		7.13	1.27	1.07		1.36	1.27				1.77
E			n.t.							n.t.		

^a Mobile phases: A: MeOH; B: EtOH; C: *n*-Hp/EtOH (90/10, v/v); D: *n*-Hp/EtOH (95/5, v/v); E: *n*-Hp/IPA (98/2, v/v). All mobile phases contained 0.1% DEA. n.t. not tested; n.a.: not applicable.

^b Mobile phase contained 0.3% TFA.

isolation of the enantiomers of a chiral molecule, being a viable route for straightforward and rapid access to both enantiomers with high optical purity and yields. Accordingly, a fast, pragmatic, and non-comprehensive column screening was the key driver for the rapid establishment of a resolution of **1** via enantioselective HPLC and supercritical fluid chromatography (SFC) on chiral stationary phases [12–14] at a (semi) preparative scale. The elution order of the two enantiomers could be switched by selection of suitable chromatographic conditions.

2. Materials and methods

2.1. Chemical and instruments

Solvents used as eluents (HPLC grade) were obtained from Aldrich (Italy). (*R/S*)-**1** was prepared by us, as already described [9].

HPLC measurements were carried out on a Jasco system (JASCO Europe, Cremella, LC, Italy) consisting of PU-2089 plus pump, AS-2055 plus autosampler and MD-2010 plus detector. Data acquisition and control were performed using the Jasco Borwin Software.

For all SFC runs an Investigator Analytical/(semi) preparative SFC system, Waters SpA (Milan, Italy) was employed. Data acquisition and control of the SFC systems were performed using the Waters SuperChrom Software Waters SpA (Milan, Italy).

Retention factors of first and second eluted enantiomer k_a and k_b , respectively, were calculated following IUPAC recommendations [15]; the dead time t_0 was considered to be equal to the peak of the solvent front for each particular run. Resolution was calculated according to Ph. Eur. 2.2.29 [16], enantioselectivity (α) was calculated according to: $\alpha = k_b/k_a$.

Optical rotations measurements were determined on a Jasco photoelectric polarimeter DIP 1000 system (JASCO Europe, Cremella, LC, Italy) with a 1 dm cell at the sodium D line ($\lambda = 589$ nm); sample concentration values c are given in $g \cdot 10^{-2} mL^{-1}$.

2.2. Chiral chromatographic resolution by HPLC

Analytical HPLC runs were performed using the commercially available Chiralcel OD-H (150 mm \times 4.6 cm, 5 μ m), Chiralcel OJ-H (150 mm \times 4.6 cm, 5 μ m), Chiralpak IC (250 mm \times 4.6 cm, 5 μ m), Chiralpak IA (150 mm \times 4.6 cm, 5 μ m) and Chiralpak AD-H (150 mm \times 4.6 cm, 5 μ m) columns (Daicel Industries Ltd., Tokyo, Japan). The mobile phase compositions as well as the chromatographic parameters are summarized in Table 1. Sample solutions of the analyte [0.5 mg mL⁻¹ in ethanol (EtOH)] were filtered through 0.45 μ m PTFE membranes (VWR International, Milan, Italy) before analysis. The injection volume was 10 μ L, the flow rate was 1.0 mL min⁻¹ and detection wavelength was 254 nm. All experiments were performed at room temperature (r.t.).

(Semi) preparative HPLC runs were carried out employing a Chiralcel OJ-H column (250 mm \times 10 mm, 5 μ m) (Daicel Industries Ltd., Tokyo, Japan), eluting with methanol (MeOH)/ diethylamine (DEA) (99.9/0.1; v/v) at a flow rate of 3 mL min⁻¹. Sample solutions of analytes (3 mg mL⁻¹ in MeOH) were filtered before analysis. The injection volume was 1 mL and the UV detection at 254 nm (r.t.). For the preparative HPLC runs the flow rate calculated from the linear scale-up (i.e. approx. 5 mL min⁻¹) led to a partial co-elution of an achiral impurity in the starting material; therefore the flow rate was reduced to 3 mL min⁻¹, for which no significant co-elution was observed.

The collected fractions were evaporated at reduced pressure. In process control was performed using an analytical Chiralcel OJ-H column.

2.3. Chiral chromatographic resolution by SFC

SFC analytical screening was carried out employing Chiralpak IA (250 mm \times 4.6 cm, 5 μ m) and Chiralpak IC (250 mm \times 4.6 cm, 5 μ m). A pilot screening was performed by gradient elution using carbon dioxide (CO₂) mixed with (i) polar modifiers (MeOH, EtOH

Table 2
Screening results for enantiomer separation of (*R/S*)-**1** via SFC.

Organic modifier ^a	Percentage [%]	Chiral stationary phase							
		Chiralpak IA				Chiralpak IC			
		<i>k</i> _A	<i>k</i> _B	α	<i>R</i> _s	<i>k</i> _A	<i>k</i> _B	α	<i>R</i> _s
MeOH	5–45 ^b	4.9	5.5	1.12	1.48	6.4	6.9		1.57
	10	6.6	8.3	1.26	1.18			n.t.	
	20	2.4	3.2	1.33	1.89				2.07
	30					4.2	5.0		1.18
EtOH	5–45 ^b		4.2	n.a.	n.a.	5.0	5.5	1.10	1.74
	IPA	5–45 ^b	3.9	4.3	1.10	1.77	5.1	5.9	1.16
IPA	15	2.2	2.9	1.32	2.95			n.t.	
	20	1.4	1.8	1.29	1.95	2.4	3.4	1.42	1.11
	25	0.9	1.2	1.33	2.12			n.t.	
	30					1.2	1.6	1.33	0.89
IPA/ <i>n</i> -Hp (9/1, v/v)	15	1.4	1.9	1.36	2.66			n.t.	
	25					1.8	2.5	1.39	4.25
	30					1.3	1.8	1.39	2.70
IPA/ <i>n</i> -Hp (8/2, v/v)	15	2.5	3.3	1.32	1.77			n.t.	
	<i>n</i> -Hp/EtOH (9/1, v/v)	30	2.4	3.0	1.25	2.56		n.t.	

^a All modifiers contained 0.1% DEA.

^b Gradient conditions: linear decrease from 95 to 55% of CO₂ from the time 0 to 10.25 min; isocratic at 55% CO₂ for 2 min; return to the initial conditions (95% CO₂) in 15 s, equilibration of the system from 12.40 min to 18 min at 95% CO₂; n.t.: not tested.

or isopropanol (IPA) added with 0.1% DEA) or (ii) mixtures of *n*-heptane (*n*-Hp) and alcohols (IPA or EtOH) added with 0.1% DEA. Successively, isocratic runs were performed. Results are summarized in Table 2. Sample solutions were prepared by dissolving the analyte at 1 mg mL⁻¹ in IPA. The injection volume was 10 μ L, the flow rate 4 mL min⁻¹ and the detection wavelength was 254 nm. All experiments were performed at 40 °C.

The (semi) preparative runs were carried out employing either a Chiralpak IA (250 mm \times 10 mm, 5 μ m) eluting with 70% of CO₂ and 30% of *n*-Hp/EtOH/DEA (9/1/0.1, v/v/v) at a flow rate of 10 mL min⁻¹, or a Chiralpak IC column (250 mm \times 10 mm, 5 μ m), eluting with 75% CO₂ and 25% of *n*-Hp/IPA/DEA (9/1/0.1, v/v/v) at a flow rate of 8 mL min⁻¹. Sample solutions of analytes (10 mg mL⁻¹ in IPA) were filtered before analysis. For the preparative SFC runs the flow rate calculated from the linear scale-up (approx. 20 mL min⁻¹) was out of the operating range of the instrument; however, it could be increased to 8 mL min⁻¹ on Chiralpak IA, due to the partial co-elution of the two enantiomers, and even to 10 mL min⁻¹ on Chiralpak IC for which the two enantiomers were separated better. Fraction collection was performed according to the UV profile; analytical in process control of collected fractions was performed using the Chiralpak IA column eluting with 70% of CO₂ and 30% of a mixture of *n*-Hp/EtOH/DEA (90/10/0.1, v/v/v). The collected fractions were evaporated under reduced pressure.

3. Results and discussion

The synthesis of racemic **1** and analogous biphenyl-alkylamines has been reported four decades ago [17]. However, no stereo-selective synthesis or enantioselective chromatographic method for obtaining the single enantiomers in g scale has been described ever before. In order to obtain both enantiomers of **1** in amounts sufficient for an exhaustive biological investigation, preparative enantioselective HPLC and SFC separations were developed, scaled-up and the obtained results compared. The design of experiments followed the general strategy recently outlined by analytical development groups working at Pfizer and Vertex focusing on methods “fit-for-purpose” in early stages of drug development [11]. “Fit-for-purpose” means that “the method used is sufficient to answer the question at the time of need, but will probably change as the development progresses” [11]. In view of the good solubility of **1** in alcohols only normal phase and polar organic solvent chromatography were tested [18].

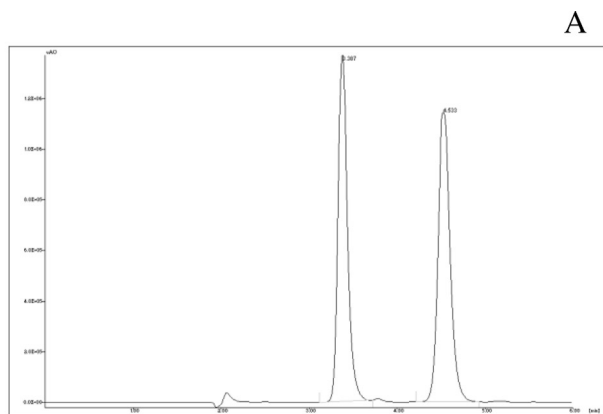
3.1. Analytical screening and development of a scalable enantiomer separation of **1**

For HPLC the screening started with a standard protocol for cellulose and amylose derived CSPs [19] which was applied to Chiralpak IC, Chiralcel OD-H and Chiralcel OJ-H (all cellulose derivatives) as well as to Chiralpak IA and Chiralpak AD-H (amylose derivatives). We intentionally narrowed our screening to some of the most versatile CSPs available in our laboratories; elution conditions in the screening included alcohols (methanol, ethanol and 2-propanol) and mixtures of *n*-heptane and polar modifiers (ethanol or 2-propanol). Results of the screening protocol are reported in Table 1 as retention factor (*k*), selectivity (α) and resolution (*R*_s) factors.

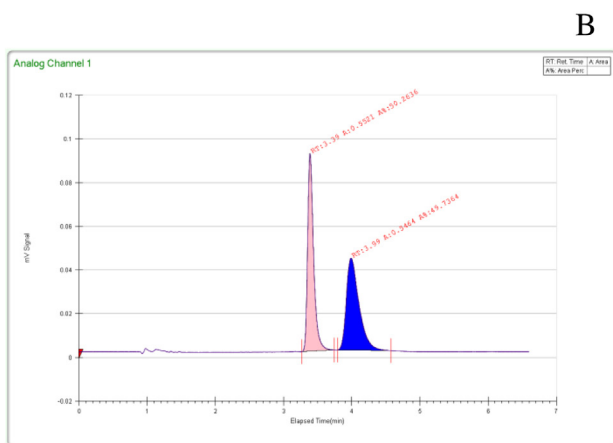
The retention times of **1**-enantiomers on Chiralpak IC and IA with non-polar eluent compositions were quite long and do not give grounds for a productive scale-up; with polar eluents no separation was observed. Enantiomer separation of **1** on Chiralcel OD-H could only be achieved when using a mobile phase with very high alkane content, while the results on Chiralcel OJ-H turned out to be quite promising for further scale-up. Interestingly Chiralpak IA (the immobilized version of Chiralpak AD-H) shows significantly longer retention times in comparison to its non-immobilized analogue employing alkane-based mobile phases, while retention behavior and enantioselectivity with methanol and ethanol as mobile phase are very similar and do not allow enantiomer separation of **1**.

Using pure methanol as eluent (with 0.1% DEA) relatively short retention times (3.4 min for the first eluted enantiomer and 4.6 min for the second), high enantioselectivity and good resolution ($\alpha = 1.8$, *R*_s = 3.9 at r.t.) could be observed on Chiralcel OJ-H (Fig. 1A). Accordingly, these experimental conditions are suitable for the scale-up to (semi) preparative scale. In view of these results no further attempts were made to extend the screening under HPLC conditions.

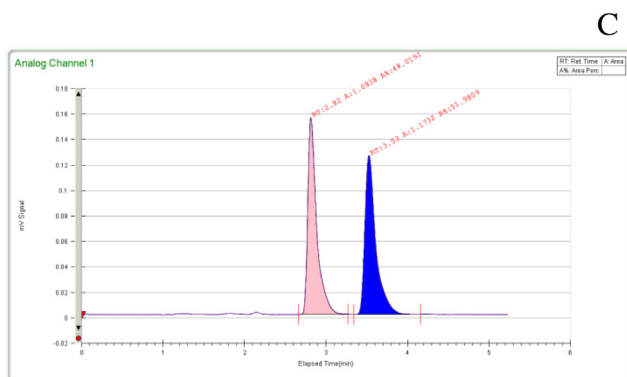
Simultaneously, we tested enantioselective SFC for the enantiomer separation of **1**, which is considered as one of the most rapid and efficient methods for obtaining directly both enantiomers in high optical purity [20–23]. Recently, the advantages of enantioselective SFC over HPLC in analytical [24,25] and preparative separations [26] have been reported by several authors. Due to lower viscosities SFC allows running chromatographic separations at faster flow rates [27] and often gives the opportunity to use less solvent in the final fraction. Therefore a straightforward and



System: **HPLC**
 Column: Chiralcel OJ-H
 Eluent: MeOH/DEA (99.9/0.1, v/v)
 Flow rate: 1.0 mL min⁻¹
 $\alpha = 1.83$; $R_s = 4.89$



System: **SFC**
 Column: Chiralpak IA
 Eluent: 70% CO₂, 30% n-Hp/
 EtOH/DEA (9/1/0.1, v/v/v)
 Flow rate: 4.0 mL min⁻¹
 $\alpha = 1.25$; $R_s = 2.56$



System: **SFC**
 Column: Chiralpak IC
 Eluent: 70% CO₂, 25% IPA/n-Hp/
 DEA (9/1/0.1, v/v/v)
 Flow rate: 4.0 mL min⁻¹
 $\alpha = 1.39$, $R_s = 4.25$

Fig. 1. Analytical enantiomer separation of (R/S)-1 on A) Chiralcel OJ-H (4.6 mm × 150 mm, $d_p = 5 \mu\text{m}$), t_{R1} : 3.4 min; t_{R2} : 4.6 min at r.t.; B) Chiralpak IA (25 cm × 0.46 cm, $d_p = 5 \mu\text{m}$), t_{R1} : 3.39 min; t_{R2} : 3.99 min at 40 °C; C) Chiralpak IC (25 cm × 0.46 cm, $d_p = 5 \mu\text{m}$), t_{R1} : 2.82 min; t_{R2} : 3.53 at 40 °C For all: Injection volume 10 μL , detection at 254 nm, eluent composition and flow rates see text in Figure.

Table 3
 Conditions and isolated amounts of (+)-(S)-1 and (-)-(R)-1 obtained by (semi) preparative enantioselective SFC or HPLC starting from racemic 1.

System	(Semi) preparative CSP	Amount of (R/S)-1 separated [mg]	No. cycles	Vol. inj (μL)	Specific productivity [kkg] ^d	Isolated amount [mg]	ee [%]	Yield [%]	$[\alpha]_D^{20}$ ^a
HPLC	Chiralcel OJ-H	21	7	1 mL ^b	0.0270	8.7	99.9	43.3	+24.0
						9.1	99.9	45.5	-24.0
SFC	Chiralpak IA	20	40	50 μL ^c	0.0072	9.1	99.9	45.5	+24.0
						8.2	94.5	41.0	-23.1
	Chiralpak IC	20	40	50 μL ^c	0.0065	9.6	99.1	48.0	-23.9
						9.5	98.9	47.5	+23.8

^a $c = 0.50\%$ in MeOH.

^b $c = 3 \text{ mg mL}^{-1}$ in MeOH.

^c $c = 10 \text{ mg mL}^{-1}$ in IPA.

^d kkg = kg racemate separated per kg CSP per day.

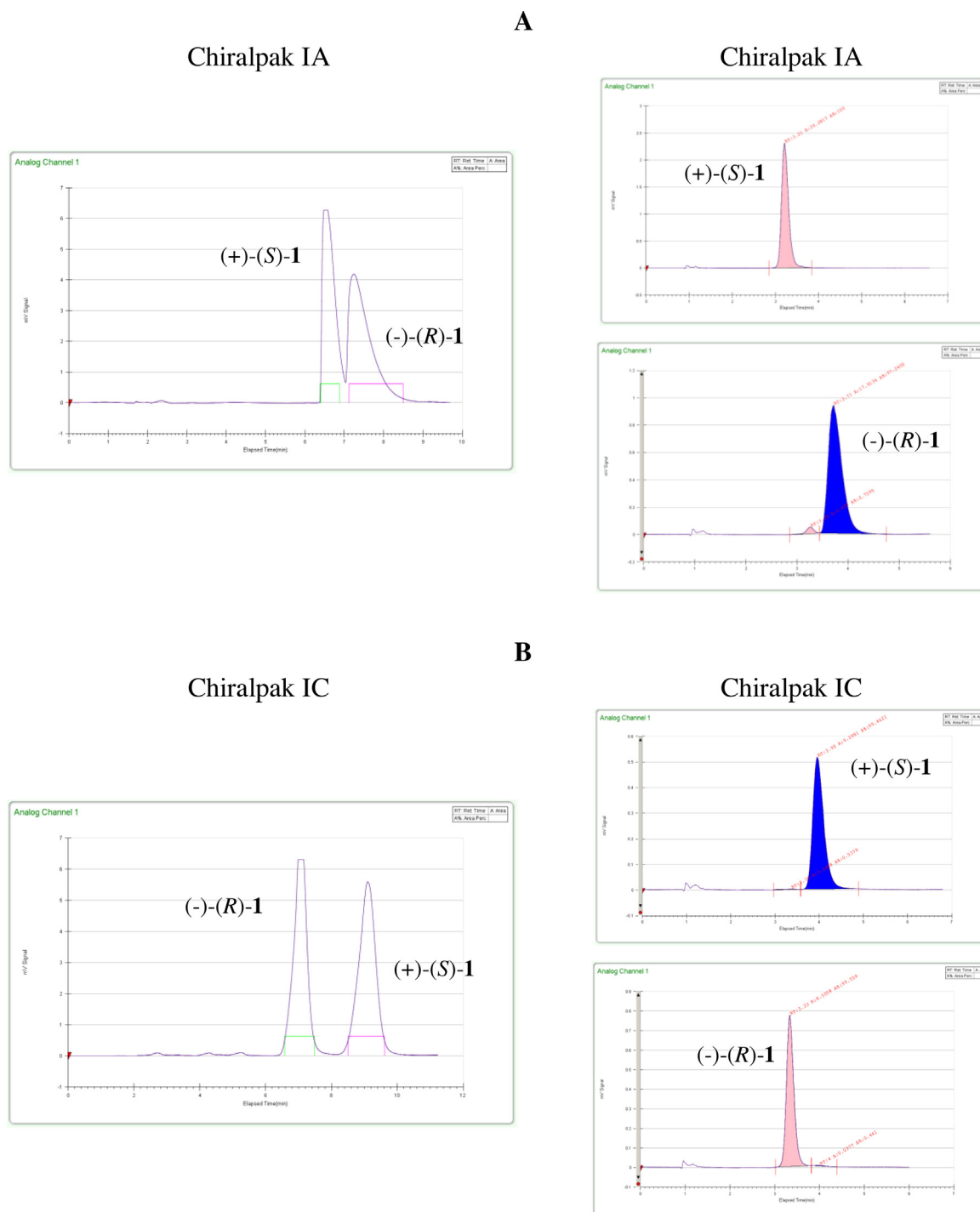


Fig. 2. (Semi) preparative enantiomer separation of **1** by SFC and final analysis.

Left: (Semi) preparative enantiomer separation of racemic **1** (A) on Chiralpak IA (10.0 mm \times 250 mm, $d_p = 5 \mu\text{m}$), eluting with 70% of CO_2 and 30% of $n\text{-Hp}/\text{EtOH}/\text{DEA}$ (9/1/0.1%, v/v/v), flow rate 10 mL min^{-1} , t_{R1} : 6.5 min, t_{R2} : 7.25 min ($\alpha = 1.16$, $R_s = 0.93$), injection volume 0.05 mL ($c = 10 \text{ mg mL}^{-1}$ in IPA); and (B) on Chiralpak IC (10.0 mm \times 250 mm, $d_p = 5 \mu\text{m}$), eluting with 75% of CO_2 and 25% of IPA/ $n\text{-Hp}/\text{DEA}$ (9/1/0.1%, v/v/v), flow rate 8 mL min^{-1} , t_{R1} : 7.1 min; t_{R2} : 9.2 min ($\alpha = 1.45$, $R_s = 2.25$). In both cases the injection volume was 0.05 mL ($c = 10 \text{ mg mL}^{-1}$ in IPA), detection at 254 nm at 40°C . Cut-points for fraction collection are indicated in the chromatogram with horizontal dashes (\square). Right: Analytical enantioselective analysis of first and second collected fraction on Chiralpak IA (4.6 mm ID \times 250 mm, $d_p = 5 \mu\text{m}$), eluting with 70% of CO_2 and 30% $n\text{-Hp}/\text{EtOH}/\text{DEA}$ (90/10/0.1, v/v/v), flow rate 4 mL min^{-1} at 40°C . Analytes were detected at 254 nm. A) t_{R1} : 3.21 min; t_{R2} : 3.71 min at 40°C ; B) t_{R1} : 3.33 min (second eluted enantiomer on Chiralpak IC) t_{R2} : 3.95 min (first eluted enantiomer on Chiralpak IC).

fast screening [28,29] of suitable chiral stationary phases and polar modifiers (MeOH, EtOH and IPA; all with 0.1% DEA) under gradient conditions (5–45%) was performed. First scouting experiments on two columns (Chiralpak IA and Chiralpak IC) using the aforementioned solvents resulted in five enantiomer separations of **1** (Table 2) under 10 min. Only the use of EtOH as polar CO_2 modifier

did not result in chiral resolution of **1** on Chiralpak IA. Also in this case the screening was not broadened considering the high success rate of the first experiments.

In a second step, the optimization of selectivity and resolution was performed under isocratic conditions, excluding unpromising experiments from the screening matrix (e.g. experiments with pure

EtOH as polar modifier on Chiralpak IA). We included also mixtures of *n*-heptane with IPA and EtOH in the screening and, at the first glance, an excellent separation on Chiralpak IA was discovered with 30 % *n*-heptane/EtOH (90/10, v/v) in CO₂ (Fig. 1B and Table 2, $\alpha = 1.25$, $R_s = 2.56$). However, as our screening under HPLC conditions (Table 1) had shown, Chiralpak IA shows good enantioselectivity employing various ratios of *n*-Hp/EtOH, even though retention times were relatively long compared to other conditions. In view of the relatively high content of modifier it can be assumed that the separation is no longer under supercritical conditions, but subcritical conditions, in which compressed CO₂ is no longer a supercritical fluid, but a liquid [30,31]. Retention times are significantly reduced in comparison to the HPLC conditions due to the fourfold higher flow rate. In a similar way also the separation conditions on Chiralcel IC were optimized. The best conditions in regard to enantioselectivity and resolution were found using 25 % IPA/ *n*-heptane (90/10, v/v) in CO₂ (Fig. 1C and Table 2, $\alpha = 1.39$, $R_s = 4.25$).

3.2. Preparation of **1** enantiomers through HPLC and SFC systems

Preparative resolution of enantiomers using HPLC and SFC is a powerful technique for rapid generation of enantiomers in pharmaceutical discovery [26]. Employing a HPLC system, among the most important prerequisites for an economic and productive preparative enantiomer separation are retention times as short as possible, a high solubility of the racemate and the enantiomers in the eluent/injection solvent and the use of a mobile phase consisting of a pure low-cost solvent, facilitating workup and re-use of mobile phase. As previously discussed, using a Chiralcel OJ-H and pure methanol as eluent (with 0.1% DEA), relatively short retention times (3.4 min for the first eluted enantiomer and 4.6 min for the second), high enantioselectivity and good resolution ($\alpha = 1.8$, $R_s = 4.9$ at r.t.) could be observed (Fig. 1A). Accordingly, these experimental conditions were selected for the scale-up to (semi) preparative scale [32]. Based on scale-up calculations [33,34] the enantiomer separation was transferred to a Chiralcel OJ-H column with an ID of 10 mm on which a maximum of 3.0 mg could be separated in one run within 16 min. 21 mg (*R/S*)-**1** have been processed in 7 cycles affording 8.7 mg of the first (yield: 43.3%; ee = 99.9%; $[\alpha]_D^{20} + 24.0$) and 9.1 mg of the second eluted enantiomer (yield: 45.5%; ee = 99.9%; $[\alpha]_D^{20} - 24.0$) at an overall yield of 88.8% (Table 3). Therefore, using the available (semi) preparative set-up per day 270 mg racemic **1** can be processed using enantioselective HPLC on Chiralcel OJ-H. Based on these experiments a specific productivity [35,36] of 27 g racemate separated per 24 h on 1 kg of CSP can be assumed.

Regarding SFC technique, both separations which gave rise to the best resolutions were scaled-up employing (semi) preparative columns with an inner diameter of 10 mm and 250 mm length packed with 5 μ m CSPs [37]. Starting from an injection volume of 50 μ L and a flow rate of 5 mL min⁻¹, as suggested by literature [38], gradual steps of both parameters were performed. The best profiles are obtained 1) on Chiralpak IA injecting 50 μ L per run and eluting at a flow rate of 10 mL min⁻¹, 2) on Chiralpak IC injecting 50 μ L per run and eluting at a flow rate of 8 mL min⁻¹. In detail, using Chiralpak IA 20 mg (*R/S*)-**1** could be processed in 40 cycles of 10 min each (Fig. 2A). 9.1 mg of the (*S*) enantiomer (first eluted, yield: 45.5%; ee = 99.9%; $[\alpha]_D^{20} + 24.0$) and 8.2 mg of the (*R*) enantiomer (second eluted yield: 41.0%; ee = 94.5%; $[\alpha]_D^{20} - 23.1$) at an overall yield of 86.5% (Table 3). On Chiralpak IC 20 mg (*R/S*)-**1** has been processed in 40 cycles of 11 min each (Fig. 2B). 9.6 mg of the (*R*) enantiomer (first eluted, yield: 48.0%; ee = 99.1%; $[\alpha]_D^{20} - 23.9$) and 9.5 mg of the (*S*) enantiomer (second eluted, yield: 47.5%; ee = 98.9%; $[\alpha]_D^{20} + 23.8$) at an overall yield of 95.5% (Table 3). In summary, using the available (semi) preparative set-up per day 72 mg racemic **1** can be separated using enantioselective SFC on Chiral-

pak IA. Based on these experiments a specific productivity of 7.2 g racemate separated per 24 h on 1 kg of CSP can be assumed [35]. On Chiralpak IC in SFC 64.8 mg of racemic **1** can be separated/24 h. The specific productivity estimated is in the range of 6.5 g per kg CSP/24 h. The specific productivities observed are at least two orders of magnitude under those observed for commercial processes [36]. Actually, productivity of SFC separation could have been improved further performing a full optimization of the process (i.e. by using mobile phase composition ensuring higher solubility of the analytes – some portion of dichloromethane for example – or stacked injections instead of batch injections). Actually, the process was not fully optimized in preparative scale, mainly due to the limited amount of the molecule available, and also considering that (i) the optimization might have taken one or two days, by which the compound was already isolated in high yield and enantiomeric excess, and, more importantly, (ii) the objective of our development work was to obtain the enantiomers in the quickest possible way with the tools at hand employing methods “fit-for-purpose”.

Our experiments show that the elution order [39] for the enantiomers of **1** is *S* before *R* on Chiralcel OJ-H in HPLC as well as on Chiralpak IA in SFC and *R* before *S* on Chiralpak IC in SFC, which allows to choose which enantiomer will be eluted as first peak (cf. Fig. 2 and Table 3).

4. Conclusions

A systematic and pragmatic screening protocol for enantioselective HPLC was established for **1**, which led to a fast and easy-to-use chiral HPLC separation suitable for a (semi) preparative scale-up. Overall time frame for screening, linear scale-up and isolation of *R*- and *S*-**1** was less than two weeks.

As a result of a first standard screening, it was found that Chiralcel OJ-H and a mixture of methanol/diethylamine (99.9/0.1, v/v) lead to relatively short retention times, high enantioselectivity and good resolution ($\alpha = 1.8$, $R_s = 3.9$). The (+)-(*S*)-**1** enantiomer elutes as the first peak on Chiralcel OJ-H. The developed method proved to be suitable for obtaining a quick access to the desired enantiomers with enantiomeric excess as high as 99.9% and amounts sufficient for preliminary biological assays.

A rapid screening protocol under SFC-conditions run in parallel made it possible to identify another number of promising conditions for the enantiomer separation of **1**. The protocol under SFC condition revealed an inversion of elution order of the enantiomers on Chiralcel IC using CO₂ with 25 % of the polar modifier IPA/*n*-heptane/diethylamine (90/10/0.1, v/v/v) as eluent.

Scale-up to (semi) preparative SFC allowed assessing productivities and recoveries under HPLC and SFC conditions. Even though recoveries and yields in (semi) preparative HPLC and SFC are in the same range and compounds with high enantiomeric excess were obtained through both technologies, the specific productivity of SFC is almost 4 times lower than the specific productivity observed in (semi) preparative HPLC.

Employing the SFC system, the bottle neck is the injection volume possible for each run (50 μ L), which turned out to be very limited. The eluent consumption on Chiralpak IA and Chiralpak IC is 3.3 and 2.6 times higher, respectively. However, under the consideration that the eluents in SFC consisted of 70 or 75 % CO₂, the organic solvent use for Chiralpak IA is equal to the amount of solvent used in (semi) preparative HPLC on Chiralcel OJ-H and one third lower on Chiralcel IC.

In summary, enantioselective (semi) preparative HPLC proved to be superior in the case of **1** in terms of specific productivity compared to SFC in our laboratory. The (–)-(*R*)-**1** and (+)-(*S*)-**1** enantiomers were obtained with an ee > 99% and therefore can be used for an in-deep comparative examination of the pharmacolog-

ical profile for the individual enantiomers of the new σ_1 receptor agonist **1**.

The recovery of the enantiomers after chromatography was in the range of 41 to 48%, equivalent to 82 up to 96% of the theoretically possible yield of the individual enantiomers.

(Semi) preparative enantioselective chromatography for compounds of interest in medicinal chemistry proves to be a straightforward, productive and robust methodology for the quick access to the desired amounts of pure enantiomers even at low specific productivities. It remains one of the most versatile and cost effective tools for fast isolation of desired enantiomers from a racemic mixture.

Analytical and semi-preparative enantiomer separations have been developed “fit-for-purpose” using a limited number of CSPs and sub-optimal equipment for scale-up. In case larger amounts of the desired enantiomers will be required an intensified and broader screening of CSPs and mobile phases will be employed, for which ample protocols exist.

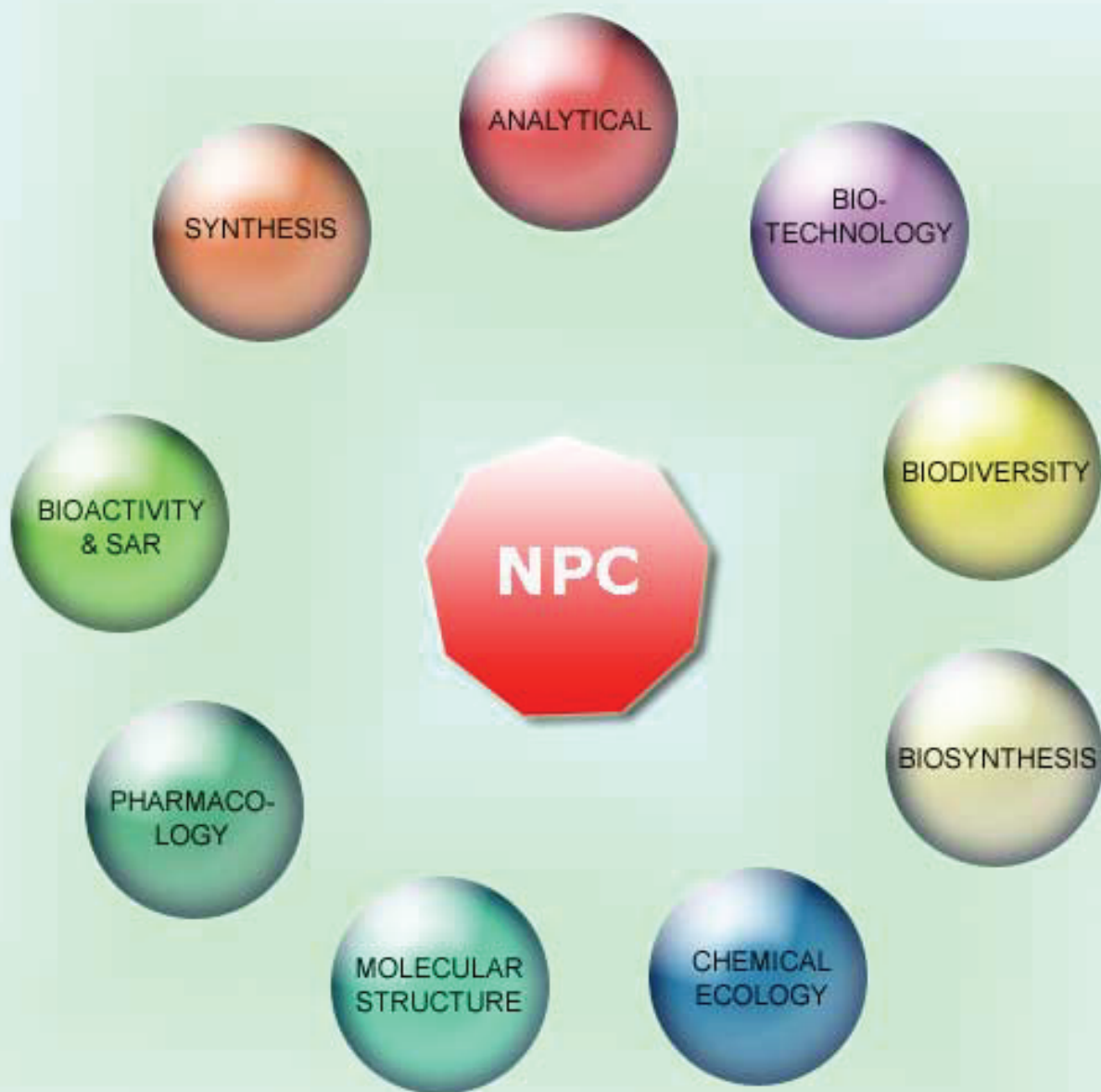
Compound **1** is one in a series of more than twenty structurally related compounds that have recently been screened and successfully separated employing the “fit-for-purpose”-protocol developed by the authors.

References

- [1] S. Collina, R. Gaggeri, A. Marra, A. Bassi, S. Negrinotti, F. Negri, D. Rossi, Sigma receptor modulators: a patent review, *Exp. Opin. Ther. Patent* 23 (2013) 597–613.
- [2] M. Peviani, F. Salvaneschi, L. Bontempi, A. Petese, A. Manzo, D. Rossi, M. Salmons, S. Collina, P. Bigini, D. Curti, Neuroprotective effects of the Sigma-1 receptor (S1R) agonist PRE-084, in a mouse model of motor neuron disease not linked to SOD1 mutation, *Neurobiol. Dis.* 62 (2014) 218–232.
- [3] S.K. Kulkarni, A. Dhir, Effects of (+) SKF 10,047, a sigma-1 receptor agonist, on anxiety, tested in two laboratory models in mice, *Expert Rev. Neurother.* 9 (2009) 1021–1034.
- [4] J.E. Bermack, G.J. Debonnel, Roles of sigma-1 receptors in Alzheimer's disease, *J. Pharmacol. Sci.* 97 (2005) 317–336.
- [5] S. Collina, G. Loddo, M. Urbano, L. Linati, A. Callegari, F. Ortuso, S. Alcaro, C. Laggner, T. Langer, O. Prezzavento, G. Ronsisvalle, O. Azzolina, Design, synthesis and SAR analysis of novel selective sigma1 ligands, *Bioorg. Med. Chem.* 15 (2007) 771–783.
- [6] D. Rossi, M. Urbano, A. Pedrali, M. Serra, D. Zampieri, M.G. Mamolo, C. Laggner, C. Zanette, C. Florio, D. Shepmann, B. Wunsch, O. Azzolina, S. Collina, Design, synthesis and SAR analysis of novel selective sigma1 ligands (Part 2), *Bioorg. Med. Chem.* 18 (2010) 1204–1212.
- [7] D. Rossi, A. Pedrali, M. Urbano, R. Gaggeri, M. Serra, L. Fernandez, M. Fernandez, J. Caballero, S. Rosinsvalle, O. Prezzavento, D. Shepmann, B. Wunsch, M. Peviani, D. Curti, O. Azzolina, S. Collina, Identification of a potent and selective σ_1 receptor agonist potentiating NGF-induced neurite outgrowth in PC12 cells, *Bioorg. Med. Chem.* 19 (2011) 6210–6224.
- [8] D. Rossi, A. Marra, P. Picconi, M. Serra, L. Catenacci, M. Sorrenti, E. Laurini, M. Fermeglia, S. Price, S. Brambilla, N. Almirante, M. Peviani, D. Curti, S. Collina, Identification of RC-33 as a potent and selective σ_1 receptor agonist potentiating NGF-induced neurite outgrowth in PC12 cells. Part 2: g-scale synthesis, physicochemical characterization and in vitro metabolic stability, *Bioorg. Med. Chem.* 21 (2013) 2577–2586.
- [9] D. Rossi, A. Marra, M. Rui, E. Laurini, M. Fermeglia, S. Pricl, D. Schepmann, B. Wunsch, M. Peviani, D. Curti, S. Collina, A step forward in the sigma1 enigma: a role for chirality in the sigma1 receptor-ligand interaction? *Med. Chem. Comm.* 6 (2015) 138–146.
- [10] R. Gaggeri, D. Rossi, S. Collina, B. Mannucci, M. Baierl, M. Juza, Quick development of an analytical enantioselective high performance liquid chromatography separation and preparative scale-up for the flavonoid Naringenin, *J. Chromatogr. A* 1218 (2011) 5414–5422.
- [11] R. DePianta, K. Douville, B. Nickerson, R. Borjas, Chiral screening methods for pharmaceutical analysis and purification in an industrial laboratory, in: S. Ahuja (Ed.), *Chiral Separation Methods for Pharmaceutical and Biotechnological Products*, John Wiley & Sons, Hoboken NJ, 2011, pp. 209–250.
- [12] Jr, W.R. Leonard, D.W. Henderson, R.A. Miller, G.A. Spencer, O.S. Sudah, M. Biba, C.J. Welch, Strategic use of preparative chiral chromatography for the synthesis of a preclinical pharmaceutical candidate, *Chirality* 19 (2007) 693–700.
- [13] L. Miller, M. Potter, Preparative chromatographic resolution of racemates using HPLC and SFC in a pharmaceutical discovery environment, *J. Chromatogr. B* 875 (2008) 230–236.
- [14] K. De Klerck, D. Mangelings, Y. Vander Heyden, Supercritical fluid chromatography for the enantioseparation of pharmaceuticals, *J. Pharm. Biomed. Anal.* 69 (2012) 77–92.
- [15] L.S. Ettre, Nomenclature for chromatography, *Pure Appl. Chem.* 65 (1993) 819–872.
- [16] European Pharmacopoeia, 2.2.29. LIQUID CHROMATOGRAPHY, 8th ed., EDQM, European Pharmacopoeia, Council of Europe, B.P. 907, 67029 Strasbourg, France, July 2013.
- [17] DE2523565 (1975); FR2288518 (1976); DE2450989 (1976).
- [18] A.A. Younesa, H. Ates, D. Mangelings, Y. Vander Heyden, A separation strategy combining three HPLC modes and polysaccharide-based chiral stationary phases, *J. Pharm. Biomed. Anal.* 75 (2013) 74–85.
- [19] M. Juza, Optimization of chiral separations in HPLC, in: S. Kromidas (Ed.), *HPLC Made to Measure—A Practical Handbook for Optimization*, Wiley-VCH, Weinheim, 2006, p. 427.
- [20] C. Roussel, A. Del Rio, J. Pierrot-Sanders, P. Piras, N. Vanthuyne, Chiral liquid chromatography contribution to the determination of the absolute configuration of enantiomers, *J. Chromatogr. A* 1037 (2004) 311–328.
- [21] K.W. Phinney, R.W. Stringham, Chiral separations using supercritical fluid chromatography, in: G. Subramanian (Ed.), *Chiral Separation Techniques*, Wiley, VCH, Weinheim, 2007, pp. 148–153.
- [22] K.L. Williams, L.C. Sander, Enantiomer separations on chiral stationary phases in supercritical fluid chromatography, *J. Chromatogr. A* 785 (1997) 149–158.
- [23] C. West, Enantioselective separations with supercritical fluids—review, *Curr. Anal. Chem.* 10 (2014) 99–120.
- [24] W. Ren-Qi, O. Teng-Teng, T. Weihua, N. Siu-Choon, Recent advances in pharmaceutical separations with supercritical fluid chromatography using chiral stationary phases, *TrAC* 37 (2012) 83–100.
- [25] D. Baudelet, N. Schifano-Faux, A. Ghinet, X. Dezitter, F. Barbotin, P. Gautret, B. Rigo, P. Chavatte, R. Millet, C. Furman, C. Vaccher, E. Lipka, Enantioseparation of pyroglutamide derivatives on polysaccharide based chiral stationary phases by high-performance liquid chromatography and supercritical fluid chromatography: a comparative study, *J. Chromatogr. A* 1363 (2014) 257–269.
- [26] J.C. Welch, Chiral chromatography in support of pharmaceutical process research, in: G. Cox (Ed.), *Preparative Enantioselective Chromatography*, Blackwell Publishing Ltd., London, 2005, pp. 10–18.
- [27] E. Lesellier, C. West, The many faces of packed column supercritical fluid chromatography—A critical review, *J. Chromatogr. A* 1389 (2015) 49–64.
- [28] C. Hamann, M. Wong, I. Aliagas, D.F. Ortwein, J. Pease, D.E. Schmidt Jr., J. Victorino, The evaluation of 25 chiral stationary phases and the utilization of sub-2.0 μm coated polysaccharide chiral stationary phases via supercritical fluid chromatography, *J. Chromatogr. A* 1305 (2013) 310–319.
- [29] M. Maftouh, C. Granier-Loyaux, E. Chavana, J. Marini, A. Pradines, Y. Vander Heyden, C. Piccard, Screening approach for chiral separation of pharmaceuticals. Part III. Supercritical fluid chromatography for analysis and purification in drug discovery, *J. Chromatogr. A* 1088 (2005) 67–81.
- [30] R.W. Stringham, K.G. Lynam, C.C. Grasso, Application of subcritical fluid chromatography to rapid chiral method development, *Anal. Chem.* 66 (1994) 1949–1954.
- [31] G. Terfloth, Enantioseparations in super- and subcritical fluid chromatography, *J. Chromatogr. A* 906 (2001) 301–307.
- [32] S. Golshan-Shirazi, G. Guiochon, Theory of optimization of the experimental conditions of preparative elution chromatography: optimization of the column efficiency, *Anal. Chem.* 61 (1989) 1368–1382.
- [33] H. Colin, in: G. Ganetsos, P.E. Parker (Eds.), *Large-Scale High Performance Preparative Liquid Chromatography*, Preparative and Production Scale Chromatography Marcel Dekker, Inc., New York, 1993, p. 15.
- [34] A.S. Rathore, A. Velayudhan, An overview of scale-up in preparative chromatography, in: A.S. Rathore, A. Velayudhan (Eds.), *Scale-Up and Optimization in Preparative Chromatography*, Marcel Dekker, Inc., New York, 2003, pp. 1–32.
- [35] M. Schulte, R. Ditz, R.M. Devant, J.N. Kinkel, F. Charton, Comparison of the specific productivity of different chiral stationary phases used for simulated moving-bed chromatography, *J. Chromatogr. A* 769 (1997) 93–100.
- [36] L. Miller, Use of dichloromethane for preparative supercritical fluid chromatographic enantioseparations, *J. Chromatogr. A* 1363 (2014) 323–330.
- [37] A. Tarafder, C. Hudalla, P. Iraneta, J.K. Fountain, A scaling rule in supercritical fluid chromatography. I. Theory for isocratic systems, *J. Chromatogr. A* 1362 (2014) 278–293.
- [38] A. Rajendran, Design of preparative-supercritical fluid chromatography, *J. Chromatogr. A* 1250 (2012) 227–249.
- [39] M. Okamoto, Reversal of elution order during the chiral separation in high performance liquid chromatography, *J. Pharm. Biomed. Anal.* 27 (2002) 401–407.

NATURAL PRODUCT COMMUNICATIONS

An International Journal for Communications and Reviews Covering all
Aspects of Natural Products Research



Volume 11. Issue 11. Pages 1631-1774. 2016
ISSN 1934-578X (printed); ISSN 1555-9475 (online)
www.naturalproduct.us

EDITOR-IN-CHIEF**DR. PAWAN K AGRAWAL**

Natural Product Inc.
7963, Anderson Park Lane,
Westerville, Ohio 43081, USA
agrawal@naturalproduct.us

EDITORS**PROFESSOR ALEJANDRO F. BARRERO**

Department of Organic Chemistry, University of Granada,
Campus de Fuente Nueva, s/n, 18071, Granada, Spain
afbarre@ugr.es

PROFESSOR MAURIZIO BRUNO

Department STEBICEF,
University of Palermo, Viale delle Scienze,
Parco d'Orleans II - 90128 Palermo, Italy
maurizio.bruno@unipa.it

PROFESSOR DE-AN GUO

National Engineering Laboratory for TCM Standardization Technology,
Shanghai Institute of Materia Medica, Chinese Academy of Sciences,
Shanghai 201203, P. R. China
gda5958@163.com

PROFESSOR VLADIMIR I. KALININ

G.B. Elyakov Pacific Institute of Bioorganic Chemistry,
Far Eastern Branch, Russian Academy of Sciences,
Pr. 100-letya Vladivostoka 159, 690022,
Vladivostok, Russian Federation
kalininv@piboc.dvo.ru

PROFESSOR YOSHIHIRO MIMAKI

School of Pharmacy,
Tokyo University of Pharmacy and Life Sciences,
Horinouchi 1432-1, Hachioji, Tokyo 192-0392, Japan
mimakiy@ps.toyaku.ac.jp

PROFESSOR STEPHEN G. PYNE

Department of Chemistry, University of Wollongong,
Wollongong, New South Wales, 2522, Australia
spyne@uow.edu.au

PROFESSOR MANFRED G. REINECKE

Department of Chemistry, Texas Christian University,
Forts Worth, TX 76129, USA
m.reinecke@tcu.edu

PROFESSOR WILLIAM N. SETZER

Department of Chemistry, The University of Alabama in Huntsville,
Huntsville, AL 35809, USA
wsetzer@chemistry.uah.edu

PROFESSOR YASUHIRO TEZUKA

Faculty of Pharmaceutical Sciences, Hokuriku University,
Ho-3 Kanagawa-machi, Kanazawa 920-1181, Japan
y-tezuka@hokuriku-u.ac.jp

PROFESSOR DAVID E. THURSTON

Institute of Pharmaceutical Science
Faculty of Life Sciences & Medicine
King's College London, Britannia House
7 Trinity Street, London SE1 1DB, UK
david.thurston@kcl.ac.uk

HONORARY EDITOR**PROFESSOR GERALD BLUNDEN**

The School of Pharmacy & Biomedical Sciences,
University of Portsmouth,
Portsmouth, PO1 2DT U.K.
axuf64@dsl.pipex.com

ADVISORY BOARD

Prof. Viqar Uddin Ahmad
Karachi, Pakistan

Prof. Giovanni Appendino
Novara, Italy

Prof. Yoshinori Asakawa
Tokushima, Japan

Prof. Roberto G. S. Berlink
São Carlos, Brazil

Prof. Anna R. Bilia
Florence, Italy

Prof. Josep Coll
Barcelona, Spain

Prof. Geoffrey Cordell
Chicago, IL, USA

Prof. Fatih Demirci
Eskişehir, Turkey

Prof. Francesco Epifano
Chieti Scalo, Italy

Prof. Ana Cristina Figueiredo
Lisbon, Portugal

Prof. Cristina Gracia-Viguera
Murcia, Spain

Dr. Christopher Gray
Saint John, NB, Canada

Prof. Dominique Guillaume
Reims, France

Prof. Duvvuru Gunasekar
Tirupati, India

Prof. Hisahiro Hagiwara
Niigata, Japan

Prof. Judith Hohmann
Szeged, Hungary

Prof. Tsukasa Iwashina
Tsukuba, Japan

Prof. Leopold Jirovetz
Vienna, Austria

Prof. Phan Van Kiem
Hanoi, Vietnam

Prof. Niel A. Koorbanally
Durban, South Africa

Prof. Chiaki Kuroda
Tokyo, Japan

Prof. Hartmut Laatsch
Gottingen, Germany

Prof. Marie Lacaillle-Dubois
Dijon, France

Prof. Shoen-Sheng Lee
Taipei, Taiwan

Prof. Imre Mathe
Szeged, Hungary

Prof. M. Soledade C. Pedras
Saskatoon, Canada

Prof. Luc Pieters
Antwerp, Belgium

Prof. Peter Proksch
Düsseldorf, Germany

Prof. Phila Raharivelomanana
Tahiti, French Polynesia

Prof. Luca Rastrelli
Fisciano, Italy

Prof. Stefano Serra
Milano, Italy

Dr. Bikram Singh
Palampur, India

Prof. John L. Sorensen
Manitoba, Canada

Prof. Johannes van Staden
Scottsville, South Africa

Prof. Valentin Stonik
Vladivostok, Russia

Prof. Ping-Jyun Sung
Pingtung, Taiwan

Prof. Winston F. Tinto
Barbados, West Indies

Prof. Sylvia Urban
Melbourne, Australia

Prof. Karen Valant-Vetschera
Vienna, Austria

INFORMATION FOR AUTHORS

Full details of how to submit a manuscript for publication in Natural Product Communications are given in Information for Authors on our Web site <http://www.naturalproduct.us>.

Authors may reproduce/republish portions of their published contribution without seeking permission from NPC, provided that any such republication is accompanied by an acknowledgment (original citation)-Reproduced by permission of Natural Product Communications. Any unauthorized reproduction, transmission or storage may result in either civil or criminal liability.

The publication of each of the articles contained herein is protected by copyright. Except as allowed under national "fair use" laws, copying is not permitted by any means or for any purpose, such as for distribution to any third party (whether by sale, loan, gift, or otherwise); as agent (express or implied) of any third party; for purposes of advertising or promotion; or to create collective or derivative works. Such permission requests, or other inquiries, should be addressed to the Natural Product Inc. (NPI). A photocopy license is available from the NPI for institutional subscribers that need to make multiple copies of single articles for internal study or research purposes.

To Subscribe: Natural Product Communications is a journal published monthly. 2016 subscription price: US\$2,595 (Print, ISSN# 1934-578X); US\$2,595 (Web edition, ISSN# 1555-9475); US\$2,995 (Print + single site online); US\$595 (Personal online). Orders should be addressed to Subscription Department, Natural Product Communications, Natural Product Inc., 7963 Anderson Park Lane, Westerville, Ohio 43081, USA. Subscriptions are renewed on an annual basis. Claims for nonreceipt of issues will be honored if made within three months of publication of the issue. All issues are dispatched by airmail throughout the world, excluding the USA and Canada.

The Use of the Comins-Meyers Amide in Synthetic Chemistry: an Overview

Serena Monticelli, Giovanna Parisi, Marta Rui, Karen de la Vega-Hernández, Irene Murgia, Raffaele Senatore, Wolfgang Holzer, Ernst Urban, Thierry Langer and Vittorio Pace*

Department of Pharmaceutical Chemistry, University of Vienna, Althanstrasse 14, 1090 Vienna, Austria

vittorio.pace@univie.ac.at

Received: February 29th, 2016; Accepted: June 26th, 2016

Dedicated to Prof. Dr. Wilhelm Fleischhacker on account of his 85th Birthday.

Formylation reactions are fundamental operations in synthetic chemistry allowing the incorporation into a given structure formyl groups amenable to further derivatization. Conceptually, the introduction of such groups through the reaction between an electrophilic donor and a nucleophilic acceptor (*i.e.* organometallic reagent) constitutes a reliable technique with widespread applications. In this Highlight, we summarize the effectiveness of the so called Comins-Meyers amide - [2-(*N*-methyl-*N*-formylamino)pyridine – in such a chemistry with vistas to the synthesis of natural products and biologically active substrates.

Keywords: Formylation, Amides, Chemoselectivity, Organic synthesis.

The formyl motif is an ubiquitous functionality in natural product chemistry (Figure 1) and represents a versatile tool in organic transformations because of the particular reactivity conferred by the classical carbonyl-type mesomerism (Scheme 1).

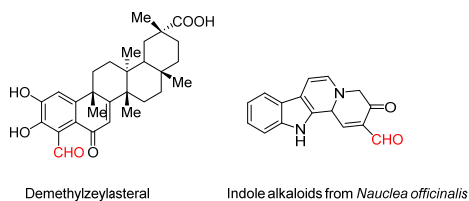
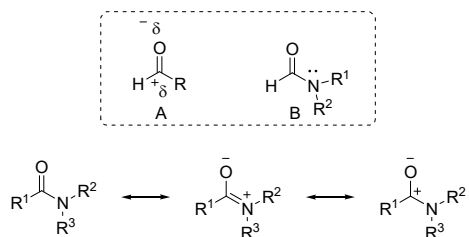


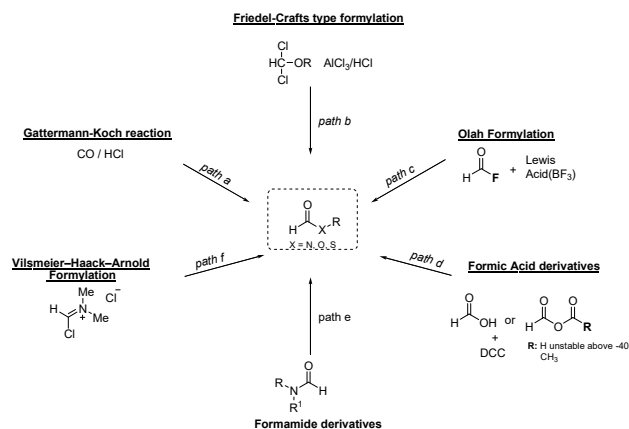
Figure 1: Examples of natural products containing formyl groups.

As such, its polarizability is reflected by the hard donor oxygen and by the fairly hard acceptor carbon behavior (A, Scheme 1). Moreover, by connecting the formyl group to a heteroatom presenting a non-bonded pair of electrons (B, Scheme 1) (e.g. nitrogen), the electrophilicity of the resulting carbonyl carbon decreases considerably: the resulting amide-type derivatives do present a tamed reactivity towards nucleophiles (Scheme 1) [1].



Scheme 1: Mesomeric effects: (A) formyl group – (B) formamide group. Characteristics of the amide bond.

Because of this outstanding importance, the installation of the formyl functionality into a given organic framework constitutes a formidable challenge for synthetic chemists and, in this context, various tactics and reagents have been designed and developed for introducing it in a chemo- and regioselective fashion [2].



Scheme 2: Overview of the main methods to introduce formyl group.

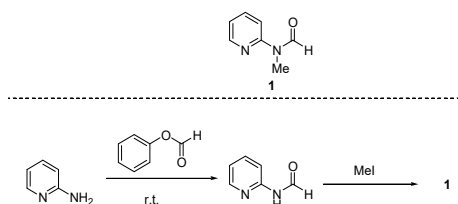
A preliminary categorization distinguishes two major classes of reagents (Scheme 2): (a) formylating agents working under acid catalysis conditions and, (b) electrophilic agents delivering the CHO group to polarized species (*i.e.* carbanions) [2].

Friedel-Craft's chemistry represents a classical method to accomplish formylations, as reported in 1897 by Gattermann and Koch who generated the highly electrophilic formyl from carbon monoxide under superacidic conditions (*path a*) [3]. Alternatively, dichloromethyl ethers and dichloromethyl amines are suitable precursors of the CHO motif under analogous conditions (*path b*) [4,5]. Formyl fluoride in the presence of a Lewis acid - introduced by Olah - shows a remarkable substrate scope as documented in the cases of alcohols, phenols, thiols, and primary and secondary amines (*path c*) [6]. Interestingly, also the relatively inert formic acid may be employed; however, performing reactions in the presence of the corresponding anhydride improves the efficiency of the processes (*path d*) [7,8]. Finally, the Vilsmeier-Haack-Arnold (VHA) reagent (*N*-chloromethylene-*N,N*-dimethylammonium chloride) is an effective precursor of formyl scaffolds, mainly for the synthesis of polycarbonyl compounds such as malondialdehyde (*path f*) (Scheme 2) [9,10].

A conceptually distinct approach relies on the direct transfer of the formyl unit to an organometallic reagent such as organomagnesium or organolithium compounds. This tactic evidently requires the design of convenient precursors which do not suffer common side reactions for these reactive species such as over addition or reduction [11a-f]. In this sense, because of the aforementioned mild reactivity of amide derivatives, *N*-formylamines are excellent scaffolds for delivering the CHO fragment.

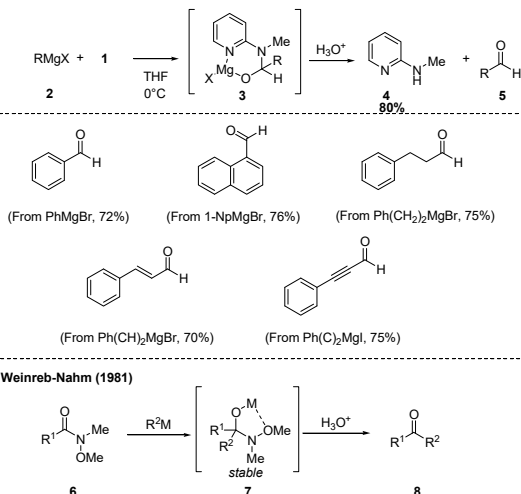
The Comins and Meyers amide

Among the plethora of reagents designed for such a purpose, a prominent role is played by [2-(*N*-methyl-*N*-formylamino)]pyridine (**1**) introduced in 1978 by Comins and Meyers for the formylation of Grignard reagents to access aldehydes in good yields and selectivities (*vide infra*) [12]. Although nowadays it is commercially available, it can be smoothly prepared from 2-aminopyridine and phenyl formate followed by methylation of the resulting 2-(*N*-formylamino)pyridine (Scheme 3).



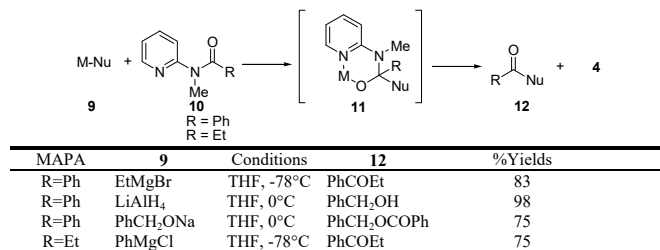
Scheme 3: Synthesis of [2-(*N*-methyl-*N*-formylamino)]pyridine.

Upon the addition of an organomagnesium reagent (**2**) to **1** the stable six-membered chelate intermediate (**3**) is formed (Scheme 4): the nitrogen at the 2-position of the pyridyl ring coordinates efficiently with the magnesium counterion (MgX) of the so generated alkoxyde, thus inhibiting overaddition phenomena. Finally, only upon acidic treatment is the desired aldehyde (**5**) released jointly with 2-*N*-methylpyridine (**4**). This method can be applied to the addition of various Grignard reagents such as aryl, alkyl, vinyl and acetylenic species [12]. It should be observed that analogous coordination effects are responsible for the effectiveness of the so called Weinreb amides (*N*-methoxy-*N*-methamides) (**6**) in the synthesis of carbonyl compounds starting from organometallic reagents [13,14]. However, the somewhat tedious access to the Weinreb amide of formic acid renders this last strategy less explored than the corresponding addition to amides of distinct acids (Scheme 4) [12,13].



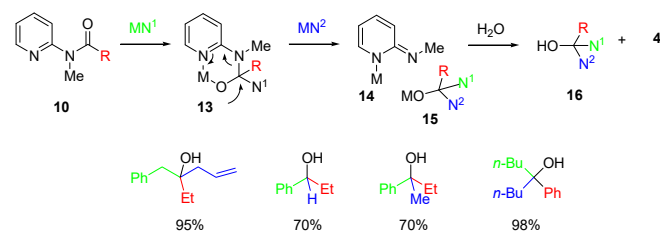
Scheme 4: Addition of organometallic reagents to formamide group.

Subsequently, Comins and Meyers reported an acylation method of different nucleophiles (**9**) using variously substituted *N*-methylamino pyridine amides (MAPA, **10**) (Scheme 5), thus expanding the versatility of the protocol to the synthesis of ketones, alcohols (under reductive conditions) and esters (**12**) [15].



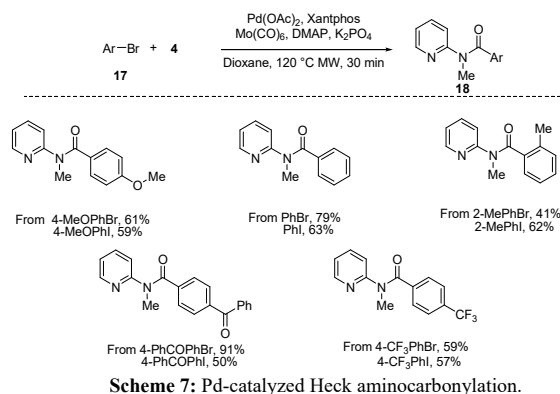
Scheme 5: Application of Comins-Meyers amide in the synthesis of ketones, alcohols and esters.

It is worth noting that Comins-Meyers amides are amenable substrates to afford the “one pot” synthesis of unsymmetrical secondary and tertiary alcohols (**16**) through the consecutive additions of two different nucleophiles (Scheme 6). Evidently, this particular behavior of non-formyl MAPAs relies on the weaker coordination of the metal in structure **13**, which renders the C-N bond labile to further attack by a second. The addition of the second nucleophile is triggered by the increase of temperature which evidently facilitates the collapse of the first intermediate (Scheme 6).



Scheme 6: “One pot” unsymmetrical synthesis of alcohols.

More recently, MAPA substrates (**18**) have been accessed by Odell *et al.* via the microwave-assisted Pd-catalyzed Heck aminocarbonylation with either Mo(CO)₆ or W(CO)₆. As shown in Scheme 7, this protocol is applicable to differently functionalized aryl bromides (**17**), which, except in rare cases, react better than the corresponding iodides [16].

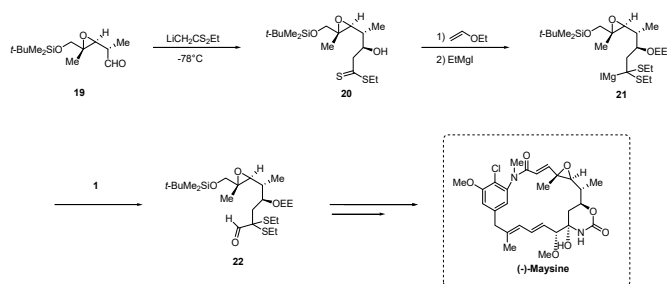


Scheme 7: Pd-catalyzed Heck aminocarbonylation.

Applications in natural products synthesis

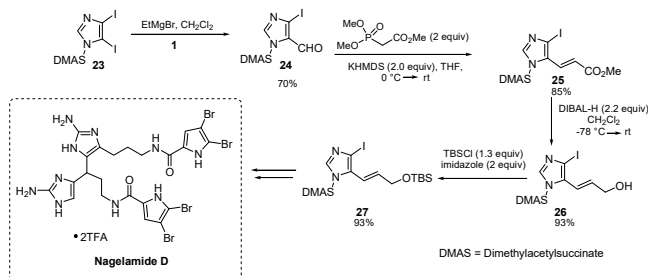
The seminal studies by Comins and Meyers provided useful insights, not only for the mechanistic aspects, but also for the

potentiality of the reagent in multi-steps synthesis. In 1983 they documented the employment of **1** during the total synthesis of the anticancer agent (-)-maysine, which required the formulation of the sulfur-stabilized Grignard reagent **21** (Scheme 8) [17].



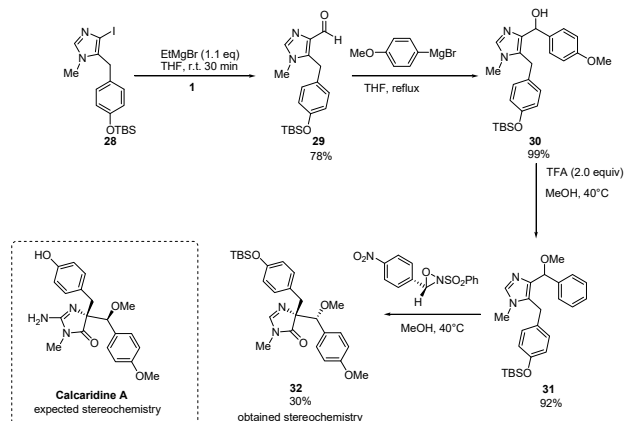
Scheme 8: Total synthesis of (-)-maysine.

In 2009 Lovely and coworkers reported the total synthesis of nagelamide D, a pyrrole-imidazole containing natural product, isolated from *Agelisia*, *Axinellida*, and *Halichondrida* spp. As depicted in Scheme 9, the crucial formylation of the protected 4,5-diiodoimidazole (**23**) was accomplished through the selective magnesiation at C5, followed by treatment with MAPA (**1**). Subsequent olefination, reduction and protection afforded **27**, the pivotal precursor of the target molecule [18].



Scheme 9: Lovely's synthesis of nagelamide D.

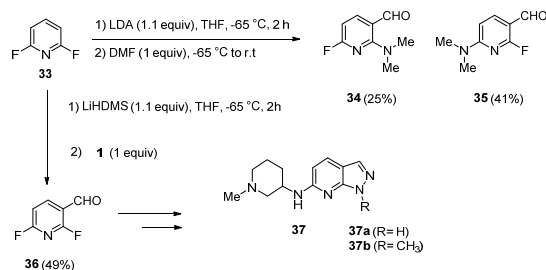
The same group adopted an analogous approach for the total synthesis of the Leucetta-derived alkaloid calcaridine A (Scheme 10). Although the formylation step in the presence of **1** worked nicely, diastereoselectivity issues motivated the switching to a different formyl source (*N*-methylformanilide) providing the correct stereoisomer required for ending the synthesis [19].



Scheme 10: Total synthesis of the Leucetta-derived alkaloid calcaridine A.

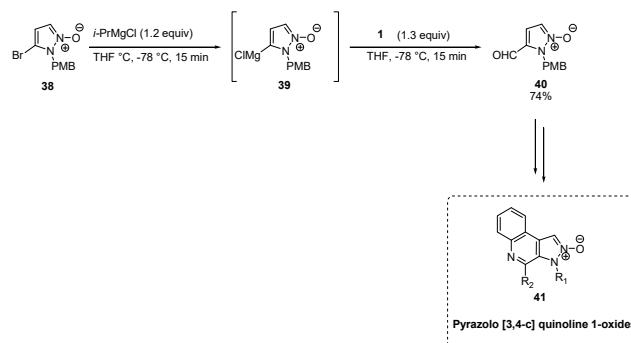
Roehr *et al.* employed **1** for the synthesis of the serotonin re-uptake inhibitors **37a** and **37b** (Scheme 11). The use of the Comins-Meyers formylating agent proved to be ideal since the desired 3-formylated

compound **36** was obtained as the exclusive reaction product upon lithiation and subsequent quenching with it. This is a big advantage compared with procedures paved on the use of different sources of CHO such as DMF, which caused severe chemoselective issues, thus lowering the synthetic appeal of the method. In fact, although the reaction of the lithiated species with DMF ensures the correct delivery of the formyl group at the 3-position, the released *N,N*-dimethylamine is able to perform an aromatic nucleophilic displacement on the fluorine-bearing 2- and 6-positions. As such, the undesired compounds **34** and **35** are formed. On the other hand, the Comins-Meyers amide generates, upon reaction with an organometallic species, the low nucleophilic 2-methylamino-pyridine (which, evidently cannot react via a S_NAr process), therefore delivering the building block with excellent selectivity, as required for finalizing the pharmaceutically oriented synthesis [20].



Scheme 11: Synthesis of the serotonin re-uptake inhibitors.

Similarly, Eskildsen *et al.* used the Meyers formylation reagent (**1**) in the synthesis of pyrazolo [3,4-*c*] quinoline 1-oxides (**41**) (Scheme 12). Such a ring system displays significant biological activities, good affinity and selectivity towards adenosine A_3 , GABA and NMDA receptors [21].



Scheme 12: Synthesis of pyrazolo [3,4-*c*] quinoline 1-oxides.

Conclusions and outlook

Comins-Meyers amide congeners are useful reagents for introducing not only a formyl group but also ketone-type carbonyls susceptible to further derivatization. The driving force for eliminating the risk of overaddition side reactions in the case of Grignard reagents is the formation of a stable chelate triggered by the coordinative capability of the pyridyl nitrogen lone pair for the MgX counterion. Remarkably, when organolithium reagents are added the resulting chelate displays an increased tendency to react further with the same or with a different nucleophile, thus affording tertiary alcohols. Although numerous applications of this versatile reagent are known, in our opinion, more detailed studies regarding the addition of functionalized organometallics (*e.g.* carbenoids) are needed to estimate better its real potentialities in C-C bond forming transformations.

Acknowledgements - The University of Vienna is gratefully thanked for financial support.

References

- [1] (a) Pace V, Holzer W, Olofsson B. (2014) Increasing the reactivity of amides towards organometallic reagents: An overview. *Advanced Synthesis and Catalysis*, **356**, 3697-3736; (b) Pace V, Holzer W. (2013) Chemoselective activation strategies of amidic carbonyls towards nucleophilic reagents. *Australian Journal of Chemistry*, **66**, 507-510.
- [2] Olah GA, Ohannesian L, Arvanaghi M. (1987) Formylating agents. *Chemical Reviews*, **87**, 671-686.
- [3] Gattermann L, Koch JA. (1897) Eine synthese aromatischer aldehyde. *Berichte der Deutschen Chemischen Gesellschaft*, **30**, 1622-1624.
- [4] Rieche A, Gross H, Höft E. (1960) Über α -Halogenäther, IV. Synthesen aromatischer aldehyde mit dichlormethyl-alkyläthern. *Chemische Berichte*, **93**, 88-94.
- [5] DeHaan FP, Delker GL, Covey WD, Bellomo, AF, Brown JA, Ferrara DM, MacArthur CJ. (1984) Electrophilic aromatic substitution. A kinetic study of the formylation of aromatics with 1, 1-dichloromethyl methyl ether in nitromethane. *The Journal of Organic Chemistry*, **49**, 3963-3966.
- [6] Olah GA, Kuhn SJ. (1960) Formylation with formyl fluoride: A new aldehyde synthesis and formylation method. *Journal of the American Chemical Society*, **82**, 2380-2382.
- [7] Olah GA, Vankar YD, Arvanaghi M, Sommer J. (1979) Formic anhydride. *Angewandte Chemie International Edition in English*, **18**, 614-614.
- [8] Huffman CW. (1958) Formylation of amines. *The Journal of Organic Chemistry*, **23**, 727-729.
- [9] Böhme HW, Viehe HG. (Eds). (1976) *Iminium salts in organic chemistry*. John Wiley & Sons, New York.
- [10] Bredereck H, Effenberger F, Hofmann A. (1963) Säureamid-Reaktionen, XXXVI. Thermische zersetzung on trisformaminomethan und bildung on s-triazin. *Chemische Berichte*, **96**, 3260-3264.
- [11] (a) Olah GA, Laali K, Farooq O. (1985) Aromatic substitution. 52. Superacid-catalyzed carbonylation of aromatics with carbon monoxide. *The Journal of Organic Chemistry*, **50**, 1483-1486; (b) Seyferth D, Hui RC. (1986) A stable 1: 1 lithium acylcyanocuprate. Dependence of the stability of acylcyanocuprates on the nature of the alkyl substituent. *Tetrahedron Letters*, **27**, 1473-1476; (c) Nudelman NS, Vitale AA. (1981) Carbonylation of aryllithium reagents in the presence of alkyl halides: one-pot synthesis of diarylalkyl carbinols and derivatives. *The Journal of Organic Chemistry*, **46**, 4625-4626; (d) Nudelman NS, Outumuro P. (1982) Insertion of carbon monoxide into carbon-lithium bonds. A convenient one-step synthesis of 1, 2-diketone diaryl derivatives. *The Journal of Organic Chemistry*, **47**, 4347-4348; (e) Tsuda T, Miwa M, Saegusa T. (1979) Lithium bis (*N,N*-diethylcarbamoyl) cuprate. A reagent for direct carbamoylation. *The Journal of Organic Chemistry*, **44**, 3734-3736; (f) Kilbourn MR, Jerabek PA, Welch MJ. (1983) Synthesis of carbon-11 labelled amides via carbonylation of lithium dialkylamides. *Journal of the Chemical Society, Chemical Communications*, **16**, 861-862.
- [12] Comins D, Meyers AI. (1978) A facile and efficient formylation of Grignard reagents. *Synthesis*, **5**, 403-404.
- [13] Nahm S, Weinreb SM. (1981) *N*-Methoxy-*N*-methylamides as effective acylating agents. *Tetrahedron Letters*, **22**, 3815-3818.
- [14] (a) Balasubramanian S, Aidhen IS. (2008) The growing synthetic utility of the Weinreb amides. *Synthesis*, **23**, 3707-3738; For recent applications of Weinreb amides from our group, see: (b) Pace V, Castoldi L, Holzer W. (2013) Synthesis of alpha, beta-unsaturated-alpha'-haloketones through the chemoselective addition of halomethylolithiums to Weinreb amides. *The Journal of Organic Chemistry*, **78**, 7764-7770; (c) Pace V, Holzer W, Verniest G, Alcántara AR, De Kimpe N. (2013) Chemoselective synthesis of *N*-substituted α -amino- α' -chloro ketones via chloromethylation of glycine-derived Weinreb amides. *Advanced Synthesis and Catalysis*, **355**, 919-926; (d) Mamuye AD, Castoldi L, Azzena U, Holzer W, Pace V. (2015) Chemoselective efficient synthesis of functionalized β -oxonitriles through cyanomethylation of Weinreb amides. *Organic and Biomolecular Chemistry*, **13**, 1969-1973; For additional examples on the use of organolithium reagents from our group, see: (e) Pace V, Castoldi L, Holzer W. (2014) Chemoselective additions of chloromethylolithium carbenoid to cyclic enones: A direct access to chloromethyl allylic alcohols. *Advanced Synthesis and Catalysis*, **356**, 1761-1766; (f) Pace V, Castoldi L, Holzer W. (2013) Addition of lithium carbenoids to isocyanates: a direct access to synthetically useful *N*-substituted 2-haloacetamides. *Chemical Communications*, **49**, 8383-8385; (g) Pace V, Castoldi L, Mamuye AD, Holzer W. (2014) Homologation of isocyanates with lithium carbenoids: A straightforward access to α -halomethyl- and α,α -dihalomethylamides. *Synthesis*, **46**, 2897-2909; (h) Pace V, Castoldi L, Monticelli S, Safranek S, Roller A, Langer T, Holzer W. (2015) A robust, eco-friendly access to secondary thioamides through the addition of organolithium reagents to isothiocyanates in cyclopentyl methyl ether (CPME). *Chemistry – A European Journal*, **21**, 18966-18970; (i) Pace V, Castoldi L, Mamuye AD, Langer T, Holzer W. (2016) Chemoselective addition of halomethylolithiums to functionalized isatins: A straightforward access to spiro-epoxyoxindoles. *Advanced Synthesis and Catalysis*, **358**, 172-177; (l) Pace V, Pelosi A, Antermite D, Rosati O, Curini M, Holzer W. (2016) Bromomethylolithium-mediated chemoselective homologation of disulfides to dithioacetals. *Chemical Communications*, **52**, 2639-2642; For reviews on the use of lithium carbenoids in analogous processes, see: (m) Pace V. (2014) Halomethylolithium carbenoids: Versatile reagents for the homologation of electrophilic carbon units. *Australian Journal of Chemistry*, **67**, 311-313. (n) Pace V, Holzer W, De Kimpe N. (2016) Lithium halomethylcarbenoids: Preparation and use in the homologation of carbon electrophiles. *Chemical Records*, **16**, 2061-2076; (n) Pace V, Monticelli S, de la Vega-Hernandez K, Castoldi L. (2016) Isocyanates and isothiocyanates as versatile platforms for accessing (thio)amide-type compounds. *Organic and Biomolecular Chemistry*, **14**, 7848-7854; (o) Pace V, Murgia I, Westermayer S, Langer T, Holzer W. (2016) Highly efficient synthesis of functionalized [small alpha]-oxyketones via Weinreb amides homologation with α -oxygenated organolithiums. *Chemical Communications*, **52**, 7584-7587; (p) Pace V, de la Vega-Hernández K, Urban, E, Langer T. (2016) Chemoselective Schwartz Reagent mediated reduction of isocyanates to formamides. *Organic Letters*, **8**, 2750-2753.
- [15] Meyers AI, Comins DL. (1978) *N*-methylamino pyridyl amides (mapa) II. An efficient acylating agent for various nucleophiles and sequential addition to unsymmetrical *tert*-alcohols. *Tetrahedron Letters*, **19**, 5179-5182.
- [16] Wieckowska A, Fransson R, Odell LR, Larhed M. (2011) Microwave-assisted synthesis of Weinreb and MAP aryl amides via Pd-catalyzed heck aminocarbonylation using Mo (CO) 6 or W (CO) 6. *The Journal of Organic Chemistry*, **76**, 978-981.
- [17] Meyers AI, Babiak KA, Campbell AL, Comins DL, Fleming MP, Henning R, Kane JM. (1983) Total synthesis of (-)-maysine. *Journal of the American Chemical Society*, **105**, 5015-5024.
- [18] Bhandari MR, Sivappa R, Lovely CJ. (2009) Total synthesis of the putative structure of nagelamide D. *Organic Letters*, **11**, 1535-1538.
- [19] Koswatta PB, Sivappa R, Dias HV, Lovely CJ. (2009) Total synthesis of the Leucetta-derived alkaloid calcaridine A. *Synthesis*, **17**, 2970-2982.
- [20] Shutske GM, Roehr JE. (1997) Synthesis of some piperazinylpyrazolo [3, 4-b] pyridines as selective serotonin re-uptake inhibitors. *Journal of Heterocyclic Chemistry*, **34**, 789-795.
- [21] Eskildsen J, Østergaard N, Vedsø P, Begtrup M. (2002) Halogen dance in pyrazole 1-oxides: synthesis of pyrazolo [3, 4-c] quinoline 1-oxides. *Tetrahedron*, **58**, 7635-7644.

Phytotoxic and Antibacterial Activity of Essential Oil of New Peppermint Cultivar Daniela Grušová, Laura De Martino, Emilia Mancini, Ludmila Tkáčiková, Ivan Šalamon, Jozef Fejer and Vincenzo De Feo	1721
Mint Flavorings from Candies Inhibit the Infectivity of <i>Chlamydia pneumoniae</i> Leena L. Hanski, Karmen Kapp, Terttu M. Tiirola, Anne Orav, Heikki J. Vuorela, Tõnu Püssa and Pia M. Vuorela	1725
<u>Accounts/Reviews</u>	
The Use of the Comins-Meyers Amide in Synthetic Chemistry: an Overview Serena Monticelli, Giovanna Parisi, Marta Rui, Karen de la Vega-Hernández, Irene Murgia, Raffaele Senatore, Wolfgang Holzer, Ernst Urban, Thierry Langer and Vittorio Pace	1729
Multidimensional Effects of Soy Isoflavone by Food or Supplements in Menopause Women: a Systematic Review and Bibliometric Analysis Simone Perna, Gabriella Peroni, Alessandra Miccono, Antonella Riva, Paolo Morazzoni, Pietro Allegrini, Stefania Preda, Valentina Baldiraghi, Davide Guido and Mariangela Rondanelli	1733
Antinociceptive Properties of St. John's Wort (<i>Hypericum perforatum</i>) and Other <i>Hypericum</i> Species Nikola M. Stojanović, Niko S. Radulović, Pavle J. Randjelović and Darko Laketić	1741
<i>Zuccagnia punctata</i>: A Review of its Traditional Uses, Phytochemistry, Pharmacology and Toxicology María Inés Isla, María Alejandra Moreno, Gabriela Nuño, Fabiola Rodríguez, Antonella Carabajal, María Rosa Alberto and Iris Catiana Zampini	1749
Leonurine, a Potential Agent of Traditional Chinese Medicine: Recent Updates and Future Perspectives Di Yang, Wanwan Jia and Yi zhun Zhu	1757
A Guidance Manual for the Toxicity Assessment of Traditional Herbal Medicines Ahmet Aydın, Göknur Aktay and Erdem Yesilada	1763

Natural Product Communications

2016

Volume 11, Number 11

Contents

Original Paper

- Constituents of *Melittis melissophyllum* subsp. *albida***
Alessandro Venditti, Claudio Frezza, Fulvia Caretti, Alessandra Gentili, Mauro Serafini and Armandodoriano Bianco 1631
- Synthesis of Ester-linked Docetaxel-glycoside Conjugate and Its Application to Drug Delivery System using Immunoliposome Targeted with Trastuzumab**
Hiroki Hamada, Shouta Okada, Kei Shimoda, Hatsuyuki Hamada and Noriyoshi Masuoka 1635
- A New Ursane-type Triterpenoid and Other Constituents from the Leaves of *Crataegus azarolus* var. *aronia***
Sarbast A. Mahmud, Omar A.M Al-Habib, Serena Bugoni, Marco Clericuzio and Giovanni Vidari 1637
- Aggregation Behavior of 6-Isocassine and N-Methyl-6-Isocassine: Insights into the Biological Mode of Action of Lipid Alkaloids**
Luis Reina, Gualberto Bottini, Zohra Bennadji, Vittorio Vinciguerra, Fernando Ferreira, Pilar Menendez and Guillermo Moyna 1641
- Antimicrobial and Cytotoxic Evaluation of New Quinazoline Derivatives**
Gülhan Turan-Zitouni, Leyla Yurttaş, Güner Saka, Zerrin Cantürk, Hülya Karaca Gencer, Merve Baysal and Zafer Asım Kaplancıklı 1645
- Synthetic Anthocyanidins from Natural Benzopyrans**
George A. Kraus and Ivan M. Geraskin 1649
- Anti-inflammatory Effects of Compounds from *Polygonum odoratum***
Siriporn Okonogi, Kantaporn Kheawfu, Wolfgang Holzer, Frank M. Unger, Helmut Viernstein and Monika Mueller 1651
- The LC/ESI-MSMS Profiles and Biological Potentials of *Vitex agnus castus* Extracts**
Hale Gamze Ağalar, Gülşen Akalın Çiftçi, Şafak Ulusoylar Yıldırım, Fatih Göger and Neşe Kırımer 1655
- Chemical Constituents of the Leaves of *Tussilago farfara* and their Aldose Reductase Inhibitory Activity**
Minpei Kuroda, Takumi Ohshima, Chihiro Kan and Yoshihiro Mimaki 1661
- Quantitative Determination by HPLC-DAD of Icaritin, Epimedin A, Epimedin B, and Epimedin C in *Epimedium* (Berberidaceae) Species Growing in Turkey**
Derya Cicek Polat and Maksut Coskun 1665
- Simultaneous Determination of the Five Marker Compounds in *Melandrium firmum* using High-Performance Liquid Chromatography with Photodiode-Array Detection**
Chang-Seob Seo and Hyeun-Kyoo Shin 1667
- Inhibitory Activities of Sesame Seed Extract and its Constituents against β -Secretase**
Shinichi Matsumura, Kazuya Murata, Nobuhiro Zaima, Yuri Yoshioka, Masanori Morimoto, Hideaki Matsuda and Masahiro Iwaki 1671
- Toxicity of Compounds Isolated from White Snakeroot (*Ageratina altissima*) to Adult and Larval Yellow Fever Mosquitoes (*Aedes aegypti*)**
Alden S. Estep, James J. Becnel and Stephen T. Lee 1675
- Compounds from *Terminalli brownii* Extracts with Toxicity against the Fish Pathogenic Bacterium *Flavobacterium columnare***
Kevin K. Schrader, Charles L. Cantrell, Jacob O. Midiwo and Ilias Muhammad 1679
- Substrate Specificity of *Aglaia loheri* Active Isolate towards P-glycoprotein in Multidrug-Resistant Cancer Cells**
Else Dapat, Sonia Jacinto and Thomas Effert 1683
- Quantitative Determination of Betaine, Choline, Acetylcholine, and 20-Hydroxyecdysone Simultaneously from *Atriplex* Species by UHPLC-UV-MS**
Yan-Hong Wang, Mallika Kumarihamy, Mei Wang, Andrew Smesler, Ikhlas A. Khan, Francisco León, Stephen J. Cutler and Ilias Muhammad 1689
- Phytochemical Content, Antioxidant and Cytotoxic Activities of *Sedum spurium***
Didem Şöhretoğlu, Yasin Genç, Ü. Şebnem Harput, Suna Sabuncuoğlu, Michal Šoral, Gülin Renda and Tibor Liptaj 1693
- Fatty Acid Methyl Ester Composition of Some Turkish Apiaceae Seed Oils: New Sources for Petroselinic Acid**
Nurgün Küçükboyacı, Fatma Ayaz, Nezaket Adıgüzel, Barış Bani and Ahmet Ceyhan Gören 1697
- Chemical Composition of Vietnamese Essential Oils of *Cinnamomum rigidifolium*, *Dasydaschalom longiusculum*, *Fissistigma maclurei* and *Goniothalamus albiflorus***
Juergen K.R. Wanner, Do N. Dai, Le T. Huong, Nguyen V. Hung, Erich Schmidt and Leopold Jirovetz 1701
- Detection and Identification of Antibacterial and Antioxidant Components of Essential Oils by TLC-Biodetection and GC-MS**
Ágnes M. Móricz, Györgyi Horváth, Andrea Böszörményi and Péter G. Ott 1705
- Essential Oils and Their Vapors as Potential Antibacterial Agents against Respiratory Tract Pathogens**
Kamilla Ács, Tímea Bencsik, Andrea Böszörményi, Béla Kocsis and Györgyi Horváth 1709
- Lantana montevidensis* Essential Oil: Chemical Composition and Mosquito Repellent Activity against *Aedes aegypti***
Eugene K. Blythe, Nurhayat Tabanca, Betül Demirci, Maia Tsikolia, Jeffrey R. Bloomquist and Ulrich R. Bernier 1713
- Chemical Composition, Antioxidant, Antimicrobial and Insecticidal Activities of Essential Oil from a Moroccan Endemic Plant: *Bubonium imbricatum***
Abdellah Aghraz, Jürgen Wanner, Erich Schmidt, Loubna Aitdra, Malika Aitsidibrahim, Nurhayat Tabanca, Ali Abbas, Lahcen Hassani, Mohammed Markouk, Leopold Jirovetz and Mustapha Larhsini 1717

Continued inside back cover



Research paper

Synthesis and biological evaluation of new aryl-alkyl(alkenyl)-4-benzylpiperidines, novel Sigma Receptor (SR) modulators, as potential anticancer-agents



Marta Rui ^{a, c, 1}, Daniela Rossi ^{a, 1}, Annamaria Marra ^a, Mayra Paolillo ^b, Sergio Schinelli ^b, Daniela Curti ^d, Anna Tesei ^e, Michela Cortesi ^e, Alice Zamagni ^e, Erik Laurini ^f, Sabrina Pricl ^{f, g}, Dirk Schepmann ^h, Bernhard Wünsch ^h, Ernst Urban ^c, Vittorio Pace ^c, Simona Collina ^{a, *}

^a Department of Drug Sciences, Medicinal Chemistry and Pharmaceutical Technology Section, University of Pavia, Viale Taramelli 6 and 12, 27100, Pavia, Italy

^b Department of Drug Sciences, Pharmacology Section, University of Pavia, Viale Taramelli 6 and 12, 27100, Pavia, Italy

^c MOSE – DEA, University of Trieste, Piazzale Europa 1, 34127, Trieste, Austria

^d Department of Biology and Biotechnology “L. Spallanzani”, Lab. of Cellular and Molecular Neuropharmacology, University of Pavia, Via Ferrata 9, 27100, Pavia, Italy

^e Biosciences Laboratory, Istituto Scientifico Romagnolo per lo Studio e la Cura dei Tumori (IRST) IRCCS, Via P. Maroncelli 40, 47014, Meldola (FC), Italy

^f MOSE – DEA, University of Trieste, Piazzale Europa 1, 34127, Trieste, Italy

^g National Interuniversity Consortium for Material Science and Technology (INSTM), Research Unit MOSE-DEA, University of Trieste, Trieste, Italy

^h Institute of Pharmaceutical and Medicinal Chemistry, University of Muenster, Correnstrasse 48, 48149, Muenster, Germany

ARTICLE INFO

Article history:

Received 20 July 2016

Received in revised form

29 August 2016

Accepted 30 August 2016

Available online 31 August 2016

Keywords:

Sigma Receptor (SR)

Pan-SR modulators

Compound 3 (RC-106)

S1R agonist/antagonist profile

Potential anticancer property

Apoptotic pathway

ABSTRACT

In the early 2000s, the Sigma Receptor (SR) family was identified as potential “druggable” target in cancer treatment. Indeed, high density of SRs was found in breast, lung, and prostate cancer cells, supporting the idea that SRs could play a role in tumor growth and progression. Moreover, a link between the degree of SR expression and tumor aggressiveness has been postulated, justified by the presence of SRs in high metastatic-potential cancer cells. As a consequence, considerable efforts have been devoted to the development of small molecules endowed with good affinity towards the two SR subtypes (S1R and S2R) with potential anticancer activity. Herein, we report the synthesis and biological profile of aryl-alkyl(alkenyl)-4-benzylpiperidine derivatives - as novel potential anticancer drugs targeting SR. Among them, **3** (RC-106) exhibited a preclinical profile of antitumor efficacy on a panel of cell lines representative of different cancer types (*i.e.* Paca3, MDA-MB 231) expressing both SRs, and emerged as a *hit* compound of a new class of SR modulators potentially useful for the treatment of cancer disease.

© 2016 Elsevier Masson SAS. All rights reserved.

1. Introduction

Sigma receptors (SRs) are an enigmatic receptor family localized in plasmatic, mitochondrial and endoplasmic reticulum membranes of several organs including liver, kidney and brain.

Radioligand binding studies and biochemical analyses have shown the presence of two SR subtypes, Sigma 1 (S1R) and Sigma 2 (S2R) receptors with different anatomical distribution, distinct physiological and pharmacological profiles [1–4].

It is well known that S1Rs play critical roles in the mammalian nervous system, indeed their involvement in different neurodegenerative and neuropsychiatric diseases has been well documented [5–8]. Their ligands can yield both cytoprotective or cytotoxic actions. In detail, S1R agonists promote neuroprotection, neurite outgrowth, trophic factor production as well as microglial activation, mitochondrial integrity and reduce production of

* Corresponding author. Department of Drug Sciences, Medicinal Chemistry and Pharmaceutical Technology Section, University of Pavia, Viale Taramelli 12, 27100, Pavia, Italy.

E-mail address: simona.collina@unipv.it (S. Collina).

¹ These Authors equally contributed to this work.

reactive oxygen species [9,10]. As a consequence, S1R agonists display a high therapeutic potential for Central Nervous System (CNS) pathologies such as Amyotrophic Lateral Sclerosis, Multiple Sclerosis, Alzheimer's disease and Parkinson disease [5,11,12]. Conversely, S1R antagonists may play a role in neuropathic pain and anticancer therapy. Overexpression of S1R in high metastatic potential cancer cells, together with the efficacy of the S1R antagonist Rimcazole (Fig. 1) in inhibiting tumor cell survival and in promoting apoptosis in breast cancer cells (MCF-7, MDA-MB-231, MDA-MB-157 and T47D) suggests a link between the degree of S1R expression and tumor growth and aggressiveness [13]. Despite the evidence supporting the importance of S1R in cancer, the mechanism of action of S1R antagonists in causing cell death is still unclear. Currently, it has been hypothesized that the observed apoptotic phenomena are related to the increase of intracellular calcium levels [14–16].

The S2R subtype is still largely unknown: it has not been cloned yet and its molecular structure has not been clarified. In the intracellular environment, S2R binding sites are localized in mitochondria, lysosomes, endoplasmic reticulum, and plasma membrane. Recent studies describe how S2R ligands trigger a cell response which inhibit the activity of the P-glycoprotein, responsible for the active extrusion of anticancer drugs, leading to cell death [17,18]. Moreover, the hypothesis of a correlation between S2R and Progesterone Receptor Membrane Component 1 (PGRMC1) [19,20] supports the idea that S2R may exert a critical role in tumorigenesis [18]. Indeed, the over-expression of PGRMC1 has been associated to tumor stage and to actively proliferating and invasive cancer cells [21]. It is also relevant that proliferating breast carcinoma cells express S2R up to ten times more than quiescent cells, and the degree of S2R expression has been correlated with tumor staging and grading [22–24]. The highest level of S2R has been detected in pancreatic cancer cell lines (Panc-02, Panc-01, CFPAC-1, AsPC-1) [25]. A recent study, carried out on mouse breast cancer (EMT-6) and human melanoma (MDA-MB-435) cell lines, demonstrate that

siramesine (Fig. 1), a S2R selective ligand commonly used as reference compound, can induce cell death (with an EC_{50} in both cell lines lower than $10 \mu\text{M}$) by three different mechanisms: caspase activation, autophagy, and impaired cell-cycle progression [26]. In the same work, it has been also demonstrated that other S2R ligands, *i.e.* SV119, WC-26 and RHM-138 (Fig. 1), possess a cytotoxic effect in the micromolar range in the aforementioned cancer cell lines [26]. Moreover, the same compounds are able to inhibit proliferation of pancreatic cancer cells (human lines: BxPC3, AsPC1, Cfpac, Panc1 and PaCa-2; murine line: Panc02) with an $IC_{50} \leq 100 \mu\text{M}$ [25].

On the bases of the above findings, we reasoned that both S1R antagonist and S2R agonists could be useful tools to address novel and more focused cancer treatments. Hence, SRs could represent an exciting target to develop anticancer drugs with novel mechanisms of action. Our group has previously prepared and characterized a wide series of compounds with preferential affinity towards S1R [29a–d]. In an intriguing observation, we documented that the presence of the bulky 4-benzylpiperidine moiety, while preserving high binding strength for S1R, increases the affinity towards S2R [29c]. Therefore, in the present study we present our efforts aimed at the identification and characterization of potent SR modulators, able to bind both receptor subtypes. Specifically, we report herein

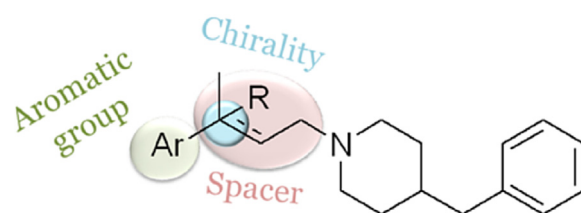


Fig. 2. SAR exploration. Structural elements subjected to variation are highlighted. (For interpretation of the references to colour in this figure legend, the reader is referred to the web version of this article.)

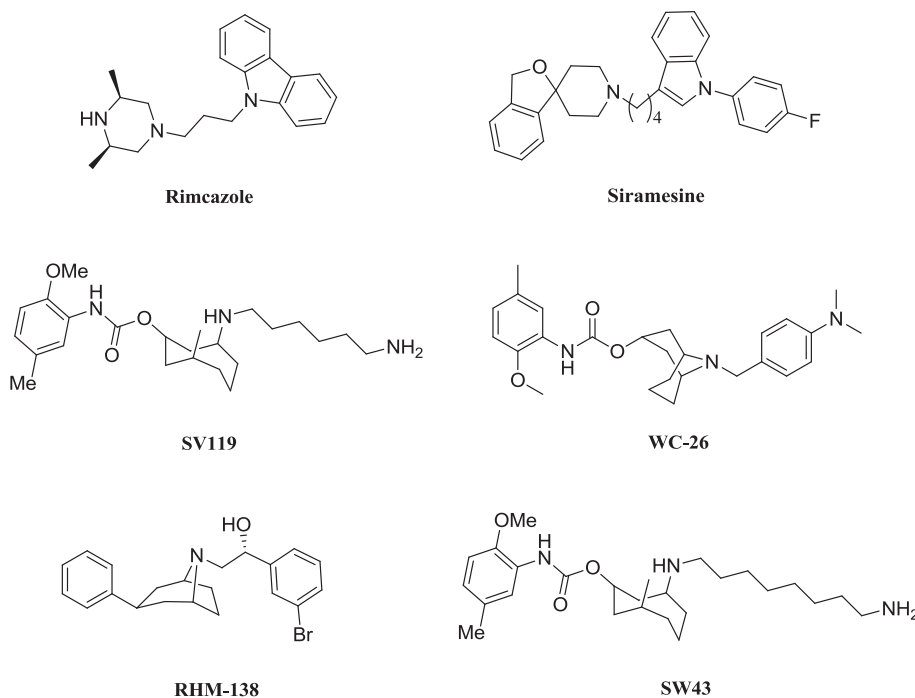


Fig. 1. S1R and S2R compounds able to promote antiproliferative effects. Rimcazole ($KiS1 = 908.0 \pm 99 \text{ nM}$; $KiS2 = 302.0 \pm 37 \text{ nM}$) [27]. Siramesine ($KiS1 = 17.0 \text{ nM}$; $KiS2 = 0.12 \text{ nM}$); SV119 ($KiS1 = 1417.0 \text{ nM}$; $KiS2 = 5.2 \text{ nM}$); WC-26 ($KiS1 = 1436.5 \pm 166.1 \text{ nM}$; $KiS2 = 2.58 \pm 0.59 \text{ nM}$); RHM-138 ($KiS1 = 544.0 \text{ nM}$; $KiS2 = 12.3 \text{ nM}$); SW43 ($KiS1 = 133.0 \text{ nM}$; $KiS2 = 19.0 \text{ nM}$) [28].

the preliminary structure-activity relationship (SAR) (Fig. 2) of arylalkyl(alkenyl)-4-benzylpiperidines with the general structure of Fig. 2. Derivatives **3** and **6** that displayed good affinity toward both receptor subtypes, from now on called pan-SR ligands, were passed for testing *in vitro* cytotoxic activity evaluation. To validate the hypothesis that S1R and S2R modulators could be effective as anticancer drugs, compound **3** was next screened towards a panel of tumor cell lines representative of various cancer types, all expressing both sigma receptors. The results of our studies showed that **3**, called by us RC-106, has interesting anticancer activities against prostate, glioblastoma, pancreas and breast cancer cell lines. The activity against pancreatic PaCa3 cells is of particular interest, being **3** (RC-106) effective against actively proliferating cells ($IC_{50} = 42 \mu\text{M}$) and against cells with reduced proliferation rate ($IC_{50} = 7.0 \mu\text{M}$). The results of this effort are described below.

2. Results

2.1. Chemistry

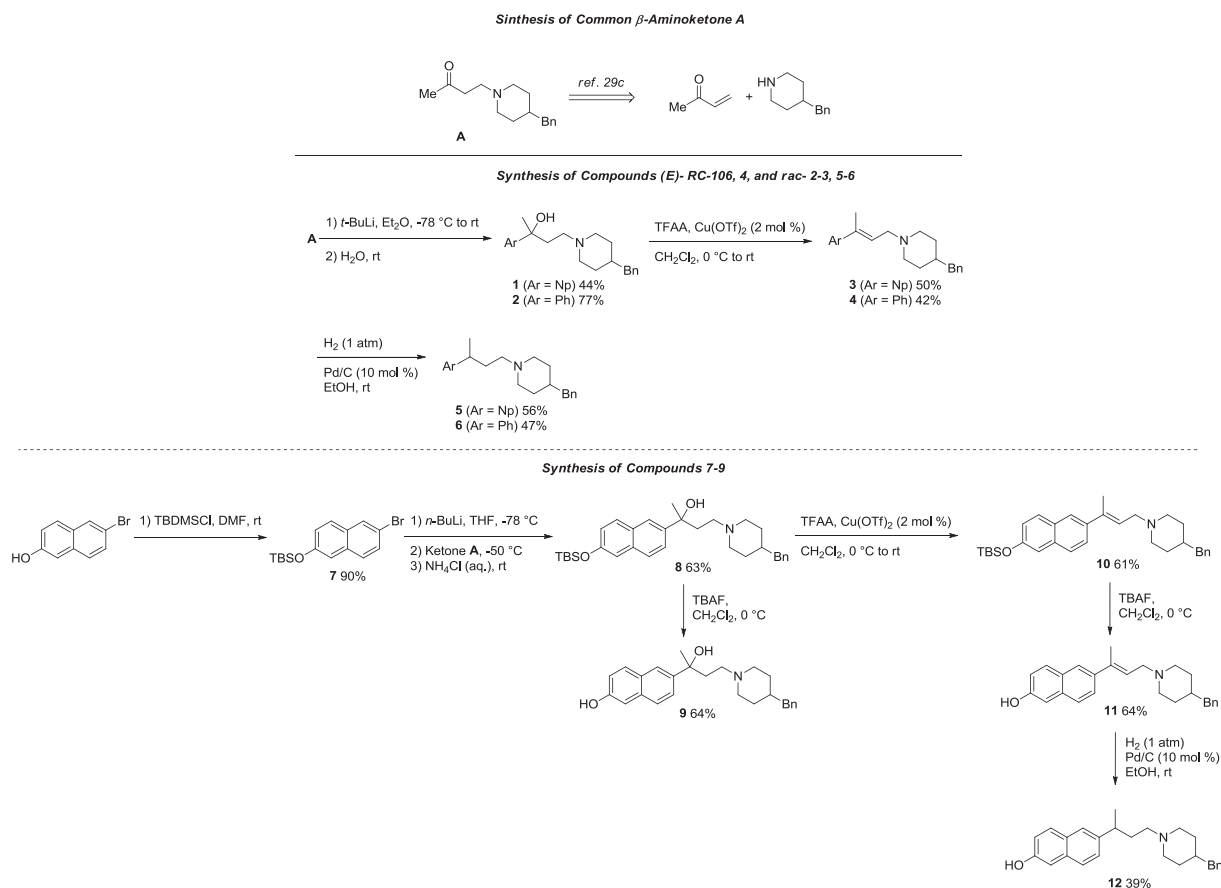
The preparation of compounds **1–12** is summarized in Scheme 1. In cases where a chiral center was present, (semi)preparative chiral chromatography was used to isolate the stereoisomers.

The key intermediate of the synthetic process is the β -aminoketone **A**. The synthetic pathway to obtain **A** was already described by us and involves a Michael addition of 4-benzylpiperidine to but-3-en-2-one in absolute ethanol and glacial acetic acid, followed by purification *via* acid/basic extraction, as reported in our previous work [29c]. The subsequent lithiation reaction at aryl-bromine in anhydrous Et₂O at -78°C with *t*-butyl lithium, followed by

addition/substitution reaction in the presence of the β -amino-ketone **A** and quenching with H₂O, led to isolate crude compounds. After purification *via* acid/basic extraction, **1** and **2** in sufficient amount for the subsequent reaction a suitable purity for biological assay were obtained, as confirmed by ¹H NMR, ¹³C NMR and UHPLC-MS analysis.

Arylalkylaminoalcohols **1** and **2** were treated with trifluoroacetic anhydride in the presence of a catalytic amount of copper triflate, according with a procedure already experimented by us [30]. In this way, compounds **3** and **4**, as (*E*) stereoisomers C2-C3, together with low amounts of the olefinic regioisomers C3-C4, were obtained as evidenced by ¹H NMR. It is worth noting that no signals related to the (*Z*) stereoisomer, which represented the minor product using the standard acidic conditions (37% HCl) [29b] were present in the ¹H NMR of crude products. As a further step, an amount of arylalkenylamines were subjected to catalytic reduction reaction in hydrogen atmosphere in the presence of Pd(0)/C 10% (p/p) in absolute EtOH, giving rise to the corresponding arylalkylamines **5** and **6**. Crude **3–6** were purified using alumina (II Brockmann degree) column chromatography, yielding pure compounds as confirmed by ¹H NMR, ¹³C NMR and UHPLC-MS analysis.

In the case of compounds bearing the hydroxyl group at the naphthyl moiety, an additional step was required, consisting in the protective reaction of the –OH group by *t*-butyldimethylsilyl chloride, thus obtaining **7** which was lithiated in anhydrous THF at -78°C using an excess of *n*-butyl lithium. After 20 min, the aminoketone **A** was added to the C-lithiated intermediate, keeping the temperature below -50°C for 1.5 h. The reaction was quenched with saturated aqueous NH₄Cl and extracted with Et₂O. The crude product was purified by column chromatography giving **8**. An



Scheme 1. Synthesis of compounds **1–12**.

amount of this compound was subjected to an elimination reaction using trifluoroacetic anhydride in the presence of a catalytic amount of copper triflate to give the arylalkenylamine **10** [(*E*) stereoisomer C2-C3] as main compound, easily isolated by column chromatography. Compounds **8** and **10** were then subjected to the deprotection of –OH-aromatic by drop wise addition of tetra-*N*-butylammonium fluoride at 0 °C in argon atmosphere in anhydrous dichloromethane (DCM), to give **9** and **11**, respectively. Lastly, the reduction reaction of **11** using a catalytic amount of Pd (0) in hydrogen atmosphere gave rise to arylalkylamine **12**. With the exception of compound **11**, which was purified by treatment with methanol, pure **9** and **12** were obtained after purification through silica column chromatography. Also in the case of naphthol-derivatives **9** and **11–12**, the identities were confirmed by ¹H NMR, ¹³C NMR and UPLC-MS analysis.

All potential SR modulators **1–6**, **9** and **11–12** were obtained in a sufficient amount and with the appropriate degree of purity for the subsequent biological investigations and, in the case of racemic compound, also for HPLC chiral resolution.

2.2. Chiral resolution

To investigate the relationship between stereochemistry and receptor binding affinity, we prepared enantiomeric **1–2**, **5–6**, **9** and **12**. On the bases of our previous experience, a direct chiral HPLC method of enantiomeric separation was applied, and the scaling up of the process was performed [31a–e]. Baseline separation of racemates was obtained using cellulose and amylose derived chiral stationary phases (Chiralcel OJ-H, Chiralpak IC and Chiralpak IA), under different elution conditions, including different mixtures of *n*-heptane and polar modifiers (methanol, ethanol or 2-propanol) and alcohols (methanol, ethanol and 2-propanol). In all cases 0.1% of diethylamine (DEA) was added to the mobile phase. Moreover, in the case of the Chiralpak IC, the analysis was carried out also in the presence of 0.3% of trifluoroacetic acid (TFA), which improves enantiomer separations. The optimized analytical methods (Table 1, Fig. S11, see Supplementary material) were suitably transferred to the (semi)preparative scale. In detail, enantiomeric **1**, **2**, **5** and **9** were resolved by a (semi)preparative Chiralcel OJ-H column, eluting with ethanol and 0.1% diethylamine (for the compound **1**) or methanol and 0.1% diethylamine (for the compounds **2**, **5** and **9**), whereas compounds **6** and **12** were resolved on (semi)preparative Chiralpak IA, using methanol and 0.1% of diethylamine, in all cases eluting at a flow rate of 2.5 mL/min. The elution conditions applied provided a quick access to the desired enantiomers (Table 2) with enantiomeric excess over than 95%, as evidenced by analytical control of the collected fractions, and in sufficient amount for preliminary biological assays.

2.3. SAR studies

The S1R and S2R binding site affinities of the tested compounds

Table 1
Analytical chiral resolution of **1–2**, **5–6**, **9** and **12**.

Compound	Column	Eluent	K ₁	K ₂	α	Rs
1	Chiralcel OJ-H	A	1.03	1.63	1.58	3.25
2	Chiralcel OJ-H	B	1.24	1.80	1.45	4.05
5	Chiralcel OJ-H	B	3.98	4.80	1.21	2.46
6	Chiralpak IA	B	0.57	0.81	1.42	3.06
9	Chiralcel OJ-H	B	1.10	1.61	1.46	2.62
12	Chiralpak IA	B	0.96	1.27	1.32	2.49

Eluent: A (100% ethanol, 0.1% diethylamine); B (methanol 100%, 0.1% diethylamine), flow rate: 1 mL/min; detection UV at 220 (compounds **2** and **6**) and at 254 nm (compounds **1**, **5**, **9** and **12**).

Table 2
Chiroptical properties of enantiomeric **1–2**, **5–6**, **9** and **12**.

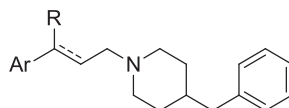
Compound	[α] _D ²⁰ (c% in MeOH)	ee (%) ^a	K
1a	+40.5 (0.2)	96.0	1.03
1b	−42.3 (0.2)	97.0	1.63
2a	+10.5 (0.6)	99.9	1.24
2b	−9.2 (0.6)	98.0	1.80
5a	+6.1 (0.2)	95.0	3.98
5b	−6.3 (0.2)	95.0	4.80
6a	+8.2 (0.3)	99.9	0.57
6b	−8.3 (0.3)	99.9	0.81
9a	+24.2 (0.1)	99.9	1.10
9b	−24.8 (0.1)	99.9	1.61
12^o	+11.8 (0.3)	99.9	0.96
12b	−12.0 (0.3)	99.9	1.27

^a Determined by chiral HPLC under the analytical conditions reported in Table 1.

were determined in competition experiments using radioligands. All compounds were tested on guinea pig brain and rat liver membranes obtained by homogenization, centrifugation, and washing of the respective tissues. S1R binding site assays were performed with [³H]-(+)-pentazocine as radioligand. The S2R binding values were evaluated using [³H]-DTG as radioligand. Compounds with high affinity were tested three times. For compounds with low SR affinity, only one measure was performed. The SR affinities of all compounds towards both S1R and S2R are presented in Table 3.

All compounds, with the only exception of **9a**, **9b** and **12**, showed an interesting affinity towards S1R (K_{S1} ≤ 50 nM) and a good/modest affinity towards S2R, with the exception of compounds **2a**, **2b**, **9** and **12**, which are weak S2R binders. Particularly, all the arylalkylaminoalcohols **1**, **2** and **9** showed a preference affinity towards S1R and the first eluted enantiomers exhibit a slight preferential interaction with the target, in accordance with our previous work [32]. Conversely, SRs do not show stereoselectivity

Table 3
Binding affinities towards S1R and S2R. Values are expressed as mean ± SEM of three experiments.



Compound	Ar	R	K _{S1} ± SEM	K _{S2} ± SEM
1	2-naphtyl	OH	6.9 ± 2	62.5
1a	2-naphtyl	OH	10 ± 2	81 ± 35
1b	2-naphtyl	OH	11 ± 1	79 ± 21
2	Phenyl	OH	9.8 ± 4	57 ± 11
2a	Phenyl	OH	27 ± 9	339 ^a
2b	Phenyl	OH	40 ± 4	240 ^a
3	2-naphtyl	–	12 ± 5	22 ± 3
4	Phenyl	–	0.7 ± 1	47 ± 13
5	2-naphtyl	H	5.6 ± 3	144 ^a
5a	2-naphtyl	H	6.0 ± 0.5	26 ± 9
5b	2-naphtyl	H	6.9 ± 1	98
6	Phenyl	H	2.1 ± 1	6.5 ± 3
6a	Phenyl	H	2.9 ± 0.4	8.9 ± 2.1
6b	Phenyl	H	3.0 ± 0.3	7.9 ± 1.9
9	6-hydroxy naphtyl	OH	27 ± 5	118 ^a
9a	6-hydroxy naphtyl	OH	70 ± 21	68 ± 8
9b	6-hydroxy naphtyl	OH	62 ± 4	905 ^a
11	6-hydroxy naphtyl	–	9.6 ± 3	305 ^a
12	6-hydroxy naphtyl	H	59 ± 5	314 ^a
12a	6-hydroxy naphtyl	H	35 ± 2	582 ^a
12b	6-hydroxy naphtyl	H	13 ± 4	105 ^a

^a Compounds with high affinity were tested three times. For compounds with low SR affinity (>100 nM), only one measure was performed.

towards the enantiomer of arylalkylamines, confirming our previous findings [31a–b]. Of particular interest are compounds **3** and **6** (racemic and enantiomeric), having a good affinity towards both S1R and S2R.

To propose a molecular rationale for the experimental affinity of the new 4-benzylpiperidine derivatives for the S1R, we used our validated three-dimensional model of the S1R [29d,31a–b,33–35]. We applied a consolidated simulation recipe based on free energy of binding (ΔG_{bind}) estimation in the framework of the Molecular Mechanics/PoissonBoltzmann Surface Area (MM/PBSA) computational methodology (Table S11, see Supplementary material) [36]. Taking the naphthalene derivative **3** as a proof-of-concept, the analysis of the corresponding MD trajectory reveals that 4-benzylpiperidine moiety establishes a strong network of polar and hydrophobic interactions with the receptor. As shown in Fig. 3A and B, the piperidine nitrogen atom is engaged in the prototypical salt bridge with the carboxylic side chain of Asp126, while the aliphatic portion of the heterocycle together with the benzyl ring are perfectly encased in the hydrophobic S1R cavity lined by residues Ile128, Phe133, Tyr173 and Leu186. Finally, the naphthalene group of **3** performs stabilizing π interactions with the side chains of Arg119 and Trp121.

For each compound, a quantitative analysis of ligand/protein interactions was next performed via a per-residue deconvolution of the enthalpic contribution to binding (Fig. S13, see Supplementary material). Taking again compound **3** as reference, Fig. 3C shows the resulting interaction spectrum. Substantially, the hydrophobic interactions of **3** with the side chains of residues Ile128, Phe133,

Tyr173, and Leu186 contribute an overall stabilization term to binding equal to -3.25 kcal/mol, while the permanent salt bridge between the N-atom of **3** and the side chain of Asp126 (average dynamic length (ADL) = 4.09 ± 0.04 Å) reflects in a stabilizing contribution of -1.87 kcal/mol. Finally, the important π/π and π/cation interactions (established between the naphthyl ring of the molecule and the indole ring of Trp121 and the cationic side chain of Arg119, respectively) result in a strong enthalpic stabilization of -2.01 kcal/mol.

To sum up, compounds **3** and both racemic and enantiomeric **6** revealed good affinity towards S1R, in agreement with the molecular modeling studies, together with a S2R affinity and therefore they have been selected for a deeper biological investigation.

2.4. Quantification of SRs expression in cancer cell lines

As stated in the introduction section, an appropriate modulation of both receptors could have a synergic effect in inducing tumor cell death. Therefore, the first step of our in depth biological investigation consisted in testing a panel of cancer cell lines representative of different human solid tumors (Table 4) for SRs expression [37–40]. In details, we determined the expression levels of mRNA of S1R and PGRMC1, considered as the S2R binding site, by Real Time RT- Polymerase Chain Reaction (RT-PCR).

The expression values of S1R and PGRMC-1 in CFPAC-1 line are very similar as evidenced by western blot and related densitometric analysis showed in supplementary data (Fig. S14) and for this reason were used as reference values (arbitrary set equal to 1) for

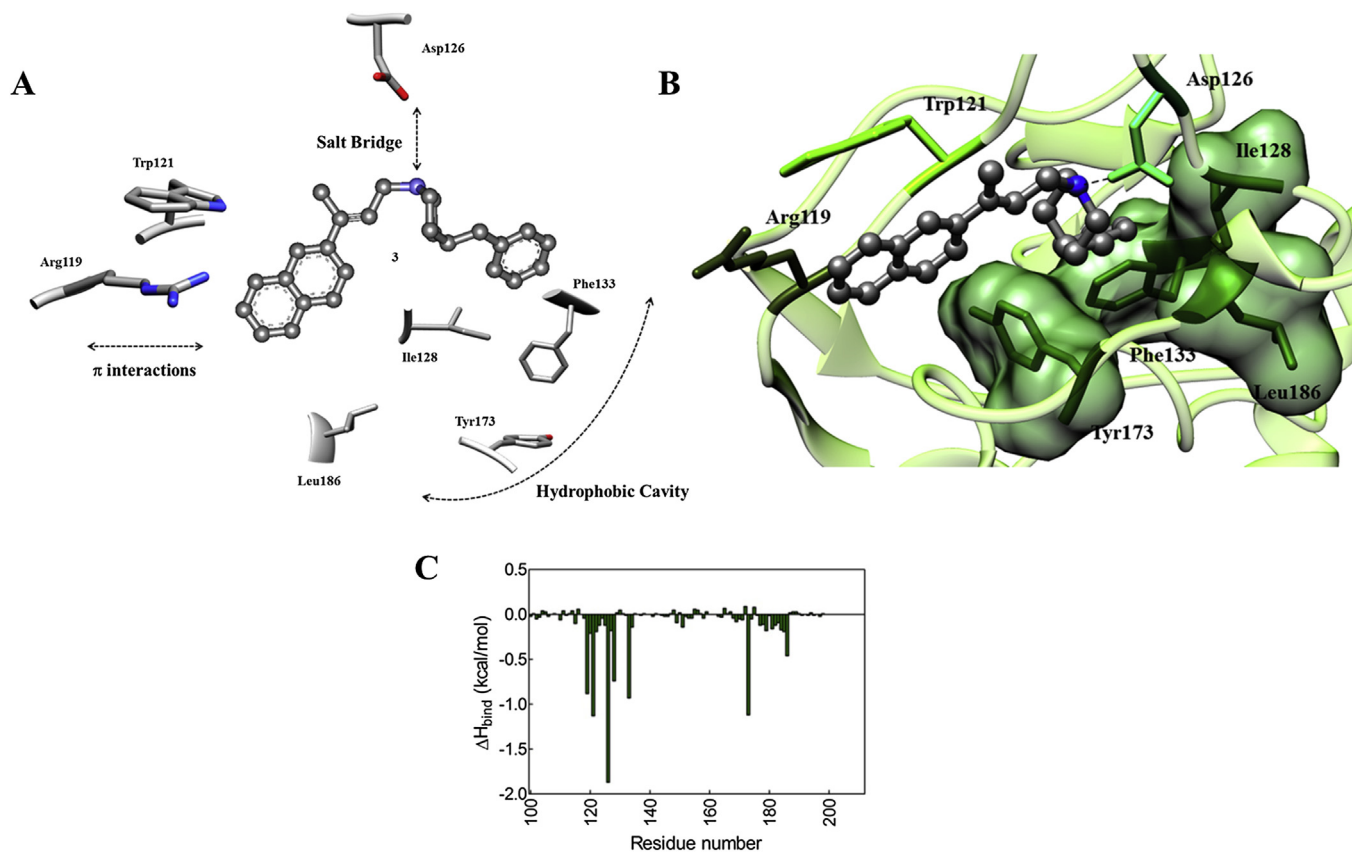


Fig. 3. (A) 2D schematic representation of the identified interactions between the S1R 3D model and **3**. (B) Zoomed view of SR1 in complex with **3**. The compound is in atom colored sticks-and-balls (C, gray; N, blue). Hydrogen atoms, water molecules, ions, and counterions are not shown for clarity. A dashed black line highlights the salt bridge between the S1R D126 side chain and the piperidine nitrogen atom of **3**. (C) Per-residue binding enthalpy ($\Delta H_{\text{bind, res}}$) decomposition for the S1R/**3** complex. Only SR1 amino acids from positions 100 to 200 – most relevant to ligand binding – are shown for clarity. (For interpretation of the references to colour in this figure legend, the reader is referred to the web version of this article.)

Table 4
Tumor cell lines expressing both SR selected for this study.

Cell line	Origin	Tumor source	Morphology
Capan-2	Pancreas	Primary tumor	Epithelial
Paca3	Pancreas	Primary tumor	Epithelial
CFPaC-1	Pancreas	Metastatic site	Epithelial
SUM 159	Breast	Primary tumor	Epithelial
MDA-MB 231	Breast	Metastatic site	Epithelial
PC3	Prostate	Metastatic site	Epithelial
LNCaP	Prostate	Metastatic site	Epithelial
U87	Glioblastoma	Primary tumor	Epithelial

Real Time RT-PCR evaluation of S1R or PGRMC-1 expression in the panel of cell line investigated. As shown in Fig. 4 the highest S1R mRNA expression levels were found in MDA-MB 231, LNCaP and PaCa3 cell lines, whereas PGRMC1 mRNA was found to be highly expressed in PC3, CAPAN-2, and PaCa3 cell lines, respectively.

2.5. Preliminary biological evaluation of **3** and **6**

We perform a preliminary assessment of the anticancer potential of compounds **3** and **6**, showing a good affinity towards SRs, on PaCa3 cells that express both SRs at high level, using siramesine, a well known commercial S2R agonist, and NE100, a S1R antagonist, as reference compounds [26,41]. The effect of compounds **3**, **6**, siramesine and NE100 on cell viability was evaluated by the MTS assay. Cell lines grown in a 10% serum-containing medium were exposed to increasing concentrations of compounds (0.1 μM - 100 μM) for 24 h. Compound **3** showed an interesting cytotoxic activity, comparable to siramesine, whereas compounds **6** and

NE100 exhibited a poor cytotoxic effect (Fig. 5). Since fetal bovine serum (FBS) is enriched in a variety of growth factors and neurosteroids that may interfere and/or mask SR binding sites, the effect of compounds **3** and **6** on PaCa3 was evaluated also in serum-free medium. Interestingly, the decrease of cell viability induced by **3** was enhanced by starvation conditions ($\text{IC}_{50} = 49.8 \pm 4.1 \mu\text{M}$ and $\text{IC}_{50} = 7.0 \pm 0.2 \mu\text{M}$, respectively). A similar effect was observed for siramesine ($\text{IC}_{50} = 45.4 \pm 2.0 \mu\text{M}$ in complete medium and $\text{IC}_{50} = 6.0 \pm 0.3 \mu\text{M}$, in starvation condition). On the contrary, starvation conditions are irrelevant for the cytotoxic properties of **6** and NE100.

According to this data, compound **3**, by now on called RC-106, was selected for further investigation.

2.6. S1R agonist/antagonist profile of compound **3** (RC-106)

Considering that the anticancer activity of a S1R ligands is related to their antagonist profile [13], we investigated the profile of **3** (RC-106) by assessing its *in vitro* ability to modulate NGF-induced neurite outgrowth in PC12 cells. Indeed, S1R agonists are known to potentiate NGF-induced neurite outgrowth when used in the low micromolar concentration range [29c,31a]. In detail, PC12 cells were incubated in a medium containing 0.5% FBS plus NGF (2.5 ng/ml), in the presence of increasing concentrations of **3** (RC-106) (0–10 μM) for 96 h. Subsequently, cells were fixed and those displaying a neurite longer than the diameter of the cell body were counted. Neurite outgrowth was not affected by the addition of **3** (RC-106) up to 1 μM concentration; on the other hand, starting from 2.5 μM neurite outgrowth was completely inhibited (Fig. S13,

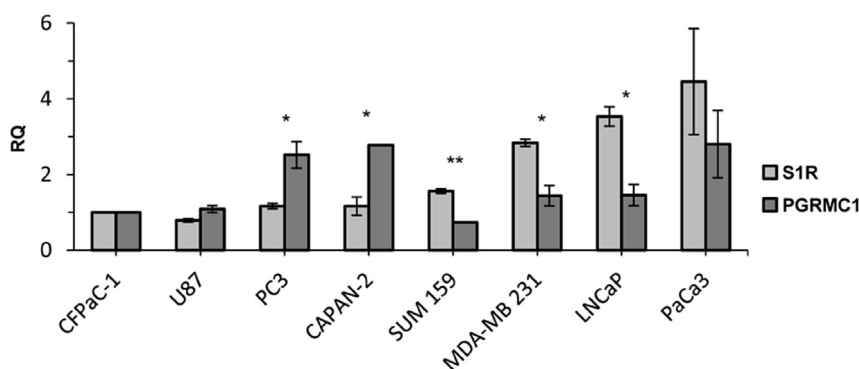


Fig. 4. Relative Quantification (RQ) of the target genes S1R and PGRMC1 RNA expression. The mRNA levels were normalized to the endogenous reference genes GAPDH and HPRT, and quantified respect to the value of S1R or PGRMC-1 found in CFPaC-1 cell line that was arbitrary set equal to 1 (RQ = 1). Values are the mean \pm SD of three independent experiments.

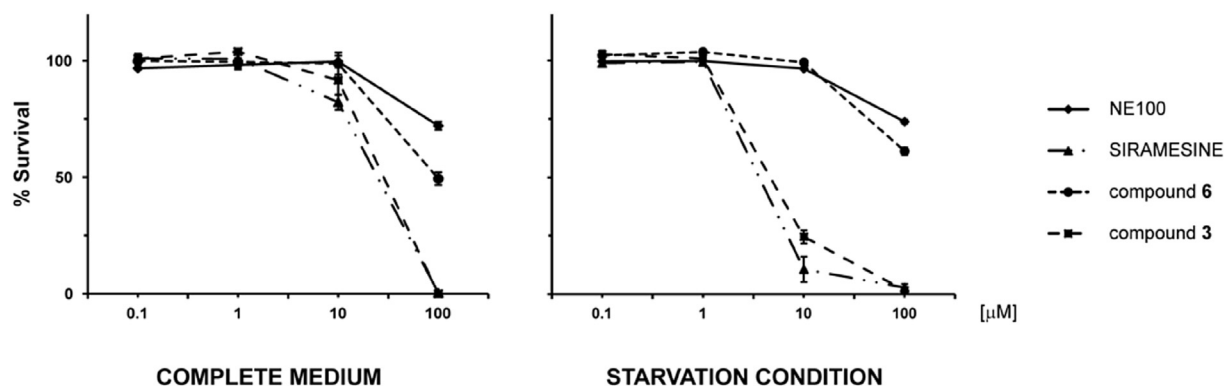


Fig. 5. Effect of different SR modulators. The cells were exposed to compounds NE100, Siramesine, **3** (RC-106) and **6**, for 24 h in the presence or in the absence of 10% FBS. The viability of the cells was determined by MTS assay (mean \pm SD of 3 independent experiments).

see Supplementary material), thus suggesting a S1R antagonist profile. To confirm this hypothesis, competition assays were performed. Specifically, PC12 cells were incubated with the standard S1R agonist PRE-084 (5, 10 and 25 μM) in the absence/presence of **3** (RC-106) at 0.25 or 2.5 μM . At 0.25 μM concentration, compound **3** (RC-106) significantly antagonized the effect of PRE-084 (10 and 25 μM) on NGF-induced neurite outgrowth (Fig. 6). At 2.5 μM concentration, **3** (RC-106) completely blocked NGF-induced neurite sprouting, even in the presence of PRE-084 (results not shown). The results confirm that **3** (RC-106) is a S1R antagonist.

2.7. Effect of **3** (RC-106) on cell viability

The cytotoxic activity of the pan-SR modulator **3** (RC-106) was evaluated by the MTS assay on the panel of cancer cell lines (LNCaP, PC3, U87, Paca3, Capan-2, MDA MB 231, SUM 159) expressing both S1R and S2R. Briefly, cell lines grown in a 10% serum-containing medium were exposed to increasing concentrations of **3** (RC-106) (0.1 μM - 100 μM) for 24 h (Fig. 7). Compound **3** (RC-106) induced a decrease of cell viability in all cell lines starting at 25 μM , with IC_{50} values ranging from 50 μM to 64 μM . The IC_{50} values did not vary significantly by increasing the incubation time up to 48 h, except for the Paca3 cell line, whose IC_{50} value markedly decreased after 48 h incubation (28.73 ± 4.6 , data not shown).

The effect of **3** (RC-106) on U87, Capan-2 and LNCaP cancer cells in the absence of serum-induced cell cycle stimulation was also evaluated. Interestingly, in all the cell lines treated with **3** (RC-106) in serum-free conditions, a marked decrease of cell survival at low compound **3** (RC-106) concentrations compared to cells treated in FBS containing medium, was shown, as evidenced by the low IC_{50} values (9.6–10.5 μM) (Fig. 8). This trend is similar to that already evidenced on PaCa3 cells.

2.8. Study of **3** (RC-106) apoptotic pathway through caspase 3 activation

Lastly, to evaluate whether the observed decrease of cell viability under both conditions was due to apoptosis, TUNEL and Annexin V stainings (analyzed by FACS) and caspase 3 activation

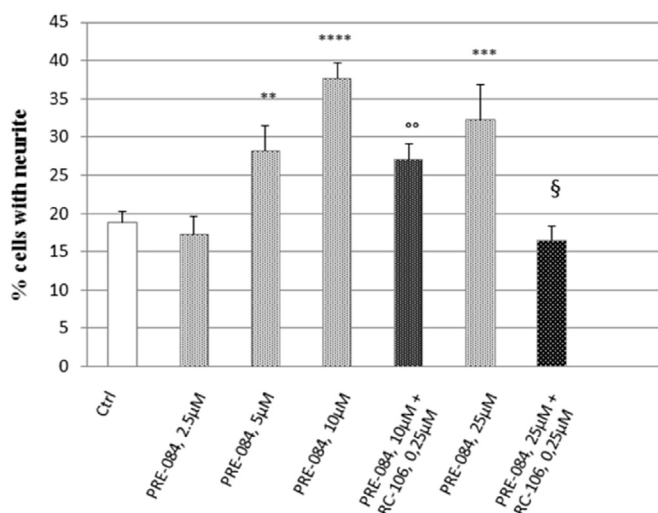


Fig. 6. Assay of NGF-induced neurite outgrowth in PC12 cells. Effect of PRE-084 alone or in combination with **3** (RC-106), at 0.25 μM . Histograms represent the mean \pm sem of at least 5 different experiments performed in triplicate. ** = $p < 0.005$; *** = $p < 0.0008$; **** = $p < 0.000004$ vs control (0 PRE-084). oo = $p < 0.007$; ooo = $p < 0.00004$ vs PRE-084 10 μM and § = $p < 0.004$ vs PRE-084 25 μM .

(western blot, WB) were performed on PaCa3 cells, the tumor line displaying also the highest PGRMC1 mRNA levels. Moreover, according to Zeng C. et al. [42] we adopted caspase 3 assay in order to clarify the S2R agonist/antagonist profile of **3** (RC-106).

The TUNEL assay showed that in serum containing medium a significant induction of apoptosis after 24 h exposure to **3** (RC-106) could be observed only at 25 μM concentration (Fig. 9A). This result is supported by the detection of the cleaved form of caspase 3 by WB analysis (Fig. 9C) and by the Annexin V assay. In these FACS experiments, a significant increase of early and late apoptotic cells ($43.1\% \pm 3.4$ and $34.1\% \pm 8.2$, respectively) at 25 μM compound **3** (RC-106) was detected (Fig. 9B).

When the same experiments were repeated under serum-free conditions (Fig. 10), a significant increase of apoptotic cells was detected by FACS analysis. In particular, at 10 μM , **3** (RC-106) induces significant apoptosis in PaCa3 cells (early apoptotic cells = $10.9\% \pm 0.0$ and late apoptotic cells = $17.2\% \pm 0.6$). The apoptosis induction was further confirmed by WB detection of cleaved caspase 3, after exposure of the cells at the same **3** (RC-106) concentration.

The apoptotic effect of compound **3** (RC-106) is caspase-dependent, as evidenced by WB assay. Therefore, through this functional assay, we can conclude that **3** (RC-106) is a S2R agonist.

PaCa3 cells were exposed to 24 h starvation-condition and to 10 μM compound **3** (RC-106) and the percentage of apoptotic cells was compared in untreated cells (UTR). (A) TUNEL assay: the values are the mean \pm SD of 3 individual experiments. * $p < 0.05$ (B) Representative images of FACS analysis of apoptosis by Annexin V test. (C) WB analysis of apoptotic-related markers. Images are representative of two independent experiments.

3. Discussion

On the basis of recent literature evidences, we hypothesized that pan-SR modulators can evoke anticancer activity. However, the design of new such compounds represents a major challenge, since no structural information is currently available on S2R, which could enable the adoption of effective techniques such as *e.g.*, computer-aided drug design. Notwithstanding these difficulties, and with this new goal in mind, we capitalized our previous work [29c], according to which the presence of a bulky aminic portion seemed to be an important feature in favoring ligand binding to both receptors. Therefore, we designed a new molecular series of aryl-alkyl(alkenyl) 4-benzylamines. The chemical strategy to obtain compounds **1–6**, **9** and **11–12** followed a divergent synthesis, based on the initial preparation of the common β -aminoketone intermediate **A**, easily obtainable via Michael chemistry (Scheme 1) [29c]. Accordingly, the smooth bromo-lithium exchange on the appropriate aryl bromide afforded the lithiated arene that, upon quenching with β -aminoketone **A**, gave the tertiary alcohols **1–2** in high yields. The subsequent dehydration with trifluoroacetic anhydride under $\text{Cu}(\text{OTf})_2$ catalysis conditions [30] afforded a mixture of olefinic regioisomers C3-C4 and the *E* stereoisomer C2-C3. After purification, olefins **3** and **4** were isolated and finally hydrogenated to access the desired amines **5** and **6**. The same strategy was applied for accessing hydroxylated compounds **9** and **11–12**. However, the protection of the aromatic alcohols as TBS ethers (and their corresponding removal) was required to avoid interference with the lithiation step. Concerning the synthetic pathway of **9** and **11–12**, two additional observations are worth at this point: *i*) the lithiation of the protected TBS-bromonaphthols with *n*-BuLi in THF performed better than the *t*-BuLi/Et₂O based method, and *ii*) keeping temperature below -50 $^{\circ}\text{C}$ after quenching with β -aminoketone **A** improved the efficiency of the alcohol synthesis. In the case of racemic compounds, a (semi)preparative chiral high performance

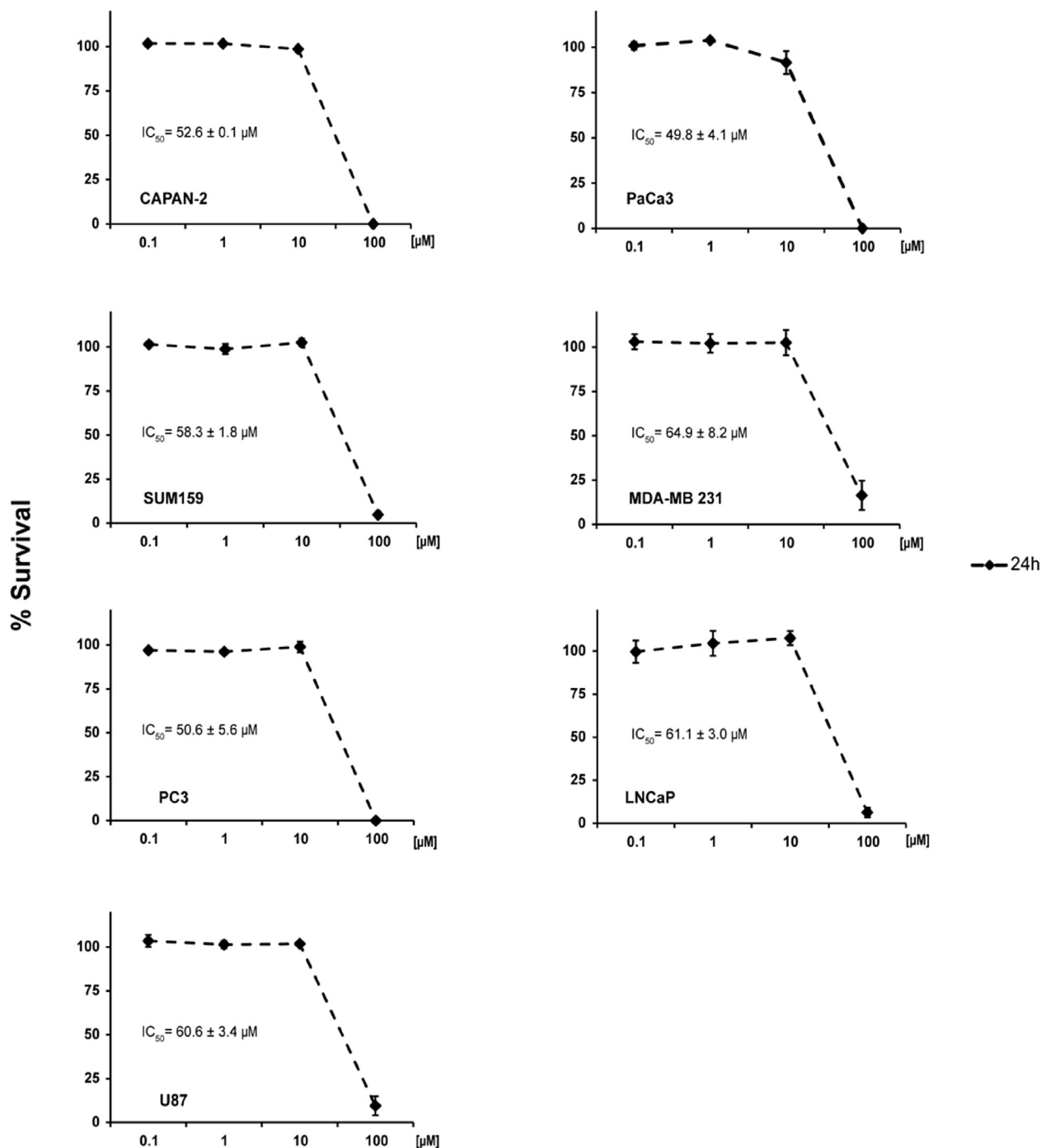


Fig. 7. Effect of **3** (RC-106) on cell viability was evaluated on a panel of cancer cell lines with different histotypes. Cells were exposed to the drug for 24 h in a 10% FBS containing medium. Cell viability was determined by the MTS assay (average of three independent experiments ± SD).

liquid chromatography (HPLC) resolution process was performed and the pure enantiomers obtained in amounts sufficient to support a preliminary biological investigation. All compounds showed – *in silico* and *in vitro* – very high/good affinity for the S1R, with K_iS1 values in the range 0.7–120 nM (Table 1, Tables S11 and S12, see Supplementary material). Molecular modeling revealed that the main molecular requirements for high S1R affinity (*i.e.*, the instauration of the prototypical salt bridge involving the ligand basic N atom and the carboxylic side chain of Asp126, the encasement of an aromatic portion of the ligand within the hydrophobic

S1R cavity lined by residues Ile128, Phe133, Tyr173 and Leu186, and the generation of a set of further stabilizing ligand/receptor π interactions) were all satisfied by the present series of compounds.

Keeping in mind that the purpose of the work was the identification of dual S1R and S2R ligands, compounds **3**, called by us RC-106, and **6** have been selected for a preliminary investigation of their cytotoxic properties, being the molecules in the full series endowed with a good affinity towards both receptor subtypes [**3** (RC-106) K_iS1 = 12.0 ± 5.0 nM; K_iS2 = 22.0 ± 3.0 nM; **6** K_iS1 = 2.1 ± 1.0; K_iS2 = 6.5 ± 3.0]. The preliminary biological

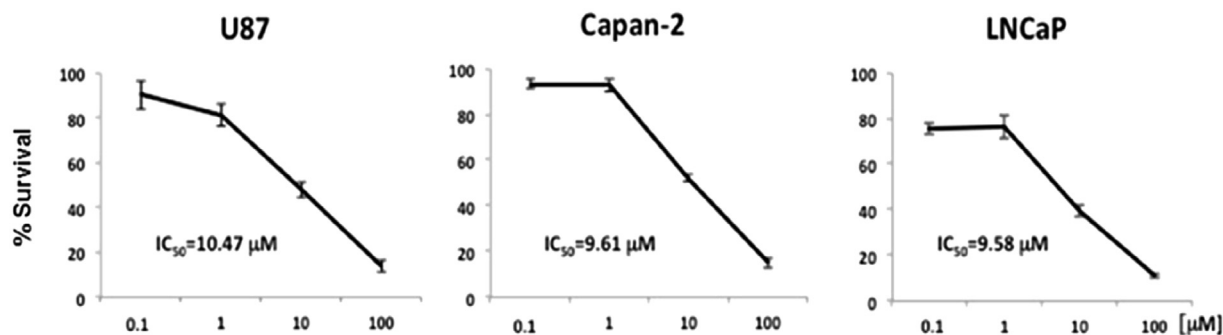


Fig. 8. MTS assay in serum-free conditions. After a 24 h starvation, cell lines were treated for 24 h with the indicated concentrations of **3** (RC-106). Data are expressed as percent of control values \pm standard deviation.

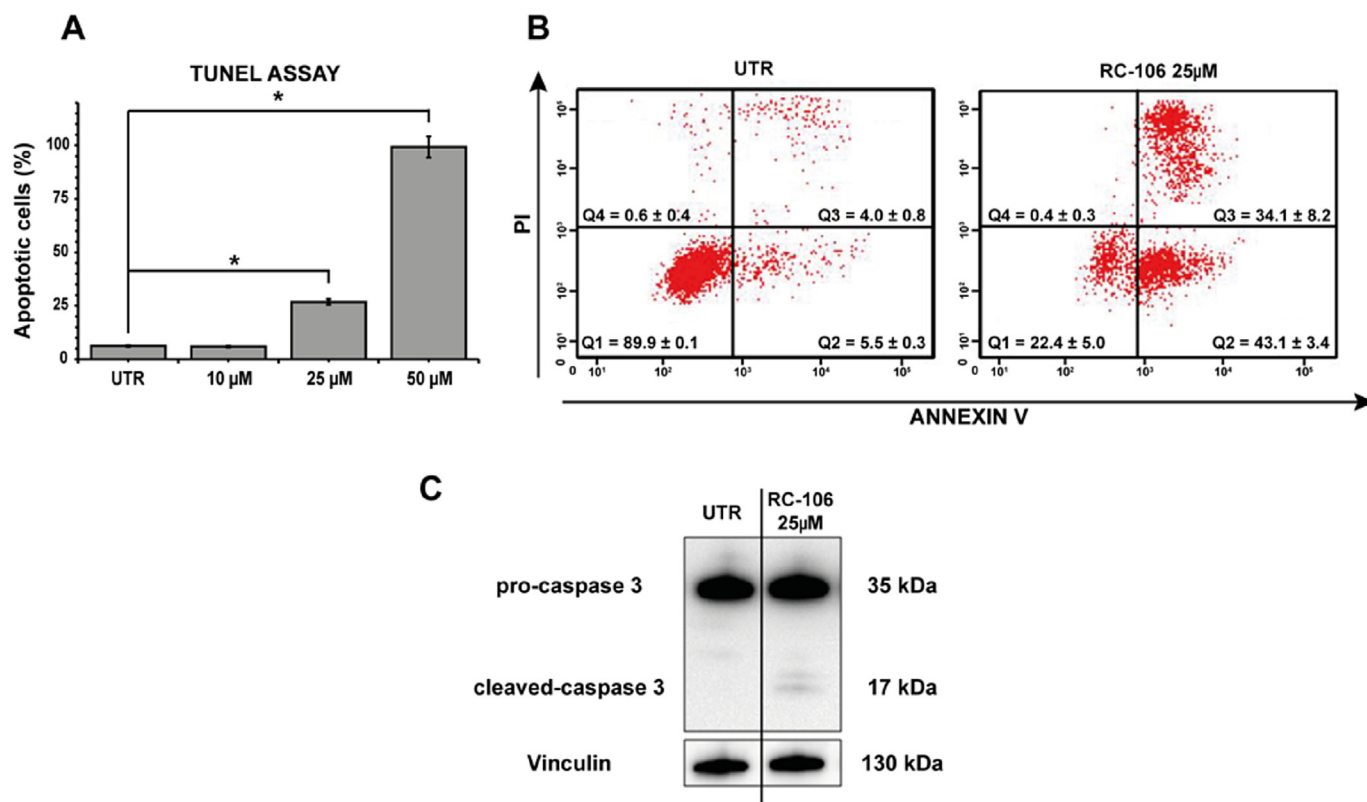


Fig. 9. Apoptosis and apoptotic-related markers analysis in Paca3 cells grown in 10% FBS complete medium. (A) TUNEL assay. Percentage of apoptotic cells after 24 h exposure to compound **3** (RC-106) at 10, 25 and 50 μ M * p < 0.05. (B) Cytofluorimetric (FACS) analysis of apoptosis by Annexin V test. Cells were exposed for 24 h to compound **3** (RC-106) (25 μ M). Q1 area represents viable cells; Q2 early-apoptotic cells; Q3 late-apoptotic cells; Q4 necrotic cells. The images are representative of three experiments. (C) WB analysis of apoptotic-related marker after 24 h exposure to **3** (RC-106) at 25 μ M. Images are representative of two independent experiments.

evaluation of **3** (RC-106) and **6** were carried out using PaCa3 cell line (MTS assay) considering the high level of expression of both SRs. For comparative purposes, the effects of siramesine (S2R agonist) and NE100 (S1R antagonist) were also evaluated. Compounds **3** (RC-106) and siramesine showed an interesting anti-proliferative activity, both in complete medium and in starvation conditions. Conversely, compound **6** and NE100 showed poor cytotoxic properties and therefore **6** were discarded.

To in depth characterize **3** (RC-106) from a functional point of view, we assessed its S1R agonist/antagonist profile on NGF-induced neuronal differentiation in PC12 cells model [43]. Indeed, it has been reported that S1R agonists, such as (+)-pentazocine, imipramine, fluvoxamine, PRE-084 and RC-33, among the others, potentiate NGF-induced neurite outgrowth in PC12 cells, and that

selective S1R antagonist (such as NE-100 and BD1063) significantly attenuate the efficacy of S1R agonists both in the same *in vitro* assay [29c,43–47]. Our results (Fig. 6) clearly show that compound **3** (RC-106) has a S1R antagonist profile.

We then investigated the cytotoxic activity of **3** (RC-106) on a panel of tumor cell lines representative of various cancer types all expressing both SRs. In particular, with regard to S2R, we evaluated PGRMC1 mRNA by RT-PCR as equivalent to S2R expression, even if the actual identity of S2R is still controversial [20,40–54]. When we tested the effect of **3** (RC-106) on actively proliferating tumor cell lines, we observed significant cytotoxicity at concentrations starting from 10 μ M in all the cell lines under investigation. Interestingly, **3** (RC-106) showed cytotoxic effect in all the cell lines tested under low proliferation conditions induced by serum deprivation.

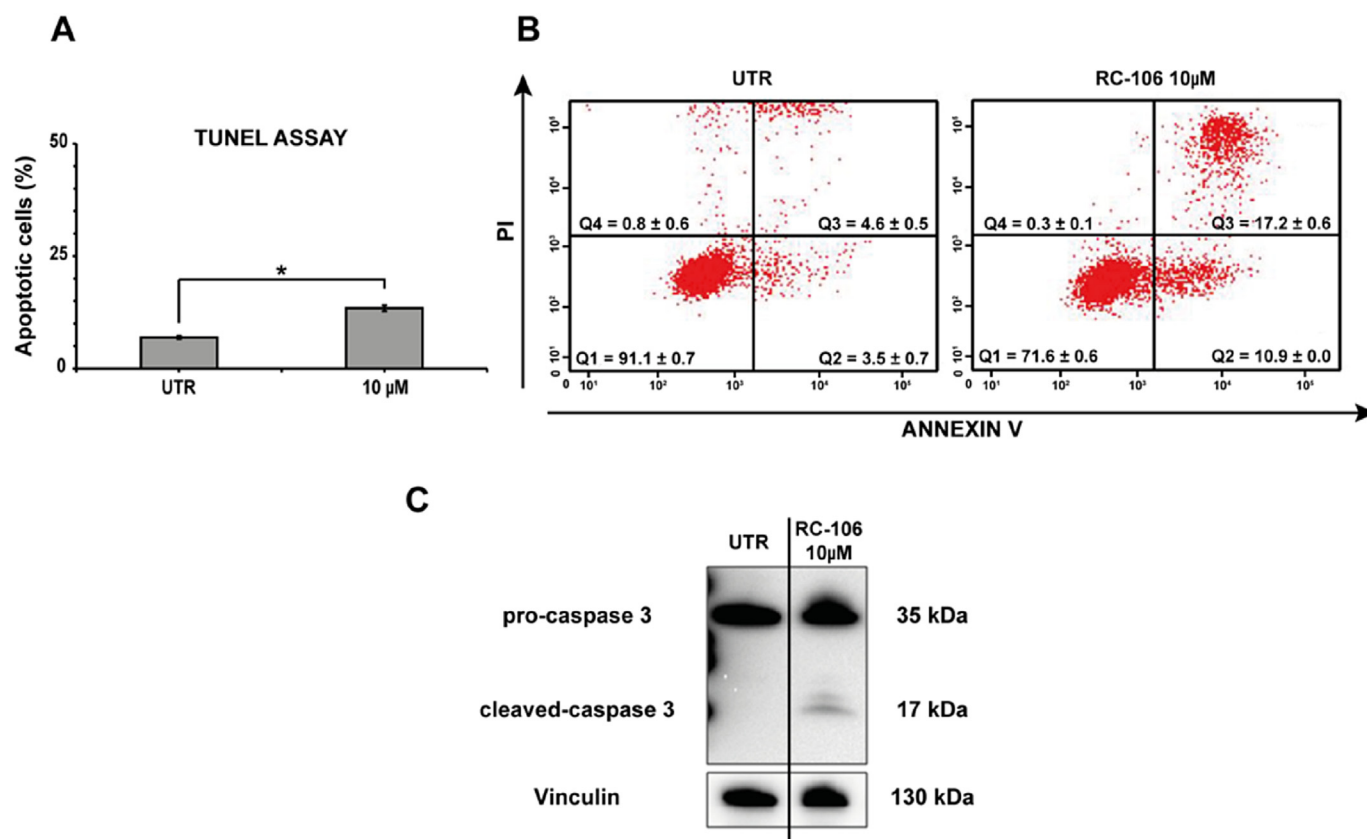


Fig. 10. Apoptosis and apoptotic-related markers analysis in Paca3 cells.

In particular, our data indicated that a short term starvation (24 h) enhances the cytotoxic effect of **3** (RC-106), as evidenced by the low IC_{50} values detected and by the low dose of **3** (RC-106) needed to trigger apoptotic mechanism under these conditions. This result is also in agreement with recent data from pre-clinical models showing that short term starvation may be able to potentiate the effectiveness of chemotherapy and radiotherapy [55–59]. Several clinical trials are currently studying the effect of fasting or fasting-mimic diets in patients undergoing chemotherapy (NCT01304251, NCT01175837, NCT00936364, NCT01175837, NCT01802346, NCT02126449). Importantly, the apoptotic effect of **3** (RC-106) is caspase-mediated both in normal and in starvation conditions, evidencing the S2R the agonist profile of **3** (RC-106).

To sum up, we identified a S1R antagonist and a S2R agonist exerting an interesting cytotoxic action toward a panel of tumor cell lines (pancreas, breast, prostate and glioblastoma) both in complete medium and under starvation conditions. Our data also suggest that the observed decrease of cell viability is due to an apoptotic process triggered by **3** (RC-106).

4. Conclusion

There is increasing evidence that both S1R and S2R play a significant role in cancer biology, therefore modulator of both SR subtypes could be of high interest for developing novel anti-cancer drugs. In this scenario, we report the design and synthesis of a compound series targeting both SR subtypes with high affinity. Among these, we identified **3** (RC-106), a compound able to induce a strong cytotoxic effect in a wide panel of cancer cell lines, all expressing SRs, both actively proliferating and in low proliferation rate in response to serum deprivation. The antitumor properties of

3 (RC-106) have been observed in all cell lines independently from tumor histotype. In particular, in pancreatic PaCa3 cells, the cell line expressing the highest levels of both receptors, **3** (RC-106) acts as pro-apoptotic drug, inducing a fast triggering of cell death program.

To sum up, **3** (RC-106) exhibited a promising cytotoxic activity on a panel of cancer cell lines of different tumors, representative of various cancer expressing both SRs. This compound could meet the requirements of new-generation drugs to enter into the so-called basket trials, consisting in treating several neoplastic diseases, all characterized by the same molecular alterations, in this case represented by high expression of S1R or S2R or both [60]. Lastly, it has to be underlined that S1R antagonists can be used for alleviating chronic pain, especially in conditions such as neuropathic pain, a pathologic condition that frequently occurs in cancer patients [61–63]. Accordingly, the identification of new, potent pan-sigma receptor modulators will be of great interest, to develop anti-tumor and analgesic drugs, representing an innovative pharmacological approach for the treatment of cancer patients with advanced disease. Therefore, **3** (RC-106) represents the *hit* compound of a new class of dual-action ligands targeting S1R and S2R potentially useful for the treatment of cancer disease. Moreover, the evaluation of the antinociceptive properties of **3** (RC-106) is under investigation and will be reported in due course.

5. Experimental section

5.1. General remarks

Reagents and solvents for synthesis were obtained from Aldrich (Italy). Solvents were purified according to the guidelines in Purification of Laboratory Chemicals. Melting points were measured on

SMP3 Stuart Scientific apparatus and are uncorrected. Analytical thin-layer-chromatography (TLC) was carried out on silica gel precoated glass-backed plates (Fluka Kieselgel 60 F254, Merck) and on aluminiumoxid precoated aluminium-backed plates (DC-Alu-folien Aluminiumoxid 60 F254 neutral, Merck); visualized by ultraviolet (UV) radiation, acidic ammonium molybdate (IV), or potassium permanganate. Flash chromatography (FC) was performed with Silica Gel 60 (particle size 230–400 mesh, purchased from Nova Chimica) and neutral aluminium oxide (particle size 0.05–0.15 mm, purchased from Fluka). Proton nuclear magnetic resonance (NMR) spectra were recorded on a Bruker Avance 500 spectrometer operating at 500 MHz. Proton chemical shifts (δ) are reported in ppm with the solvent reference relative to tetramethylsilane (TMS) employed as the internal standard (CDCl_3 , $\delta = 7.26$ ppm). The following abbreviations are used to describe spin multiplicity: s = singlet, d = doublet, t = triplet, q = quartet, m = multiplet, br = broad signal, dd = doublet-doublet, td = triplet-doublet. The coupling constant values are reported in Hz. ^{13}C NMR spectra were recorded on a 500 MHz spectrometer, with complete proton decoupling. Carbon chemical shifts (δ) are reported in ppm relative to TMS with the respective solvent resonance as the internal standard (CDCl_3 , $\delta = 77.23$ ppm).

UHPLC-UV-ESI/MS analysis were carried out on a Acquity UPLC Waters LCQ FLEET system using an ESI source operating in positive ion mode, controlled by ACQUITY PDA and 4 MICRO (Waters). Analyses were run on a ACQUITY BEH C18 (50×2.1 mm, $1.7 \mu\text{m}$) column, at room temperature, with gradient elution (solvent A: water containing 0.1% of formic acid; solvent B: methanol containing 0.1% of formic acid; gradient: 10% B in A to 100% B in 3 min, followed by isocratic elution 100% B for 1.5 min, return to the initial conditions in 0.2 min) at a flow rate of 0.5 mL min^{-1} . All of the final compounds had 95% or greater purity.

Chiral HPLC runs were conducted on a Jasco (Cremella, LC, Italy) HPLC system consisting of PU-1580 pump, 851-AS auto-sampler, and MD-1510 Photo Diode Array (PDA) detector. Experimental data were acquired and processed by Jasco Borwin PDA and Borwin Chromatograph Software. Solvents used for chiral chromatography were HPLC grade and supplied by Carlo Erba (Milan, Italy). Chiral analytical columns: Chiralcel OJ-H (4.6 mm diameter \times 150 mm length, $\text{dp } 5 \mu\text{m}$), Chiralpak IC (4.6 mm diameter \times 250 mm length, $\text{dp } 5 \mu\text{m}$) and Chiralpak IA (4.6 mm diameter \times 250 mm length, $\text{dp } 5 \mu\text{m}$). Analytes were detected photometrically at 220 and 254 nm. Unless otherwise specified, sample solutions were prepared dissolving analytes at 1 mg/mL in ethanol and filtered through $0.45 \mu\text{m}$ PTFE membranes before analysis. The injection volume was $10 \mu\text{L}$. Detection was performed at 220 and 254 nm. The retention factor (k) was calculated using the equation $k = (t_{\text{R}} - t_0)/t_0$, where t_{R} is the retention time and t_0 the dead time (t_0 was considered to be equal to the peak of the solvent front and was taken from each particular run). The enantioselectivity (α) and the resolution factor (R_s) were calculated as follows: $\alpha = k_2/k_1$ and $R_s = 2(t_{\text{R}2} - t_{\text{R}1})/(w_1 + w_2)$ where $t_{\text{R}2}$ and $t_{\text{R}1}$ are the retention times of the second and the first eluted enantiomers, and w_1 and w_2 are the corresponding base peak widths. All HPLC analyses were performed at room temperature.

The best conditions found by the screening protocol were applied to a (semi)preparative scale-up. The enantiomers of **1**, **2**, **5** and **9** were then completely resolved by a (semi)preparative process using a Chiralcel OJ-H column (10 mm diameter \times 250 mm length, $5 \mu\text{m}$), eluting with ethanol (for the compound **2**) or methanol (for the compounds **3**, **5** and **8**) at RT with a flow rate of 2.5 mL/min. Compounds **6** and **12** were resolved on Chiralpak IA (10 mm diameter \times 250 mm length, $5 \mu\text{m}$) using MeOH at a flow rate of 2.5 mL/min as eluent. The eluate was fractionated according to the UV profile (detection performed at 220 and 254 nm). The

fractions obtained containing the enantiomers were evaporated at reduced pressure. Analytical control of collected fractions was performed using the analytical columns.

Optical rotation values of enantiomeric compounds were measured on a Jasco photoelectric polarimeter DIP 1000 using a 0.5 dm cell and a sodium and mercury lamp ($\lambda = 589 \text{ nm}$, 435 nm); sample concentration values are given in $10^{-2} \text{ g mL}^{-1}$ (Table 2).

5.2. General procedure for the preparation of compounds **1** and **2**

Under nitrogen atmosphere, *tert*-BuLi (2.5 equiv, 1.7 M in pentane) was added dropwise to a -78°C cooled solution of the appropriate aryl bromide (1.25 equiv) in anhydrous diethyl ether (20 mL). After 20 min the reaction was slowly allowed to reach room temperature. The stirring was continued for 1 additional hour and a solution of 4-(4-benzylpiperidin-1-yl)-butan-2-one (1.0 equiv) in anhydrous diethyl ether (6 mL) was then added dropwise at -78°C . The reaction mixture was slowly warm to 0°C , stirred for 3 h and then quenched with water (12 mL); after an acid (pH = 3–4)/base (pH = 8–9) work-up, the combined organic phases were evaporated under vacuum to get the desired compounds.

5.2.1. 4-(4-benzylpiperidin-1-yl)-2-(naphthalen-2-yl)butan-2-ol, [**1**]

Yield: 44%; white solid; mp: $105\text{--}107^\circ\text{C}$; IR (cm^{-1}): 3434, 2918, 1653, 1438, 1156, 1112, 820; ^1H NMR (500 MHz) (CDCl_3) δ (ppm): 8.01 (s, 1H), 7.86–7.81 (m, 3H), 7.47–7.45 (m, 3H), 7.28 (t, $J = 7.8$ Hz, 2H), 7.19 (t, $J = 7.0$ Hz, 1H), 7.13 (d, $J = 7.1$ Hz, 2H), 3.19 (d, 1H), 2.54–2.50 (m, 3H), 2.31 (m, 1H), 2.22–2.14 (m, 2H), 1.92 (d, 1H), 1.84 (m, 1H), 1.76 (m, 1H), 1.68 (m, 1H), 1.60 (m, 1H), 1.57 (s, 3H), 1.50 (m, 1H), 1.31 (m, 2H); ^{13}C NMR (500 MHz) (CDCl_3) δ (ppm): 146.3, 140.5, 133.3, 132.0, 129.1, 128.2, 128.1, 127.6, 127.4, 125.8, 125.4, 123.8, 123.6, 75.7, 55.1, 54.8, 52.6, 43.1, 37.8, 37.4, 32.6, 32.1, 31.4; UHPLC-ESI-MS: $t_{\text{R}} = 2.03$, >99.9% pure ($\lambda = 225 \text{ nm}$), $m/z = 374$ [$\text{M} + \text{H}$] $^+$

5.2.1.1. (+)-4-(4-benzylpiperidin-1-yl)-2-(naphthalen-2-yl)butan-2-ol, [(+)-**1**]. White solid; $[\alpha]_{\text{D}}^{20} = +40.5$ (c 0.2, CH_3OH). The IR and NMR spectra are identical to that of **1**. HPLC: $t_{\text{R}} = 8.5$ min, ee 96.0%.

5.2.1.2. (-)-4-(4-benzylpiperidin-1-yl)-2-(naphthalen-2-yl)butan-2-ol, [(-)-**1**]. White solid; $[\alpha]_{\text{D}}^{20} = -42.3$ (c 0.2, CH_3OH). The IR and NMR spectra are identical to that of **1**. HPLC: $t_{\text{R}} = 11.1$ min, ee 97.0%.

5.2.2. 4-(4-benzylpiperidin-1-yl)-2-phenylbutan-2-ol, [**2**]

Yield: 77%; white solid; mp: $90.9\text{--}93^\circ\text{C}$; IR (cm^{-1}): 3184, 3125, 1602, 1369, 1343, 1156, 846, 699; ^1H NMR (500 MHz) (CDCl_3) δ (ppm): 7.45 (d, $J = 8.9$ Hz, 2H), 7.33 (t, $J = 8.1$ Hz, 2H), 7.27 (t, $J = 7.4$ Hz, 2H), 7.21–7.19 (m, 2H), 7.13 (d, $J = 7.0$ Hz, 2H), 3.15 (d, 1H), 2.54 (m, 1H), 2.52 (m, 2H) 2.30 (m, 1H), 2.22 (m, 1H), 2.07 (m, 1H), 1.86 (m, 1H), 1.80 (m, 1H) 1.75 (m, 1H), 1.67 (m, 1H) 1.60 (m, 1H), 1.50 (m, 1H), 1.49 (s, 3H) 1.31 (m, 2H); ^{13}C NMR (500 MHz) (CDCl_3) δ (ppm): 148.9, 140.5, 129.1, 127.9, 128.2, 126.0, 125.8, 125.0, 75.5, 55.1, 54.8, 52.6, 43.1, 37.8, 37.7, 32.6, 32.1, 31.4; UHPLC-ESI-MS: $t_{\text{R}} = 1.75$, >97% pure ($\lambda = 210 \text{ nm}$), $m/z = 324$ [$\text{M} + \text{H}$] $^+$

5.2.2.1. (+)-4-(4-benzylpiperidin-1-yl)-2-phenylbutan-2-ol, [(+)-**2**]. Yellow oil; $[\alpha]_{\text{D}}^{20} = +10.5$ (c 0.6, CH_3OH). The IR and NMR spectra are identical to that of **2**. HPLC: $t_{\text{R}} = 3.4$ min, ee 99.9%.

5.2.2.2. (-)-4-(4-benzylpiperidin-1-yl)-2-phenylbutan-2-ol, [(-)-**2**]. Yellow oil; $[\alpha]_{\text{D}}^{20} = -9.2$ (c 0.6, CH_3OH). The IR and NMR spectra are identical to that of **2**. HPLC: $t_{\text{R}} = 4.2$ min, ee 98.0%.

5.3. General procedure for the preparation of compounds **3** and **4**

Under argon atmosphere trifluoroacetic anhydride (2.0 equiv) was added dropwise to a solution of the tertiary alcohol (1.0 equiv) and copper triflate (2 mol %) in anhydrous dichloromethane (5 mL) cooled to 0 °C. After stirring the reaction a solution of NaHCO_{3(aq)} (5%) was added. The phases were separated and the organic phase was dried over anhydrous Na₂SO₄ and concentrated under reduced pressure. The obtained crude was purified by alumina (II Brockmann degree) column chromatography (9 *n*-hexane – 1 ethyl acetate).

5.3.1. (*E*)-4-benzyl-1-[3-(naphthalen-2-yl)but-2-en-1-yl]piperidine, [**3**]

Yield: 50%, yellow solid; mp: 221–222 °C; IR (cm⁻¹): 3049–2977, 2926, 2848, 2514, 1597, 1482, 1453–1434, 1287–1157, 1039, 940, 895, 855, 819, 744, 689; ¹H NMR (500 MHz) (CDCl₃) δ (ppm): 7.82–7.80 (m, 3H), 7.78 (d, *J* = 9.0 Hz, 1H), 7.61 (d, *J* = 8.6 Hz, 1H), 7.46–7.44 (m, 2H), 7.29 (t, *J* = 7.4 Hz, 2H), 7.20 (t, *J* = 7.1 Hz, 1H), 7.16 (d, *J* = 7.6 Hz, 2H), 6.09 (t, *J* = 6.6 Hz, 1H), 3.22 (d, *J* = 6.5 Hz, 2H), 3.03 (d, 2H) 2.57 (d, *J* = 6.9 Hz, 2 H), 2.16 (s, 3H), 1.98 (t, 2H), 1.68 (d, 2H), 1.57 (m, 1H), 1.38 (m, 2 H); ¹³C NMR (500 MHz) (CDCl₃) δ (ppm): 140.7, 140.4, 136.9, 133.4, 132.5, 129.1, 128.1, 128.0, 127.6, 127.5, 126.0, 125.7, 125.6, 124.2, 124.1, 57.2, 54.1, 43.2, 37.9, 32.2, 16.1; UHPLC-ESI-MS: t_R = 2.20, >98% pure (λ = 245 nm), *m/z* = 356 [M + H]⁺

5.3.2. (*E*)-4-benzyl-1-(3-phenylbut-2-en-1-yl)piperidine, [**4**]

Yield: 42%; yellow solid; mp: 220–222 °C; IR (cm⁻¹): 3085–2979, 2926, 2488, 1641–1580, 1484–1401, 1273–1160, 1038, 943, 835, 765–748, 689; ¹H NMR (500 MHz) (CDCl₃) δ (ppm): 7.40 (d, *J* = 7.9, 2H), 7.31–7.28 (m, 4H); 7.24 (m, 1H), 7.19 (t, *J* = 7.6 Hz, 1H), 7.15 (d, *J* = 7.3 Hz, 2H), 5.92 (t, *J* = 6.4 Hz, 1H), 3.16 (d, *J* = 6.5 Hz, 2H), 2.99 (d, 4H), 2.55 (d, *J* = 6.8 Hz, 2H), 2.05 (s, 3H), 1.95 (t, 2H), 1.66 (d, 2H), 1.54 (m, 1H), 1.36 (m, 2H); ¹³C NMR (500 MHz) (CDCl₃) δ (ppm): 143.3, 140.7, 137.1, 129.1, 128.2, 128.1, 126.9, 125.7, 125.6, 124.9, 57.0, 54.0, 43.2, 37.6, 32.1, 16.1; UHPLC-ESI-MS: t_R = 1.97, >98% pure (λ = 205 nm), *m/z* = 306 [M + H]⁺

5.4. General procedure for the preparation of compound **5** and **6**

To a solution of olefin (1.0 equiv) in absolute ethanol (10 mL) was added a catalytic amount of Pd (0)/C 10% (*p/p*, 0.06 equiv). The suspension was stirred vigorously under hydrogen atmosphere (1 atm). The reaction mixture was then filtered through Celite, using dichloromethane as solvent. The crude was purified by alumina (II Brockmann degree) column chromatography (9 *n*-hexane – 1 ethyl acetate).

5.4.1. 4-benzyl-1-[3-(naphthalen-2-yl)butyl]piperidine, [**5**]

Yield: 56%, yellow oil; IR (cm⁻¹): 3025, 2924, 2508, 1631, 1602, 1542, 1496, 1453; ¹H NMR (500 MHz) (CDCl₃) δ (ppm): 7.79–7.77 (t, *J* = 8.7 Hz, 3H), 7.59 (s, 1H), 7.45–7.42 (m, 2H), 7.32 (d, *J* = 8.8 Hz, 1H), 7.25 (m, 2H), 7.17 (m, 1H), 7.08 (m, 2H), 3.30 (broad peak, 2H), 2.90 (m, 1H), 2.76 (m, 1H), 2.55 (d, *J* = 7.4 Hz, 2H), 2.46 (m, 1H), 2.27–2.13 (m, 4H), 1.82–1.71 (m, 4H), 1.59 (m, 1H), 1.36 (d, *J* = 6.5 Hz, 3H); ¹³C NMR (500 MHz) (CDCl₃) δ (ppm): 142.4, 139.3, 133.4, 132.3, 128.9, 128.5, 128.3, 127.6, 127.5, 126.1, 125.5, 125.3, 124.8, 56.1, 52.4, 41.9, 38.3, 36.5, 31.8, 29.1, 22.7; UHPLC-ESI-MS: t_R = 2.17, >97% pure (λ = 220 nm), *m/z* = 358 [M + H]⁺

5.4.1.1. (+)-4-benzyl-1-(3-(naphthalen-2-yl)butyl)piperidine, [(+)-**5**]. Yellow oil; [α]_D²⁰ = +6.1 (c 0.2, CH₃OH). The IR and NMR spectra are identical to that of **5**. HPLC: t_R = 7.7 min, ee 95.0%.

5.4.1.2. (-)-4-benzyl-1-(3-(naphthalen-2-yl)butyl)piperidine, [(-)-**5**]. Yellow oil; [α]_D²⁰ = -6.3 (c 0.2, CH₃OH). The IR and NMR spectra are identical to that of **5**. HPLC: t_R = 9.0 min, ee 95.0%.

5.4.2. 4-benzyl-1-(3-phenylbutyl)piperidine, [**6**]

Yield: 47%, yellow oil; IR (cm⁻¹): 3682, 3019, 2929, 2856, 2434, 2400, 1230; ¹H NMR (500 MHz) (CDCl₃) δ (ppm): 7.28–7.27 (m, 4H), 7.17 (m, 4H), 7.13 (d, *J* = 7.0 Hz, 2H), 2.86 (broad peak, 2H), 2.71 (m, 1H), 2.52 (d, *J* = 6.6 Hz, 2H), 2.26 (m, 1H), 2.14 (m, 1H), 1.87–1.72 (m, 4H), 1.61 (d, 2H), 1.49 (m, 1H), 1.29 (m, 2H), 1.24 (d, *J* = 7.3 Hz, 3H); ¹³C NMR (500 MHz) (CDCl₃) δ (ppm): 147.3, 140.7, 129.1, 128.3, 128.1, 126.9, 125.9, 125.7, 57.3, 54.1, 53.9, 43.2, 38.4, 37.9, 35.4, 32.1, 22.6; UHPLC-ESI-MS: t_R = 1.92, >97% pure (λ = 200 nm), *m/z* = 308 [M + H]⁺

5.4.2.1. (+)-4-benzyl-1-(3-phenylbutyl)piperidine, [(+)-**6**]. Yellow oil; [α]_D²⁰ = +8.2 (c 0.3, CH₃OH). The IR and NMR spectra are identical to that of **6**. HPLC: t_R = 3.7 min, ee 99.9%.

5.4.2.2. (-)-4-benzyl-1-(3-phenylbutyl)piperidine, [(-)-**6**]. Yellow oil; [α]_D²⁰ = -8.3 (c 0.3, CH₃OH). The IR and NMR spectra are identical to that of **6**. HPLC: t_R = 5.3 min, ee 99.9%.

5.5. (6-bromonaphthalen-2-yloxy)-tert-butyl dimethylsilane, [**7**]

Under argon atmosphere 6-bromo-2-naphthol (1.0 equiv), imidazole (1.0 equiv) and *tert*-butyldimethylsilyl chloride (1.2 equiv) were solubilized in anhydrous dimethylformamide (20 mL). After stirring the solution overnight, the reaction mixture was extracted by dichloromethane (x 2) and brine (x 5). The organic phase was dried over Na₂SO₄, and concentrated under reduced pressure. The crude was purified by column chromatography (10 *n*-hexane).

Yield: 90%, white solid; mp: 62–64 °C; IR (cm⁻¹): 3743, 2954, 1735, 1653, 1560, 1470, 1256, 1062; ¹H NMR (500 MHz) (CDCl₃) δ (ppm): 7.92 (s, 1H), 7.64 (d, *J* = 8.9 Hz, 1H), 7.57 (d, *J* = 8.9 Hz, 1H), 7.48 (dd, *J* = 9.2 and 2.3 Hz, 1H), 7.16 (ds, *J* = 2.4 Hz, 1H), 7.10 (dd, *J* = 8.5 and 2.2 Hz, 1H), 1.02 (s, 9H), 0.25 (s, 6H); ¹³C NMR (500 MHz) (CDCl₃) δ (ppm): 153.8, 133.1, 130.2, 129.6, 129.4, 128.4, 128.3, 123.1, 117.3, 114.9, 25.7, 18.2, -4.4; ESI-MS: *m/z* = 338 [M + H]⁺

5.6. 4-(4-benzylpiperidin-1-yl)-2-[6-(*tert*-butyldimethylsilyloxy)-naphthalen-2-yl]-butan-2-ol, [**8**]

Compound **7** (1.5 equiv) was dissolved in anhydrous tetrahydrofuran (5 mL) under argon atmosphere. The solution was cooled to -78 °C, then was added dropwise *n*-butyl-lithium (4.4 equiv, 2.5 M in *n*-hexane). After 20 min, the temperature was increased up to -50 °C and a solution of 4-(4-benzyl-piperidin-1-yl)-butan-2-one (1.0 equiv) in anhydrous tetrahydrofuran (5.0 mL) was added dropwise. The reaction mixture was stirred for 1.5 h, keeping the temperature below -50 °C. The solution was quenched with 10 mL of saturated solution of NH₄Cl(aq) and extracted with Et₂O. The organic phase was dried over Na₂SO₄. The solvent was removed under reduced pressure and the crude was purified by alumina (II Brockmann degree) column chromatography (8 *n*-hexane – 2 ethyl acetate).

Yield: 63%; bright yellow oil; IR (cm⁻¹): 3336, 3026, 2926, 2856, 2349, 2310, 1603, 1496, 1471, 1453, 1371, 1260; ¹H NMR (500 MHz) (CDCl₃) δ (ppm): 7.92 (s, 1H), 7.72 (d, *J* = 9.1 Hz, 1H), 7.65 (d, *J* = 8.6 Hz, 1H), 7.42 (d, *J* = 8.6 Hz, 1H), 7.27 (m, 2H), 7.18 (t, *J* = 7.7 Hz, 2H), 7.12 (t, *J* = 8.6 Hz, 2H), 7.06 (dd, *J* = 8.4 and 1.8 Hz, 1H), 3.18 (broad peak, 1H), 3.02 (broad peak, 1H), 2.61 (broad peak, 1H), 2.53 (m, 2H), 2.31 (d, 1H), 2.12 (t, 1H), 1.92–1.86 (m, 2H), 1.75 (m, 1H), 1.65–1.63 (m, 2H), 1.54 (s, 3H), 1.51 (m, 1H), 1.29 (m, 2H), 1.02 (s,

9H), 0.24 (s, 6H); ^{13}C NMR (500 MHz) (CDCl_3) δ (ppm): 153.2, 144.2, 140.5, 133.1, 129.4, 129.1, 129.0, 128.2, 126.4, 125.8, 124.1, 123.3, 122.0, 114.5, 75.6, 55.1, 54.7, 54.2, 53.7, 52.6, 43.1, 37.8, 37.4, 32.5, 32.1, 31.4, 25.7, 18.2, -4.3; APCI-MS: $m/z = 504$ [$\text{M} + \text{H}$] $^+$

5.7. (E)-4-benzyl-1-{3-[6-(tert-butylidimethyl-silyloxy)-naphthalen-2-yl]-but-2-en-1-yl}-piperidine, [10]

Under argon atmosphere trifluoroacetic anhydride (2.0 equiv) was added dropwise to a solution of compound **8** (1.0 equiv) and copper triflate (2 mol %) in anhydrous dichloromethane (5 mL) cooled to 0 °C. After stirring the reaction a solution of $\text{NaHCO}_3(\text{aq})$ (5%) was added. The phases were separated and the organic phase was dried over anhydrous Na_2SO_4 and concentrated under reduced pressure. The obtained crude was purified by alumina (II Brockmann degree) column chromatography (9 *n*-hexane – 1 ethyl acetate).

Yield: 61%; yellow solid; mp: 102–104 °C; IR (cm^{-1}): 3027, 2926, 2856, 2801, 2349, 1597, 1497, 1478, 1374, 1318, 1257; ^1H NMR (500 MHz) (CDCl_3) δ (ppm): 7.74 (s, 1H), 7.69 (d, $J = 9.0$ Hz, 1H), 7.63 (d, $J = 8.9$ Hz, 1H), 7.56 (d, $J = 8.7$ Hz, 1H), 7.28 (m, 2H), 7.19–7.15 (m, 4H), 7.06 (d, $J = 9.1$ Hz, 1H), 6.04 (t, $J = 6.7$ Hz, 1H), 3.21 (d, 2H), 3.02 (broad peak, 2H), 2.56 (d, $J = 7.0$ Hz, 2H), 2.13 (s, 3H), 1.97 (broad peak, 2H), 1.68 (broad peak, 2H), 1.55 (broad peak, 1H), 1.36 (m, 2H), 1.02 (s, 9H), 0.25 (s, 6H); ^{13}C NMR (500 MHz) (CDCl_3) δ (ppm): 153.4, 140.7, 138.5, 136.9, 133.7, 129.4, 129.1, 128.1, 126.4, 125.7, 125.0, 124.5, 123.9, 122.2, 114.7, 57.2, 54.1, 43.2, 37.9, 32.2, 25.7, 18.2, 16.1, -4.4; ESI-MS: $m/z = 486$ [$\text{M} + \text{H}$] $^+$

5.8. General procedure for the preparation of compounds **9** and **11**

Tetra-*N*-butylammonium fluoride (1.5 equiv, 1.0 M in tetrahydrofuran) was added dropwise to a solution of compounds **8** and **10** (1.0 equiv) in anhydrous dichloromethane (5.0 mL), at 0 °C, in argon atmosphere. After 2 h the reaction mixture was extracted by a solution of NaHCO_3 (5%). In the case of compound **9**, the crude was purified by column chromatography (9 dichloromethane – 1 methanol – 0.1% NH_3 in methanol); on the contrary for compound **11**, it was been enough to do a precipitation of the solid impurities using methanol.

5.8.1. 6-[4-(4-benzylpiperidin-1-yl)-2-hydroxybutan-2-yl]naphthalen-2-ol, [9]

Yield: 64%; yellow oil; IR (cm^{-1}): 3452, 2925, 1633, 1605, 1560, 1454, 1381; ^1H NMR (500 MHz) (CDCl_3) δ (ppm): 7.91 (s, 1H), 7.72 (d, $J = 8.4$ Hz, 1H), 7.60 (d, $J = 8.4$ Hz, 1H), 7.40 (d, $J = 8.8$ Hz, 1H), 7.25 (t, $J = 6.9$ Hz, 2H), 7.18–7.14 (m, 3H), 7.07 (d, $J = 8.0$ Hz, 2H), 3.20 (broad peak, 1H), 2.61 (broad peak, 1H), 2.46 (d, $J = 6.5$ Hz, 2H), 2.34 (m, 2H), 2.18 (m, 1H), 1.96 (broad peak, 1H), 1.88 (broad peak, 1H), 1.80 (broad peak, 1H), 1.66 (broad peak, 2H), 1.59 (s, 1H), 1.49 (broad peak, 1H), 1.34 (broad peak, 2H); ^{13}C NMR (500 MHz) (CDCl_3) δ (ppm): 154.0, 143.0, 140.3, 133.3, 129.8, 129.0, 128.5, 128.2, 126.2, 125.8, 124.1, 123.4, 118.3, 109.2, 75.8, 55.0, 54.7, 52.6, 42.9, 37.6, 37.4, 31.7, 31.3; UHPLC-ESI-MS: $t_R = 1.68$, >97% pure ($\lambda = 230$ nm), $m/z = 390$ [$\text{M} + \text{H}$] $^+$

5.8.1.1. (+)-6-[4-(4-benzylpiperidin-1-yl)-2-hydroxybutan-2-yl]naphthalen-2-ol, [(+)-**9**]. Yellow oil; $[\alpha]_D^{20} = +24.2$ (c 0.1, CH_3OH). The IR and NMR spectra are identical to that of **9**. HPLC: $t_R = 4.0$ min, ee 99.9%.

5.8.1.2. (-)-6-[4-(4-benzylpiperidin-1-yl)-2-hydroxybutan-2-yl]naphthalen-2-ol, [(-)-**9**]. Yellow oil; $[\alpha]_D^{20} = -24.8$ (c 0.1, CH_3OH). The IR and NMR spectra are identical to that of **9**. HPLC: $t_R = 5.0$ min, ee 99.9%.

5.8.2. (E)-6-[4-(4-benzylpiperidin-1-yl)but-2-en-2-yl]naphthalen-2-ol, [11]

Yield: 64%; bright yellow solid; mp: 157–159 °C; IR (cm^{-1}): 3629, 2926, 2854, 2349, 1601, 1454; ^1H NMR (500 MHz) (CDCl_3) δ (ppm): 7.50 (s, 1H), 7.44 (d, $J = 8.7$ Hz, 1H), 7.28 (t, $J = 8.1$ Hz, 2H), 7.19 (t, $J = 8.0$ Hz, 1H), 7.15–7.11 (t, $J = 7.8$ Hz, 2H), 7.03–7.01 (m, 3H), 6.89 (ds, 1H), 5.89 (t, $J = 7.2$ Hz, 1H), 3.28 (ds, 2H), 3.21 (ds, 2H), 2.57 (d, $J = 7.5$ Hz, 2H), 2.13 (m, 2H), 2.12 (s, 3H), 1.74 (m, 2H), 1.63 (m, 1H), 1.53 (m, 2H); ^{13}C NMR (500 MHz) (CDCl_3) δ (ppm): 154.5, 140.4, 136.7, 134.0, 130.0, 129.1, 128.2, 128.0, 125.9, 124.0, 123.7, 122.7, 119.2, 109.9, 56.8, 53.9, 42.9, 37.8, 31.3, 15.7; UHPLC-ESI-MS: $t_R = 1.92$, >97% pure ($\lambda = 245$ nm), $m/z = 372$ [$\text{M} + \text{H}$] $^+$

5.9. 6-[4-(4-benzylpiperidin-1-yl)butan-2-yl]naphthalen-2-ol, [12]

To a solution of compound **11** (1.0 equiv) in absolute ethanol (10 mL) was added a catalytic amount of Pd (0)/C 10% (*p/p*, 0.06 equiv). The suspension was stirred vigorously under hydrogen atmosphere (1 atm). The reaction mixture was then filtered through Celite, using dichloromethane as solvent. The crude was purified by column chromatography (9 dichloromethane – 1 methanol – 0.1% NH_3 in methanol).

Yield: 39%; yellow oil; IR (cm^{-1}): 3297, 2924, 2349, 2309, 1604, 1453, 1376, 1269; ^1H NMR (500 MHz) (CDCl_3) δ (ppm): 7.42 (d, $J = 9.0$ Hz, 1H), 7.37 (s, 1H), 7.24 (t, 2H), 7.17 (d, $J = 8.0$ Hz, 1H), 7.17 (m, 1H), 7.06 (m, 3H), 6.98 (d, $J = 9.0$ Hz, 1H), 6.81 (s, 1H), 3.26 (broad peak, 1H), 3.10 (broad peak, 1H), 2.73 (m, 1H), 2.50–2.49 (broad peak, 4H), 2.14–2.12 (m, 2H), 2.04 (m, 2H), 1.67 (m, 2H), 1.60–1.54 (m, 3H), 1.28 (overlapped peak, 3H); ^{13}C NMR (500 MHz) (CDCl_3) δ (ppm): 154.6, 139.5, 133.6, 129.0, 128.3, 126.8, 126.0, 125.1, 125.0, 118.7, 109.2, 56.5, 53.7, 52.9, 42.3, 38.1, 37.0, 33.2, 30.0, 22.9; UHPLC-ESI-MS: $t_R = 1.86$, >95% pure ($\lambda = 230$ nm), $m/z = 374$ [$\text{M} + \text{H}$] $^+$

5.9.1. (+)-6-[4-(4-benzylpiperidin-1-yl)butan-2-yl]naphthalen-2-ol, [(+)-**12**]

Yellow oil; $[\alpha]_D^{20} = +11.8$ (c 0.3, CH_3OH). The IR and NMR spectra are identical to that of **12**. HPLC: $t_R = 4.9$ min, ee 99.9%.

5.9.2. (-)-6-[4-(4-benzylpiperidin-1-yl)butan-2-yl]naphthalen-2-ol, [(-)-**12**]

Yellow oil; $[\alpha]_D^{20} = -12.0$ (c 0.3, CH_3OH). The IR and NMR spectra are identical to that of **12**. HPLC: $t_R = 5.7$ min, ee 99.9%.

5.10. Molecular modeling

The optimized structures of selected compounds were docked into the putative binding pockets for the S1R by applying a consolidated procedure [29d,31a,32–35,64]. The resulting docked conformations for each complex were clustered and visualized; then, for each compound, only the molecular conformation satisfying the combined criteria of having the lowest (i.e., more favorable) energy and belonging to a highly populated cluster was selected to carry for further modeling. The ligand/receptor complexes obtained from the docking procedure was further refined in Amber 14 [65] using the quenched molecular dynamics (QMD) method, as previously described [29d,31a,32–35,64]. According to QMD, the best energy configuration of each complex resulting from this step was subsequently solvated by a cubic box of TIP3P [66] water molecules extending at least 10 Å in each direction from the solute. The system was neutralized and the solution ionic strength was adjusted to the physiological value of 0.15 M by adding the required amounts of Na^+ and Cl^- ions. Each solvated system was relaxed by 500 steps of steepest descent followed by 500 other conjugate-gradient minimization steps and then

gradually heated to a target temperature of 300 K in intervals of 50 ps of NVT MD, using a Verlet integration time step of 1.0 fs. The Langevin thermostat was used to control temperature, with a collision frequency of 2.0 ps^{-1} . The protein was restrained with a force constant of $2.0 \text{ kcal}/(\text{mol} \text{ \AA})$, and all simulations were carried out with periodic boundary conditions. Subsequently, the density of the system was equilibrated *via* MD runs in the isothermal-isobaric (NPT) ensemble, with isotropic position scaling and a pressure relaxation time of 1.0 ps for 50 ps with a time step of 1 fs. All restraints on the protein atoms were then removed, and each system was further equilibrated using NPT MD runs at 300 K, with a pressure relaxation time of 2.0 ps. Three equilibration steps were performed, each 2 ns long and with a time step of 2.0 fs. To check the system stability, the fluctuations of the rmsd of the simulated position of the backbone atoms of the receptor with respect to those of the initial protein were monitored. All chemophysical parameters and rmsd values showed very low fluctuations at the end of the equilibration process, indicating that the systems reached a true equilibrium condition. The equilibration phase was followed by a data production run consisting of 40 ns of MD simulations in the canonical (NVT) ensemble. Only the last 20 ns of each equilibrated MD trajectory were considered for statistical data collections. A total of 1000 trajectory snapshots were analyzed the each ligand/receptor complex. The binding free energy, ΔG_{bind} , between the ligands and the sigma1 receptor was estimated by resorting to the MM/PBSA approach implemented in Amber 14. According to this well validated methodology [36], the free energy was calculated for each molecular species (complex, receptor, and ligand), and the binding free energy was computed as the difference:

$$\Delta G_{\text{bind}} = G_{\text{complex}} - (G_{\text{receptor}} + G_{\text{ligand}}) = \Delta E_{\text{MM}} + \Delta G_{\text{sol}} - T\Delta S$$

in which ΔE_{MM} represents the molecular mechanics energy, ΔG_{sol} includes the solvation free energy and $T\Delta S$ is the conformational entropy upon ligand binding. The per residue decomposition of the enthalpic term of ΔG_{bind} was performed exploiting the equilibrated MD trajectory of each given compound/receptor complex. This analysis was carried out using the MM/GBSA approach [67,68], and was based on the same snapshots used in the binding free energy calculation. All simulations were carried out using the Pmemd modules of Amber 14, running on the MOSE CPU/GPU calculation cluster.

5.11. Binding assays

5.11.1. Materials

Guinea pig brains for the S1R binding assays were commercially available (Harlan–Winkelmann, Borcheln, Germany). Homogenizer: Elvehjem Potter (B. Braun Biotech International, Melsungen, Germany) and Soniprep 150, MSE, London, UK. Centrifuges: Cooling centrifuge model Rotina 35R (Hettich, Tuttlingen, Germany) and high-speed cooling centrifuge model Sorvall RC-5C plus (Thermo Fisher Scientific, Langenselbold, Germany). Multiplates: standard 96-well multiplates (Diagonal, Muenster, Germany). Shaker: self-made device with adjustable temperature and tumbling speed (scientific workshop of the institute). Vortexer: Vortex Genie 2 (Thermo Fisher Scientific, Langenselbold, Germany). Harvester: MicroBeta FilterMate-96 Harvester. Filter: Printed Filtermat Type A and B. Scintillator: Meltilex (Type A or B) solid-state scintillator. Scintillation analyzer: MicroBeta Trilux (all PerkinElmer LAS, Rodgau-Jügesheim, Germany). Chemicals and reagents were purchased from various commercial sources and were of analytical grade.

5.11.2. Preparation of membrane homogenates from guinea pig brain cortex

Five guinea pig brains were homogenized with the potter (500–800 rpm, 10 up-and-down strokes) in six volumes of cold 0.32 M sucrose. The suspension was centrifuged at 1200 g for 10 min at 4 °C. The supernatant was separated and centrifuged at 23,500 g for 20 min at 4 °C. The pellet was resuspended in 5–6 volumes of buffer (50 mM Tris, pH 7.4) and centrifuged again at 23,500 g (20 min, 4 °C). This procedure was repeated twice. The final pellet was resuspended in 5–6 volumes of buffer and frozen (–80 °C) in 1.5 mL portions containing $\sim 1.5 \text{ (mg protein)/mL}^{-1}$.

5.11.3. Protein determination

The protein concentration was determined by the method of Bradford modified by Stoscheck. The Bradford solution was prepared by dissolving 5 mg of Coomassie Brilliant Blue G 250 in 2.5 mL EtOH (95% v/v). Deionized H₂O (10 mL) and phosphoric acid (85% w/v, 5 mL) were added to this solution, and the mixture was stirred and filled to a total volume of 50 mL with deionized water. Calibration was carried out using bovine serum albumin as a standard in nine concentrations (0.1, 0.2, 0.4, 0.6, 0.8, 1.0, 1.5, 2.0, and 4.0 mg mL⁻¹). In a 96-well standard multiplate, 10 mL of the calibration solution or 10 mL of the membrane receptor preparation were mixed with 190 mL of the Bradford solution. After 5 min, the UV absorption of the protein–dye complex at $\lambda = 595 \text{ nm}$ was measured with a plate reader (Tecan Genios, Tecan, Crailsheim, Germany).

5.11.4. General protocol for binding assays

The test compound solutions were prepared by dissolving $\sim 10 \text{ mmol}$ (usually 2–4 mg) of test compound in DMSO so that a 10 μM stock solution was obtained. To obtain the required test solutions for the assay, the DMSO stock solution was diluted with the respective assay buffer. The filtermats were presoaked in 0.5% aqueous polyethylenimine solution for 2 h at RT before use. All binding experiments were carried out in duplicate in 96-well multiplates. The concentrations given are the final concentrations in the assay. Generally, the assays were performed by addition of 50 μL of the respective assay buffer, 50 μL test compound solution at various concentrations (10^{-5} , 10^{-6} , 10^{-7} , 10^{-8} , 10^{-9} and 10^{-10} M), 50 μL of corresponding radioligand solution, and 50 μL of the respective receptor preparation into each well of the multiplate (total volume 200 μL). The receptor preparation was always added last. During the incubation, the multiplates were shaken at a speed of 500–600 rpm at the specified temperature. Unless otherwise noted, the assays were terminated after 120 min by rapid filtration using the harvester. During the filtration each well was washed five times with 300 mL of water. Subsequently, the filtermats were dried at 95 °C. The solid scintillator was melted on the dried filtermats at 95 °C for 5 min. After solidifying of the scintillator at RT, the trapped radioactivity in the filtermats was measured with the scintillation analyzer. Each position on the filtermat corresponding to one well of the multiplate was measured for 5 min with the [³H]-counting protocol. The overall counting efficiency was 20%. The IC₅₀ values were calculated with GraphPad Prism 3.0 (GraphPad Software, San Diego, CA, USA) by nonlinear regression analysis. The IC₅₀ values were subsequently transformed into K_i values using the equation of Cheng and Prusoff. The K_i values are given as mean value \pm SEM from three independent experiments.

5.11.5. S1R binding assay

The assay was performed with the radioligand [³H](+)-pentazocine ($22.0 \text{ Ci mmol}^{-1}$; PerkinElmer). The thawed membrane preparation of guinea pig brain cortex ($\sim 100 \text{ mg protein}$) was incubated with various concentrations of test compounds, 2 nM

[³H](+)-pentazocine, and Tris buffer (50 mM, pH 7.4) at 37 °C. The nonspecific binding was determined with 10 mM unlabeled (+)-pentazocine. The K_d value of (+)-pentazocine is 2.9 nM.

5.11.6. S2R binding assay

The assay was performed using 150 µg of rat liver homogenate were incubated for 120 min at room temperature with 3 nM [³H]-DTG (Perkin–Elmer, specific activity 58.1 Ci mmol⁻¹) in 50 mM Tris–HCl, pH 8.0, 0.5 mL final volume. (+)-pentazocine (100 nM) and haloperidol (10 µM) were used to mask S1R and to define non-specific binding, respectively.

5.12. Cell lines

PC12 cells were grown in RPMI 1640 (Mediatech, Manassas, VA) supplemented with 10% heat inactivated horse serum (HS) and 5% fetal bovine serum (FBS) (Biochrom) 1% Glutamax, 1% penicillin/streptomycin (pen/strep). Cell differentiation was induced by exposure to a medium containing RPMI 1640 supplemented with 0.5% HS, Glutamax 1%, pen/strep 1% and NGF 2.5 ng/ml. PRE-084 and BD-1063 were prepared at 10 mM stock solutions in apyrogenic water. Pancreatic adenocarcinoma Capan-2 and PaCa3, breast adenocarcinoma MDA-MB 231 and SUM 159 cell line and prostatic adenocarcinoma PC3 cell lines were grown in culture medium composed of DMEM/Ham's F12 (1:1) (Euroclone) supplemented with fetal calf serum (FCS) (10%) (Euroclone), glutamine (2 mM) (Euroclone) and insulin (10 µg/ml) (Sigma-Aldrich, St. Louis, MO, USA). Glioblastoma cell line U87 was grown in EMEM culture medium (Euroclone) supplemented with FCS (10%) and glutamine (2 mM). Prostatic adenocarcinoma cell line LNCaP was grown in RPMI culture medium (Euroclone) supplemented with FCS (10%) and glutamine (2 mM). Serum restriction was done by incubating cells in low glucose culture medium without FCS for 24 h. All cell lines were purchased by the American Type Culture Collection (ATCC) except for SUM 159 that was purchased from Amsterand plc (Detroit, MI, USA).

All experiments were performed on cells in the exponential growth phase and checked periodically for mycoplasma contamination by MycoAlert™ Mycoplasma Detection Kit (Lonza, Basel, Switzerland).

5.13. Cytotoxicity test

5.13.1. MTS assay

CellTiter 96[®] AQueous One Solution Cell Proliferation Assay (Promega, Milan, Italy) was used on cells seeded onto a 96-well plate at a density of 3×10^3 cells per well. The effect of the drugs was evaluated after 24 h of continued exposure. Three independent experiments were performed in octuplicate. The optical density (OD) of treated and untreated cells was determined at a wavelength of 490 nm using a plate reader. Dose response curves were created by Excel software. IC₅₀ values were determined graphically from the plot.

5.13.2. Flow cytometry

Flow cytometric analysis was performed using a FACS Canto flow cytometer (Becton Dickinson, San Diego, CA). Data acquisition and analysis were performed using FACSDiva software (Becton Dickinson). Samples were run in triplicate and 10,000 events were collected for each replicate.

5.13.3. Annexin-V assay

After exposure to compound, medium was removed and cell were detached by trypsinization, washed once in PBS 1× and incubated with 25 µl/ml Annexin V-FITC in binding buffer

(Affimetrix eBioscience, San Diego, USA) for 15 min at 37 °C in a humidified atmosphere in the dark. Cells were then washed in PBS and suspended in binding buffer.

Immediately before flow cytometric analysis, propidium iodide was added to a final concentration of 5 µg/ml to discriminate between apoptotic (Ann-V positive and PI positive or PI negative) and necrotic cells (Ann-V negative and PI positive).

5.13.4. TUNEL assay

Cells were fixed in 1% formaldehyde in PBS on ice for 15 min, suspended in 70% ice cold ethanol and stored overnight at 20 °C. Cells were then washed twice in PBS and re-suspended in PBS containing 0.1% Triton X-100 for 5 min at 4°C. Thereafter, samples were incubated in 50 µl of solution containing TdT and FITC conjugated dUTP deoxynucleotides 1:1 (Roche Diagnostic GmbH, Mannheim, Germany) in a humidified atmosphere for 90 min at 37 °C in the dark, washed in PBS, counterstained with propidium iodide (2.5 µg/ml, MP Biomedicals, Verona, Italy) and RNase (10 kU/ml, Sigma–Aldrich) for 30 min at 48 °C in the dark and analyzed by flow cytometry.

5.13.5. Western blot

Cell proteins were extracted with M-PER Mammalian Protein Extraction Reagent (Thermo Fisher Scientific) supplemented with Halt Protease Phosphatase Inhibitor Cocktail (Thermo Fisher Scientific). Mini-PROTEANTGX™ precast gels (4–20%) (BIO-RAD) were run using Mini-PROTEAN Tetra electrophoresis cells and then electroblotted by Trans-BlotTurbo™ Mini PVDF Transfer Packs (BIORAD). The unoccupied membrane sites were blocked with T-TBS 1× (Tween 0.1%) and 5% non-fat dry milk to prevent nonspecific binding of antibodies and probed with specific primary antibodies overnight at 4 °C. This was followed by incubation with the respective secondary antibodies. The antibody-antigen complexes were detected with Immun-Star™ WesternC™ kit (BIO-RAD).

The following primary antibodies were used: anti-caspase-3 (Cell Signaling Technology, Inc., Celbio, Pero, Milan, Italy). Antivinculin (sc-5573) from Santa Cruz Biotechnology was used as housekeeping. Quantity One Software was used for analysis.

5.14. Real time RT-PCR

Total cellular RNA was extracted using TRIzol reagent (Life technologies) in accordance with manufacturer's instruction and quantified using the Nanodrop MD-1000 spectrophotometer system. Reverse transcription reactions were performed in 20 µL of nuclease free water containing 400 ng of total RNA using iScript cDNA Synthesis kit (Bio-Rad Laboratories, Hercules, CA). Real-Time PCR was run using 7500 Fast Real-Time PCR system (Applied Biosystems) and TaqMan assays to detect the expression of SIGMAR1 and PGRMC1 genes.

Reactions were carried out in triplicate at a final volume of 20 µL containing 40 ng of cDNA template, TaqMan universal PCR Master Mix (2×), and selected TaqMan assays (20×). Samples were maintained at 50 °C for 2 min, then at 95 °C for 10 min followed by 40 amplification cycles at 95 °C for 15 s, and at 60 °C for 30 s.

The amount of mRNA was normalized to the endogenous genes GAPDH and HPRT-1.

5.15. Statistical analysis

All statistical analyses were done using standard software packages GraphPad Prism (GraphPad Software, San Diego California USA, version 5.0). The comparison between groups was performed by applying the Student “t” test for 2-group comparisons or one-way ANOVA followed by appropriate post hoc tests for multiple

comparisons. p-values lower than 0.05 were considered statistically significant.

Acknowledgement

The Authors gratefully acknowledge Ilaria Rocchio for the experimental support and Stefania Brambilla for UHPLC-ESI-MS analysis.

Appendix A. Supplementary data

Supplementary data related to this article can be found at <http://dx.doi.org/10.1016/j.ejmech.2016.08.067>.

References

- [1] S.B. Hellewell, A. Bruce, G. Feinstein, J. Orringer, W. Williams, W.D. Bowen, Rat liver and kidney contain high densities of sigma 1 and sigma 2 receptors: characterization by ligand binding and photoaffinity labeling, *Eur. J. Pharmacol.* 268 (1994) 9–18.
- [2] R. Quirion, W. Bowen, Y. Itzhak, J.L. Junien, J.M. Musacchio, R.B. Rothman, T.P. Su, S.W. Tam, D.P. Taylor, A proposal for the classification of sigma binding sites, *Trends Pharmacol. Sci.* 13 (1992) 85–86.
- [3] M. Hanner, F.F. Moebius, A. Flandofer, H.G. Knaus, J. Striessnig, E. Kempner, H. Glossmann, Purification, molecular cloning, and expression of the mammalian sigma1-binding site, *Proc. Natl. Acad. Sci. U.S.A.* 93 (1996) 8072–8077.
- [4] W.D. Bowen, Sigma receptors: recent advances and new clinical potentials, *Pharm. Acta Helvetiae* 74 (2000) 211–218.
- [5] S. Collina, R. Gaggeri, A. Marra, A. Bassi, S. Negrinotti, F. Negri, D. Rossi, Sigma receptor modulators: a patent review, *Exp. Opin. Ther. Pat.* 23 (2013) 597–613.
- [6] S.Y. Tsai, T. Hayashi, T. Mori, T.P. Su, Sigma-1 receptor chaperones and diseases, *Cent. Nerv. Syst. Agents Med. Chem.* 9 (2009) 184–189.
- [7] V.L. Phan, G. Alonso, F. Sandillon, A. Privat, T. Maurice, Therapeutic potentials of sigma1 (sigma 1) receptor ligands against cognitive deficits in aging, *Soc. Neurosci. Abstr.* 26 (2000) 2172.
- [8] A. Marra, D. Rossi, L. Pignataro, C. Bigogno, A. Canta, N. Oggioni, A. Malacrida, M. Corbo, G. Cavaletti, M. Peviani, D. Curti, G. Dondio, S. Collina, Toward the identification of neuroprotective agents: g-scale synthesis, pharmacokinetic evaluation and CNS distribution of (R)-RC-33, a promising Sigma1 receptor agonist, *Future Med. Chem.* 8 (2016) 287–295.
- [9] S.Y. Tsai, T. Hayashi, B.K. Harvey, Y. Wang, W.W. Wu, R.F. Shen, Y. Zhang, K.G. Becker, B.J. Hoffer, T.P. Su, Sigma-1 receptors regulate hippocampal dendritic spine formation via a free radical-sensitive mechanism involving Rac1xGTP pathway, *Proc. Natl. Acad. Sci. U.S.A.* 106 (2009) 22468–22473.
- [10] B. Wang, R. Rouzier, C.T. Albarracin, A. Sahin, P. Wagner, Y. Yang, T.L. Smith, F. Meric Bernstam, A.C. Marcelo, G.N. Hortobagyi, L. Pusztai, Expression of sigma 1 receptor in human breast cancer, *Breast Cancer Res. Treat.* 87 (2004) 205–214.
- [11] T. Maurice, T.P. Su, The pharmacology of sigma-1 receptors, *Pharmacol. Ther.* 124 (2009) 195–206.
- [12] M. Peviani, E. Salvaneschi, L. Bontempi, A. Petese, A. Manzo, D. Rossi, M. Salmona, S. Collina, P. Bigini, D. Curti, Neuroprotective effects of the Sigma-1 receptor (S1R) agonist PRE-084, in a mouse model of motor neuron disease not linked to SOD1 mutation, *Neurobiol. Dis.* 62 (2014) 218–232.
- [13] B.A. Spruce, L.A. Campbell, N. McTavish, M.A. Cooper, M.V. Appleyard, M. O'Neill, J. Howie, J. Samson, S. Watt, K. Murray, D. McLean, N.R. Leslie, S.T. Safrany, M.J. Ferguson, J.A. Peters, A.R. Prescott, G. Box, A. Hayes, B. Nutley, F. Raynaud, C.P. Downes, J.J. Lambert, A.M. Thompson, S. Eccles, Small molecule antagonists of the sigma-1 receptor cause selective release of the death program in tumor and self-reliant cells and inhibit tumor growth in vitro and in vivo, *Cancer Res.* 64 (2004) 4875–4886.
- [14] E. Aydar, P. Onganer, R. Perrett, M.B. Djamgoz, C.P. Palmer, The expression and functional characterization of sigma (sigma) 1 receptors in breast cancer cell lines, *Cancer Lett.* 242 (2006) 245–257.
- [15] D. Crottes, H. Guizouarn, P. Martin, F. Borgese, O. Soriani, The sigma-1 receptor: a regulator of cancer cell electrical plasticity? *Front. Physiol.* 4 (2013) 175.
- [16] M. Happy, J. Dejoie, C.K. Zajac, B. Cortez, K. Chakraborty, J. Aderemi, M. Sauane, Sigma 1 Receptor antagonist potentiates the anti-cancer effect of p53 by regulating ER stress, ROS production, Bax levels, and caspase-3 activation, *Biochem. Biophysical Res. Commun.* 456 (2015) 683–688.
- [17] C. Zeng, S. Vangveravong, J. Xu, K.C. Chang, J. Xu, R.S. Hotchkiss, L. Jones, K.T. Wheeler, D. Shen, Z.P. Zhuang, H.F. Kung, R.H. Mach, Subcellular localization of sigma-2 receptors in breast cancer cells using two-photon and confocal microscopy, *Cancer Res.* 67 (2007) 6708–6716.
- [18] G. Cassano, G. Gasparre, M. Niso, M. Contino, V. Scaleria, N.A. Colabufo, F281, synthetic agonist of the sigma-2 receptor, induces Ca²⁺ efflux from the endoplasmic reticulum and mitochondria in SK-N-SH cells, *Cell Calcium* 45 (2009) 340–345.
- [19] J. Xu, C. Zeng, W. Chu, F. Pan, J.M. Rothfuss, F. Zhang, Z. Tu, D. Zhou, D. Zeng, S. Vangveravong, F. Johnston, D. Spitzer, K.C. Chang, R.S. Hotchkiss, W.G. Hawkins, K.T. Wheeler, R.H. Mach, Identification of the PGRMC1 protein complex as the putative sigma-2 receptor binding site, *Nat. Comm.* 2 (2011) 380.
- [20] S.B. Hellewell, W.D. Bowen, A sigma-like binding site in rat pheochromocytoma (PC12) cells: decreased affinity for (+)-benzomorphans and lower molecular weight suggest a different sigma receptor form from that of Guinea pig brain, *Brain Res.* 527 (1990) 244–253.
- [21] I.S. Ahmed, H.J. Rohe, K.E. Twist, M.N. Mattingly, R.J. Craven, Progesterone receptor membrane component 1 (Pgrmc1): a heme-1 domain protein that promotes tumorigenesis and is inhibited by a small molecule, *J. Pharmacol. Exp. Ther.* 333 (2010) 564–573.
- [22] R.H. Mach, C.R. Smith, I. Al-Nabulsi, B.R. Whirret, S.R. Childers, K.T. Wheeler, Sigma 2 receptors as potential biomarkers of proliferation in breast cancer, *Cancer Res.* 57 (1997) 156–161.
- [23] K.T. Wheeler, L.M. Wang, C.A. Wallen, S.R. Childers, J.M. Cline, P.C. Keng, R.H. Mach, Sigma-2 receptors as a biomarker of proliferation in solid tumours, *Br. J. Cancer* 82 (2000) 1223–1232.
- [24] N.A. Colabufo, F. Berardi, M. Contino, S. Ferorelli, M. Niso, R. Perrone, A. Pagliarulo, P. Sapanuro, V. Pagliarulo, Correlation between sigma2 receptor protein expression and histopathologic grade in human bladder cancer, *Cancer Lett.* 237 (2006) 83–88.
- [25] H. Kashivagi, J.E. McDunn, P.O. Simon, P.S. Goedegeure, J. Xu, L. Jones, K. Chang, F. Johnston, K. Trinkaus, R.S. Hotchkiss, R.H. Mach, W.G. Hawkins, Selective sigma-2 ligands preferentially bind to pancreatic adenocarcinomas: applications in diagnostic imaging and therapy, *Mol. Cancer* 6 (2007) 48.
- [26] C. Zeng, J. Rothfuss, J. Zhang, W. Chu, S. Vangveravong, Z. Tu, F. Pan, K.C. Chang, R. Hotchkiss, R.H. Mach, Sigma-2 ligands induce tumour cell death by multiple signalling pathways, *Br. J. Cancer* 106 (2012) 693–701.
- [27] S.M. Husbands, S. Izenwasser, T. Kopajtic, W.D. Bowen, B.J. Vilner, J.L. Katz, A.H. Newman, Structure-Activity Relationships at the Monoamine transporters and σ receptors for a novel series of 9-[3-(*cis*-3,5-dimethyl-1-piperazinyl)-propyl]carbazole (Rimcazone) analogues, *J. Med. Chem.* 42 (1999) 4446–4455.
- [28] Y.S. Huang, H.L. Lu, L.J. Zhang, Z. Wu, Sigma-2 receptor ligands and their perspectives in Cancer diagnosis and therapy, *Med. Res. Rev.* 34 (2014) 532–566.
- [29] (a) S. Collina, G. Loddio, M. Urbano, L. Linati, A. Callegari, F. Ortuso, S. Alcaro, C. Laggner, T. Langer, O. Prezzavento, G. Ronsisvalle, O. Azzolina, Design, synthesis, and SAR analysis of novel selective sigma1 ligands, *Bioorg. Med. Chem.* 15 (2007) 771–783;
(b) D. Rossi, M. Urbano, A. Pedrali, M. Serra, D. Zampieri, M.G. Mamolo, C. Laggner, C. Zanette, C. Florio, D. Schepmann, B. Wünsch, O. Azzolina, S. Collina, Design, synthesis and SAR analysis of novel selective sigma1 ligands (Part 2), *Bioorg. Med. Chem.* 18 (2010) 1204–1212;
(c) D. Rossi, A. Pedrali, M. Urbano, R. Gaggeri, M. Serra, L. Fernandez, M. Fernandez, J. Caballero, S. Rosinsvalle, O. Prezzavento, D. Schepmann, B. Wünsch, M. Peviani, D. Curti, O. Azzolina, S. Collina, Identification of a potent and selective σ 1 receptor agonist potentiating NGF-induced neurite outgrowth in PC12 cells, *Bioorg. Med. Chem.* 19 (2011) 6210–6224;
(d) D. Rossi, A. Marra, P. Picconi, M. Serra, L. Catenacci, M. Sorrenti, E. Laurini, M. Fermeglia, S. Priel, S. Brambilla, N. Almirante, M. Peviani, D. Curti, S. Collina, Identification of RC-33 as a potent and selective σ 1 receptor agonist potentiating NGF-induced neurite outgrowth in PC12 cells. Part 2: g-scale synthesis, physicochemical characterization and in vitro metabolic stability, *Bioorg. Med. Chem.* 21 (2013) 2577–2586.
- [30] V. Pace, F. Martínez, M. Fernández, J.V. Sinisterra, A.R. Alcántara, Highly efficient synthesis of new α -Arylamino- α -chloropropan-2-ones via oxidative hydrolysis of vinyl chlorides promoted by calcium hypochlorite, *Adv. Synthesis Catal.* 351 (2009) 3199–3206.
- [31] (a) D. Rossi, A. Pedrali, R. Gaggeri, A. Marra, L. Pignataro, E. Laurini, V. DalCol, M. Fermeglia, S. Priel, D. Schepmann, B. Wünsch, M. Peviani, D. Curti, S. Collina, Chemical, pharmacological, and in vitro metabolic stability studies on enantiomerically pure RC-33 compounds: promising neuroprotective agents acting as σ 1 receptor agonists, *Chem. Med. Chem.* 8 (2013) 1514–1527;
(b) D. Rossi, A. Pedrali, A. Marra, L. Pignataro, D. Schepmann, B. Wünsch, L. Ye, K. Leuner, M. Peviani, D. Curti, O. Azzolina, S. Collina, Studies on the enantiomers of RC-33 as neuroprotective agents: isolation, configurational assignment, and preliminary biological profile, *Chirality* 25 (2013) 814–822;
(c) R. Gaggeri, D. Rossi, S. Collina, B. Mannucci, M. Baierl, M. Juza, Quick development of an analytical enantioselective high performance liquid chromatography separation and preparative scale-up for the flavonoid Narigenin, *J. Chromatogr. A* 1218 (2011) 5414–5422;
(d) D. Rossi, A. Marra, M. Rui, S. Brambilla, M. Juza, S. Collina, “Fit-for-purpose” development of analytical and (semi)preparative enantioselective high performance liquid and supercritical fluid chromatography for the access to a novel σ 1 receptor agonist, *J. Pharm. Biomed. Anal.* 118 (2016) 363–369;
(e) D. Rossi, V. Talman, G. Boije Af Gennäs, A. Marra, P. Picconi, R. Nasti, M. Serra, J. Ann, M. Amadio, A. Pascale, R.K. Tuominen, J. Yli-Kauhalauma, J. Lee, S. Collina, Beyond the affinity for protein kinase C: exploring 2-phenyl-3-hydroxypropyl pivalate analogues as C1 domain-targeting ligands, *Med. Chem. Comm.* 6 (2015) 547–554.

- [32] D. Rossi, A. Marra, M. Rui, E. Laurini, M. Fermeglia, S. Pricl, D. Schepmann, B. Wünsch, M. Peviani, D. Curti, S. Collina, A step forward in the sigma enigma: a role for chirality in the sigma1 receptor–ligand interaction? *MedChemComm* 6 (2015) 138–146.
- [33] E. Laurini, V. Dal Col, M.G. Mamolo, D. Zampieri, P. Posocco, M. Fermeglia, V. Vio, S. Pricl, Homology model and docking-based virtual screening for ligands of the σ_1 receptor, *ACS Med. Chem. Lett.* 2 (2011) 834–839.
- [34] E. Laurini, D. Marson, V. Dal Col, M. Fermeglia, M.G. Mamolo, D. Zampieri, L. Vio, S. Pricl, Another brick in the wall. Validation of the σ_1 receptor 3D model by computer-assisted design, synthesis, and activity of new σ_1 ligands, *Mol. Pharm.* 9 (2012) 3107–3126.
- [35] S. Brune, D. Schepmann, K.H. Klempnauer, D. Marson, V. Dal Col, E. Laurini, M. Fermeglia, B. Wünsch, S. Pricl, The sigma enigma: in vitro/in silico site-directed mutagenesis studies unveil σ_1 receptor ligand binding, *Biochem.* 53 (2014) 2993–3003.
- [36] I. Massova, P.A. Kollman, Combined molecular mechanical and continuum solvent approach (MM-PBSA/GBSA) to predict ligand binding, *Perspect. Drug Discov. Des.* 18 (2000) 113–135.
- [37] Y. Zhang, Y. Huang, P. Zhang, X. Gao, R.B. Gibbs, S. Li, Incorporation of a selective sigma-2 receptor ligand enhances uptake of liposomes by multiple cancer cells, *Int. J. Nanomedicine* 7 (2012) 4473–4485.
- [38] V. Mégallizi, V. Mathieu, T. Mijatovic, P. Gailly, O. Debeir, N. De Neve, M. Van Damme, G. Bontempi, B. Haibe-Kains, C. Decaestecker, Y. Kondo, R. Kiss, F. Lefranc, 4-IBP, a sigma1 receptor agonist, decreases the migration of human cancer cells, including glioblastoma cells, in vitro and sensitizes them in vitro and in vivo to cytotoxic insults of proapoptotic and proautophagic drugs, *Neoplasia* 9 (2007) 358–369.
- [39] D. Das, L. Persaud, J. Dejoie, M. Happy, O. Brannigan, D. De Jesus, M. Sauane, Tumor necrosis factor-related apoptosis-inducing ligand (TRAIL) activates caspases in human prostate cancer cells through sigma 1 receptor, *Biochem. Biophys. Res. Commun.* (2016 Jan 11 pii: S0006–291X(16)30055–9).
- [40] C.S. John, B.J. Vilner, B.C. Geyer, T. Moody, W.D. Bowen, Targeting sigma receptor-binding benzamides as in vivo diagnostic and therapeutic agents for human prostate tumors, *Cancer Res.* 59 (1999) 4578–4583.
- [41] S. Okuyama, A. Nakazato, NE-100: a novel sigma receptor antagonist, *CNS Drug Rev.* 2 (1999) 226–237.
- [42] C. Zeng, J.M. Rothfuss, J. Zhang, S. Vangveravong, W. Chu, S. Li, Z. Tu, J. Xu, R.H. Mach, Functional assays to define agonists and antagonists of the sigma-2 receptor, *Anal. Biochem.* 448 (2014) 68–74.
- [43] M. Takebayashi, T. Hayashi, T.P. Su, Nerve growth factor-induced neurite sprouting in PC12 cells involves sigma-1 receptors: implications for antidepressants, *J. Pharmacol. Exp. Ther.* 303 (2002) 1227–1237.
- [44] T. Nishimura, T. Ishima, M. Iyo, K. Hashimoto, Potentiation of nerve growth factor-induced neurite outgrowth by fluvoxamine: role of sigma-1 receptors, IP3 receptors and cellular signaling pathways, *PLoS One* 3 (2008) e2558.
- [45] T. Ishima, K. Hashimoto, Potentiation of nerve growth factor-induced neurite outgrowth in PC12 cells by ifenprodil: the role of sigma-1 and IP3 receptors, *PLoS One* 7 (2012) e37989.
- [46] M.J. Robson, B. Noorbakhsh, M.J. Seminerio, R.R. Matsumoto, Sigma-1 receptors: potential targets for the treatment of substance abuse, *Curr. Pharm. Des.* 18 (2012) 902–919.
- [47] T. Ishima, Y. Fujita, K. Hashimoto, Interaction of new antidepressants with sigma-1 receptor chaperones and their potentiation of neurite outgrowth in PC12 cells, *Eur. J. Pharmacol.* 727 (2014) 167–173.
- [48] I.S. Ahmed, C. Chamberlain, R.J. Craven, S2R (Pgrmc1): the cytochromerelated sigma-2 receptor that regulates lipid and drug metabolism and hormone signaling, *Expert Opin. Drug Metab. Toxicol.* 8 (2012) 361–370.
- [49] S.U. Mir, I.S. Ahmed, S. Arnold, R.J. Craven, Elevated progesterone receptor membrane component 1/sigma-2 receptor levels in lung tumors and plasma from lung cancer patients, *Int. J. Cancer* 131 (2012) E1–E9.
- [50] S.U. Mir, S.R. Schwarze, L. Jin, J. Zhang, W. Friend, S.S. Miriyala, D. Clair, R.J. Craven, Progesterone receptor membrane component 1/Sigma-2 receptor associates with MAP1LC3B and promotes autophagy, *Autophagy* 9 (2013) 1566–1578.
- [51] C. Abate, M. Niso, V. Infantino, A. Menga, F. Berardi, Elements in support of the 'non-identity' of the PGRMC1 protein with the σ_2 receptor, *Eur. J. Pharmacol.* 5 (2015) 16–23.
- [52] U.B. Chu, T.A. Mavlyutov, M.L. Chu, H. Yang, A. Schulman, C. Mesangeau, C.R. McCurdy, L.W. Guo, A.E. Ruoho, The Sigma-2 receptor and progesterone receptor membrane component 1 are different, *E. Bio. Med.* 11 (2015) 1806–1813.
- [53] A.E. Ruoho, L.W. Guo, A.R. Hajjipour, K. Karaoglu, T.A. Mavlyutov, U.B. Chu, J. Yang, Will the True Sigma-2 Receptor Please Stand up?, San Diego, 2013 (Neuroscience Meeting).
- [54] A. van Waarde, A.A. Ryzczynska, N.K. Ramakrishnan, K. Ishiwata, P.H. Elsinga, R.A. Dierckx, Potential applications for sigma receptor ligands in cancer diagnosis and therapy, *Biochim. Biophys. Acta* 1848 (2014) 2703–2714.
- [55] C. Lee, L. Raffaghello, S. Brandhorst, F.M. Safdie, G. Bianchi, A. Martin-Montalvo, V. Pistoia, M. Wei, S. Hwang, A. Merlino, L. Emionite, R. de Cabo, V.D. Longo, Fasting cycles retard growth of tumors and sensitize a range of cancer cell types to chemotherapy, *Sci. Transl. Med.* 4 (2012) 124–127.
- [56] L. Raffaghello, C. Lee, F.M. Safdie, M. Wei, F. Madia, G. Bianchi, V.D. Longo, Starvation-dependent differential stress resistance protects normal but not cancer cells against high-dose chemotherapy, *Proc. Natl. Acad. Sci. U. S. A.* 105 (2008) 8215–8220.
- [57] F. Safdie, S. Brandhorst, M. Wei, W. Wang, C. Lee, S. Hwang, P.S. Conti, T.C. Chen, V.D. Longo, Fasting enhances the response of glioma to chemo- and radiotherapy, *PLoS One* 7 (2012) e44603.
- [58] I. Caffa, V. D'Agostino, P. Damonte, D. Soncini, M. Cea, F. Monacelli, P. Odetti, A. Ballestrero, A. Provenzani, V.D. Longo, A. Nencioni, Fasting potentiates the anticancer activity of tyrosine kinase inhibitors by strengthening MAPK signaling inhibition, *Oncotarget* 6 (2015) 11820–11832.
- [59] S. de Groot, M.P. Vreeswijk, M.J. Welters, G. Gravesteyn, J.J. Boei, A. Jochems, D. Houtsmma, H. Putter, J.J. van der Hoeven, J.W. Nortier, H. Pijl, J.R. Kroep, The effects of short-term fasting on tolerance to (neo) adjuvant chemotherapy in HER2-negative breast cancer patients: a randomized pilot study, *BMC Cancer* 15 (2015) 652.
- [60] J. Menis, B. Hasan, B. Besse, New clinical research strategies in thoracic oncology: clinical trial design, adaptive, basket and umbrella trials, new endpoints and new evaluations of response, *Eur. Respir. Rev.* 23 (2014) 367–378.
- [61] A.S. Bura, T. Guegan, D. Zamanillo, J.M. Vela, R. Maldonado, Operant self-administration of a sigma ligand improves nociceptive and emotional manifestations of neuropathic pain, *Eur. J. Pain* 17 (2013) 832–843.
- [62] L. Romero, D. Zamanillo, X. Nadal, R. Sanchez-Arroyos, I. Rivera-Arconada, A. Dordal, A. Montero, A. Muro, A. Bura, C. Segalés, M. Laloya, E. Hernández, E. Portillo-Salido, M. Escriche, X. Codony, G. Encina, J. Burguño, M. Merlos, J.M. Baeyens, J. Giraldo, J.A. López-García, R. Maldonado, C.R. Plata-Salamán, J.M. Vela, Pharmacological properties of S1RA, a new sigma-1 receptor antagonist that inhibits neuropathic pain and activity-induced spinal sensitization, *Br. J. Pharmacol.* 166 (2012) 2289–2306.
- [63] J.L. Diaz, D. Zamanillo, J. Corbera, J.M. Baeyens, R. Maldonado, M.A. Pericas, J.M. Vela, A. Torrens, Selective sigma-1 (sigma1) receptor antagonists: emerging target for the treatment of neuropathic pain, *Cent. Nerv. Syst. Agents Med. Chem.* 9 (2009) 172–183.
- [64] F. Weber, S. Brune, K. Korpis, P.J. Bednarski, E. Laurini, V. Dal Col, S. Pricl, D. Schepmann, B. Wünsch, Synthesis, pharmacological evaluation, and σ_1 receptor interaction analysis of hydroxyethyl substituted piperazines, *J. Med. Chem.* 57 (2014) 2884–2894.
- [65] D.A. Case, J.T. Berryman, R.M. Betz, D.S. Cerutti, T.E. Cheatham III, T.A. Darden, R.E. Duke, T.J. Giese, H. Gohlke, A.W. Goetz, N. Homeyer, S. Izadi, P. Janowski, J. Kaus, A. Kovalenko, T.S. Lee, S. LeGrand, P. Li, T. Luchko, R. Luo, B. Madej, K.M. Merz, G. Monard, P. Needham, H. Nguyen, H.T. Nguyen, I. Omelyan, A. Onufriev, D.R. Roe, A. Roitberg, R. Salomon-Ferrer, C.L. Simmerling, W. Smith, J. Swails, R.C. Walker, J. Wang, R.M. Wolf, X. Wu, D.M. York, P.A. Kollman, AMBER 2015, University of California, San Francisco, 2015.
- [66] W.L. Jorgensen, J. Chandrasekhar, J.D. Madura, R.W. Impey, M.L. Klein, Comparison of simple potential functions for simulating liquid water, *J. Chem. Phys.* 79 (1983) 926–935.
- [67] V. Tsui, D.A. Case, Theory and applications of the generalized Born solvation model in macromolecular simulations, *Biopolymers* 56 (2000) 275–291.
- [68] A. Onufriev, D. Bashford, D.A. Case, Modification of the generalized Born model suitable for macromolecules, *J. Phys. Chem. B* 104 (2000) 3712–3720.

Supporting Information

Synthesis and biological evaluation of new aryl-alkyl(alkenyl)-4-benzylpiperidines, novel Sigma Receptor (SR) modulators, as potential anticancer-agents.

Marta Rui^{1,3#}, Daniela Rossi^{1#}, Annamaria Marra¹, Mayra Paolillo², Sergio Schinelli², Daniela Curti⁴, Anna Tesei⁵, Michela Cortesi⁵, Alice Zamagni⁵, Erik Laurini⁶, Sabrina Pricl^{6,7}, Dirk Schepmann⁸, Bernhard Wünsch⁸, Ernst Urban³, Vittorio Pace³, Simona Collina^{1*}

¹*Department of Drug Sciences, Medicinal Chemistry and Pharmaceutical Technology section, University of Pavia, Viale Taramelli 6 and 12, 27100 Pavia (Italy)*

²*Department of Drug Sciences, Pharmacology section, University of Pavia, Viale Taramelli 6 and 12, 27100 Pavia (Italy)*

³*Department of Pharmaceutical Chemistry, University of Vienna, Althanstrasse 14, 1090 Vienna (Austria)*

⁴*Department of Biology and Biotechnology “L. Spallanzani”, Lab. of Cellular and Molecular Neuropharmacology, University of Pavia, Via Ferrata 9, 27100 Pavia (Italy)*

⁵*Radiobiology and Preclinical Pharmacology Laboratory, Biosciences Laboratory, Istituto Scientifico Romagnolo per lo Studio e la Cura dei Tumori (IRST) IRCCS, Via P. Maroncelli 40, 47014 Meldola (FC), Italy*

⁶*MOSE – DEA, University of Trieste, Piazzale Europa 1, 34127 Trieste (Italy)*

⁷*National Interuniversity Consortium for Material Science and Technology (INSTM), Research Unit MOSE-DEA University of Trieste, Trieste, Italy*

⁸*Institute of Pharmaceutical and Medicinal Chemistry, University of Muenster, Correnstrasse 48, 48149 Muenster (Germany)*

Table of contents

1. Chiral resolution	S2
2. Molecular Modelling	S2
3. S1R agonist/antagonist profile of compound 3 (RC-106)	S5
4. Expression of S1R and PGRMC-1 in CFPAC-1 line	S5
4. ¹ H and ¹³ C NMR spectra	S6
5. References	S19

1. Chiral resolution

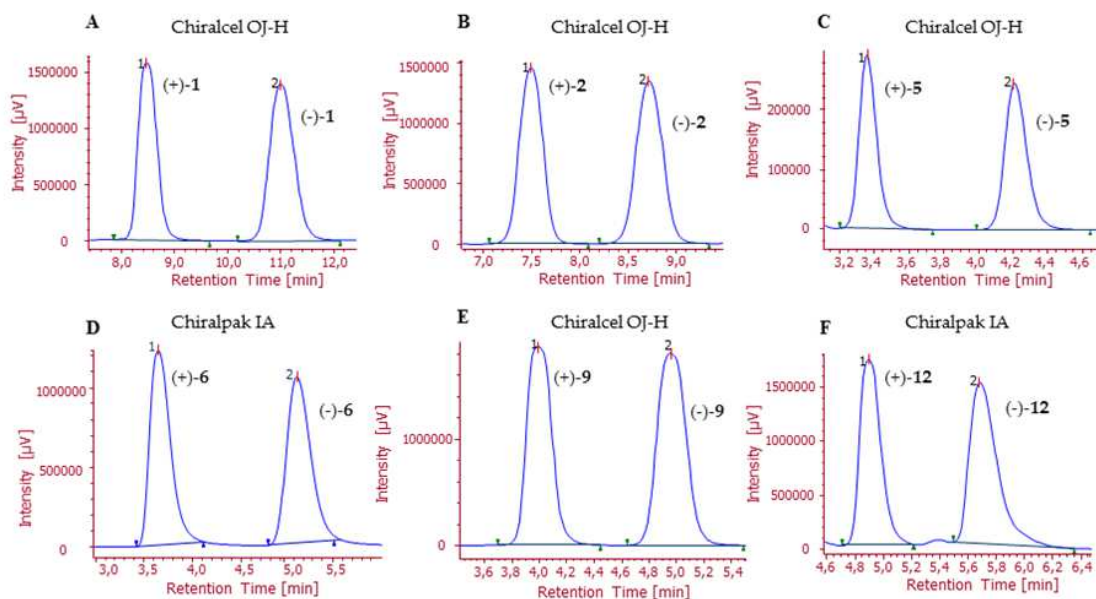


Figure S11. Selected analytical chromatographic profiles of A) **1**, B) **2**, C) **5**, D) **6**, E) **9**, F) **12**.

2. Molecular Modelling

Table S11. Free energy components (ΔH_{bind} and $-T\Delta S_{\text{bind}}$) and total binding free energies (ΔG_{bind}) for compounds **1-6** and **9, 11-12** in complex with S1R. Errors are given in parenthesis as standard errors of the mean.

Compound	ΔH_{bind} (kcal/mol)	$-T\Delta S_{\text{bind}}$ (kcal/mol)	ΔG_{bind} (kcal/mol)
1a	-23.71 (0.08)	-13.77 (0.17)	-9.94 (0.19)
1b	-23.81 (0.10)	-13.72 (0.19)	-10.09 (0.21)
2a	-24.33 (0.08)	-13.71 (0.19)	-10.62 (0.21)
2b	-24.44 (0.11)	-13.70 (0.16)	-10.74 (0.19)
3	-25.11 (0.09)	-14.15 (0.16)	-10.96 (0.18)
4	-25.61 (0.08)	-14.19 (0.17)	-11.42 (0.19)
5a	-24.59 (0.11)	-13.91 (0.18)	-10.68 (0.21)
5b	-24.77 (0.09)	-13.95 (0.20)	-10.82 (0.22)

6a	-25.26 (0.09)	-14.07 (0.15)	-11.19 (0.17)
6b	-25.08 (0.09)	-14.03 (0.18)	-11.05 (0.20)
9a	-23.62 (0.12)	-13.70 (0.21)	-9.92 (0.24)
9b	-24.04 (0.09)	-13.86 (0.20)	-10.18 (0.22)
11	-25.20 (0.09)	-14.21 (0.18)	-10.99 (0.20)
12a	-24.64 (0.13)	-14.04 (0.17)	-10.60 (0.21)
12b	-24.62 (0.08)	-13.95 (0.18)	-10.67 (0.20)

The computational analysis of the free energy of binding confirms that all compounds are able to bind S1R with high affinity, in agreement with experimental data. Although all molecules are provided with the molecular requirement to aptly bind the target receptor, our approach explains how the different aryl moiety and the carbonic spacer between this aromatic portion and the piperidine nitrogen atom, can affect ligand/receptor interactions. The per residue deconvolution of the binding enthalpy $\Delta H_{\text{bind, res}}$ was extended to all new derivatives **1-6**, **9**, **11-12**, in order to dissect the main structural features responsible for similarities/differences in their S1R affinity (Fig. SI2). This approach allowed us to quantitatively corroborate the SAR presented above on the effect of the different aryl/spacer moiety. Furthermore, the receptor/ligand interaction pattern determined for the present derivatives is highly reminiscent of the one previously reported for other arylalkylamines and arylalkylaminoalcohols [1-4].

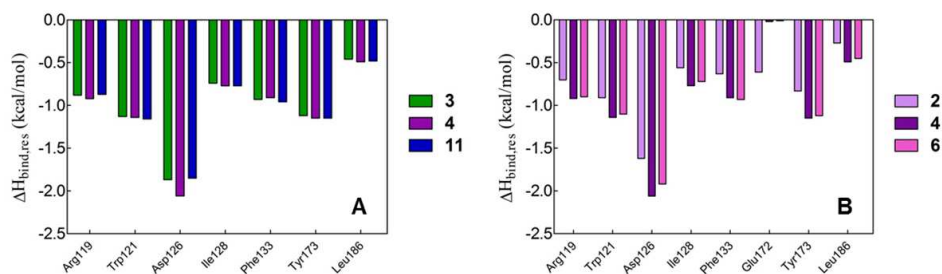


Figure SI2. Comparison of per-residue binding enthalpy decomposition for compounds **3**, **4** and **11** (A) and **2**, **4**, and **6** (B) in complex with the S1R. Only the receptor residues for which $\Delta H_{\text{bind, res}} < -0.40$ kcal/mol

are shown. Molecules **2** and **6** are chiral compounds and, for the sake of a quicker interpretation, the reported $\Delta H_{\text{bind, res}}$ values for these compounds represent the average between the computational binding affinities of each enantiomer, since they can be considered equivalent (see Table SI2), in agreement with our previous works [1-4].

The effect of the different aryl moieties was analyzed with the aim of explaining the most favorable free energy of binding of the benzyl substituted compound **4** ($\Delta G_{\text{bind}} = -11.42$ kcal/mol, Table SI1). The phenyl moiety adopts an optimal configuration in the binding site (Fig. SI2A), and the confined difference in the binding affinity with respect to the naphthalene and hydroxynaphthalene derivatives **3** and **11** can be ascribed to an overall, more favorable adaptation of the aryl moiety to perform π interaction with the residues Arg119 and Trp121 in the receptor binding pocket (Fig. SI2A).

Regarding the second purpose of our analysis, a common trend among the affinity of the molecules can be observed: the more rigid but-2-enyl spacer insured the best binding performances. Within the phenyl-bearing derivatives **2**, **4**, and **6**, the results confirmed that molecule **4**, provided with a but-2-enyl spacer, exerted the best binding interactions. The replacement of this linker with an alkyl chain in the compound **6** led to a slight reduction of the same stabilizing contribution, as shown in the comparison of the corresponding interaction spectra (Fig. SI2B). This was somewhat an expected result, as the differences between the two molecules fundamentally reside in the ability of the rigid alkenyl spacer to adopt an optimal conformation within the receptor binding site, with the most productive orientation of the interacting groups. On the other hand, the behaviour of derivative **2** deserves a more detailed examination of the results: the presence of the hydroxybutan-2-yl linker adds an extra pharmacophoric opportunity in compounds **2**, absent in derivatives **4** and **6**. This, in turn, reflects in the occurrence of an additional hydrogen bond between the -OH group on the compound linker and the side chain of Glu172, which provides a stabilizing contribution of -0.61 kcal/mol (Fig. SI2B). Despite the presence of this further feature, the contribution afforded by the other receptor residues involved in ligand binding in the case of **2** is lower than the one estimated for **4** and **6** (Fig. SI2B), and this, eventually, results in significantly lower affinity of **2** for the S1R.

3. S1R agonist/antagonist profile of compound 3 (RC-106).

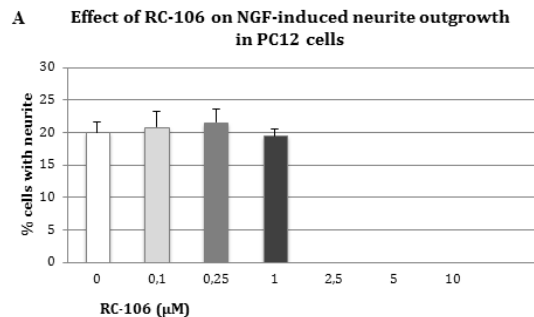


Figure SI3. Assay of NGF-induced neurite outgrowth in PC12 cells. Effect of RC-106 alone in the concentration range 0.1-10 µM. RC-106 does not affect NGF-induced neurite outgrowth in PC12 cell assay in the concentration range 0.1-1 µM. Conversely, NGF-induced neurite outgrowth is completely inhibited by in the range 2.5-10 µM. Histograms represent the mean \pm sem of at least 4 different experiments performed in triplicate.

4. Expression of S1R and PGRMC-1 in CFPaC-1 line

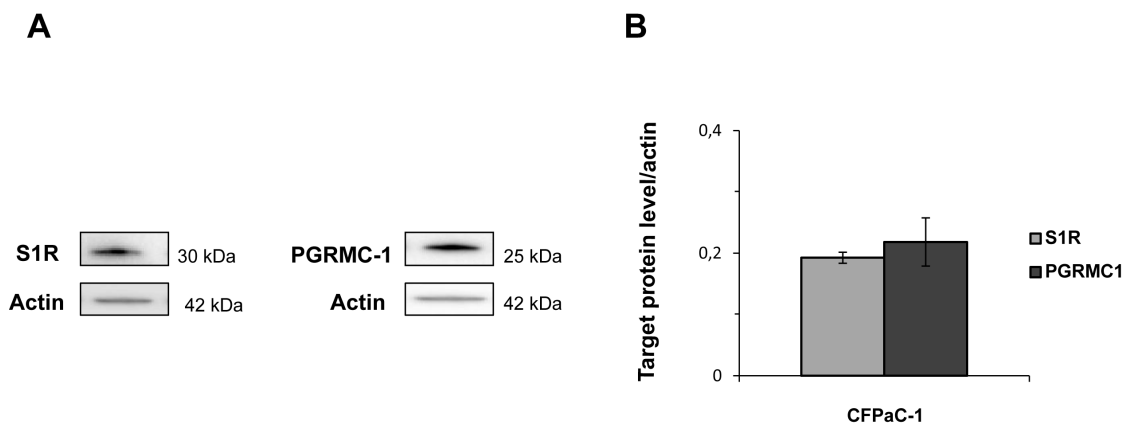
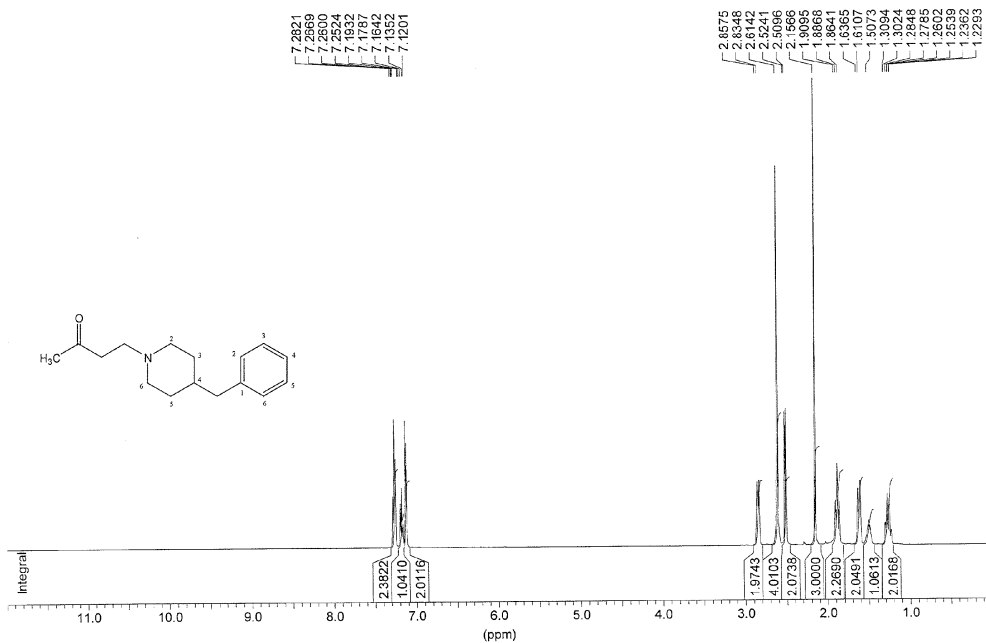


Figure SI4. Western blot and densitometry analysis of S1R and PGRMC-1 proteins CFPaC-1 cell line. (A) Immunoblotting reveal that CFPaC-1 cell line expresses both S1R and PGRMC-1 at the same level. (B) Relative protein levels were quantified by densitometry and normalized to β -actin expression. Densitometric analysis was made with Quantity One software (BIO-RAD). Immunoblotting data are representative of experiments performed in duplicate. No significant difference was noted using Student's *t*-test comparisons ($p < 0.05$, and $p < 0.01$).

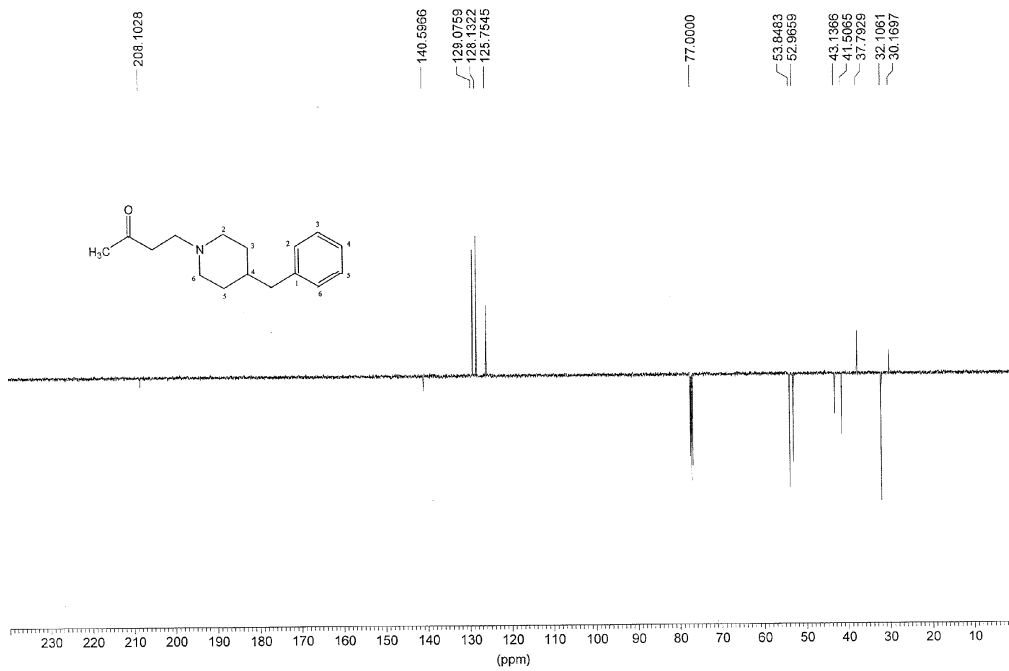
5. ^1H and ^{13}C NMR Spectra

3.1. β -aminoketone A

MR000a in cdd3 (Proton), 28.11.2014

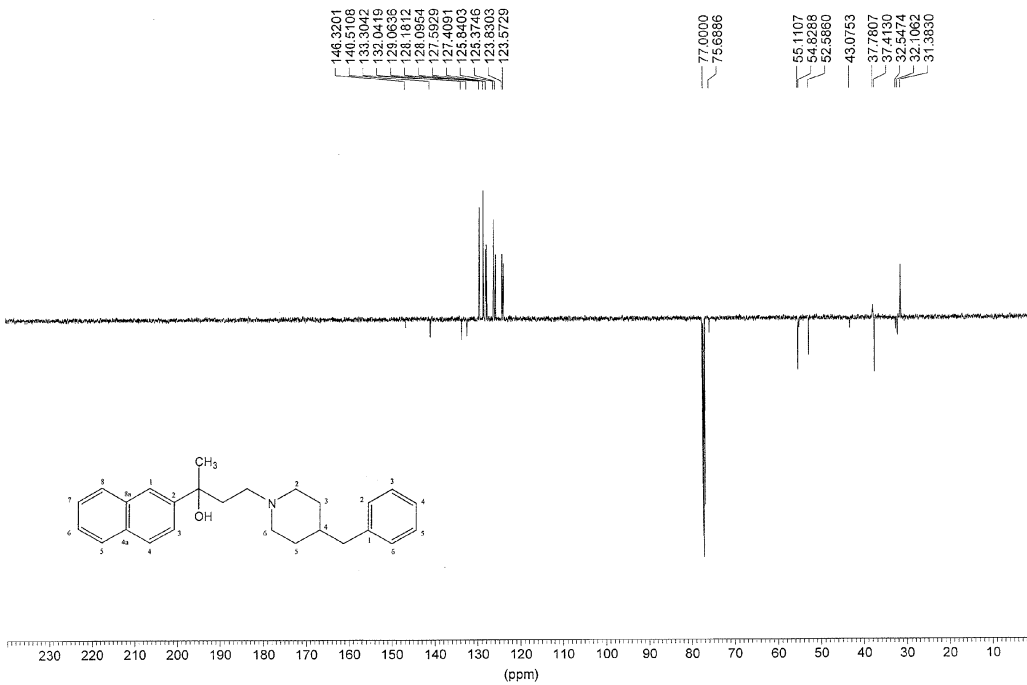
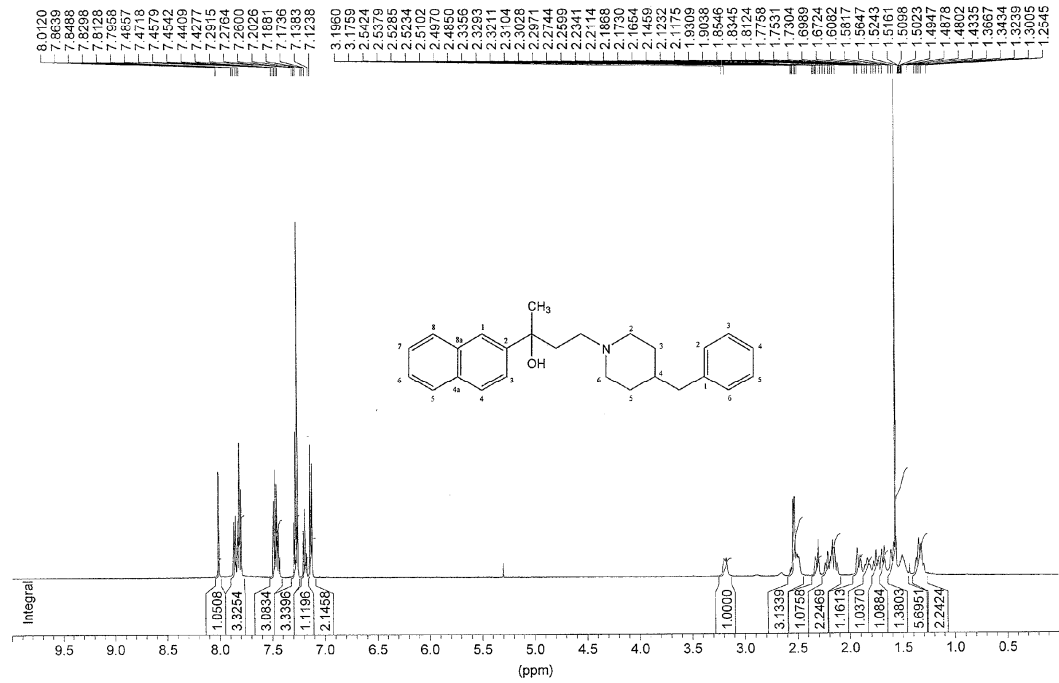


MR000a in cdd3 (APT), 28.11.2014



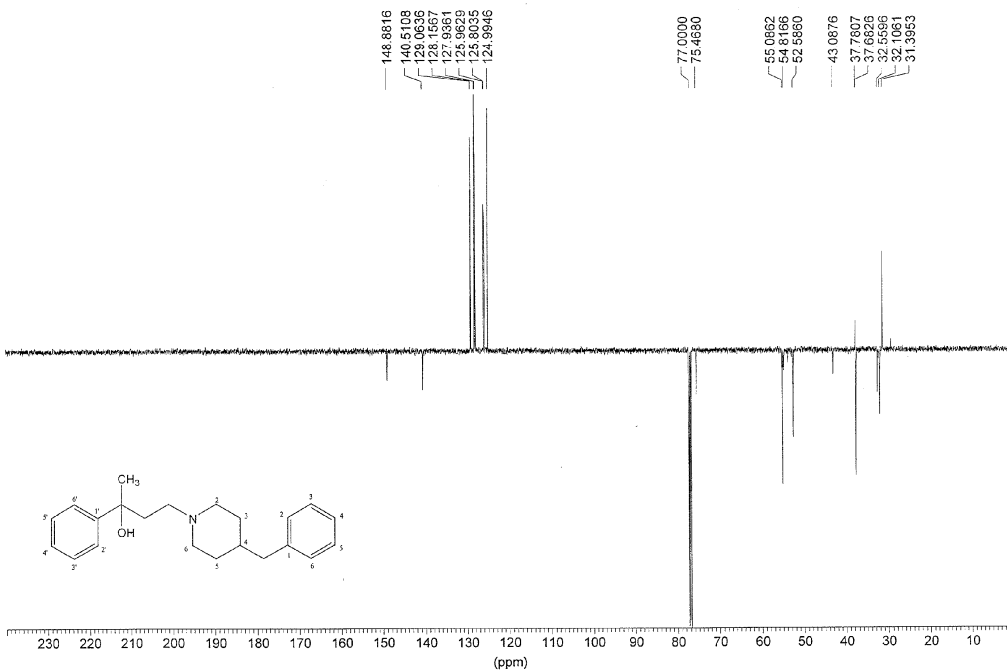
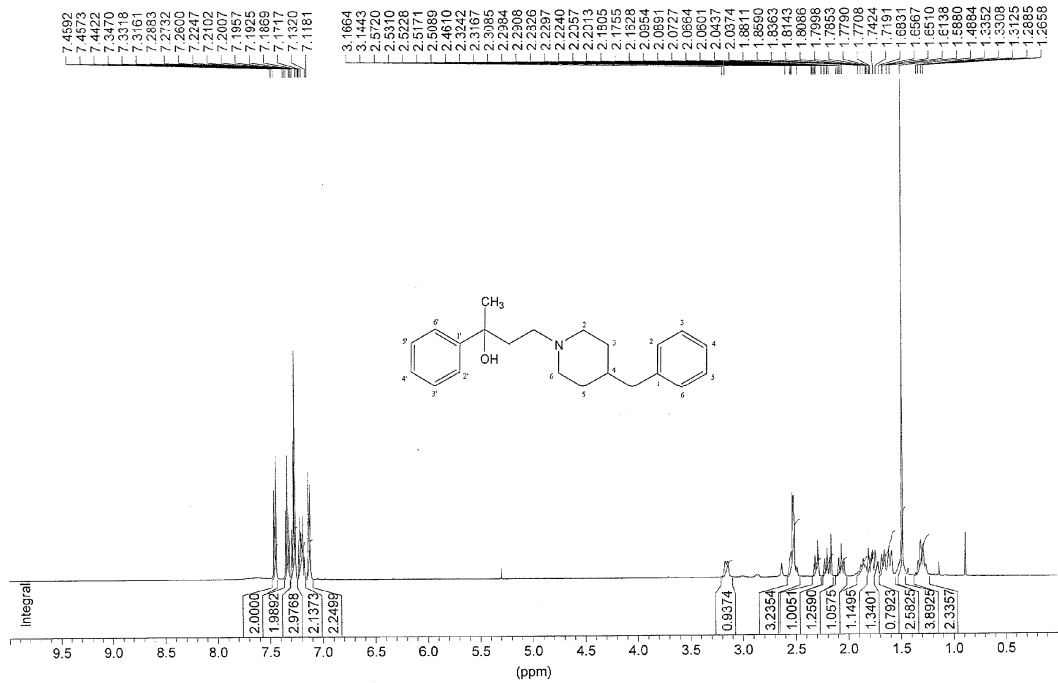
Compound 1

PV169 in cdd3 (Proton), 7.2.2015



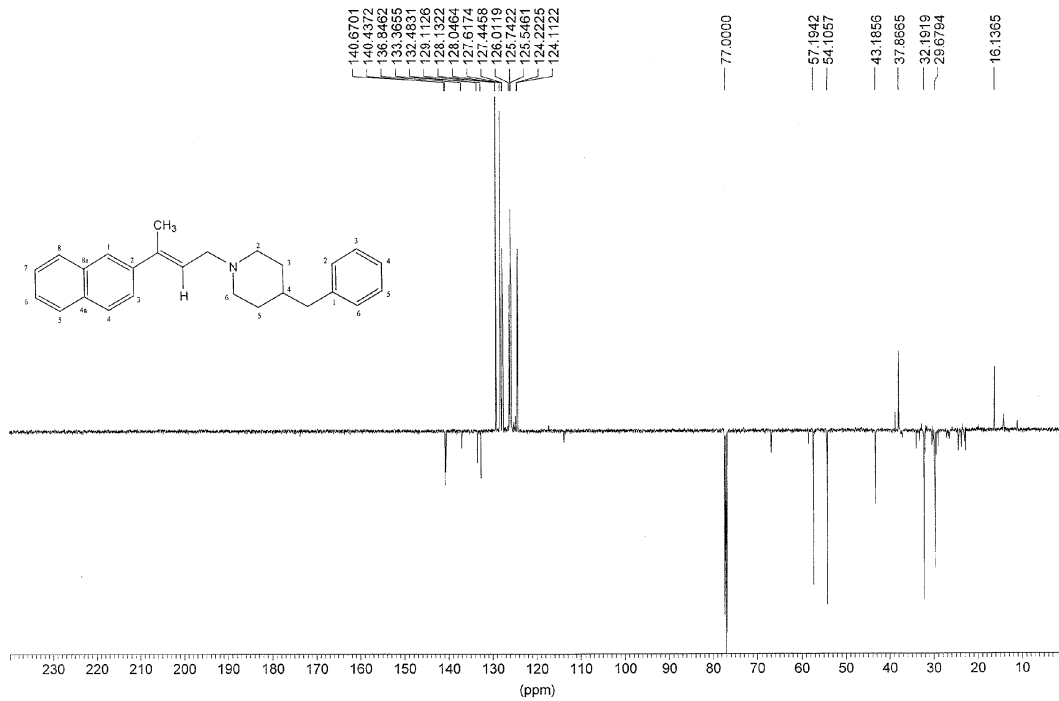
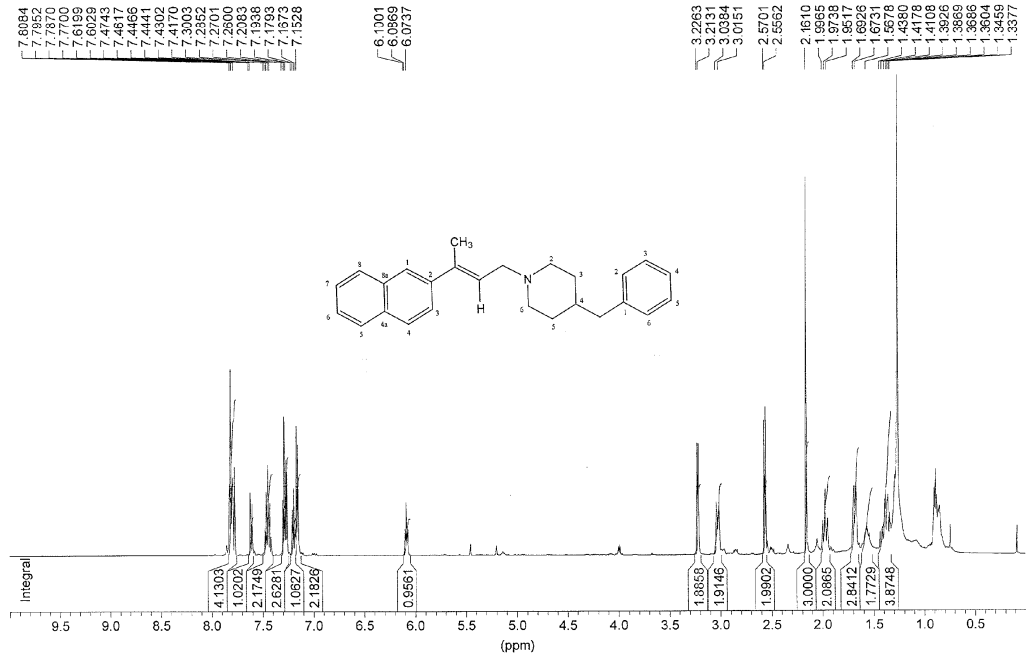
Compound 2

PV170 in cdc3 (Proton), 8.2.2015



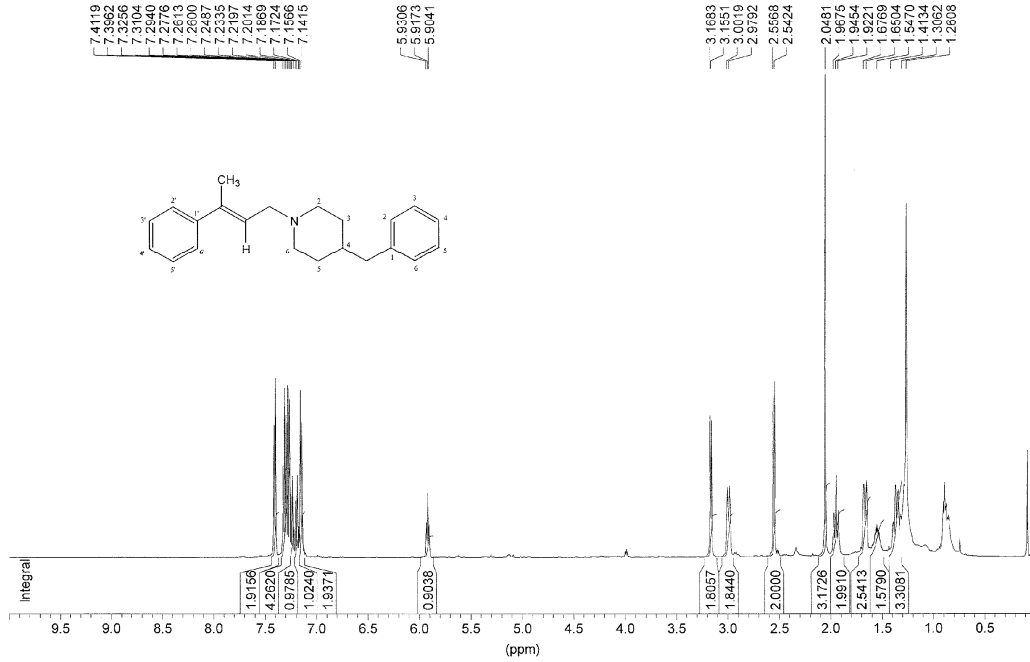
Compound 3 (RC-106)

MR126_1 (96-116) in cdcl3 (Proton), 13.2.2016

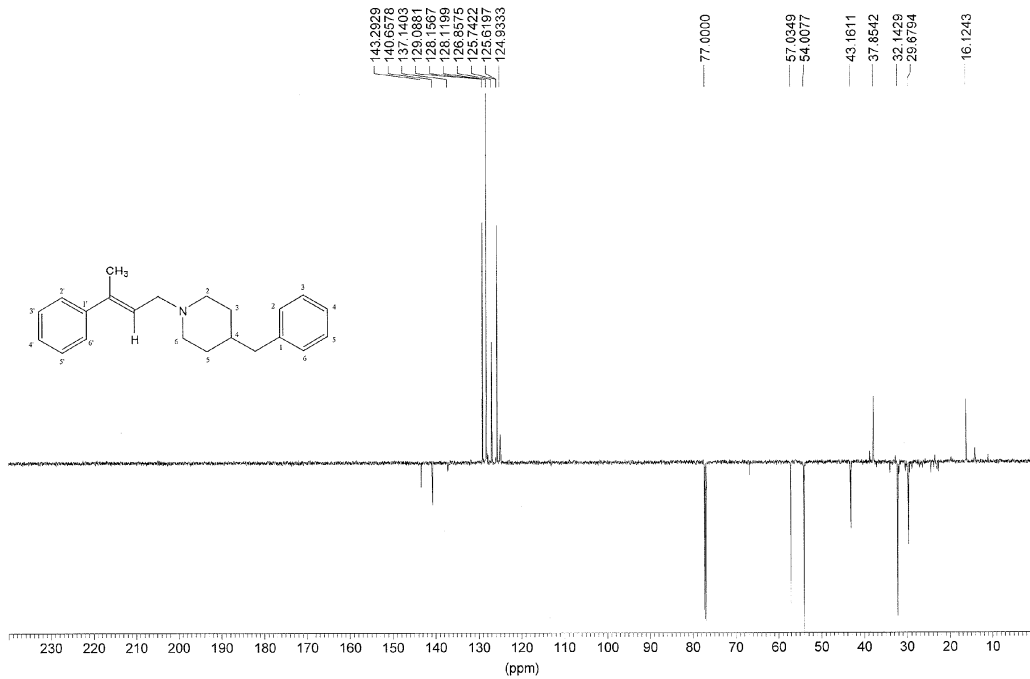


Compound 4

MR105_3 in cdcl3 (Proton), 23.4.2015

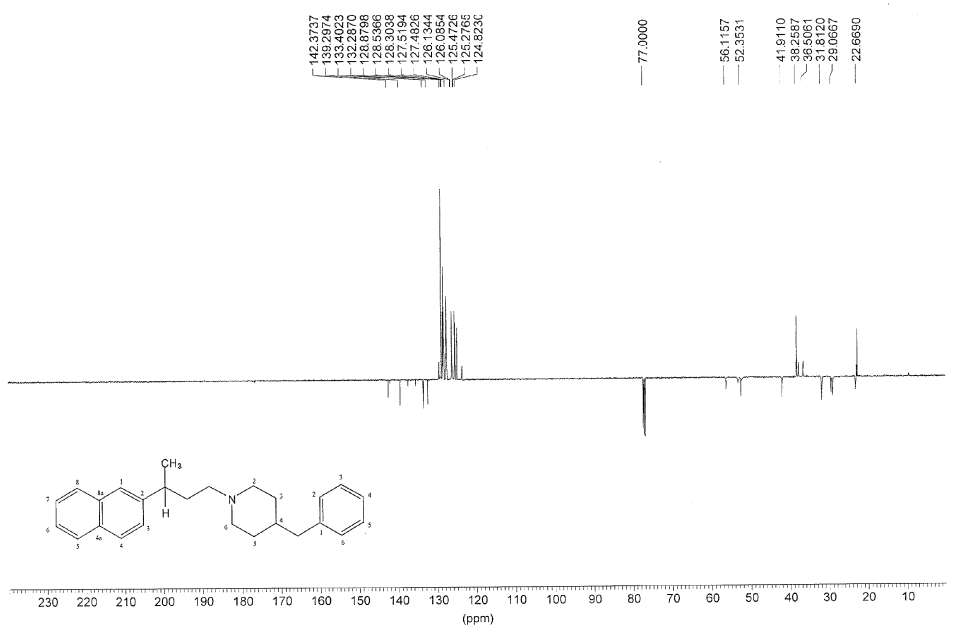
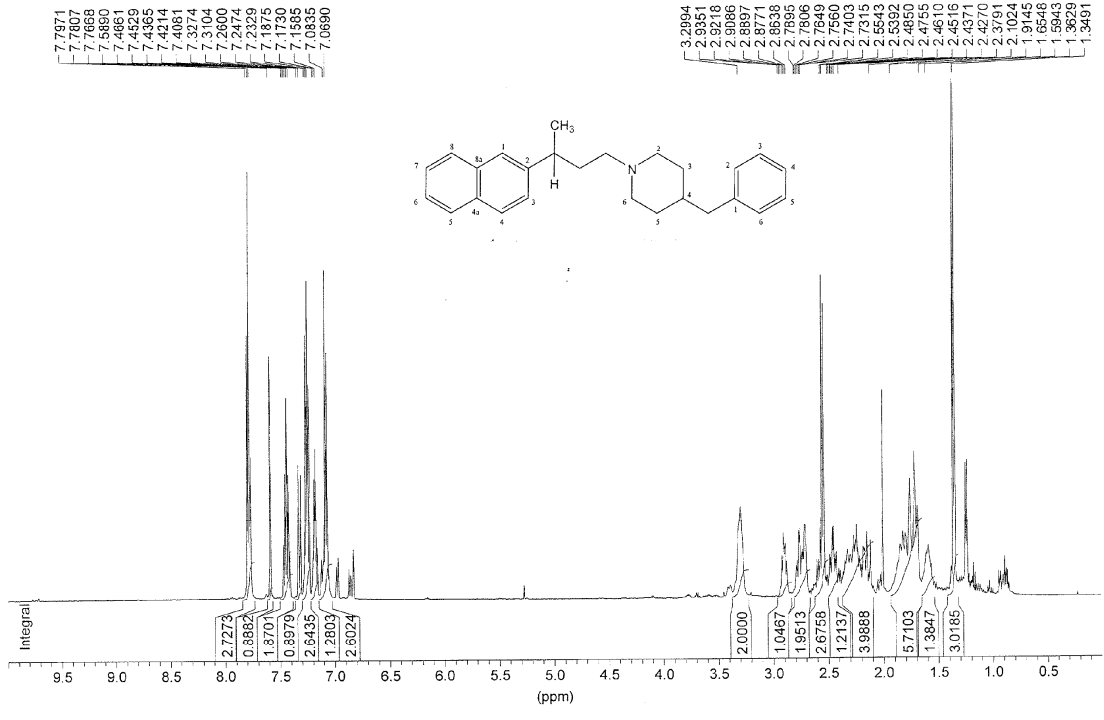


MR105_3 in cdcl3 (APT), 23.4.2015



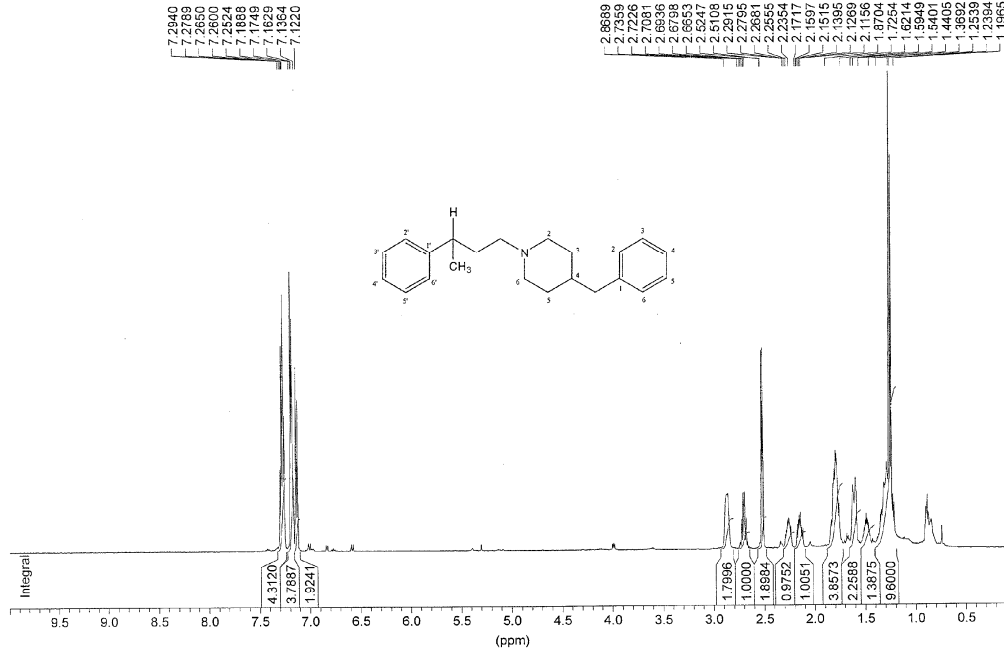
Compound 5

MR172_2 in cdcl3 (Proton), 24.3.2015

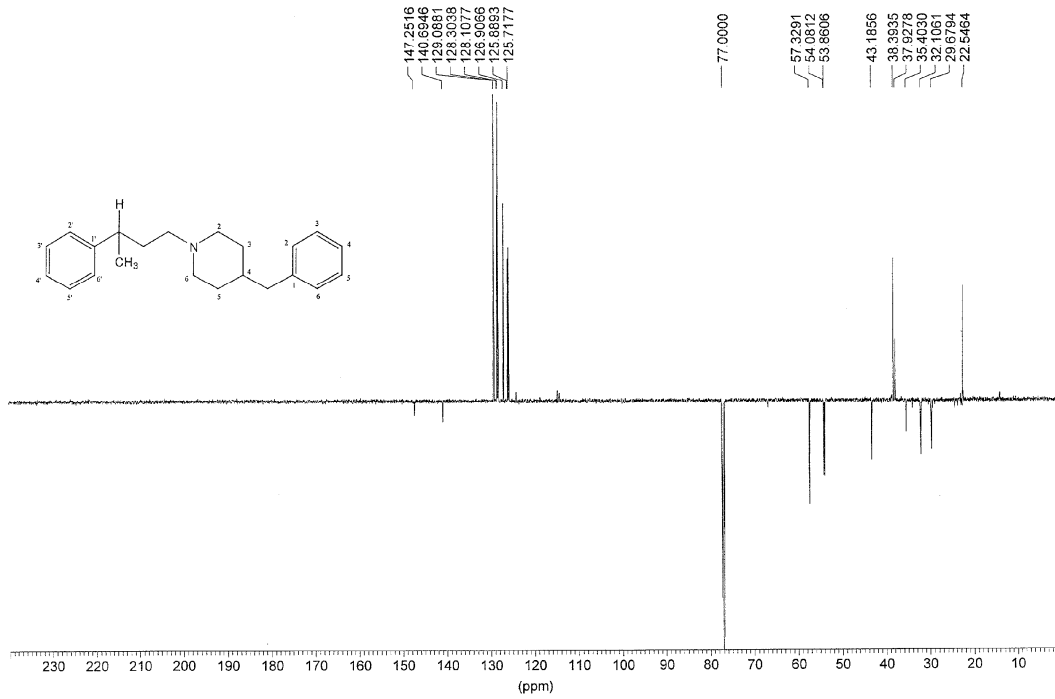


Compound 6

MR122_1 in cdcl3 (Proton), 5.2.2015

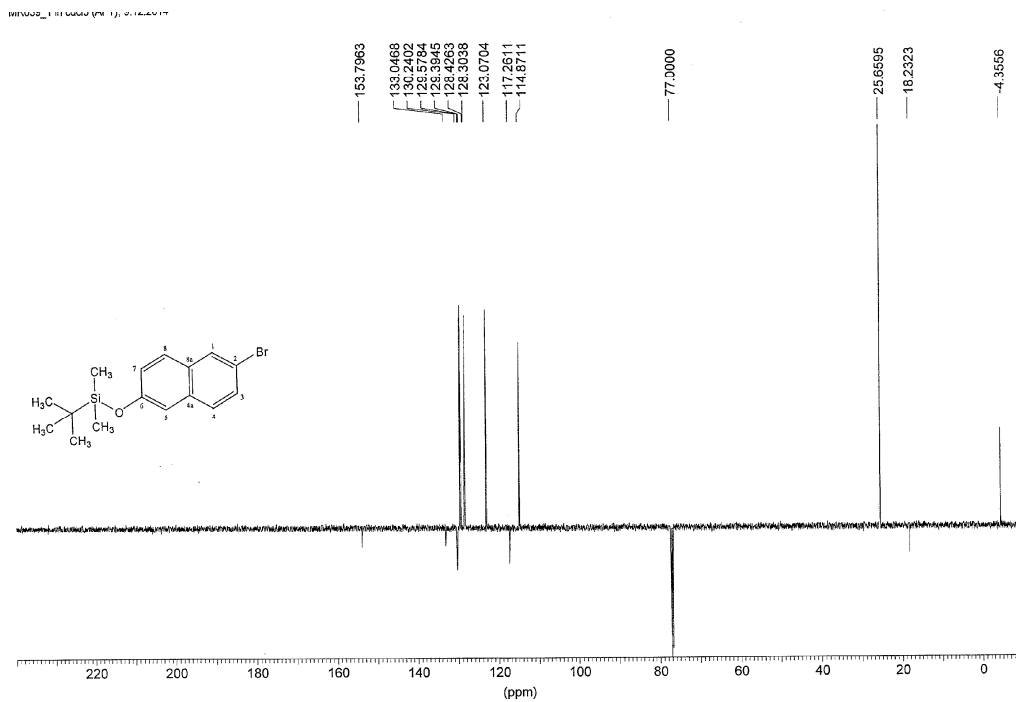
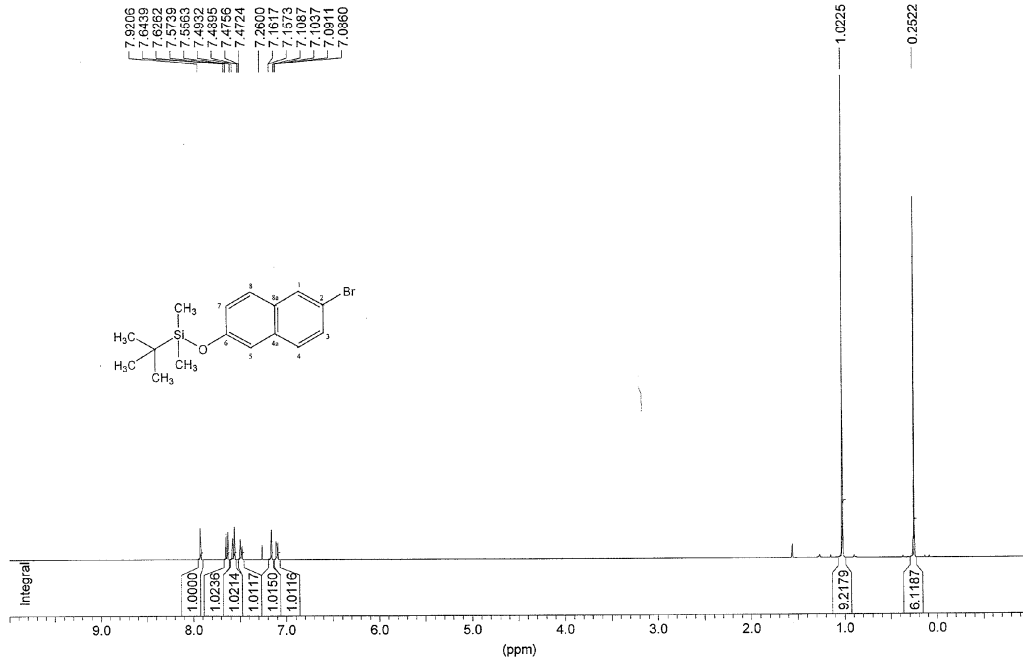


MR122_1 in cdcl3 (APT), 5.2.2015



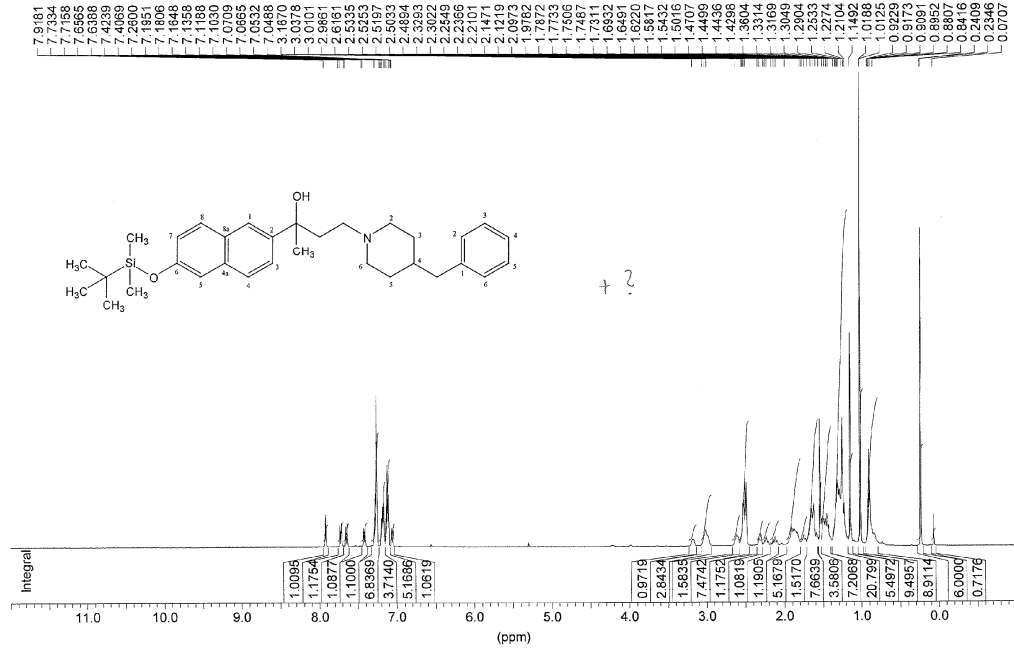
Compound 7

MR039_1 in cdcl3 (Proton), 9.12.2014

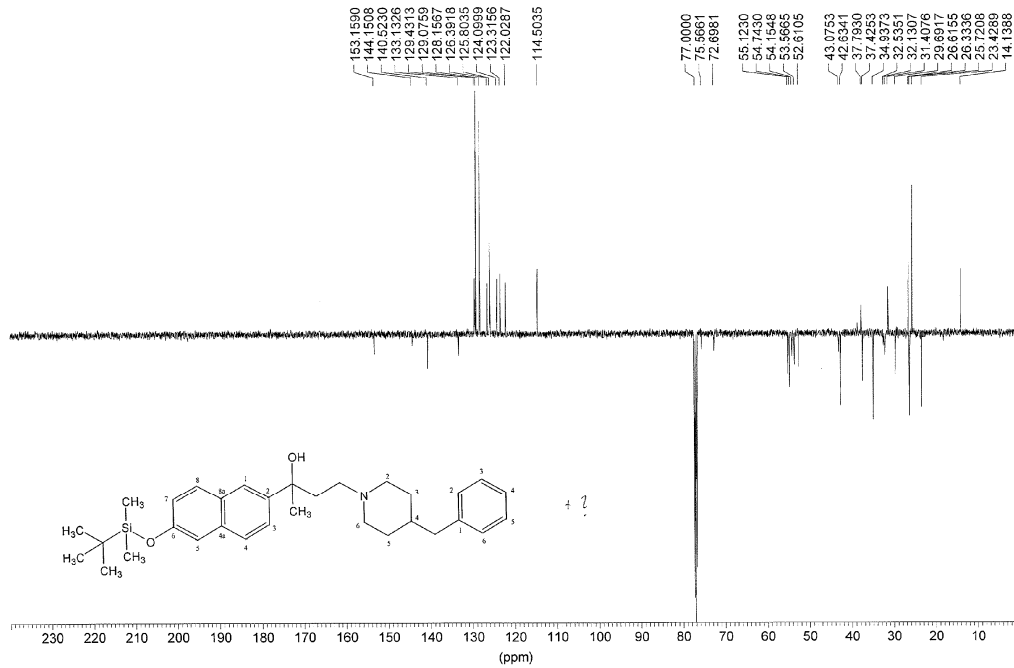


Compound 8

MR005_1 in cdc3 (Proton), 19.11.2014

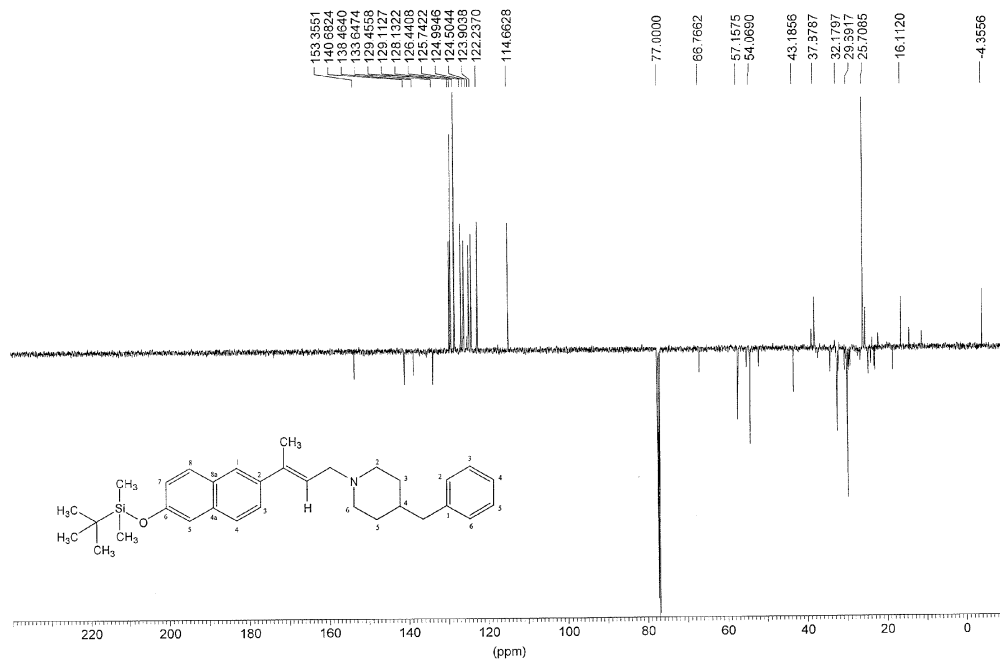
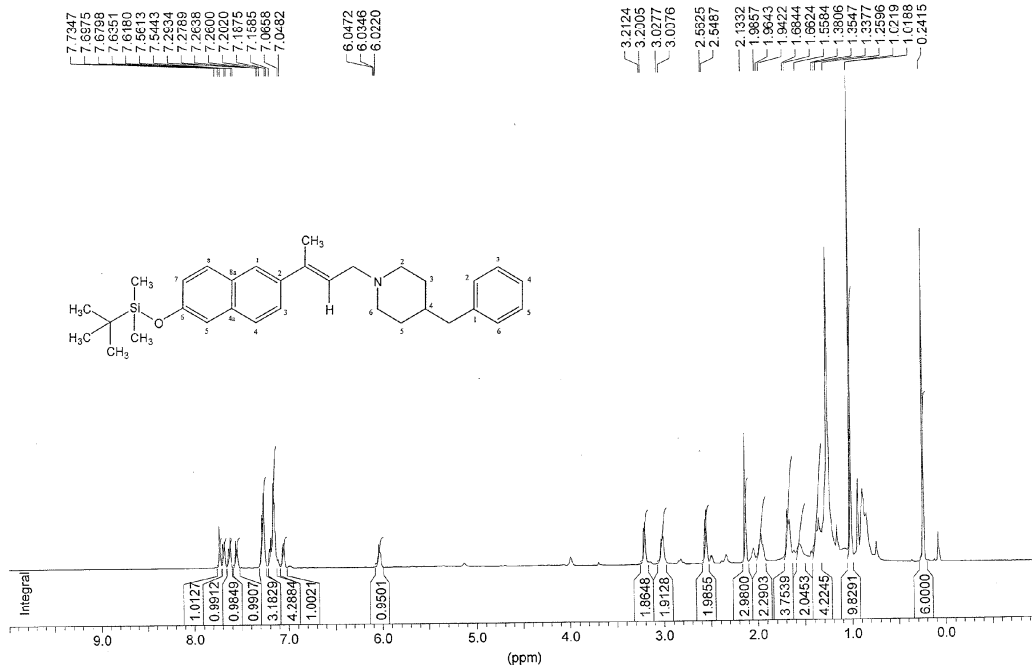


MR006_1 in cdc3 (APT), 19.11.2014



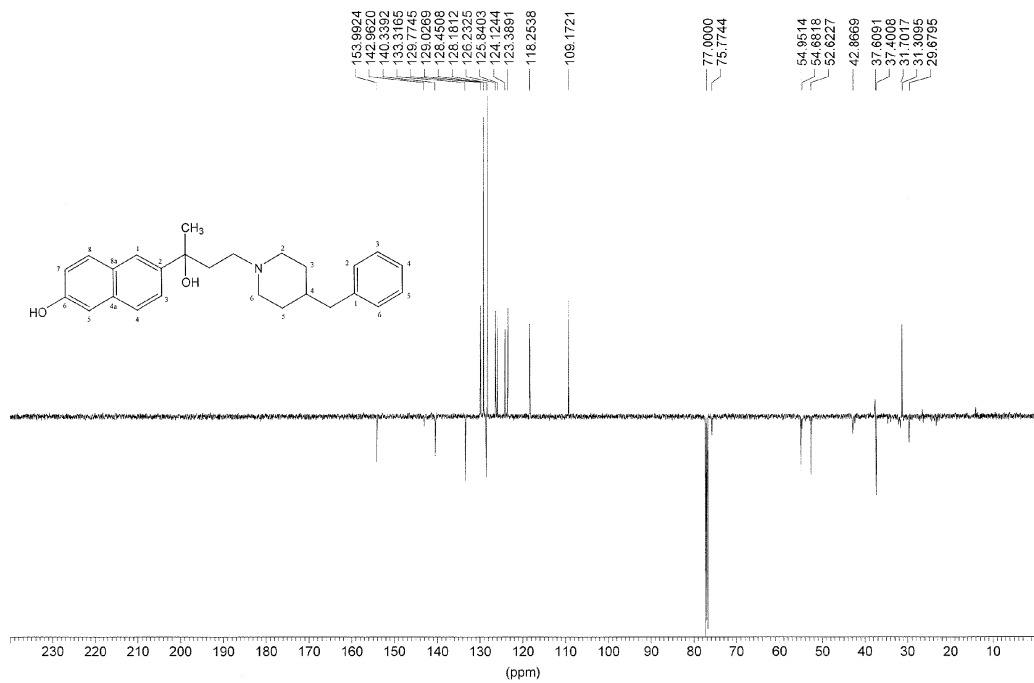
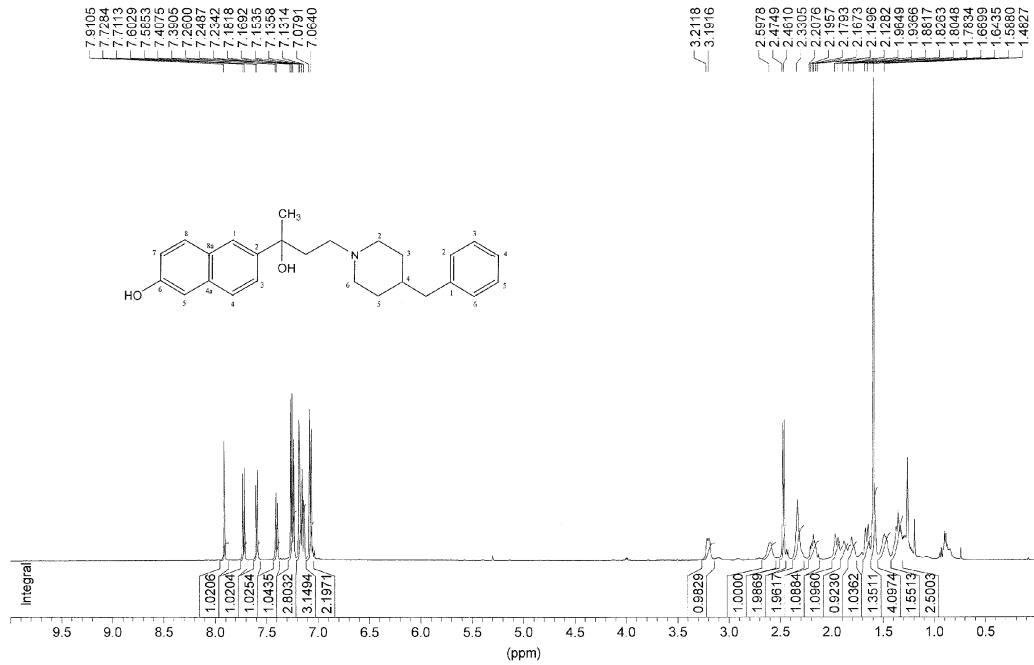
Compound 10

MR127_2 in odci3 (Proton), 11.2.2015



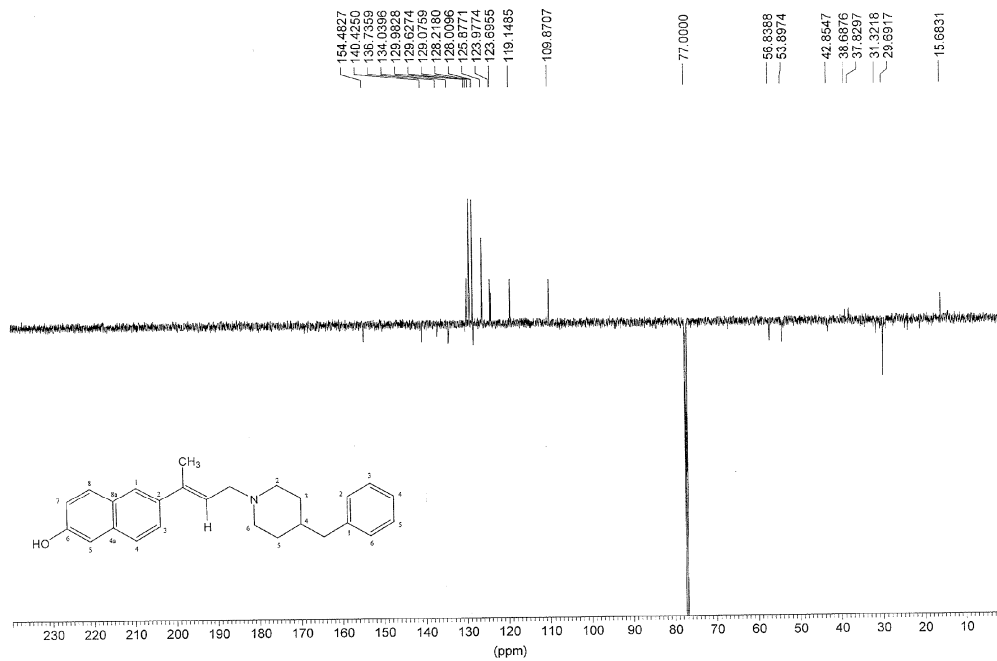
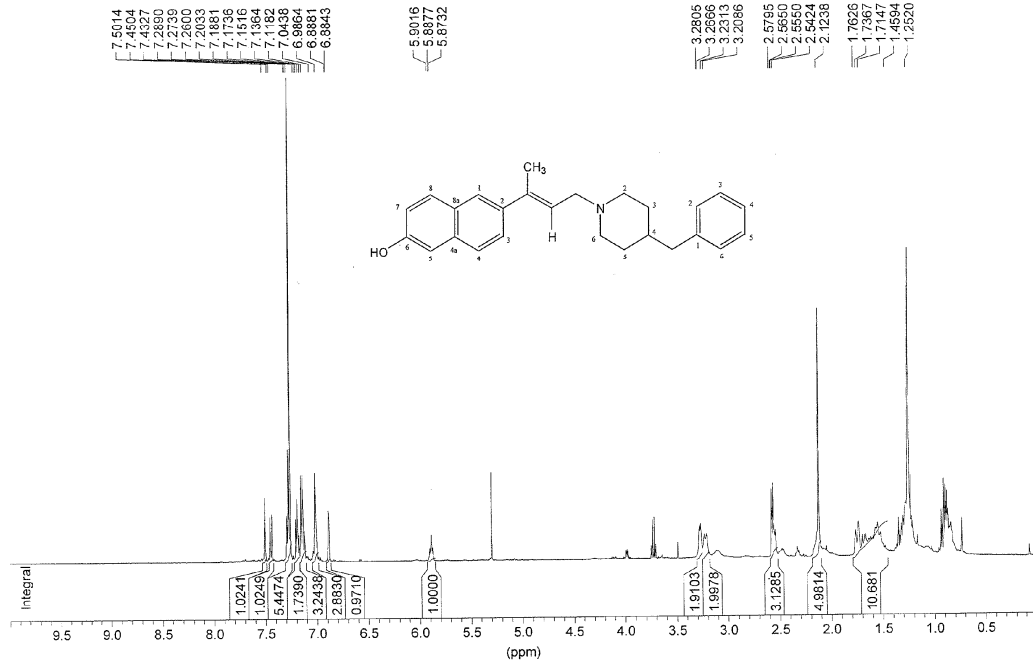
Compound 9

MR220_1 in cdCl3 (Proton), 24.4.2015



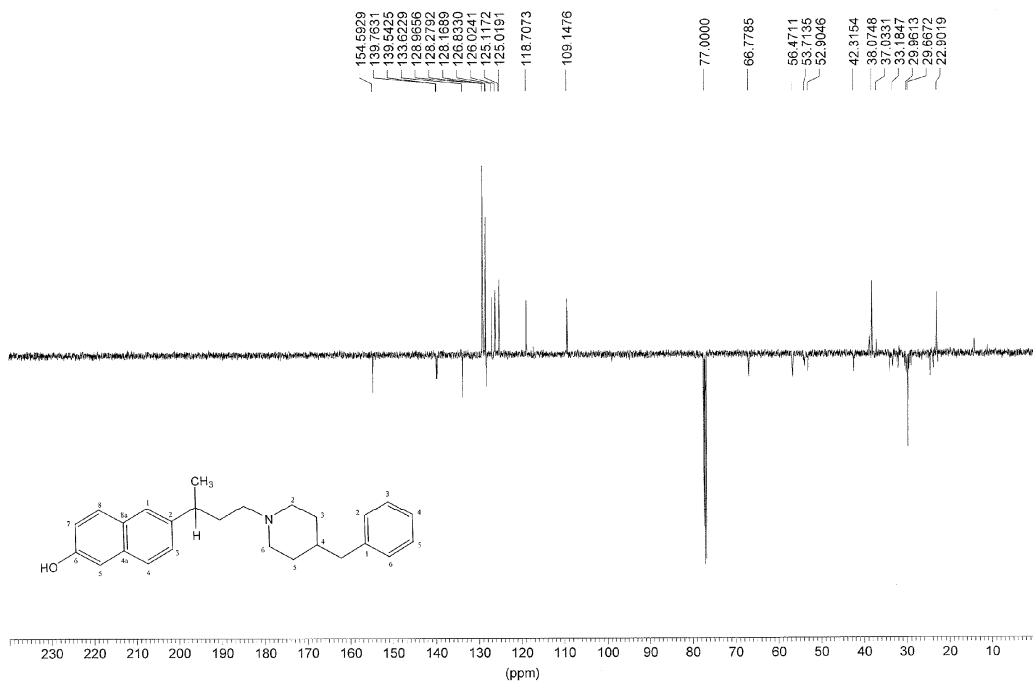
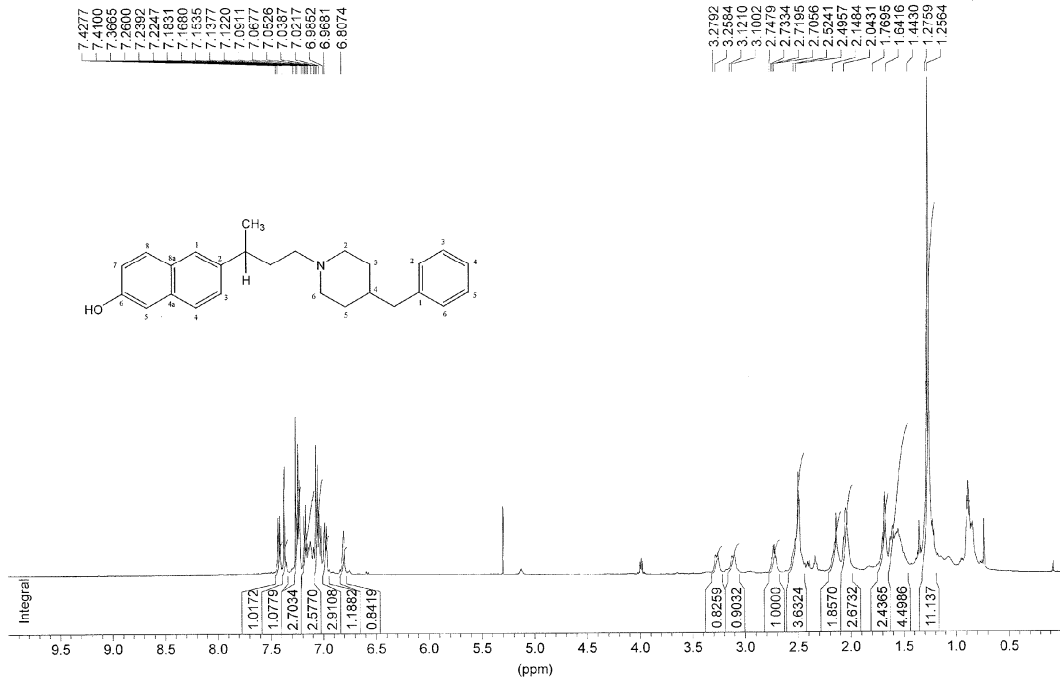
Compound 11

MR211_1 in cdd3 (Proton), 14.4.2015



Compound 12

MR219_1 in cdd3 (Proton), 27.4.2015



6. References

- [1] D. Rossi, A. Marra, P. Picconi, M. Serra, L. Catenacci, M. Sorrenti, E. Laurini, M. Fermeglia, S. Pricl, S. Brambilla, N. Almirante, P. Peviani, D. Curti, S. Collina. Identification of RC-33 as a potent and selective σ_1 receptor agonist potentiating NGF-induced neurite outgrowth in PC12 cells. Part 2: g-scale synthesis, physicochemical characterization and in vitro metabolic stability, *Bioorg. Med. Chem.* 21 (2013) 2577-2586.
- [2] D. Rossi, A. Pedrali, R. Gaggeri, A. Marra, L. Pignataro, E. Laurini, V. DalCol, M. Fermeglia, S. Pricl, D. Schepmann, B. Wünsch, M. Peviani, D. Curti, S. Collina. Chemical, pharmacological, and in vitro metabolic stability studies on enantiomerically pure RC-33 compounds: promising neuroprotective agents acting as σ_1 receptor agonists, *Chem. Med. Chem.* 8 (2013) 1514-1527.
- [3] D. Rossi, A. Marra, M. Rui, E. Laurini, M. Fermeglia, S. Pricl, D. Schepmann, B. Wünsch, M. Peviani, D. Curti, S. Collina. Chemical, pharmacological, and in vitro metabolic stability studies on enantiomerically pure RC-33 compounds: promising neuroprotective agents acting as σ_1 receptor agonists, *MedChemComm.* 6 (2015) 138-146.
- [4] D. Rossi, A. Pedrali, A. Marra, L. Pignataro, D. Schepmann, B. Wünsch, L. Ye, K. Leuner, M. Peviani, D. Curti, O. Azzolina, S. Collina. Studies on the enantiomers of RC-33 as neuroprotective agents: isolation, configurational assignment, and preliminary biological profile, *Chirality* 25 (2013) 814-822.

Article

Novel Enantiopure Sigma Receptor Modulators: Quick (Semi-)Preparative Chiral Resolution via HPLC and Absolute Configuration Assignment

Marta Rui ^{1,2}, Annamaria Marra ¹, Vittorio Pace ², Markus Juza ³, Daniela Rossi ¹ and Simona Collina ^{1,*}

¹ Department of Drug Sciences, Medicinal Chemistry and Pharmaceutical Technology Section, University of Pavia, Viale Taramelli 12, Pavia 27100, Italy; marta.rui01@universitadipavia.it (M.R.); annamaria.marra@unipv.it (A.M.); daniela.rossi@unipv.it (D.R.)

² Department of Pharmaceutical Chemistry, University of Vienna, Althanstrasse 14, Vienna 1090, Austria; vittorio.pace@univie.ac.at

³ Corden Pharma Switzerland LLC, Eichenweg 1, Liestal 4410, Switzerland; markus.juza@cordenpharma.com

* Correspondence: simona.collina@unipv.it; Tel.: +39-0382-987-379

Academic Editors: Claudio Villani and Derek J. McPhee

Received: 20 July 2016; Accepted: 6 September 2016; Published: 10 September 2016

Abstract: The identification of novel pan-sigma receptor (SR) modulators, potentially useful in cancer treatment, represents a new goal of our research. Here, we report on the preparation of novel chiral compounds characterized by a 3-C alkyl chain bridging an aromatic portion to a 4-benzyl-piperidine moiety. All of the studied compounds have been prepared both in racemic and enantiomerically-pure form, with the final aim to address the role of chirality in the SR interaction. To isolate and characterize enantiomeric compounds, high-performance liquid chromatography (HPLC) procedures were set up. A systematic analytical screening, involving several combinations of chiral stationary and mobile phases, allowed us to optimize the analytical resolution and to set up the (semi-)preparative chromatographic conditions. Applying the optimized procedure, the enantiomeric resolution of the studied compounds was successfully achieved, obtaining all of the compounds with an enantiomeric excess higher than 95%. Lastly, the absolute configuration has been empirically assigned to enantiopure compounds, combining the electronic circular dichroism (ECD) technique to the elution order study.

Keywords: sigma receptor (SR) modulators; amylose- and cellulose-derived CSPs; chiral resolution; enantioselective HPLC; electronic circular dichroism (ECD)

1. Introduction

Sigma receptors (SRs) are involved in different pharmacological and pathological pathways. They modulate cell survival and excitability and sub-serve many critical functions in the human body. To date, two subtypes have been identified: Sigma 1 (S1R) and Sigma 2 receptors (S2R). S1Rs are overexpressed in the central nervous system (CNS), while S2Rs are overexpressed in tumor cells and tissues in proliferation [1]. Accordingly, S1R modulators could be useful for the treatment of several CNS diseases, such as anxiety, depression, schizophrenia, drug addiction, Parkinson's and Alzheimer's diseases [2], whereas S2R ligands could have a relevant role in cancer diagnosis and therapy [3]. Since some research groups identified an overexpression of S1R in different typologies of cancer cells and demonstrated a strict correlation between S1R and this pathological manifestation, S1R has been also proposed as a potential target for treating cancer conditions [4–6]. As a result, therapies that have S1R and S2R as targets might play a role against a wide spectrum of cancer types. Indeed, recent literature highlights the anticancer potential of ligands able to bind both receptor subtypes,

called pan-SR ligands [7]. The work presented here falls into this field, and it is a part of our ongoing research focused on the identification of novel SR modulators. Along the years, we prepared and studied a wide compound library of SR modulators [8]. The SAR analysis evidenced that a good affinity towards both SRs is related to the presence of a bulky aminic moiety [9,10]. Particularly, the 4-benzylpiperidine derivative RC-106 (Figure 1) is characterized by a good affinity toward both S1R and S2R (K_i S1R = 12.0 nM \pm 6.0; K_i S2R = 22.0 nM \pm 1.1). Moreover, the SAR studies of chiral SR modulators showed that small changes in the ligand structure markedly influence the ability of SRs to discriminate the enantiomeric form. For example, racemic and enantiomeric RC-33 (Figure 1) interact in a non-stereoselective manner with SRs, both enantiomers showing a similar affinity toward both S1R and S2R [11–13]. A different behavior was observed for the analogue RC-34, characterized by the presence of an electronegative element (the only structural difference with respect to RC-33). In this case, the (*S*)-configured enantiomer resulted in being the eutomer, with the following eudismic ratio (ER, K_i distomer/ K_i eutomer): $ER_{S1R} = 8.3$ and $ER_{S2R} = 2.5$ [14]. According to these results, the capability of SRs to discriminate between the enantiomers of a ligand seems to be strictly related to its structural features [15].

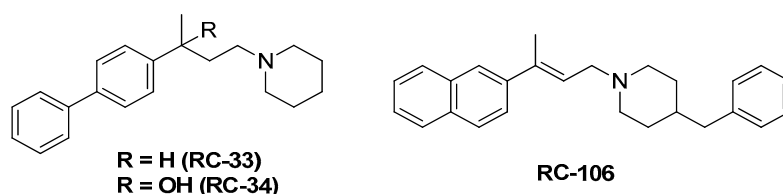


Figure 1. Structures of RC-33, RC-34 and RC-106.

In this paper, we report on the preparation of the potential chiral SR modulators 1–6, characterized by an alkyl or alcoholic spacer bridging an aromatic moiety to the 4-benzyl-piperidine portion (Table 1) and discuss in detail our efforts to develop easy-to-use chiral chromatographic methods, this approach being effective for both analytical and preparative purposes [16–19]. Moreover, we report on absolute configuration assignment studies of enantiomerically-pure 1–6, combining electronic circular dichroism (ECD) and elution order studies. Our final aim is to have enantiopure 1–6 in a sufficient amount for the biological investigation, in order to study the intriguing aspect of the influence of chirality in SR interaction.

Table 1. Molecules under investigation.

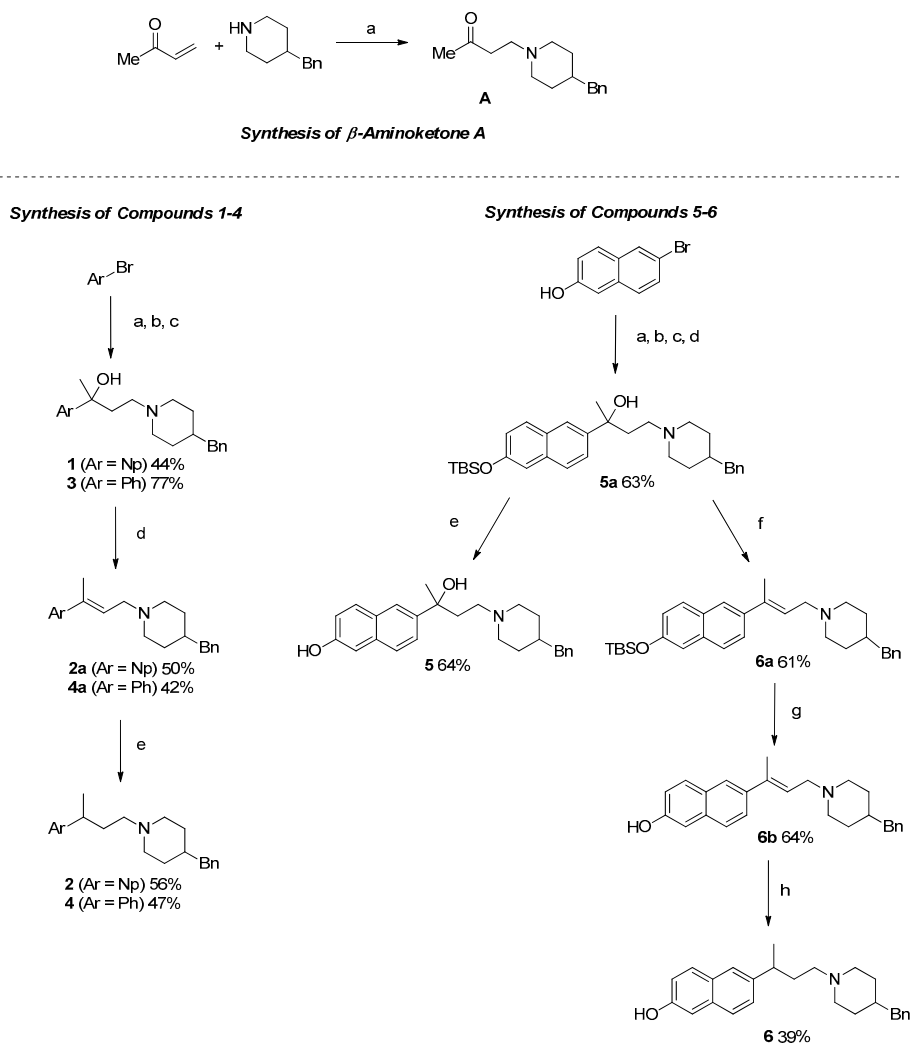
Compound	Ar	R
1		OH
2		H
3		OH
4		H
5		OH
6		H

2. Results and Discussion

2.1. Synthesis

As reported in Scheme 1, the synthesis of 4-(4-benzyl-piperidin-1-yl)-butan-2-one, common intermediate (A), was accomplished in a good yield via the Michael addition of 4-benzyl piperidine to

but-3-en-2-one in absolute ethanol and glacial acetic acid. Briefly, Compounds **1** and **3** were obtained adopting a nucleophilic addition strategy of in situ-generated organolithium species to ketones. The appropriate aryl-bromine was lithiated with an excess of *tert*-butyllithium (*t*-BuLi) in anhydrous diethyl ether (Et₂O) at $-78\text{ }^{\circ}\text{C}$, followed by the addition of **A**: the desired tertiary alcohols **1** and **3** were obtained in practical yields. Subsequently, the so-obtained alcohols were subjected to dehydration with trifluoroacetic anhydride under copper(I) triflate catalytic conditions [20]. Purification on alumina column chromatography provided the olefins **2a** and **4a**, which were hydrogenated (Pd (0)/C 10% (*p/p*)) to give the corresponding reduced amines **2** and **4**. The same tactic was applied for accessing naphthol derivatives **5** and **6**. However, prior to lithiation, the protection of the aromatic alcohol as TBS-ether was required to prevent interference during the metalation step. Additional points merit mention: (1) keeping the temperature at $-50\text{ }^{\circ}\text{C}$ after the quenching with **A**, (2) employing THF as the solvent and (3) using the less basic *n*-BuLi as the lithiating agent resulted in being beneficial to maximize the yield. Lastly, under identical conditions to those ones reported for the synthesis of **2** and **4**, Compound **6** was obtained in a good yield.



Scheme 1. Synthesis of Compounds **1–6**. Experimental conditions: β -aminoketone **A**: (a) glacial acetic acid, abs EtOH, rt; Compounds **1–4**: (a) *t*-BuLi, anhydrous Et₂O, $-78\text{ }^{\circ}\text{C}$ to rt; (b) ketone **A**, $-78\text{ }^{\circ}\text{C}$ to $0\text{ }^{\circ}\text{C}$; (c) H₂O rt; (d) Cu(OTf)₂, (CF₃O)₂O, anhydrous DCM, $0\text{ }^{\circ}\text{C}$ to rt; (e) H₂, Pd(0)/C 10% (*p/p*), abs EtOH, rt; Compounds **5–6**: (a) TBDMSCl, DMF; (b) *n*-BuLi, THF, $-78\text{ }^{\circ}\text{C}$; (c) ketone **A**, $-50\text{ }^{\circ}\text{C}$; (d) NH₄Cl (aq.), rt; (e) TBAF, CH₂Cl₂, $0\text{ }^{\circ}\text{C}$; (f) TFAA, Cu(OTf)₂ (2 mol-%) CH₂Cl₂, $0\text{ }^{\circ}\text{C}$ to rt; (g) TBAF, CH₂Cl₂; (h) H₂ (1 atm) Pd/C (10 mol %) EtOH, rt.

2.2. Analytical Screening and Development of a Scalable Resolution Method

The strategy we adopted for obtaining enantiopure **1–6** is based on our knowledge and extensive experience in chiral liquid chromatography that led us to have a wide range of chiral analytical and (semi-)preparative columns in-house. As a first choice, we used amylose- and cellulose-based CSPs immobilized on silica gel chiral columns, due to their wide solvent compatibility, versatility and robustness. In details, Chiralpak IC (cellulose tris(3,5-dichlorophenylcarbamate immobilized on silica gel) and Chiralpak IA (amylose tris(3,5-dimethylphenylcarbamate, immobilized on silica gel) have been used, eluting with alcohols (MeOH or /and EtOH) or with *n*-hep in the presence of polar modifiers (EtOH or IPA), DEA 0.1% and TFA 0.3%.

Therefore, the HPLC screening protocol of Table 2 was applied, and only when the results of this screening were encouraging, but not fully successful, the mobile phase was slightly modified in order to achieve a compound baseline separation. Since no satisfactory chiral separation for all compounds was obtained, conventional cellulose-based chiral column Chiralcel OJ-H (cellulose tris(4-methylbenzoate, coated on silica gel) was also experimented with, again eluting with alcohols (MeOH or /and EtOH) or *n*-hep in the presence of IPA as polar modifier and adding DEA 0.1%. Results of the analytical screening are reported in Tables 3–5 and are expressed as retention (*k*), selectivity (α) and resolution (*R*_s) factors.

Table 2. Screening protocol: mobile phase composition.

Entry	Mobile Phase Composition (%)			
	MeOH	EtOH	<i>n</i> -hep	IPA
1	100	-	-	-
2	50	50	-	-
3	-	10	90	-
4	-	-	90	10

Chiralpak IC provided a baseline separation of Compounds **1**, **2**, **4** and **6**, even if the chromatographic conditions were not suitable for a productive scale-up (Table 3). In detail, no enantioresolution was observed eluting with alcohols (data not shown), while modest or good values of α and *R*_s were obtained eluting with *n*-hep/EtOH or *n*-hep/IPA, even if the retention times (*t*_R) are quite long (*t*_R of the second eluted enantiomer ranging from 30–90 min). Moreover, to solve Compound **1**, a slight modification of the mobile phase composition of the screening protocol, eluting with *n*-hep/IPA (92/8, *v/v*), has been necessary. Nevertheless, a modest resolution was achieved ($\alpha = 1.12$ and *R*_s = 1.44).

Table 3. Analytical screening on Chiralpak IC with different mobile phases containing 0.1% DEA and 0.3% TFA.

Compound	Mobile Phase			<i>K</i> ₁	<i>K</i> ₂	<i>A</i>	<i>R</i> _s
	<i>n</i> -hep (%)	EtOH (%)	IPA (%)				
<i>(R/S)</i> -1	90	10	-	1.52		1	-
	90	-	10	4.45		1	-
	92	-	8	7.76	8.72	1.12	1.44
<i>(R/S)</i> -2	90	10	-	1.93		1	-
	90	-	10	7.83	9.62	1.23	2.36
<i>(R/S)</i> -3	90	10	-	1.29		1	-
	90	-	10	1.35		1	-
<i>(R/S)</i> -4	90	10	-	1.56		1	-
	90	-	10	6.52	8.68	1.33	3.08
<i>(R/S)</i> -5	90	10	-	3.24		1	-
	90	-	10	15.79		1	-
<i>(R/S)</i> -6	90	10	-	4.07		1	-
	90	-	10	27.14	29.97	1.11	1.26

Flow rate: 1 mL/min. Detection: 254 nm (Compounds **1**, **2**, **5**, **6**) and 220 nm (Compounds **3**, **4**).

Chiralpak IA gave rise to better results, being effective in resolving Compounds 1–6 (Table 4). Interestingly, the presence of *n*-hep in the mobile phase was essential for the separation of 1, 3 and 5 and gave rise to quite long retention times (t_R of the second eluted enantiomer ranging from 15–65 min). Conversely, 2, 4 and 6 (endowed with an alkyl spacer) have been successfully resolved eluting with pure MeOH in short times (t_R second eluted enantiomer less than 10 min).

Table 4. Analytical screening on Chiralpak IA with different mobile phases containing 0.1% DEA.

Compound	Mobile Phase				K_1	K_2	α	R_s
	<i>n</i> -hep (%)	MeOH (%)	EtOH (%)	IPA (%)				
(R/S)-1	-	100	-	-	5.48		1	-
	90	-	10	-	3.48		1	-
	90	-	-	10	5.00	5.55	1.11	1.69
(R/S)-2	-	100	-	-	1.00	1.24	1.24	1.73
	90	-	10	-	2.62		1	-
	90	-	-	10	4.24	5.07	1.19	2.08
(R/S)-3	-	100	-	-	0.53		1	-
	90	-	10	-	2.77	3.25	1.17	1.67
	90	-	-	10	3.84		1	-
(R/S)-4	-	100	-	-	0.57	0.81	1.42	3.06
	90	-	10	-	1.99		1	-
	90	-	-	10	3.21		1	-
(R/S)-5	-	100	-	-	0.35		1	-
	90	-	10	-	13.72	17.38	1.27	3.04
	90	-	-	10	14.68	18.55	1.26	2.95
(R/S)-6	-	100	-	-	0.96	1.27	1.32	2.49
	90	-	10	-	8.90	10.45	1.18	3.22
	90	-	-	10	19.76	23.86	1.21	2.94

Flow rate: 1 mL/min. Detection: 254 nm (Compounds 1, 2, 5, 6) and 220 nm (Compounds 3, 4).

On the basis of these results and keeping in mind that our purpose is to set up an economic and productive preparative enantiomer separation for 1–6, we turned our attention to a further analytical screening, using the Chiralcel OJ-H column. Baseline separation of Compounds 1–3 and 5 has been obtained in short retention times, less than 12 min (referred to the second eluted enantiomer). Results are reported in Table 5. Interestingly, high enantioselectivity and good resolution have been achieved eluting only with alcohols, while no separation occurs eluting with *n*-hep, with the only exception of Compound 1.

Table 5. Analytical screening on Chiralcel OJ-H with different mobile phases containing 0.1% DEA.

Compound	Mobile Phase				K_1	K_2	α	R_s
	<i>n</i> -hep (%)	MeOH (%)	EtOH (%)	IPA (%)				
(R/S)-1	-	100	-	-	2.5		1	-
	-	50	50	-	1.77	2.40	1.36	3.14
	-	-	100	-	1.03	1.63	1.58	3.25
	90	-	-	10	1.56	2.27	1.46	2.35
(R/S)-2	-	100	-	-	3.98	4.80	1.21	2.46
	-	50	50	-	1.87	2.25	1.20	1.97
	-	-	100	-	1.23	1.46	1.19	1.83
	90	-	-	10	9.61		1	-

Table 5. Cont.

Compound	Mobile Phase				K_1	K_2	α	R_s
	<i>n</i> -hep (%)	MeOH (%)	EtOH (%)	IPA (%)				
<i>(R/S)</i> -3	-	100	-	-	1.24	1.80	1.45	4.05
	-	50	50	-	0.70	0.93	1.33	2.32
	-	-	100	-	2.24		1	-
	90	-	-	10	0.46		1	-
<i>(R/S)</i> -4	-	100	-	-	1.52		1	-
	-	50	50	-	0.74		1	-
	-	-	100	-	0.46		1	-
	90	-	-	10	0.54		1	-
<i>(R/S)</i> -5	-	100	-	-	1.10	1.61	1.46	2.62
	-	50	50	-	0.74	1.07	1.45	1.99
	-	-	100	-	0.39	0.70	1.79	1.92
	90	-	-	10	0.32		1	-
<i>(R/S)</i> -6	-	100	-	-	2.20		1	-
	-	50	50	-	1.25		1	-
	-	-	100	-	0.73		1	-
	90	-	-	10	0.61		1	-

Flow rate: 0.5 mL/min. Detection: 254 nm (Compounds 1, 2, 5, 6) and 220 nm (Compounds 3, 4).

To sum up, we set up methods able to give baseline separation of 1–6 in a relatively short analysis time. In detail, the methods foresee the use of Chiralpak IA for solving Compounds 4 and 6 and of Chiralcel OJ-H for solving 1–3 and 5. In view of these results, we considered the developed methodologies suitable for the scale-up to the (semi-)preparative scale, and accordingly, no further attempts were made to extend the screening under HPLC conditions. Figure 2 shows chromatograms of racemic 1–6, when the highest resolution was reached, that is using Chiralpak IA or Chiralcel OJ-H columns, eluting with 100% methanol (Compounds 2–6) or with 100% ethanol (Compound 1).

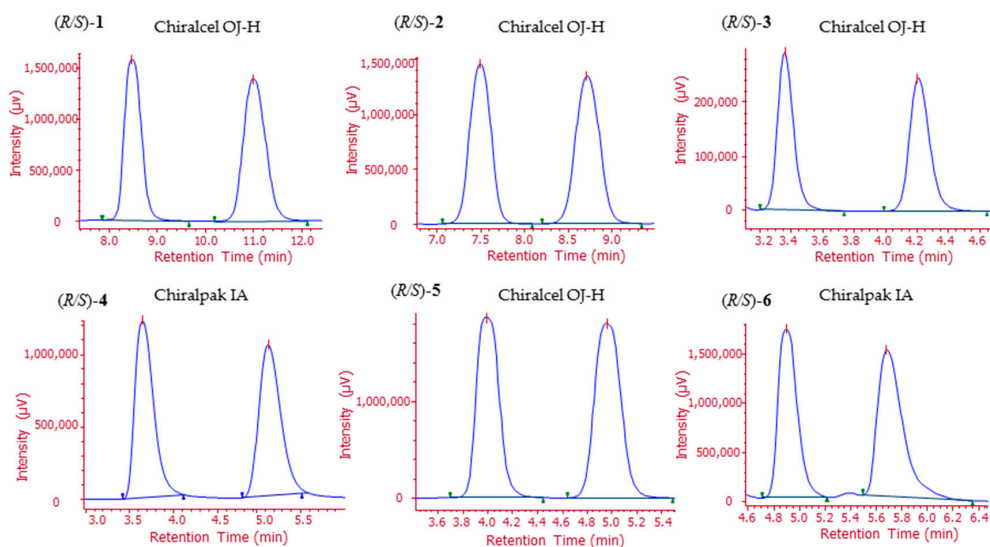


Figure 2. Analytical enantiomer separation of *(R/S)*-1, *(R/S)*-2, *(R/S)*-3, *(R/S)*-5 on Chiralcel OJ-H (4.6 mm × 150 mm, dp = 5 µm) and of *(R/S)*-4 and *(R/S)*-6 on Chiralpak IA (4.6 mm × 250 mm, dp = 5 µm). *(R/S)*-1 elution condition: 100% EtOH, DEA 0.1%, flow rate 0.5 mL/min. *(R/S)*-2, *(R/S)*-3 and *(R/S)*-5 elution condition: 100% MeOH, DEA 0.1%, flow rate 1.0 mL/min. *(R/S)*-4 and *(R/S)*-6 elution condition: 100% MeOH, 0.1% DEA, flow rate 1 mL/min. For all: injection volume 10 µL.

2.3. Preparation of Enantiomeric 1–6 through HPLC

During the drug discovery process, (semi-)preparative resolution of enantiomers using HPLC is a powerful technique for the rapid preparation of enantiomers. Employing this technique, important prerequisites for an economic and productive preparative enantiomer separation are: (i) retention times as short as possible; (ii) high solubility of the racemate and the enantiomers in the eluent/injection solvent; and (iii) the use of a mobile phase consisting of a pure low-cost solvent, facilitating work-up and re-use of the mobile phase. As previously discussed, using Chiralpak IA or Chiralcel OJ-H columns and eluting with alcohols added with DEA (0.1%), relatively short retention times (less than 12 min for the second eluted enantiomer), high enantioselectivity and good resolution could be observed (Figure 2). Accordingly, these experimental conditions were transferred to a Chiralpak IA and a Chiralcel OJ-H columns with an ID of 10 mm, on which a maximum of 12.5 mg could be separated in one run, depending on the solubility of the compound in the mobile phase. Therefore, racemic 1–6 were processed in a low number of cycles (Table 6), leading to enantiopure 1–6 in satisfactory amounts and yields, with an ee \geq 95% (Table 6), as evidenced by analytical control of the collected fractions (Figure S1).

Table 6. (Semi-)preparative resolution of (*R/S*)-1, (*R/S*)-2, (*R/S*)-3, (*R/S*)-5 on Chiralcel OJ-H (10 mm \times 250 mm, dp = 5 μ m) and of (*R/S*)-4 and (*R/S*)-6 on Chiralpak IA (10 mm \times 250 mm, dp = 5 μ m).

Compound	CSP	Processed Amount (mg)	No. Cycles	Enantiomer	Isolated Amount (mg)	ee (%)	Yield (%)	$[\alpha]_D^{20}$ (MeOH)
<i>(R/S)</i> -1	Chiralcel OJ-H	30	3	(+)-1	14.1	96.0	94.0	+40.5
				(-)-1	14.3	97.0	95.3	-42.3
<i>(R/S)</i> -2	Chiralcel OJ-H	30	3	(+)-2	13.8	95.0	92.0	+6.1
				(-)-2	12.5	95.0	83.3	-6.3
<i>(R/S)</i> -3	Chiralcel OJ-H	50	4	(+)-3	22.9	99.9	91.6	+10.5
				(-)-3	23.0	98.0	92.0	-9.2
<i>(R/S)</i> -4	Chiralpak IA	16	2	(+)-4	6.1	99.9	76.3	+8.2
				(-)-4	6.3	99.9	78.8	-8.3
<i>(R/S)</i> -5	Chiralcel OJ-H	22	4	(+)-5	9.1	99.9	82.7	+24.2
				(-)-5	8.9	99.9	80.9	-24.8
<i>(R/S)</i> -6	Chiralpak IA	25	3	(+)-6	10.5	99.9	84.0	+11.8
				(-)-6	9.8	99.9	78.4	-12.0

Flow rate: 2.5 mL/min. Detection: 254 nm (Compounds 1, 2, 5, 6) and 220 nm (Compounds 3, 4). Injection volume: 1.0 mL.

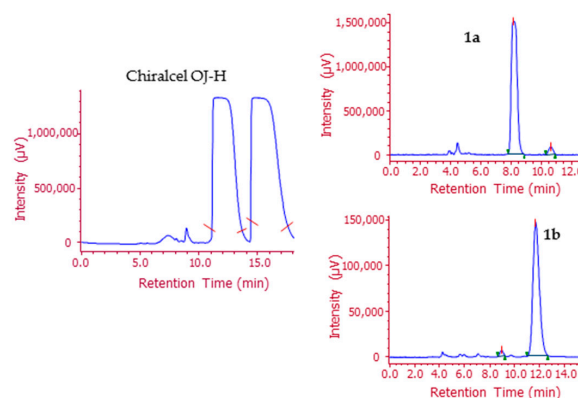


Figure 3. Representative chromatogram of (semi-)preparative resolution: compound (*R/S*)-1, Chiralcel OJ-H (10 mm \times 250 mm, dp = 5 μ m). Elution condition: 100% EtOH, DEA 0.1%, flow rate 2.5 mL/min. Injection volume 1.0 mL. **1a:** (+)-1, **1b:** (-)-1.

A representative example of (semi-)preparative resolution is reported in Figure 3. Actually, 30 mg of racemic **1** were processed in three runs (45 min in total) at a flow rate of 2.5 mL/min at room temperature. According to the chromatographic profile (Figure 3), a small intermediate fraction was collected. Final analysis of **1** enantiomers is shown in Figure 3.

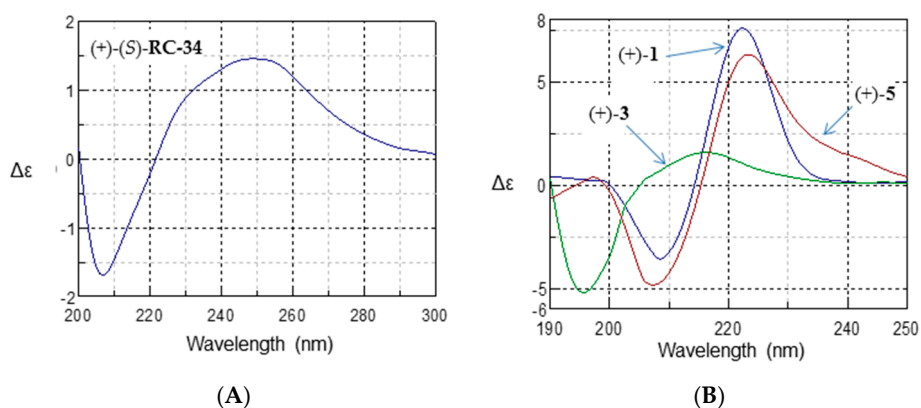
2.4. Absolute Configurational Assignment

As the last step of this work, the absolute configuration at the stereogenic center of enantiomeric **1–6** was established by combining electronic circular dichroism (ECD) and chiral HPLC analysis. The electronic circular dichroism (ECD) spectra have been compared with the ECD curves of structural analogues RC-33 and RC-34, whose configuration was already assigned by us [13,14]. In detail, the ECD spectra of enantiomeric arylamino alcohols **1**, **3** and **5** were compared with that of (*S*)-RC-34 (Figure 1) and the ECD spectra of enantiomeric **2**, **4** and **6**, with that of (*S*)-RC-33.

Briefly, comparable Cotton effects (CEs) for (+)-**1**, (+)-**3**, (+)-**5** and (+)-(*S*)-RC-34 compounds are evident in two ranges of wavelengths. Between 195 and 207 nm, there are negative CEs, and between 216 and 223 nm there are positive CE, attributable to 1L_a and 1L_b electronic transitions of benzene and naphthalene (Figure 4). The sign of the CEs of 1L_a is consistently opposite that at the longer wavelength (1L_b). Some evident differences in the profile of the curves are in agreement with the UV spectra and could depend on the substitution pattern of the aromatic moiety. Basing on these considerations, the (*S*) absolute configuration of (+)-(*S*)-RC-34 may be proposed also for (+)-**1**, (+)-**3** and (+)-**5**, because the sequence around the stereogenic center is the same for all four compounds.

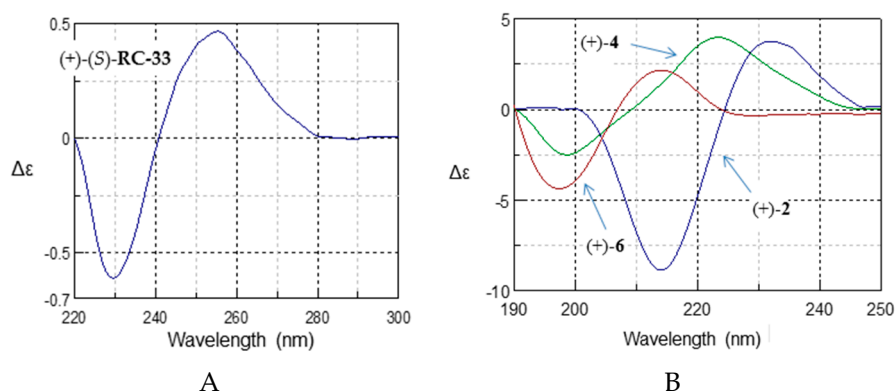
Further support to this configurational assignment was derived from the study of the elution order of chiral HPLC analysis, taking into account that the absolute configuration of structurally-related compounds usually follows the same chiral recognition mechanism in the chromatographic process on a given chiral stationary phase, using the same mobile phase. Accordingly, (*S*)-RC-34, (+)-**1**, (+)-**3** and (+)-**5** were analyzed under the same chromatographic conditions (Chiralcel OJ-H, 50% MeOH and 50% EtOH, 0.1% DEA) and resulted in all cases in the first eluted enantiomers. The elution order results confirmed that the (*S*) absolute configuration may be attributed also to (+)-**1**, (+)-**3** and (+)-**5**.

Empirical absolute configuration assignment of **2**, **4**, **6** was effected applying a similar approach. ECD spectra of **2**, **4**, **6** have been compared with that of the structurally-related compound (*S*)-RC-33, as a reference of known stereochemistry. The enantiomers (+)-**2**, (+)-**4**, (+)-**6** and (*S*)-RC-33 displayed a similar negative CE in the wavelength range between 198 and 230 nm and a CE between 214 and 255 nm, associated with 1L_a and 1L_b electronic transitions of the aromatic chromophores, respectively. Again, the sign of the CEs of 1L_a is consistently opposite that at the longer wavelength (1L_b), and the differences in the profile of the curves could depend on the different aromatic nucleus. Based on these considerations, the (*S*) absolute configuration of (+)-(*S*)-RC-33 may be proposed also for (+)-**2**, (+)-**4** and (+)-**6** (Figure 5), having the same substituents around the stereogenic center. Again, (*S*)-RC-33 and (+)-**2** were analyzed under the same chromatographic conditions (Chiralcel OJ-H, 50% MeOH and 50% EtOH, 0.1% DEA) and resulted in both cases in the first eluted enantiomers. Unfortunately, the OJ-H column is not able to solve Compounds **4** and **6**. To confirm that a set of structurally-related compounds is characterized by the same absolute configuration, they must be analyzed under the same chromatographic conditions. Indeed, chiral recognition mechanisms on chiral stationary phases may be sensitive to even minor structural or conditional changes. Therefore, we took into consideration the chromatographic profiles of (*S*)-RC-33, (+)-**2**, (+)-**4** and (+)-**6** on Chiralpak IC (90/10 *n*-hep/IPA, 0.1% DEA), a condition that ensures the baseline separation of all of the studied compound enantiomers. (*S*)-RC-33, (+)-**2**, (+)-**4** and (+)-**6** showed the same behaviors, confirming that all of the first eluted enantiomers are characterized by the same absolute configuration, that is the (*S*) configuration. These results are in agreement with the data collected through ECD technique, and the (*S*) absolute configuration may be attributed also to (+)-**1**, (+)-**3** and (+)-**5**.



Compound	λ_{\min}	$\Delta\epsilon_{\min}$	λ_{\max}	$\Delta\epsilon_{\max}$
(S)-RC-34	206.5	-2.78	253.0	1.09
(+)-1	208.5	-3.58	222.5	7.59
(+)-3	195.5	-5.19	216.5	1.57
(+)-5	207.5	-4.82	223.5	6.31

Figure 4. ECD curves of (A) (+)-(S)-RC-34 and (B) (+)-1, (+)-3, (+)-5 and their Cotton effect (CE) in the wavelength range 190–300 nm.



Compound	λ_{\min}	$\Delta\epsilon_{\min}$	λ_{\max}	$\Delta\epsilon_{\max}$
(S)-RC-33	229.8	-0.61	255.0	0.47
(+)-2	214.0	-9.04	232.5	3.56
(+)-4	198.5	-2.26	223.0	3.85
(+)-6	198.0	-4.34	214.0	2.18

Figure 5. ECD curves of (A) (+)-(S)-RC-33, (B) (+)-2, (+)-4, (+)-6 and their Cotton effect (CE) in the wavelength range of 190–300 nm.

3. Experimental Section

3.1. HPLC-UV Chiral Resolution

In order to identify the best conditions to be properly scaled up to the (semi-)preparative scale, an analytical screening of cellulose- and amylose-based CSPs was firstly performed using Chiralcel OJ-H (Chiral technologies Europe, Illkirch-Cedex, France, Europe, 4.6 mm diameter \times 150 mm length, dp 5 μm), Chiralpack IC (Chiral technologies Europe, Illkirch-Cedex, France, Europe, 4.6 mm diameter \times 250 mm length, dp 5 μm) and Chiralpack IA (Chiral technologies Europe, Illkirch-Cedex,

France, Europe, 4.6 mm diameter \times 250 mm length, dp 5 μ m) columns and eluting with a flow rate of 0.5 mL/min, 1 mL/min and 1 mL/min, respectively. Analytes were detected photometrically at 220 and 254 nm. Unless otherwise specified, sample solutions were prepared dissolving analytes at 1 mg/mL in ethanol and filtered through 0.45- μ m PTFE membranes before analysis. The injection volume was 10 μ L. The mobile phases consisted of alcohols (MeOH or/and EtOH) or mixtures of *n*-hep and polar modifiers (EtOH or IPA). In all cases, 0.1% of DEA was added to the mobile phase. In the case of the Chiralpak IC columns, the analyses were carried out also in the presence of 0.3% of TFA. The retention factor (*k*) was calculated using the equation $k = (t_R - t_0)/t_0$, where t_R is the retention time and t_0 the dead time (t_0 was considered to be equal to the peak of the solvent front and was taken from each particular run). The enantioselectivity (α) and the resolution factor (*R*_s) were calculated as follows: $\alpha = k_2/k_1$ and $R_s = 2(t_{R2} - t_{R1})/(w_1 + w_2)$, where t_{R2} and t_{R1} are the retention times of the second and the first eluted enantiomers and w_1 and w_2 are the corresponding base peak widths. The best conditions found by the screening protocol were applied to a (semi-)preparative scale-up. The enantiomers of **1**, **2**, **3** and **5** were then completely resolved by a (semi-)preparative process using a Chiralcel OJ-H column (10 mm diameter \times 250 mm length, 5 μ m), eluting with EtOH (for Compound **1**) or MeOH (for Compounds **2**, **3** and **5**) at rt with a flow rate of 2.5 mL/min. Compounds **4** and **6** were resolved on Chiralpak IA (10 mm diameter \times 250 mm length, 5 μ m) using MeOH at a flow rate of 2.5 mL/min as the eluent.

The eluate was fractioned according to the UV profile (detection at 220 and 254 nm). The fractions obtained containing the enantiomers were evaporated at reduced pressure. Analytical control of the collected fractions was performed using the analytical columns.

3.2. Electronic Circular Dichroism

The solutions of **1–6** enantiomers: (+)-**1** (*c*: 2.68×10^{-5} M, in *n*-hexane), (+)-**2** (*c*: 1.90×10^{-5} M in *n*-hexane), (+)-**3** (*c*: 3.09×10^{-5} M in *n*-hexane), (+)-**4** (*c*: 2.21×10^{-5} M in *n*-hexane), (+)-**5** (*c*: 6.29×10^{-6} M in *n*-hexane), (+)-**6** (*c*: 1.31×10^{-5} M in *n*-hexane; optical pathway 1 cm), (+)-(*S*)-RC-34 (*c*: 2.5×10^{-5} M in *n*-hexane; optical pathway 1 cm) and (+)-(*S*)-RC-33 (*c*: 9.12×10^{-5} M in *n*-hexane; optical pathway 1 cm) were analyzed in a nitrogen atmosphere. ECD spectra were scanned at 50 nm/min with a spectral band width of 2 nm and a data resolution of 0.5 nm (Figures 4 and 5).

4. Conclusions

In this paper, we presented the synthesis of the novel potential SR modulators **1–6** and their enantioseparation via HPLC chiral resolutions on cellulose- and amylose-based CSPs. A systematic screening protocol for enantioselective HPLC was established leading to fast and easy-to-use chiral HPLC separations suitable for a (semi-)preparative scale-up. The separation of the enantiomers was optimized by varying the chromatographic parameters. Baseline separations were obtained for all of the studied compounds under optimized chromatographic conditions. The recovery of the enantiomers after chromatography was in the range of 76%–95%, for the individual enantiomers. (Semi-)preparative enantioselective chromatography for compounds of interest proves to be a straightforward, productive and robust methodology for the quick access to the desired amounts of pure enantiomers. It remains one of the most versatile and cost effective tools for the fast isolation of desired enantiomers from a racemic mixture. The absolute configuration at the chiral center of enantiomeric **1–6** was empirically assigned by combining electronic circular dichroism (ECD) and chiral HPLC analysis.

The bioactivity of each enantiomer is now under investigation in order to deeply understand the role of chirality in the SRs-ligand interaction.

Supplementary Materials: Supplementary materials can be accessed at: <http://www.mdpi.com/1420-3049/21/9/1210/s1>.

Acknowledgments: The authors gratefully acknowledge Michela Culanti Indiano for the experimental support.

Author Contributions: S.C. conceived of the work and contributed to reviewing the whole manuscript. She was also responsible for the correctness of all of the studies. M.R. and A.M. performed the research, analyzed the data and contributed to the writing of the manuscript. V.P. provided guidance on the synthesis of the racemates. D.R. and M.J. provided guidance on the design of the screening and the up-scaling of the enantiomer separations.

Conflicts of Interest: The authors declare no conflict of interest.

Abbreviations

The following abbreviations are used in this manuscript:

MDPI	Multidisciplinary Digital Publishing Institute
DOAJ	Directory of Open Access Journals
DEA	Diethylamine
ECD	Electronic circular dichroism
EtOH	Ethanol
IPA	Isopropanol
MeOH	Methanol
<i>n</i> -hep	<i>n</i> -Heptane
TFA	Trifluoroacetic acid
UV	Ultraviolet

References

1. Aydar, E.; Palmer, C.P.; Djamgoz, M.B. Sigma receptors and cancer: Possible involvement of ion channels. *Cancer Res.* **2004**, *64*, 5029–5035. [[CrossRef](#)] [[PubMed](#)]
2. Collina, S.; Gaggeri, R.; Marra, A.; Bassi, A.; Negrinotti, S.; Negri, F.; Rossi, D. Sigma receptor modulators: A patent review. *Exp. Opin. Ther. Pat.* **2013**, *23*, 597–613. [[CrossRef](#)] [[PubMed](#)]
3. Huang, Y.S.; Lu, H.L.; Zhang, L.J.; Wu, Z. Sigma-2 receptor ligands and their perspectives in cancer diagnosis and therapy. *Med. Res. Rev.* **2014**, *34*, 532–566. [[CrossRef](#)] [[PubMed](#)]
4. Wang, B.; Rouzier, R.; Albarracin, C.T.; Sahin, A.; Wagner, P.; Yang, Y.; Smith, T.L.; Meric Bernstam, F.; Marcelo, A.C.; Hortobagyi, G.N.; Puzstai, L. Expression of sigma 1 receptor in human breast cancer. *Breast Cancer Res. Treat.* **2004**, *87*, 205–214. [[CrossRef](#)] [[PubMed](#)]
5. Aydar, E.; Onganer, P.; Perrett, R.; Djamgoz, M.B.; Palmer, C.P. The expression and functional characterization of sigma (sigma) 1 receptors in breast cancer cell lines. *Cancer Lett.* **2006**, *242*, 245–257. [[CrossRef](#)] [[PubMed](#)]
6. Crottes, D.; Guizouarn, H.; Martin, P.; Borgese, F.; Soriani, O. The sigma-1 receptor: A regulator of cancer cell electrical plasticity? *Front. Physiol.* **2013**, *4*, 175. [[CrossRef](#)] [[PubMed](#)]
7. Megalizzi, V.; le Mercier, M.; Decaestecker, C. Sigma receptors and their ligands in cancer biology: Overview and new perspectives for cancer therapy. *Med. Res. Rev.* **2012**, *32*, 410–427. [[CrossRef](#)] [[PubMed](#)]
8. Collina, S.; Loddo, G.; Urbano, M.; Linati, L.; Callegari, A.; Ortuso, F.; Alcaro, S.; Laggner, C.; Langer, T.; Prezzavento, O.; et al. Design, synthesis, and SAR analysis of novel selective sigma1 ligands. *Bioorg. Med. Chem.* **2007**, *15*, 771–783. [[CrossRef](#)] [[PubMed](#)]
9. Rossi, D.; Urbano, M.; Pedrali, A.; Serra, M.; Zampieri, D.; Mamolo, M.G.; Laggner, C.; Zanette, C.; Florio, C.; Shepman, D.; et al. Design, synthesis and SAR analysis of novel selective sigma1 ligands (Part 2). *Bioorg. Med. Chem.* **2010**, *18*, 1204–1212. [[CrossRef](#)] [[PubMed](#)]
10. Rossi, D.; Pedrali, A.; Urbano, M.; Gaggeri, R.; Serra, M.; Fernandez, L.; Fernandez, M.; Caballero, J.; Rosinsvalle, S.; Prezzavento, O.; et al. Identification of a potent and selective σ_1 receptor agonist potentiating NGF-induced neurite outgrowth in PC12 cells. *Bioorg. Med. Chem.* **2011**, *19*, 6210–6224. [[CrossRef](#)] [[PubMed](#)]
11. Rossi, D.; Marra, A.; Picconi, P.; Serra, M.; Catenacci, L.; Sorrenti, M.; Laurini, E.; Fermeiglia, M.; Pricl, S.; Brambilla, S.; et al. Identification of RC-33 as a potent and selective σ_1 receptor agonist potentiating NGF-induced neurite outgrowth in PC12 cells. Part 2: G-scale synthesis, physicochemical characterization and in vitro metabolic stability. *Bioorg. Med. Chem.* **2013**, *21*, 2577–2586. [[CrossRef](#)] [[PubMed](#)]
12. Rossi, D.; Pedrali, A.; Gaggeri, R.; Marra, A.; Pignataro, L.; Laurini, E.; DalCol, V.; Fermeiglia, M.; Pricl, S.; Schepman, D.; et al. Chemical, pharmacological, and in vitro metabolic stability studies on enantiomerically pure RC-33 compounds: promising neuroprotective agents acting as σ_1 receptor agonists. *Chem. Med. Chem.* **2013**, *8*, 1514–1527. [[CrossRef](#)] [[PubMed](#)]

13. Rossi, D.; Pedrali, A.; Marra, A.; Pignataro, L.; Schepmann, D.; Wünsch, B.; Ye, L.; Leuner, K.; Peviani, M.; Curti, D.; Azzolina, O.; Collina, S. Studies on the Enantiomers of as Neuroprotective Agents: Isolation, Configurational Assignment, and Preliminary Biological Profile. *Chirality* **2013**, *25*, 814–822. [[CrossRef](#)] [[PubMed](#)]
14. Rossi, D.; Marra, A.; Rui, M.; Laurini, E.; Fermeglia, M.; Pricl, S.; Schepmann, D.; Wuensch, B.; Peviani, M.; Curti, D.; et al. A step forward in the sigma enigma: A role for chirality in the sigma1 receptor-ligand interaction? *MedChemComm* **2014**, *6*, 138–146. [[CrossRef](#)]
15. Walker, J.M.; Bowen, W.D.; Walker, F.O.; Matsumoto, R.R.; De Costa, B.; Rice, K.C. Sigma receptors: Biology and function. *Pharmacol. Rev.* **1990**, *42*, 355–402. [[PubMed](#)]
16. Collina, S.; Loddo, G.; Urbano, M.; Rossi, D.; Mamolo, M.G.; Zampieri, D.; Alcaro, S.; Gallelli, A.; Azzolina, O. Enantioselective chromatography and absolute configuration of N,N-dimethyl-3-(naphthalen-2-yl)-butan-1-amines: Potential Sigma1 ligands. *Chirality*. **2006**, *18*, 245–253. [[CrossRef](#)] [[PubMed](#)]
17. Rossi, D.; Nasti, R.; Marra, A.; Meneghini, S.; Mazzeo, G.; Longhi, G.; Memo, M.; Cosimelli, B.; Greco, G.; Novellino, E.; et al. Enantiomeric 4-Acylamino-6-alkyloxy-2 Alkylthiopyrimidines As Potential A3 Adenosine Receptor Antagonists: HPLC Chiral Resolution and Absolute Configuration Assignment by a Full Set of Chiroptical Spectroscopy. *Chirality* **2016**. [[CrossRef](#)] [[PubMed](#)]
18. Gaggeri, R.; Rossi, D.; Collina, S.; Mannucci, B.; Baierl, M.; Juza, M. Quick development of an analytical enantioselective high performance liquid chromatography separation and preparative scale-up for the flavonoid Naringenin. *J. Chromatogr. A* **2011**, *1218*, 5414–5422. [[CrossRef](#)] [[PubMed](#)]
19. Rossi, D.; Marra, A.; Rui, M.; Brambilla, S.; Juza, M.; Collina, S. “Fit-for-purpose” development of analytical and (semi)preparative enantioselective high performance liquid and supercritical fluid chromatography for the access to a novel σ_1 receptor agonist. *J. Pharm. Biomed. Anal.* **2016**, *118*, 363–369. [[CrossRef](#)] [[PubMed](#)]
20. Pace, V.; Martínez, F.; Fernández, M.; Sinisterra, J.V.; Alcántara, A.R. Highly Efficient Synthesis of New α -Arylamino- α' -chloropropan-2-ones via Oxidative Hydrolysis of Vinyl Chlorides Promoted by Calcium Hypochlorite. *Adv. Synth. Catal.* **2009**, *351*, 3199–3206. [[CrossRef](#)]

Sample Availability: Samples of all compounds are available from the authors.



© 2016 by the authors; licensee MDPI, Basel, Switzerland. This article is an open access article distributed under the terms and conditions of the Creative Commons Attribution (CC-BY) license (<http://creativecommons.org/licenses/by/4.0/>).

Supplementary Materials: Novel Enantiopure Sigma Receptor (SR) Modulators: Quick (Semi)-Preparative Chiral Resolution via HPLC and Absolute Configuration Assignment

Marta Rui, Annamaria Marra, Vittorio Pace, Markus Juza, Daniela Rossi and Simona Collina

1. Materials and Methods

1.1. General

Optical rotation values were measured on a Jasco photoelectric polarimeter DIP 1000 using a 0.5-dm cell and a sodium and mercury lamp ($\lambda = 589$ nm, 435 nm, 405 nm); sample concentration values (c) are given in 10^{-2} g·mL⁻¹.

Proton nuclear magnetic resonance (NMR) spectra were recorded on a Bruker Avance 500 spectrometer operating at 500 MHz. Proton chemical shifts (δ) are reported in ppm with the solvent reference relative to tetramethylsilane (TMS) employed as the internal standard (CDCl₃, $\delta = 7.26$ ppm). The following abbreviations are used to describe spin multiplicity: s = singlet, d = doublet, t = triplet, q = quartet, m = multiplet, br = broad signal, dd = doublet-doublet, td = triplet-doublet. The coupling constant values are reported in Hz. ¹³C-NMR spectra were recorded on a 500-MHz spectrometer, with complete proton decoupling. Carbon chemical shifts (δ) are reported in ppm relative to TMS with the respective solvent resonance as the internal standard (CDCl₃, $\delta = 77.23$ ppm). UPLC-UV-ESI/MS analyses were carried out on an Acquity UPLC Waters LCQ FLEET system using an ESI source operating in positive ion mode, controlled by ACQUITY PDA and 4 MICRO (Waters S.A.S., Saint-Quentin En Yvelines Cedex, France). Analyses were run on a ACQUITY BEH C18 (Waters S.A.S.) 50 × 2.1 mm, 1.7 μ m) column, at room temperature, with gradient elution (Solvent A: water containing 0.1% of formic acid; Solvent B: methanol containing 0.1% of formic acid; gradient: 10% B in A to 100% B in 3 min, followed by isocratic elution 100% B for 1.5 min, return to the initial conditions in 0.2 min) at a flow rate of 0.5 mL·min⁻¹. All of the final compounds had 95% or greater purity.

1.2. Compound Characterization

(+)-(S)-4-(4-Benzyl-piperidin-1-yl)-2-naphthalen-2-yl-butan-2-ol, [(+)-(S)-1]: White solid; $[\alpha]_D^{20} = +40.5$ (c 0.2, CH₃OH). IR (cm⁻¹): 3434, 2918, 1653, 1438, 1156, 1112, 820; ¹H-NMR (500 MHz) (CDCl₃) δ (ppm): 8.01 (s, 1H), 7.86–7.81 (m, 3H), 7.47–7.45 (m, 3H), 7.28 (t, $J = 7.8$ Hz, 2H), 7.19 (t, $J = 7.0$ Hz, 1H), 7.13 (d, $J = 7.1$ Hz, 2H), 3.19 (d, 1H), 2.54–2.50 (m, 3H), 2.31 (m, 1H), 2.22–2.14 (m, 2H), 1.92 (d, 1H), 1.84 (m, 1H), 1.76 (m, 1H), 1.68 (m, 1H), 1.60 (m, 1H), 1.57 (s, 3H), 1.50 (m, 1H), 1.31 (m, 2H); ¹³C-NMR (500 MHz) (CDCl₃) δ (ppm): 146.3, 140.5, 133.3, 132.0, 129.1, 128.2, 128.1, 127.6, 127.4, 125.8, 125.4, 123.8, 123.6, 75.7, 55.1, 54.8, 52.6, 43.1, 37.8, 37.4, 32.6, 32.1, 31.4. HPLC: $t_R = 8.5$ min, ee 96.0%.

(-)-(R)-4-(4-Benzyl-piperidin-1-yl)-2-naphthalen-2-yl-butan-2-ol, [(-)-(R)-1]: White solid; $[\alpha]_D^{20} = -42.3$ (c 0.2, CH₃OH). The IR and NMR spectra are identical to that of (+)-(S)-1. HPLC: $t_R = 11.1$ min, ee 97.0%.

(+)-(S)-4-Benzyl-1-(3-naphthalen-2-yl-butyl)-piperidine, [(+)-(S)-2]: Yellow oil; $[\alpha]_D^{20} = +6.1$ (c 0.2, CH₃OH). IR (cm⁻¹): 3025, 2924, 2508, 1631, 1602, 1542, 1496, 1453; ¹H-NMR (500 MHz) (CDCl₃) δ (ppm): 7.79–7.77 (t, $J = 8.7$ Hz, 3H), 7.59 (s, 1H), 7.45–7.42 (m, 2H), 7.32 (d, $J = 8.8$ Hz, 1H), 7.25 (m, 2H), 7.17 (m, 1H), 7.08 (m, 2H), 3.30 (broad peak, 2H), 2.90 (m, 1H), 2.76 (m, 1H), 2.55 (d, $J = 7.4$ Hz, 2H), 2.46 (m, 1H), 2.27–2.13 (m, 4H), 1.82–1.71 (m, 4H), 1.59 (m, 1H), 1.36 (d, $J = 6.5$ Hz, 3H); ¹³C-NMR (500 MHz) (CDCl₃) δ (ppm): 142.4, 139.3, 133.4, 132.3, 128.9, 128.5, 128.3, 127.6, 127.5, 126.1, 125.5, 125.3, 124.8, 56.1, 52.4, 41.9, 38.3, 36.5, 31.8, 29.1, 22.7. HPLC: $t_R = 7.7$ min, ee 95.0%.

(-)-(R)-4-Benzyl-1-(3-naphthalen-2-yl-butyl)-piperidine, [(-)-(R)-2]: Yellow oil; $[\alpha]_{\text{D}}^{20} = -6.3$ (c 0.2, CH₃OH). The IR and NMR spectra are identical to that of (+)-(S)-2. HPLC: $t_{\text{R}} = 9.0$ min, ee 95.0%.

(+)-(S)-4-(4-Benzyl-piperidin-1-yl)-2-phenyl-butan-2-ol, [(+)-(S)-3]: Yellow oil; $[\alpha]_{\text{D}}^{20} = +10.5$ (c 0.6, CH₃OH). IR (cm⁻¹): 3184, 3125, 1602, 1369, 1343, 1156, 846, 699; ¹H-NMR (500 MHz) (CDCl₃) δ (ppm): 7.45 (d, $J = 8.9$ Hz, 2H), 7.33 (t, $J = 8.1$ Hz, 2H), 7.27 (t, $J = 7.4$ Hz, 2H), 7.21-7.19 (m, 2H), 7.13 (d, $J = 7.0$ Hz, 2H), 3.15 (d, 1H), 2.54 (m, 1H), 2.52 (m, 2H), 2.30 (m, 1H), 2.22 (m, 1H), 2.07 (m, 1H), 1.86 (m, 1H), 1.80 (m, 1H), 1.75 (m, 1H), 1.67 (m, 1H), 1.60 (m, 1H), 1.50 (m, 1H), 1.49 (s, 3H), 1.31 (m, 2H); ¹³C-NMR (500 MHz) (CDCl₃) δ (ppm): 148.9, 140.5, 129.1, 127.9, 128.2, 126.0, 125.8, 125.0, 75.5, 55.1, 54.8, 52.6, 43.1, 37.8, 37.7, 32.6, 32.1, 31.4. HPLC: $t_{\text{R}} = 3.4$ min, ee 99.9%.

(-)-(R)-4-(4-Benzyl-piperidin-1-yl)-2-phenyl-butan-2-ol, [(-)-(R)-3]: Yellow oil; $[\alpha]_{\text{D}}^{20} = -9.2$ (c 0.6, CH₃OH). The IR and NMR spectra are identical to that of (+)-(S)-3. HPLC: $t_{\text{R}} = 4.2$ min, ee 98.0%.

(+)-(S)-4-Benzyl-1-(3-phenyl-butyl)-piperidine, [(+)-(S)-4]: Yellow oil; $[\alpha]_{\text{D}}^{20} = +8.2$ (c 0.3, CH₃OH). IR (cm⁻¹): 3682, 3019, 2929, 2856, 2434, 2400, 1230; ¹H-NMR (500 MHz) (CDCl₃) δ (ppm): 7.28-7.27 (m, 4H), 7.17 (m, 4H), 7.13 (d, $J = 7.0$ Hz, 2H), 2.86 (broad peak, 2H), 2.71 (m, 1H), 2.52 (d, $J = 6.6$ Hz, 2H), 2.26 (m, 1H), 2.14 (m, 1H), 1.87-1.72 (m, 4H), 1.61 (d, 2H), 1.49 (m, 1H), 1.29 (m, 2H), 1.24 (d, $J = 7.3$ Hz, 3H); ¹³C-NMR (500 MHz) (CDCl₃) δ (ppm): 147.3, 140.7, 129.1, 128.3, 128.1, 126.9, 125.9, 125.7, 57.3, 54.1, 53.9, 43.2, 38.4, 37.9, 35.4, 32.1, 22.6. HPLC: $t_{\text{R}} = 3.7$ min, ee 99.9%.

(-)-(R)-4-Benzyl-1-(3-phenyl-butyl)-piperidine, [(-)-(R)-4]: Yellow oil; $[\alpha]_{\text{D}}^{20} = -8.3$ (c 0.3, CH₃OH). The IR and NMR spectra are identical to that of (+)-(S)-4. HPLC: $t_{\text{R}} = 5.3$ min, ee 99.9%.

(+)-(S)-6-[3-(4-Benzyl-piperidin-1-yl)-1-hydroxy-1-methyl-propyl]-naphthalen-2-ol, [(+)-(S)-5]: Yellow oil; $[\alpha]_{\text{D}}^{20} = +24.2$ (c 0.1, CH₃OH). IR (cm⁻¹): 3452, 2925, 1633, 1605, 1560, 1454, 1381; ¹H-NMR (500 MHz) (CDCl₃) δ (ppm): 7.91 (s, 1H), 7.72 (d, $J = 8.4$ Hz, 1H), 7.60 (d, $J = 8.4$ Hz, 1H), 7.40 (d, $J = 8.8$ Hz, 1H), 7.25 (t, $J = 6.9$ Hz, 2H), 7.18-7.14 (m, 3H), 7.07 (d, $J = 8.0$ Hz, 2H), 3.20 (broad peak, 1H), 2.61 (broad peak, 1H), 2.46 (d, $J = 6.5$ Hz, 2H), 2.34 (m, 2H), 2.18 (m, 1H), 1.96 (broad peak, 1H), 1.88 (broad peak, 1H), 1.80 (broad peak, 1H), 1.66 (broad peak, 2H), 1.59 (s, 1H), 1.49 (broad peak, 1H), 1.34 (broad peak, 2H); ¹³C-NMR (500 MHz) (CDCl₃) δ (ppm): 154.0, 143.0, 140.3, 133.3, 129.8, 129.0, 128.5, 128.2, 126.2, 125.8, 124.1, 123.4, 118.3, 109.2, 75.8, 55.0, 54.7, 52.6, 42.9, 37.6, 37.4, 31.7, 31.3. HPLC: $t_{\text{R}} = 4.0$ min, ee 99.9%.

(-)-(R)-6-[3-(4-Benzyl-piperidin-1-yl)-1-hydroxy-1-methyl-propyl]-naphthalen-2-ol, [(-)-(R)-5]: Yellow oil; $[\alpha]_{\text{D}}^{20} = -24.8$ (c 0.1, CH₃OH). The IR and NMR spectra are identical to that of (+)-(S)-5. HPLC: $t_{\text{R}} = 5.0$ min, ee 99.9%.

(+)-(S)-6-[3-(4-Benzyl-piperidin-1-yl)-1-methyl-propyl]-naphthalen-2-ol, [(+)-(S)-6]: Yellow oil; $[\alpha]_{\text{D}}^{20} = +11.8$ (c 0.3, CH₃OH). IR (cm⁻¹): 3297, 2924, 2349, 2309, 1604, 1453, 1376, 1269; ¹H-NMR (500 MHz) (CDCl₃) δ (ppm): 7.42 (d, $J = 9.0$ Hz, 1H), 7.37 (s, 1H), 7.24 (t, 2H), 7.17 (d, $J = 8.0$ Hz, 1H), 7.17 (m, 1H), 7.06 (m, 3H), 6.98 (d, $J = 9.0$ Hz, 1H), 6.81 (s, 1H), 3.26 (broad peak, 1H), 3.10 (broad peak, 1H), 2.73 (m, 1H), 2.50-2.49 (broad peak, 4H), 2.14-2.12 (m, 2H), 2.04 (m, 2H), 1.67 (m, 2H), 1.60-1.54 (m, 3H), 1.28 (overlapped peak, 3H); ¹³C-NMR (500 MHz) (CDCl₃) δ (ppm): 154.6, 139.5, 133.6, 129.0, 128.3, 126.8, 126.0, 125.1, 125.0, 118.7, 109.2, 56.5, 53.7, 52.9, 42.3, 38.1, 37.0, 33.2, 30.0, 22.9. HPLC: $t_{\text{R}} = 4.9$ min, ee 99.9%.

(-)-(R)-6-[3-(4-Benzyl-piperidin-1-yl)-1-methyl-propyl]-naphthalen-2-ol, [(-)-(R)-6]: Yellow oil; $[\alpha]_{\text{D}}^{20} = -12.0$ (c 0.3, CH₃OH). The IR and NMR spectra are identical to that of (+)-(S)-6. HPLC: $t_{\text{R}} = 5.7$ min, ee 99.9%.

1.3. (Semi-)Preparative Chromatograms and Analytical Controls

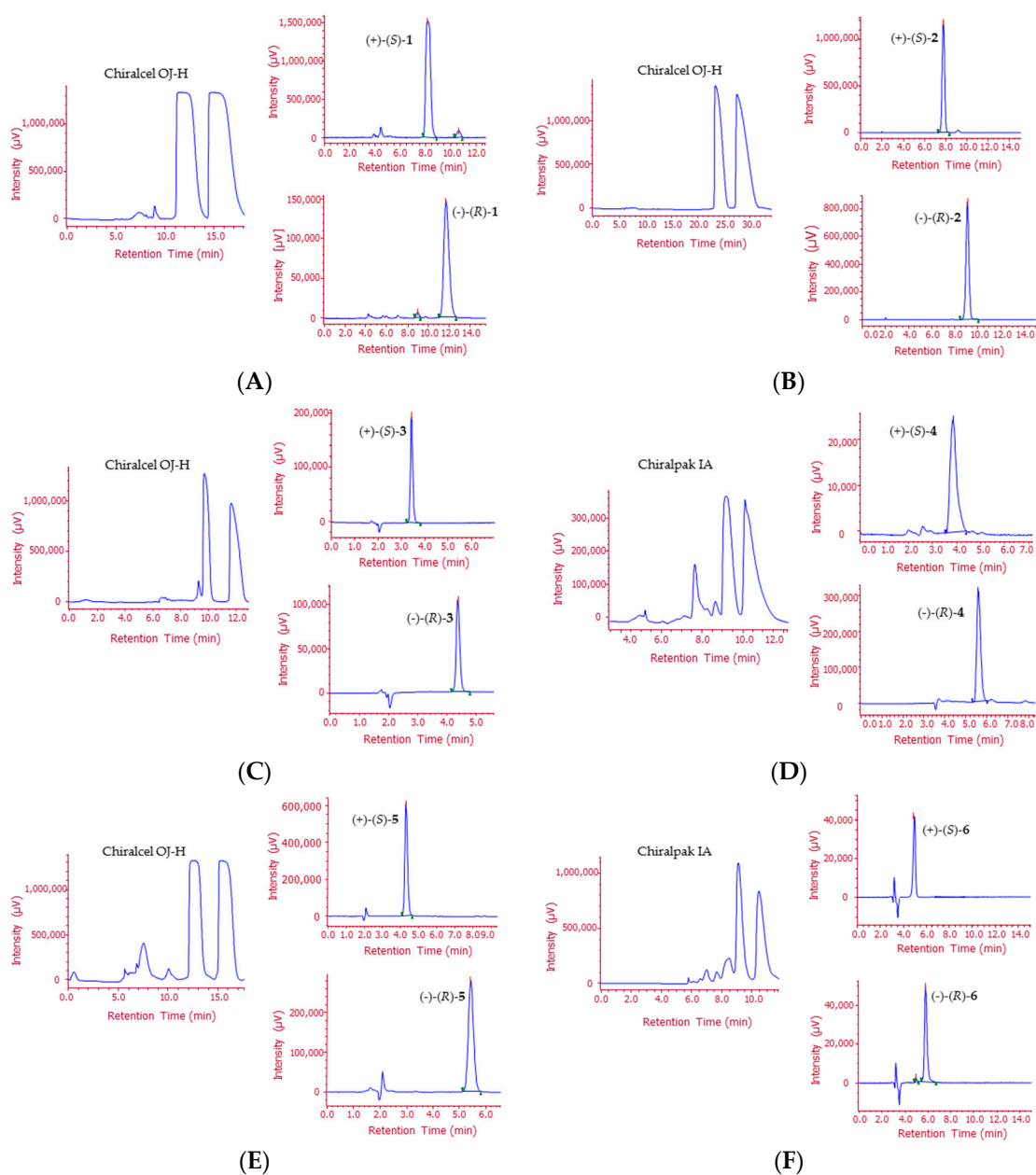


Figure S1. (Semi-)preparative enantiomer separations and analytical enantioselective analysis of first and second collected fractions of (A) 1, (B) 2, (C) 3, (D) 4, (E) 5, (F) 6. Elution conditions: (A) 100% EtOH, DEA 0.1%, flow rate 2.5 mL/min for (semi-)preparative analysis and 0.5 mL/min for analytical analysis; (B, C, E) 100% MeOH, DEA 0.1%, flow rate 2.5 mL/min for (semi-)preparative analysis and 0.5 mL/min for analytical analysis; and (D, F) 100% MeOH, 0.1% DEA, flow rate 2.5 mL/min for (semi-)preparative analysis and 1 mL/min for analytical analysis. Injection volume: 1 mL for (semi-)preparative analysis and 10 μL for analytical analysis. Detection: 254 nm (Compounds 1, 2, 5, 6) and 220 nm (Compounds 3, 4).



Gaining in pan-affinity towards sigma 1 and sigma 2 receptors. SAR studies on arylalkylamines



Daniela Rossi^{a,†}, Marta Rui^a, Marcello Di Giacomo^a, Dirk Schepmann^b, Bernhard Wunsch^b, Stefania Monteleone^{c,†}, Klaus R. Liedl^c, Simona Collina^{a,*}

^a Department of Drug Sciences, Medicinal Chemistry and Pharmaceutical Technology Section, University of Pavia, Viale Taramelli 12, 27100 Pavia, Italy

^b Institute of Pharmaceutical and Medicinal Chemistry, University of Muenster, Correnstrasse 48, 48149 Muenster, Germany

^c Institute of General, Inorganic and Theoretical Chemistry, Center of Molecular Biosciences, University of Innsbruck, Innrain 80/82, 6020 Innsbruck, Austria

ARTICLE INFO

Article history:

Received 1 September 2016

Revised 30 September 2016

Accepted 6 October 2016

Available online 11 October 2016

Keywords:

Sigma receptors

Arylalkylamine

Pan-affinity

QSAR

ABSTRACT

Sigma Receptor (SR) modulators are involved in different signal transduction pathways, representing important pharmacological/therapeutic tools in several pathological conditions, such as neurodegenerative diseases and cancers. To this purpose, numerous compounds have been developed in order to target selectively one of the two subtypes (S1R and S2R) as chemotherapeutic agent. However, experiments have also shown that ligands which are able to bind both SR subtypes can be useful for the diagnosis and/or the treatment of cancers. Therefore, the discovery of compounds with good affinity towards both S1R and S2R ('pan-modulators') is also of great interest and still represents a challenge up to now. For this reason, we synthesized novel arylalkylamines with the aim to obtain compounds with S1R and S2R affinity in the nM range and, by modeling quantitative structure–activity relationships (QSARs), we identified the essential structural features to obtain promising pan-compounds.

© 2016 Elsevier Ltd. All rights reserved.

1. Introduction

The term Sigma Receptor (SR) was coined in 1976 to identify a new opioid receptor subtype; Martin et al. showed the high affinity presented by the benzomorphan analog (\pm)-SKF-10,047 (Fig. 1) toward this receptor subtype class.¹ Subsequent studies established that the previous classification was not proper, since the opioid antagonists, naloxone and naltrexone, were ineffective toward SR.^{2–4} Another hypothesis, mistakenly described, proposed SR as the binding site of phencyclidine (Fig. 1), located on the ionic channel associated to the *N*-methyl-D-aspartate (NMDA) receptor.⁵

Two subtypes have been discovered so far, Sigma 1 Receptor (S1R) and Sigma 2 Receptor (S2R), with different distribution and pharmacological/pathological behavior.^{6,7}

The gene encoding S1R, cloned in 1996, expresses an integral membrane protein composed by 223 amino acids, resulting in a molecular weight of 23–30 kDa. S1R is highly conserved among different animal species, which share a sequence similarity of 90–96%.^{8–10} These data, collected during the years, laid the foundation for accessing to the first three-dimensional (3D) model of S1R through homology modeling techniques and to the design of

numerous ligands.¹¹ Indeed, the structural model allowed the design of several compounds with a good binding profile toward S1R and the rationalization of the binding results that were obtained by ligand-based drug design.^{12,13}

Only in 2016, the crystal structure of the human S1R has been determined in complex with two ligands endowed with high S1R affinity (pdb codes 5hk1, 5hk2); it is constituted by a trimer, with a single transmembrane helix and a cytosolic domain for each monomer.¹⁴ The ligand binding pocket is placed in the β -barrel region of the cytosolic domain and is constituted mainly by hydrophobic residues. The binding is triggered by an ionic interaction with a highly conserved Glu residue (E172), that is involved in a network of hydrogen bonds with Asp126 and Tyr103. Therefore, only positively charged molecules show S1R activity. Moreover, ligands form hydrophobic π – π interactions with Tyr103 and other hydrophobic amino acids in the binding site. The previous homology model presents high degree of similarity with the crystal structure. However, the presence of a single transmembrane domain is in disagreement with the constructs reported by antecedent studies.^{11,15} These results represent an important starting point for deepening the knowledge about this poorly understood molecular target.

From a biological point of view some questions are still open; only in the last decade several studies focused their attention on the transduction signal cascades associated with S1R. It is localized

* Corresponding author. Tel.: +39 0382 987379; fax: +39 0382 422975.

E-mail address: simona.collina@unipv.it (S. Collina).

† These authors equally contributed to this work.

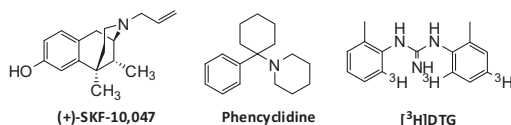


Figure 1. Chemical structures of the benzomorphan analog (\pm)-SKF-10,047, NMDA antagonist phencyclidine and tritiated 1,3-di(2-tolyl)-guanidine.

in a region, called MAM (Mitochondria-Associated-ER Membrane) domain, between the ER and the mitochondria interface.¹⁶ In physiological conditions, S1R is associated with BiP (Binding immunoglobulin Protein) as a silent complex; instead, under stressful conditions or pharmacological manipulation, the receptor acts as molecular chaperone, controlling a broad network of proteins (voltage and ligand-gated channels, G-protein coupled receptors, kinases) and interrupting the cellular death.^{17,18} Its protective action can be explained by decreasing the concentration of reactive oxygen species (ROS) produced by mitochondria, through still unclear mechanisms. Another important role played by S1R is related to its capability to promote the communication among different cellular districts, regulating the membrane lipid composition.^{19,20}

In contrast, little information on S2R is available; the gene encoding this receptor has not been cloned yet and the protein has not been purified. However, it has been identified by photoaffinity labeling, using tritiated 1,3-di(2-tolyl)-guanidine ([³H]DTG) (Fig. 1): results revealed a protein of 18–21 kDa.⁷ Considering these evidences and the unsuccessful attempt to identify the endogenous ligand, the design of selective S2R molecules represent still a challenge today. Recently, the Progesterone Receptor Membrane Component 1 (PGRMC1) has been proposed as S2R binding site and partially crystallized (pdb code 4x8y).^{21,22} Despite some experimental data support this theory, Chu and coworkers recently stated that the genes encoding S2R and PGRMC1 are different. Indeed, sequence alignment of PGRMC1 and S1R reveals sequence similarity below 30%, indicating a low probability to be homologs. Also their structural comparison shows different folds and putative binding sites. Even though PGRMC1 is supposed to be anchored to the membrane by an α helix as S1R, its crystallized cytosolic domain is not trimeric, but only upon binding to heme is able to form a dimer. Therefore, the S2R putative binding site would be highly different with respect to S1R. In contrast, S2R binding assays show that S1R and S2R ligands have similar chemical properties, indicating that the binding sites should be also similar. In conclusion, further investigations are still necessary to provide a better understanding of the S2R binding pocket.²³

From a pharmacological standpoint, S1R is closely related to the Central Nervous System and involved in neuroprotection^{24–26}; accordingly, two S1R ligands, the agonist ANAVEX and the antagonist S1RA, are currently in phase II of clinical trials as potential drugs for the treatment of Alzheimer's disease and neuropathic pain respectively (Fig. 2).^{27,28} Furthermore, recent studies evidenced the potential in cancer therapy of S1R antagonist. Indeed, S1R is overexpressed in lung, breast and prostate cancer cell lines.²⁹ Also S2R is linked to several cancerous conditions,^{30–32} making selective S2R ligands useful tools in tumor diagnosis and S2R selective agonists useful in cancer treatment.

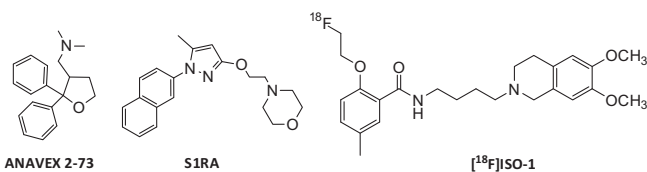


Figure 2. Chemical structures of S1R and S2R ligands that are currently in clinical trials.

To date, the molecular panorama related to S2R modulators is wide. They belong to four main chemical classes: (i) 6,7-dimethoxytetrahydroisoquinoline, (ii) granatane- or tropane-related bicycle, (iii) indole and (iv) cyclohexylpiperazine analogs. Although they represent promising pharmaceutical and/or therapeutic tools, only compound [¹⁸F]ISO-1, a PET marker of cell proliferation, is in phase I clinical trial (Fig. 2).^{33,34}

In the past years we focused our attention on SR modulators, preparing and characterizing a wide compound library of SR ligands. These molecules possess a common arylalkyl(alkenyl) amine scaffold. Among them, **RC-33** (1-[3-(1,1'-biphen)-4-yl]-butylpiperidine) showed excellent S1R affinity (K_i S1R = 0.70 ± 0.3 nM), selectivity over S2R (K_i S2R/ K_i S1R = 147,1) and good in vitro metabolic stability (Table 1).^{35–39} Considering the discovery of a new S1R lead compound (**RC-33**) and keeping in mind the high interest in S2R modulators as promising therapeutic tools, in this paper we present our efforts in better understanding the structure activity relationships (SARs) of novel **RC-33** analogs. In detail, we investigated the relevance of functional groups in obtaining a gain of affinity towards both receptors. Our aim is the discovery of molecules with mixed affinity. Taking into account our reported molecules and especially compound **RC-33**,³⁵ we designed and synthesized a small compound library (Scheme 1), in order to examine the importance of the aryl group and the amine moiety. Moreover, to better identify the chemical properties that are essential for improving the binding affinity, we generated a Quantitative Structure–Activity Relationship (QSAR) model, based on the activity data published in literature and our in-house library. This model has been, afterwards, tested on the new class of compounds that we present here.

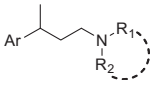
2. Results

2.1. Chemistry

The synthesis of arylalkylamines **10–13a–d** followed the synthetic pathway reported in Scheme 1. The key step is the C–C bond generation, consisting in the nucleophilic addition of the corresponding aryl-lithium reagents **1–4** to carbonyl group of the appropriate β -aminoketone **5a–d** (Scheme 1). The intermediates **5a–d** were prepared via Michael addition of the corresponding secondary amine to but-3-en-2-one, according to the methodology reported in our previous works (anhydrous toluene at reflux or PEG 400, rt)³⁷ Once prepared, **5a–d** were added to the appropriate aryllithium reagents (generated by aryl bromine **1–4** through Br/Li exchange using *t*-butyllithium at -78 °C) to give the corresponding tertiary aminoalcohols. Without any purification, the alcohols were dehydrated in situ under acidic condition (37% HCl, stirring at rt for 12 h), thus providing the desired compounds **6–9a–d**. The elimination reaction of alcoholic intermediates resulted in highly regio- and (*E*)-stereoselective for all alkenylamines synthesized, as confirmed by ¹HNMR analysis and NOESY experiments of crude compounds, in accordance with our previous experience. Arylalkenylamines **6–9 a–d** obtained as (*E/Z*)-mixture after chromatographic purification or crystallization could be converted into (*E*)-alkenylamines in satisfactory yields (30–77%). The final step of our synthetic strategy consisted in the conversion of **6–9a–d** into the corresponding arylalkylamines **10–13a–d** by catalytic hydrogenation of C–C double bond under hydrogen atmosphere using Pd(0) EnCat™ 30NP. In this way, arylalkylamines **10–13a–d**, easily isolated by solid phase extraction (SPE, SCX cartridge), were obtained with acceptable yields (43–95%) and in suitable amounts for the biological investigations.

6–13a–d structures were confirmed by ¹H NMR and MS analysis.

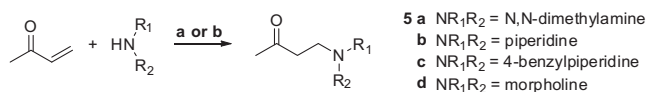
Table 1
Binding affinities towards S1R and S2R. Values are expressed as mean \pm SEM of three experiments



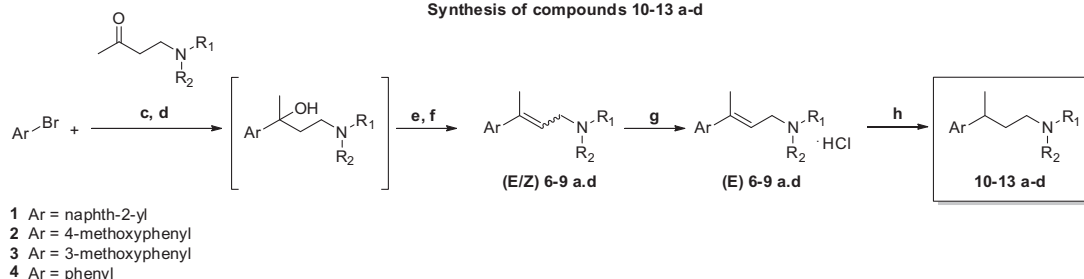
Compound	Ar	$\begin{matrix} \text{N} \\ \\ \text{R}_1 \\ \\ \text{R}_2 \end{matrix}$	K _i S1R (nM) \pm SEM	K _i S2R (nM) \pm SEM	S2R/S1R
(R/S)-RC-33	4-Biphenyl	Piperidine	0,70 \pm 0,3	103 \pm 10	147,1
(R/S)-10a	Naphth-2-yl	N,N-Dimethylamine	1,95 \pm 0,2	43,8 \pm 5,2	22
(R/S)-10b	Naphth-2-yl	Piperidine	1,5 \pm 0,6	50 \pm 6,4	33,3
(R/S)-10c	Naphth-2-yl	4-Benzylpiperidine	19 \pm 2,1	144 ^a	7,6
(R/S)-10d	Naphth-2-yl	Morpholine	5,4 \pm 1,4	33 \pm 2	6,1
(R/S)-11a	4-Methoxyphenyl	N,N-Dimethylamine	116 \pm 22	255 ^a	2,2
(R/S)-11b	4-Methoxyphenyl	Piperidine	20 \pm 5,8	58 \pm 9,4	2,9
(R/S)-11c	4-Methoxyphenyl	4-Benzylpiperidine	3,5 \pm 0,4	18 \pm 4,4	5,14
(R/S)-11d	4-Methoxyphenyl	Morpholine	76 \pm 7,0	68 \pm 13	0,89
(R/S)-12a	3-Methoxyphenyl	N,N-Dimethylamine	239 ^a	864 ^a	3,62
(R/S)-12b	3-Methoxyphenyl	Piperidine	36 \pm 4,1	35 \pm 4,8	0,97
(R/S)-12c	3-Methoxyphenyl	4-Benzylpiperidine	2,9 \pm 0,7	14 \pm 1,4	4,83
(R/S)-12d	3-Methoxyphenyl	Morpholine	137 \pm 40	92 \pm 0,2	0,67
(R/S)-13a	Phenyl	N,N-Dimethylamine	427 ^a	>1000 ^a	N.D.
(R/S)-13b	Phenyl	Piperidine	46 \pm 6,2	56 \pm 9,2	1,22
(R/S)-13c	Phenyl	4-Benzylpiperidine	2,1 \pm 1,0	6,5 \pm 3	3,1
(R/S)-13d	Phenyl	Morpholine	85 \pm 6,3	71 \pm 3,2	1,2

^a Compounds with high affinity were tested three times. For compounds with low SR affinity (>100 nM), only one measure was performed.

Synthesis of compounds 5 a-d



Synthesis of compounds 10-13 a-d



Scheme 1. Synthesis of β -aminoketones **5a–d**. Reagents and conditions: (a) anhydrous toluene, reflux for **5a**; (b) PEG 400 for compounds **5b–d**. Synthesis of compounds **10–13a–d**. Reagents and conditions: (c) *t*-BuLi, anhydrous Et₂O, –78 °C to rt; (d) ketone **5a–d**, –78 °C to rt; (e) 37% HCl, rt; (f) 1 N NaOH; (g) crystallization from acetone; (h) H₂, Pd (0) EnCatTM 30 NP, abs EtOH, rt.

2.2. Binding assays

We measured the affinity towards S1R and S2R of our new compounds **10–13 a–d** through radioligand receptor binding studies. The assay for S1R is based on the use of membranes from guinea pig cerebral cortex, a receptor source, in the presence of a potent and selective S1R radioligand (i.e. [³H]-(+)-pentazocine). Nonspecific binding values were determined using non-radiolabeled (+)-pentazocine and haloperidol in large excess. Conversely, in the case of S2R, we used the membranes of rat liver as receptor source. This test was performed using a nonselective radioligand ([³H]-DTG), since no S2R selective radioligand are commercially available. Moreover, it is important to mask S1R: for this reason, an excess of non-tritiated (+)pentazocine was added to the assay solution.

In order to determine nonspecific binding, a high concentration of non-tritiated DTG was used.^{7,40}

Table 1 reports S1R and S2R affinities of all tested compounds in their racemic form, in comparison with the affinity of **RC-33** as reference compound. With the only exception of compound **13a**, which presents weak affinities toward both receptor subtypes, all compounds generally show from modest to good S1R affinity. Naphthalene and 4-benzylpiperidine derivatives (**10a–d**) exhibit the best S1R affinities for the presence of bulky aromatic portion, which fits well in the receptor pocket (Fig. 3). Moreover, 4-benzylpiperidine derivatives (**11c**, **12c**, **13c**) show also interesting S2R affinity values. In this case, a bulky amine moiety constitutes the main feature for interacting with the S2R binding site. Indeed, N,N-dimethylamine derivatives (**11a**,

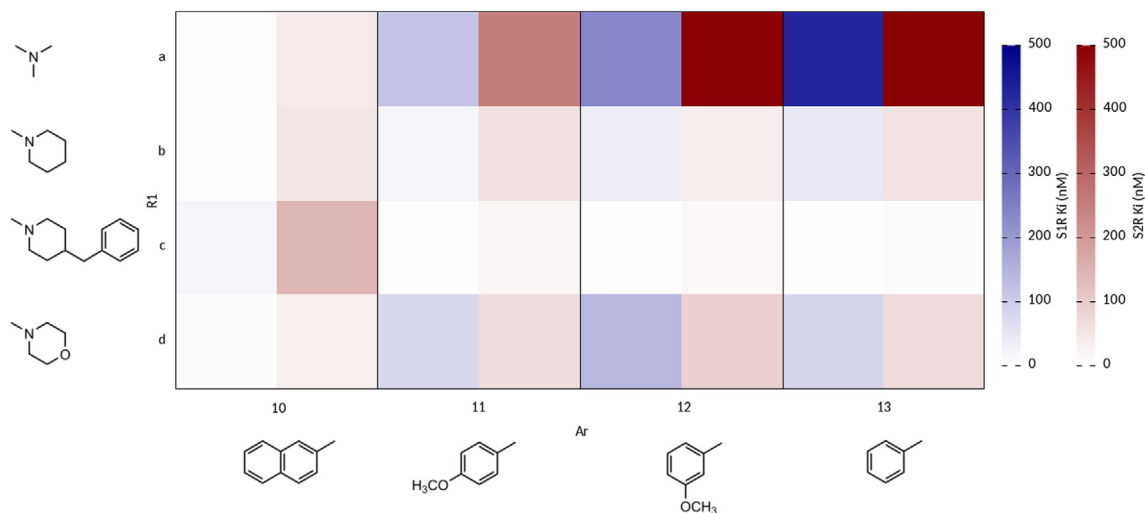


Figure 3. Comparison of S1R and S2R K_i binding affinity values. High affinity towards S1R (indicated by white to light blue colors) is achieved by naphthalene and 4-benzylpiperidine derivatives. Whereas, the highest affinity towards S2R (marked with white to light red colors) is achieved by 4-benzylpiperidine derivatives only.

12a, 13a), presenting a small amine moiety, are characterized by a very weak affinity toward S2R. Lastly, we also identified compounds (**11d, 12b, 12d, 13b**) with mixed affinity toward both receptors subtypes, from now on called pan-selective SR ligands.

2.3. QSAR modeling

Based on previously published affinity data, we modeled quantitative structure–activity relationships (QSARs) in order to rationally interpret the experimental data and to design further ligands.

From the linear regression models we found that the binding affinity to the receptors is increased mainly by two molecular features: flexibility (expressed by 'b_rotN') and hydrophobicity (expressed by 'BCUT_SLOGP_3'). On one hand, flexible molecules are characterized by higher number of rotational bonds: therefore, they can easily orient in the binding pocket in order to form molecular interactions with key residues. On the other hand, the descriptor that calculates hydrophobicity (SlogP) takes additionally into consideration if determined atoms are bonded and their atomic distance. For instance, if the nitrogen atom is placed between two aromatic rings (4-benzylpiperidine series), the BCUT_SLOGP_3 value is relatively high and results in better binding affinity towards both receptors; however, if one aromatic and one aliphatic ring (piperidine) are present, its value is lower and the binding affinity is modest. Consequently, dimethylamines show the lowest values of hydrophobicity and binding affinity. However, compounds **10a** and **10b** constitute exceptions, as they possess high affinity towards S1R despite their relatively low values of BCUT_SLOGP_3. Indeed, this descriptor is identified as more important for binding to S2R than S1R, and the correlation between pK_i and BCUT_SLOGP_3 is higher for S2R than S1R (R 0.61 for S2R, 0.59 for S1R).

Moreover, given hydrophobic molecules, we assume that their solvation energy (E_{sol}) is higher than for water soluble compounds and, consequently, it increases pK_i values for both receptors. Indeed, morpholine derivatives show the lowest energy values, whereas 4-benzylpiperidine derivatives the highest ones.

Another molecular descriptor identified by our QSAR model is globularity (expressed by 'glob'), that indicates if compounds have a spherical, flat or rod-like shape: in this case, our models reveals that the binding affinity is disfavored by high globularity values,

that reveal spherical shapes. Therefore, it is clear that planar or rod-like compounds fit better to the binding site.

The binding affinity is also decreased by high dipole moment (expressed by 'dipole'), that is calculated from the partial charges of the molecule. For instance, compounds of series **a** (dimethylamines) are characterized by high dipole moment, whereas compounds of series **c** (4-benzylpiperidines) by low dipole moment. This descriptor is more relevant for binding to S2R than S1R receptor, that correlates better to the ionization potential (expressed by 'AM1_IP'): for instance, compounds with a notable S1R affinity (**10a** and **10b**) have lower values than the other ligands (**13a**). Furthermore, the binding affinity is penalized by H-bond donors that do not include basic atoms like nitrogen: indeed, 'a_don' counts only for atoms that are both H-bond donor and acceptors such as the hydroxyl group. The compounds that we present in this paper do not contain any hydroxyl group; however, we built the QSAR models on a library that included also compounds presenting this group attached to the alkylic chain. Comparing their affinity values, we can conclude that in average the presence of this H-bond donor feature does not improve, but instead decreases the affinity to both receptors.

In our QSAR models, we did not include the descriptor for the number of nitrogen atoms, because it constitutes a common feature to all compounds in the series and it is well known that a positively charged atom is essential for binding both receptors. Therefore, it would not add any information and improve the quality of the models.

3. Discussion

The identification of pan-modulators, i.e. compounds that are able to bind both SR subtypes, is of great interest for the development of chemotherapeutic drugs targeting SRs. We report here the design and synthesis of pan-modulators in the class of arylalkylamines. We designed a series of **RC-33** analogues, in order to deepen the role played by the hydrophobic ring and the basic portion, in the interaction with the molecular targets.

The synthetic protocol provides few steps for accessing to the final alkyl-compounds. The lithium chemistry was essential to obtain the alcoholic precursors. Indeed, as reported in our previous publication,³⁷ a Li/Br exchange, at the aromatic ring, guaranteed

the lithiated species formation. The subsequent quenching with the appropriate β -aminoketone, led to crude alcohols. Without any additional manipulation, 37% HCl was added at the reaction environment. Therefore, the dehydration reaction gave the (*E/Z*) stereoisomer mixture, which was subjected to a purification, using crystallization or chromatographic purification methods, in order to obtain the (*E*)-compounds, as only isomer. Hydrogenation allowed the obtaining of the desired compounds **10–13a–d**, in good/modest yields and in sufficient amounts to perform the biological investigations.

The affinities to S1R and S2R of **10–13a–d** compounds were evaluated through binding assays and compared with the **RC-33** respective values, in order to understand which structural changes improve the affinity toward S1R or S2R and which ones are necessary to decrease the S2R/S1R ratio.

First of all, mixed affinity is obtained by the presence of the nitrogen atom, that is expected to be charged and to form ionic interactions with Glu172 in the binding site of S1R. As the sequence of S2R is not known yet, we suppose that also the binding pocket of S2R includes an acidic amino acid that can interact with the nitrogen.

Another essential molecular property is hydrophobicity: the nitrogen atom is placed between two hydrophobic features, which can be either aromatic or aliphatic. Aromatic rings are expected to form π - π interactions with aromatic residues in the binding site, as Tyr103 in S1R. Also the binding to S2R requires two hydrophobic features around the nitrogen atom: if one of these is missing (as in the dimethylamine derivatives) the binding affinity is penalized. Although S1R receptor is also likely to bind two hydrophobic groups, it does not require a second feature if the first is a naphthalene (compounds **10a–d**). Effectively, the S2R/S1R K_i ratio clearly shows that compounds **10a–d** are selective towards S1R (Fig. 4). Therefore, in order to gain in affinity to both SRs, the naphthalene moiety has to be excluded.

Series **c**, i.e. 4-benzylpiperidine derivatives, is relatively more selective towards S1R than S2R, but the binding affinities are very good in both cases, indicating that the presence of a second

aromatic ring, bound to the piperidine, favors mixed binding properties.

On the other hand, **11–12–13d** are the least selective ligands, as they present a morpholine and an aryl. Indeed, these compounds can bind both receptors for the presence of the nitrogen and the aromatic ring, but they show low binding affinity because of lower hydrophobicity and solvation energy.

Methoxy substituent does not change substantially the selectivity: for piperidines the S2R/S1R K_i ratio decreases only if the substitution is in *meta* (**12b**), for morpholine in both cases (**11d** and **12d**), whereas for 4-benzylpiperidines it increases resulting in higher selectivity towards S1R (**11c** and **12c**).

It has to be pointed out that *N*-(3-(3-fluorophenyl)propyl)pyrrolidine (compound number 44 from Banister et al.⁴¹), shows similar binding affinity towards S2R, but inactivity towards S1R (K_i S2R = 39 nM, S1R K_i >10 μ M, S1R K_i /S2R K_i = 256). Its molecular structure is similar to **12b** with a F atom in *meta* position of the phenyl ring and pyrrolidine instead of piperidine. This confirms the importance of the substituent in *meta* position rather than in *para* to improve S2R binding affinity. On the other side, the pyrrolidine ring is more rigid than piperidine and the fluorine atom acts as H-bond acceptor beside its hydrophobic properties. Therefore, these features should be investigated also on piperidine derivatives to explain the complete loss of affinity towards the S1R receptor.

In summary, our data clearly show that a satisfactory compromise between affinity and selectivity is achieved by the 4-benzylpiperidine derivatives (series **c**). Moreover, molecules with a piperidine or a morpholine (series **b** and **d** respectively), with the exception of the naphthalene derivatives (**10b** and **10d**), lose in affinity toward both receptor subtypes, unless thus maintaining a good pan-affinity (S2R/S1R K_i ratio < 3). However, molecules with a small amine group as *N,N*-dimethylamine (series **a**) exhibit unsatisfactory binding values towards both receptors, except for compound **10a** that possesses high affinity toward S1R. From this analysis we conclude that the driving force to obtain a SR pan-modulator is represented by the right choice of the aminic moiety.

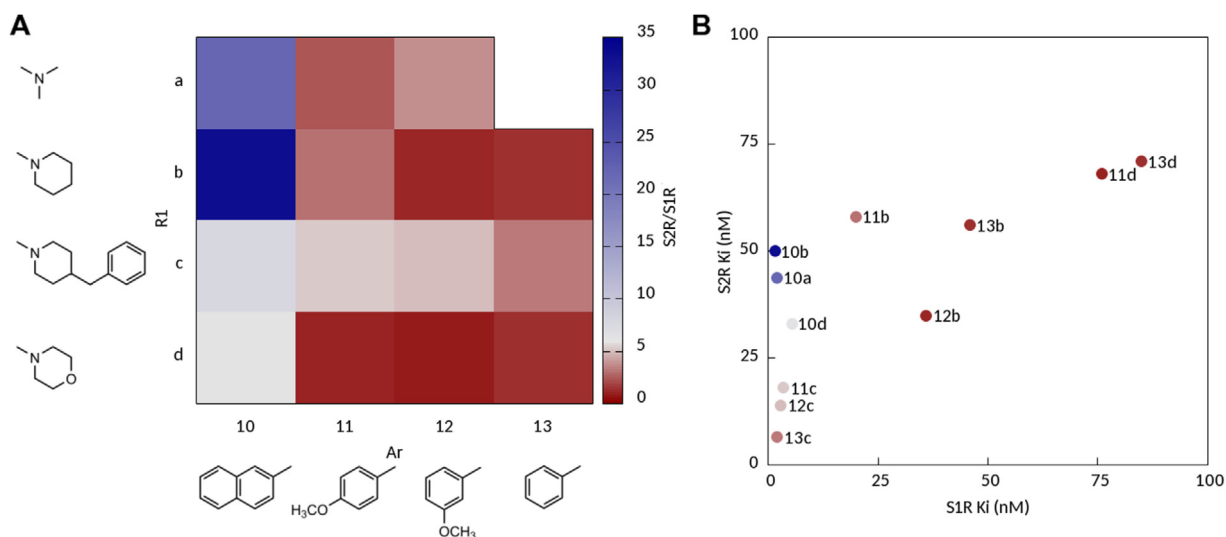


Figure 4. S2R/S1R K_i ratio (A) in relation to S1R and S2R affinity values (B). (A) Compound **13a** is not shown as its S2R K_i value has not been determined with accuracy. Substitutions at amine and aromatic positions are shown and colored according to the S2R/S1R K_i ratio. Low values (marked by dark red color) indicate mixed affinity of compounds towards both receptors. Instead, selective compounds show high ratio values (highlighted by dark blue color). It is clear that enhanced mixed affinity cannot be achieved by naphthalene derivatives, that are the most active towards S1R. (B) Compounds with both S1R and S2R affinity values lower than 100 nM are displayed and colored according to the S2R/S1R K_i ratio. It is evident that all 4-benzylpiperidine derivatives (series **c**), but the naphthalene substituted (10c), present the higher affinities towards both receptors, as they cluster in the bottom left corner of the plot. However, their S2R/S1R ratio is in the range 3–8, as indicated by their red to gray color; whereas morpholine and piperidine compounds (series **b** and **d**), excluding the naphthalene substitution, show very good mixed properties (marked by dark red color), but also low affinity values towards both receptors, as they cluster in the top right corner of the graph.

4. Conclusions

A novel series of arylalkylamines has been prepared and their affinity towards S1R and S2R evaluated. To clarify the structural features leading to the affinity for both receptor subtypes, robust QSAR models have been developed. QSAR modeling revealed that the substitution of the nitrogen with a benzylpiperidine allows the achievement of pan-activity without losing in affinity. The only exception is compound **10c**: despite the high hydrophobicity, the presence of a bulky aromatic portion, as a naphth-2-yl, causes a loss in affinity toward S2R.

Noteworthy is compound **13c**, which represents a good compromise between affinity (K_i S1R = 2.1 ± 1.0 ; K_i S2R = 6.5 ± 3) and pan-activity (S2R/S1R K_i ratio = 3.1). Therefore, **13c** could be considered the *hit* compound of this pan-ligand series.

In conclusion, our study opens the way to the design of further pan-modulators as potential novel chemotherapeutic candidates. It is important to underline that all compounds possess a stereogenic center and at this stage of the research have been tested as racemate. Our current efforts are directed to obtain homochiral compounds, in order to investigate the role of chirality in the interaction with the SRs.

5. Material and methods

5.1. Chemistry

General remarks: Reagents and solvents for synthesis were obtained from Aldrich (Italy). Solvents were purified according to the guidelines in Purification of Laboratory Chemicals.⁴² Melting points were measured on SMP3 Stuart Scientific apparatus and are uncorrected. Analytical thin-layer-chromatography (TLC) was carried out on silica gel precoated glass-backed plates (Fluka Kieselgel 60 F254, Merck) and on aluminumoxide precoated aluminum-backed plates (DC-Alufolien Aluminumoxide 60 F254 neutral, Merck); visualized by ultra-violet (UV) radiation, acidic ammonium molybdate (IV), or potassium permanganate. Flash chromatography (FC) was performed with Silica Gel 60 (particle size 230–400 mesh) purchased from NovaChimica and neutral aluminum oxide (particle size 0.05–0.15 mm) purchased from Fluka. Bond Elute SCX cartridges were purchased from Varian. IR spectra were recorded on a Jasco FT/IR-4100 spectrophotometer; only noteworthy absorptions are given. ¹H NMR spectra were measured with an AVANCE 400 spectrometer Bruker, Germany at rt. Chemical shifts (*d*) are given in ppm, coupling constants (*J*) are in Hertz (Hz) and signals are designated as follows: (s) singlet, (br s) broad singlet, (d) doublet, (t) triplet, (q) quartet, and (m) multiplet. TMS was used as internal standard. MS spectra were recorded on a Finnigan LCQ Fleet system (Thermo Finnigan, San Jose, CA, USA), using an ESI source operating in positive ion mode. The purities of target compounds were determined on a Jasco HPLC system equipped with a Jasco autosampler (model AS-2055 plus), a quaternary gradient pump (model PU-2089 plus), and a multiwavelength detector (model MD-2010 plus). For the HPLC analysis of the arylalkylamines a Chromolith® column (50 × 4.6 mm), eluting with H₂O (0.1% formic acid, solvent A) and ACN (0.1% formic acid, solvent B) under gradient condition (Methods A, B, C, D) at room temperature. Method A (compounds **10b–10d**, **11b**, **12c**, **13b–13d**): 0 min 95% A and 5% B, 3 min 95% A and 5% B, 13 min 5% A and 95% B, 15 min, 5% A and 95% B, 20 min, 95% A and 5% B. Flow rate 1.5 mL/min. Method B (compounds **11c–11d**, **12d**, and **13a**): 0 min 95% A and 5% B, 3 min 95% A and 5% B, 23 min 5% A and 95% B, 25 min, 5% A and 95% B, 30 min, 95% A and 5% B. Flow rate 1.5 mL/min. Method C (compound **10a** and **12b**): gradient conditions as Method B, Flow rate 2 mL/min. Method D (compounds

11a and **12a**): 0 min 90% A and 10% B, 10 min 10% A and 90% B, 20 min 10% A and 90% B, 25 min, 90% A and 10% B. Flow rate 2 mL/min. For the general procedure and characterization of compounds **6–9a–d** see [Supplementary material](#).

5.1.1. General procedure for the preparation of compound 10–13a–d

Before use, Pd(0) EnCat™ 30NP (supplied as a water wet solid with water content 45% w/w) was washed thoroughly with absolute ethanol to remove water. Pre-washed Pd(0) EnCat™ 30NP (0.20 equiv) was added to a stirred solution of the appropriate arylalkenylamine as free base (0.14 mmol) in absolute ethanol (11 mL) and the reaction mixture was left at room temperature in hydrogen atmosphere (balloon) for 30 h. The catalyst was then filtered off and washed with absolute ethanol; the organic phases were lastly dried in vacuo. In this way, pure **13b** was obtained as yellow oils. In the case of compounds **10–12 a–d**, **13a** and **13c** the crudes were loaded on SCX cartridge and eluted with 1 M NH₃ in methanol, pure compounds were obtained in good yield.

5.1.1.1. (R/S)-N,N-Dimethyl-(3-naphthalen-2-yl-butyl)-amine [(R/S)-10a]. Yield: 59%, white solid, mp: 177–179 °C; IR (cm⁻¹): 3362, 3010, 2776, 2577, 2467, 1599, 1474, 1190, 1014, 963, 751; ¹H NMR (400 MHz) (CD₃OD) δ (ppm): 7.80 (m, 3H), 7.63 (s, 1H), 7.40 (m, 3H), 2.87 (m, 1H), 2.30 (m, 2H), 2.18 (s, 6H), 1.89 (m, 2H), 1.35 (d, *J* = 7.1 Hz, 3H); ESI-MS *m/z* = 228.21 [M+H]⁺. HPLC *t_R* = 5.42 min, >98% purity (λ = 270 nm).

5.1.1.2. (R/S)-1-(3-Naphthalen-2-yl-butyl)piperidine [(R/S)-10b]. Yield: 77%, white solid; IR (cm⁻¹): 3050, 2928, 1908, 1600, 1122, 816, 742; ¹H NMR (400 MHz) (CDCl₃) δ (ppm): 7.83–2.76 (m, 3H), 7.60 (s, 1H), 7.48–7.26 (m, 3H), 2.90 (sextuplet, *J* = 7.1 Hz, 1H), 2.44–2.26 (m, 4H), 2.25–2.17 (m, 1H), 1.97–1.83 (m, 3H), 1.62–1.57 (m, 4H), 1.37–1.25 (m, 2H), 1.24 (d, *J* = 7.1 Hz, 3H); ESI-MS *m/z* = 268.24 [M+H]⁺. HPLC *t_R* = 7.41 min, >97% purity (λ = 270 nm).

5.1.1.3. (R/S)-4-Benzyl-1-(3-naphthalen-2-yl-butyl)piperidine [(R/S)-10c]. Yield: 56%, yellow oil; IR (cm⁻¹): 3025, 2924, 2508, 1631, 1602, 1542, 1496, 1453; ¹H NMR (400 MHz) (CDCl₃) δ (ppm): 7.79–7.77 (t, 3H), 7.59 (s, 1H), 7.45–7.42 (m, 2H), 7.32 (m, 1H), 7.26–7.23 (m, 2H), 7.19–7.17 (m, 1H), 7.08 (m, 2H), 3.30 (br d, 2H), 2.93–2.86 (m, 1H), 2.78–2.73 (m, 1H), 2.55 (d, *J* = 7.0 Hz, 2H), 2.48–2.43 (m, 1H), 2.27–2.13 (m, 4H), 1.82–1.71 (m, 4H), 1.61–1.59 (m, 1H), 1.36 (d, *J* = 6.9 Hz, 3H); ESI-MS *m/z* = 358.62 [M+H]⁺. HPLC *t_R* = 11.12 min, >95% purity (λ = 270 nm).

5.1.1.4. (R/S)-4-(3-Naphthalen-2-yl-butyl)morpholine [(R/S)-10d]. Yield: 80%, yellow oil; IR (cm⁻¹): 3053–3026, 2954, 2923–2806, 1599, 1485, 1448, 1115, 836, 763, 732, 696; ¹H NMR (400 MHz) (CDCl₃) δ (ppm): 7.78–7.81 (m, 3H), 7.61 (s, 1H), 7.48–7.40 (m, 2H), 7.35 (dd, 1H), 3.71 (t, 4H), 2.93 (m, *J* = 7.1 Hz, 1H), 2.40 (br s, 4H), 2.17–2.34 (m, 2H), 1.93–1.84 (m, 2H), 1.35 (d, *J* = 7.0 Hz, 3H); ESI-MS *m/z* = 270.13 [M+H]⁺. HPLC *t_R* = 6.88 min, >95% purity (λ = 270 nm).

5.1.1.5. (R/S)-N,N-Dimethyl-[3-(4-methoxy-phenyl)-butyl]-amine [(R/S)-11a]. Yield: 98%, white solid; mp: 194–195 °C; IR (cm⁻¹): 2951, 2599, 2362, 2350, 1681, 1514, 1238, 1173, 1031, 828, 668; ¹H NMR (400 MHz) (CDOD) δ (ppm): 7.18 (d, *J* = 8.7 Hz, 2H), 6.9 (d, *J* = 8.7 Hz, 2H), 3.78 (s, 3H), 3.15–3.09 (m, 1H), 2.83 (s, 6H), 2.84–2.76 (m, 1H), 2.02–1.94 (m, 2H) 1.31 (d, *J* = 7.34 Hz, 3H); ESI-MS *m/z* = 208.15 [M+H]⁺, HPLC *t_R* = 4.51 min, >95% purity (λ = 270 nm).

5.1.1.6. (R/S)-1-[3-(4-Methoxy-phenyl)-butyl]piperidine [(R/S)-11b]. Yield: 58%, yellow oil; IR (cm⁻¹): 3030–2994, 2930, 2852–2762, 1611, 1511, 1245, 1176, 1089, 1036, 1010, 827, 790; ¹H NMR (400 MHz) (CDCl₃) δ (ppm): 7.10 (d, *J* = 8.7 Hz, 2H), 6.82 (d, *J* = 8.7 Hz, 2H), 3.79 (s, 3H), 2.73–2.62 (sextuplet, *J* = 7.1 Hz, 1H), 2.39–2.21 (m, 5H), 2.16–2.09 (m, 1H), 1.78–1.73 (q, *J* = 7.7 Hz, 2H), 1.59–1.51 (m, 4H), 1.41 (m, 2H), 1.22 (d, *J* = 7.7 Hz, 3H); ESI-MS *m/z* = 248.12 [M+H]⁺. HPLC *t*_R = 7.00 min, >95% purity (λ = 270 nm).

5.1.1.7. (R/S)-4-Benzyl-1-[3-(4-methoxy-phenyl)-butyl]piperidine [(R/S)-11c]. Yield: 76%, yellow oil; IR (cm⁻¹): 3060–3024, 2916, 2833–2766, 1609, 1510, 1453, 1243, 1176, 1036, 827, 744, 698; ¹H NMR (400 MHz) (CDCl₃) δ (ppm): 7.23–7.20 (m, 2H), 7.18–7.10 (m, 3H), 7.09 (d, *J* = 8.7 Hz, 2H), 6.82 (d, *J* = 8.7 Hz, 2H), 3.78 (s, 3H), 2.85 (br d, 2H), 2.65–2.52 (sextuplet, *J* = 7.1 Hz, 1H), 2.51 (d, *J* = 7.1 Hz, 2H), 2.26–2.09 (m, 2H), 1.82–1.63 (m, 4H), 1.62–1.56 (m, 2H), 1.47–1.41 (m, 1H), 1.34–1.27 (m, 2H), 1.21 (d, *J* = 7.7 Hz, 3H); ESI-MS *m/z* = 338.22 [M+H]⁺. HPLC *t*_R = 10.37 min, >96% purity (λ = 270 nm).

5.1.1.8. (R/S)-4-[3-(4-Methoxy-phenyl)-butyl]morpholine [(R/S)-11d]. Yield: 78%, yellow oil; IR (cm⁻¹): 3030–2993, 2954, 2852–2806, 1611, 1512, 1456, 1245, 1116, 1035, 829; ¹H NMR (400 MHz) (CDCl₃) δ (ppm): 7.12 (d, *J* = 8.7 Hz, 2H), 6.86 (d, *J* = 8.7 Hz, 2H), 3.81 (s, 3H), 3.72 (t, 4H), 2.72 (sext, *J* = 7.1 Hz, 1H), 2.41 (br s, 4H), 2.33–2.16 (m, 2H), 1.79–1.70 (m, 2H), 1.25 (d, *J* = 7.0 Hz, 3H); ESI-MS *m/z* = 250.45 [M+H]⁺. HPLC *t*_R = 6.93 min, >95% purity (λ = 276 nm).

5.1.1.9. (R/S)-N,N-Dimethyl-[3-(3-methoxy-phenyl)]amine [(R/S)-12a]. Yield: 72%, white solid; mp: 130–131 °C; IR (cm⁻¹): 3169, 2350, 2326, 1771, 1696, 1484, 1245, 1013, 860, 795, 701; ¹H NMR (400 MHz) (CDOD) δ (ppm): 7.29–7.23 (t, 1H), 6.82–6.75 (m, 3H), 3.80 (s, 3H), 3.20–3.11 (m, 1H), 2.84 (s, 6H), 2.84–2.75 (m, 1H), 2.12–2.00 (m, 2H), 1.33 (d, *J* = 6.85 Hz, 3H); ESI-MS *m/z* = 208.22 [M+H]⁺. HPLC *t*_R = 3.96 min, >99% purity (λ = 270 nm).

5.1.1.10. (R/S)-1-[3-(3-Methoxy-phenyl)-butyl]piperidine [(R/S)-12b]. Yield: 77%, yellow oil; IR (cm⁻¹): 3027–2995, 2930, 2852–2736, 1599, 1583, 1486, 1453, 1437, 1257, 1157, 1042, 871, 776, 700; ¹H NMR (400 MHz) (CDCl₃) δ (ppm): 7.21 (t, *J* = 7.0 Hz, 1H), 6.78 (d, *J* = 7.6 Hz, 1H), 6.74–6.70 (m, 2H), 3.80 (s, 3H), 2.68 (m, *J* = 7.1 Hz, 1H), 2.33 (br m, 5H), 2.29–2.11 (m, 1H), 1.84–1.71 (m, 2H), 1.59–1.53 (m, 4H), 1.52–1.41 (m, 2H), 1.24 (d, *J* = 6.9 Hz, 3H); ESI-MS *m/z* = 248.04 [M+H]⁺. HPLC *t*_R = 6.16 min, >98% purity (λ = 270 nm).

5.1.1.11. (R/S)-4-Benzyl-1-[3-(3-methoxy-phenyl)-butyl]piperidine [(R/S)-12c]. Yield: 52%, colorless oil; IR (cm⁻¹): 3082–3024, 2916, 2845–2766, 1599, 1583, 1485, 1452, 1436, 1258, 1044, 776, 744, 698; ¹H NMR (400 MHz) (CDCl₃) δ (ppm): 7.35–7.25 (m, 2H), 7.24–7.14 (m, 4H), 6.80 (d, *J* = 7.7 Hz, 1H), 6.78–6.73 (m, 2H), 3.82 (s, 3H), 2.89 (br d, 2H), 2.71 (sext, *J* = 6.9 Hz, 1H), 2.54 (d, 2H), 2.36–2.18 (m, 2H), 1.88–1.76 (br m, 4H), 1.62 (br d, 2H), 1.57–1.46 (m, N(CH₂CH₂)₂CH, 1H), 1.38–1.28 (m, 2H), 1.26 (d, *J* = 6.9 Hz, 3H); ESI-MS *m/z* = 338.36 [M+H]⁺. HPLC *t*_R = 8.21 min, >96% purity (λ = 270 nm).

5.1.1.12. (R/S)-4-[3-(3-Methoxy-phenyl)-butyl]morpholine [(R/S)-12d]. Yield: 43%, yellow oil; IR (cm⁻¹): 3050–3024, 2954, 2852–2806, 1607, 1598, 1583, 1486, 1454, 1259, 1116, 1043, 867, 778, 700; ¹H NMR (400 MHz) (CDCl₃) δ (ppm): 7.21 (t, *J* = 7.7 Hz, 1H), 6.78 (d, *J* = 7.7 Hz, 1H), 6.74–6.72 (m, 2H), 3.80 (s, 3H), 3.70 (t, 4H), 2.72 (m, *J* = 7.1 Hz, 1H), 2.39 (br s, 4H), 2.31–2.16 (m, 2H), 1.79–1.72 (m, 2H), 1.25 (d, *J* = 7.0 Hz, 3H); ESI-MS

m/z = 250.16 [M+H]⁺. HPLC *t*_R = 6.25 min, >95% purity, (λ = 270 nm).

5.1.1.13. (R/S)-N,N-Dimethyl-(3-phenyl-butyl)-amine [(R/S)-13a]. Yield: 95%, white solid; mp: 220–222 °C; IR (cm⁻¹): 2957, 2462, 2362, 2313, 1471, 1315, 1173, 1017, 959, 764, 708; ¹H NMR (500 MHz) (CDOD) δ (ppm): 7.37–7.25 (m, 2H), 7.25–7.12 (m, 3H), 3.21–3.10 (m, 1H), 2.83 (s, 6H), 2.79–2.75 (m, 1H), 2.03–1.95 (m, 2H), 1.32 (d, *J* = 6.8 Hz, 3H); ESI-MS *m/z* = 178.23 [M+H]⁺. HPLC *t*_R = 17.12 min, >95% purity (λ = 276 nm).

5.1.1.14. (R/S)-1-(3-Phenyl-butyl)piperidine [(R/S)-13b]. Yield: 58%, yellow oil; IR (cm⁻¹): 3083–3026, 2929, 2852–2762, 1602, 1493, 1451, 1154, 1120, 759, 698; ¹H NMR (400 MHz) (CDCl₃) δ (ppm): 7.29 (t, *J* = 8.1 Hz, 2H), 7.19–7.16 (m, 3H), 2.73–2.68 (sextuplet, *J* = 7.1 Hz, 1H), 2.36–2.26 (m, 5H), 2.19–2.12 (m, 1H), 1.84–1.78 (m, 2H), 1.61–1.56 (m, 2H), 1.41 (m, 2H), 1.25 (d, *J* = 6.9 Hz, 3H); ESI-MS *m/z* = 218.17 [M+H]⁺. HPLC *t*_R = 9.27 min, >95% purity (λ = 250 nm).

5.1.1.15. (R/S)-4-Benzyl-1-(3-phenyl-butyl)piperidine [(R/S)-13c]. Yield: 47%, yellow oil; IR (cm⁻¹): 3682, 3019, 2929, 2856, 2434, 2400, 1230; ¹H NMR (400 MHz) (CDCl₃) δ (ppm): 7.36–7.25 (m, 4H), 7.24–7.13 (m, 6H), 2.86 (br d, 2H), 2.71 (sext, *J* = 7.0 Hz, 1H), 2.52 (d, *J* = 7.1 Hz, 2H), 2.34–2.21 (m, 1H), 2.20–2.11 (m, 1H), 1.89–1.72 (m, 4H), 1.61 (br d, 2H), 1.58–1.42 (m, 1H), 1.39–1.30 (m, 2H), 1.28 (d, *J* = 7.2 Hz, 3H). ESI-MS *m/z* = 308.19 [M+H]⁺. HPLC *t*_R = 8.40 min, >98% purity (λ = 270 nm).

5.1.1.16. (R/S)-4-(3-Phenylbutyl)morpholine [(R/S)-13d]. Yield: yellow oil; IR (cm⁻¹): 2972, 2857, 1602, 1492, 1445, 1370, 1265, 1116, 914, 860. ¹H NMR (400 MHz) (CDCl₃) δ (ppm): 7.40–7.35 (m, 2H), 7.30–7.22 (m, 1H), 7.18–7.10 (m, 2H), 3.66–3.62 (m, 4H), 2.73 (m, 1H), 2.54–2.49 (m, 2H), 2.37–2.24 (m, 2H), 2.22–2.14 (m, 2H), 1.82–1.71 (m, 2H), 1.27 (d, *J* = 7.0 Hz, 3H). ESI-MS *m/z* = 220.42 [M+H]⁺. HPLC *t*_R = 8.72 min, >96% purity (λ = 250 nm).

5.2. Binding assays

The affinities of compounds **10–13a–d** towards S1R and S2R were evaluated by radioligand receptor binding studies.

The assay for S1R is based on the use of membrane from guinea pig cerebral cortex, which represents a receptor source in the presence of a potent and selective S1R radioligand (i.e. [³H]-(+)-pentazocine). Nonspecific binding values were determined using non-radiolabeled (+)-pentazocine and haloperidol in large excess.

Instead, in the case of S2R, we used the membrane of rat liver as receptor source. This test was performed using a nonselective radioligand ([³H]-DTG), since no S2R selective radioligand are commercially available. Moreover, it is important to mask the S1R: for this reason, an excess of non-tritiated (+)pentazocine was added to the assay solution. In order to determine nonspecific binding, a high concentration of non-tritiated DTG was used.

5.2.1. Materials

Guinea pig brains for the S1R binding assays were commercially available (Harlan–Winkelmann, Borcheln, Germany). Homogenizer: Elvehjem Potter (B. Braun Biotech International, Melsungen, Germany) and Soniprep 150, MSE, London, UK). Centrifuges: Cooling centrifuge model Rotina 35R (Hettich, Tuttlingen, Germany) and High-speed cooling centrifuge model Sorvall RC-5C plus (Thermo Fisher Scientific, Langensfeld, Germany). Multiplates: standard 96-well multiplates (Diagonal, Muenster, Germany). Shaker:

self-made device with adjustable temperature and tumbling speed (scientific workshop of the institute). Vortexer: Vortex Genie 2 (Thermo Fisher Scientific, Langensfeld, Germany). Harvester: MicroBeta FilterMate-96 Harvester. Filter: Printed Filtermat Type A and B. Scintillator: Meltilex (Type A or B) solid-state scintillator. Scintillation analyzer: MicroBeta Trilux (all PerkinElmer LAS, Rodgau-Jügesheim, Germany). Chemicals and reagents were purchased from various commercial sources and were of analytical grade.

5.2.1.1. Preparation of membrane homogenates from guinea pig brain cortex.

Five guinea pig brains were homogenized with the potter (500–800 rpm, 10 up-and-down strokes) in six volumes of cold 0.32 M sucrose. The suspension was centrifuged at 1200 g for 10 min at 4 °C. The supernatant was separated and centrifuged at 23,500g for 20 min at 4 °C. The pellet was resuspended in 5–6 volumes of buffer (50 mM Tris, pH 7.4) and centrifuged again at 23,500g (20 min, 4 °C). This procedure was repeated twice. The final pellet was resuspended in 5–6 volumes of buffer and frozen (–80 °C) in 1.5 mL portions containing ~1.5 (mg protein)mL⁻¹.

5.2.2. Protein determination

The protein concentration was determined by the method of Bradford⁴³ modified by Stoscheck.⁴⁴ The Bradford solution was prepared by dissolving 5 mg of Coomassie Brilliant Blue G 250 in 2.5 mL EtOH (95% v/v). Deionized H₂O (10 mL) and phosphoric acid (85% w/v, 5 mL) were added to this solution, and the mixture was stirred and filled to a total volume of 50 mL with deionized water. Calibration was carried out using bovine serum albumin as a standard in nine concentrations (0.1, 0.2, 0.4, 0.6, 0.8, 1.0, 1.5, 2.0, and 4.0 mg mL⁻¹). In a 96-well standard multiplate, 10 mL of the calibration solution or 10 mL of the membrane receptor preparation were mixed with 190 mL of the Bradford solution. After 5 min, the UV absorption of the protein–dye complex at $\lambda = 595$ nm was measured with a plate reader (Tecan Genios, Tecan, Crailsheim, Germany).

5.2.3. General protocol for binding assays

The test compound solutions were prepared by dissolving ~10 mmol (usually 2–4 mg) of test compound in DMSO so that a 10 μ M stock solution was obtained. To obtain the required test solutions for the assay, the DMSO stock solution was diluted with the respective assay buffer. The filtermats were presoaked in 0.5% aqueous polyethyleneimine solution for 2 h at rt before use. All binding experiments were carried out in duplicate in 96-well multiplates. The concentrations given are the final concentrations in the assay. Generally, the assays were performed by addition of 50 μ L of the respective assay buffer, 50 μ L test compound solution at various concentrations (10^{-5} , 10^{-6} , 10^{-7} , 10^{-8} , 10^{-9} and 10^{-10} M), 50 μ L of corresponding radioligand solution, and 50 μ L of the respective receptor preparation into each well of the multiplate (total volume 200 μ L). The receptor preparation was always added last. During the incubation, the multiplates were shaken at a speed of 500–600 rpm at the specified temperature. Unless otherwise noted, the assays were terminated after 120 min by rapid filtration using the harvester. During the filtration each well was washed five times with 300 mL of water. Subsequently, the filtermats were dried at 95 °C. The solid scintillator was melted on the dried filtermats at 95 °C for 5 min. After solidifying of the scintillator at rt, the trapped radioactivity in the filtermats was measured with the scintillation analyzer. Each position on the filtermat corresponding to one well of the multiplate was measured for 5 min with the [³H]-counting protocol. The overall

counting efficiency was 20%. The IC₅₀ values were calculated with GraphPad Prism 3.0 (GraphPad Software, San Diego, CA, USA) by nonlinear regression analysis. The IC₅₀ values were subsequently transformed into K_i values using the equation of Cheng and Prussoff.⁴⁵ The K_i values are given as mean value \pm SEM from three independent experiments.

5.2.4. S1R binding assay

The assay was performed with the radioligand [³H](+)-pentazocine (22.0 Ci mmol⁻¹; PerkinElmer). The thawed membrane preparation of guinea pig brain cortex (~100 mg protein) was incubated with various concentrations of test compounds, 2 nM [³H](+)-pentazocine, and Tris buffer (50 mM, pH 7.4) at 37 °C. The non-specific binding was determined with 10 mM unlabeled (+)-pentazocine. The K_d value of (+)-pentazocine is 2.9 nM.

5.2.5. S2R binding assay

The assay was performed using 150 μ g of rat liver homogenate were incubated for 120 min at room temperature with 3 nM [³H]-DTG (Perkin–Elmer, specific activity 58.1 Ci mmol⁻¹) in 50 mM Tris–HCl, pH 8.0, 0.5 mL final volume. (+)-pentazocine (100 nM) and haloperidol (10 μ M) were used to mask S1R and to define non-specific binding, respectively.

6. QSAR modeling

We generated 3D structures of 75 arylalkylamine derivatives by using MOE dedicated tools.⁴⁷ Before calculating descriptors, we prepared the structures by using its ‘wash’ function to protonate them at physiological pH. Energy minimization followed using MMFF94x and applying default settings.⁴⁶

We divided our dataset into training and test set: the training set contained 61 derivatives, that were already published in literature and other in-house compounds (unpublished data). We generated the QSAR models based on the training set. We calculated and scaled all available 2D and 3D descriptors in MOE: the most important seven descriptors were selected out of 338 by considering their correlation to the assay data (Supplemental Material Table 1). Affinity data were converted to pK_i ($-\log_{10}K_i$) values in order to normalize the range of data and perform a linear regression. More negative pK_i values indicate higher K_i values and, hence, lower affinity. QSAR models were generated by Partial Least Square analysis with a limit of three principal components and validated by cross validation.

QSAR models have been validated internally by Leave-One-Out (LOO) cross validation and externally by testing our new derivatives.

The model for receptor S1R has a correlation coefficient R² 0.64 and root mean square error RMSE 0.64; cross-validated correlation coefficient (Q²) is 0.55, with RMSE of 0.72, indicating that the prediction is reliable. We modeled QSARs also for S2R receptor, by using the same procedure and descriptors (correlation coefficient R² 0.58, root mean square error RMSE 0.44, cross-validated correlation coefficient Q² 0.48, cross-validated RMSE 0.49).

$$\begin{aligned} pK_{iS1R} &= -1.44302 + 0.23255 * BCUT_SLOGP_3 - 0.33249 * a_don \\ &\quad + 0.27685 * E_sol + 0.20083 * b_rotN - 0.13502 * glob \\ &\quad - 0.03737 * dipole - 0.46869 * AM1_IP \\ pK_{iS2R} &= -2.23985 + 0.27149 * BCUT_SLOGP_3 - 0.20203 * a_don \\ &\quad + 0.12047 * E_sol + 0.14450 * b_rotN - 0.11578 * glob \\ &\quad - 0.24609 * dipole - 0.02238 * AM1_IP \end{aligned}$$

The equation that describes the linear correlation indicates that the descriptors contribute to the binding affinity with positive or negative coefficients. Descriptors, which contribute to the

predicted pK_i values with a negative coefficient, decrease the binding affinity. On the opposite, descriptors, which contribute to the predicted pK_i values with a positive coefficient, increase it.

To estimate whether selected descriptors are not inter-correlated, we generated a correlation matrix by using the respective MOE tool: we found that the absolute correlation is lower than 0.5 for all descriptors, but E_{sol} that is orthogonal to AM1_IP and dipole descriptors with correlation of 0.73 and 0.64 respectively. However, AM1_IP and dipole do not exceed the threshold of 0.5 (correlation 0.22). Figures have been generated by GnuPlot tools.⁴⁸

Acknowledgements

We would like to thank Alice Pedrali for the contribution to compounds synthesis, Alessandra Lacetera, Susanne von Grafenstein and Julian E. Fuchs for their contributions to QSAR modeling.

A. Supplementary data

Supplementary data associated with this article can be found, in the online version, at <http://dx.doi.org/10.1016/j.bmc.2016.10.005>.

References and notes

- Martin, W. R.; Eades, C. G.; Thompson, J. A.; Huppler, R. E.; Gilbert, P. E. *J. Pharmacol. Exp. Ther.* **1976**, *197*, 517.
- Su, T. P. *J. Pharmacol. Exp. Ther.* **1982**, *223*, 284.
- Maurice, T.; Lockhart, B. P. *Prog. Neuro-Psychopharmacol.* **1997**, *21*, 69.
- Vaupel, D. B. *Eur. J. Pharmacol.* **1983**, *92*, 269.
- Skuzza, G. *Pol. J. Pharmacol.* **2003**, *55*, 923.
- Hellewell, S. B.; Bowen, W. D. *Brain Res.* **1990**, *527*, 244.
- Hellewell, S. B.; Bruce, A.; Feinstein, G.; Orringer, J.; Williams, W.; Bowen, W. D. *Eur. J. Pharmacol., Mol. Pharmacol. Sect.* **1994**, *268*, 9.
- Hanner, M.; Moebius, F. F.; Flandorfer, A.; Knaus, H. G.; Striessnig, J.; Kempner, E.; Glossmann, H. *Proc. Natl. Acad. Sci. U.S.A.* **1996**, *93*, 8072.
- Kekuda, R.; Prasad, P. D.; Fei, Y. J.; Leibach, F. H.; Ganapathy, V. *Biochem. Biophys. Res. Commun.* **1996**, *229*, 553.
- Seth, P.; Leibach, F. H.; Ganapathy, V. *Biochem. Biophys. Res. Commun.* **1997**, *241*, 535.
- Laurini, E.; Dal Col, V.; Mamolo, M. G.; Zampieri, D.; Posocco, P.; Fermeglia, M.; Vio, L.; Pricl, S. *ACS Med. Chem. Lett.* **2011**, *2*, 834.
- Weber, F.; Brune, S.; Borgel, F.; Lange, C.; Korpis, K.; Bednarski, P. J.; Laurini, E.; Fermeglia, M.; Pricl, S.; Schepmann, D.; Wunsch, B. *J. Med. Chem.* **2016**, *59*, 5505.
- Zampieri, D.; Laurini, E.; Vio, L.; Fermeglia, M.; Pricl, S.; Wuensch, B.; Schepmann, D.; Mamolo, M. G. *Eur. J. Med. Chem.* **2015**, *90*, 797.
- Schmidt, H. R.; Zheng, S. D.; Gurpinar, E.; Koehl, A.; Manglik, A.; Kruse, A. C. *Nature* **2016**, *532*, 527.
- Ortega-Roldan, J. L.; Ossa, F.; Amin, N. T.; Schnell, J. R. *FEBS Lett.* **2015**, *589*, 659.
- Hayashi, T.; Su, T. P. *Cell* **2007**, *131*, 596.
- Hayashi, T.; Su, T. P. *J. Pharmacol. Exp. Ther.* **2003**, *306*, 718.
- Tsai, S. Y.; Hayashi, T.; Mori, T.; Su, T. P. *Cent. Nerv. Syst. Agents Med. Chem.* **2009**, *9*, 184.
- Marra, A.; Rossi, D.; Pignataro, L.; Bigogno, C.; Canta, A.; Oggioni, N.; Malacrida, A.; Corbo, M.; Cavaletti, G.; Peviani, M.; Curti, D.; Dondio, G.; Collina, S. *Future Med. Chem.* **2016**, *8*, 287.
- Tsai, S. Y.; Hayashi, T.; Harvey, B. K.; Wang, Y.; Wu, W. W.; Shen, R. F.; Zhang, Y.; Becker, K. G.; Hoffer, B. J.; Su, T. P. *Proc. Natl. Acad. Sci. U.S.A.* **2009**, *106*, 22468.
- Xu, J.; Zeng, C.; Chu, W.; Pan, F.; Rothfuss, J. M.; Zhang, F.; Tu, Z.; Zhou, D.; Zeng, D.; Vangveravong, S.; Johnston, F.; Spitzer, D.; Chang, K. C.; Hotchkiss, R. S.; Hawkins, W. G.; Wheeler, K. T.; Mach, R. H. *Nat. Commun.* **2011**, *2*, 380.
- Kabe, Y.; Nakane, T.; Koike, I.; Yamamoto, T.; Sugiura, Y.; Harada, E.; Sugase, K.; Shimamura, T.; Ohmura, M.; Muraoka, K.; Yamamoto, A.; Uchida, T.; Iwata, S.; Yamaguchi, Y.; Krayukhina, E.; Noda, M.; Handa, H.; Ishimori, K.; Uchiyama, S.; Kobayashi, T.; Suematsu, M. *Nat. Commun.* **2016**, *7*, 11030.
- Chu, U. B.; Mavlyutov, T. A.; Chu, M. L.; Yang, H.; Schulman, A.; Mesangeau, C.; McCurdy, C. R.; Guo, L. W.; Ruoho, A. E. *eBio Med.* **2015**, *2*, 1806.
- Alonso, G.; Phan, V.; Guillemain, I.; Saunier, M.; Legrand, A.; Anoa, M.; Maurice, T. *Neuroscience* **2000**, *97*, 155.
- V.A. Phan, G.; Sandillon, F.; Privat, A.; Maurice, T., *Therapeutic Potentials of Sigma1 Receptor Ligands Against Cognitive Deficits in Aging*, in: S.F.N. Abstracts (Ed.), 2000.
- Collina, S.; Gaggeri, R.; Marra, A.; Bassi, A.; Negrinotti, S.; Negri, F.; Rossi, D. *Expert Opin. Ther. Pat.* **2013**, *23*, 597.
- Stephen Macfarlane, M. C.; Moore, Dennis; Zografidis, Tasos; Missling, Christopher *Alzheimer's Dementia* **2015**, *11*, 900.
- Montserrat Abadías, M. E.; Vaqué, Anna; Sust, Mariano; Encina, Gregorio *Br. J. Clin. Pharmacol.* **2013**, *75*, 103.
- Aydar, E.; Onganer, P.; Perrett, R.; Djamgoz, M. B.; Palmer, C. P. *Cancer Lett.* **2006**, *242*, 245.
- Mach, R. H.; Smith, C. R.; AlNabulsi, I.; Whirrett, B. R.; Childers, S. R.; Wheeler, K. T. *Cancer Res.* **1997**, *57*, 156.
- Wheeler, K. T.; Wang, L. M.; Wallen, C. A.; Childers, S. R.; Cline, J. M.; Keng, P. C.; Mach, R. H. *Br. J. Cancer* **2000**, *82*, 1223.
- Colabufo, N. A.; Berardi, F.; Contino, M.; Ferorellia, S.; Niso, M.; Perrone, R.; Pagliarulo, A.; Saponaro, P.; Pagliarulo, V. *Cancer Lett.* **2006**, *237*, 83.
- Dehdashti, F.; Laforest, R.; Gao, F.; Shoghi, K. I.; Aft, R. L.; Nussenbaum, B.; Kreisel, F. H.; Bartlett, N. L.; Cashen, A.; Wagner-Johnson, N.; Mach, R. H. *J. Nucl. Med.* **2013**, *54*, 350.
- van Waarde, A.; Rybczynska, A. A.; Ramakrishnan, N. K.; Ishiwata, K.; Elsinga, P. H.; Dierckx, R. A. *Biochim. Biophys. Acta* **2015**, *1848*, 2703.
- Collina, S.; Loddo, G.; Urbano, M.; Linati, L.; Callegari, A.; Ortuso, F.; Alcaro, S.; Laggner, C.; Langer, T.; Prezzavento, O.; Ronsisvalle, G.; Azzolina, O. *Bioorg. Med. Chem.* **2007**, *15*, 771.
- Rossi, D.; Urbano, M.; Pedrali, A.; Serra, M.; Zampieri, D.; Mamolo, M. G.; Laggner, C.; Zanette, C.; Florio, C.; Schepmann, D.; Wuensch, B.; Azzolina, O.; Collina, S. *Bioorg. Med. Chem.* **2010**, *18*, 1204.
- Rossi, D.; Pedrali, A.; Urbano, M.; Gaggeri, R.; Serra, M.; Fernandez, L.; Fernandez, M.; Caballero, J.; Ronsisvalle, S.; Prezzavento, O.; Schepmann, D.; Wuensch, B.; Peviani, M.; Curti, D.; Azzolina, O.; Collina, S. *Bioorg. Med. Chem.* **2011**, *19*, 6210.
- Rossi, D.; Marra, A.; Picconi, P.; Serra, M.; Catenacci, L.; Sorrenti, M.; Laurini, E.; Fermeglia, M.; Pricl, S.; Brambilla, S.; Almirante, N.; Peviani, M.; Curti, D.; Collina, S. *Bioorg. Med. Chem.* **2013**, *21*, 2577.
- Rossi, D.; Pedrali, A.; Gaggeri, R.; Marra, A.; Pignataro, L.; Laurini, E.; Dal Col, V.; Fermeglia, M.; Pricl, S.; Schepmann, D.; Wunsch, B.; Peviani, M.; Curti, D.; Collina, S. *ChemMedChem* **2013**, *8*, 1514.
- Zampieri, D.; Mamolo, M. G.; Laurini, E.; Florio, C.; Zanette, C.; Fermeglia, M.; Posocco, P.; Paneni, M. S.; Pricl, S.; Vio, L. *J. Med. Chem.* **2009**, *52*, 5380.
- Banister, S. D.; Rendina, L. M.; Kassiou, M. *Bioorg. Med. Chem. Lett.* **2012**, *22*, 4059.
- Tan, F.; Guio-Aguilar, P. L.; Downes, C.; Zhang, M.; O'Donovan, L.; Callaway, J. K.; Crack, P. J. *Neuropharmacology* **2010**, *59*, 416.
- Bradford, M. M. *Anal. Biochem.* **1976**, *72*, 248.
- Stoscheck, C. M. *Methods Enzymol.* **1990**, *182*, 50.
- Cheng, Y.; Prusoff, W. H. *Biochem. Pharmacol.* **1973**, *22*, 3099.
- Halgren, T. A. *J. Comput. Chem.* **1996**, *17*, 490.
- Molecular Operating Environment (MOE). 2015.1001; Chemical Computing Group Inc., 1010 Sherbooke St. West, Suite #910, Montreal, QC, Canada, H3A 2R7, 2016.
- Williams, T.; Kelley, C.; Lang, R.; Kotz, D.; Campbell, J.; Elber, G.; Woo, A., et al. *GnuPlot 5.0* **2015**.

Supplemental Material

Gaining in Pan-Affinity Towards Sigma 1 and Sigma 2 Receptors. SAR studies on arylalkylamines.

Authors

D. Rossi^{a#}, M. Rui^a, M. Di Giacomo^a, D. Schepmann^b, B. Wuensch^b, S. Monteleone^{c#}, K. R. Liedl^c, S. Collina^{a*}

^a Department of Drug Sciences, Medicinal Chemistry section, University of Pavia, Viale Taramelli 12, 27100 Pavia, Italy

^b Institute of Pharmaceutical and Medicinal Chemistry, University of Muenster, Correnstrasse 48, 48149 Muenster, Germany

^c Institute of General, Inorganic and Theoretical Chemistry, Center of Molecular Biosciences, University of Innsbruck, Innrain 80/82, 6020 Innsbruck, Austria

Table of Contents

1. Experimental procedures and Spectroscopic Data	S2
3. QSAR Modelling	S5
4. References	S5

1. Experimental procedures and Spectroscopic Data

General remarks: Reagents and solvents for synthesis were obtained from Aldrich (Italy). Solvents were purified according to the guidelines in Purification of Laboratory Chemicals [1]. Melting points were measured on SMP3 Stuart Scientific apparatus and are uncorrected. Analytical thin-layer-chromatography (TLC) was carried out on silica gel precoated glass-backed plates (Fluka Kieselgel 60 F254, Merck) and on aluminiumoxid precoated aluminium-backed plates (DC-Alufohlen Aluminiumoxid 60 F254 neutral, Merck); visualized by ultra-violet (UV) radiation, acidic ammonium molybdate (IV), or potassium permanganate. Flash chromatography (FC) was performed with Silica Gel 60 (particle size 230–400 mesh) purchased from NovaChemica and neutral aluminium oxide (particle size 0.05-0.15 mm) purchased from Fluka. Bond Elute SCX cartridges were purchased from Varian. IR spectra were recorded on a Jasco FT/IR-4100 spectrophotometer; only noteworthy absorptions are given. ¹H-NMR spectra were measured with an AVANCE 400 spectrometer Bruker, Germany at rt. Chemical shifts (δ) are given in ppm, coupling constants (J) are in Hertz (Hz) and signals are designated as follows: (s) singlet, (br s) broad singlet, (d) doublet, (t) triplet, (q) quartet, and (m) multiplet. TMS was used as internal standard. MS spectra were recorded on a Finnigan LCQ Fleet system (Thermo Finnigan, San Jose, CA, USA), using an ESI source operating in positive ion mode. The purities of target compounds were determined on a Jasco HPLC system equipped with a Jasco autosampler (model AS-2055 plus), a quaternary gradient pump (model PU-2089 plus), and a multiwavelength detector (model MD-2010 plus). The HPLC method for the arylalkenylamines was as follows: column XBridge™ Phenyl, 4.6 mm x 150 mm, 5 μ m; column temperature, ambient; flow rate, 1 mL/min; gradient elution, 10% methanol in phosphate buffer (5 mM, pH 7.6) to 90% methanol in phosphate buffer (5 mM, pH 7.6) in 10 min, followed by isocratic elution, 90% methanol in phosphate buffer (5 mM, pH 7.6) for 10 min. The HPLC method for the arylalkanylamine was as followed: column Chromolith®, column temperature, ambient; flow 1.5-2 mL/min; gradient elution, 5% acetonitrile with formic acid to 95% acetonitrile with formic acid in 10-20 min, followed by isocratic elution, 95% acetonitrile with formic acid for 2 min. All of the final compounds had 95% or greater purity. Elemental analyses (C, H, N) were performed on a Carlo Erba 1106 analyzer and the analysis results were within $\pm 0.4\%$ of the theoretical values.

General procedure for the preparation of compounds 6-9 a-d: *t*-BuLi (2.5 equiv, 1.7 M in pentane) was added dropwise to a solution of the appropriate aromatic precursor (1.25 equiv) in anhydrous diethyl ether (0.2 M) cooled to -78 °C, under nitrogen atmosphere, keeping the temperature for 20 min. The reaction was then slowly allowed to warm to room temperature. Stirring was continued for 1h and a solution of the corresponding β -aminoketone (1.0 equiv) in anhydrous diethyl ether (0.6 M) was then added dropwise at -78 °C. The reaction mixture was slowly warm to 0 °C, stirred for 3 h and then quenched with 37% HCl until pH 2 and stirred overnight. Reaction work-up for compounds **6b-c** and **7c**: the organic phase was separated from the aqueous one containing a white-yellow solid, which was isolated by filtration and dissolved in water. The aqueous solution was then made alkaline with 1 N NaOH (pH 10) and extracted with EtOAc. The combined organic phases were dried over anhydrous Na₂SO₄ and concentrated in vacuo, yielding crude **6b-c** and **7c** as free bases. Compounds **6b** and **7b** were then converted into the corresponding hydrochlorides and crystallized from acetone to give pure (E)-**6b** HCl and (E)-**7b** HCl as white solids. Compound **6c** was further purified by crystallization from CH₂Cl₂ and then converted into the corresponding hydrochloride, which was crystallized from acetone affording pure (E)-**6c** HCl, as white solid.

Reaction work-up for compounds **6-9a**, **7-9b**, **8-9c**, **6-8d**: the organic layer was extracted with 10% HCl and the aqueous phase washed with diethyl ether. The combined acid aqueous phases were then made alkaline with 1 N NaOH (pH 10) and extracted with EtOAc. The organic phases were dried over anhydrous Na₂SO₄, treated with 37% HCl and crystallized from acetone to give the desired pure (E) hydrochlorides salts as white solids. For compounds **7b** and **7d**, a further purification by flash chromatography on silica gel (n-hexane/EtOAc/methanol/7 N NH₃ in methanol 9:1:0.5:0.1 v/v/v/v and n-hexane/EtOAc/diethylamine 5:5:0.1 v/v/v, respectively) was performed prior to salification; crystallization from acetone furnished the expected pure (E)-**7b** HCl and **7d** HCl as white solids.

(*E*)-dimethyl-(3-naphthalen-2-yl-but-2-enyl)amine hydrochloride (**6a**): Yield: 76%, white solid; mp: 201-2013 °C; IR (cm⁻¹): 3051, 2892, 2563, 2477, 2366, 2310, 1632, 1475, 1384, 1130, 950, 820, 741; ¹H-NMR (400 MHz) (CD₃OD) δ (ppm): 7.95 (s, 1H),

7.80 (m, 3H), 7.64 (d, $J = 7.8$ Hz, 1H), 7.48 (m, 2H), 6.02 (t, $J = 7.8$ Hz, 1H), 4.03 (d, $J = 7.8$ Hz, 2H), 2.94 (s, 6H), 2.30 (s, 3H). Anal. Calcd. for $C_{16}H_{20}NCl$: C, 73.41; H, 7.70; N, 5.35. Found: C, 73.14; H, 7.57; N, 5.16.

(*E*)-1-(3-(naphthalen-2-yl)but-2-en-1-yl)piperidine hydrochloride (**6b**): Yield: 77%; white solid; mp: 209–210 °C. IR (cm^{-1}): 3058, 2931, 2859, 2607, 2484, 2413–2395, 1646–1595, 1439, 1399–1280, 1160–1078, 1038, 957–944, 896, 850, 818, 741; 1H -NMR (400 MHz) (D_2O) δ (ppm): 7.73–7.86 (m, 4H), 7.50 (dd, $J = 1.8, 7.7$ Hz, 1H), 7.39–7.47 (m, 2H), 5.76 (t, $J = 7.8$ Hz, 1H), 3.72 (d, $J = 7.8$ Hz, 2H), 3.38 (br. d, 2H, $J = 11.5$ Hz), 2.78 (br. t, $J = 12.1$ Hz, 2H), 2.05 (s, 3H), 1.74–1.86 (m, 2H), 1.64–1.74 (m, 1H), 1.46–1.64 (m, 2H), 1.22–1.40 (m, 1H); HPLC Tr = 14.14 min; MS: $m/z = 266.13 [M+H^+]$.

(*E*)-4-benzyl-1-(3-naphthalen-2-yl-but-2-enyl)piperidine (**6c**): Yield: 30%, white solid; mp: 221–222 °C; IR (cm^{-1}): 3049–2977, 2926, 2848, 2514, 1597, 1482, 1453–1434, 1287–1157, 1039, 940, 895, 855, 819, 744, 689; 1H -NMR (400 MHz) (CD_3OD) δ (ppm): 7.82–7.80 (m, 3H) 7.78 (d, $J = 17$ Hz, 1H), 7.61 (d, $J = 17$ Hz, 1H), 7.46–7.44 (m, 2H), 7.29 (t, $J = 15.1$ Hz, 2H), 7.20 (t, $J = 14.5$ Hz, 1H), 7.16 (d, $J = 14.5$ Hz, 2H), 6.09 (t, $J = 13.2$ Hz, 1H), 3.22 (d, $J = 13.2$ Hz, 2H), 3.03 (d, $J = 23.3$ Hz, 2H), 2.57 (d, $J = 13.9$ Hz, 2H), 2.16 (s, 3H), 1.98 (t, $J = 22.7$ Hz, 2H), 1.68 (d, $J = 19.5$ Hz, 2H), 1.57 (m, 1H), 1.38 (m, 2H); HPLC Tr = 16.21 min; MS: $m/z = 356.21 [M+H^+]$.

(*E*)-4-(3-naphthalen-2-yl)-but-2-en-1-yl)morpholine hydrochloride (**6d**): Yield: 57%, white solid; mp: 221–222 °C, IR (cm^{-1}): 3056, 2976–2939, 2526–2453, 1639, 1440–1399, 1123, 1081, 961, 812, 740. 1H -NMR (400 MHz) (D_2O) δ (ppm): 7.88 (d, $J = 1.2$ Hz, 1H), 7.87–7.80 (m, 3H), 7.56 (dd, $J = 1.8, 8.7$ Hz, 1H), 7.51–7.46 (m, 2H), 5.83 (qt, $J = 1.2, 8.0$ Hz, 1H), 3.88 (d, $J = 7.9$ Hz, 2H), 4.19–3.60 (br, 4H), 3.57–2.99 (br, 4H), 2.13 (d, $J = 1.2$ Hz, 3H); HPLC Tr = 13.16 min; MS: $m/z = 268.01 [M+H^+]$.

(*E*)-[3-(4-methoxy-phenyl)-but-2-enyl]-dimethyl-amine (**7a**): Yield: 46%, white solid; mp: 200–201 °C; IR (cm^{-1}): 3006, 2573, 2481, 2362, 2310, 1511, 1250, 1182, 1029, 1009, 954, 835; 1H -NMR (400 MHz) (CD_3OD) δ (ppm): 7.42–7.37 (m, 2H), 6.94–6.87 (m, 2H), 5.69 (qt, $J = 1.3, 6.8$ Hz, 1H), 3.82 (d, $J = 7.8$ Hz, 2H), 3.73 (s, 3H), 2.78 (s, 6H), 2.02 (d, $J = 1.3$ Hz, 3H). Anal. Calcd. for $C_{13}H_{20}NOCl$: C, 64.59; H, 8.34; N, 5.79. Found: C, 64.72; H, 8.03; N, 5.81. HPLC Tr = 12.06 min; MS: $m/z = 206.15 [M+H^+]$.

(*E*)-1-(3-(4-methoxyphenyl)but-2-en-1-yl)piperidine hydrochloride (**7b**): Yield: 48%, white solid; mp: 210–212 °C; IR (cm^{-1}): 2934, 2614, 2520, 1607, 1509, 1464, 1454, 1287, 1244, 1173, 1033, 958, 830, 817. 1H -NMR (400 MHz) (D_2O) δ (ppm): 7.42 (d, $J = 8.8$ Hz, 2H), 6.94 (d, $J = 8.8$ Hz, 2H), 5.71 (t, $J = 7.9$ Hz, 1H), 3.80 (d, $J = 8.0$ Hz, 2H), 3.76 (s, 3H), 3.46 (br. d, 2H), 2.88 (dt, $J = 2.5, 12.6$ Hz, 2H), 2.04 (s, 3H), 1.91–1.80 (m, 2H), 1.78–1.69 (m, 1H), 1.68–1.53 (m, 2H), 1.44–1.31 (m, 1H); HPLC Tr = 13.27 min; MS: $m/z = 246.01 [M+H^+]$.

(*E*)-4-benzyl-1-(3-(4-methoxyphenyl)but-2-en-1-yl)piperidine hydrochloride (**7c**): Yield: 50%, white solid, mp: 190–193 °C; IR (cm^{-1}): 3061–3030, 2973–2837, 2506, 1605, 1511, 1449, 1242, 1027, 821, 751. 1H -NMR (400 MHz) (D_2O) δ (ppm): 7.46–7.38 (m, 2H), 7.35–7.26 (m, 2H), 7.25–7.16 (m, 3H), 7.00–6.91 (m, 2H), 5.701 (t, $J = 7.6$ Hz, 1H), 3.81 (d, $J = 7.7$ Hz, 2H), 3.77 (s, 3H), 3.49 (br. d, $J = 12.6$ Hz, 2H), 2.86 (br. t, $J = 12.4$ Hz, 2H), 2.55 (d, $J = 6.4$ Hz, 2H), 2.03 (s, 3H), 1.89–1.74 (m, 3H), 1.47–1.30 (m, 2H); HPLC Tr = 15.10 min; MS: $m/z = 336.25 [M+H^+]$.

(*E*)-4-(3-(4-methoxyphenyl)but-2-en-1-yl)morpholine hydrochloride (**7d**): Yield: 53%, white solid, mp: 209–210 °C; IR (cm^{-1}): 3032–3000, 2934, 2866, 2433, 1512, 1244, 1128, 1026, 970, 827. 1H -NMR (400 MHz) (D_2O) δ (ppm): 7.37 (d, $J = 8.8$ Hz, 2H), 6.88 (d, $J = 8.8$ Hz, 2H), 5.66 (qt, $J = 8.0$ Hz, 1H), 3.82 (d, $J = 8.0$ Hz, 2H), 3.94–3.73 (br, 4H), 3.71 (s, 3H), 3.33–3.09 (br, 4H), 2.00 (d, $J = 1.2$ Hz, 3H); HPLC Tr = 12.25 min; MS: $m/z = 248.02 [M+H^+]$.

[3-(3-methoxy-phenyl)-but-2-enyl]-dimethyl-amine hydrochloride (**8a**): Yield: 60%, white solid; mp: 156–157 °C; IR (cm^{-1}): 3031, 2364, 2310, 1606, 1574, 1424, 1338, 1213, 1051, 950, 869, 771. 1H -NMR (400 MHz) (CD_3OD) δ (ppm): 7.27 (t, $J = 8.0$ Hz, 1H),

7.04 (d, $J = 7.8$ Hz, 1H), 6.95 (t, $J = 2.2$ Hz, 1H), 6.89 (dd, $J = 2.3, 8.0$ Hz, 1H), 5.73 (qt, $J = 1.4, 7.8$ Hz, 1H), 3.84 (d, $J = 7.9$ Hz, 2H), 3.73 (s, 3H), 2.79 (s, 6H), 2.03 (d, $J = 1.4$ Hz, 3H). Anal. Calcd. for $C_{13}H_{20}NOCl$: C, 64.59; H, 8.34; N, 5.79. Found: C, 64.73; H, 7.97; N, 5.63. HPLC Tr = 12.23 min; MS: $m/z = 206.01$ $[M+H^+]$.

(*E*)-1-[3-(3-methoxy-phenyl)-but-2-enyl]piperidine hydrochloride (**8b**): 60%, white solid; mp: 163-165 °C; IR (cm^{-1}): 2998–3068, 2944, 2834–2856, 2611, 2507, 1600, 1572, 1486, 1427, 1291, 1211, 1158, 1047, 941–958, 878, 827, 780, 697. 1H -NMR (400 MHz) (D_2O) δ (ppm): 7.31 (t, $J = 8.0$ Hz, 1H), 7.10 (d, $J = 8.0$ Hz, 1H), 6.99 (t, $J = 2.3$ Hz, 1H), 6.93 (dd, $J = 2.5, 8.1$ Hz, 1H), 5.75 (qt, $J = 1.3, 7.9$ Hz, 1H), 3.82 (d, $J = 7.9$ Hz, 2H), 3.77 (s, 3H), 3.48 (br. d, $J = 12.1$ Hz, 2H), 2.80 (dt, $J = 2.7, 12.7$ Hz, 2H), 2.06 (d, $J = 1.3$ Hz, 3H), 1.82–1.92 (m, 2H), 1.70–1.79 (m, 1H), 1.55–1.70 (m, 2H), 1.32–1.46 (m, 1H). HPLC Tr = 13.39 min; MS: $m/z = 246.09$ $[M+H^+]$.

(*E*)-4-benzyl-1-[3-(3-methoxy-phenyl)-but-2-enyl]piperidine hydrochloride (**8c**): Yield: 45%, white solid; mp: 169-173 °C; IR (cm^{-1}): 3079–3024, 2998–2919, 2490, 1576, 1454–1432, 1287, 1210, 1046, 776, 743, 698, 692. 1H -NMR (400 MHz) (D_2O) δ (ppm): 7.26–7.35 (m, 3H), 7.16–7.24 (m, 3H), 7.09–7.03 (m, 1H), 6.97–7.01 (m, 1H), 6.93 (dd, $J = 2.5, 8.2$ Hz, 1H), 6.75 (t, $J = 7.8$ Hz, 1H), 3.82 (d, $J = 7.9$ Hz, 2H), 3.78 (s, 3H), 3.50 (br. d, $J = 11.8$ Hz, 2H), 2.87 (br. t, $J = 12.6$ Hz, 2H), 2.55 (d, $J = 6.7$ Hz, 2H), 2.05 (s, 3H), 1.74–1.90 (m, 3H), 1.32–1.47 (m, 2H). HPLC Tr = 15.23 min; MS: $m/z = 336.15$ $[M+H^+]$.

(*E*)-4-[3-(3-methoxy-phenyl)-but-2-enyl]morpholine hydrochloride (**8d**): Yield: 39%, white solid; mp: 203-212 °C; IR (cm^{-1}): 3021, 2834–2999, 2454–2469, 1580, 1444–1464, 1213, 1125, 1080, 1032, 962, 865, 840, 783, 709, 689. 1H -NMR (400 MHz) (D_2O) δ (ppm): 7.24 (t, $J = 8.0$ Hz, 1H), 7.00 (d, $J = 7.9$ Hz, 1H), 6.93 (t, $J = 2.1$ Hz, 1H), 6.87 (dd, $J = 2.2, 8.2$ Hz, 1H), 5.69 (qt, $J = 1.2, 7.9$ Hz, 1H), 3.85 (d, $J = 7.9$ Hz, 2H), 3.71 (s, 3H), 3.56–3.95 (br, 4H), 2.99–3.45 (br, 4H), 2.01 (d, $J = 1.1$ Hz, 3H). HPLC Tr = 12.29 min; MS: $m/z = 248.02$ $[M+H^+]$.

(*E*)-*N,N*-dimethyl-3-phenylbut-2-en-1-amine hydrochloride (**9a**): Yield: 39%, white solid; mp: 199-200 °C; IR (cm^{-1}): 3113, 2350, 2310, 1548, 1515, 1182, 1020, 950, 870, 757, 691; 1H -NMR (500 MHz) (CD_3OD) δ (ppm): 7.54–7.48 (m, 2H), 7.43–7.31 (m, 3H), 5.88 (t, $J = 1.2, 6.9$ Hz, 1H), 4.00 (d, $J = 7.8$ Hz, 2H), 2.94 (s, 6H), 2.22 (s, $J = 1.2$ Hz, 3H). Anal. Calcd. for $C_{12}H_{18}NCl$: C, 68.07; H, 8.57; N, 6.62. Found: C, 68.52; H, 8.22; N, 6.57. HPLC Tr = 12.06 min; MS: $m/z = 176.01$ $[M+H^+]$.

(*E*)-1-(3-phenyl-but-2-enyl)piperidine hydrochloride (**9b**): Yield: 30%; white solid; mp: 2943, 2609, 2489, 1649, 1434–1454, 947, 846, 758, 691. 1H -NMR (400 MHz) (D_2O) δ (ppm): 7.34–7.42 (m, 2H), 7.21–7.34 (m, 3H), 5.67 (t, $J = 7.7$ Hz, 1H), 3.75 (d, $J = 7.8$ Hz, 2H), 3.40 (br. d, $J = 12.1$ Hz, 2H), 2.82 (br. t, $J = 12.0$ Hz, 2H), 2.00 (s, 3H), 1.73–1.86 (m, 2H), 1.63–1.72 (m, 1H), 1.47–1.62 (m, 2H), 1.24–1.39 (m, 1H). HPLC Tr = 13.25 min; MS: $m/z = 216.04$ $[M+H^+]$.

(*E*)-4-benzyl-1-(3-phenyl-but-2-enyl)piperidine hydrochloride (**9c**): Yield: 45%; white solid; mp: 220-222 °C; IR (cm^{-1}): 3055-3025, 2922, 2493, 1650-1598, 1455-1442, 758, 744, 693; 1H -NMR (400 MHz) (D_2O) δ (ppm): 7.48-7.40 (d, 2H), 7.40-7.27 (m, 5H); 7.25-7.17 (m, 3H), 5.75 (qt, $J = 1.3, 7.9$ Hz, 1H), 3.83 (d, $J = 7.9$ Hz, 2H), 3.51 (br. d, $J = 12.8$ Hz, 2H), 2.88 (br. t, $J = 12.7$ Hz, 2H), 2.55 (d, $J = 6.7$ Hz, 2H), 2.06 (d, $J = 1.3$ Hz, 3H), 1.89-1.77 (m, 3H), 1.47-1.32 (m, 2H). HPLC Tr = 15.05; MS: $m/z = 306.17$ $[M + H]^+$.

2. QSAR Modelling

The design of pan-modulators can be achieved by considering molecular descriptors, that show similar relative importance towards both receptors. Whereas chemo-physical properties, that show different importance for the receptor subtypes, can be considered to design selective ligands. Relative importance values have been calculated by MOE QSAR tools [2].

Table 1: molecular descriptors that were used to model quantitative structure activity relationships.

Descriptors	S1R Relative importance	S2R Relative importance

a_don	Number of H-bond donor atoms	0.72	0.78
AMI_IP	Ionization potential (kcal/mol)	1.00	0.08
b_rotN	Number of rotatable bonds	0.42	0.54
BCUT_SLOGP_3	Atoms connection and contribution to logP	0.48	1.00
Dipole	Dipole moment calculated from the partial charges of the molecule	0.08	0.89
E_sol	Solvation energy	0.60	0.47
Glob	Globularity	0.26	0.39

3. References

- [1] F. Tan, P.L. Guio-Aguilar, C. Downes, M. Zhang, L. O'Donovan, J.K. Callaway, P.J. Crack, The sigma 1 receptor agonist 4-PPBP elicits ERK1/2 phosphorylation in primary neurons: a possible mechanism of neuroprotective action, *Neuropharmacology*, 59 (2010) 416-424.
- [2] Molecular Operating Environment (MOE), Chemical Computing Group Inc.

Are sigma modulators an effective opportunity for cancer treatment? A patent overview (1996-2016)

Simona Collina, Emanuele Bignardi, Marta Rui, Daniela Rossi, Raffaella Gaggeri, Alice Zamagni, Michela Cortesi & Anna Tesei

To cite this article: Simona Collina, Emanuele Bignardi, Marta Rui, Daniela Rossi, Raffaella Gaggeri, Alice Zamagni, Michela Cortesi & Anna Tesei (2017): Are sigma modulators an effective opportunity for cancer treatment? A patent overview (1996-2016), Expert Opinion on Therapeutic Patents, DOI: [10.1080/13543776.2017.1276569](https://doi.org/10.1080/13543776.2017.1276569)

To link to this article: <http://dx.doi.org/10.1080/13543776.2017.1276569>



Accepted author version posted online: 04 Jan 2017.
Published online: 13 Jan 2017.



Submit your article to this journal [↗](#)



Article views: 3



View related articles [↗](#)



View Crossmark data [↗](#)

REVIEW

Are sigma modulators an effective opportunity for cancer treatment? A patent overview (1996-2016)

Simona Collina^a, Emanuele Bignardi^a, Marta Rui^a, Daniela Rossi^a, Raffaella Gaggeri^b, Alice Zamagni^c, Michela Cortesi^c and Anna Tesei^d

^aDrug Sciences Department, Medicinal Chemistry and Pharmaceutical Technology Section, University of Pavia, Pavia, Italy; ^bPharmacy Unit, Istituto Scientifico Romagnolo per lo Studio e la Cura dei Tumori (IRST), IRCCS, Meldola, Italy; ^cBiosciences Laboratory, Istituto Scientifico Romagnolo per lo Studio e la Cura dei Tumori (IRST), IRCCS, Meldola, Italy; ^dMBiochem, Biosciences Laboratory, Istituto Scientifico Romagnolo per lo Studio e la Cura dei Tumori (IRST), IRCCS, Meldola, Italy

ABSTRACT

Introduction: Although several molecular targets against cancer have been identified, there is a continuous need for new therapeutic strategies. Sigma Receptors (SRs) overexpression has been recently associated with different cancer conditions. Therefore, novel anticancer agents targeting SRs may increase the specificity of therapies, overcoming some of the common drawbacks of conventional chemotherapy.

Areas covered: The present review focuses on patent documents disclosing SR modulators with possible application in cancer therapy and diagnosis. The analysis reviews patents of the last two decades (1996–2016); patents were grouped according to target subtypes (S1R, S2R, pan-SRs) and relevant Applicants. The literature was searched through Espacenet, ISI Web, PatentScope and PubMed databases.

Expert opinion: The number of patents related to SRs and cancer has increased in the last twenty years, confirming the importance of this receptor family as valuable target against neoplasias. Despite their short history in the cancer scenario, many SR modulators are at pre-clinical stage and one is undergoing a phase II clinical trial. SRs ligands may represent a powerful source of innovative antitumor therapeutics. Further investigation is needed for validating SR modulators as anti-cancer drugs. We strongly hope that this review could stimulate the interest of both Academia and pharmaceutical companies.

ARTICLE HISTORY

Received 19 October 2016
Accepted 14 December 2016

KEYWORDS

Cancer; diagnostic and therapeutic tools; drug conjugates; sigma receptors (SRs); pan-SR ligands; S1R and S2R modulators

1. Introduction

The incidence of cancer is increasing over the years, as reported by the International Agency for Research on Cancer, with estimated 14.1 million new cancer cases and 8.2 million cancer deaths in 2012 worldwide [1]. Finding innovative and more effective treatments for this pathology remains indeed an urgent medical need. This fact appears even more relevant when considering the therapies available as standard chemotherapy, which is the first-choice treatment for the majority of patients [2–4]. In the past decades, anticancer drugs have become more effective and specific although with many hurdles. Poor selectivity and high toxicity levels in nonneoplastic tissues are frequently associated with anticancer drugs: fast replicating cells, such as gut epithelia, bone marrow cells, or hair follicles are most affected [5,6]. Chemotherapy mainly targets one of the principal hallmarks of cancer, i.e. sustaining proliferative signaling, which is shared with these normal tissues. In developing innovative and effective anticancer drugs, it is essential to consider also the other main features of cancer cells, whose progressive acquisition contributes to tumor development. These hallmarks include sustaining

proliferative signaling, evading growth suppression, resisting cell death, enabling replicative immortality, inducing angiogenesis, activating invasion, and metastasis [7]. Understanding the molecular basis underlying tumorigenesis and finding new molecules acting on them are therefore of primary importance, and research on novel targets for anticancer therapy has been extremely intense [8]. In the last decade, dissection of tumorigenesis mechanisms and efforts to find new and more efficient therapies have provided strong evidence that sigma receptors (SRs) play a crucial role in cancer progress and development. SRs were discovered in 1976 by Martin et al. and classified as orphan receptor family [9–14] after several experimental evidence. Biological assays allowed the identification of two receptor subtypes: sigma 1 (S1R) and sigma 2 (S2R) [15]. Increasing evidence suggests that both S1R and S2R may regulate cell proliferation and survival: S1Rs seem to promote cell growth and inhibit apoptosis, whereas S2R activation through both selective and nonselective ligands induces growth arrest and cell death in various cell lines [16]. Nonetheless, S1R has been proposed for years as molecular target for treating neurodegenerative diseases. Accordingly, the first S1Rs-related patents disclosed the great potential of

Article highlights

- Conventional chemotherapy is becoming more and more effective. However, it brings important issues, such as poor specificity and side effects. The need for novel therapeutic targets is still unmet;
- In the last two decades, Sigma Receptors overexpression has been observed in several tumour types (e.g. pancreatic adenocarcinoma and breast cancer);
- SRs have been only recently associated to cancer conditions, although growing evidence supports their value as potential targets for anticancer drugs;
- Despite the numerous SR ligands designed, only [18F]-ISO-1 is undergoing a Phase II clinical trial for the diagnosis of primary breast cancer;
- Multiple strategies have been employed for developing new anticancer agents targeting SRs. S1R ligands re-evaluation and drug conjugates seem the most promising approaches in the patent literature.

This box summarizes key points contained in the article.

S1R modulators against neurological disorders (e.g. epilepsy, addiction, Alzheimer's disease, and Parkinson's disease), as we previously discussed [17]. Only recently, S1R has been regarded as a 'druggable' target in cancer conditions, as several research groups pointed out [18,19]. Indeed, high expression levels of S1R have been found in different cancer types [20–22]. S1R may also be involved in apoptosis as suggested by its location at the mitochondria-associated membranes (MAM) [23]. Accordingly, this hypothesis is supported by the fact that mitochondria are involved in regulating cellular stress response and apoptosis, especially under pathological conditions (Figure 1) [24].

While S1R properties and function have been widely elucidated [25], S2R biological characterization is still to be completely defined, since it has been neither cloned nor its amino acid sequence deciphered. However, there is growing

evidence to consider S2R as a promising therapeutic target in cancer conditions when the receptor is often highly expressed [26–28]. S2R modulators mainly with agonist profile are currently under investigation as valuable pharmacological tools with antiproliferative properties (Figure 1) [29]. Prompted by the increasing interest, the scientific community has postulated several S2R pharmacophoric models for designing new compounds characterized by different scaffolds and high degree of structural novelty. Several compounds have been synthesized and evaluated for affinity towards S2R. Some of them are being pharmacologically investigated [30].

In summary, SRs have gained greater value in oncology, and many medicinal chemistry programs have been launched to discover new anticancer drugs acting via SRs. Considering the present scenario and future prospects of SR-related anticancer drugs, in this review we analyze the patent applications that (1) disclose new SR modulators, in view of their potential in cancer therapy or diagnosis, and (2) propose anticancer therapeutic application for SR ligands.

2. New SR modulators for cancer therapy and diagnosis

SR ligands with potential anticancer applications have increased in number, as clearly demonstrated by the trend in the literature of the last 20 years (Figure 2). A similar trend was observed for patent applications. In this section, patents are discussed according to the binding profile of the compounds and grouped according to the applicants.

2.1. S1R ligands

Patent references: WO199620928 (Australian Nuclear Science & Technology Organization), WO2008055932, WO2011147910 (Laboratorios del Dr. Esteve S.A.), US20100179111, US8349898,

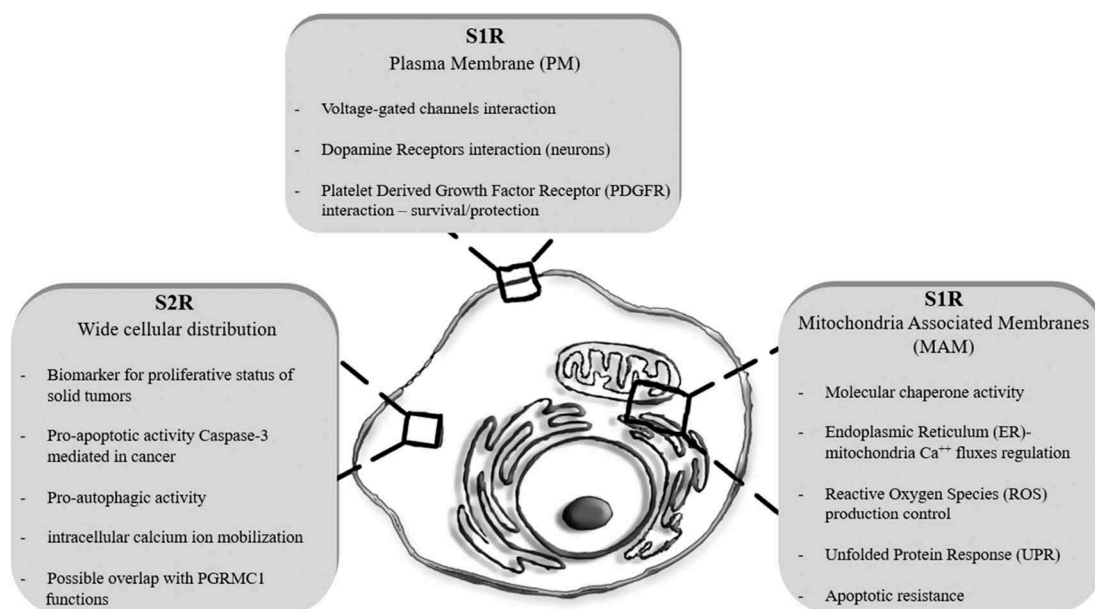


Figure 1. Summary of the Sigma Receptors (SRs) functions in the cell. Sigma 1 Receptor (S1R) exerts its role at both at Mitochondria Associated Membranes (MAM) of Endoplasmic Reticulum (ER) and at Plasma Membrane (PM), where it can translocate after stimulation. Sigma 2 Receptor (S2R) localization is widely distributing in the cell compartments, including mitochondria, ER, lysosomes and PM. S2R role has been mostly associated to pathological conditions, such as cancer.

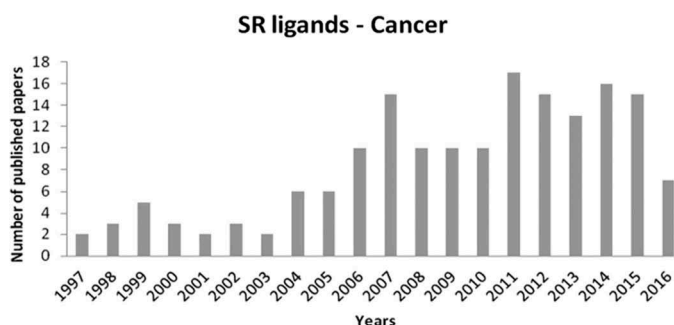


Figure 2. Literature overview of scientific papers related to Sigma Receptor (SR) ligands and Cancer.

US2013102571, US8946302 (Wisconsin Alumni Research Foundation), and WO2015132733 (Università degli Studi di Pavia).

2.1.1. Patent reference: WO199620928 (Australian Nuclear Science & Technology Organization)

In 1996, researchers of the Australian Nuclear Science & Technology Organization deposited a patent describing a series of piperidine derivatives **I** (Figure 3) [31] characterized by a good affinity towards S1 receptors (K_i values, ranging 0.38 – 4.3 nM) and negligible affinity for S2R and other receptors. The applicants proposed these compound classes for therapy of SR-related pathological conditions, such as psychosis and cancer. The patent also pointed out the unavailability of a

commercial S1R radio-ligand for computed tomography investigation [32]. Therefore, the applicants disclosed radiolabeled piperidine derivatives, which are able to cross the blood–brain barrier. These compounds are claimed to be useful tools for cancer diagnosis. Among them, compound **1**, ^{123}I -HEPIE (Figure 3, K_i S1R = 2.3 nM, K_i S2R = 139 nM), is characterized by a good biodistribution in nude mice with B16 melanomas, displaying positive tumor/tissue ratios at 24 h in most organs, such as brain (5.2), muscle (22.8), and lung (5.3). Based on this evidence, the inventors suggest ^{123}I -HEPIE applications as both imaging of malignant melanoma and therapeutic agent.

2.1.2. Patent references: WO2008055932 and WO2011147910 (Laboratorios del Dr. Esteve S.A.)

In 2008, researchers from Laboratorios del Dr. Esteve S.A. claimed a family of compounds based on a 1,2,4-triazole scaffold decorated with different substituents (general formula **II**, Figure 3) [33]. All the patented compounds have an S1R binding profile. The inventors claim that compounds belonging to 1,2,4-triazole series may be used in the treatment of S1R-related conditions, suggesting a wider application, from central nervous system (CNS) disorders to cancer. Besides S1R affinity values, the pharmacological profiles of these triazole derivatives have not been reported. It is noteworthy that this is the first patent with anticancer applications for S1R ligands from the company ‘Lab. Del Dottor Esteve,’ a leader in S1R modulators research and development.

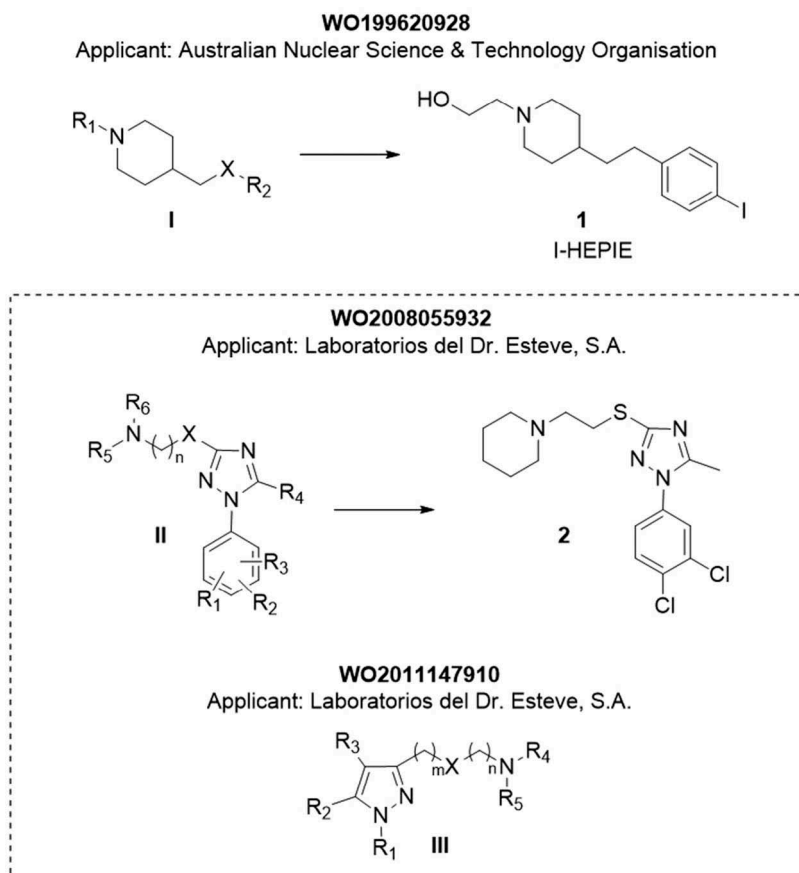


Figure 3. General formulas and most promising compounds based on piperidine, 1,2,4-triazol and pyrazol scaffolds.

In 2011, the same applicant [34] discussed novel pyrazole-derived compounds, characterized by the presence of an alkylamine chain (general formula III, Figure 3) in position 3. Some representative molecules have been tested for S1R affinity. The K_i values range from micromolar to nanomolar; in particular, three compounds in the full series have promising binding affinity (K_i values: 2.1, 3.2, and 2.13 nM). However, unless the authors claim that the disclosed compounds are S1R antagonists, the patent includes no evaluation of agonistic/antagonistic profile. As a consequence, the inventors do not specify particular pathological conditions and propose a wide range of therapeutic applications including cancer and neuropathic pain: Laboratorios del Dr. Esteve S.A. promoted S1RA, an S1R antagonist with a pyrazole core, which is being tested in a Phase II clinical trial for the treatment of neuropathic pain [35,36].

2.1.3. Patent references: US20100179111, US8349898, US2013102571, and US8946302 (Wisconsin Alumni Research Foundation)

In the same years, Ruoho et al. of the Wisconsin Alumni Research Foundation claimed the N,N-dimethylphenylpropyl aminic scaffold as a crucial moiety for binding to S1R (general formula IV, Figure 4). The patents cover both the preparation of novel S1R ligands and their *in vitro* biological characterization [37–40]. An in-depth Structure Activity Relationship (SAR) exploration of alkylamine derivatives allowed identifying molecules with good affinity towards S1R. First, the applicant evaluated whether the length of alkyl chain had a role in the influence of the S1R binding profile. The affinities for S1R increased with the length of carbon chain, showing the dodecylamine moiety the highest affinity ($K_i = 0.02 \mu\text{M}$). Attention has also been paid to the phenylpropyl group bound to the aminic portion of the molecules. This SAR investigation

resulted in N-phenylpropyl derivatives of the N-alkylamines with a 100–1000-fold increase in S1R affinity. The inventors studied the effect of an electron-withdrawing group (e.g. nitro group) as a substituent of the phenyl ring. The nitro derivatives showed an even higher affinity towards S1R. Furthermore, biological investigation of the presented compounds revealed their ability to inhibit the proliferation of several cancer cell lines. In particular, compounds 3 and 4 (Figure 4) displayed the highest cytotoxicity towards many cancer types. The applicants disclosed also a further series of tertiary amines (N,N'-dialkyl or N-alkyl-N'-arylalkyl derivatives). Compound 6 (Figure 4) emerged for its cytotoxic properties in almost all the cell lines tested, unless it does not display high S1R affinity ($K_i = 7.24 \mu\text{M}$). On the other hand, compound 5 (Figure 4) showed a good compromise between S1R affinity ($K_i = 0.3 \text{ nM}$) and inhibition activity (IC_{50} ranging from 28 to 58 μM) towards a panel of cancer cell lines (i.e. NCI-H460, SKOV-3, Du145, MCF7, and MB-MDA-231). The inventors performed broad studies on the S1R binding site, using both radiolabeled ligands and cross-linking reagents. The data disclosed have been supported by scientific publications [41].

In summary, the applicants proposed for the first time the use of S1R modulators in cancer therapy, claiming that the disclosed molecules may inhibit tumor proliferation, prevent metastasis, suppress angiogenesis, and potentially induce the death of cancerous cells. Administration to patients may result in a reduced number or size of cancerous growths. Although the inventors claim that disclosed molecules are S1R inhibitors, they provide no data on the evaluation of agonistic/antagonistic profile. The studies described herein can be considered as a milestone in the history S1R research, given the results reported in the patents, especially on the suggested anticancer mechanisms.

US20100179111; US8349898; US2013102571; US8946302
Applicant: Wisconsin Alumni Research Foundation

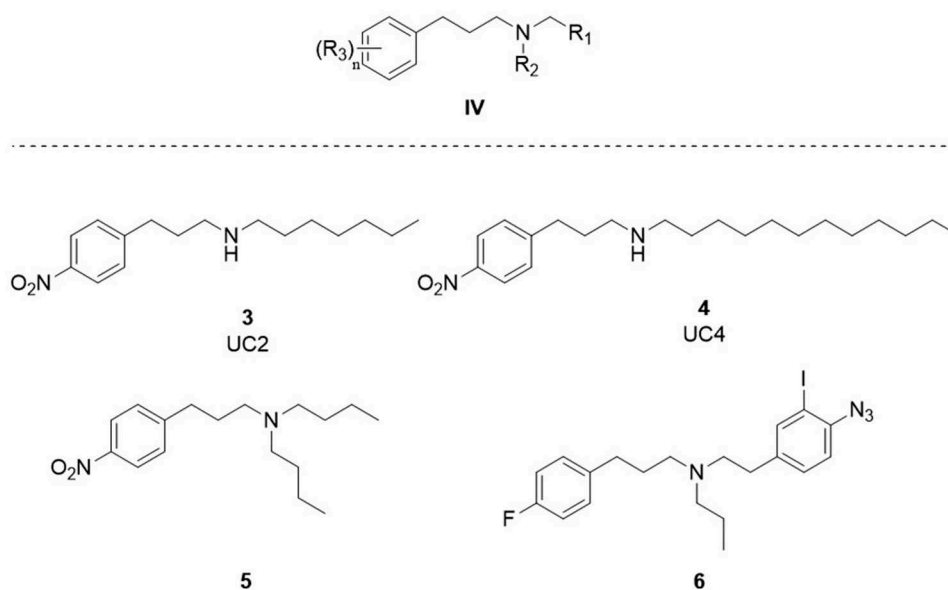


Figure 4. General formula and most promising compounds based on phenylpropylamine scaffold.

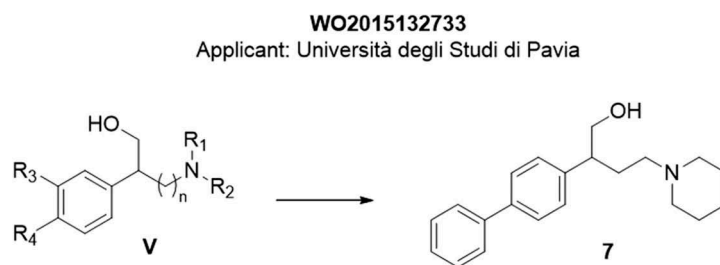


Figure 5. General formula and most promising compound based on aryl-alkylamine scaffold.

2.1.4. Patent reference: WO2015132733 (University of Pavia)

In 2015, Collina and co-workers of the University of Pavia patented a wide series of aryl-alkylamines derivatives (general formula **V**, Figure 5) as S1R ligands, potentially useful for the treatment of neuropathic pain and cancer [42]. Compound 2-((1,1'-biphenyl)-4-yl)-4-(piperidin-1-yl)butan-1-ol (**7** – Figure 5) was selected for a deeper investigation on account of its potency and selectivity. The analysis focused on evaluating its *in vitro* S1R-antagonizing effects, *in vitro* metabolic stability, and ability to reduce inflammatory pain (formalin test).

Compound **7** has an S1R K_i of 6.3 nM, displaying S1R antagonist profile, able to significantly reduce inflammatory pain in mice injected with 20% formalin solution at the lowest dose tested (1 mg/kg). Moreover, it shows a high metabolic stability in the considered biological matrices. All of these results can be of high interest as S1R is a useful antagonist for alleviating neuropathic pain, frequently occurring in cancer patients. Combining this dual effect in one drug would be an innovative approach to treat patients with advanced cancer disease. No information is reported on the investigation of anticancer effect of the compounds.

2.2. S2R ligands

Patent references: US20080161343, US7612085, US20100048614, US8168650, US8168650 (Washington University), and US20120190710 (Adejare A, Mantua, NJ, USA).

2.2.1. Patent reference: US20080161343, US7612085, US20100048614, US8168650, and US7893266 (Washington University)

From 2008 to 2015, Mach et al. of the Washington University deposited several patents [43–46] disclosing the synthesis of S2R ligands, belonging to N-substituted 9-azabicyclo[3.3.1]nonan-3 α -yl-phenylcarbamate analogs. Among them, compounds **8** (WC26), **9** (SV119), and **10** (RHM-138) reported in Figure 6 have been deeply investigated. Compounds **8**, **9**, and **10** are able to induce apoptosis in murine mammary carcinoma cell lines (EMT-6) cancer cells, via both caspase-dependent and caspase-independent manners. In the first case, cell death is mediated by caspase-3 activation, unless a caspase inhibitor partially blocks the apoptosis. Accordingly, the applicants claimed that the presented compounds may be used as anticancer drugs, both alone or in combination with other chemotherapy agents (e.g. doxorubicin and others). The EC₅₀

(after 48 h of treatment in EMT-6 cells) of compounds **8**, **9**, and **10** are 12.5, 11, and 16 μ M, respectively.

To increase the intracellular amount of S2R-selective ligands in cancer cells, the applicants proposed the derivatization of patented compounds with biotin. Several studies demonstrated that biotin transporter (sodium-dependent multi-vitamin transporter) is overexpressed in different aggressive cancer lines [47–50]. The applicant disclosed the synthesis of biotinylated compounds **14–17** (Figure 6), obtained by the reaction between **9** and biotin, using spacers of different length. Surprisingly, SR affinities and S2R selectivity dramatically collapse when biotin group is incorporated into the structure, lowering S2R affinity from 70 (compound **9**) to 1351 nM. From this first attempt, the biotin derivatization seemed to be ineffective in improving tumor uptake. Different drug conjugates comprising S2R ligands and anticancer drugs have been explored in other patent applications, as reported below in this review.

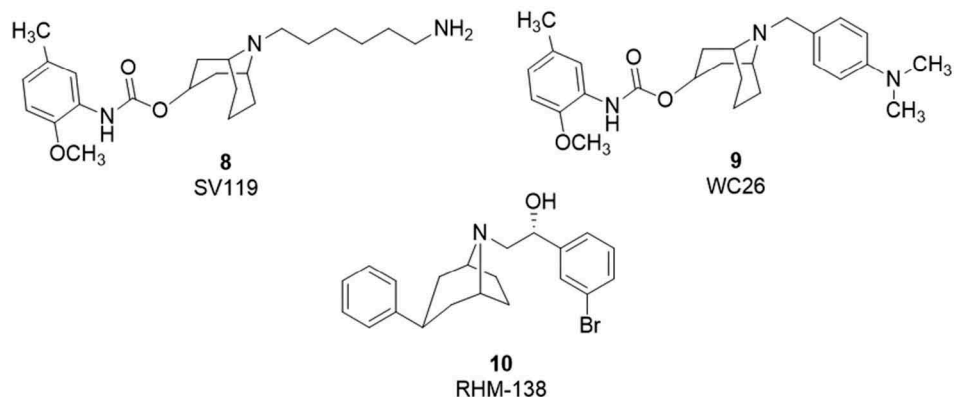
The applicant focused also on the development of S2R ligands as diagnostic agents. The preparation of radiolabeled and fluorescent molecules (compounds **11**, **12**, and **13** – Figure 4) and their evaluation in xenograft models of pancreatic tumor, displaying high S2R expression, have been described. Using micro-Positron Emission Tomography/Computed Tomography (PET/CT) imaging techniques, the inventors demonstrated the uptake of compound **13** into the tumor, thus showing the potential of this molecule as a powerful diagnostic agent.

In 2011, the inventors explored novel benzamidic compounds [51] with the general structures **VI**, **VII**, and **VIII** as shown in Figure 7 and proposed their applications as radiotracers for S2R-expressing tumor types, such as breast cancer. The invention covers the synthesis, biological evaluation, SR affinity, and biodistribution analysis, performed both *in vitro* and *in vivo*. The patent particularly focuses on compounds with general formula **VI**, which are already broadly investigated. Moreover, 12 compounds of this 'series' have been evaluated for their SR-binding affinity, 4 of which showed interesting values of K_i against S2R, equal to or below 10 nM. These compounds also display a high selectivity towards S2R when K_i values are compared with those for D2, D3, and S1R. The most interesting compound seems to be **18**, which has been radiolabeled with ⁷⁶Br for biodistribution and tumor intake experiments. In detail, compound **18** has been studied in Balb/C mice, which were implanted with EMT-6-derived mammary tumors. The results showed that ⁷⁶Br-**18** has a high tumor uptake and could be used for breast cancer

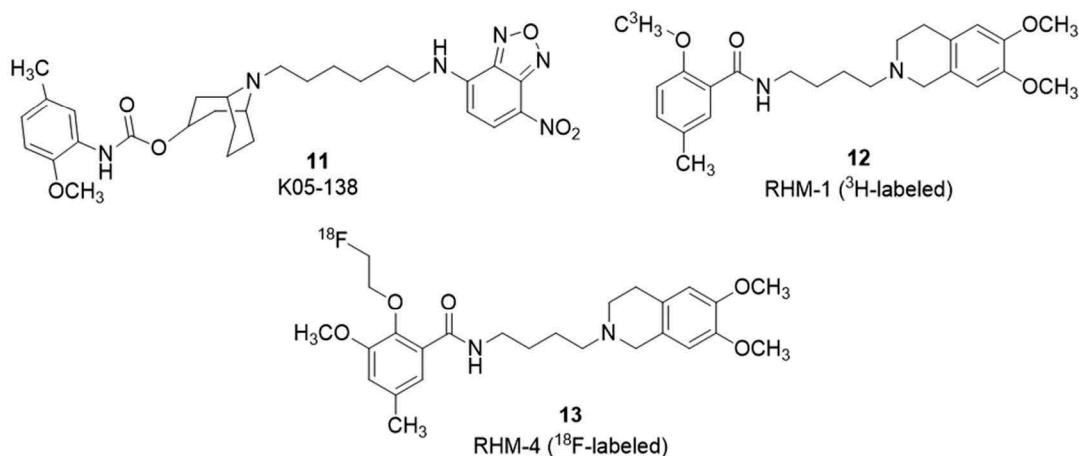
US20080161343, US7612085, US20100048614, US8168650

Applicant: Washington University

S2R Ligands



Labeled S2R Ligands



Biotinilated compounds

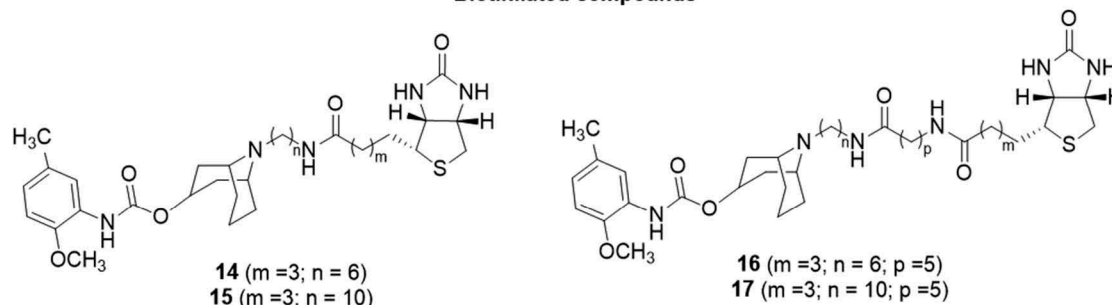


Figure 6. Sigma 2 Receptor (S2R) specific-ligands (8–10), labelled S2R specific-ligands (11–13) and biotinilated S2R specific-ligands (14–17).

detection and diagnosis with noninvasive techniques, such as PET, SPECT, and others.

The findings of the patents from Washington University are of great interest, since they present innovative and valuable S2R ligands, having good antiproliferative and diagnostic properties.

2.2.2. Patent reference: US20120190710 (Adejare A)

The invention is related to the synthesis and characterization of S2R ligands [52], which may find applications in the treatment of pathological conditions where S2R is overexpressed (e.g. cancer). The compounds presented in the patent are bicyclo-2-

amines with general formula **IX** detailed in Figure 8 and include a phenyl ring, a bicyclo-heptane, and a secondary amine group. The patent covers a wide range of chemical entities and possible pharmaceutical formulations of the compounds. Broad therapeutic uses are suggested although the treatment of cancer and neurological disorders is presented as more reliable. Three compounds have been evaluated for their SR-binding affinity profile and for the effect on the viability of different cancer cell lines. Selected compounds, namely **19**, **20**, and **21**, displayed an interestingly high affinity for S2Rs, being their K_i in the nanomolar range (9.6, 16, and 5.5 nM, respectively). Moreover, they are

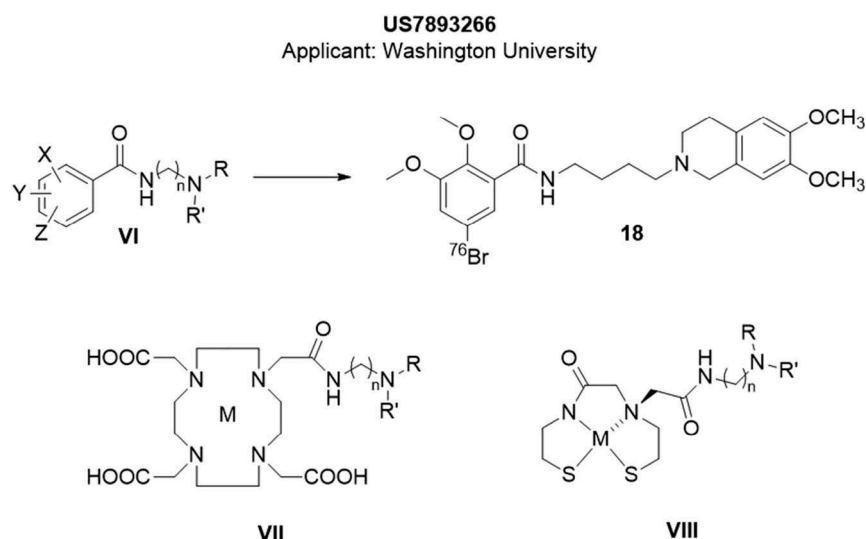


Figure 7. General formulas of Sigma 2 Receptor (S2R) ligands with potential application as radiotracers (VI-VIII). 18 is the most promising compound derived from VI.

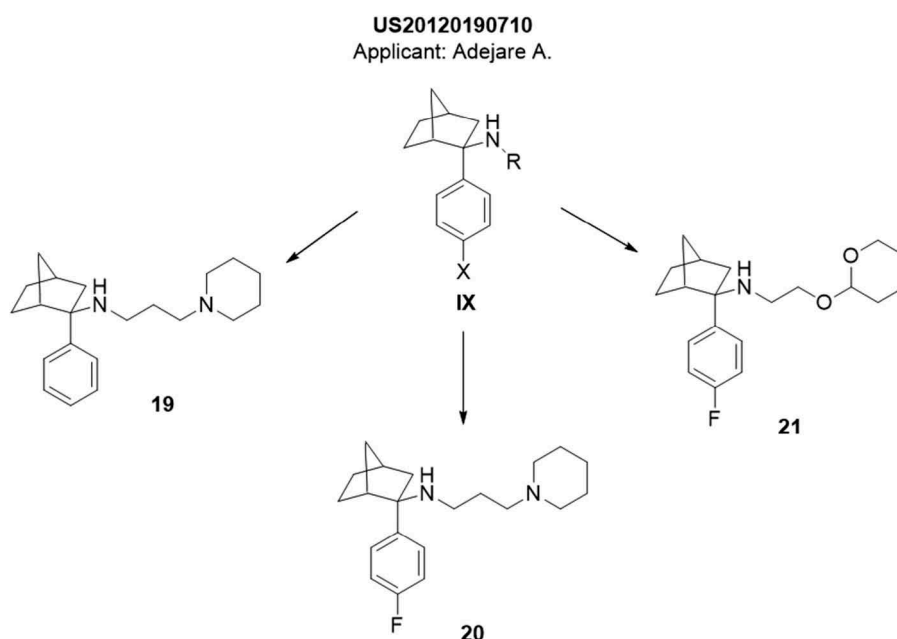


Figure 8. General formula and most promising compounds based on bicycle-heptane-2-amine scaffold.

S2R selective, having very low affinities for S1R ($K_i > 10,000$ nM) and other receptors (i.e. 5-HT_{2A}, D1, D2, μ -, and k-opioid receptors). The compounds **19**, **20**, and **21** have been evaluated in murine neuroblastoma cancer cells (N2a) for the viability tests, as well as in human glioma and breast cancer lines (U-138 and MCF-7, respectively). In both cases, there is a dose-dependent viability inhibition of cancer cells when compared to normal cells.

2.2.3. Patent reference: US2009176705 and WO2015153814 (Washington University)

The patents disclosed S2R ligands (selected among those present in a previous patent US2009176705 by the same inventors) conjugated with a well-established anticancer drug [53,54].

The proposed drug conjugates are claimed to selectively target S2R-highly expressing tumors, given the role of SR ligands

as an effective carrier of potentiated anticancer molecules. In the patent, the antitumor agent des-methyl analog of Erastin (Figure 9) selectively killed cells expressing the small T oncoprotein and oncogenic Ras, causing an alteration of the intracellular ion homeostasis and leading to oxidative cell death. The conjugates included either Erastin or des-methyl analog, which are linked to an S2R-selective ligand, either SV119 or SW V-43 (Figure 9). Among the compounds, SW V-49s has been extensively evaluated for anticancer properties in tumor pancreatic cell lines (CFPAC-1, BxPC-3, AsPC-1, PANC-1, and Mia PaCa-2) and in SYO-1, a synovial sarcoma cell line. In detail, SW V-49s displayed an IC₅₀ in the low micromolar field for all the cancer cell lines tested, while the IC₅₀ values for Erastin and SV119 alone were >100 and >54 μ M, respectively. The inventors demonstrated that cytotoxicity of SW V-49s towards pancreatic cell lines is mediated by both apoptosis and ferroptosis, being the

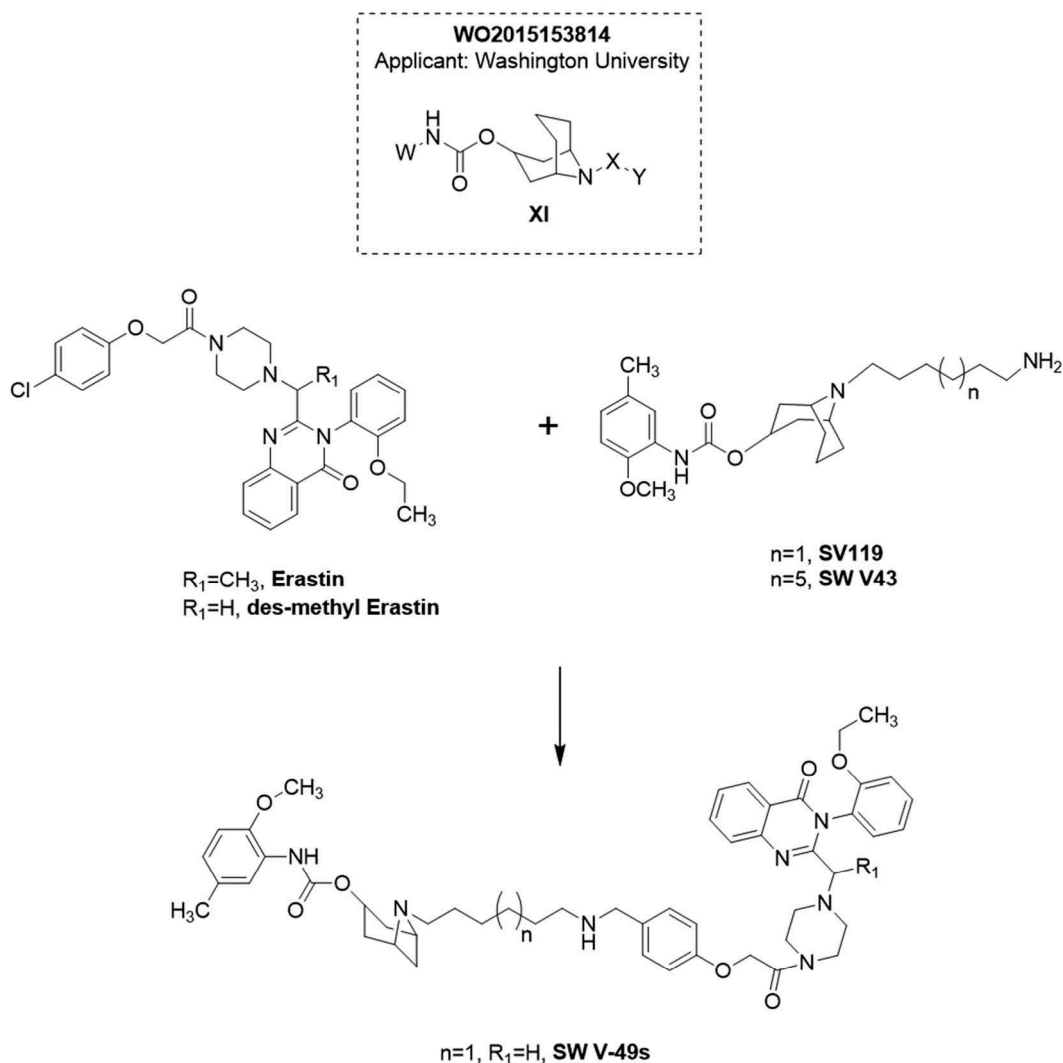


Figure 9. General formula (XI) of Sigma 2 Receptor (S2R) ligands based on N-substituted 9-azabicyclo[3.3.1]nonan-3-yl carbamate scaffold. S2R ligands (SV119, SW V43) are conjugated to Erastin or des-methyl Erastin to obtain SW V49s.

latter an iron-dependent oxidative cell death [55–57]. Moreover, SW V49s is able to reduce the volume of subcutaneous KCKI mouse pancreatic tumor in C57BL/6 mice. Interestingly, Erastin, SV119, or a combination of them had no effect on the reduction of mouse xenografts. The patent provides both novel S2R ligands and innovative uses for existing anticancer drugs (i.e. Erastin [58]). Ultimately, the conjugates disclosed may have future prospects in targeted anticancer therapy, with greater effectiveness and reduced side effects, due to the high level of cytotoxicity of standard chemotherapy.

2.3. S1R and S2R (pan-SRs) ligands

Patent references: WO200230422 (Merck Patent GMBH), WO2008087458, and WO2010097641 (Vamvakides).

2.3.1. Patent reference: WO200230422 (Merck Patent GMBH)

The inventors presented a compound library, characterized by piperidine or piperazine ring systems with general formulas **XII** and **XIII** (Figure 10) [59]. The document shows the affinity/selectivity values of novel SR ligands. The affinities have been

expressed as IC_{50} for both receptor subtypes. The values suggest that the presented molecules display low selectivity between SRs with possible mixed activity. The patent claims that the compounds may be used for the treatment of cancer, in particular lung carcinoma, melanoma, and sarcoma tumor types.

2.3.2. Patent reference: WO2008087458 and WO2010097641 (Vamvakides)

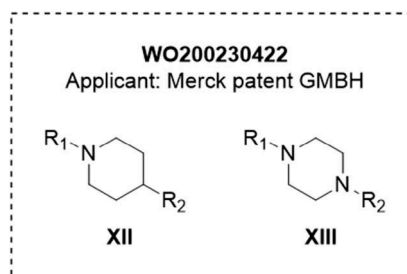


Figure 10. General Formulas of compounds based on piperidine (XII) or piperazine (XIII) scaffold.

The invention [60] is related to previously synthesized SR ligands [61] with anti-/proapoptotic properties and neuroprotective, anticancer, antimetastatic, and anti-inflammatory actions. The molecules have general formula **XIV** (Figure 11) characterized by the presence of mono- or di-substituted adamantyl ring. The most interesting compounds are claimed to have a mixed activity, i.e. S1R antagonist/S2R agonist profile, although no experimental data are provided. Only structures are displayed, together with physicochemical characterization. The inventors claim that all S1R/S2R-mixed modulators have a strong (nanomolar) affinity towards S1R, whereas the affinity towards S2R ranges from nanomolar to micromolar. These molecules seem to be toxic to cancer cells, showing a very low toxicity *in vivo* (data not shown). In 2010, the same applicant submitted another patent [62], referring to a previous application [60].

The inventors concretize the concept of bio-modulatory activity, by analyzing the previously synthesized compounds and classifying them based on their agonistic/antagonistic action on S1R and S2R. The patent discloses two different 'classes' of molecules, which are described in the *Example Section*: (i) S1R agonists with antiapoptotic properties, which may be used for cytoprotective and/or cytoregenerative purposes (mainly in the CNS), by virtue of their ability to counteract the endoplasmic reticulum stress and prevent apoptosis; (ii) weak S1R agonist and S1R antagonists/S2R agonists, which have the ability to promote apoptosis in cancer cells. They may be used alone or in combination with other commercially available drugs for treating cancer, metastasis, and neuropathic pain.

As previously reported for WO2008087458, the biological investigation and the pharmacological profiling are poorly detailed. However, the inventors provided some data about cytotoxic concentrations of the pan-SR ligands. Besides this aspect, the patent is one of the first to have disclosed pan-SR ligands as antiproliferative agents. The applicants claim that cytotoxicity has been evaluated in many cancer cell types (i.e. colorectal, prostate, ovarian, renal, pancreas, lung, gliomas, glioblastomas leukemia, lymphomas, melanomas, sarcomas, and hepatoma), as IC_{50} values are less than 10 μ M. For comparative purposes, antiprotozoal drug quinacrine and the antihistaminic astemizole have been evaluated. The IC_{50} values range 3–5 μ M *in vitro* against the mentioned cancer types, whereas for drug-resistant melanoma, breast cancer, colon, and glioblastoma, the IC_{50} ranges 1 to 2 μ M. *In vivo* evaluation has been carried out in order to confirm *in vitro* results.

The inventors claimed that the presented SR ligands could be used for both inducing and preventing apoptosis. This

property may be exploited for preparing new drugs against cancer, neurodegenerative diseases, and neuropathic pain, depending on the SR-binding profile and on the doses. Cytoprotection is accomplished using S1R agonists at low doses, whereas anticancer activity may be exerted via pan-SR ligands at higher doses.

3. Anticancer applications for well-established SR ligands

Several scientific original articles and patents have been published on the discovery of new SR ligands, potentially useful in CNS disease treatment. Since the 2000s, well-known SR modulators have been used as standard compounds with the aim to establish a correlation between SR modulation and cancer. This section focuses on patents claiming novel anticancer applications for SR modulators, either alone or in combination with other anticancer drugs.

3.1. Patent references: WO200000599, WO200174359, and WO2009074809 (University of Dundee)

The first patent from the University of Dundee presented different methods for selectively inducing nuclear factor kappa-light-chain-enhancer of activated B cells (NF- κ B)-mediated apoptosis in cancer cells [63]. The inventors used different 'apoptosis inducers,' comprising opioid-, opioid-like-, and sigma-receptor ligands. Among the latter class, SRs and dopamine receptors antagonist haloperidol, as well as SR-selective antagonist Rimcazole (Figure 12) [64], are used as inducers of apoptosis in several cell lines, both tumorous and healthy control cells. The apoptotic mechanism observed in lung cancer cell lines involved NF- κ B pathway; the coadministration of the compounds with opioid-like agents (i.e. tumor necrosis factor) results in an increase of cellular death. To further confirm these results, the inventors tested haloperidol and Rimcazole in Hodgkin's lymphoma cells and breast cancer cell lines (MCF7 and MDA), where NF- κ B is constitutively activated. For comparative purposes, the same investigation was performed in healthy cell line. According to experimental data, haloperidol and Rimcazole promote apoptosis especially in cancerous rather than normal control cells. The inventors demonstrated that two S1R ligands with opposite action (Rimcazole and cis-U50488 [65] – Figure 12) cooperate in the apoptosis induction, when coadministered to MDA-MB-468 breast cancer cell line.

Last, when p53 activators and SR ligands are used in combination, there is an increased percentage of apoptotic cells compared to Rimcazole and p53-activators alone. Besides these *in vitro* experiments, the patent also provides data about the effective growth inhibition of human breast carcinoma xenografts in athymic mice.

In 2001, the same applicants presented a new patent [66], claiming new methods for using SR ligands to regulate endothelial cell proliferation and/or survival, thereby controlling the angiogenesis. The main example molecules are selective S1R antagonists Rimcazole and IPAG [67] (Figure 12). The patent stems from two considerations: (1) angiogenesis is

WO199730983, WO2008087458,
WO2010097641
Applicant: Vamvakides A.

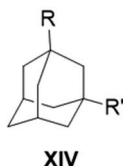


Figure 11. General formula of compounds based on adamantyl ring scaffold.

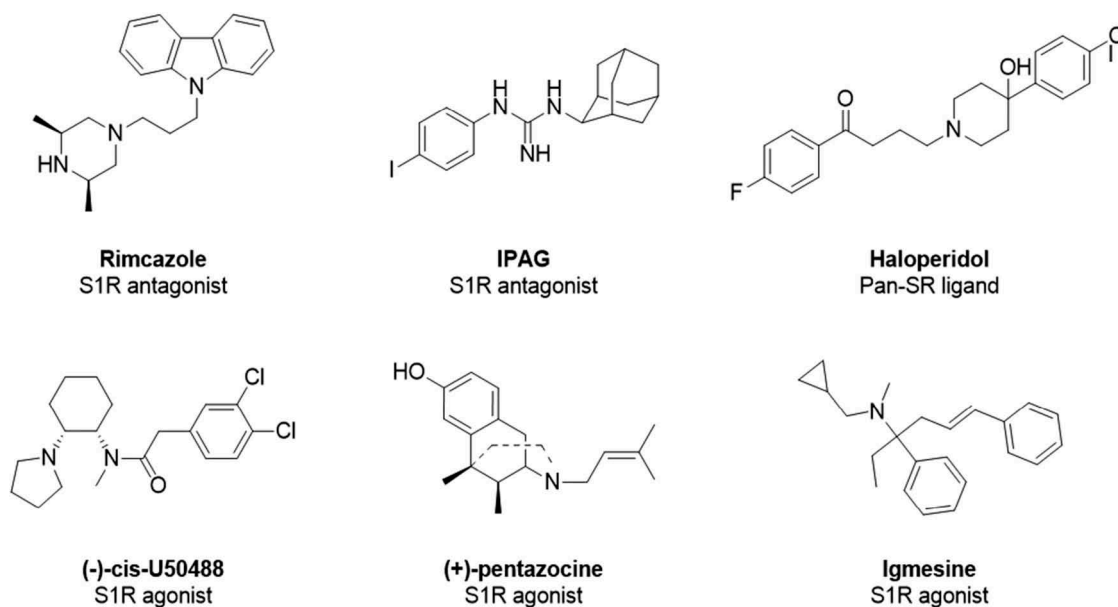


Figure 12. Binding affinity values towards Sigma 1 Receptor (K_{iS1R}) and Sigma 2 Receptor (K_{iS2R}): Rimcazole ($K_{iS1R} = 908.0$ nM; $K_{iS2R} = 302.0$ nM), IPAG ($K_{iS1R} = 2.8$ nM), Haloperidol ($K_{iS1R} = 3.7$ nM; $K_{iS2R} = 12$ nM), (-)-cis-U50488 ($K_{iS1R} = 81.0$ nM; $K_{iS2R} = 250.0$ nM), (+)-pentazocine ($K_{iS1R} = 3.1$ nM; $K_{iS2R} = 1500$ nM) and Igmesine ($K_{iS1R} = 39$ nM).

required for tumor development, and endothelial cells are necessary for this process; (2) endothelial cells are extremely sensitive to opioid- and sigma-mediated inhibition of survival. The investigation begins with the expression profile of S1R in human endothelial cells, followed by the evaluation of S1R antagonistic effects in this cell type. The IC_{50} values of Rimcazole and IPAG are 50 and 11 μ M, respectively. The inventors demonstrated that S1R antagonists are characterized by antiproliferative and antiangiogenic properties both *in vitro* and *in vivo*. In particular, S1R antagonists inhibit the growth of breast carcinoma xenograft. Last, the involvement of S1R overexpression in cancer is further confirmed, since high expression levels of the receptor are able to repress p53- and Bax-induced apoptosis. The patent has an innovative approach to develop alternative anticancer therapies. The presented molecules act on normal cells (i.e. endothelial cells) rather than on tumorous cells, which are usually more difficult to be effectively targeted by drugs.

In 2009, the applicants focused on the possible use of I- κ B kinase (IKK)/NF- κ B pathway inhibitors [68,69] in combination with S1R antagonists, such as Rimcazole [70], aiming to enhance activity through a synergic effect. As previously mentioned, Rimcazole is able to selectively induce apoptosis in cancer cell lines, through the activation of NF- κ B pathway. However, the stimulation of IKK/NF- κ B pathway branch may lead to severe side effects and antiapoptotic activity. The aim of the inventors was to provide a method to avoid the toxicity linked with hyperactivation of NF- κ B. For this purpose, the applicants suggested the use of some histone deacetylase inhibitors (i.e. sodium valproate) and a proteasome inhibitor MG132, which have demonstrated to block the antiapoptotic arm of the pathway (IKK/NF- κ B). The combination with Rimcazole leads to a synergic effect and promotes the Rimcazole-mediated cancer cell death.

3.2. Patent reference: WO2010128309 (Modern Biosciences PLC)

In 2010, Patel and co-workers proposed the use of Rimcazole and some of its derivatives in combination with microtubule-stabilizing agents (e.g. taxanes) [71] for treating tumor conditions such as breast cancer. *In vitro* studies have been performed, but results showed that Rimcazole and taxol exhibit a slightly antagonistic effect against each other. However, *in vivo* studies in breast cancer xenografts (MDA-MB-231 xenografts) demonstrated that the tumor growth had reduced, thanks to the combination of Rimcazole and taxol, rather than to the molecules alone. Besides these promising results, the inventors excluded a synergic action between Rimcazole and taxanes.

3.3. Patent reference: US20150182550 (Centre National de La Recherche Scientifique – CNRS, Paris, France/ Univerite Nice Sophia Antipolis, Nice, France)

The patent application [72] relates to the use of S1R modulators to regulate the ion channel expression at a posttranscriptional level. The patent focuses on human Ether-à-go-go-Related Gene (hERG) ion channel modulation in K562 cells (chronic myeloid leukemia) and MDA-MD-435s (breast cancer cell model). The inventors demonstrated that S1R is part of the signaling that regulates the cell adhesion to extracellular matrix, a hallmark of cancer cells. The patent application suggests a method for modulating ion channels (i.e. hERG) through S1R, by using selective agonists (igmesine and (+)-pentazocine [73,74] – Figure 12) and by silencing S1R expression in the selected cell models. The main finding is that igmesine and (+)-pentazocine are able to reduce the number of active channels at the cell membrane, without affecting the electrical characteristics of hERG. In conclusion,

the patent indicates a possible strategy to affect multiple cancer features, such as proliferation, invasion, apoptosis, and others, in which hERG seems to be involved. Remarkably, since S1R agonists do not affect hERG electrical properties, they would not trigger the side effects that are observed with conventional hERG inhibitors [75].

4. Conclusions

Despite the long-standing interest in SRs as potential drug targets, these receptors remain quite enigmatic. Early studies led to several controversies and wrong assumptions about SR classification: they have been recently classified as orphan receptor family, with broad spectra of potential therapeutic applications, especially in CNS-related pathologies. Some pharmaceutical companies included S1R agonists in their pipelines at different stages of clinical research [17]. In the past 20 years, the scientific community reported several data on the involvement of SRs in cancer. These receptors are overexpressed in a series of tumor types, supporting the use of SR ligands to control disease progression. The patent analysis demonstrated that SR ligands belong to three major classes, S1R, S2R, and pan-SRs modulators, suggesting the involvement of both SR subtypes in cancer.

5. Expert opinion

The scientific community is only recently recognizing the potential of SRs in oncology, unless since the 1990s an increasing number of intellectual property documents disclosed the application of SR ligands in cancer treatment (Figure 13). Growing evidence suggests that both S1R and S2R ligands display antiproliferative properties although triggering distinct molecular cascades [27,76,77].

Among the early approaches in developing novel anticancer drugs targeting SRs, the re-evaluation of well established S1R modulators as antiproliferative agents plays a crucial role, since SRs-regulated mechanisms are still unclear.

The seminal works by Spruce and Soriani identified the relationship between S1R ligands and well documented anticancer targets (e.g. IKK/NF- κ B pathway and hERG ion channel).

Although 'patent of use' can be considered as a milestone in developing novel SR-related anticancer therapies, the synthesis of new S1R ligands with antitumor properties has gained importance over the years. In particular, Ruoho and colleagues, as well as Lab. Del Dr. Esteve S.A., presented interesting compounds, which have been claimed to be selective S1R inhibitors, with broad applications in cancer and neuropathic pain treatment. In the effort to produce S1R antagonists as anticancer agents, Collina et al. presented the synthesis and the biological evaluation of a novel class of S1R inhibitors (aryl-alkylamines derivatives). This patent is the sole that provides data on the agonist/antagonist profile of the disclosed compounds although other applicants do not focus on this aspect. Collina et al. claimed that the presented S1R antagonists might address both tumor growth and pain, which is often associated with cancer pathologies. Concerning S1R-selective ligands with specific applications in diagnostics, ^{123}I -HEPIE is worth mentioning for its good biodistribution properties and high specificity for cancer tissues. In this context, the recently solved S1R crystal structure [78] will foster the design of more focused and specific ligands, thus broadening the possibility of innovative anticancer discovery.

Unlike S1R, S2R subtype has been associated with cancer conditions since its identification. Several researchers focused on the synthesis of new chemical entities targeting S2R, in virtue of the high expression of S2R subtype in cancer cell lines and tissues [79]. The evidence that S2R stimulation selectively inhibits cancer proliferation gave a further boost to the design and development of S2R agonists. All these data have been concretized in pharmacophoric model definition [80–83] to ultimately design novel molecules with both high affinity and selectivity towards S2R. The compounds synthesized so far can be grouped into four main structural classes: (i) 6,7-dimethoxytetrahydroisoquinoline derivatives; (ii) granatane- or tropane-related bicycle

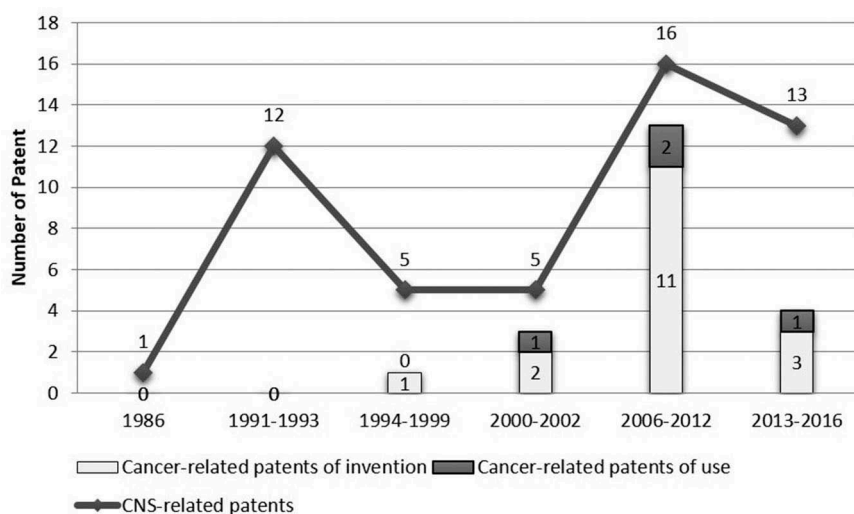


Figure 13. Overview of Sigma Receptors (SRs)-related patents from 1986 to 2016. Among the early approaches in developing novel anticancer drugs targeting SRs, the re-evaluation of well established S1R modulators as antiproliferative agents plays a crucial role, since SRs-regulated mechanisms are still unclear. The seminal works by Spruce and Soriani identified the relationship between S1R ligands and well documented anticancer targets (e.g. IKK/NF- κ B pathway and hERG ion channel).

structures; (iii) indole derivatives; and (iv) cyclohexylpiperazine analogs [29,84]. Within these categories, many S2R ligands have been suggested as valuable compounds for cancer therapy and diagnosis, as previously reviewed [29,85]. In addition, patent literature offers an interesting scenario, including several molecules with potential diagnostic and therapeutic applications in different cancer types. Mach and co-workers have been very active since 2008 in demonstrating the high tumor uptake of fluorescent and radiolabeled S2R ligands (i.e. **11**, **12**, and **13** – Figure 6). We have to outline the high potential of S2R-selective ligands as diagnostic tools rather than anticancer agents. These receptors are indeed highly expressed in cancer cell lines (e.g. pancreatic carcinoma and breast cancer) [28,86–88]. As detailed below, the most promising molecules are those displaying a pan-SR affinity.

Since the conjugation of S2R ligands with biotin did not result in improved anticancer molecules, a different approach was claimed in the patents from Hawkins et al. and Mach et al., who proposed the combination of an S2R ligand and a well-established anticancer drug (i.e. Erastin). The rationale of the latter strategy is based on the cooperative action between the two molecules, in which the binding to S2R is aimed to increase the antiproliferative effect of the anticancer agent. This approach has also been published in scientific literature [89], and it may be considered as a ‘Hybrid’ strategy between *de novo* synthesis and the ‘Patents of Use.’

A further way to exploit SRs in cancer therapy is represented by compounds with a mixed-S1R/S2R activity (pan-modulators) [60]. The idea of pan-SR ligands was introduced when Kashiwagi et al. evaluated the cytotoxic activity of haloperidol [86]. Afterward, a metabolite of this drug, with pan-SRs activity, showed antiproliferative behavior in prostate cancer cell lines [90]. This class of compounds may be considered as a starting point for developing dual-target anticancer agents. The manipulation of two molecular targets may improve the therapeutic efficacy, addressing the multiple factors that occur in this pathological condition [91].

The increasing interest for SRs in the oncology field concretizes in the presence of SR modulators in pharmaceutical companies’ pipelines, thus supporting the urgency for broader research on these molecules. Going into details, Anavex Corp. is carrying out preclinical studies on five compounds, claimed to be SR modulators, with possible anticancer and analgesic applications. Among these, ANAVEX 1037 displays high S1R and low S2R affinities, along with the interaction with sodium channels. Conjugate compounds represent other potential anticancer candidates, comprising an S2R agonist and Erastin. These molecules are present in the pipeline of the small company Accuronix, founded by the applicants of a previously analyzed patent [53]. This young company may serve as a good example of translating research results into commercially available products.

As for SR-targeting diagnostic tools, two clinical trials involve the compound [18F]ISO-1 (a highly selective S2R ligand) as radiotracer for positron emission tomography [92]. The Washington University School of Medicine completed a Phase I clinical trial for the assessment of cellular proliferation in different cancer types, using [18F]ISO-1 and PET/CT [93]. The study had the aim to determine which tissues and organs of

the body take up [18F]-ISO-1 naturally. The Abramson Cancer Center of Pennsylvania University has started a second clinical trial (Phase II) very recently [94]. The main objective is to determine the [18F]ISO-1 uptake in primary breast cancer patients.

Acknowledgments

The authors would like to thank Dr. Francesca Negri (University of Pavia) for the support in patent literature search and analysis.

Funding

No funding to declare.

Declaration of interest

The authors have no relevant affiliations or financial involvement with any organization or entity with a financial interest in or financial conflict with the subject matter or materials discussed in the manuscript. This includes employment, consultancies, honoraria, stock ownership or options, expert testimony, grants or patents received or pending, or royalties.

References

Papers of special note have been highlighted as either of interest (*) or of considerable interest (**) to readers.

1. Torre LA, Siegel RL, Ward EM, et al. Global cancer incidence and mortality rates and trends – an update. *Cancer Epidemiol Biomarkers Prev.* 2016;25:16–27.
2. Tripodo G, Mandracchia D, Collina S, et al. New perspectives in cancer therapy: the biotin-antitumor molecule conjugates. *Med Chem.* 2014;S1:1–8.
3. Chimento A, Sala M, Gomez-Monterrey IM, et al. Biological activity of 3-chloro-azetidin-2-one derivatives having interesting antiproliferative activity on human breast cancer cell lines. *Bioorg Med Chem Lett.* 2013;23:6401–6405.
4. Saturnino C, Buonerba M, Boatto G, et al. Synthesis and preliminary biological evaluation of a new pyridocarbazole derivative covalently linked to a thymidine nucleoside as a potential targeted antitumoral agent. *J Chem Pharm Bulletin.* 2003;51:971–974.
5. Timmers L, Boons CC, Kropff F, et al. Adherence and patients’ experiences with the use of oral anticancer agents. *Acta Oncol.* 2014;53:259–267.
6. Cavaletti G, Marmiroli P. Chemotherapy-induced peripheral neurotoxicity: *curr. Opin Neurol.* 2015;28:500–507.
7. Hanahan D, Weinberg RA. Hallmarks of cancer: the next generation. *Cell.* 2011;144:646–674.
8. Huang M, Shen A, Ding J, et al. Molecularly targeted cancer therapy: some lessons from the past decade. *Trends Pharmacol Sci.* 2014;35:41–50.
9. Martin WR, Eades CG, Thompson JA, et al. Effects of morphine-like and nalorphine-like drugs in nondependent and morphine-dependent chronic spinal dog. *J Pharmacol Exp Ther.* 1976;197:517–532.
- In this publication, the discovery of sigma receptors is reported.
10. Su TP. Evidence for sigma opioid receptor: binding of [3H]skf-10047 to etorphine-inaccessible sites in guinea-pig brain. *J Pharmacol Exp Ther.* 1982;223:284–290.
11. Maurice T, Lockhart BP. Neuroprotective and anti-amnesic potentials of sigma (sigma) receptor ligands. *Prog Neuropsychopharmacol Biol Psychiatry.* 1997;21:69–102.
12. Vaupel DB. Naltrexone fails to antagonize the sigma effects of PCP and SKF 10,047 in the dog. *Eur J Pharmacol.* 1983;92:269–274.

13. Quirion R, Chicheportiche R, Contreras PC, et al. Classification and nomenclature of phencyclidine and sigma receptor sites. *Trends Neurosci.* **1987**;10:444–446.
14. Skuza G. Potential antidepressant activity of sigma ligands. *Pol J Pharmacol.* **2003**;55:923–934.
15. Hanner M, Moebius FF, Flandorfer A, et al. Purification, molecular cloning, and expression of the mammalian sigma1-binding site. *Proc Natl Acad Sci.* **1996**;93:8072–8077.
16. Rui M, Rossi D, Marra A, et al. Synthesis and biological evaluation of new aryl-alkyl(alkenyl)-4-benzylpiperidines, novel sigma receptor (SR) modulators, as potential anticancer-agents. *Eur J Med Chem.* **2016**;124:649–665.
17. Collina S, Gaggeri R, Marra A, et al. Sigma receptor modulators: a patent review. *Expert Opin Ther Pat.* **2013**;23:597–613.
- **A previous review about SR modulators' therapeutic potential.**
18. Spruce BA, Campbell LA, McTavish N, et al. Small molecule antagonists of the σ -1 receptor cause selective release of the death program in tumor and self-reliant cells and inhibit tumor growth in vitro and in vivo. *Cancer Res.* **2004**;64:4875–4886.
19. Cassano G, Gasparre G, Niso M, et al. F281, synthetic agonist of the sigma-2 receptor, induces Ca^{2+} efflux from the endoplasmic reticulum and mitochondria in SK-N-SH cells. *Cell Calcium.* **2009**;45:340–345.
20. Aydar E, Palmer CP, Djamgoz MB. Sigma receptors and cancer: possible involvement of ion channels. *Cancer Res.* **2004**;64:5029–5035.
21. Aydar E, Onganer P, Perrett R, et al. The expression and functional characterization of sigma (σ) 1 receptors in breast cancer cell lines. *Cancer Lett.* **2006**;242:245–257.
22. Wang B, Rouzier R, Albarracin CT, et al. Expression of sigma 1 receptor in human breast cancer. *Breast Cancer Res Treat.* **2004**;87:205–214.
23. Su TP, Hayashi T, Maurice T, et al. The sigma-1 receptor chaperone as an inter-organelle signaling modulator. *Trends Pharmacol Sci.* **2010**;31:557–566.
- **An important experimental study showing that sigma receptors are chaperones.**
24. Marchi S, Giorgi C, Oparka M, et al. Oncogenic and oncosuppressive signal transduction at mitochondria-associated endoplasmic reticulum membranes. *Mol Cell Oncol.* **2014**;1:e956469.
25. Su TP, Su TC, Nakamura Y, et al. The sigma-1 receptor as a pluripotent modulator in living systems. *Trends Pharmacol Sci.* **2016**;37:262–278.
- **An extensive report about S1R functions and interactions.**
26. Wheeler KT, Wang LM, Wallen CA, et al. Sigma-2 receptors as a biomarker of proliferation in solid tumours. *Br J Cancer.* **2000**;82:1223–1232.
27. Zeng C, Rothfuss J, Zhang J, et al. Sigma-2 ligands induce tumour cell death by multiple signalling pathways. *Br J Cancer.* **2012**;106:693–701.
28. Zeng C, Vangveravong S, Xu J, et al. Subcellular localization of sigma-2 receptors in breast cancer cells using two-photon and confocal microscopy. *Cancer Res.* **2007**;67:6708–6716.
29. Huang YS, Lu HL, Zhang LJ, et al. Sigma-2 receptor ligands and their perspectives in cancer diagnosis and therapy: sigma-2 receptor ligands. *Med Res Rev.* **2014**;34:532–566.
30. Abate C, Niso M, Marottoli R, et al. Novel derivatives of 1-cyclohexyl-4-[3-(5-methoxy-1,2,3,4-tetrahydronaphthalen-1-yl)propyl] piperazine (PB28) with improved fluorescent and σ receptors binding properties. *J Med Chem.* **2014**;57:3314–3323.
31. Australian Nuclear Science & Technology Organisation. Piperidine-based sigma receptor ligands. WO9620928; **1996**
32. Gilligan PJ, Cain GA, Christos TE, et al. Novel piperidine sigma receptor ligands as potential anti-psychotic drugs. *J Med Chem.* **1992**;35:4344–4361.
33. Laboratorios del Dr. Esteve S.A. 1,2,4-triazole derivative as Sigma receptor inhibitors. WO2008055932; **2008**
34. Laboratorios del Dr. Esteve S.A. Pyrazole compounds as Sigma Receptor inhibitors. WO2011147910; **2011**
35. Abadias M, Escriche M, Vaqué A, et al. Safety, tolerability and pharmacokinetics of single and multiple doses of a novel sigma-1 receptor antagonist in three randomized phase I studies: new sigma-1 receptor antagonist: safety, tolerability and pharmacokinetics. *Br J Clin Pharmacol.* **2013**;75:103–117.
36. Vela JM, Merlos M, Almansa C. Investigational sigma-1 receptor antagonists for the treatment of pain. *Expert Opin Investig Drugs.* **2015**;24:883–896.
37. Wisconsin Alumni Research Foundation. Sigma1 receptor ligands and methods of use. US8349898; **2013**
38. Wisconsin Alumni Research Foundation. Sigma-1 receptor ligands and methods of use. US20100179111; **2010**
39. Wisconsin Alumni Research Foundation. Selective Sigma-1 receptor ligands. US20130102571; **2013**
40. Wisconsin Alumni Research Foundation. Selective sigma-1 receptor ligands. US8946302; **2015**
41. E Ruoho A, Chu U, Ramachandran S, et al. The ligand binding region of the sigma-1 receptor: studies utilizing photoaffinity probes, sphingosine and N-alkylamines. *Curr Pharm Des.* **2012**;18:920–929.
42. Collina S, Rossi D, Marra A, et al. Università degli Studi di Pavia. Use of arylalkanolamines as sigma-1 receptor antagonists. WO2015132733; **2015**.
- **This patent is the only one providing evidences about the agonist/antagonist profile of disclosed molecules.**
43. Mach RH, Tu Z, Chu W, et al. Washington University. Sigma 2 receptor ligands and therapeutic uses therefor. US2008161343; **2008**
44. Mach RH, Tu Z, Chu W, et al. Washington University. Sigma 2 receptor ligands and therapeutic uses therefor. US7612085; **2009**
45. Mach RH, Hotchkiss R, Hawkins W, et al. Washington University. Therapeutic uses of bicyclic ligands of Sigma-2 receptor. US20100048614; **2010**
46. Mach RH, Hotchkiss R, Hawkins W, et al. Washington University. Therapeutic uses of bicyclic ligands of sigma2 receptor. US8168650; **2012**
47. Luo S, Kansara VS, Zhu X, et al. Functional characterization of sodium-dependent multivitamin transporter in mdck-mdr1 cells and its utilization as a target for drug delivery. *Mol Pharm.* **2006**;3:329–339.
48. Shi JF, Wu P, Jiang ZH, et al. Synthesis and tumour cell growth inhibitory activity of biotinylated annonaceous acetogenins. *Eur J Med Chem.* **2014**;71:219–228.
49. Vadlapudi AD, Vadlapatla RK, Pal D, et al. Functional and molecular aspects of biotin uptake via SMVT in human corneal epithelial (HCEC) and retinal pigment epithelial (D407) cells. *Aaps J.* **2012**;14:832–842.
50. Chen S, Zhao X, Chen J, et al. Mechanism-based tumor-targeting drug delivery system. Validation of efficient vitamin receptor-mediated endocytosis and drug release. *Bioconjug Chem.* **2010**;21:979–987.
51. Washington University. Detection of cancer cells in vitro using S2R ligands as radiotracers. US7893266; **2011**
52. Adejare A Bicyclo-heptan-2-amines. US20120190710; **2012**
53. Washington University. Sigma-2 receptor ligand drug conjugates as antitumor compounds, methods of synthesis and uses thereof. WO2015153814; **2015**
54. Washington University. Modular platform for targeted therapeutic delivery. US20090176705; **2009**
55. Xie Y, Hou W, Song X, et al. Ferroptosis: process and function. *Cell Death Differ.* **2016**;23:369–379.
56. Cao JY, Dixon SJ. Mechanisms of ferroptosis. *Cell Mol Life Sci.* **2016**;73:2195–2209.
57. Yagoda N, Von Rechenberg M, Zaganjor E, et al. RAS-RAF-MEK-dependent oxidative cell death involving voltage-dependent anion channels. *Nature.* **2007**;447:865–869.
58. Gangadhar NM, Stockwell BR. Chemical genetic approaches to probing cell death. *Curr Opin Chem Biol.* **2007**;11:83–87.

59. Merk Patent GMBH Use of defined substances that bind to the sigma receptor for combating sarcoma and carcinoma. WO200230422; 2002
60. Vamvakides A. New sigma receptor ligands with antiapoptotic and or proapoptotic properties over cellular biochemical mechanisms, with neuroprotective, anticancer, antimetastatic and anti(chronic) inflammatory action. WO2008087458; 2008
61. Vamvakides A. Tetrahydro-n,n-dimethyl-2,2-diphenyl-3-feranemetiianamine, its enantiomers, and their pharmaceutically acceptable acid addition salts. WO9730983; 1997
62. Vamvakides A. Sigma receptors ligands with anti-apoptotic and/or pro-apoptotic properties, over cellular mechanisms, exhibiting prototypical cytoprotective and also anti-cancer activity. WO2010097641; 2010
63. University of Dundee. Materials and methods relating to the induction of apoptosis in target cells. WO200000599; 2000
64. Gilmore DL, Liu Y, Matsumoto RR. Review of the pharmacological and clinical profile of rimcazole. CNS Drugs Rev. 2004;10:1–22.
65. De Costa BR, Bowen WD, Hellewell SB, et al. Alterations in the stereochemistry of the kappa-selective opioid agonist U50, 488 result in high-affinity. sigma. ligands. J Med Chem. 1989;32:1996–2002.
66. University of Dundee. Sigma Receptor ligands and their medical uses. WO200174359; 2001.
- **Patent disclosing seminal approaches for the reuse of S1R modulators as anticancers.**
67. Whittemore ER, Ilyin VI, Woodward RM. Antagonism of N-methyl-D-aspartate receptors by sigma site ligands: potency, subtype-selectivity and mechanisms of inhibition. J Pharmacol Exp Ther. 1997;282:326–338.
68. Appel S, Rupf A, Weck MM, et al. Effects of imatinib on monocyte-derived dendritic cells are mediated by inhibition of nuclear factor-kB and Akt signaling pathways. Clin Cancer Res. 2005;11:1928–1940.
69. An J, Rettig MB. Epidermal growth factor receptor inhibition sensitizes renal cell carcinoma cells to the cytotoxic effects of bortezomib. Mol Cancer Ther. 2007;6:61–69.
70. University of Dundee. Sigma ligands and IKK/NF-kB inhibitors for medical treatment. WO2009074809; 2009
71. Patel L, Williams S, Wilding I, et al. Modern Biosciences PLC. Combination therapy comprising a taxane and a sigma receptor ligand such as rimcazole. WO2010128309; 2010
72. Centre National de la Recherche Scientifique – CNRS, Paris, France/Univerite Nice Sophia Antipolis, Nice, France. Inhibitors of the interaction of the sigma-1 receptor with hERG for use in the treatment of cancer. US2015182550A1; 2015
73. Renaudo A, L'Hoste S, Guizouarn H, et al. Cancer cell cycle modulated by a functional coupling between sigma-1 receptors and Cl-channels. J Biol Chem. 2007;282:2259–2267.
74. Renaudo A, Watry V, Chassot AA, et al. Inhibition of tumor cell proliferation by ligands is associated with K⁺ channel inhibition and p27kip1 accumulation. J Pharmacol Exp Ther. 2004;311:1105–1114.
75. Sanguinetti MC, Tristani-Firouzi M. hERG potassium channels and cardiac arrhythmia. Nature. 2006;440:463–469.
76. Cottès D, Guizouarn H, Martin P, et al. The sigma-1 receptor: a regulator of cancer cell electrical plasticity? front. Physiol. 2013;4:1–10.
77. Happy M, Dejoie J, Zajac CK, et al. Sigma 1 receptor antagonist potentiates the anti-cancer effect of p53 by regulating ER stress, ROS production, Bax levels, and caspase-3 activation. Biochem Biophys Res Commun. 2015;456:683–688.
78. Schmidt HR, Zheng S, Gurpinar E, et al. Crystal structure of the human sigma1 receptor. Nature. 2016;532:527–530.
79. Colabufo NA, Berardi F, Contino M, et al. Correlation between sigma2 receptor protein expression and histopathologic grade in human bladder cancer. Cancer Lett. 2006;237:83–88.
80. Cratteri P, Romanelli MN, Cruciani G, et al. GRIND-derived pharmacophore model for a series of alpha-tropanyl derivative ligands of the sigma-2 receptor. J Comput Aided Mol Des. 2004;18:361–374.
81. Abate C, Mosier PD, Berardi F et al. A Structure-Affinity and comparative molecular field analysis of sigma-2 (sig2) receptor ligands. Cent Nerv Syst Agents Med Chem Former Curr Med Chem-Cent Nerv Syst Agents. 2009;9:246–257.
82. Laurini E, Zampieri D, Mamolo MG, et al. A 3D-pharmacophore model for sigma2 receptors based on a series of substituted benzo[d]oxazol-2(3H)-one derivatives. Bioorg Med Chem Lett. 2010;20:2954–2957.
83. J Rhoades D, H Kinder D, M Mahfouz T. A comprehensive ligand based mapping of the sigma2 receptor binding pocket. Med Chem. 2014;10:98–121.
84. Zeng C, Rothfuss JM, Zhang J, et al. Functional assays to define agonists and antagonists of the sigma-2 receptor. Anal Biochem. 2014;448:68–74.
85. van Waarde A, Rybczynska AA, Ramakrishnan NK, et al. Potential applications for sigma receptor ligands in cancer diagnosis and therapy. Biochim Biophys Acta BBA Biomembr. 2015;1848:2703–2714.
86. Kashiwagi H, McDunn JE, Simon PO, et al. Selective sigma-2 ligands preferentially bind to pancreatic adenocarcinomas: applications in diagnostic imaging and therapy. Mol Cancer. 2007;6:48.
87. Kashiwagi H, McDunn JE, Simon PO, et al. Sigma-2 receptor ligands potentiate conventional chemotherapies and improve survival in models of pancreatic adenocarcinoma. J Transl Med. 2009;7:24.
88. Mach RH, Zeng C, Hawkins WG. The sigma2 receptor: a novel protein for the imaging and treatment of cancer. J Med Chem. 2013;56:7137–7160.
89. Ohman KA, Hashim YM, Vangveravong S, et al. Conjugation to the sigma-2 ligand SV119 overcomes uptake blockade and converts dm-Erastin into a potent pancreatic cancer therapeutic. Oncotarget. 2016;7:33529–33541.
90. Marrazzo A, Fiorito J, Zappalà L, et al. Antiproliferative activity of phenylbutyrate ester of haloperidol metabolite II [(±)-MRJF4] in prostate cancer cells. Eur J Med Chem. 2011;46:433–438.
91. Meunier B. Hybrid molecules with a dual mode of action: dream or reality? Acc. Chem Res. 2008;41:69–77.
92. Shoghi KI, Xu J, Su Y, et al. Quantitative receptor-based imaging of tumor proliferation with the sigma-2 ligand [18F]ISO-1. Plos ONE. 2013;8:e74188.
93. Dehdashti F, Laforest R, Gao F, et al. Assessment of cellular proliferation in tumors by PET using 18F-ISO-1. J Nucl Med. 2013;54:350–357.
94. Abramson Cancer Center of University of Pennsylvania. Imaging of in vivo sigma-2 receptor expression with [18F]ISO-1 positron emission tomography (PET/CT) in primary breast cancer. 2016. Available from: <https://clinicaltrials.gov/show/NCT02762110>

New Perspectives in Lithium Carbenoids Mediated Homologations

Vittorio Pace*^a
 Laura Castoldi^a
 Serena Monticelli^a
 Marta Rui^b
 Simona Collina^b

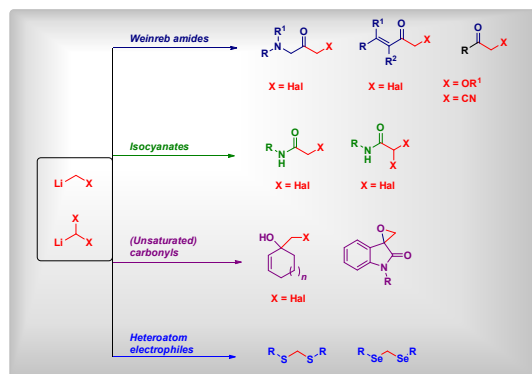
^a University of Vienna - Department of Pharmaceutical Chemistry, Althanstrasse, 14, 1090, Vienna (Austria).

^b Department of Drug Sciences - University of Pavia, Viale Taramelli 6, 27100, Pavia (Italy)

* indicates the main/corresponding author.

e-mail_vittorio.pace@univie.ac.at

Dedicated to Professor Friedrich Hammerschmidt in the occasion of his retirement



Received:

Accepted:

Published online:

DOI:

Abstract α -Functionalized organolithium reagents (*e.g.* LiCH_2X) are versatile reagents for accomplishing homologations of carbon- and heteroatom-type electrophiles. The proper selection of the reaction conditions allows one to direct their intrinsic ambiphilicity towards the nucleophilic character. Herein, the homologation of various electrophiles ranging from Weinreb amides to isocyanates, carbonyl derivatives and chalcogenides – with a particular focus on the chemoselectivity of the processes – is contextualized.

1. Introduction
2. Homologation of Weinreb Amides
3. Homologation of Cyclic Ketones
4. Homologation of Isocyanates
5. Homologation of Disulfides and Diselenides
6. Conclusions

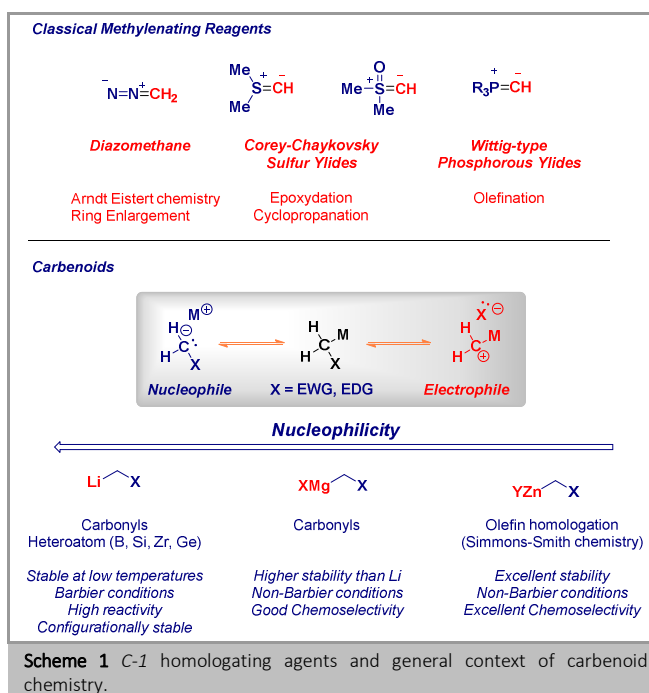
Key words Carbenoids; Lithium; Homologation; Chemoselectivity; Organometallic.

Introduction

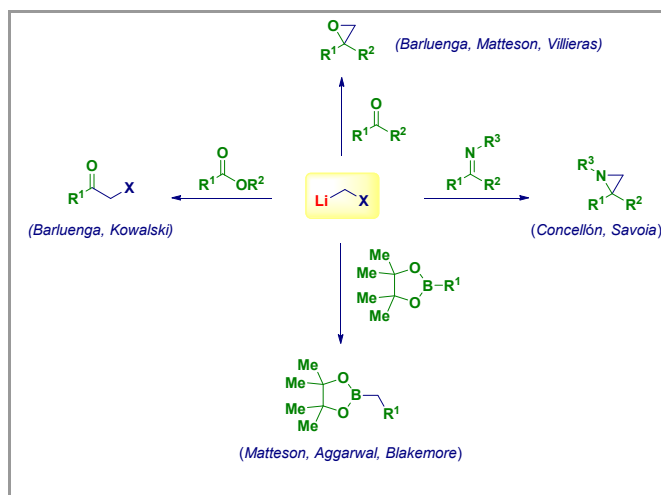
The formal addition of a substituted methylene unit (*e.g.* $-\text{CH}_2\text{X}$, X = Halogen, CN, OR) to an electrophile is a fundamental synthetic operation enabling the delivery of a given fragment with the *exact* degree of functionalization.¹ As such, the formation of a new carbon-carbon or carbon-heteroatom bond is accomplished under high chemocontrol and thus, issues arising from the late-functionalization of an unsubstituted precursor could be advantageously overcome.²

In this context, classical reagents versatile for this co-called homologation reactions³ are halocarbenoids introduced in organic synthesis during the 1960s by Köbrich.⁴ Although at first sight they may be considered analogues of similar reagents such as diazomethane⁵ or Corey-Chaykovsky ylides,⁶ their capability to switch the reactivity from nucleophilic to electrophilic renders them unique species within the panorama of organometallic reagents (Scheme 1). Indeed, two main parameters are governing the equilibrium between the nucleophilic and the electrophilic reactivity: 1) the nature of the metal and, 2) the temperature. Nowadays, it is quite well

recognized that the employment of lithium species (*e.g.* LiCH_2X) guarantees the predominance of the nucleophilic behavior,^{4d-g,4i,7} while switching to carbenoids of less electropositive metals (*e.g.* Zn)⁸ allows the electrophilic reactivity to come in to play, as for example exemplified by the powerful Simmons-Smith chemistry for the olefin homologation.⁹ As a consequence of the tamed nucleophilicity of magnesium organometallics (compared to lithium counterparts), the corresponding carbenoids can be conveniently used for designing high chemoselective protocols.¹⁰ Clososki and coworkers were able to selectively add $\text{ClMgCH}_2\text{Cl}\cdot\text{LiCl}$ to an aldehyde even in the presence of concomitant electrophilic functionalities such as ketones, esters, nitriles or amides.¹¹

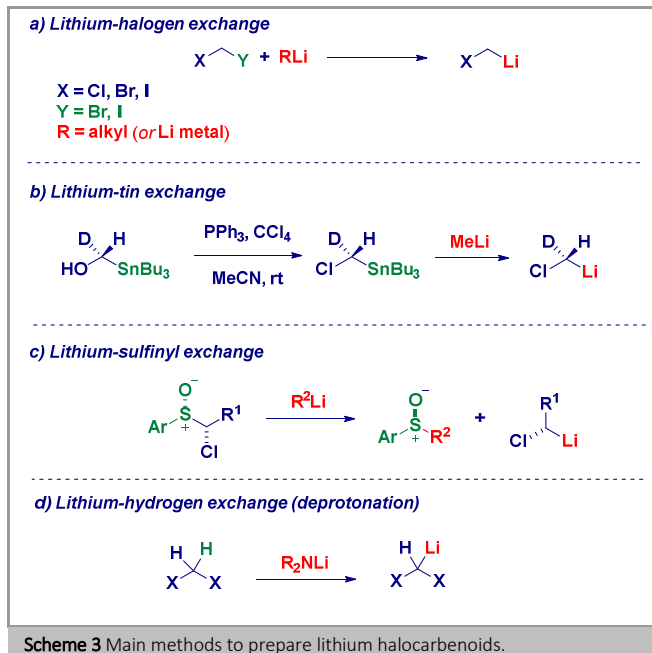


The introduction of a reactive halomethylene unit provides *de facto* the possibility to exploit the inherent reactivity of this motif. Since seminal contributions in the 1960s and 1970s by Köbrich,^{4a,12} – followed by in depth studies by Matteson,¹³ Barluenga,¹⁴ Villieras,¹⁵ Concellón¹⁶ and Savoia¹⁷ – the addition of LiCH₂Hal to carbonyl type compounds such as aldehydes, ketones, esters or activated imines – followed by the easy ring-closure, has been regarded as an effective alternative to the Corey-Chaykovsky chemistry (Scheme 2).⁶ Analogously, the elegant homologation of boron electrophiles introduced by Matteson in the 1980s¹⁸ put the bases for exploiting this chemistry in outstanding transformations recently developed by Aggarwal¹⁹ and Blakemore.²⁰



Scheme 2 Classical applications of lithium carbenoid chemistry in homologation processes.

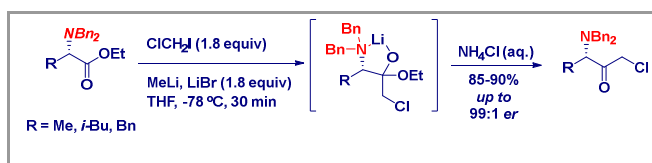
Despite the high potential of lithium halocarbenoids, the limited thermal instability has somewhat represented the Achilles's heel because of the almost strict requirement of employing Barbier-type conditions.^{4f} Accordingly, the three following methods can be employed for the generation of monohalocarbenoids (Scheme 3): *a*) halogen-metal exchange with organolithium reagents (with both RLi or Li metal);^{4f} *b*) tin-lithium exchange;²¹ *c*) sulfinyl-lithium exchange.^{20a} The latter two methods allow to access configurationally stable carbenoids and, notably the Sn-Li exchange could be used for the generation of the high chemically (*but not* configurationally) unstable fluoromethylithium.²² A breakthrough in the area has been recently introduced by Luisi and coworkers who documented the formation of LiCH₂Cl under *non*-Barbier conditions (*i.e.* a wide range of electrophiles could be added *after* the generation of the carbenoid) by using in flow chemistry technology.²³ This approach is highly promising since the Kirmse α -elimination²⁴ to a free carbene and LiCl can be conveniently inhibited through this method thus, providing an additional tool to classically employed coordinative strategies (*i.e.* addition of lithium salts or use of Lewis base solvents).^{15,25} Finally, *d*) the relative high acidity of dihalomethanes enables the selective deprotonation with lithium amide bases thus, constituting an efficient way to dihalocarbenoids.^{4f}



Scheme 3 Main methods to prepare lithium halocarbenoids.

Homologation of Weinreb Amides

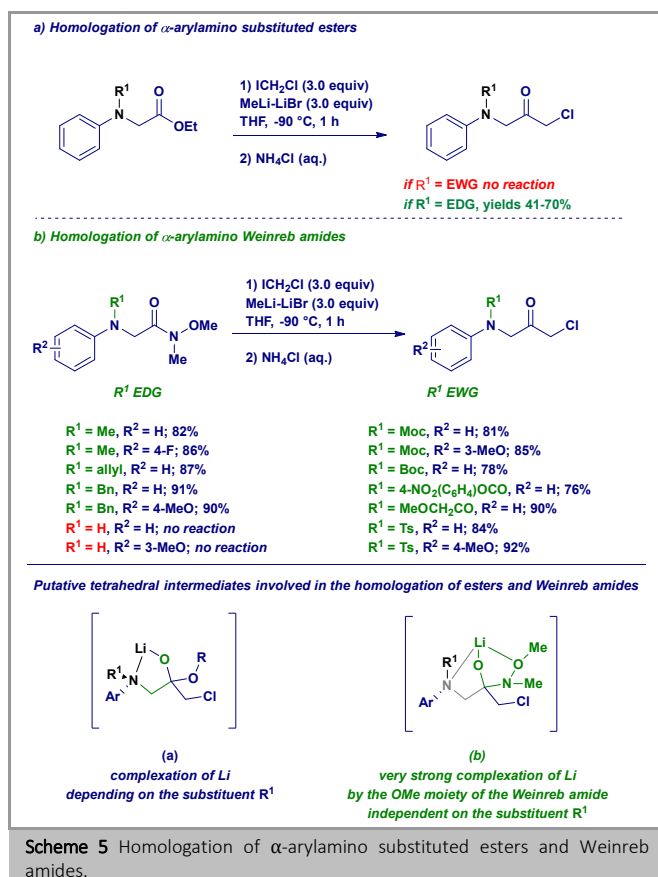
In 2013 our group launched a research program focused on the halomethylation of suitable acylating agents such as esters introduced by Barluenga during the 1990s.^{14b,14c} This chemistry proved to be successful – also because of the almost full retention of the stereochemical information during the process – as also demonstrated by various applications in the synthesis of highly valuable building blocks required for obtaining HIV protease inhibitors.²⁶ Applications of the Barluenga's ester homologation strategy to industrial processes pointed out the dramatic effect displayed by the substituent at the α -nitrogen (Scheme 4).²⁷ The presence of a free N-H functionality were not tolerated as a consequence of the competing deprotonation of the carbenoid could trigger.



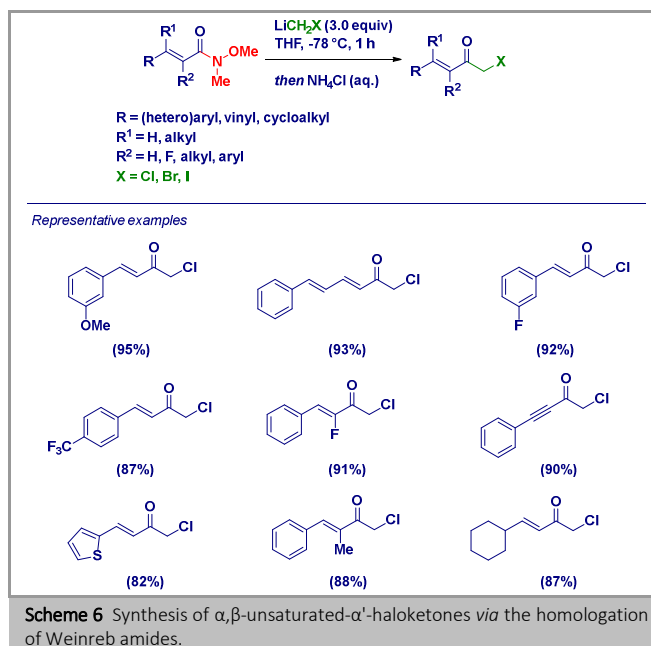
Scheme 4 Barluenga's homologation of α -amino esters.

Because of our needing of 3-arylamino-1-chloroacetones presenting an *electron-withdrawing group* (EWG) at nitrogen, we were surprised by the lack of reactivity of esters presenting an analogous substituent (Scheme 5 – *path a*).²⁸ These particular – fully functionalized at nitrogen – acyl placeholders could not evidently be considered belonging to the *secondary*-amine type category above discussed and, the experimentally observed chemical inertness should be caused by different factor(s). Additionally, the good reactivity displayed by α -arylamino esters presenting an alkyl type (*i.e.* with electron-donating properties) moiety, suggested us to consider the stability of the putative tetrahedral intermediate²⁹ – formed upon the addition of the carbenoid to the ester – as the key parameter governing

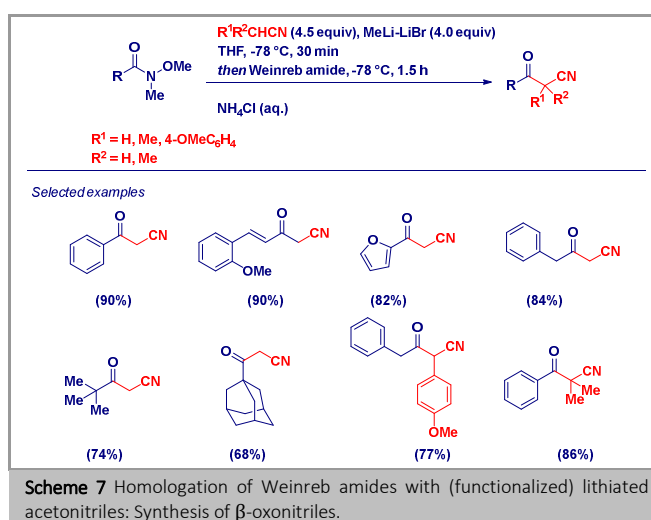
the process. The simple switching to Weinreb amides³⁰ - well known as exceptional substrates for the acylation of organometallic reagents - allowed us to realize the desired chloromethylation in high yield (Scheme 5 - *path b*). In agreement with the hypothesis of the tetrahedral intermediates' stability, the complexing effect of the constitutively present -OMe group (in Weinreb amides) overcomes *de facto* the electronic density-depending coordinative capability of the nitrogen.²⁸



The excellent performance of Weinreb amides in reactions with halocarbene reagents is even more evident in the case of more complex targets as α,β -unsaturated- α' -haloketones (Scheme 6).³¹ Indeed, the employment of esters posed serious chemoselective issues because of the preferential double addition of the carbenoid to give carbinols instead of the required α -haloketones. In this case, the halomethylation of Weinreb amides proceeds with full chemocontrol. The outstanding chemoselectivity of the method is further highlighted by the lack of carbenoid-mediated cyclopropanation-type phenomena.³² The protocol is quite general and is not dependent on the particular halomethyl fragment employed ($-\text{CH}_2\text{X}$, X = Cl, Br or I).

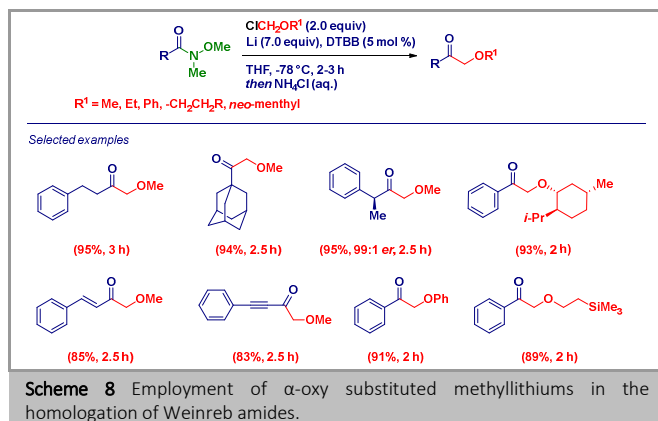


Weinreb amides could serve as acylating agents also for lithiated acetonitriles species ($\text{LiR}^1\text{R}^2\text{CN}$), which - remarkably - due to higher intrinsic stability (compared to halocarbenoids), did not require the employment of Barbier-type conditions (Scheme 7).³³ Again, the protocol manifests a large scope allowing the direct, high yielding synthesis not only of α -cyanomethylketones (*i.e.* β -oxonitriles) but also of α,α -disubstituted analogues. This is quite interesting since functionalization procedures dealing with the alkylation or arylation of unsubstituted α -cyanomethylketones are often complicated by electronic and sterical effects.³⁴



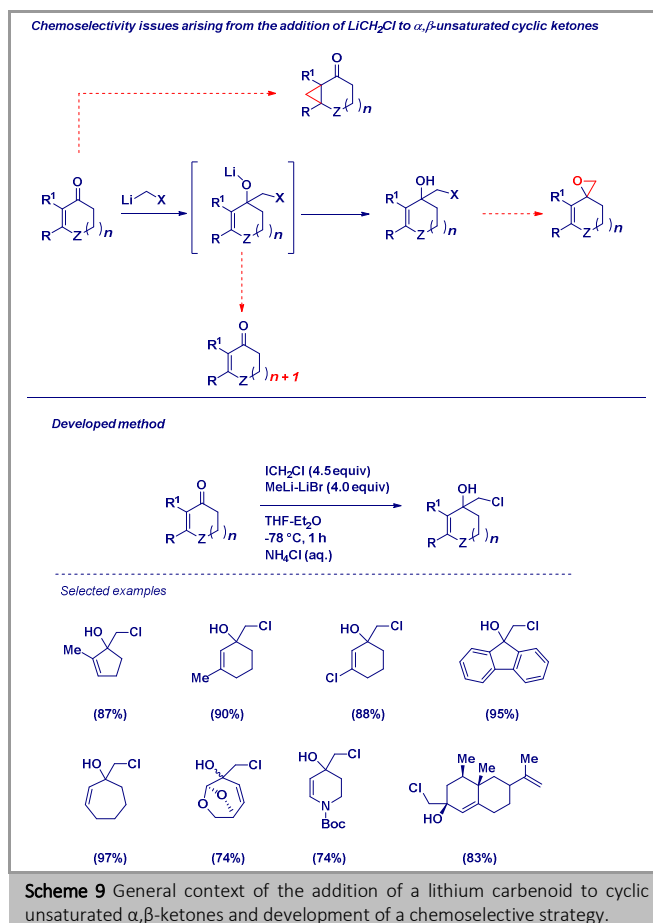
Our investigations in the area continued with the development of a strategy enabling the homologation with α -oxy substituted methyl lithium carbanions - prepared according to the Yus' arene-catalyzed reductive lithiation of chloromethyl ethers³⁵ - in order to prepare α -oxygenated ketones (Scheme 8).³⁶ Key features of the method are: 1) very wide substrate scope in terms of both Weinreb amides and halo functionalized ether

(primary, secondary (cyclo)alkyl-, aryl-; 2) uniformly high yields regardless the electronic and steric factors eventually present on the starting materials; 3) full preservation of the optical purity of the starting materials during the process (through both the employment of enantioenriched Weinreb amides and optically active organolithium species) thus, accounting for a rapid, highly efficient access to enantiopure substituted α -oxygenated ketones.

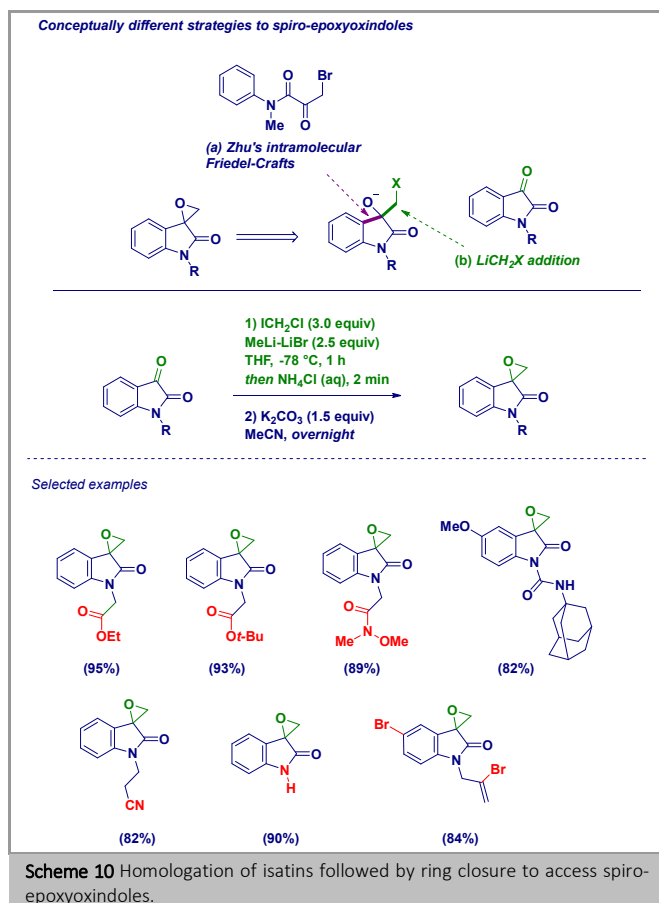


Homologation of Cyclic Ketones

Considering the feasibility of lithium α -halocarbenoids mediated epoxidations of carbonyl-type functionalities,^{13,15,37} we wondered if these reagents could be added to more challenging substrates such as α,β -unsaturated cyclic ketones. In principle, the addition of $-\text{CH}_2\text{X}$ units to the $\text{C}=\text{O}$ group of ketones could yield the following products: a) halohydrin upon acidic quenching; b) epoxide through temperature-triggered ring closure; c) homologation of the cyclic system to the $(n+1)$ cycle. Moreover the conjugated $\text{C}=\text{C}$ bond could be considered a placeholder for Simmons-Smith-type chemistry (Scheme 9). Chloromethylithium has been found to add in a 1,2-fashion with almost full selectivity, thus enabling the easy formation of quaternary allylic chlorohydrins.³⁸ Key features disclosed are: 1) LiBr not only acts as a carbenoid stabilizer but, also as a mild Lewis acid activator of the $\text{C}=\text{O}$ bond;³⁹ 2) the protocol is tolerant to various ring-sized enones (5, 6, 7 membered and, also complex natural product structures) bearing eventually different substitution patterns.



Cognizant of the good performance of the ring-closure strategy of β -halohydrins to access important targets such as spiroepoxyoxindoles recently shown by Zhu *et al.*,⁴⁰ we designed a different retrosynthetic approach (to access **xx**) based on the homologation of widely available functionalized isatins (Scheme 10).⁴¹ Conceptually, our protocol, which differs from the Zhu's intramolecular Fridel-Crafts tactic, is paved on the straightforward addition of the LiCH_2Cl carbenoid to the extremely highly electrophilic isatin carbonyl.⁴² The full chemoselectivity of the process is quite remarkable: the addition of the carbenoid takes place exclusively to the isatin carbonyl even in the presence of additional electrophilic functionalities [e.g. (Weinreb) amides, esters, nitriles] decorating the isatins' core. Significantly, exchangeable C-sp^2 bromine atoms did not influence the proper generation of the carbenoid from ICH_2Cl during the lithiation step.

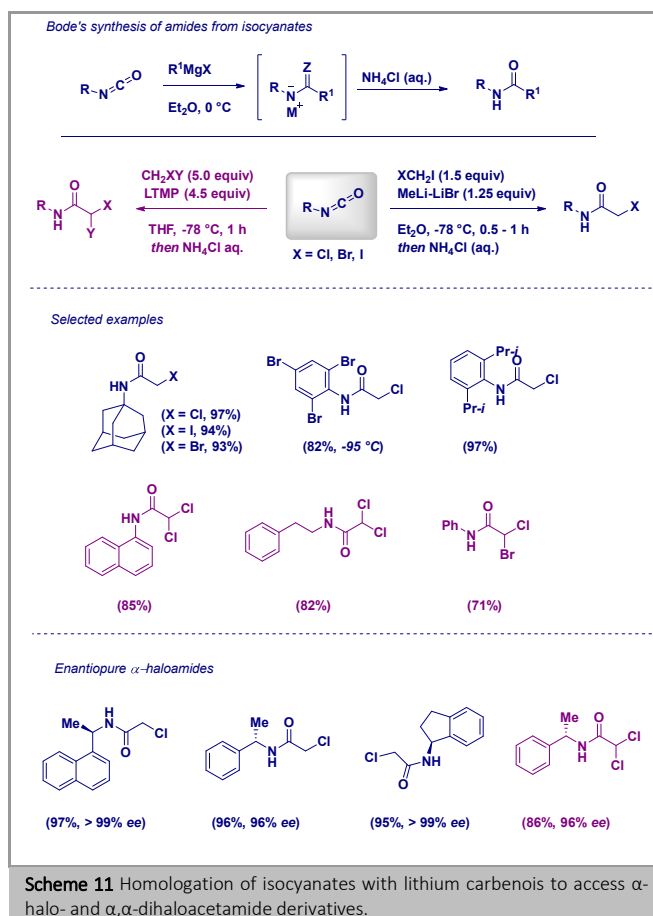


Homologation of Isocyanates

The intrinsic potentiality of delivering a CH_2X fragment through an unique, chemoselective synthetic operation - which would have overcome the chemo- and regio- issues arising from the introduction of halogens *via* classical mechanistically based approaches (*e.g.* electrophilic or radical halogenations) - motivated us to investigate the reaction of carbenoids with isocyanates.² This class of highly electrophilic heterocumulene compounds⁴³ have been recognized as excellent partners in reactions with carbanions since the 1920s when Gilman⁴⁴ proposed the use of these species for the titration of RM reagents. Astoundingly, applications of such a straightforward tactic for constructing (thio)amide linkage at preparative level were occasional⁴⁵ before Bode fully demonstrated its usefulness in the synthesis of sterically hindered amides non easily accessible through classic condensation procedures.⁴⁶

We documented the applicability of the technique to the chemoselective, high-yielding synthesis of α -halomethyl amides (Scheme 11).⁴⁷ The reaction showcases an excellent substrate scope allowing the chemoselective addition of LiCH_2X to a wide range of isocyanates with different substitution pattern at nitrogen. No differences have been observed switching from aliphatic to aromatic materials. The protocol is amenable for the synthesis of highly sterically hindered and functionalized α -haloamides. Further points of interest are: a) The tactic provides haloamides in almost quantitative yields, without needing to perform chromatography purifications; b) the different monohalocarbenoids react equally; c) the stereochemical information contained in the starting isocyanate is fully

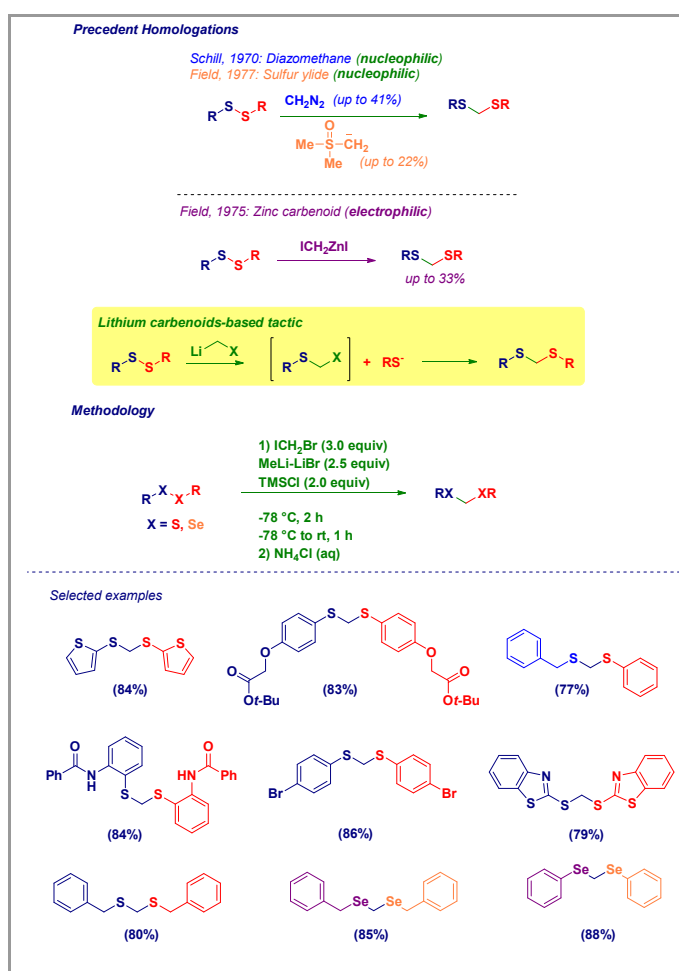
transferred to the α -haloamide. The methodology could also be extended to the synthesis of α,α -dihaloamides, which is a demanding task because of the chemoselective difficulties associated with the use of halogenation procedures.⁴⁸ The generation of dihalolithium carbenoids (LiCH_2XY) through the deprotonation of a dihalomethane with a lithium amide base under Barbier conditions in the presence of the isocyanate gives the expected compounds in high yields and optical purity. We found LTMP as the optimal base able to selectively generate the dihalocarbenoids. Again, the addition of dihalolithium carbenoids does not alter the enantiopurity of the starting isocyanates.⁴⁸



The scope of the nucleophilic addition to isocyanates worked out also with hydride species.⁴⁹ This long standing issue - affected by the overreduction of formamides to amines - could be easily solved by selecting the highly chemoselective Schwartz reagent as the hydride donor. We were delighted in observing full chemoselectivity during the LiCH_2I -mediated Matteson homologation of the boronic ester featuring a formamido substituent. Isothiocyanates reacted extremely well with α -oxygenated (Hoppe carbamate)⁵⁰ or α -nitrogenated (*N*-Boc-pyrrolidine)⁵¹ chiral organolithium reagents (generated in the presence of asymmetric ligands, *i.e.* (-)- or (+)-sparteine.⁵² On the other hand, the synthesis of analogous α -halothioamides resulted non feasible probably because of the alkylating effect displayed by the isothiocyanates' sulfur on the carbenoid precursor (ICH_2Cl).

Homologation of Disulfides and Diselenides

With the aim of designing new homologation protocols for heteroatom-type electrophiles,⁵³ we focused our attention on disulfides which, as evidenced in prior studies by Field⁵⁴ and Schill,⁵⁵ resulted reluctant towards methylenating agents such as zinc carbenoids, diazomethane or sulfur ylides. The homologation to the corresponding dithioacetal could be nicely performed by employing LiCH_2Br (Scheme 12).⁵⁶ Mechanistically, the attack of the latter to the disulfide to form the (isolable) intermediate α -halomethyl sulfide, releases a mercapto anion able to displace the halogen upon increasing of temperature. The methodology features a wide substrate scope and, functionalized disulfides reacted efficiently regardless the substitution pattern. It is worth highlighting the success in the case of an asymmetric disulfide and in the homologation of diselenides to the corresponding diselenoacetals. The synthetic applicability of bromo-containing dithioacetals is well demonstrated by the palladium-catalyzed Feringa-Fañánas-Martín cross coupling with an heteroaromatic organolithium, thus consisting in a valid alternative to commonly employed Suzuki-type chemistry for accessing poliaromatic structures.⁵⁷



Scheme 12 LiCH_2Br -based homologation of disulfides and diselenides.

Conclusions

Since the seminal studies by Köbrich, lithium halomethylcarbenoids emerged as synthetically versatile

reagents for accomplishing homologation reactions on a plethora of electrophiles not limited to carbon species. They allow the formal incorporation of a (reactive) halomethylene fragment into an electrophile thus, overcoming additional steps needed for the transformations of similar intermediates (e.g. diazoketones, sulfur ylides) into the desired adducts. We showed the effectiveness in performing highly chemocontrolled homologations in the presence of additional electrophilic substrates.

Nowadays, the recently developed Luisi's protocol for generating LiCH_2X reagents with microfluidic techniques - at temperatures up to -20°C without the requirement of Barbier-type conditions - would certainly allow to further exploit the synthetic potential of these reagents in broader contexts.

Without any doubt, the important contributions by Hammerschmidt and coworkers on the configurational stability of halo-[D₁]-methyl lithium will open the field to the establishment of chiral carbenoid-mediated homologation techniques to access enantiomerically pure functionalized halomethyl-derivatives.

In this regard, the generation of chiral, fully substituted carbenoids (i.e. LiCRR^1X) ensued by application to homologation processes is certainly a major challenge which will deserve in-depth studies to provide robust and versatile tools for organic transformations.

Acknowledgment

The University of Vienna is deeply acknowledged for supporting this research through two doctoral grants to L. C. and S. M. We also thank the University of Pavia for a mobility doctoral fellowship to M. R.

V. P. is indebted to all the students who joined his laboratory during these years and allowed the success of this research. V. P. also thanks the Austrian Chemical Society for being selected to represent Austria at the 8th Young Investigator Workshop hold in Islantilla, Huerva, Spain.

References

- (1) a) Knochel, P.; Molander, G. A.; Eds., In *Comprehensive Organic Synthesis (Second Edition)*, Elsevier, **2014**; b) Pace, V. New Perspectives in Homologation Processes for Synthetic Medicinal Chemistry: Lithium Halocarbonoids at the Helm. Habilitation Thesis, University of Vienna, Vienna, 2016.
- (2) Pace, V.; Monticelli, S.; de la Vega-Hernandez, K.; Castoldi, L. *Org. Biomol. Chem.* **2016**, *14*, 7848.
- (3) Li, J. J. *Name Reactions for Homologation*; Wiley: Hoboken, **2009**.
- (4) For reviews, see: a) Köbrich, G.; Akhtar, A.; Ansari, F.; Breckhoff, W. E.; Büttner, H.; Drischel, W.; Fischer, R. H.; Flory, K.; Fröhlich, H.; Goyert, W.; Heinemann, H.; Hornke, I.; Merkle, H. R.; Trapp, H.; Zündorf, W. *Angew. Chem. Int. Ed.* **1967**, *6*, 41; b) Boche, G.; Lohrenz, J. C. W. *Chem. Rev.* **2001**, *101*, 697; c) Braun, M., In *The Chemistry of Organolithium Compounds*, Rappoport, Z.; Marek, I., ed.; John Wiley and Sons: Chichester, **2004**; d) Capriati, V., In *Contemporary Carbene Chemistry*, ed.; John Wiley & Sons, Inc: **2013**; e) Capriati, V.; Florio, S. *Chem. Eur. J.* **2010**, *16*, 4152; f) Pace, V.; Holzer, W.; De Kimpe, N. *Chem. Rec.* **2016**, *16*, 2061; g) Pace, V. *Aust. J. Chem.* **2014**, *67*, 311; h) Luisi, R.; Capriati, V., *Lithium Compounds in Organic*

- Synthesis: From Fundamentals to Applications*. ed.; Wiley-VCH: Weinheim, 2014; 'Vol.' p; i) Clayden, J. *Organolithiums: Selectivity for Synthesis*; Pergamon: Oxford, **2002**; j) Gessner, V. H. *Chem. Commun.* **2016**,
- (5) a) Arndt, F.; Eistert, B.; Ender, W. *Chem. Ber.* **1929**, 62, 44; b) Candeias, N. R.; Paterna, R.; Gois, P. M. P. *Chem. Rev.* **2016**, 116, 2937; c) Ford, A.; Miel, H.; Ring, A.; Slattery, C. N.; Maguire, A. R.; McKervey, M. A. *Chem. Rev.* **2015**, 115, 9981; d) Maas, G. *Angew. Chem. Int. Ed.* **2009**, 48, 8186; e) Pace, V.; Verniest, G.; Sinisterra, J. V.; Alcántara, A. R.; De Kimpe, N. *J. Org. Chem.* **2010**, 75, 5760.
- (6) a) Corey, E. J.; Chaykovsky, M. *J. Am. Chem. Soc.* **1962**, 84, 867; b) Gololobov, Y. G.; Nesmeyanov, A. N.; Iysenko, V. P.; Boldeskul, I. E. *Tetrahedron* **1987**, 43, 2609.
- (7) For excellent novel applications of lithium carbenoids as electrophiles, see: a) Molitor, S.; Gessner, V. H. *Synlett* **2015**, 26, 861; b) Molitor, S.; Feichtner, K.-S.; Kupper, C.; Gessner, V. H. *Chem. Eur. J.* **2014**, 20, 10752; c) Molitor, S.; Becker, J.; Gessner, V. H. *J. Am. Chem. Soc.* **2014**, 136, 15517; d) Kupper, C.; Molitor, S.; Gessner, V. H. *Organometallics* **2014**, 33, 347; e) Molitor, S.; Gessner, V. H. *Chem. Eur. J.* **2013**, 19, 11858; f) Gessner, V. H.; Däschlein, C.; Strohmam, C. *Chem. Eur. J.* **2009**, 15, 3320.
- (8) Pasco, M.; Gilboa, N.; Mejuch, T.; Marek, I. *Organometallics* **2013**, 32, 942.
- (9) a) Simmons, H. E.; Smith, R. D. *J. Am. Chem. Soc.* **1958**, 80, 5323; b) Charette, A. B.; Beauchemin, A., In *Organic Reactions*, ed.; John Wiley & Sons, Inc.: **2004**.
- (10) For reviews, see: a) Satoh, T. *Heterocycles* **2012**, 85, 1; b) Satoh, T. *Chem. Soc. Rev.* **2007**, 36, 1561; c) Avolio, S.; Malan, C.; Marek, I.; Knochel, P. *Synlett* **1999**, 1820; For leading references, see: d) Hoffmann, R. W.; Nell, P. G.; Leo, R.; Harms, K. *Chem. Eur. J.* **2000**, 6, 3359; e) Hoffmann, R. W.; Nell, P. G. *Angew. Chem. Int. Ed.* **1999**, 38, 338.
- (11) a) Nishimura, R. H. V.; Murie, V. E.; Soldi, R. A.; Lopes, J. L. C.; Clososki, G. C. *J. Braz. Chem. Soc.* **2015**, 26, 2175; b) Nishimura, R. H. V.; Murie, V. E.; Soldi, R. A.; Clososki, G. C. *Synthesis* **2015**, 47, 1455; c) Nishimura, R. H. V.; Toledo, F. T.; Lopes, J. L. C.; Clososki, G. C. *Tetrahedron Lett.* **2013**, 54, 287.
- (12) Köbrich, G. *Angew. Chem. Int. Ed.* **1972**, 11, 473.
- (13) Sadhu, K. M.; Matteson, D. S. *Tetrahedron Lett.* **1986**, 27, 795.
- (14) a) Barluenga, J.; Llavona, L.; Concellón, J. M.; Yus, M. *J. Chem. Soc., Perkin Trans. 1* **1990**, 417; b) Barluenga, J.; Baragaña, B.; Alonso, A.; Concellón, J. M. *J. Chem. Soc., Chem. Commun.* **1994**, 969; c) Barluenga, J.; Baragaña, B.; Concellón, J. M. *J. Org. Chem.* **1995**, 60, 6696.
- (15) Tarhouni, R.; Kirschleger, B.; Rambaud, M.; Villieras, J. *Tetrahedron Lett.* **1984**, 25, 835.
- (16) a) Concellón, J. M.; Cuervo, H.; Fernández-Fano, R. *Tetrahedron* **2001**, 57, 8983; b) Concellón, J. M.; Rodríguez-Solla, H.; Simal, C. *Org. Lett.* **2008**, 10, 4457; c) Concellón, J. M.; Rodríguez-Solla, H.; Bernad, P. L.; Simal, C. *J. Org. Chem.* **2009**, 74, 2452.
- (17) Savoia, D.; Alvaro, G.; Di Fabio, R.; Gualandi, A.; Fiorelli, C. *J. Org. Chem.* **2006**, 71, 9373.
- (18) a) Matteson, D. S. *J. Org. Chem.* **2013**, 78, 10009; b) Matteson, D. S.; Majumdar, D. *Organometallics* **1983**, 2, 1529; c) Matteson, D. S.; Majumdar, D. *J. Am. Chem. Soc.* **1980**, 102, 7588.
- (19) a) Sonawane, R. P.; Jheengut, V.; Rabalakos, C.; Larouche-Gauthier, R.; Scott, H. K.; Aggarwal, V. K. *Angew. Chem. Int. Ed.* **2011**, 50, 3760; b) Pulis, A. P.; Blair, D. J.; Torres, E.; Aggarwal, V. K. *J. Am. Chem. Soc.* **2013**, 135, 16054; c) Burns, M.; Essafi, S.; Bame, J. R.; Bull, S. P.; Webster, M. P.; Balieu, S.; Dale, J. W.; Butts, C. P.; Harvey, J. N.; Aggarwal, V. K. *Nature* **2014**, 513, 183; d) Rasappan, R.; Aggarwal, V. K. *Nat Chem* **2014**, 6, 810; e) Unsworth, P. J.; Leonori, D.; Aggarwal, V. K. *Angew. Chem. Int. Ed.* **2014**, 53, 9846; f) Watson, C. G.; Balanta, A.; Elford, T. G.; Essafi, S.; Harvey, J. N.; Aggarwal, V. K. *J. Am. Chem. Soc.* **2014**, 136, 17370; g) Balieu, S.; Hallett, G. E.; Burns, M.; Bootwicha, T.; Studley, J.; Aggarwal, V. K. *J. Am. Chem. Soc.* **2015**, 137, 4398.
- (20) a) Emerson, C. R.; Zakharov, L. N.; Blakemore, P. R. *Chem. Eur. J.* **2013**, 19, 16342; b) Blakemore, P. R.; Burge, M. S. *J. Am. Chem. Soc.* **2007**, 129, 3068; c) Blakemore, P. R.; Marsden, S. P.; Vater, H. D. *Org. Lett.* **2006**, 8, 773; d) Wu, Z.; Sun, X.; Potter, K.; Cao, Y.; Zakharov, L. N.; Blakemore, P. R. *Angew. Chem. Int. Ed.* **2016**, 55, 12285.
- (21) Kapeller, D. C.; Hammerschmidt, F. *J. Am. Chem. Soc.* **2008**, 130, 2329.
- (22) Kail, D. C.; Malova Krizkova, P.; Wieczorek, A.; Hammerschmidt, F. *Chem. Eur. J.* **2014**, 20, 4086.
- (23) Degennaro, L.; Fanelli, F.; Giovine, A.; Luisi, R. *Adv. Synth. Catal.* **2015**, 357, 21.
- (24) Kirmse, W. *Angew. Chem. Int. Ed.* **1965**, 4, 1.
- (25) Loupy, A.; Tchoubar, B. *Salt Effects in Organic and Organometallic Chemistry*; VCH: Weinheim, **1992**.
- (26) a) Reeder, M. R.; Anderson, R. M. *Chem. Rev.* **2006**, 106, 2828; b) Honda, Y.; Katayama, S.; Kojima, M.; Suzuki, T.; Kishibata, N.; Izawa, K. *Org. Biomol. Chem.* **2004**, 2, 2061; c) Izawa, K.; Onishi, T. *Chem. Rev.* **2006**, 106, 2811; d) Pace, V.; Castoldi, L.; Pregno, M. *Mini-Rev. Med. Chem.* **2013**, 13, 988.
- (27) a) Onishi, T.; Hirose, N.; Nakano, T.; Nakazawa, M.; Izawa, K. *Tetrahedron Lett.* **2001**, 42, 5883; b) Onishi, T.; Nakano, T.; Hirose, N.; Nakazawa, M.; Izawa, K. *Tetrahedron Lett.* **2001**, 42, 5887; c) Onishi, T.; Otake, Y.; Hirose, N.; Nakano, T.; Torii, T.; Nakazawa, M.; Izawa, K. *Tetrahedron Lett.* **2001**, 42, 6337; d) Gohring, W.; Gokhale, S.; Hilpert, H.; Roessler, F.; Schlageter, M.; Vogt, P. *Chimia* **1996**, 50, 532.
- (28) Pace, V.; Holzer, W.; Verniest, G.; Alcántara, A. R.; De Kimpe, N. *Adv. Synth. Catal.* **2013**, 355, 919.
- (29) Adler, M.; Adler, S.; Boche, G. *J. Phys. Org. Chem.* **2005**, 18, 193.
- (30) a) Nahm, S.; Weinreb, S. M. *Tetrahedron Lett.* **1981**, 22, 3815; b) Balasubramaniam, S.; Aidhen, I. S. *Synthesis* **2008**, 3707; c) Pace, V.; Holzer, W.; Olofsson, B. *Adv. Synth. Catal.* **2014**, 356, 3697; d) Pace, V.; Holzer, W. *Aust. J. Chem.* **2013**, 66, 507.
- (31) Pace, V.; Castoldi, L.; Holzer, W. *J. Org. Chem.* **2013**, 78, 7764.
- (32) Ke, Z.; Zhou, Y.; Gao, H.; Zhao, C.; Phillips, D. L. *Chem. Eur. J.* **2007**, 13, 6724.

- (33) Mamuye, A. D.; Castoldi, L.; Azzena, U.; Holzer, W.; Pace, V. *Org. Biomol. Chem.* **2015**, *13*, 1969.
- (34) a) Fetter, J.; Nagy, I.; Giang, L. T.; Kajtar-Peredy, M.; Rockenbauer, A.; Korecz, L.; Czira, G. *J. Chem. Soc., Perkin Trans. 1* **2001**, 1131; b) Rasmussen, J. K.; Hassner, A. *Synthesis* **1973**, 682; c) Chiba, T.; Okimoto, M. *J. Org. Chem.* **1991**, *56*, 6163.
- (35) a) Guijarro, A.; Yus, M. *Tetrahedron Lett.* **1993**, *34*, 3487; b) Guijarro, A.; Mancheño, B.; Ortiz, J.; Yus, M. *Tetrahedron* **1996**, *52*, 1643.
- (36) Pace, V.; Murgia, I.; Westermayer, S.; Langer, T.; Holzer, W. *Chem. Commun.* **2016**, *52*, 7584.
- (37) Lautens, M.; Maddess, M. L.; Sauer, E. L. O.; Ouellet, S. G. *Org. Lett.* **2001**, *4*, 83.
- (38) Pace, V.; Castoldi, L.; Holzer, W. *Adv. Synth. Catal.* **2014**, *356*, 1761.
- (39) Pace, V.; Castoldi, L.; Hoyos, P.; Sinisterra, J. V.; Pregnotato, M.; Sánchez-Montero, J. M. *Tetrahedron* **2011**, *67*, 2670.
- (40) Gorokhovik, I.; Neuville, L.; Zhu, J. *Org. Lett.* **2011**, *13*, 5536.
- (41) Mamuye, A. D.; Monticelli, S.; Castoldi, L.; Holzer, W.; Pace, V. *Green Chem.* **2015**, *17*, 4194.
- (42) a) Pace, V.; Castoldi, L.; Mamuye, A. D.; Langer, T.; Holzer, W. *Adv. Synth. Catal.* **2016**, *358*, 172; For isatins homologation with diazomethane, see: b) Chodnekar, M. S.; Crowther, A. F.; Hepworth, W.; Howe, R.; McLoughlin, B. J.; Mitchell, A.; Rao, B. S.; Slatcher, R. P.; Smith, L. H.; Stevens, M. A. *J. Med. Chem.* **1972**, *15*, 49; c) Kennewell, P. D.; Miller, D. J.; Scrowston, R. M.; Westwood, R. *J. Chem. Soc. Miniprint* **1995**, *10*, 2380; For isatins homologation with sulfur ylides, see d) Chouhan, M.; Senwar, K. R.; Sharma, R.; Grover, V.; Nair, V. A. *Green Chem.* **2011**, *13*, 2553; e) Hajra, S.; Maity, S.; Maity, R. *Org. Lett.* **2015**, *17*, 3430.
- (43) a) Allen, A. D.; Tidwell, T. T. *Chem. Rev.* **2013**, *113*, 7287; b) Delebecq, E.; Pascault, J.-P.; Boutevin, B.; Ganachaud, F. *Chem. Rev.* **2013**, *113*, 80.
- (44) Gilman, H.; Kinney, C. R. *J. Am. Chem. Soc.* **1924**, *46*, 493.
- (45) a) Padwa, A.; Crawford, K. R.; Rashatasakhon, P.; Rose, M. *J. Org. Chem.* **2003**, *68*, 2609; b) Antczak, M. I.; Ready, J. M. *Chem. Sci.* **2012**, *3*, 1450; c) Ach, D.; Reboul, V.; Metzner, P. *Eur. J. Org. Chem.* **2002**, *2002*, 2573.
- (46) a) Schäfer, G.; Bode, J. W. *Chimia* **2014**, *68*, 252; b) Schäfer, G.; Matthey, C.; Bode, J. W. *Angew. Chem. Int. Ed.* **2012**, *51*, 9173.
- (47) Pace, V.; Castoldi, L.; Holzer, W. *Chem. Commun.* **2013**, *49*, 8383.
- (48) Pace, V.; Castoldi, L.; Mamuye, A. D.; Holzer, W. *Synthesis* **2014**, *46*, 2897.
- (49) Pace, V.; de la Vega-Hernández, K.; Urban, E.; Langer, T. *Org. Lett.* **2016**, *18*, 2750.
- (50) Hoppe, D.; Hintze, F.; Tebben, P. *Angew. Chem. Int. Ed.* **1990**, *29*, 1422.
- (51) Kerrick, S. T.; Beak, P. *J. Am. Chem. Soc.* **1991**, *113*, 9708.
- (52) Pace, V.; Castoldi, L.; Monticelli, S.; Safraneck, S.; Roller, A.; Langer, T.; Holzer, W. *Chem. Eur. J.* **2015**, *21*, 18966.
- (53) a) Dixon, S.; Fillery, S. M.; Kasatkin, A.; Norton, D.; Thomas, E.; Whitby, R. *J. Tetrahedron* **2004**, *60*, 1401; b) Lhermet, R.; Ahmad, M.; Fressigné, C.; Silvi, B.; Durandetti, M.; Maddaluno, J. *Chem. Eur. J.* **2014**, *20*, 10249; c) Boddaert, T.; François, C.; Mistico, L.; Querolle, O.; Meerpoel, L.; Angibaud, P.; Durandetti, M.; Maddaluno, J. *Chem. Eur. J.* **2014**, *20*, 10131; d) Negishi, E.; Akiyoshi, K.; O'Connor, B.; Takagi, K.; Wu, G. *J. Am. Chem. Soc.* **1989**, *111*, 3089.
- (54) a) Field, L.; Banks, C. H. *J. Org. Chem.* **1975**, *40*, 2774; b) Field, L.; Chu, H.-K. *J. Org. Chem.* **1977**, *42*, 1768.
- (55) Petragani, N.; Schill, G. *Chem. Ber.* **1970**, *103*, 2271.
- (56) Pace, V.; Pelosi, A.; Antermite, D.; Rosati, O.; Curini, M.; Holzer, W. *Chem. Commun.* **2016**, *52*, 2639.
- (57) a) Giannerini, M.; Fañanás-Mastral, M.; Feringa, B. L. *Nat. Chem.* **2013**, *5*, 667; b) Giannerini, M.; Hornillos, V.; Vila, C.; Fañanás-Mastral, M.; Feringa, B. L. *Angew. Chem. Int. Ed.* **2013**, *52*, 13329; c) Vila, C.; Giannerini, M.; Hornillos, V.; Fananas-Mastral, M.; Feringa, B. L. *Chem. Sci.* **2014**, *5*, 1361; For highlights, see: d) Pace, V.; Luisi, R. *ChemCatChem* **2014**, *6*, 1516; e) Capriati, V.; Perna, F. M.; Salomone, A. *Dalton Transactions* **2014**, *43*, 14204; f) Firth, J. D.; O'Brien, P. *ChemCatChem* **2015**, *7*, 395.

Biosketches

Paste photo in this space	Overwrite this text with the author's short biography. Add more table rows as required (one per author).
---------------------------	---

For **Accounts**, include photos and short biographical text for all authors. If the photo is of a group of people, specify who is shown where.

For **Synpacts**, restrict the photo and biographical text to the main (starred) author(s). If the photo displays co-workers, however, they can be mentioned briefly within the main author's short biography.

Photographs (.jpg or .tif format) must be a minimum of 300 dpi in order to reproduce well in print.

Checklist (have these on hand for manuscript submission in ScholarOne):

- cover letter, including a statement of the work's significance
- full mailing address, telephone and fax numbers, and e-mail address of the corresponding author
- email address for each author
- original Word file
- original graphics files zipped into one zip file
- eye-catching graphical abstract as an individual file
- 5–8 key words

Useful links:

- [SYNLETT homepage](#)
- [SYNLETT information and tools for authors](#)
- [Graphical abstract samples](#) (PDF file download)
- [What is "Primary Data"?](#)
- [ScholarOne](#) (manuscript submission)
-

(1) a) Knochel, P.; Molander, G. A.; Eds., In *Comprehensive Organic Synthesis (Second Edition)*, Elsevier, **2014**,

; b) Pace, V. *New Perspectives in Homologation Processes for Synthetic Medicinal Chemistry: Lithium Halocarbenoids at the Helm*. Habilitation Thesis, University of Vienna, Vienna, 2016.

(2) Pace, V.; Monticelli, S.; de la Vega-Hernandez, K.; Castoldi, L. *Org. Biomol. Chem.* **2016**, *14*, 7848.

(3) Li, J. J. *Name Reactions for Homologation*; Wiley: Hoboken, **2009**.

- (4) a) Köbrich, G.; Akhtar, A.; Ansari, F.; Breckoff, W. E.; Büttner, H.; Drischel, W.; Fischer, R. H.; Flory, K.; Fröhlich, H.; Goyert, W.; Heinemann, H.; Hornke, I.; Merkle, H. R.; Trapp, H.; Zündorf, W. *Angew. Chem. Int. Ed.* **1967**, *6*, 41; b) Boche, G.; Lohrenz, J. C. W. *Chem. Rev.* **2001**, *101*, 697; c) Braun, M., In *The Chemistry of Organolithium Compounds*, Rappoport, Z.; Marek, I., ed.; John Wiley and Sons: Chichester, **2004**; d) Capriati, V., In *Contemporary Carbene Chemistry*, ed.; John Wiley & Sons, Inc: **2013**; e) Capriati, V.; Florio, S. *Chem. Eur. J.* **2010**, *16*, 4152; f) Pace, V.; Holzer, W.; De Kimpe, N. *Chem. Rec.* **2016**, *16*, 2061; g) Pace, V. *Aust. J. Chem.* **2014**, *67*, 311; h) Luisi, R.; Capriati, V., *Lithium Compounds in Organic Synthesis: From Fundamentals to Applications*. ed.; Wiley-VCH: Weinheim, 2014; 'Vol.' p; i) Clayden, J. *Organolithiums: Selectivity for Synthesis*; Pergamon: Oxford, **2002**; j) Gessner, V. H. *Chem. Commun.* **2016**,
- (5) a) Arndt, F.; Eistert, B.; Ender, W. *Chem. Ber.* **1929**, *62*, 44; b) Candeias, N. R.; Paterna, R.; Gois, P. M. P. *Chem. Rev.* **2016**, *116*, 2937; c) Ford, A.; Miel, H.; Ring, A.; Slattery, C. N.; Maguire, A. R.; McKervey, M. A. *Chem. Rev.* **2015**, *115*, 9981; d) Maas, G. *Angew. Chem. Int. Ed.* **2009**, *48*, 8186; e) Pace, V.; Verniest, G.; Sinisterra, J. V.; Alcántara, A. R.; De Kimpe, N. *J. Org. Chem.* **2010**, *75*, 5760.
- (6) a) Corey, E. J.; Chaykovsky, M. *J. Am. Chem. Soc.* **1962**, *84*, 867; b) Gololobov, Y. G.; Nesmeyanov, A. N.; Iysenko, V. P.; Boldeskul, I. E. *Tetrahedron* **1987**, *43*, 2609.
- (7) a) Molitor, S.; Gessner, V. H. *Synlett* **2015**, *26*, 861; b) Molitor, S.; Feichtner, K.-S.; Kupper, C.; Gessner, V. H. *Chem. Eur. J.* **2014**, *20*, 10752; c) Molitor, S.; Becker, J.; Gessner, V. H. *J. Am. Chem. Soc.* **2014**, *136*, 15517; d) Kupper, C.; Molitor, S.; Gessner, V. H. *Organometallics* **2014**, *33*, 347; e) Molitor, S.; Gessner, V. H. *Chem. Eur. J.* **2013**, *19*, 11858; f) Gessner, V. H.; Däschlein, C.; Strohmann, C. *Chem. Eur. J.* **2009**, *15*, 3320.
- (8) Pasco, M.; Gilboa, N.; Mejuch, T.; Marek, I. *Organometallics* **2013**, *32*, 942.
- (9) a) Simmons, H. E.; Smith, R. D. *J. Am. Chem. Soc.* **1958**, *80*, 5323; b) Charette, A. B.; Beauchemin, A., In *Organic Reactions*, ed.; John Wiley & Sons, Inc.: **2004**.
- (10) a) Satoh, T. *Heterocycles* **2012**, *85*, 1; b) Satoh, T. *Chem. Soc. Rev.* **2007**, *36*, 1561; c) Avolio, S.; Malan, C.; Marek, I.; Knochel, P. *Synlett* **1999**, 1820; d) Hoffmann, R. W.; Nell, P. G.; Leo, R.; Harms, K. *Chem. Eur. J.* **2000**, *6*, 3359; e) Hoffmann, R. W.; Nell, P. G. *Angew. Chem. Int. Ed.* **1999**, *38*, 338.
- (11) a) Nishimura, R. H. V.; Murie, V. E.; Soldi, R. A.; Lopes, J. L. C.; Clososki, G. C. *J. Braz. Chem. Soc.* **2015**, *26*, 2175; b) Nishimura, R. H. V.; Murie, V. E.; Soldi, R. A.; Clososki, G. C. *Synthesis* **2015**, *47*, 1455; c) Nishimura, R. H. V.; Toledo, F. T.; Lopes, J. L. C.; Clososki, G. C. *Tetrahedron Lett.* **2013**, *54*, 287.
- (12) Köbrich, G. *Angew. Chem. Int. Ed.* **1972**, *11*, 473.
- (13) Sadhu, K. M.; Matteson, D. S. *Tetrahedron Lett.* **1986**, *27*, 795.
- (14) a) Barluenga, J.; Llavona, L.; Concellón, J. M.; Yus, M. *J. Chem. Soc., Perkin Trans. 1* **1990**, 417; b) Barluenga, J.; Baragaña, B.; Alonso, A.; Concellón, J. M. *J. Chem. Soc., Chem. Commun.* **1994**, 969; c) Barluenga, J.; Baragaña, B.; Concellón, J. M. *J. Org. Chem.* **1995**, *60*, 6696.
- (15) Tarhouni, R.; Kirschleger, B.; Rambaud, M.; Villieras, J. *Tetrahedron Lett.* **1984**, *25*, 835.
- (16) a) Concellón, J. M.; Cuervo, H.; Fernández-Fano, R. *Tetrahedron* **2001**, *57*, 8983; b) Concellón, J. M.; Rodríguez-Solla, H.; Simal, C. *Org. Lett.* **2008**, *10*, 4457; c) Concellón, J. M.; Rodríguez-Solla, H.; Bernad, P. L.; Simal, C. *J. Org. Chem.* **2009**, *74*, 2452.
- (17) Savoia, D.; Alvaro, G.; Di Fabio, R.; Gualandi, A.; Fiorelli, C. *J. Org. Chem.* **2006**, *71*, 9373.
- (18) a) Matteson, D. S. *J. Org. Chem.* **2013**, *78*, 10009; b) Matteson, D. S.; Majumdar, D. *Organometallics* **1983**, *2*, 1529; c) Matteson, D. S.; Majumdar, D. *J. Am. Chem. Soc.* **1980**, *102*, 7588.
- (19) a) Sonawane, R. P.; Jheengut, V.; Rabalakos, C.; Larouche-Gauthier, R.; Scott, H. K.; Aggarwal, V. K. *Angew. Chem. Int. Ed.* **2011**, *50*, 3760; b) Pulis, A. P.; Blair, D. J.; Torres, E.; Aggarwal, V. K. *J. Am. Chem. Soc.* **2013**, *135*, 16054; c) Burns, M.; Essafi, S.; Bame, J. R.; Bull, S. P.; Webster, M. P.; Balieu, S.; Dale, J. W.; Butts, C. P.; Harvey, J. N.; Aggarwal, V. K. *Nature* **2014**, *513*, 183; d) Rasappan, R.; Aggarwal, V. K. *Nat Chem* **2014**, *6*, 810; e) Unsworth, P. J.; Leonori, D.; Aggarwal, V. K. *Angew. Chem. Int. Ed.* **2014**, *53*, 9846; f) Watson, C. G.; Balanta, A.; Elford, T. G.; Essafi, S.; Harvey, J. N.; Aggarwal, V. K. *J. Am. Chem. Soc.* **2014**, *136*, 17370; g) Balieu, S.; Hallett, G. E.; Burns, M.; Bootwicha, T.; Studley, J.; Aggarwal, V. K. *J. Am. Chem. Soc.* **2015**, *137*, 4398.
- (20) a) Emerson, C. R.; Zakharov, L. N.; Blakemore, P. R. *Chem. Eur. J.* **2013**, *19*, 16342; b) Blakemore, P. R.; Burge, M. S. *J. Am. Chem. Soc.* **2007**, *129*, 3068; c) Blakemore, P. R.; Marsden, S. P.; Vater, H. D. *Org. Lett.* **2006**, *8*, 773; d) Wu, Z.; Sun, X.; Potter, K.; Cao, Y.; Zakharov, L. N.; Blakemore, P. R. *Angew. Chem. Int. Ed.* **2016**, *55*, 12285.
- (21) Kapeller, D. C.; Hammerschmidt, F. *J. Am. Chem. Soc.* **2008**, *130*, 2329.
- (22) Kail, D. C.; Malova Krizkova, P.; Wiczorek, A.; Hammerschmidt, F. *Chem. Eur. J.* **2014**, *20*, 4086.
- (23) Degennaro, L.; Fanelli, F.; Giovine, A.; Luisi, R. *Adv. Synth. Catal.* **2015**, *357*, 21.
- (24) Kirmse, W. *Angew. Chem. Int. Ed.* **1965**, *4*, 1.
- (25) Loupy, A.; Tchoubar, B. *Salt Effects in Organic and Organometallic Chemistry*; VCH: Weinheim, **1992**.
- (26) a) Reeder, M. R.; Anderson, R. M. *Chem. Rev.* **2006**, *106*, 2828; b) Honda, Y.; Katayama, S.; Kojima, M.; Suzuki, T.; Kishibata, N.; Izawa, K. *Org. Biomol. Chem.* **2004**, *2*, 2061; c) Izawa, K.; Onishi, T. *Chem. Rev.* **2006**, *106*, 2811; d) Pace, V.; Castoldi, L.; Pregnotato, M. *Mini-Rev. Med. Chem.* **2013**, *13*, 988.
- (27) a) Onishi, T.; Hirose, N.; Nakano, T.; Nakazawa, M.; Izawa, K. *Tetrahedron Lett.* **2001**, *42*, 5883; b) Onishi, T.; Nakano, T.; Hirose, N.; Nakazawa, M.; Izawa, K. *Tetrahedron Lett.* **2001**, *42*, 5887; c) Onishi, T.; Otake, Y.; Hirose, N.; Nakano, T.; Torii, T.; Nakazawa, M.; Izawa, K. *Tetrahedron Lett.* **2001**, *42*, 6337; d) Gohring, W.; Gokhale, S.; Hilpert, H.; Roessler, F.; Schlageter, M.; Vogt, P. *Chimia* **1996**, *50*, 532.
- (28) Pace, V.; Holzer, W.; Verniest, G.; Alcántara, A. R.; De Kimpe, N. *Adv. Synth. Catal.* **2013**, *355*, 919.
- (29) Adler, M.; Adler, S.; Boche, G. *J. Phys. Org. Chem.* **2005**, *18*, 193.
- (30) a) Nahm, S.; Weinreb, S. M. *Tetrahedron Lett.* **1981**, *22*, 3815; b) Balasubramaniam, S.; Aidhen, I. S. *Synthesis* **2008**, 3707; c) Pace, V.; Holzer, W.; Olofsson, B. *Adv. Synth. Catal.* **2014**, *356*, 3697; d) Pace, V.; Holzer, W. *Aust. J. Chem.* **2013**, *66*, 507.

- (31) Pace, V.; Castoldi, L.; Holzer, W. *J. Org. Chem.* **2013**, *78*, 7764.
- (32) Ke, Z.; Zhou, Y.; Gao, H.; Zhao, C.; Phillips, D. L. *Chem. Eur. J.* **2007**, *13*, 6724.
- (33) Mamuye, A. D.; Castoldi, L.; Azzena, U.; Holzer, W.; Pace, V. *Org. Biomol. Chem.* **2015**, *13*, 1969.
- (34) a) Fetter, J.; Nagy, I.; Giang, L. T.; Kajtar-Peredy, M.; Rockenbauer, A.; Korecz, L.; Czira, G. *J. Chem. Soc., Perkin Trans. 1* **2001**, 1131; b) Rasmussen, J. K.; Hassner, A. *Synthesis* **1973**, 682; c) Chiba, T.; Okimoto, M. *J. Org. Chem.* **1991**, *56*, 6163.
- (35) a) Guijarro, A.; Yus, M. *Tetrahedron Lett.* **1993**, *34*, 3487; b) Guijarro, A.; Mancheño, B.; Ortiz, J.; Yus, M. *Tetrahedron* **1996**, *52*, 1643.
- (36) Pace, V.; Murgia, I.; Westermayer, S.; Langer, T.; Holzer, W. *Chem. Commun.* **2016**, *52*, 7584.
- (37) Lautens, M.; Maddess, M. L.; Sauer, E. L. O.; Ouellet, S. G. *Org. Lett.* **2001**, *4*, 83.
- (38) Pace, V.; Castoldi, L.; Holzer, W. *Adv. Synth. Catal.* **2014**, *356*, 1761.
- (39) Pace, V.; Castoldi, L.; Hoyos, P.; Sinisterra, J. V.; Pregolato, M.; Sánchez-Montero, J. M. *Tetrahedron* **2011**, *67*, 2670.
- (40) Gorokhovik, I.; Neuville, L.; Zhu, J. *Org. Lett.* **2011**, *13*, 5536.
- (41) Mamuye, A. D.; Monticelli, S.; Castoldi, L.; Holzer, W.; Pace, V. *Green Chem.* **2015**, *17*, 4194.
- (42) a) Pace, V.; Castoldi, L.; Mamuye, A. D.; Langer, T.; Holzer, W. *Adv. Synth. Catal.* **2016**, *358*, 172; b) Chodnekar, M. S.; Crowther, A. F.; Hepworth, W.; Howe, R.; McLoughlin, B. J.; Mitchell, A.; Rao, B. S.; Slatcher, R. P.; Smith, L. H.; Stevens, M. A. *J. Med. Chem.* **1972**, *15*, 49; c) Kennewell, P. D.; Miller, D. J.; Scrowston, R. M.; Westwood, R. J. *Chem. Soc. Miniprint* **1995**, *10*, 2380; d) Chouhan, M.; Senwar, K. R.; Sharma, R.; Grover, V.; Nair, V. A. *Green Chem.* **2011**, *13*, 2553; e) Hajra, S.; Maity, S.; Maity, R. *Org. Lett.* **2015**, *17*, 3430.
- (43) a) Allen, A. D.; Tidwell, T. T. *Chem. Rev.* **2013**, *113*, 7287; b) Delebecq, E.; Pascault, J.-P.; Boutevin, B.; Ganachaud, F. *Chem. Rev.* **2013**, *113*, 80.
- (44) Gilman, H.; Kinney, C. R. *J. Am. Chem. Soc.* **1924**, *46*, 493.
- (45) a) Padwa, A.; Crawford, K. R.; Rashatasakhon, P.; Rose, M. J. *Org. Chem.* **2003**, *68*, 2609; b) Antczak, M. I.; Ready, J. M. *Chem. Sci.* **2012**, *3*, 1450; c) Ach, D.; Reboul, V.; Metzner, P. *Eur. J. Org. Chem.* **2002**, *2002*, 2573.
- (46) a) Schäfer, G.; Bode, J. W. *Chimia* **2014**, *68*, 252; b) Schäfer, G.; Matthey, C.; Bode, J. W. *Angew. Chem. Int. Ed.* **2012**, *51*, 9173.
- (47) Pace, V.; Castoldi, L.; Holzer, W. *Chem. Commun.* **2013**, *49*, 8383.
- (48) Pace, V.; Castoldi, L.; Mamuye, A. D.; Holzer, W. *Synthesis* **2014**, *46*, 2897.
- (49) Pace, V.; de la Vega-Hernández, K.; Urban, E.; Langer, T. *Org. Lett.* **2016**, *18*, 2750.
- (50) Hoppe, D.; Hintze, F.; Tebben, P. *Angew. Chem. Int. Ed.* **1990**, *29*, 1422.
- (51) Kerrick, S. T.; Beak, P. J. *J. Am. Chem. Soc.* **1991**, *113*, 9708.
- (52) Pace, V.; Castoldi, L.; Monticelli, S.; Safranek, S.; Roller, A.; Langer, T.; Holzer, W. *Chem. Eur. J.* **2015**, *21*, 18966.
- (53) a) Dixon, S.; Fillery, S. M.; Kasatkin, A.; Norton, D.; Thomas, E.; Whitby, R. J. *Tetrahedron* **2004**, *60*, 1401; b) Lhermet, R.; Ahmad, M.; Fressigné, C.; Silvi, B.; Durandetti, M.; Maddaluno, J. *Chem. Eur. J.* **2014**, *20*, 10249; c) Boddaert, T.; François, C.; Mistico, L.; Querolle, O.; Meerpoel, L.; Angibaud, P.; Durandetti, M.; Maddaluno, J. *Chem. Eur. J.* **2014**, *20*, 10131; d) Negishi, E.; Akiyoshi, K.; O'Connor, B.; Takagi, K.; Wu, G. *J. Am. Chem. Soc.* **1989**, *111*, 3089.
- (54) a) Field, L.; Banks, C. H. *J. Org. Chem.* **1975**, *40*, 2774; b) Field, L.; Chu, H.-K. *J. Org. Chem.* **1977**, *42*, 1768.
- (55) Petraghani, N.; Schill, G. *Chem. Ber.* **1970**, *103*, 2271.
- (56) Pace, V.; Pelosi, A.; Antermite, D.; Rosati, O.; Curini, M.; Holzer, W. *Chem. Commun.* **2016**, *52*, 2639.
- (57) a) Giannerini, M.; Fañanás-Mastral, M.; Feringa, B. L. *Nat. Chem.* **2013**, *5*, 667; b) Giannerini, M.; Hornillos, V.; Vila, C.; Fañanás-Mastral, M.; Feringa, B. L. *Angew. Chem. Int. Ed.* **2013**, *52*, 13329; c) Vila, C.; Giannerini, M.; Hornillos, V.; Fananas-Mastral, M.; Feringa, B. L. *Chem. Sci.* **2014**, *5*, 1361; d) Pace, V.; Luisi, R. *ChemCatChem* **2014**, *6*, 1516; e) Capriati, V.; Perna, F. M.; Salomone, A. *Dalton Transactions* **2014**, *43*, 14204; f) Firth, J. D.; O'Brien, P. *ChemCatChem* **2015**, *7*, 395.
-

